THE COMPOSITION AND STATE OF GOLD TAILINGS

NICOLAAS JOHANNES VERMEULEN

A thesis submitted in partial fulfilment of the requirements for the degree

PHILOSOPHIAE DOCTOR (ENGINEERING)

in the

FACULTY OF ENGINEERING, BUILT ENVIRONMENT AND INFORMATION TECHNOLOGY

UNIVERSITY OF PRETORIA

PRETORIA

January 2001

UNIVERSITEIT VAN PRETORIA
UNIVERSITY OF PRETORIA
YUNIBESITHI YA PRETORIA

DIE SAMESTELLING EN TOESTAND VAN GOUDSLIK

NICOLAAS JOHANNES VERMEULEN

'n Proefskrif voorgelê ter gedeeltelike vervulling van die vereistes vir die graad

PHILOSOPHIAE DOCTOR (INGENIEURSWESE)

in die

FAKULTEIT INGENIEURSWESE, BOU-OMGEWING EN INLIGTINGTEGNOLOGIE

UNIVERSITEIT VAN PRETORIA

PRETORIA

Januarie 2001

Sole Deo Gloria

UNIVERSITEIT VAN PRETORIA
UNIVERSITY OF PRETORIA
YUNIBESITHI YA PRETORIA

THESIS SUMMARY

THE COMPOSITION AND STATE OF GOLD TAILINGS

N.J. VERMEULEN

Supervisor: Professor E. Rust (University of Pretoria)
Co-Supervisor: Professor C.R.I. Clayton (University of Southampton, UK)
Department: Civil Engineering
University: University of Pretoria
Degree: Philosophiae Doctor (Engineering)

Tailings dams are generally not designed with the same conservatism as conventional water-retention dams for economical reasons. The safe design, construction, operation and reclamation of these structures require an understanding of the nature and behaviour of tailings as a construction material. The composition of this man-made material and its influence on the in-situ state of tailings is of particular importance. A research program was therefore initiated at the University of Pretoria, to investigate the composition and state of South African gold tailings on the far West Rand gold reefs. Samples for this project were collected from the pond areas of two impoundments, and from the tailings delivery slurry.

Individual layers in a tailings deposit, whether fine or coarse, are made up of mixtures of tailings sands (particles larger than 63 μm) and tailings slimes (particles smaller than 63 μm). Tailings sands are shown to be almost pure silica quartz with approximately 10% illite. Tailings slimes, on the other hand, contain considerable amounts of clay minerals (20% muscovite, 15% illite and 20% pyrophyllite, kaolin and clinochlore) and traces of pyrite and other sulphides in addition to the quartz. Tailings, consequently, have a significant amount of clay fines, which can be expected to have a major effect on the mechanical behaviour of the material. Tailings sands are highly angular to sub-rounded, bulky, but flattened particles, whereas the finer slimes are made-up of thin and plate-like particles characteristic of clay minerals. Particle surface textures can range from smooth to rough on a micro scale.

The material considered in this study had an abundance of slimes in both fine and coarse samples, which controlled its behaviour. Fully dispersed gradings were uniformly distributed in the fine sand

UNIVERSITEIT VAN PRETORIA
UNIVERSITY OF PRETORIA
YUNIBESITHI YA PRETORIA

SAMEVATTING VAN PROEFSKRIF

DIE SAMESTELLING EN TOESTAND VAN GOUDSLIK

N.J. VERMEULEN

Promotor: Professor E. Rust (Universiteit van Pretoria)
Medepromotor: Professor C.R.I. Clayton (Universiteit van Southampton, VK)
Departement: Siviele Ingenieurswese
Universiteit: Universiteit van Pretoria
Graad: Pholisophiae Doctor (Ingenieurswese)

Slikdamme word as gevolg van ekonomiese oorwegings, nie ontwerp volgens dieselfde konserwatiewe benadering waarmee konvensionele damme ontwerp word nie. Die veilige ontwerp, konstruksie, bedryf en herwinning van slikdamme vereis 'n deeglike kennis van die aard en gedrag van slik as 'n boumateriaal. Die samestelling van goudslik en die invloed daarvan op die toestand en meganiese gedrag van die materiaal is van besondere belang. Ten einde hierdie eienskappe te ondersoek is 'n navorsingsprojek gestig by die Universiteit van Pretoria. Vir die doel is slikmateriaal gemonster vanaf twee slikdamme in die verre Wesrand.

Individuele lae in 'n slikdam bestaan uit mengsels van sliksande (greine groter as 63 μm) en slikslym (greine kleiner as 63 μm). In hierdie studie word getoon dat die sliksand hoofsaaklik bestaan uit suiwer silika kwarts met 'n klein persentasie (ongeveer 10%) klei-minerale. In teenstelling daarmee bevat slikslym aansienlik meer klei-minerale (ongeveer 45%), sowel as klein hoeveelhede piriet en ander sulfiede. Dit is dus duidelik dat goudslik genoeg klei-minerale bevat om die meganiese gedrag daarvan te beïnvloed. Sliksande het 'n hoekige vorm, alhoewel die korrels meer plat as kubies of rond is. In teenstellings hiermee bestaan slikslym uit dun plaatjies soos tipiese klei-minerale. Die oppervlak van individuele greine wissel van glad tot grof op 'n mikroskaal.

Die materiaal wat bestudeer is het 'n oormaat fyn materiaal gehad in beide die fyn en growwe slikmonsters. Die gedrag van hierdie slikke word dus beheer deur die fyn materiaal. In 'n gedispergeerde toestand, lê die graderings univorm verprei in die slik- en fynsand-areas met min greine kleiner as 2 μm of groter as 200 μm. Die verskil tussen fyn en growwe graderings is hoofsaaklik geleë in die medium greingrootte wat wissel tussen 6 en 60 μm. Wanneer monsters nie

ACKNOWLEDGEMENTS

I wish to express my appreciation to the following organisations and persons who made this thesis possible:

- Professors *Eben Rust* and *Chris Clayton* for their professional and personal guidance and motivation throughout the duration of this project.
- Professors *A.W. Rohde* and *E. Horak* for allowing me the time and resources to complete this work within a reasonable timeframe.
- *Vaal River Operations (Anglo Gold)*: Chris Robertse, and his staff for their on-site assistance.
- *University of Pretoria Electron Microscopy Laboratory*: Andre Botha for teaching me how to fish with a scanning electron microscope.
- *University of Pretoria X-ray Diffraction Services*: Sabina Verryn.
- *University of Pretoria Civil Engineering Laboratory*: Jaap Peens and his team for their assistance with the piezocone fieldwork.
- My wife *Kona* for her support and encouragement throughout the project and for editing the final manuscript.
- My parents for instilling in me a desire for knowledge and an appreciation for quality.
- Funding for this project was provided by: *SRK Tailings* (Adriaan Meintjes), *Jones and Wagener* (Dr. Fritz Wagener) and the *University of Pretoria Research Development Programme*. The work was also partially supported by a grant from the Technology and Human Resources for Industry Programme (THRIP); a partnership programme funded by the Department of Trade and Industry (DTI) and managed by the National Research Foundation (NRF) of South Africa.

TABLE OF CONTENTS

LIST OF TABLES

LIST OF FIGURES

CHAPTER 1

INTRODUCTION

1.1 BACKGROUND

A catastrophic failure of the Merriespruit gold tailings dam in February 1994, resulted in 17 fatalities, more than 200 injured, 80 houses destroyed, a further 200 houses severely damaged and more than R75mil in damage as 600,000 m^3 of liquefied slurry engulfed the township on the evening of the 22nd. Apart from graphically illustrating the risk of a tailings dam failure, the disaster sparked a campaign of renewed investigation into the safety of impoundment structures in South Africa. Tailings have been the subject of research in many countries around the world, especially those where mineral resources form a major part of the economy - South Africa being a good example. Nevertheless, very little research has concentrated on the fundamental composition of tailings and the influence thereof on the mechanical behaviour of this man-made material. Consequently a research programme has been initiated at the University of Pretoria to study the properties and behaviour of tailings.

This thesis constitutes the first step in defining the composition and state of typical South African gold tailings. Notable features include the use of the electron microscope and x-ray technology to examine the composition of tailings; exposure of a 5 m undisturbed tailings profile near the penstock of an impoundment; use of high quality undisturbed samples; as well as extensive laboratory tests to improve the interpretation of in-situ cone penetration data.

1.2 OBJECTIVE

The objective of this study was to investigate the composition and state of gold mine tailings to advance the state-of-the-art in understanding the mechanical behaviour of this material. The characterisation of tailings in their undisturbed state has always been complicated by difficulties in extracting undisturbed samples for controlled laboratory tests. For this study, both bulk and undisturbed samples of gold tailings have been subjected to methodical in-situ and laboratory testing to determine the in-situ composition and state. The material selected is representative of typical Witwatersrand gold tailings.

The behaviour of a tailings impoundment, as a geotechnical structure, is controlled by the state and composition of the in-situ material. For the purposes of this report these terms are defined below:

a) **Mechanical behaviour**: Stress-strain behaviour of a material described in terms of parameters that describe the fundamental and structural properties of the material, for example the effective angle of internal friction, ϕ', shear stiffness, G', and Poisson's ratio, ν. These parameters are used in design calculations or theoretical models to predict the load response for safety and serviceability assessments.

b) **Composition**: The composition of a soil is determined by the physical constituents and their properties together with the properties of the pore fluid. Physical properties that are of interest include: mineralogy, specific gravity, size distribution, shape and surface texture, whereas pH, colloidal solids and soluble solids are of importance in the pore fluid.

c) **State**: The state of a soil is governed by the state of the skeletal structure, i.e. the state of the packing arrangement including density and fabric as well as the nature of the inter-particle interactions or bonds. The state is partly a function of the history of loading and the current stress levels. Stress is usually defined in terms of effective stress resulting from the combined effect of the total stress and pore pressure regimes.

A tailings impoundment exists as a highly layered deposit of finely ground, silt sized, particles with mechanical properties intermediate between those of sands and clays. Generally, a raised impoundment is constructed with the coarser tailings sands serving as an embankment wall, and the finer slimes as internal fill. However, at any given location on an impoundment, individual layers can vary significantly in composition. Composition together with state will define the geotechnical behaviour under load. Factors that may be of importance in this regard include changes in composition between finer and coarser grades of tailings, as well as variances in state as a function of composition and structure. Of particular interest is the role of inter-particle forces including body-force components, surface charge effects and inter-particle bonding.

This study aims at defining the composition and state of gold tailings to serve as a basic model for understanding its geotechnical properties and behaviour, as follows:

a) Characterisation of the fundamental properties of the tailings solid particles including mineralogy, specific gravity, size distribution, particle shape and surface texture.

b) Determination of the compressibility and stiffness characteristics of fine and coarse tailings grades.

c) Investigation of the strength characteristics as a function of state and composition including in-situ structure.

d) Comparison of test results on reconstituted laboratory samples with tests on high quality undisturbed samples as well as in-situ piezocone tests.

1.3 SCOPE

Due to the extended nature of the study certain limitations have been imposed to permit a manageable project. These can be summarised as follows:

a) Subject material has been restricted to a gold tailings product from Vaal River Operations in the far west of the Witwatersrand.

b) Two impoundment sites were identified as relevant to the study. The first, Pay Dam - one of the older dams, was being recycled to extract remaining valuable content. The northern penstock on this dam had been washed open to a depth of 5 m by hydro-cannon. The site was used extensively for undisturbed sampling of fine and coarse deposits next to the penstock. It was also used to compare directly visual profiles with those deduced from in-situ piezocone tests. The second site, Mizpah - the latest addition on the mine, was representative of a well designed working impoundment. Bulk samples of fine and coarse deposits were collected from the beach-pond interface and a series of piezocone tests made from the daywall, across the beach and into the pond.

c) Samples were collected mainly from the pond areas of the impoundments where access is normally very difficult. In addition, a representative sample of the tailings delivery pulp was also taken.

d) Only saturated conditions were considered in this study, although samples were taken and piezocone probes made in the area above the water table, where de-saturation may have occurred. All laboratory tests concerned with compression and shear strength were performed on saturated samples, either as reconstituted slurries or by saturation of undisturbed specimens in the triaxial apparatus.

e) The study concentrated on the physical properties of the tailings particles and their effect on mechanical behaviour, although it is recognised that the pore fluid chemistry must play an important role. Wherever possible, the original pore fluid was retained in the undisturbed samples and for preparing specimens for indicator tests. In other cases, distilled water was added for grading and other purposes.

1.4 METHODOLOGY

To realise the objectives of this study samples of tailings were subjected to a comprehensive series of controlled laboratory tests. Results from these tests have been

compiled to describe the state and composition of the tailings and correlated with in-situ piezocone tests. Laboratory tests were performed using both reconstituted remoulded slurries and undisturbed samples. Test methods employed can be summarised as:

a) Basic indicator tests including particle size grading, specific gravity and Atterberg limits.

b) Use of electron microscope imagery for indications of particle size, shape and surface texture as well as undisturbed fabric.

c) X-ray emission spectrometry in the scanning electron microscope for elemental composition.

d) X-ray powder diffraction for mineral identification.

e) Compression and consolidation in the triaxial apparatus to examine stiffness and density states as a function of stress level and composition.

f) Undrained triaxial shear to examine strength dependency of the material on composition and state.

1.5 ORGANISATION OF THE THESIS

The thesis consists of the following chapters:

- *Chapter 1* serves as an introduction to the report.
- *Chapter 2* presents a review of the state-of-the-art on gold tailings and tailings structures from a survey of published literature.
- *Chapter 3* summarises all experimental work including site selection, sampling, laboratory as well as in-situ tests.
- *Chapter 4* discusses the results of the experimental program in terms of defining the in-situ composition and state of typical South African gold tailings.
- *Chapter 5* closes the thesis with a summary of the main conclusions.

CHAPTER 2

LITERATURE REVIEW

2.1 INTRODUCTION

The objective of this chapter is to present a literature review of tailings dam design and construction in general, as well as a critical review of the engineering properties of gold tailings. A brief history of the South African gold mining industry is given with emphasis on the geology and mineralogy of the two principal gold producing areas: the Witwatersrand Gold Fields and the Barberton Gold Fields. This is followed by a detailed examination of the physical and chemical processes employed to recover the gold valuables, which produce the tailings by-product to be disposed of. The design and construction of tailings impoundments are considered, highlighting the differences in philosophy between the mining companies and regulatory authorities. Alternative layouts and construction methods are discussed and it will be seen that the most popular arrangement used in South Africa, although economical, is also the least desirable from a safety point of view. The chapter ends with a comprehensive review of the mechanical properties of gold tailings, laying the groundwork for the rest of the thesis.

2.2 A BRIEF HISTORY OF THE GOLD MINING INDUSTRY IN S.A.

2.2.1 Introduction

The earliest documented discoveries of gold were made in river beds or shallow excavations in ancient Egypt, Russia and later during the gold rushes in California, Australia and Alaska. However, it was South Africa that became the scene of the greatest gold find of all - the gold-bearing Witwatersrand reefs which constitute the largest known deposits of gold in the world. The discovery of gold in South Africa has had a profound effect on the development of this country, not only in sustaining a precious metal based economy, but also in providing job opportunities for millions and supporting a vast range of subsidiary industries. South Africa has been the world leader in gold production for many years and at stages produced more gold than all the other countries combined. The following presents a short chronology of significant events in the gold mining industry in South Africa as reported by Stanley (1987):

1806 The Secretary Governor of the Cape announces the discovery of gold between the Witwatersrand and the town of Magaliesberg, 154 years after Jan van Riebeek and the V.O.I.C. "Vereenigde Oost-Indische Compagnie" sailed around Cape Point.

1836 Reports are heard of gold mining actives in the Soutpansberg in the far north of the country.

1850 Cape farmers discover gold nuggets in the Gamka river.

1868 Gold is discovered in the Olifants river and Murchison range in the Transvaal.

1871 Organised mining of the Natalia reef starts on the farm Eersteling in the northern town of Pietersburg.

1872 Low veld alluvial gold deposits are found in the Sabie-Pilgrim's Rest area. A town rises out of the dust and becomes a mecca for gold diggers, panners and swindlers alike.

1874 Alluvial gold is found near the town of Magaliesberg on the West Rand.

1875 Alluvial and vein gold is discovered near Barberton on the East Rand and leads to the Barberton Boom from 1877 to 1883.

1881 First discovery of gold quartz veins at Kromdraai.

1884 Vein gold in the Confidence Reef west of Johannesburg on the Central Rand leads to the discovery of the greatest gold strike in history - the legendary Witwatersrand Gold Reefs.

1886 The highly profitable Main Reef of the Witwatersrand is first discovered in March 1886 as an exposed conglomerate.

1891 Mining is established along the outcrop reefs of the Witwatersrand.

1894 East Rand Proprietary Mines (ERPM) the oldest operating mine, declared gold in September 1894 and has produced roughly 1,500 tons of gold at an average grade of 7,23 grams per metric ton to date.

1932 Discovery of the continuation of the Witwatersrand Reefs on the West Wits Line leads to the establishment of the country's wealthiest and deepest mines on the far West Rand.

1939 Basal Reef becomes a major contributor of gold in the Orange Freestate.

1952 By this time the broad outline of the Witwatersrand Basin had been established as outcrops and "Shallow" Reefs stretching from Germiston to Randfontein comprising the East, Central and West Rand gold fields, from which the reef dips south and stretches to the "Deep" Reefs of the West Wits Line near Carltonville, and eventually into the Freestate goldfields.

1977 With the development of more effective metallurgical processes, the recycling of old slimes dams and waste dumps becomes popular.

A number of large mining houses have been established in South Africa to co-ordinate mining activities with co-operative organisation from the Chamber of Mines of South Africa,

which also functions as a spokesman for the industry. The first Chamber of Mines was formed on 7 December 1887 in the Central Hotel in Johannesburg and was succeeded by the modern Chamber on 5 October 1889. The establishment of a number of significant mining houses soon followed:

1887 Gold Fields of South Africa (GFSA), operates mainly in the far West Rand.

1893 Rand Mines, specialises in deep level mining and once controlled 15% of world richest mines.

1895 Durban Roodepoort Deep, was formed to exploit the first payable gold deposit discovered on the farm Langlaagte on the western side of the Witwatersrand in 1886 near what is now called the town of Roodepoort.

1895 General Mining Corporation (GENCOR), widely diversified today.

1917 Anglo American Corporation, active in the East Rand, West Rand and Orange Freestate, has recently split into a number of subsidiaries of which Anglo Gold is responsible for gold mining operations.

1933 Anglovaal Ltd, has active gold mining interests in the Free State.

2.2.2 Terms and Definitions

Terms and definitions used in the mining industry for the various components associated with hard rock mining and tailings, which are useful for the purposes of this study, include (Truscott, 1923; Gilchrist, 1989, Cowey, 1994):

- **Country Rock**: The rock bordering and containing the gold bearing reef, typically quartzite, sandstone, granite, rhyolite, andesite, etc. In South Africa the Country Rock is mostly shales and clays.
- **Effluent:** Liquid fraction of the tailings slurry or pulp with soluble chemicals.
- **Gangue**: Gangue, consisting of minerals associated with the gold in the ore and country rock, constitutes the valueless portion to be removed and disposed of. Gangue minerals associated with gold ore are generally non-metalliferous and may include quartz (SiO_2), calcite ($CaCO_3$), silver (Ag) alloyed with the gold, pyrites (FeS_2), arsenopyrite (FeAsS) and chalcopyrite ($CuFeS_2$).
- **Ore**: Metalliferous rock from which metal or metallic compounds are extracted as valuables. The Witwatersrand gold ore, or Banket as it is known, consists of consolidated pebbles and gravels fast cemented in a quartzite matrix, which is hard and tough.
- **Ore-mineral**: The valuable portion of the ore typically gold, uranium, platinum, coal etc. In all cases in South Africa, gold is disseminated extremely finely within the ore, nuggets being very rare.
- **Pulp density or Solids Concentration (S_c):** The ratio of the mass of the solids to the mass of the total slurry, or $S_c = 1/(1 + w)$, where the moisture content, w, represents

the ratio of the mass of water to the mass of solids. Pulp densities can range between 15 and 55% in tailings, but is usually between 40 and 50%.

- **Rate-of-Rise (ROR):** Term used to describe the rate of increase in height with time as deposition proceeds on a tailings impoundment, usually in meters per year. Rate-of-rise is the single most important construction related factor controlling impoundment stability.
- **Tailings Sands:** Fraction by weight coarser than 75 μm, but for the purposes of this thesis measured at 63 μm.
- **Tailings Slimes:** Fraction by weight finer than 75 μm, but for the purposes of this thesis measured at 63 μm.
- **Tailings**: The by-product of the extraction process, tailings consist of finely ground and chemically treated rock flower in a slurry with process water. Tailings in South Africa are usually disposed of in perimeter dyke surface impoundments or slimes dams. Occasionally it is put to use as underground backfill for mined out areas.
- **Waste Rock**: Mostly country rock extracted in developing access to the reefs. These rocks do not enter the metallurgical works and are usually disposed of in large rock dumps.

2.2.3 Geology and Mineralogy of the Witwatersrand gold fields

The sediments of the Witwatersrand Goldfields or Triad were laid down between 2.7 and 3 billion years ago in a large basin south of Johannesburg and are derived from the surrounding Archian granite-greenstone terrains (Stanley 1987). The deposits lie in an oval area of approximately 42,000 km^2 in Gauteng, North-West Province and the Freestate Province. The gold was originally introduced in the deposit as detrital particles that underwent the low grade metamorphism which led to re-crystallisation. The Witwatersrand reefs are the largest contributor of gold in the world. More than 40 million kilograms of fine gold have been recovered up to 1985, with an average grade in all reefs mined until 1962 of 8.74 g/t. Undoubtedly, many more kilograms have been recovered to date, but at reduced yields, as the richest areas have become mined out.

Throughout the Witwatersrand, gold ores occur in sheets or reefs originally deposited horizontally under water. The reefs were subsequently covered by material up to thousands of meters deep. Following the consolidation and cementation of these layers, geological movements transformed it into tilted and faulted strata. The thickness of the reefs ranges between a line of grit to several meters, with an average of 300 mm. The sediments were also intersected by dykes and sills of dolerite, diabase and syenite intruding existing faults.

The reefs can be in the form of either coarse conglomerates or, less frequently, greyish metamorphosed sedimentary rock formations. In the conglomerates, rock pebbles are cemented in a silicate matrix. Pebbles, usually derived from vein quartz, may also consist of quartzite, chert jasper and quartz porphyry and vary in composition, size and colour. The matrix consists of pure silica, but also contains minute flakes of muscovite and pyrophyllite as well as visible pyrite and other sulphides. Table 2-1 summarises the mineral composition of a typical gold reef on the Witwatersrand.

Table 2-1: Mineral composition of a typical Witwatersrand gold reef (Stanley, 1987).

Mineral	Abundance
Quartz (SiO_2), primary and secondary	70 - 90%
Muscovite and other phyllosilicates	10 - 30%
Pyrites	3 - 4%
Other sulphides	1 - 2%
Grains of primary minerals	1 - 2%
Uraniferous Kerogen	1%
Gold	~45 ppm in the Vaal Reef

The gold is usually confined to the matrix and tends to be concentrated along bedding planes. Visible gold is relatively rare. Table 2-2 presents a summary of the major types of gold to be found in the Witwatersrand reefs.

Table 2-2: Major types of gold occurrences in the Witwatersrand reefs.

Type of Gold	Relative Abundance
Detrital gold	Up to 90% of total gold in some reefs occur as clusters of grains
Biochemical redistributed gold	An important source if present
Metamorphosed gold	5 - 40% depending on local conditions
Primary gold in allergenic sulphides	Mainly pyrite, less than 2%
Gold in secondary quartz veins	Extremely rare but highly concentrated
Surface outcrops	Highly weathered, oxidised and friable
Other minerals of economic interest	Silver, Pyrite (Sulphuric acid), Uranium, Platinum and Sulphides

2.2.4 The Barberton gold fields

The Barberton gold fields are situated in a volcanic sedimentary greenstone belt of Archian granite-greenstones in the Mpumalanga and Swaziland low-veld. The gold is largely found in refractory ores containing significant amounts of sulphide minerals, such as pyrite. Gold is also recovered from quartz veins and weathered and oxidised outcrops that have been enriched by the removal of the sulphides. In the refractory ores gold extraction is adversely affected by cyanide-consuming sulphide minerals, the presence of coarse gold particles which require extended contact for dissolution as well as by impervious coatings (iron oxides) on the gold particles which hinder contact with the leachate. Economical extraction of gold from these ores requires very fine grinding and roasting (calcining) to oxidise the iron sulphide minerals and thus expose the gold.

2.3 THE GOLD EXTRACTION PROCESS

2.3.1 Winning mineral ores

The winning of mineral ores can be summarised as: drilling, blasting and moving broken ore to the mill. When gold reserves are discovered, usually by diamond core drilling, a shaft is sunk in an optimal location. From the main shaft horizontal development tunnels are advanced at different levels to intercept the dipping ore bearing reefs. Winzes (connecting tunnels) are then created in the reef dip between the horizontal drives. From these winzes the reef is mined by drilling and blasting in stopes or working areas extending on the reef dip. Actual stoping widths are usually of the order of 1m. The broken ore is shovelled into the paths of mechanical scrapers, which move the ore down the stopes to be collected in "koekepanne" or underground rail-mounted hoppers. From the stopes the ore is transported to central, near vertical, shafts known as ore-passes, which collect the material from several levels before hoisting it to the surface in ore-cages. Reef and development waste is handled separately. Some sorting of waste rock and reef is sometimes employed in the stopes, where the broken ore ranges in size from about 300 mm to very fine fractions. Once at the surface the material is transported to the mill either by conveyer belt, train or truck.

2.3.2 Ore-dressing

Ore dressing comprises the mechanical preparation of ore rocks by crushing, grinding and separation, in order to liberate, expose and concentrate the valuable mineral for metallurgical extraction (Ritcey, 1989). The objectives of ore-dressing include: reducing the ore to a proper size for the metallurgical extraction, removal of the gangue as far as possible, increasing the concentration of valuable minerals for transport or extraction,

removal of impurities that can hinder metallurgical processes and separation of different ore-minerals that might occur together. All this has to be done in the most economical way, i.e. using the least number of machines of the largest capacity. Liberation of the mineral is governed by factors such as grain size and complexity of mineralisation. The gangue can often provide clues as to the possibility of excessive reagent consumption during leaching, which would require calcining prior to the metallurgical processes to convert the ores to a reduced or oxidised state for enhanced metal recovery. On the Witwatersrand 5 - 10% of the gold is encased in sulphides, but in Barberton deposits up to 100% is encased in the refractory ores. Calcining is thus required with the Barberton refractory ores to reduce the iron sulphide minerals.

Many properties of the ore minerals make separating it from the gangue possible. Colour, lustre and general appearance have often been used in the past to hand-pick valuable pieces from the waste. Density and surface energy effects influence the rate of sedimentation of the different constituents in water and other fluids. Magnetic permeability and electric conductivity may also be used to concentrate the ore mineral by magnetic and electrostatic separation. Other useful properties include fusibility, friability, fracture, hardness, texture, aggregation etc.

The ore-dressing program on a gold mine may consist of the following, (Truscott, 1923):

(a) **Washing and Sorting:** Washing cleans the crude-ore for subsequent sorting and crushing, and is sometimes sufficient to release some of the mineral-ore from the gangue. Separation of different constituents or classes of ore is usually done by hand. The operators pick out pieces of ore clean enough for direct metallurgical treatment, whilst sorting out worthless pieces of gangue. Removal of minerals and foreign objects such as tramp metal and wood chips that interfere with the rest of the process is a major advantage. However, hand-sorting is limited to a certain size fraction by practical and economical factors.

(b) **Comminution (Crushing):** Comminution denotes the whole operation of reducing crude ore in successive stages to the fine slurry or pulp required for metallurgical treatment. Crushing is often the most expensive part of ore-dressing because of the fineness required. The old workhorses of the reduction works, gravity stamps and steam stamps, have since been replaced by more efficient machines, which reduce the ore to expose the valuable mineral in the following stages:

- *Preliminary Comminution or Breaking*: Jaw and/or Cone Breakers, Figure 2-1 and Figure 2-2, are used to break the rocks by applying direct pressure without adding any water. Breaking rarely releases or exposes the mineral but reduces the size of the material for subsequent crushing. With jaw breakers

the ore is broken between fixed and moving jaws actuated by a pitman lever within a massive iron or steel frame. In the cone breakers the ore is caught and broken inside a outer concave ring by the eccentric gyration of an inner conical cylinder. In the 1950's Run-of-Mine (ROM) milling was introduced negating the need for preliminary breaking by sending the mined ore directly to the mills. Nevertheless, breakers are still being used widely in preliminary comminution today.

- *Primary Comminution or Crushing*: In the beginning the stamp mill reigned supreme as the primary mill, fed from gyratory crushers, but was eventually replaced by primary Tube Mills and Ball Mills, Figure 2-3. These mills, fed from the breakers or directly by hoisted material (ROM), crush the ore by shear and impact caused by the rolling and falling of metal balls or rods within a revolving cylinder. Crushing results in a substantial release and exposure of the mineral as the ore is completely slimed with very little sand fraction remaining. Crushing can also be done using Pressure Rolls, Pendulum Rollers and Edge Runners.
- *Secondary Comminution or Grinding*: Secondary comminution completes the release or exposure of the mineral and is basically a continuation of primary comminution.

Table 2-3 gives an indication of the size reduction ratios and capacities of different plant used for comminution in the gold mining industry.

(c) **Sizing and Classification:** In dressing it often becomes necessary to eliminate variability in size in order to improve staged comminution. Sizing and classification comprise the division and separation of broken, crushed or ground material into classes according to the average diameter (sizing) and density (classification). Sizing can be done efficiently by screening, and classification by separating particles in a rising column of water. Depending on whether mechanical or chemical processes follow, flocculants or de-flocculants may be added to the slurry. Flocculants are added in small amounts to promote settlement in preparation for chemical treatments such as cyanidation. Flocculants used include inorganic acids, sulphuric acid, ferrous sulphate, lime, neutral salts, calcium chloride, magnesium sulphate, alum and iron salts, with lime being most popular. Mine water is usually a flocculant in itself and inhibits mechanical separation by trapping ore-minerals in the gangue. De-flocculation is then brought about using dispersants such as alkalis and alkali salts, sodic carbonate, organic acids and tannic acid.

(d) **Concentration:** Optimisation of ore-dressing techniques require maximum release of the ore-mineral but at the same time avoiding excessive comminution. In addition, gold

Table 2-3: Ratings of crushing plant used commonly in the gold industry.

Machine	Size Reduction			Crushing Rate	Daily capacity
	Feed	Out	Factor		
	(mm)	*(mm)*		*(kg/kW.hr)*	*(Tons)*
Jaw and Cone Breakers	..	50	4	1200	120-1200
Gravity Stamp	50	4	12	200	8-20
	50	1	50	125	5-8
	50	0.4	120	75	2-4
Steam Stamp	100	12.5	8	150	250-400
Tube-mill, short	4	0.2	20	125	50-250
Tube-mill, long	1	0.1	10	50	25-100
Ball Tube-mill	50	1.25	40	250	50-400
	50	0.3	160	100	40-200
Ball-mill	75	0.5	150	100	40-100
Rolls, coarse	50	12.5	4	600	100-400
Rolls, fine	12.5	1.25	10	350	100-400
Pendulum, wet	19	0.8	24	100	30-60
Pendulum, dry	38	0.4	90	50	10-20
Edge-runner, slow	50	0.4	120	100	20-40
Edge-runner, fast	9	0.6	15	100	50-80

values and sulphides (pyrite) have to be extracted efficiently form the gangue after the mineral ore has been detached or liberated. Water concentration (gravity), flotation and other methods attempt to separate the valuable ore-mineral from poor gangue, thus avoiding wasteful and useless comminution and providing a concentration of the valuable ore-mineral.

- Water concentration requires the mineral to be of a different density than the gangue, allowing the division of ore-mineral from gangue by density if already sized, or by size if classified. Gold ores lend themselves to gravity extraction as the gold and pyrite are much denser than the silica carrier.
- Flotation Concentration relies on the wetting and non-wetting properties of the ore-mineral by water and other contaminants (oils). Oil has an affinity for mineral ores and floats on water to be collected as overflow - oil flotation. Flotation can also be effected by rising gas bubbles, where the non-wetting property of the mineral allows it to be carried off by the bubbles - gas-froth flotation. Flotation concentration is mostly used to treat refractory ores for roasting (calcining) prior to cyanidation, but has grown in popularity elsewhere.

- Other separation techniques include: magnetic separation, electrostatic separation, pneumatic separation and centrifugal separation. These, however, are not commonly used in the gold mining industry.

(e) **Heat Treatments:** Ores may be heat treated during the dressing stages to remove excess water, or to expose the ore-mineral in refractory ores. This process is known as calcining. During calcining the ore is heated to between 450 and 800°C. The iron sulphides (typically pyrite) decompose into porous haematite, rendering the gold amenable to chemical treatment as follows:

$$4FeS_2 + 11O_2 \rightarrow 2Fe_2O_3 \text{ (Red Haematite)} + 8SO_2 \qquad \textbf{Eq. 2-1}$$

$$3FeS_2 + 8O_2 \rightarrow Fe_3O_4 \text{ (Black Magnetite)} + 6SO_2 \qquad \textbf{Eq. 2-2}$$

Several intermediate materials are formed and the sulphur dioxide may be used in the manufacturing of sulphuric acid. Roasting also volatilises cyanides (cyanide consuming agents) such as antimony and arsenic.

2.3.3 Metallurgical extraction

Once the valuable ore-mineral has been liberated, exposed and concentrated by ore-dressing techniques, it may be extracted chemically through the processes of amalgamation or cyanidation, Stanley (1987).

(a) **Amalgamation:** The first step in the amalgamation process is to bring the gold into contact with mercury, whereby the gold dissolves in the mercury. This is done by either passing the pulp over mercury laden copper plates, or by tumbling the pulp with mercury in an amalgam drum with the addition of caustic soda to help oxidation of the sulphides. The resultant amalgam is washed clear of sulphides. Excess mercury may be pressed out through canvas in an amalgam press followed by retorting. Retorting comprises the separation and recovery of mercury from pressed gold amalgam through distillation and condensation. The retorted gold, spongy in appearance, is melted with flux and poured into bullion bars. The drawbacks of this process are the obvious health and safety hazards it poses, together with labour intensiveness and large floor space requirements. The process has largely been superseded by cyanidation.

(b) **Cyanidation:** During cyanidation the gold is leached from a thickened pulp with soluble cyanide salts (sodium cyanide, NaCN or calcium cyanide, CaCN) according to the following equation:

$$2Au + 4NaCN + ½O_2 + H_2O = 2NaAu(CN)_2 + 2NaOH \quad \textbf{Eq. 2-3}$$

Other essentials are oxygen and calcium hydroxide, $Ca(OH)_2$, to stabilise the cyanide radical, control alkalinity and maintain a minimum pH of 10 to 11. The pulp is usually prevented from sedimenting by mechanical or compressed-air agitation to facilitate leaching. Depending on the grade of the ore up to 98% gold can be extracted in the leaching process. Cyanide leaching results in a solution containing anionic metal cyanide complexes from which the gold complexes must be recovered. Two major routes for recovery may be followed. The first, zinc precipitation, requires the liquid (gold in solution) to be separated from any insoluble material before recovery; the second, carbon-in-pulp (CIP) process, is able to recover the gold directly from the leached pulp. Separation of liquid and solids is usually done through continuous vacuum filtration followed by filtrate clarification, to remove the remaining fine suspended solids.

- *Zinc Precipitation or Cementation*: Vacuum de-aeration is applied to remove dissolved oxygen, since this greatly improves the efficiency and economics of the process. Soluble lead salts (lead nitrate) are then added together with zinc shavings or dust, whilst satisfactory cyanide and alkalinity levels (using calcium oxide, CaO) have to be maintained for efficient operation. Mixing can take place prior to precipitation in a small emulsifier tank. Zinc precipitates the gold due to its high electro-negative charge in relation to gold's electro-positive charge, according to the following formula:

  $$2NaAu(CN)_2 + Zn = Na_2Zn(CN)_4 + 2Au \quad \textbf{Eq. 2-4}$$

  The slime of gold and zinc salts produced in this way is recovered by filtration and then treated with dilute sulphuric acid to remove as much zinc and other impurities as possible. The resulting precipitate is then calcined to dry the pulp and to oxidise impurities such as lead and zinc prior to smelting with a flux of borax and silica. Smelting oxidises the base metals in the gold slime and combines them with silica to form a slag, which separates from the gold and silver due to its lower density. Gold smelts at 1063°C, requiring the ovens to work at between 1200 - 1400°C. The bullion is poured into bars, cleaned, numbered and assayed before dispatch to the Rand Refinery. The slag is also dispatched to the Rand Refinery as a by-product.
- *Carbon-In-Pulp Process*: Activated carbon is used to recover gold by adsorption directly from the leachate. The carbon must be coarser than the pulp (usually > 1 mm) so that it can be readily screened from the pulp in the end. Adsorption occurs as the pulp flows continuously by gravity through a series of tanks and inter-stage screens. The inter-stage screens ensure that the carbon remains in the tanks but allows the pulp to pass. The pulp loses

gold progressively down the train, with barren value in the last tank. The carbon, removed once a day by counter current from the last to the first tank, is then washed by dilute hydrochloric acid (HCl), followed by washing with water to remove tramp material (wood chips etc.) as well as slime. During washing the system is raised to the desired elution temperature of 110 - 120°C. Eluates such as potassium cyanide, sodium sulphide or caustic cyanide (NaCN + NaOH) are then used to release the gold and bring it into solution. Gold is recovered from the eluate either by electro winning or zinc precipitation. A similar technique called the carbon-in-solution (CIS) process may be used to scavenge gold from other solutions that arise from existing mine circuits.

- *Carbon-in-Leach (CIL) Process*: The leach and adsorption circuits are occasionally combined. The carbon enhances the leach efficiency by removing surface coatings and has advantages from a capital cost point of view. However, CIL presents considerable operational problems.

Other methods employed include: resin-in-pulp (RIP) using ion-exchange resins instead of carbon, solvent-in-pulp (SIP), reverse osmosis and membrane technology, electro winning, pressure elution and electro elution.

2.3.4 Refining

The Rand Refinery, based in Germiston near Johannesburg, was established in 1920 to provide a gold refining service to the South African mining industry (Cowey, 1994). It is the largest and most modern gold refinery in the world, processing South Africa's entire production of newly-mined gold. In addition to gold refining services, the Rand Refinery also provides analytical services, produces silver and gold granules of various caratages and delivers high purity export products and gold chemicals, such as gold potassium cyanide used for gold plating.

At the refinery bullion is upgraded to at least 99.5% pure by either the Miller chlorination process or electrolytic refining. Miller chlorination involves chlorine gas being blown through the molten bullion, which converts base metals and silver to chlorides or slag. Electrolytic refining may be used to extract the remaining impurities from the chlorination process to render 99.99% pure gold by removing the platinum group metals. This process is also used to recover gold from mine by-products such as sweepings, dust, clothes, etc.

2.4 TAILINGS IMPOUNDMENTS

2.4.1 Introduction

It is generally recognised that mining industries provide an essential input into the economy of various regions around the world. It is equally well known that mines can also be a source of immense environmental concerns. More than 5 t of solid and liquid wastes have to be generated in the mining and milling processes to obtain about 10 g of gold, (Ripley et al., 1982). Only a small percentage of these wastes can potentially be backfilled into worked-out areas underground and the bulk of the waste has to be stored in large surface impoundments. However, point of view can often colour one's perceptions of these waste impoundments, as illustrated by two quotes from the same era:

> *"Many Massive 'Manhill's that Mark the Mortals' Map*
> *Make Magnificent and Mighty Monuments to*
> *- the Miner's Muscle*
> *- the Metallurgists Magic and*
> *- the Meaningful Meditations of the Master*
> *of Mud Mechanics, the Mill Manager"*
>
> Smith (1972)

> *"In the view of conservationists, there is something special about dams, something - as conservation problems go - that is disproportionately and metaphysically sinister. The outermost circle of the Devil's world seems to be a moat filled mainly with DDT. Next to it is a moat of burning gasoline. Within that is a ring of pinheads each covered with a million people - and so on past phalanxed bulldozers and bicuspid chain saws into the absolute centre of hell on earth, where stands a 'Tailings' dam."*
>
> McPhee (1971)

Tailings, the by-product of ore-dressing and metallurgical extraction processes, contain the waste fraction of the processed mineral-ores, usually in the form of a fine grained slurry or pulp. Until the mid-1800's mining and smelting technologies were primitive and only the highest grade ores could be mined profitably with the result that little waste was produced. As mining, smelting and transportation technologies improved, lower grade ores could be mined, leading to increased volumes of tailings as well as a finer grind, (USCOLD, 1994). During 1900 - 1930 the first dams were constructed specifically to retain tailings in the USA. Before that, tailings were disposed of directly into rivers and other water bodies. The first dams, designed by trial and error by mine operators, were often constructed across stream channels employing upstream methods and did not survive long. After the 1928 Barahona

dam failure in Chile, the downstream method was employed for the first time, as were cycloned sands for constructing the embankment walls. In the 1940's earthmoving equipment made conventional water retention dams viable, and by 1950 engineering principles of seepage and foundation stability were applied. The 1965 seismic failures in Chile gave impetus to liquefaction research in tailings and issues related to groundwater contamination were introduced in the 1970's.

Tailings impoundments are arguably the largest structures built by man (Hoare & Hill, 1970), with significance for engineers, regulatory authorities and the public alike. They can and often do have a greater environmental impact than any other aspect of the mine, including, for example, the mine excavation. Tailings structures are primarily geotechnical structures; built on soils and rocks, with soil and rock materials to contain the tailings product that behaves essentially as a soil. The amount of tailings produced in the world, $5x10^9$ t/yr in 1994, greatly exceeds the amount of fill handled by the civil engineering profession in the construction of embankment dams, motorway embankments, and all other earthworks (Penman, 1994). By far the greatest amount of tailings is produced by the processing of metal ores. South African mines were producing in excess of 250 million tons of mine tailings waste annually in 1987, with an average mine producing roughly 100,000 tons of tailings per month over an expected lifetime of 25 years (Donaldson, 1965). This much waste requires impoundment structures that pose huge risks of environmental destruction and possible disaster in the event of a failure. Fortunately such disasters have been relatively infrequent. Nevertheless, more than 1,000 fatalities have been reported since 1917 as a result of incidents on all types of tailings impoundments. These and similar incidents have caused countless millions of rand in damages to property, not to mention devastating the environment.

The main components of a residue disposal system according to McPhail and Wagner (1989) are (see Figure 2-4):

- *Delivery system*: Pipe work, valves and discharge points to convey and deposit the tailings pulp onto the impoundment.
- *Containment wall or Embankment*: Either as a raised wall composed of deposited tailings and a small compacted earth starter wall, or as a conventional retaining earth and/or rock dam wall.
- *Under-drainage system*: System of filter drains to control seepage from within the dam.
- *Decant system*: Penstock or floating barge type drainage facilities for the removal of clarified slurry water and storm water from the pond.
- *Stromwater diversion system*: Trenches and/or bunds around the dam to divert storm water runoff.

- *Stromwater catchment system*: Paddocks arranged around the dam to control water and tailings sediment from the dam slopes.
- *Return water system*: System of dams, sumps and pipes for handling effluent from the dam.
- *Ancillary systems*: Access roads, power supply, etc.

2.4.2 Siting and Layout

As with conventional water-retaining dams, each tailings impoundment constitutes an individual project, dependent for its detailed design on the site conditions, the type and rate of delivery of the tailings, availability of other waste materials from the mining or industrial processes, climatic conditions and many other factors.

The most important restraint in siting a proposed impoundment is storage capacity, i.e. the ability of the structure to accommodate daily demands for tailings disposal with rate-of-rise (ROR) being the restraining factor. Should the structure rise too quickly, the development of pore pressures in excess of equilibrium levels can adversely affect the stability of impoundments constructed of low permeability tailings products. For gold tailings, of relatively high permeability, the ROR becomes critical in controlling densification of embankment material through desiccation. Environmental aspects such as air and water pollution have become major issues recently. Blight (1987) estimates the rate of surface erosion on a typical South African gold ring dyke dam to be as much as 500 t/ha per year.

Prior to actual commencement of the design of any tailings impoundment structure, other studies must be developed. These include a preliminary decision regarding the volume of ore to be treated daily and yearly, the general order of the size of the ore body to estimate the total volume of tailings, metallurgical studies to assess the probable tailings gradation and recovery process and potential plant layout. In South Africa it is common practice to start the design with an estimated final height of the impoundment in the order of 35 - 40 m. Rates-of-rise commonly employed range between 1 and 3 m/yr as a function of pulp density and foundation conditions (Wates, 1983) resulting in a life expectancy of at least 10 years. Measurements of settled dry densities range between 1250 and 1650 kg/m^3 as a function of depth, so a value of ρ_d = 1450 kg/m^3 is used in general for design purposes. These values can be used to estimate the required area of the impoundment, which will influence the possibilities of siting and layout. Siting considerations, after Cowey (1994), should also take consideration of:

- *Transportation costs*: Distance and elevation relative to the mill.
- *Topography*: Layout, fill volume requirements and diversion feasibility.
- *Hydrology*: To minimise inflow or diversion requirements.

- *Geology*: Foundation stability, seepage and requirements for borrow fill material.
- *Groundwater*: Seepage contamination.

In addition to the area required for the actual tailings fill, area has to be allocated for stormwater cut-off trenches, access roads, water and pulp services, catchment paddocks as well as area for the handling of returnwater. Usually a 50 m zone around the perimeter is sufficient, but this can make up as much as 25% of tailings dam area.

Areas obviously not suited for tailings dams are those that

- are too far from the metallurgical plant,
- are of a too steep topography,
- pose difficulties with access,
- comprise too large a water catchment area,
- include unsuitable geology or mineralisation,
- include important land use zones and
- are in a sensitive ecological zone.

In defining alternative solutions for a tailings impoundment the following aspects of materials selection and internal arrangement have to be taken into consideration (Caldwell & Stevenson, 1984):

(a) **Embankment type**: The choice of embankment type is governed by mill related factors such as type and output of tailings and effluent as well as site related factors including seismicity, climate, water handling and available materials.

(b) **Phreatic surface**: The free water level in a tailings impoundment governs to a large degree the overall stability of the structure and has to be kept as low as possible near the embankment faces. Seepage breakout on the embankment could lead to mass instability as well as seepage related problems of piping, erosion and sloughing. The phreatic surface is governed by the arrangement of internal permeabilities, which should ideally decrease towards the decant facility, as well as by the permeability of the foundation material relative to the tailings. The only aspect influencing the level of the phreatic surface that can be controlled during operation is the location of the surface pond relative to the embankment walls. Structural aspects that are used to control the phreatic surface in the embankment include low permeability cores and high permeability zones (drainage chimneys, blanket drains or finger drains) to extract water near the embankment face. Filters should be properly designed and constructed and often constitute a disproportionally large fraction of the total cost of construction.

(c) **The starter dike**: By providing a starter dike more pervious than the tailings, an extra measure for phreatic surface control is provided. Typical construction materials for starter dikes include:

- *Natural soils*: Maximum use should be made of natural accessible material, where borrow areas inside the impoundment is most advantageous. Factors which influence selection are: moisture content, permeability and compactibility.
- *Mine waste other than tailings*: Using mine waste may present a major cost advantage, but should balance production rates with rate-of-rise requirements. These materials require careful attention to filter design and construction.
- *Cycloned tailings*: The use of tailings offers major cost advantages over borrowed material, but requires less than 60%, non-plastic slimes in the feed. Cyclone construction is rarely used on gold tailings impoundments due to its low sand content.

According to a parametric study by Nelson et al. (1977) the starter dyke permeability is the most important factor influencing the phreatic surface location in upstream constructed dams, with blanket drains having a lesser effect.

(d) **Foundation conditions**: The design must be compatible with foundation conditions. Problem materials include organic material, normally consolidated soft clays and collapsible soils. If these cannot be removed prior to construction, embankment slopes have to be adjusted accordingly. Notably it is the internal structures that suffer most through settlement damage.

Mining companies and regulatory agencies have fundamentally different objectives in choosing a design alternative for a tailings impoundment. Whereas the mine is concerned with economics, regulatory agencies are concerned with environmental factors, often of equal or greater importance than economic issues, on behalf of the public. The gold market is not controlled by mining companies, but by a free market system of supply and demand. The extra cost of mine waste disposal cannot be passed on to the consumer but must be absorbed within the economic constraints of the project (Van Zyl, 1993). The disposal of mine waste represents, therefore, capital and operating costs to a mining operation. For this reason, mine waste has historically been disposed of at the lowest cost, often with considerable environmental impact. However, any failure in the disposal system could shut down the processing plant causing loss of profit plus payment to unemployed staff, as well as cost of repair and any claims that could arise from the failure. Compounding the economics of these structures is the fact that they have to provide for cost-effective reclamation when the dam is decommissioned (Caldwell & Robertson, 1986). Tailings

structures become part of the environment after they have served their purpose and must be left in a durable and safe state.

The Systems Approach (Roth, 1991) of generating and selecting alternatives has been successfully implemented to meet the interests of all groups concerned in tailings dam design. The final selection of a proposed site and layout is ultimately dependent on:

- visual impact,
- land use,
- airborne dust release,
- seepage water release,
- stability,
- operational requirements and
- cost.

2.4.3 Statutory Requirements in South Africa

Prior to 1998 the main acts controlling the design, construction and operation of tailings impoundments were the Mines and Works Act (Act 27 of 1956), the Atmospheric Pollution Prevention Act (Act 45 of 1965), the Water Act (Act 54 of 1956, as amended from time to time), the Health Act (Act 63 of 1977) and the Soil Conservation Act (Act 54 of 1956). Although the Water Act (as amended by Act No. 96 of 1984) was used to classify a tailings dam structure on the basis of size and hazard potential, a Government Notice in 1986 exempted the Mines from the provisions of the regulations (except regulation 15 regarding registration) for a period of 5 years. This was extended in 1991 for a further period of 2 years, and again for a further period of exemption of 2 years in 1993. No license or permit was required to operate gold residue disposal facilities, but permits regarding slimes dams had to be acquired from the Department of Mineral and Energy Affairs in terms of Section 8(1)(a) and Section 6B/4(2) of the Physical Planning Act (Act 88 of 1967) as well as from the Department of Water Affairs in terms of Section 12,21 and Section 30(5) of the Water Act. In addition, an environmental impact assessment was required as a formal approach to evaluate the effects of the project on the environment and to minimise environmental degradation in the most cost effective manner. Regardless of legislative requirements, emphasis on environmental aspects had the additional benefits of establishing a good public image by preservation or actual improvement of the environment, and demonstrated that industrial development could go hand-in-hand with environmental protection.

After the 1994 Merriespruit disaster (Wagener et al., 1998), work started on the drafting of an obligatory Code of Practice for the design, operation management, rehabilitation and closure of tailings dams. After a trial period in 1997 the draft code was finalised in 1998 and

encoded under South African mining legislation as SABS 0286. Under this code a tailings dam is classified in terms of its hazard potential, requiring certain mandatory procedures depending on the hazard classification. A professional engineer, experienced in tailings dam engineering, is required to review and audit each tailings dam on a regular basis including the monitoring and reporting on rates of rise, piezometer levels, drain outflows, freeboard and pond control. Emphasis is also placed in the code on ensuring that the owner of a tailings dam appoints appropriately experienced and trained operators. In addition to SABS 0286, construction and operation of tailings impoundments are currently controlled by the National Water Act (Act No. 36 of 1998) and regulations incorporating the Water Services Act (Act No. 108 of 1997) Volumes 1 and 2, the Mine Health and Safety Act (Act No. 29 of 1996) and the Occupational Health and Safety Act (Act No. 85 of 1993).

2.4.4 Embankment layouts

When deciding on an embankment layout the designer aims to optimise embankment height and fill area to accommodate daily production rates and final storage capacity, without compromising the safety and serviceability of the structure in the most economical manner. Other factors that have to be taken into account are: earthworks requirements, availability of construction materials, reclamation and seepage control measures.

Typical layout designs that are used worldwide include:

(a) **Perimeter or Ring Dyke**, Figure 2-5a: As the name implies the ring dyke impoundment requires an embankment wall to be constructed around the perimeter of the dam prior to or during filling. This type of layout is used extensively in South Africa due to the flat topography in the gold producing areas, which affords little opportunity for valley type impoundments. Ring dykes require relatively high quantities of embankment fill in relation to their storage capacity and are therefore ideally suited to constructing the embankment wall from the tailings product that is produced over the operational life of the dam. Another advantage of this type of layout is that runoff inflow to the surface is eliminated.

(b) **Cross Valley Impoundments**, Figure 2-5b: The cross valley impoundment requires only one embankment to cross a valley or depression from wall to wall downstream of the storage area. The storage area should ideally be located near the head of the drainage basin to minimise flood inflow quantities that must be handled either by storage, spillways or separate upstream water control dams.

(c) **Side-hill Impoundments**, Figure 2-5c: Best suited to side-hill slopes of less than 10%.

(d) **Valley Bottom or Incised Impoundments**, Figure 2-5d: A compromise between cross valley and side-hill layouts, valley bottom impoundments must be provided with a diversion channel to carry flood inflow around the impoundment.

(e) **Multiple Impoundments vs. Single Impoundment**: A large tailings storage facility can be constructed either as a single impoundment or as a number of separate, but connected impoundment units or compartments. Multiple compartments demand greater volumes of embankment fill material and may require excessive flood control measures in a small upstream section. However, they allow better phreatic surface and seepage control in ring dike systems and may be the only viable option in the restricted space at valley bottoms. Multiple impoundment units can also be used to spread initial construction costs if sequentially constructed.

2.4.5 Transportation and Discharge

In the early gold mining days, the stamp mills produced a coarse sand tailings that was dumped dry using an endless rope cocopan method and more recently belt conveyors (Gowan & Williamson, 1987). Today's reduction product is extremely fine, with a high water content, and does not allow free stacking or dumping. It requires engineered impoundment structures. The most economic materials used to construct a tailings impoundment are often the coarse (sand) fractions of the tailings. The sands can be separated from the fines in the tailings either gravitationally following discharge onto a beach, or centrifugally by hydraulic cycloning.

The tailings slurry is usually pumped at the highest concentration practicable to reduce the bulk of material and the cost of transportation. Pulp concentration is increased at the metallurgical plant by classifiers, cyclones, screens, filters or thickeners, the cost of which should be offset against the benefits of higher rates-of-rise attainable, the value and re-use potential of recovered water as well as reduced costs of return water recovery. The maximum concentration is limited by metallurgical plant processes or by the pumping plant. In a typical gold tailings pulp the ratio of water to solids varies between 2.8 and 1.0 by mass, which relates to a moisture content of between 280 and 100%. For underground filling purposes pulp concentration is further increased to a moisture content of 50% to enhance the dewatering and consolidation characteristics of the fill.

The delivery system comprises rubber lined centrifugal pumps, pipelines - sometimes rubber lined to reduce corrosion and wear, and valves. The options available for discharge

onto the tailings impoundment are sub-aqueous deposition and sub-aerial deposition, either using open ended pipe discharge, spigotting or cycloning.

(a) **Sub-aqueous Deposition**: Usually in the form of uncontrolled discharge within a body of water. The tailings settle as a soft bottom sediment, or are transported and dispersed over a large area under water. The resulting low density material is generally very soft and may require special construction techniques and reclamation procedures. The soft sediments can also retain excess pore pressures for a very long time under self-weight consolidation and can be expected to be under-consolidated[1] in many cases.

(b) **Sub-aerial Deposition:**

- *Open Ended Pipe Discharge*: Open ended pipe discharge is often used in South Africa as an inexpensive delivery system. Deposition is typically accomplished by discharging the slurry from one or more open ended pipe outlets or stations around the perimeter of the dam area. The discharge sequence is cycled to allow a freshly deposited layer time to dry and increase in density before the next layer is deposited. This has been standard practice in South Africa since the early 1900's (Ruhmer, 1974) and results in a significant improvement in the mechanical properties of the deposit. The discharged slurry leaving the pipe forms a deep hole or plunge pool at the base of the pipe outlet from where the slurry breaches and flows towards the central area containing a semi-permanent pond. Flow is fast and concentrated on the beach (sloped area above water level) before fanning out in a delta as it approaches the pond area. The idea is for segregation to take place on the beach, leaving coarser particles closer to the embankment and the finer fraction in the central area. Although there is a general trend of increasing fineness towards the pond area, flow on the upper beach tends to concentrate in meandering channels with flow velocities high enough to pass most of the material to the pond with little opportunity for segregation and deposition on the beach (Penman, 1994).
- *Spigotting*: Similar to open ended discharge, but with the objective of reducing the velocity of the deposited stream and encouraging sheet flow across the beach to aid segregation. This form of deposition effectively separates the coarse sandy fraction from the slimes by gravity segregation on the beach and is therefore generally used when the tailings have a wide grading and high percentage of clay sized material. Spigotting is

[1] Under-consolidation, in the context of this document, implies that primary consolidation and therefore the process of excess pore pressure dissipation has not yet been completed.

accomplished by partly covering the delivery pipe orifice with a faceplate, leaving only a small half-moon opening. This results in a spraying of the discharged slurry over a large area on the beach with more uniform sheet-like flow towards the pond. The same effect can be accomplished by punching holes into a ring-type tailings delivery pipe. With delivery points spaced at 1 to 5 m intervals and operated in groups of 20 to 40 spigots at a time. A ring main around the toe of the dam feeds the spigot pipe, which together with supports and extension pipes has to be raised periodically as the dam rises.

- *Cycloning*: Cyclones mechanically separate the feed pulp into coarse and fine fractions providing competent sands at a reduced water content for embankment building and high water content slimes for interior filling. Operation of a cycloning system requires planning and a significant amount of management if the system is to function properly. It is only practicable when the tailings product has a wide grading with sufficient coarse underflow for embankment wall construction. The Witwatersrand uniformly graded gold ores and general flat terrain makes this type of construction prohibitively expensive. Under special circumstances it might, however, find application in short valley impoundments, where seismic activity is of particular concern or in small operations of limited life.

2.4.6 Methods of Construction

Methods of impoundment construction vary considerably from one tailings product to another as a result of the grading, solids content and solids density of the slurry. These aspects control the tendency of the material to segregate or separate into size fractions following discharge onto the impoundment structure. Copper and platinum tailings being well graded between 2 mm and 1 μm, segregate readily and disposal methods can be designed to optimise the effects of this segregation (McPhail & Wagner, 1989). Gold tailings, on the other hand, are fairly uniformly graded between 200 μm and 2 μm with a reduced tendency to segregate and the design can not rely on the benefits of gravity segregation in the method of disposal (Wates et al., 1987; McPhail & Wagner, 1989). The most important factor controlling segregation of gold tailings slurries is the density of the pulp discharged, and to a lesser extent variations in grading.

In addition to the segregating properties of the slurry, the choice of method of constructing the impoundment structure will be determined by the following factors:

- Capital and operating costs.
- Previous experience and preferences.
- Site topography.

- Climatic conditions which affect drying characteristics and freeboard requirements.

Direct Disposal into a Water body

Historically tailings were discharged from the mill directly into the nearest water course or body. Eventually farmers supporting the mining communities started to complain about plugged irrigation ditches as well as contaminated farmlands. Today, the environmental impact or pre-treatment costs of this method of disposal virtually eliminates the option.

Offshore Disposal

Where the mill effluent is relatively innocuous, sub-aqueous offshore disposal outside of biological productive or sensitive zones, may be considered. However the tailings product should be coarse or flocculated to settle without causing excessive turbidity. Offshore disposal may be the only viable method of disposal in coastal areas with extreme high precipitation, steep terrain and high seismicity.

Conventional Earth or Rock-fill Dam Wall

Tailings impoundments can be constructed in the same way as a conventional water retaining dam using natural materials such as rock-fill with a clay core to construct the retaining wall.

Advantages: Suitable for any type of tailings.
Any discharge procedure may be used.
Suitable for high water storage capacity.
Good seismic resistance.
An engineered upstream filter can readily be included in the wall.

Disadvantage: Construction of entire embankment wall usually in one stage.
Requires natural soil borrow for construction.
High cost of embankment construction.

This method is best suited to impoundments with:

- high water storage requirements and high runoff inputs,
- no re-circulation of tailings water required,
- high clay content tailings requiring large evaporation areas and
- toxic leachate tailings, utilising natural or artificial seepage barriers.

Raised Embankments (Brawner & Campbell, 1972; Mittal & Morgenstern, 1977; Vick, 1983)

To minimise the cost of a tailings impoundment structure the most economical design must be employed. This frequently requires consideration of the use of tailings to construct the dam wholly. Staged construction may then be utilised with the height of the embankment structure maintained minimally above the storage level required. This procedure minimises initial capital investment and spreads the cost of construction over many years.

Construction starts with a small starter dyke of natural materials designed to impound the initial 2 to 3 years of tailings with some flood protection. Thereafter the embankment is raised periodically using tailings material to keep ahead of the main impoundment level with sufficient freeboard for flood control. In areas of low to no seismic activity, tailings embankments can be placed to acceptable densities by carefully controlled hydraulic procedures without additional mechanical compaction. However, in areas of moderate to high seismic activity, additional densification must be achieved by mechanical compaction (Mittal & Morgenstern, 1977). Relative small reductions in the slope of a raised embankment can result in large increases in the dam height and storage capacity. Embankment slope is normally restricted by erosion and stormwater control requirements rather than stability concerns, resulting in quite steep slopes. These are effectively reduced for stability purposes, generally to 25°, by using step-back berms.

There are fundamental differences between conventional earth-fill dams and raised embankment tailings dams that should be taken into account when designing a tailings impoundment (Kealy & Busch, 1979). Tailings from the reduction plant have different characteristics to materials used in natural earth-fill dams, and the method and sequence of construction are entirely different. Consequently embankments built with tailings have the following unique features:

- Unlike earth and rock-fill dams, tailings embankments are active and have an average annual growth rate of 1 to 3 m/yr, depending on the tonnages produced and areas available for disposal. Thus each embankment is under continuous construction until abandonment.
- Due to continuous construction, the seepage regime takes on a different geometry compared with that of a standard water-retention dam.
- Because of the method of hydraulic deposition, each sector of a cross section of the impoundment is highly layered and can have different properties. Furthermore, the methods of deposition and rate-of-rise can change with time and climatic seasons.
- Unlike conventional dams, construction takes place without the use of certified inspectors. Extended field monitoring programs are, therefore, required to provide the data necessary to increase confidence levels in the factor of safety, or to amend

construction techniques. This method of continuous assessment lends itself to the Observational Method of construction as discussed by Peck (1969).

- Finally there is a finite life planned for a tailings embankment, after which land reclamation and re-use should be considered.

Raised embankments may be constructed using one of the following techniques:

- Upstream.
- Downstream.
- Centreline.
- Daywall-nightpan paddock.
- Cyclone.
- Thickened discharge.

(a) **Upstream Raised Embankment (Figure 2-6a):** The upstream technique is the oldest method of constructing tailings dams and is a natural development from considerations of disposing of tailings as cheaply as possible. An initial starter wall is constructed at the downstream toe. This starter wall should be sufficiently pervious to pass seepage water, but designed to resist piping. Tailings are then discharged from the top of the starter dam by spigotting or cycloning to develop a dyke composed of the coarser fraction. The centreline of the top of the embankment is shifted towards the pond area as the height of the dam increases. The downstream toe of each subsequent dyke is supported on top of the previous dyke, with the upstream portion placed over the finer tailings. As the height of the dam increases, the potential failure surface is located at an increasingly greater distance from the downstream face and possibly through layers of soft slimes deposited under backponding due to careless earlier discharge practices. As a result, the outside competent shell contributes less to stability as the height increases.

Harper et al. (1992) label upstream raised embankments as most susceptible to excessive post earthquake deformations and liquefaction (Dobry & Alvarez, 1967; Finn 1982). They stress the importance of water management (Kealy & Busch, 1971; Abadjiev, 1976; Nelson et al., 1977), especially pond location relative to the embankment crest and construction quality control as crucial to the safety of these impoundments. As most historical dams have been built this way, the authors recommend the following methods of improving or stabilising upstream dams: provision of drainage under and within the embankment, reduction of slope angle, use of compaction to improve the density and construction of a rock-fill toe berm against the downstream face to increase stability. Nevertheless, Casagrande and McIver (1970) describe an upstream dam built to a height of 92 m with a slope of 1 in 0.58.

Advantages: Simplest and least costly method of construction.
Smaller quantities of coarse tailings required.
Can use natural soil borrow or tailings in the embankment.
Large initial dam area and high storage capacity.

Disadvantages: Phreatic surface control requires well controlled pond location.
Low pulp density required to promote segregation after deposition.
Low shear strength results from low in-situ densities.
Does not provide for internal drainage facilities.
Limited safe rate-of-rise.
Seismic liquefaction susceptibility - inappropriate in seismic areas.
Cannot be used for water retention.
More prone to cracking due to differential settlements.

(b) **Downstream Raised Embankment (Figure 2-6b):** The downstream method of construction is similar to the upstream method with the centreline of the top of the embankment shifting downstream as the dam is raised. Each subsequent stage of dyke construction, is therefore supported on the top of the downstream slope of the previous section. This method of construction eliminates the possibility of a slip surface passing through earlier backponded slimes as might be the case with the upstream method. If the dam is located in a seismic active area the downstream extensions must be compacted to increase in-place density and minimise the risk of liquefaction. To minimise seepage through an embankment constructed with tailings, the upstream face may be sealed with a layer of impervious soil.

Advantages: Suitable for any type of tailings.
Can use natural soil borrow or tailings for embankment construction.
Rate-of-rise essentially unrestricted.
Can readily incorporate internal drainage systems.
Storage of significant water volumes possible.
Embankment compaction is no problem.
Liquefaction resistant, can be used in areas of high seismicity.
The embankment is not built over previously deposited slimes.

Disadvantages: High initial costs.
Large volume of embankment fill required; increases exponentially.
High cost of embankment construction.
Small initial dam area, but increases with time.
Erosion protection cannot be applied until the dam is completed.

(c) **Centreline Raised Embankment (Figure 2-6c):** The centreline method is a compromise between the upstream and downstream methods. In the centreline

method, the crest of the dam is maintained at the same horizontal position as the height of the dam increases. The dam is raised by spreading and compacting additional coarse tailings on the top, on the upstream shoulder and on the downstream slope. If the upstream slope of the embankment relies on the buttressing effect of the impounded slimes and the slimes undergo large post deposition settlement leaving the upstream face unsupported, localised slope instability may occur. A coarse gradation of the tailings is necessary to afford rapid drainage to provide access for construction and compaction equipment. This method shares advantages with both the upstream and downstream methods, while mitigating many of the disadvantages.

Advantages: Requires less embankment fill than the downstream method.
Moderate cost of embankment construction.
Can use natural soil borrow or tailings for embankment construction.
Acceptable seismic resistance.

Disadvantages: High initial costs.
Requires more sand or coarse fraction than upstream methods.
High restrictions on the rate-of-rise.
Not recommended for permanent water storage.
Erosion protection cannot be applied until the dam is completed.

(d) **Daywall-Nightpan Paddock System (Figure 2-7):** This form of construction relies on a temperate to semi-arid climate and low water table conditions or acceptable evaporation rates to improve the properties of the deposited material. Upstream, downstream and centreline configurations may be employed. The upstream paddock system, developed empirically over the last 100 years, is used almost exclusively in South Africa with its prevailing dry and hot climate in the mining areas. On the Witwatersrand evaporation generally exceeds precipitation and dams up to 60 m high have been built successfully (Penman, 1994). Desiccation suctions of up to 1 MPa have been measured (Blight, 1969), however, these will be destroyed upon re-wetting of the material, and the only reliable increase in strength is thought to be due to densification as a result of the high suctions (Donaldson, 1965).

Compacted earth starter walls and under-drainage are constructed initially so that the rate-of-rise does not exceed 2.5 m/yr by the time the starter wall is overtopped. The tailings then take over from the starter wall as the main embankment wall. The dam is divided into two sections, the perimeter wall or daywall and the interior or night area also known as the nightpan or floor. The daywall is designed to provide sufficient freeboard to retain the accumulated water from deposited tailings and that from the design storm. The daywall is generally 10 - 30 m wide (Wagener & Jacobsz, 1999), at an average slope (Section 2.4.7) of 35° (Blight, 1988) and is sectioned into paddocks around the perimeter, each paddock being filled from its midpoint by a delivery station.

Wall raising is done by building up the rim of a paddock using the deposited tailings, either by tractor-plough or by labour-intensive shovel packing. During the day-shift pulp is delivered into these daywall paddocks to a depth of about 150 - 200 mm and distributed by gravity. Delivery stations are fed from a ring-main around the toe of the dam and are usually not more than 400 m apart. Excess or supernatant water is decanted into the night area via decant pipes through the inner wall of the daywall. The daywall is left to dry, consolidate and crack for up to 3 weeks before the next lift, thus improving the mechanical properties of the material as a result of densification (Blight & Steffen 1979). The need for supervision and close control of the pulp depth makes daywall raising entirely a daytime procedure, hence the name. The daywall is not compacted in South Africa and is approximately 1 - 2 m higher than the interior of the dam.

During the night, tailings are discharged into the interior of the dam (night area or nightpan) from delivery stations located just inside the daywall. Supernatant water is drawn off the next day by penstock decant or barge pump. A natural beach forms in the night area from the delivery point towards the pond surrounding the decant facility. The location of this semi-permanent pond in the night area is controlled by the spacing, sequence of operation and duration of delivery of the internal delivery stations.

Paddock deposition is successful when the tailings product is fairly uniform in grading, remains well in suspension at a constant density until placed, and when the rate-of-rise matches the drying time of the tailings (Gowan & Williamson, 1987). These conditions result in a deposited slurry that is reluctant to segregate and therefore does not result in too weak a region in the low point between delivery stations on the daywall. The method is particularly successful in South Africa for most gold, tin, calcine and gypsum products, aided by the highly evaporative climate. The paddock system results in a daywall which is normally well consolidated and reasonably firm, while the material in the night area and especially in the pond area is significantly less consolidated and soft (Wagener & Jacobsz, 1999).

(e) **Cyclone Construction (Figure 2-8):** Cyclone construction methods can be applied in an upstream, centreline, downstream or combination configuration, depending on the pulp grading and topography. The feed pulp is separated into sand underflow and slimes overflow by hydro-cyclone. The low permeability, fine, overflow contains most of the water and is used to fill the interior of the dam, this is ideal to limit seepage losses to the foundation. The underflow contains the coarser particles with significantly less water content, which greatly reduces its susceptibility to liquefaction (Watermeyer & Williamson, 1979). The improved strength and permeability properties of this fraction makes it the ideal material for constructing the embankment wall.

The percentage of coarse material in the feed pulp is important as it dictates the split percentages and therefore the ratio of coarse building material to fine impound material. Coarse splits of 15 - 25% are normally required for embankment construction and can be achieved by proper choice of cyclone. South African practice is to use the cyclones on site, connected to a manifold pipe maintained along the crest of the dam, where the discharged underflow forms cone shaped piles. The number, size and positions of cyclones are governed by operator preferences, ease of moving and handling, quantity of tailings and the need to distribute the overflow around the perimeter for pond control. Growth of the coarse embankment must exceed the growth of the inner fines beach. This requires careful design of the dam shape and size to ensure adequate embankment fill material.

Cycloned walls usually perform better under seismic loading conditions and are able to handle higher rates-of-rise at the expense of operating costs. These advantages are not as great with the more uniform gold tailings with its poor split. Cyclone construction is therefore used only in specialised applications where high rates-of-rise, steep topography, large freeboard requirements and high rainfall conditions warrant the extra expense.

(f) **Thickened Discharge Method:** First proposed by Shields (1974) and later developed by Robinsky (1975; 1978) the thickened discharge method comprises the dumping of de-watered tailings slurry into a conical pile. Seepage is collected in a small dam downstream of the pile. Palmer and Krizek (1987) developed a flow prediction model for the thickened slurry to determine the thickness and lateral extent of a deposited layer and thus the shape and volume of the pile.

Advantages:
- No risk of static failure.
- Cost of embankment construction virtually eliminated.
- Smaller surface area required.
- Moderately resistant to liquefaction (Jeyapalan, 1982a).
- Seepage contamination drastically reduced.
- Less time for consolidation.

Disadvantages:
- High cost of thickener construction and operation.
- Pumping of thickened slurry difficult and costly.
- Susceptible to erosion from runoff water, best suited to flat areas.

Underground Disposal

Underground disposal of tailings is primarily used for backfill and open pit infill purposes. Disposal purely for storage is of secondary importance. Only the coarse tailings sands are used for underground disposal. The slimes need to be disposed of on the surface and may

cause additional problems not offset by the benefits of underground storage. Artificially cemented and thickened tailings slurries have been used successfully to infill the rock-skeleton of stiff underground support systems (Blight, 1988). These support systems are mainly used to augment highly stressed pillars. Another use of underground tailings disposal is to provide point supports in the form of yielding, horizontally reinforced, tailings packs. The yielding properties of these packs are ideally suited for this purpose.

Advantages: Can be used to provide underground support or a working floor.
Maximises ore recovery by allowing pillars to be mined in backfilled areas

Disadvantages: Requires coarse tailings of high permeability and low compressibility.
May require the addition of cement when used as structural support.
Requires surface disposal of slimes.

2.4.7 Water control in and around surface impoundments

Water plays a leading role in any impoundment failure whether by overtopping, slope stability failure, seepage related failure, liquefaction or erosion of the embankment wall. The Water Balance or difference between inflow and outflow is used to predict long term accumulation of excess water in an impoundment. Water inputs to a tailings impoundment originate from three major sources, mill water discharge (process water), direct precipitation and external runoff or flood water. Water leaves the impoundment either as mill reclaim water, evaporation, seepage, direct discharge by overtopping, or might be stored in inter-particle voids on the dam. The water balance is controlled by implementation of flood handling and inflow control mechanisms of which adequate freeboard is the most important, as well as surface water decant facilities and seepage water drain systems. After balancing the water storage needs, a further 0.5 m freeboard is usually required by regulation (McPhail & Wagner, 1989). Van Zyl and Harr (1977) provide some guidelines as to the sizing of blanket drains to aid in the control of the phreatic surface near the embankment wall. Water balance is becoming a key issue in environmental and regulatory evaluations so that control measures should be selected to minimise environmental impact through contamination. To this extent seepage barriers, seepage return systems and effluent modification prior to deposition may be required.

The position of the phreatic surface in a tailings impoundment (Figure 2-10b) is determined by the water balance (Figure 2-10a) and plays a major role in controlling slope stability of the embankment. It is essential that the pond remains located over the settled tailings in the pond and kept at a safe distance from the dam crest, thus maintaining as wide a beach as possible. This helps to prevent the phreatic surface from moving too close to the downstream slope of the embankment and assists the task of any drains that have been provided to limit the downstream advance of the phreatic surface. Keeping the phreatic

surface well below the beach and embankment wall not only helps to control the phreatic surface, but also improves densification in these areas due to desiccation suctions. This leads to increased strength and stability, as well as a reduction in the volume of the impounded mass leading to increased storage capacity.

Originally (pre 1960) tailings dams did not provide for drainage systems at the toe of the embankment. For these dams seepage erosion on the embankment slopes are critical in undermining slope stability. Fortunately the rate-of-rise and foundation drainage provided stability in most cases with feasible dam heights in the order of 15 to 20 m. Since 1959, toe and blanket under drains have been incorporated in dam design, which provides a control point well inside the structure for drawing down the phreatic surface (Wagener & Wates, 1982), and to intercept seepage water percolating through the upper soil horizons. The drainage system may consist of granular blankets, strip drains or drainage pipes located beneath the downstream slope of the embankment. Water entering the blanket and toe drains is transported to a solution trench (Figure 2-4) by drain outfall pipes. The solution trench is usually an open, trapezoidal, unlined channel located around the perimeter of the dam. The word solution indicates that it collects contaminated water from the impoundment, either as surface runoff or seepage water. The solution trench usually drains into the penstock drain channel (Figure 2-10) towards a water reservoir or evaporation dam. Depending on the depth of the channel the solution trench may in addition function as a cut-off trench.

Drainage layers must be carefully designed if they are to function satisfactorily on a long term basis. The drain must be more permeable than the adjacent soil to allow free drainage, but should be graded to prevent clogging of the drain by passage of soil particles into the drainage layer. With drainage systems in place feasible dam heights have increased to 60 m and more. However, poor deposition practice, rapid rate-of-rise and poor pond control, negates this advantage. Seepage erosion at the toe of an embankment has in the past been remedied by rock-fill buttressing with a proper filter, at considerable expense.

In a discussion on the effect of drainage layers below the embankment, Van Zyl (1993), agrees that, during initial stages of deposition, the drainage layer enhances dewatering of the deposited tailings. After the drain is covered with tailings, however, the permeability of the tailings directly above the drainage layer can reduce to as low as $5x10^{-7}$ cm/s through consolidation, effectively forming a seepage barrier. This process is dependent on the fineness and clay content of the tailings immediately above the drain. If the area below the pond becomes "lined" in this way, it can effectively reduce seepage losses and contamination of groundwater. Kealy and Busch (1979) have found that pond fines, in contact with the natural soil foundation, can be consolidated to a greater extent than the

material immediately above it due to suctions in the natural soil, thus reducing its permeability and forming a similar liner to that over blanket drains.

Penstock decant facilities (Figure 2-10a) and floating barge pumps are commonly used to extract supernatant tailings water and stormwater from the surface of an impoundment. The number and size of these structures are dictated by minimum freeboard requirements. A penstock consists of a series of inlet boxes with vertical risers (concrete rings or steel pipe sections typically 500 mm in diameter) connecting to a horizontal steel or concrete pipe outlet in the foundation of the dam. The outlet discharges decant water for reclamation outside the dam area. After a storm, one or more riser rings may be removed to accelerate de-watering of the pond and to maintain freeboard, but management of the riser rings is hazardous due to the suction effect of the inflowing water. Hydrological studies indicate that a freeboard of at least 0.5 m is sufficient to accommodate a 1:100 year storm of 24 hour duration (Smith et al., 1987). As the geometry of the basin can change during the operational life of an impoundment, it is common practice to maintain a minimum vertical freeboard of 1.0 m between the storage area and the embankment wall. The majority of minor incidents on tailings impoundments are from penstock failures (Wagener & Jacobsz, 1999). These failures require the installation of a floating barge type decant system or a floating penstock system to keep the dam operational.

With barge systems, a primed pump is located centrally in the pond area with the decant pipe floated across the pond to the embankment. Barge systems are considered structurally more reliable but require a lot more maintenance, and are only practicable where there is a large year-round pond.

Where penstock drains are used, access is provided by pond walls and catwalks. Pond walls are extensions of the daywall into the night area, which are raised with the daywall. These walls stretch from the closest external wall to near the penstock. Only a limited length of catwalk then connects the pond wall with the penstock inlet. Catwalks consist of gumpole uprights and wooden plank walking surfaces. These have to be raised periodically by extending the uprights. Pond walls can be useful to maintain pond control over the penstock and increase the effective length of the beach, providing longer flow paths to the penstock and more time for segregation to take effect.

Storage policies under return water management dictate that water should not be stored on the surface of a tailings impoundment unless the structure is specifically designed for this purpose. The pond area should be kept at minimum and just deep enough to ensure water clarity for decant purposes. A return water system should discharge, treat or store water at

rates above the rate of decant. Return water should either be recycled or allowed to evaporate, thus minimising loss of recycle water and the risk of discharge pollution.

In addition to internal and surface drainage measures, ground level catchment paddocks are provided around the perimeter of the dam to intercept runoff from the side slopes of the impoundment. These paddocks are designed to hold and eventually evaporate the runoff water. It is common practice on many operational dams not to store water in the paddocks, which is drained into the solution trench by penstock drain systems similar to that of the main dam. The paddocks also serve to limit siltation pollution by material eroded from the slopes. Side slopes of the embankment wall are protected against stormwater erosion by providing a stepped profile with horizontal berms. The berms are drained after a storm to the catchment paddocks by berm decant penstocks if necessary. Water should never be retained or stored on the berms since this can lead to instability problems of the embankment wall. Factors influencing the frequency and size of step-back berms include stability constraints of the intermediate sections (i.e. between step-backs), erosion potential of the material on the side slopes and sufficient width to permit access to operations tractors and vehicles on the berm (Smith et al., 1987).

2.4.8 Design Considerations and Stability Analyses

Tailings dams are generally not designed with the same conservatism as conventional dams. The aim is to balance safety (stability) and economics (storage capacity) with embankment slope. The design of tailings structures must recognise that stability is required not only during the operational life of the structure, but also for generations after mining has been completed. Most embankment failures, with the exception of liquefaction related failures, occur as flow slides, triggered by a rotational type slide. In line with this, most stability calculations rely on common slope stability methods based on limit equilibrium. Invariably these procedures will identify a shallow critical failure, approaching the infinite slope condition. The designer has to be careful and experienced to interpret the results from these classical procedures.

According to Vick, (1983), errors result mainly from incorrect input parameters and not from analysis procedures. A typical analysis can be broken down into the following steps:

(a) **Phreatic Surface**: A critical step in the analysis of embankment stability is determining the location of the phreatic surface and pore pressure distributions. In a simplified model the pore pressure distribution can be derived from assumptions of steady state gravity seepage in an homogeneous and anisotropic (typically $k_h/k_v \approx 10$, Pettibone & Kealy, 1971; Vick, 1983) material. However, this does not account for permeability variations due to segregation across a section through the dam. For more accurate

results non-steady, transient flow in an inhomogeneous and anisotropic material has to be modelled and account be taken of unsaturated capillary flow in addition. Other aspects that are of importance include variations of void ratio and permeability with depth and increased confinement stress as well as consolidation related seepage for rapid rate-of-rise situations.

(b) **Stress Distribution**: Total stresses are calculated from the vertical overburden pressures based on in-situ densities. The effective stress distribution can then be determined as the difference between the total stress distribution and the pore pressure distribution and estimates of the earth pressure coefficient.

(c) **Failure Criterion**: A Mohr-Coulomb type failure envelope is developed from laboratory triaxial or shear box tests on reconstituted samples. Stress levels correspond to the calculated in-situ effective stresses. Stress relief and recompression cycles may be employed to simulate field loading conditions as well as overconsolidation due to suction pressures.

(d) **Embankment Stability Analysis - Static**: Design for static stability requires a design shear strength from the assumed failure criterion, usually Mohr-Coulomb, and is carried out for the following scenarios:

- *End of construction*: Applied to starter dikes and conventional earth dam walls approaching fast undrained loading conditions following construction.
- *Staged construction*: Especially useful for raised embankments that are constructed to allow dissipation of excess pore pressures. Vick (1983) reports that if the rate-of-rise is less than 5 to 10 m/yr, complete dissipation of excess pore pressures is usually assumed with a corresponding drained effective strength. Regardless, pore pressure dissipation appears to be faster than rates predicted from one-dimensional consolidation theory, principally due to the presence of thin sand seams and horizontal consolidation. Ladd, in the 1991 Terzaghi Lecture, emphasises the need for stability analyses to use a shear strength consistent with the most likely drainage condition during a potential failure. Many assumed drained failures have shown no dissipation of excess pore pressures during shear. Loading conditions that can lead to undrained instability include: normal operation at too high a rate-of-rise in low permeability tailings preventing excess pore pressures from fully dissipating, excessive foundation strains and slope oversteepening caused by rapid internal or surface erosion (Lo et al., 1988). For these cases a conservative, undrained, failure strength should be chosen based on in-situ effective stresses taken as equal to the consolidation stresses at the time of failure.

Ladd argues that such an undrained strength method of analysis should be used for staged construction problems where full dissipation of excess pore pressures have not occurred. Another point for consideration is the strain history and stress-strain behaviour of the material in terms of peak vs. steady state strengths coupled with conditions of strain hardening vs. strain softening. Peak strengths can only be relied upon if the designer can be certain that the material has never been strained beyond the level of peak shear stress; on the other hand post peak softening in a collapsible soil structure can lead to liquefaction.

- *Long term steady seepage*: Intended for raised embankments at their maximum height. Excess pore pressures are assumed to be fully dissipated and redistribution of internal stresses completed. The assumption of steady state seepage is a conservative measure and the structure is assumed not to fail in the long term. Therefore, shear induced pore pressures can be ignored.
- *Rapid draw down*: Only applicable to impoundments designed to retain substantial amounts of flood water, where the water breaches the embankment or is released to induce a rapid draw down situation. This method can also be applied to investigate the stability of an embankment wall following liquefaction of the impounded slimes during a seismic event.

(e) **Embankment Stability Analysis - Dynamic (Seismic)**: According to Lo et al. (1988), undrained instability and liquefaction of a tailings impoundment may be brought about by dynamic loading from earthquake shaking and blasting shocks. Often processes responsible for ore genesis are associated with seismic activity. Cyclic loading of this nature may result in a loss of strength caused by excess pore pressure build-up, strain softening and remoulding. Liquefaction of the impounded slimes alone may lead to embankment instability by increasing the external load on the upstream slope of the embankment (Klohn & Maartman, 1973; Finn & Byrne, 1976; Klohn et al., 1978). Liquefaction of the internal slimes can amount to 25% increase in load on the embankment wall as a result of hydrostatic conditions in the liquefied pond. Even if a liquefaction type flow failure is not likely, excessive deformations resulting from the seismic loads can cause overtopping of free water on the dam and result in a failure (Harper et al., 1992). Blasting shocks on the other hand are of too high a frequency to influence a dam of typical low natural frequency.

Seismic risk at a specific location can be estimated from seismic coefficient charts based on historical data, probabilistic methods which in addition take into account probabilities of larger events, or from deterministic methods which predict the maximum credible acceleration based on site geology and give no regard to seismic history. The design acceleration should be based on the hierarchy of accelerations

given by the above methods. For low level activity the historic approach may be enough. In more active areas the probabilistic methods should be used and in areas of high seismicity with active faults, both the probabilistic and deterministic predictions should be considered.

Factors influencing the liquefaction susceptibility of tailings during a seismic event are reported to be:

- *Stress related factors*: Initial effective consolidation stress and stress anisotropy, magnitude and direction of cyclic applied stresses and the number of cycles of stress reversal.
- *Material related factors*: These include, grain characteristics and grading, method of deposition, ageing, strain history, and the state of consolidation or relative density (Harper et al, 1992). Vick (1983) states that tailings are more susceptible to liquefaction than natural soils due to the fact that in most cases tailings structures consist of loose, uncompacted, fine sands with excess pore pressures likely to be induced by stress reversal.

Design approaches are either empirically based on the histories of other similar tailings dams or on analytical procedures using simplified liquefaction analyses (steady state analysis), pseudo static methods, total stress equivalent linear dynamic analyses or complete effective stress dynamic analyses using sophisticated numerical techniques.

Klohn et al., 1978 propose a pseudo static analysis with seismic coefficients corrected for dynamic response as a conservative approach using the following assumptions:

- *Dilatency during shear*: Strength recovery (Castro & Christian, 1976) due to dilatency for uncompacted fills is neglected; with compacted fills strength recovery is a definite possibility.
- *Principal stress ratio*: Assume the stress ratio (σ'_h/σ'_v) on the failure plane to be equal K_o, the earth pressure coefficient at rest.
- *Pore pressure migration from a liquefied pond*: If beach and embankment zones are significantly saturated, excess pore pressures will migrate from the pond into these saturated outer zones as well as into saturated foundations. Pore pressure migration can be ignored for dams with proper drainage.
- *Redistribution of stresses*: As sections fail due to rising dynamic pore pressures, stress redistribution follows and may result in instability of previously stable areas.

In seismically active areas, the risk cost of seismic failure has to be added to construction cost to evaluate alternative design alternatives, (Vick et al., 1985).

2.4.9 Seepage and Contaminant Transport Analyses

The objectives of seepage analysis are to determine the amounts of seepage losses and the risk of groundwater contamination. The design of drainage structures is determined by dam geometry, tailings properties and the nature of the foundations, which influence the seepage regime (Wates, 1991). Design takes account of prior geologic, hydrologic and geochemical conditions, as well as the physical and chemical characteristics of the tailings, effluent and natural soils, to predict the need for seepage control and to pose alternative measures that will minimise environmental impact at a reasonable cost. Seepage quantities can be estimated using closed-form solutions for simple geometries and seepage assumptions, or from more complicated numerical techniques in critical situations. The buffering effect of chemical reactions with natural soils can play a major part in controlling contamination of groundwater systems, especially if these soils are partially saturated and above the groundwater table.

Seepage Analysis

Flow quantities from a tailings impoundment can be estimated quite accurately from approximate methods based on analytical equations or flow net solutions (Van Zyl, 1987). In these cases it is standard to assume:

- steady state unconfined flow with respect to the boundary conditions,
- Darcy's law to be valid,
- saturated flow, neglecting any unsaturated flow and
- spatially varied isotropic or anisotropic hydraulic conductivity.

However, the calculations are most sensitive to changes in hydraulic conductivity. Mittal and Morgenstern (1976) show that due to rapid rates-of-rise, slimes can be under-consolidated in the pond, locking in high excess pore pressures and violating the conditions of steady state seepage.

Barrett (1987), gives a summary of commonly used closed form seepage analysis methods:

- *Flow net:* Although well developed and able to predict seepage quantities accurately, the method is cumbersome to use and results in unreliable estimates of the pore pressure distribution.
- *DuPuit:* The DuPuit solution assumes vertical equipotential lines between sections and an impervious foundation, which results in a small inclination of the phreatic surface.
- *Kozeny (1931):* Solution to Kozeny's equations prove accurate for a parabolic phreatic surface assuming an impervious foundation and a continuous drainage blanket on the downstream side of the embankment.

- *Kealy and Busch (1969):* By solving the LaPlace and Richards' equations for phreatic surface location and axisymmetric plane flow in a porous medium this method is able to account for spatial variation and anisotropy in permeabilities.
- *Abadjiev (1976):* Abadjiev attempts to account for variations in vertical permeability due to stress increase with depth and provides solutions that are accurate within the assumption of an impervious foundation.

Van Zyl and Harr (1977) present a number of standard solution charts for homogeneous isotropic seepage conditions in tailings impoundments. These charts are based on assumptions stated to model the most conservative condition including homogeneous and isotropic material properties, steady state flow and full discharge of all water entering the drainage systems at atmospheric pressure. Solutions are given for the following cases:

- *Material extends to infinite depth with a drainage layer at finite depth*: Nelson-Skornyakov (1949), gave a closed form solution to this problem for horizontal and near vertical upstream faces by applying conformal mapping techniques. Equations are derived for the phreatic surface and the effective length of the drain. Harr also presents an equation for the factor of safety against piping.
- *Horizontal drain underlain by impervious material of infinite extent*.
- *Impervious base*: Solution follows directly from Kozeny's equations.

Special conditions that are not easily analysed by simplified models include: consolidation which has the effect of decreasing hydraulic conductivity as the void ratio decreases and the effect of evaporation on seepage characteristics in the unsaturated zone. In addition, the pore pressure regime is not as easily predicted with approximate methods as the flow quantity. The phreatic surface is usually conservatively placed for stability calculations.

For more advanced analyses techniques reference should be made to:

(a) **Consolidation Effect** - Gibson et al. (1967 & 1981): Gibson and his co-workers made use of a one-dimensional, finite non-linear strain, numerical method in modelling the effect of consolidation on seepage quantities from sub-aqueously deposited material. All theories of one-dimensional consolidation are special cases of this method and no closed-form solution has yet been found. Numerical procedures have been developed and are discussed by the authors. The method requires as input, relationships between void ratio and effective confinement stress as well as between void ratio and permeability. These relationships can be established from standard laboratory tests. They found permeability reductions of up to one order of magnitude or more as a result of consolidation. These reductions can show the blinding effect on under drains that can push up the phreatic surface; on the other hand they may be of benefit in modelling the reduced seepage to the groundwater below the pond.

(b) **Evaporation Effect (Sub-aerial deposition)** - Bartlett and Van Zyl (1984): Unsaturated flow in the flat beach areas can either be vertical downwards seepage of water bleeding from subsequent depositions, or vertical upwards flow due to evaporation from surface. Evaporation has a greater influence on reducing water content in fine tailings than in coarse tailings, although the fine tailings reach equilibrium at a higher water content. The authors show that neglecting unsaturated flow can lead to underestimates of seepage losses.

Contaminant Transport Analysis

Methods that are commonly used in simplified contaminant transport analysis include the following:

(a) **Lumped Parameter Methods**: Used for preliminary design and to check the results of other methods. This method incorporates: water and salt balances, storage in partially saturated zones, neutralisation capacity and attenuation distances.

(b) **Analytical Methods**: These methods are employed when preliminary estimates indicate a high contamination potential, or if the tailings contain a high degree of toxic compounds. In some cases it is required by regulatory agencies. One-dimensional saturated and partially saturated flow according to Darcy's law is assumed together with a uniform geometry and uniform material properties to allow direct calculations.

(c) **Numerical Methods**: Highly sophisticated numerical techniques are only justified in cases where it may provide significant cost advantages such as with very complex dam geometry and geology, or if detailed analysis of two dimensional partial saturated flow is required. These methods attempt to model simultaneous and interactive processes of dilution of contaminant concentration, changes in contaminant solubility due to pH, contaminant adsorption, etc.

2.4.10 Tailings Dam Disasters

According to mining folklore, no tailings dam has ever been completed without at least one failure occurring during construction (Smith, 1972). Although the term failure is rarely defined in these stories, it can be assumed to include everything from a slight nonconformity with the design to complete collapse. It has been estimated that over 70% of large Canadian mining operations have experienced waste dump failures of some kind or the other (Hoare & Hill, 1970). Numerous waste embankment failures have occurred worldwide but were not reported as they did not involve any fatalities. The consequences of

failure have three major components: property damage costs, environmental damage and loss of life. By far the most common cause of distress is the control of the phreatic surface and maintaining adequate freeboard for stormwater confinement. Past failures indicate that designers often underestimate the probable maximum rainfall, and that the pond is operated with less than the required minimum freeboard or is allowed to encroach on the embankment wall due to poor deposition practices or too high a rate-of-rise.

Failure of a tailings impoundment can arise from a number of mechanisms, including:

- Foundation failure.
- Liquefaction.
- Slope instability from local sloughing to massive circular arc slides.
- Overtopping by floodwaters.
- Erosion of the face - Blight (1989).
- Piping in either the dyke or foundations - Wates et al. (1999).
- Failure in the decant facility - Wagener and Jacobsz (1999).

Except for liquefaction, all types of failure give some warning signs. Liquefaction events occur rapidly with little or no warning and the consequences and impact they have on their surroundings, the environment, and on human lives can be catastrophic, (Papageorgiou et al., 1997). For other types of distress, signals such as cracking, wet-spots on the downstream embankment face, critical settlement, and piezometric trends all indicate deficiencies in the structure. Without proper instrumentation and supervision it may be difficult to interpret accurately the extent of the problem.

The United States Committee on Large Dams has recorded failures, accidents and groundwater-related incidents for tailings dams, USCOLD (1994). The compilation of 185 incidents (21 in gold tailings) is intended to emphasise those potential failure modes of greatest significance in design. The major causes of tailings dam incidents and failures are reported to be:

- Slope instability of the embankment wall.
- Seepage instability of the embankment.
- Foundation failure.
- Overtopping of the dam crest.
- Structural deficiency of spillways, decant structures or discharge pipes.
- Earthquake (seismic) shaking.
- Mine subsidence caused by underground workings.
- Erosion damage.

Most failures involve active dams with only a small percentage of incidents on inactive dams. Slope instability is reported to be the leading cause of incidents, especially due to earthquakes. Other than that, the majority of failures have been due to erosion by water, either overtopping the dam or piping through some weakness (Penman, 1994). Upstream dams dominate failure records but may be disproportionately represented. Upstream dams are especially prone to slope instability and excessively vulnerable to earthquakes. Table 2-4 provides a list of some of the incidents mentioned in the USCOLD report.

The most important lessons learned from a study of past failures in tailings impoundments are the need for a comprehensive monitoring program and continuous detailed analysis of all data, backed up by rapid remedial action on identifying possible problems.

2.5 TAILINGS AS AN ENGINEERING MATERIAL

This section presents a summary of the mechanical properties of gold tailings as reported in the literature. It is intended as a basis for interpreting experimental test results and to augment such results for the purposes of defining the state and composition of gold tailings. Knowledge of the composition and state should enable the engineer to predict the engineering behaviour of tailings impoundments under typical load conditions. Where applicable, publications on tailings other than gold are listed separately.

2.5.1 The Nature of Gold Tailings Slurries

Following comminution and chemical extraction of the gold valuables the by-product of the reduction plant, tailings, are transported to the impoundment in the form of a slurry or pulp for disposal. It is the properties of this slurry, governing its soil forming behaviour on the impoundment, which are the subject of this section.

Tailings Slurries

Gold tailings have been classified as a fine, hard and angular rock flour, with 0 - 15% fine sand, 80% silt and 0 - 10% clay sized particles slurried with process water, (Vick, 1983; McPhail & Wagner, 1989). Cowey (1994), breaks down the mineral constituents of gold tailings into non-sulphide components (silicates, oxides, carbonates, etc.) and sulphide minerals (pyrites, etc.). In a typical South African gold tailings slurry pulp density varies between 25 and 50%, which relates to a moisture content of between 280 and 100% (Wagener & Wates, 1982).

Table 2-4: Summary of some significant tailings dam incidents since 1917.

Year	Location	Tailings	Cause	Fatalities	Reference
1917	South Africa	Gold			White, 1917
1928	Barahona, Chilly	Copper	EQ[2]	54	Dobry & Alvarez, 1967
1937	Simmer & Jack, South Africa	Gold	SI		Donaldson et al., 1976
1938	Fort Peck, USA	Sand	SI	80	Casagrande, 1965
1944	Hollinger, Canada	Gold	FN		Blackshaw, 1951
1956	Grootvlei, South Africa	Gold	SI		Donaldson et al., 1976
1961	Jupille, Belgium	Fly-ash	SI	11	Bishop, 1973
1965	El Cobre, Chilly	Copper	EQ	200	Dobry & Alvarez, 1967
1966	Aberfan, UK	Coal	SI	144	Bishop et al. 1969
1970	Mulfulira, Zambia	Copper	MS	89	Brawner, 1979
1972	Buffalo Creek, USA	Coal	SI	118	Jeyapalan et al., 1982a & b
1974	Bafokeng, South Africa	Platinum	SE	12	Jennings, 1979
1978	Mochikoshi, Japan	Gold	EQ	1	Okusa & Anma, 1980
1978	Hirayama, Japan	Gold	EQ		Okusa et al., 1980
1978	Norosawa, Japan	Gold	EQ		Okusa et al., 1980
1978	Arcturus, Zimbabwe	Gold	SI	1	Shakesby & Whitlow, 1991
1980	Phelps-Dodge, USA	Copper	SI	54	
1981	Freestate, South Africa	Gold	SI		Sully, 1985
1983	Golden Sunlight, USA	Gold	GR		
1983	Grey Eagle, USA	Gold	GR		Hutchinson et al., 1985
1984	Battle Mt. Gold, USA	Gold	SI		
1985	Olinghouse, USA	Gold	SE		
1985	Stava, Italy	Fluorite	SI	268	Berti et al., 1988 Chandler & Tosatti, 1995
1987	Montana Tunnels, USA	Gold	GR		Clark et al., 1989
1994	Merriespruit, South Africa	Gold	OT/SI	17	Wagener, 1997 Wagener et al., 1997a, 1998
1995	Omai, Guyana	Gold	ER		Vick, 1996
1995	Golden Cross, New Zealand	Gold	O		WISE Uranium Project, 1998
1995	Placer, Philippines	Gold	FN	12	WISE Uranium Project, 1998
1995	Simmergo, South Africa	Gold	SI		Blight, 1997

[2] SI - Slope instability, SE - Seepage, FN - Foundation, OT - Overtopping, EQ - Earthquake, MS - Mine subsidence GR - Groundwater, O - Other.

It appears that gold tailings fines generally exist in a flocculated state in a typical delivery slurry. When subjected to sedimentation tests, significant differences are noticed in the results of tests, whether performed with a dispersing agent or not. Non-dispersed slurries immediately form an interface between clear solution above and a shrinking mobile mass below the interface. It is as if the flocculated particles, in the absence of a dispersant, sweep the water clear of colloids as it "consolidates" in an homogeneous shrinking mass of low density, Truscott (1923). If treated with dispersant, the fines segregate and settle to form a dense sediment at the bottom of the sedimentation cylinder in the normal manner. There is also a significant time difference between the two processes, with non-dispersed sedimentation taking only a fraction of the time of sedimentation in a dispersed state. Hamel and Gunderson (1973) also report the differences in settlement behaviour between dispersed and non-dispersed tailings slurries. Having studied the effect of flocculants and dispersants on the settled density of Australian high clay content gold tailings, Fell (1988) concluded that the settled density could be improved by adding small quantities of dispersants. Fell also concluded that the settling properties did not alter with time, provided the material did not dry out. Furthermore, the density was not affected by initial water content, provided it was high enough.

A great deal of research has been carried out at the University of the Witwatersrand by Blight and his co-workers on the shear strength properties of tailings slurries (Blight & Bentel, 1983; Blight, 1988; Blight, 1994). These studies were aimed at modelling the flow properties and friction losses of tailings slurries in pipes, channels and on dam beaches, as well as predicting the extent of post failure debris flows from breached tailings impoundments. Tailings slurries have been found to behave somewhere between a Bingham plastic and a Newtonian fluid. The shear strength of a Newtonian fluid can be expressed by,

$$\tau = \frac{d\gamma}{dt}\eta \qquad \textbf{Eq. 2-5}$$

where τ = shear strength

γ = shear strain

η = Newtonian or 'true' viscosity

t = time

and that of Bingham plastics by,

$$\tau = \tau_o + \eta\frac{d\gamma}{dt} \qquad \textbf{Eq. 2-6}$$

where τ_o = strength when the rate of shear strain $d\gamma/dt$ is zero, a type of yield stress.

Using a variable speed coaxial-cylinder type viscometer the apparent viscosity, η_a, can be determined and used to approximate the rheological behaviour of a tailings slurry using the relationship:

$$\eta_a = \frac{\tau_o}{d\gamma/dt} \qquad \textbf{Eq. 2-7}$$

Eq. 2-7 in effect approximates the tailings slurry to a Newtonian fluid. The approximate viscosity of water is one, and that of a mixture of soil and water is greater than one, depending on solids content. The dilute mixtures of sediment and water in rivers still have apparent viscosities close to one, whereas in gold tailings slurries the apparent viscosity ranges between 2 and 7. Changes in water content have a major influence on the apparent viscosity and shear strength of the slurry. Shear strength, detectable by the viscometers, only develops at a water content of less than 30%, where the slurries behave more like Bingham plastics than Newtonian fluids. At lower water contents a threshold shear strength starts to dominate the viscosity.

Hungr (1995) also developed a continuum model to simulate post failure debris flow, based on a Lagrangean solution of the equations of motion and a semi-empirical numerical model of unsteady flow. The model allows selection of a variety of material rheologies as well as variances in rheologies along the slide path, or within the sliding mass. Effects of lateral confinement are accounted for in a simplified manner. The model compares favourably with results from laboratory experiments and other analytical methods. Han and Wang (1996) used the assumption of a Bingham plastic to successfully model a breach failure in China.

Effluent

Gold tailings water is often slightly alkaline with high concentrations of soluble salts. It often contains soluble sulphates, chlorides, sodium, calcium and low concentrations of organic chemicals (Vick, 1983). The effluent chemistry is the result of a combination of the ore minerals and chemical treatments in the reduction plant.

Oxidation, Ageing and Cementing

In the presence of water and oxygen, the reactive sulphide minerals in tailings can produce an acid leachate that favours the solution of heavy metals, thus becoming a severe threat to local ecosystems. In pyrite-rich tailings some crusting of the dried out exposed surfaces on a dam may occur. This crusting, however, is purely superficial.

The iron sulphides are mostly pyrite (FeS_2) in gold tailings slurries, and are especially susceptible to oxidation in the presence of water and oxygen or by anaerobic biological oxidation to ferrous and ferric oxides, ferric hydroxide and sulphuric acid (Cowey, 1994). The products of oxidation may result in volume changes as well as acidic conditions in the tailings, which are conducive to the solution and leaching of toxic heavy metals. Under saturated conditions with no access to free oxygen the oxidation of the sulphides can only take place by means of anaerobic bacterial oxidation through *Thiobacillus ferrooxidans* and *Thiobacillus thiooxidans* (Kleinmann et al., 1981). Stanley (1987) argues that the interior of a tailings dam is more or less impenetrable to air and free oxygen and that the slime is preserved in the laid down condition. However, where air and water penetrate the beaches and embankment slopes rapid oxidation of the surface sulphide minerals will take place, within one month, up to a depth of 0.5 to 1 m.

A number of workers have commented on the self cementing properties of tailings (Patton, 1952; Thomas, 1971; Pettibone & Kealy, 1971). Cementation may take the form of:

- Chemical bonds between clay mineral as a function of their pore water chemistry.
- Thixotropic hardening caused by clay minerals.
- Crystal bridges between grains formed by precipitating soluble salts.
- Hard cementing between grains on precipitation of sulphates
- Precipitation cementing by silicates, metal oxides or calcium carbonate following pH changes as a result of pyrite oxidation.

Solubility of natural soil bonding agents such as silica, iron and carbonate, known to be present in gold tailings slurries, are affected by the pH, oxidation potential, temperature and pressure of the solution. Changes in these parameters caused by pyrite oxidation, can lead to precipitation bonding. Silica is highly soluble in an alkaline environment but relatively insoluble in neutral to acidic conditions. Iron precipitation usually follows neutralisation of acidic conditions. Carbonates are soluble in acidic conditions.

For work published on tailings slurries other than gold, reference can be made to: Copper: Finn et al. (1978), Volpe (1979), Chen et al. (1988), Mlynarek et al. (1991), Mlynarek et al. (1994); Iron: Guerra (1972); Uranium: Matyas et al. (1984); Larson and Mitchell (1986); Lead-Zinc: Mabes et al. (1977); Molybdenum: Klohn (1984); Lignite: Kotzias et al. (1984); Coal: Siriwardane and Ho (1985); Canadian Oil Sands: Suthaker and Scott (1997); non-ferrous: Abadjiev (1985), Abadjiev (1988).

2.5.2 Deposition and Sedimentation of Tailings

The formation of a hydraulic fill is very much like the formation of natural sediments; transportation is followed by deposition, sedimentation and eventually by consolidation due

to self-weight and external loading (Imai, 1981; Schiffman et al., 1988). The difference is age; compared with natural sediments, hydraulic fills are young with a very recent stress history. The study of the sedimentation and consolidation behaviour of tailings following deposition is of major concern in the design of tailings impoundments, not only from a stability point of view but also in determining the storage capacity and allowable rate-of-rise on these structures.

Transportation of sediments, sedimentation and consolidation are simultaneous parts of the tailings deposition process (Consoli & Sills, 2000). It is important to note that much of the work on sedimentation-consolidation of natural sediments and tailings slurries has thus far been restricted to the solution of one dimensional vertical settling problems. The study of the sedimentation of tailings should not be limited to the modelling of vertical sedimentation only, but should also include the effects of horizontal transportation. Tailings particles should be regarded as moving through and being carried along by water following deposition.

From a stress history point of view the profile in a tailings impoundment should be soft, normally consolidated, with high void ratios and low effective stresses. In reality, desiccation suctions developed from evaporation on the beach surfaces and embankment walls can build in large pre-consolidation stresses with heavily overconsolidated states existing below these surfaces. Benefits from sub-aerial deposition and desiccation include increased storage capacity, reduced permeability and seepage, reduced compressibility and increased shear strength due to densification. Another consequence of desiccation is the development of drying cracks. These cracks, even if filled in by successive depositions, remain weak surfaces within the dam, presenting potential piping channels and preferential paths for pyrite oxidation as the dam ages (Blight & Bentel, 1983).

A consistent feature of tailings impoundments is the highly layered nature of the profile as a result of depositional practices, soil forming processes and variations in milling consistencies, (McPhail & Wagner, 1989). Often this layering takes the form of alternating fine and coarse deposits, with up to 50% variation in fineness over a depth of 10 to 200 mm.

Sedimentation Behaviour

Compared with natural sediments, predicting the sedimentation behaviour of tailings is complicated by a number of factors, (Lappin, 1997):

- Small depth of flow.
- High sediment load.
- Turbulent flow close to the discharge point and in scour channels on the beach.

- Particles being trapped in the bed load or in flocculated structures.
- Coarse particles held in suspension or rolled along the bed.
- Suctions in the bed trapping fine particles.

In addition to these difficulties, account has to be taken of both the slurry properties including particle size, shape and specific gravity, water content and viscosity as well as deposition-related flow conditions on the beach (sub-aerial), compared with those in the pond (sub-aqueous).

Under sub-aerial conditions on the beach, sedimentation is more or less instantaneous followed by consolidation effected by desiccation, and saturated or unsaturated compression due to overburden pressures (Senevirante et al., 1996). Under sub-aqueous conditions in the pond, sedimentation is initially rapid forming a loose soil of no strength, which gradually changes into a very low strength loose soil structure consolidating under its own weight and overburden pressures. Sub-aqueous sedimentation can be modelled using Kynch's theory of hindered settling by considering continuity of the solid phase together with the particle velocities as a function of porosity. This leads to Kynch's "flux-plot" used in the design of sedimentation processes (Kynch; 1952, Been, 1980; Imai, 1980 & 1981; McRoberts & Nixon, 1976; Schiffman et al., 1986). Ulrich and Valera (1995) point out that, being a ground product, tailings particles are usually quite angular. In addition the fines seldom exhibit cohesion. This results in high void ratio packing arrangements with little particle-to-particle contact following sub-aqueous deposition, which must be susceptible to liquefaction.

Consolidation Behaviour

Consolidation involves primary consolidation as a result of the dissipation of excess pore pressures and secondary consolidation or creep as a function of the viscosity of the soil skeleton. Both occur simultaneously but primary consolidation, together with sedimentation, is believed to dominate in tailings materials.

The first coherent formulation of the consolidation phenomenon was developed by Terzaghi (1923), based on the conservation of momentum (equilibrium) and mass (continuity) for infinitesimal strain and one-dimensional flow and settlement. It is doubtful whether small strain theory can be applied adequately to the consolidation of tailings with the large reductions in void ratio under self-weight consolidation (Carrier et al., 1983; Van Zyl, 1993). Still considering a one-dimensional theory, Gibson et al. (1967) added the consequences of non-linear finite strain using the Lagrangean co-ordinate system. The large strain non-linear consolidation theory, using Lagrangean co-ordinates has been applied successfully to tailings by Gibson et al. (1967) and specifically to gold tailings by Caldwell et al. (1984) and

Senevirante et al. (1996). Horizontal permeability can dominate the consolidation process as a result of the severe anisotropy in permeability with k_h typically an order of magnitude larger than k_v. However, global anisotropy can significantly be affected by desiccation cracks and the properties of their infill material. For example, a desiccation crack filled with coarser material can vertically connect two free draining layers across a relatively low permeability layer. Biot (1941) formulated the first general and coherent multidimensional consolidation theory, taking into consideration the interdependency between deformation of the soil skeleton and the flow of interstitial fluid. With the development of finite element and finite difference numerical methods, the solution of realistic boundary problems with the three-dimensional Biot coupled consolidation theory became possible.

Recently, there has been a move towards the development of unified sedimentation-consolidation models for tailings. Experimental and theoretical studies linking sedimentation and consolidation of settling tailings have been proposed by Pane (1985) and Toorman (1996). Been (1980) and Been & Sills (1981) pointed out the relation which existed between the theories of hindered settling developed by Kynch (1952) and finite deformation consolidation developed by Gibson et al. (1967). Schiffman et al. (1984) and Pane (1985) presented a single theoretical basis for sedimentation and consolidation processes of solid-water mixtures. Studying phenomena concerning the end of sedimentation and beginning of consolidation phases, Been and Sills (1981) concluded that the basic difference between a suspension (sedimentation phase) and a solid skeleton consisting of the same particles (consolidation phase) is the presence of effective stresses (see also Carrier et al., 1983). The maximum density at which a soil slurry can exist as a suspension without the presence of effective stresses is termed the structural density. One way of determining this separation is by measuring the state (density) at which the suspension starts to exhibit shear stiffness. Another way is to take the void ratio that exists at the top of the sediment bed after a considerable period of self-weight consolidation has occurred. Although both these values correspond by definition to zero effective stress, Been and Sills have shown that there can be a significant difference in their magnitudes as a result of creep at the surface of the sediment bed. Carrier et al. (1983) proposed the following equation to calculate the void ratio at the end of sedimentation,

$$e_{sed} = 7G_s \frac{LL}{100} \qquad \textbf{Eq. 2-8}$$

where e_{sed} = void ratio at the end of sedimentation start of consolidation
G_s = specific gravity
LL = liquid limit as a %

Swarbrick and Fell have worked on a unified model which includes the effects of desiccation and re-wetting for high clay content tailings at the University of New South Wales in Australia (Swarbrick & Fell, 1990; Swarbrick & Fell, 1991; Swarbrick, 1992; Swarbrick & Fell, 1992; Swarbrick, 1993; Swarbrick, 1994). Input parameters for the model are derived from large column settling tests and lysimeter drying tests. Tailings properties that influence its depositional behaviour were found to be particle density, net negative charge on the clay particles, soil water diffusion and thermal conductivity. Their model has been comprehensively evaluated against laboratory and field tests for iron, coal and bauxite tailings. However, the authors warn against the use of this and similar models for tailings with high salt concentrations, where surface crust formation will inhibit evaporation and result in erroneous predictions, see also Fahey and Fujiyasu (1994).

Hydraulic Sorting

Sub-aerial deposition and the progression of flow and sedimentation of the tailings slurry on a typical South African impoundment are well described by Bentel (1981). The slurry, discharged from an open ended pipe forms a plunge pool where the stream hits the beach. In the plunge pool the slurry swirls around and deposits tailings, dissipating much of the energy as it does so. Where the pool-rim is breached, a stream of tailings discharges onto the beach. Flow is supercritical on the upper beach and concentrated in individual scoured rivulets or channels with deposition of material taking place as a result of energy losses at hydraulic jumps. Further down the beach there are fewer hydraulic jumps spaced further apart and a gradual decline in the slope of the profile. The individual rivulets widen, meander and eventually coalesce at the end of the beach. As the slurries approach the beach-pond interface the rivulets fan out in deltas with slow sub-critical sheet flow and ripple bedding, resulting in a low profile gradient. The sudden reduction in energy at the edge of the pond leads to increased deposition.

The in-place physical properties or state of tailings, especially permeability, compressibility and strength, are often assumed to be related to the beach profile or surface geometry of the impoundment. Many authors agree that there is a tendency for decreasing permeability towards the pond as a result of increasing fineness (Jerabek & Hartman, 1965; Kealy & Busch, 1971). It is the particle segregation and hydraulic sorting processes that are responsible for this increase in fineness. Figure 2-9 shows the reduction in the normalised median particle diameter, $D_{50}/D_{50(max)}$, with distance from the point of deposition on a diamond tailings dam. The resulting beach geometry, discussed in detail in the next section, is a result of particle sorting processes, which in turn are a function of the properties of the tailings slurry and of the depositional conditions. On gold tailings dams, the beach profile is more a function of pulp density than of the slurry properties due to the generally uniform

grading of these materials. The lower the pulp density the more effective the sorting processes.

In addition to horizontal sorting on a beach, size sorting also occurs vertically resulting in the highly layered structure and anisotropy of the tailings profile (Blight & Bentel, 1983).

Deriving equations for the unhindered settling velocity of suspended sediment in a quiescent fluid undergoing laminar flow, Blight and Bentel (1983) predict the grading properties of a tailings beach as follows:
The vertical settling velocity, v_v, is calculated from,

$$v_v^2 = \frac{4(\rho_s - \rho_w)g \cdot D}{3C \cdot \rho_w} \qquad \textbf{Eq. 2-9}$$

where: ρ_s = density of the particle

ρ_w = density of the slurry liquid

D = diameter of the particle

C = coefficient of drag, constant for Reynolds numbers greater than 400

and the horizontal settling velocity v_h, from,

$$v_h = C(\delta \cdot i)^2 \qquad \textbf{Eq. 2-10}$$

where: δ = depth of flow

i = hydraulic gradient

thus,

$$D = \frac{C \cdot \delta^{3/2} \cdot \sqrt{i}}{K \cdot x} \qquad \textbf{Eq. 2-11}$$

$$\text{where: } K = \frac{4(\rho_s - \rho_w)g}{3C \cdot \rho_w} \qquad \textbf{Eq. 2-12}$$

Eq. 2-11 gives the maximum diameter, D, of a particle expected at a distance x along the flow path down a beach.

Alternatively, a similar equation can be derived following Stokes' Law, as:

$$v_v = \frac{(\rho_s - \rho_w)g \cdot D^2}{18\eta} \qquad \textbf{Eq. 2-13}$$

where η = viscosity of the slurry

then

$$D = \left[\frac{C' \cdot \delta^{3/2} \cdot i}{K' \cdot x} \right]^{1/2} \qquad \textbf{Eq. 2-14}$$

where $K' = \dfrac{(\rho_s - \rho_w)g}{18\eta}$ **Eq. 2-15**

These equations are approximate and do not account for:

- Interference of adjacent particles.
- Variations of the hydraulic gradient with beach gradient.
- The change in depth of flow (δ) with distance.
- Transportation of material after settlement or rolling sorting.
- Scour and re-deposition of previously deposited material.
- Deposition of fine material high up on the beach due to turbulent flow and hydraulic jumps.
- The flocculated nature of tailings.

Blight (1987 & 1994) suggests using an exponential ratio between the median particle at a distance down the beach compared with that of the whole tailings mix to predict particle size sorting:

$$D_{50(at\,x)} = D_{50(Total)} \cdot \exp\left(-B \frac{x}{L} \right) \qquad \textbf{Eq. 2-16}$$

where: D_{50} = median particle diameter

B = constant as a function of tailings type and the rate of deposition

L = total length of the beach.

Morris (1993) derives a similar sediment sorting equation based on the assumption of constant specific gravity, G_s, as:

$$D = D_{50(Total)} \exp(-\alpha \cdot x) \qquad \textbf{Eq. 2-17}$$

where D = expected particle diameter at a distance of x down the beach

α = constant, so that $\alpha = \varepsilon/(1+b)$

ε = constant defining the local slope of the beach

b = transport constant relating the bed shear stress to particle properties

For a sediment with variable G_s, particle sorting by specific gravity results in:

$$G_s - 1 = (G_s - 1)_{Total} \exp(-\beta \cdot x) \qquad \textbf{Eq. 2-18}$$

where β = constant and is related to α and ε by,

$$\varepsilon = \alpha(1+b) + \beta\left(1+\frac{b}{3}\right) \qquad \text{Eq. 2-19}$$

Morris is of the opinion that the specific gravity, G_s, of gold tailings is not constant and is actually related to the particle sizes. Abadjiev (1997) stresses that not only D_{50}, but the whole grading curve should be investigated for its influence on the particle sorting processes.

Beach Profiles

A review of tailings literature soon reveals the significance of predicting beach profiles on impoundment structures. Being able to predict the beach slope or profile allows not only better management of the pond, but also improved estimates of storage volumes and freeboard. As a result of difficulties with sampling and testing, a number of researchers have also sought indirect measures of estimating the settled physical properties of tailings based on the beach profile.

It has been shown that particle-size sorting processes, the strength of the settling slurry and requirements of continuity and conservation of energy are responsible for the shape of a hydraulic fill beach. As the slurry flows from the discharge point down the beach coarser particles will settle out, increasing the moisture content of the remaining slurry and lowering the pulp density, which results in a general flattening of the beach slope. Beach slopes on tailings impoundments range typically from up to 2% at the discharge point down to possibly 0.1% at the pond (Vick, 1983). Gold and uranium tailings, however, possess relatively uniform gradings and a narrow range in particle sizes, which virtually eliminate horizontal segregation. Changes in the grading of these materials, therefore, have little effect on the beach slope. Moisture content or solids concentration dominates the beach profile on gold and uranium tailings impoundments.

As the solids concentration of the feed pulp, S_c, increases and gravitational sorting becomes less effective, the overall slope or steepness of the beach also increases (Blight, 1994). As long as gravitational sorting is effective the slurry will be in a particle sorting regime. At some point, S_c > 55% in gold tailings, a mudflow regime commences, where there is no horizontal sorting and the slurry moves as a homogeneous viscous fluid or mud to the pond. Following the onset of a mudflow regime the overall beach slope will start to decrease. The rate of deposition does not appear to have a large effect on the beach profile provided deposition is on a wet beach. When deposition takes place on a dry beach, the slurry looses water to the beach, which increases the pulp concentration and results in a more curved profile and steeper overall beach slope. Increasing the number of discharge points around the perimeter of a dam also results in a steeper beach slope.

The first empirical attempt at predicting hydraulic fill beach profiles was made by Melent'ev et al. (1973), on beached natural alluvial soils and mine tailings in Russia. Melent'ev observed that geometrically similar beaches are formed for a specific type of particulate material, solids content of the slurry at placing and rate of placement. This Master or Melent'ev Profile applies within limits regardless of the length of beach and the difference in elevation between the point of deposition and the pond.

For conditions of sub-aerial deposition the master profile, Figure 2-11a, is expressed as,

$$y = i_{av} \cdot L(1 - x_o)^n \qquad \textbf{Eq. 2-20}$$

where y = vertical height of the beach measured upwards from the pond edge
i_{av} = overall slope of the beach or H/L
H = total height of the beach
L = total length of the beach
$x_o = x/L$
x = horizontal distance along the beach measured from the discharge point
n = beach parameter

The beach parameter, n, is a function of the particle size distribution and solids concentration of the slurry and is constant for a particular tailings type, grading and pulp density, (Blight, 1987). It controls the shape and curvature of the beach profile so that for a flat beach n is equal to one, for a concave-up beach n is greater than 1, and n is less than 1 for a convex-up beach. Values of n between 1.33 and 1.66 was found by Melent'ev for fine to coarse tailings. Blight (1994) quotes a value of $n = 4.0$ on a gold tailings beach.
In a non-dimensional or normalised form Eq. 2-20 becomes,

$$\frac{y}{H} = \left(1 - \frac{x}{L}\right)^n \qquad \textbf{Eq. 2-21}$$

For conditions of sub-aqueous deposition the master profile, Figure 2-11b, is expressed as,

$$y = H\left(1 - \exp^{a \cdot x/L}\right) \qquad \textbf{Eq. 2-22}$$

where y = vertical height of the beach measured down from the pond water level
H = total depth of the pond
L = beach length
x = horizontal distance measured negative from the edge of the pond
a = dimensionless coefficient

Bentel (1981) in studying the beach profiles of sub-aqueously deposited gold tailings, found the beach parameter, $n = 2$, in other words concave-up.

Melent'ev and his co-workers also derived an expression for predicting the overall slope of the beach, H/L,

$$\frac{H}{L} = a \cdot S_c^{1/3} \left(\frac{D_{50}}{h^*} \right)^{1/6} \qquad \textbf{Eq. 2-23}$$

where a = constant

S_c = solids concentration of the slurry

D_{50} = median particle size

h^* = stream depth associated with the scour velocity of the water

Since the groundbreaking work of Melent'ev, many researchers have investigated, or tried to improve on the simple master profile concept:

(a) Smith et al. (1986) experimented with an exponential function, which best fit the geometries of the beaches on gold tailings impoundments, but found the Melent'ev power function to be more generally applicable.

(b) Using scaled laboratory tests Blight et al. (1985), Wates et al. (1987) and Fan and Masliyah (1990) found the simple Melent'ev master profile to predict successfully flume profiles, which were representative of field beach profiles. In addition they also showed that:

- Increased solids content of the slurry resulted in steeper beach slopes close to the discharge point and flatter slopes at the pond.
- Increasing the coarseness of the pulp had the same effect.
- Increased solids content resulted in an increase in the rate-of-rise of the beach.
- Total slurry discharge rate at constant solids content had no significant effect on the slope of the beach, but higher flow rates lead to an increased rate-of-rise.
- Shear strength decreased towards the pond corresponding to the decreasing slope angle of the beach profile.

(c) Morris (1993), used river-transport dynamics with engineering hydraulics as a theoretical basis to solve the three fundamental differential equations for two dimensional flow over a mobile bed. The resulting exponential relationship seemed promising for modelling the profiles on coal and platinum beaches, but lacks the simplicity of the master profile.

(d) More recently McPhail (1995) and McPhail and Blight (1997) used the stream power function and entropy maximisation for predicting the large scale beaching characteristics of a tailings slurry. The resulting exponential integral is dependent on the hydraulics of the plunge pool at the discharge end, as well as a variable, μ, as a function of the initial slope of the stream power curve.

Publications on the deposition and sedimentation behaviour of other tailings materials include: Coal, Iron and Bauxite: Fourie (1988); Uranium Chen et al. (1988), Emerson et al. (1994); Consoli (1997); Consoli & Sills (2000).

2.5.3 Sampling and Testing

The sampling and testing of tailings present a number of challenges. As a geo-material, tailings exhibit behaviour somewhere between that of a sand and a clay, depending on the state and composition of the material. This causes difficulties in the interpretation of in-situ tests, where assumptions of fully drained or fully undrained shear cannot be relied upon. The low density and low effective stress levels, which result from hydraulic deposition processes, make sampling and specimen preparation for laboratory testing extremely difficult. If undisturbed samples cannot be recovered, representative specimens have to be prepared artificially using techniques that simulate the soil formation processes on the actual impoundment. Once a test specimen is prepared, the actual testing is often assisted by the quick draining characteristics of the material. However, quite large strains may be required to develop the full stress-strain response. Another difficult aspect to address is the behaviour of the partially saturated material on the embankment wall and beach areas. Although not critical to the safety and serviceability of the dam, these zones play a defining role in determining the state and composition of material which may subsequently become critical. This section highlights some of the aspects concerned with the sampling and testing of tailings material.

Sampling

The properties of tailings in an impoundment are highly dependent on location, ranging from semi-dry coarse tailings near the discharge point to normally consolidated soft liquefiable fines in the penstock pond. This may call for different and specialised sampling techniques depending on location and whether bulk or undisturbed samples are required.

Collecting bulk samples for basic tests can be as simple as shovelling tailings into a bag from a dry beach, or virtually impossible in trying to separate and collect a specific layer, which might be only 10 mm thick, from the pond area below the water surface. In collecting

bulk samples, the highly layered nature of the tailings profile has to be taken into account. In some cases a mixed sample of material spreading over several layers of alternating fine and coarse tailings may be collected. In others, a specific layer has to be isolated and carefully sampled.

With undisturbed sampling it is important to retain the soil structure and prevent liquefaction disturbance during handling and transportation. The most difficult part of undisturbed sampling in tailings is recovery from below the water table. Liquefaction and withdrawal suctions make recovery of samples extremely difficult, if not impossible. Sampling is usually done by simple piston sampler (Mittal & Morgenstern, 1976; Carrier et al., 1983), thin-walled tube sampler (East et al., 1988) or coring techniques (Plewes et al., 1988). Donaldson (1965), using the shoestring method after Collins (1954), was able to extract 76 mm undisturbed samples with a thin walled tube sampler. Kealy and Busch (1979), working from a floating barge in the pond, used a plastic air line attached to a Shelby tube sampler to break suction when withdrawing the tube from the hole. Follin et al. (1984) used the Delft stocking net sampler to recover successfully 18 m continuous samples with virtually no sampling disturbance evident. They concluded that the Delft sampler is an excellent tool for sampling tailings, but that it is not effective in dry sands of medium to high relative density due to excessive forces on the nylon stocking. Controlled ground freezing techniques have been employed by Yoshimi and Goto (1996), but disturbance caused by the formation of ice-lenses must be of concern. Roe and Zahl (1986) recovered undisturbed samples from the beach surface by impregnation with a low viscosity resin. The method is only viable above the water table, to allow impregnation by the resin. After the resin has set the sample is extracted and prepared for microscopic analysis of the structure.

Testing in the Laboratory

Tests in the laboratory are performed on either undisturbed or reconstituted samples. As a result of difficulties in obtaining quality undisturbed samples, most laboratory tests for determining compressibility, consolidation and strength of tailings have been performed on reconstituted specimens.

Provided that a high quality undisturbed sample can be delivered to the laboratory, due care has to be exercised in cutting and trimming the test specimen to prevent physical disturbance and moisture loss. Alternatively, representative reconstituted specimens have to be artificially prepared. There are numerous methods for preparing reconstituted tailings samples including compaction (Hamel & Gunderson, 1973), wet-tamping (Highter & Tobin, 1980), pluviation (Kuerbis et al., 1988), and slurry sedimentation (Donaldson, 1965), but these should be carefully tailored and calibrated with field measurements to ensure that it is

representative. Donaldson (1965) has described a method of preparing triaxial specimens by pouring the tailings slurry directly into a triaxial split mould and applying a small initial consolidation pressure with the split mould still attached. After 2 hours of consolidation the mould could be successfully removed and the test continued.

The effect of pre-treatment procedures should be determined when performing all laboratory tests; particularly the effect of changing the pore water chemistry and the make-up of the dissolved constituents when using tap or distilled water for specimen preparation and saturation (Emerson & Self, 1994). On the other hand, drying out of samples may cause precipitation of the dissolved constituents as hydrate solids, which will influence many test results. The flocculated nature of gold tailings slurries has already been mentioned and should be taken into account when specifying and performing grading analyses and indicator tests (Hamel & Gunderson, 1973). Duplicate tests should be specified at all times to give an indication of the effect of pre-treatment procedures on the test results and material behaviour.

The use of laboratory flumes in studying the depositional processes and profiles on tailings beaches has already been mentioned in Section 2.5.2. Flume tests have also been used to examine the post failure flow behaviour of breached tailings by simulating overtopping and pond encroachment failures by Papageorgiou et al. (1997).

Knowledge of the location of the phreatic surface in a tailings impoundment is arguably the most valuable piece of information for design and auditing purposes. Unfortunately, permeability, as the defining parameter controlling the seepage regime, is also one of the most difficult to determine in the laboratory, either directly using permeameters or indirectly based on consolidation data. Barrett (1987) summarises some of the shortcomings of permeability testing in the laboratory:

(a) **Sampling related problems**: Difficulties with access and sampling conditions can lead to sampling bias, and physical disturbance, pore pressure changes and stress relief all have an influence on the measured permeability. Generally, permeability samples must be big enough to allow for the influence of macrostructure (cracks, layering etc.). On a gold tailings impoundment desiccation cracks typically form in grid pattern at roughly one meter intervals. These cracks and the properties of their infill material greatly influence the anisotropy of permeability. The seepage regime in a tailings dam is further complicated by the highly layered nature of the deposit, which makes the choice of preferred drainage direction very difficult during testing. However, it might be worthwhile determining the permeabilities of individual representative layers as well as the macro-permeability.

(b) **Equipment related problems**: Seepage against the sides of permeameters, stress levels during testing and seepage force induced consolidation (Suthaker & Scott, 1996) are some of the problems that have to be addressed during testing.

Suthaker and Scott (1996) reviewed a number of methods for determining hydraulic conductivity in the laboratory including constant and falling head permeameters, flow pump tests (Olsen, 1966), restricted flow tests (Sills et al., 1986) and seepage tests, but found conventional measurement techniques not suited to measure permeability, especially in the fine tailings slimes. The authors subsequently designed a slurry consolidometer to prevent seepage induced consolidation by locking the top cap of the consolidometer during permeability measurements.

Mittal and Morgenstern (1976) and Lappin (1997) argue that compressibility and consolidation characteristics should preferably be tested in Rowe cell type oedometers. The Rowe cell allows variations of the boundary conditions together with pore pressure control and measurement, which allows constant head permeability tests between loading stages. However, it is doubtful whether the drainage facilities of the Rowe cell are permeable enough to allow free drainage of tailings. The Rowe cell also allows only limited settlement of the loading diaphragm and excessive frictional effects and low sensitivity restrict the use of the apparatus at very low stress levels. Compressibility and permeability, for the early stages of self weight consolidation, can better be determined from density and pore pressure measurements during sedimentation column tests (Lappin, 1997). These tests can also be used to determine the rate of sedimentation.

Sully (1985), suggests that permeabilities should rather be determined from a large number of in-situ infiltration tests, to account for macrostructure.

Stress-strain and strength measurements are usually performed in the direct shear box or triaxial apparatus, Vick (1983). The shear box test suffers from many limitations (Atkinson & Bransby, 1978):

- Stresses and strains are non-uniform
- States of stress and strain cannot be determined completely
- The specimen is forced to shear more or less along a horizontal plane

The apparatus is better suited for the determination of stresses that cause failure on a particular plane, and is particularly suited for finding the strength of pre-existing failure surfaces in a soil specimen. Even with the more sophisticated simple shear device (Bjerrum & Landva, 1966; Roscoe, 1970), either the stress distribution or boundary deformations are not sufficiently controlled (Airey & Wood, 1987).

The shear device that is most commonly used both for design and research is the triaxial apparatus, as described originally by Bishop and Henkel (1962), with all its modern adaptations. However, the isotropic consolidation conditions in the triaxial may not conform to the field loading situation, and drainage conditions are limited to being either fully drained or fully undrained. Typical results of triaxial tests on tailings indicate, (Vick, 1983; East et al., 1988; Van der Berg et al., 1998):

- Relatively high strains to failure.
- Zero effective cohesion with undrained effective friction angles ranging between 32 and 42°. The high angles of friction are likely the result of the angularity of the tailings particles. Both coarse and fine tailings appear to give similar results in terms of friction angle.
- At densities and stress levels relevant to in-situ saturated conditions, dilation seldom occurs prior to failure with no strain softening or strength reduction following peak shear strength.
- At low stress and high density states, typical of samples recovered from desiccated beaches and subsequently saturated in the laboratory, dilation does occur and strength reduction may be a possibility as a result of the overconsolidated states of these specimens.
- In undrained shear, the coarser material is particularly prone to phase transfer dilation as described by Ishihara et al. (1975), followed by strain hardening at the critical state.

Feasibility studies of using physical simulation techniques, especially centrifuge modelling, to simulate failure mechanisms and phreatic surface development on tailings structures have been published for coal tailings by Al-Hussaini et al. (1981), Sutherland and Rechard (1984) and Stone et al. (1994). These studies indicated good performance in modelling staged filling, Lappin (1997).

In-situ Testing

In-situ testing offers an attractive alternative to sampling and laboratory testing, but difficulties in defining boundary and drainage conditions hamper the interpretation of these tests.

The in-situ vane shear test (VST) has been used extensively in tailings investigations, but there is no assurance regarding drainage conditions during shear. Usually attempts are made to ensure either fully undrained (rapid rate of shear) or fully drained (very slow rate of shear) conditions. However, these attempts are not necessarily successful (Blight, 1970; Blight & Steffen, 1979; Vick, 1983).

The cone penetration test and piezocone (CPT & CPTU) suffer from the same limitations concerning drainage conditions during shear as the vane shear test, but have the advantage of providing excellent information on sub-surface layering and, in the case of the piezocone, the seepage regime within a tailings impoundment (East et al., 1988a). Stratigraphy from the piezocone provides almost an historic record of mine operations over the life of the tailings dam. The material type changes, the rate of deposition and any major stoppages are reflected in the penetration record. The use of friction ratios is limited in tailings due to the highly layered nature of these deposits, where the friction sleeve can be located across a number of different layers simultaneously.

Jones et al. (1981) used the piezocone extensively on platinum and gold tailings dams and developed the first version of the Jones and Rust soil classification chart for the piezocone using normalised cone resistance and pore pressure parameters, Figure 2-12. Subsequent development of this chart is discussed in Jones and Rust (1982, 1983). Classification is based on the principle that penetration through coarse material results in high penetration resistance together with low or negative generated excess pore pressure. In fine material, penetration resistance is low with large positive excess pore pressure. The identification chart proposed by Robertson and Campanella, (Robertson, 1990), is also popular for classification purposes in tailings. For more information and other identification systems, reference can be made to Campanella et al. (1983); Larson and Mitchell (1986), Mlynarek et al. (1991) and Tschuschke et al. (1995).

Standpipe piezometers, preferably with water sampling capabilities, are widely used on tailings dams to monitor the pore water regime, phreatic surface and in-situ permeabilities (Kealy & Busch, 1979; Follin et al., 1984; Wagener et al., 1997). Piezometers are either installed in boreholes or are of the push-in type, but care must be taken to ensure that the measuring tip is sealed off properly after installation. The accuracy of a standpipe piezometer is of the order of ± 150 mm provided it is properly installed, however, due to the time lag of response of the water level inside the piezometer, accuracies of better than ± 300 mm cannot be expected (Wagener et al., 1997). In order to determine the level of the phreatic surface accurately a number of piezometers have to be installed at a specific location to account for the effect of vertical flow. The error resulting from assuming the phreatic surface to be located at the level of the water inside a single standpipe is not always conservative in a tailings impoundment. When seepage flow has a vertical downwards component the water level in a piezometer will be below the actual phreatic surface and vice versa.

The piezocone, in turn, gives reliable estimates of the equilibrium or ambient pore pressure distribution as well as the location of the phreatic surface, from dissipation tests (Rust et al.,

1984). By comparing the ambient pore pressure increase with depth to that resulting from hydrostatic water pressures the following conclusions may be drawn:

- If equilibrium pore pressures are hydrostatic, then there is no component of vertical flow at the location of the sounding.
- If equilibrium pore pressures are below hydrostatic, then a vertical downwards flow component exists.
- If equilibrium pore pressures are above hydrostatic, then a vertical upwards flow component exists.

A non-hydrostatic profile of equilibrium pore pressures in the pond area is often the result of ongoing consolidation resulting in vertical movement of the dissipation water.

Coefficients of consolidation and a good indication of permeability can also be derived from piezocone dissipation data based on theories of consolidation, plasticity and cavity expansion (Rust et al., 1995; Rust, 1996). Van der Berg (1995) noted the unique relationship between the slope of the phreatic surface, the rate of increase in ambient pore pressure with depth and anisotropy in permeability. Piezocone dissipation data enables the determination of the slope of the phreatic surface, α, in the horizontal direction, and the slope of the equilibrium pore pressure increase with depth, β, in the vertical direction. These parameters can then be used to calculate the anisotropy in permeability at the phreatic surface as,

$$\frac{k_x}{k_z} = \frac{\tan\beta}{\tan^2\alpha} \qquad \textbf{Eq. 2-24}$$

Permeability ratios of 7 to 22 and even as high as 25 (Wagener et al., 1998), have been found in this way, and take into account in-situ structure and macro permeability.

The density state or relative density is a critical parameter in determining the stability and liquefaction potential of a tailings impoundment. Relative density, D_r, can be estimated from cone penetration results with reference to Schmertmann (1978) using,

$$D_r(\%) = \frac{100}{2.91}\ln\left(\frac{q_c}{12.31\sigma'^{0.71}_{vo}}\right) \qquad \textbf{Eq. 2-25}$$

where q_c = measured cone resistance

σ'_{vo} = effective vertical overburden pressure

Mlynarek et al. (1995) suggest that the density state in a tailings dam can only be determined from cone results if site specific correlations are first established using in-situ void ratio's from undisturbed sampling and estimates of the maximum and minimum void ratio's from laboratory tests; see also Jones et al. (1981), Baldi et al. (1982), Klohn (1984) and Matyas et al. (1984). Alternatively interpretation of relative densities from cone results

should be accompanied by calibration chamber tests (East et al., 1988a). However, tailings data lie in areas with high uncertainty compared with typical chamber sands.

According to Mittal (1974), penetration tests are unreliable tools for in-situ density measurements. As an alternative down-hole nuclear density logging may be used, which is reported to give reliable results (Mittal & Morgenstern, 1975 & 1976; Carrier et al., 1983; Klohn, 1984; Tjelta et al., 1987; Plewes et al., 1988).

Jones et al. (1981) derived an equation for profiling the in-situ variations in the angle of internal friction, ϕ', in tailings by assuming zero cohesion and making use of bearing capacity relations after Harr (1977) and Parez et al. (1976),

$$\frac{q_c + \Delta u((q_c/\sigma'_{vo}) - 1)}{\sigma'_{vo}} = (1 + \tan\phi')\tan^2\left(45 + \frac{\phi'}{2}\right)\exp(\pi \tan\phi') \qquad \textbf{Eq. 2-26}$$

where q_c = measured cone resistance, adjusted according to Parez et al. (1976)

Δu = excess pore pressure

σ'_{vo} = effective vertical overburden pressure

Other empirical attempts at relating shear strength parameters in cohesionless tailings to cone penetration results include:

(a) Sugawara and Chikaraishi (1982) - gold tailings:

$$\frac{q_c}{\sigma'_{vo}} = 1.5\exp\left[2\pi\tan\left(\frac{\sin\phi'}{(1 - 2A_p\sin\phi')}\right) - 1\right]\cos\left(\frac{\sin\phi'}{(1 - 2A_p\sin\phi')}\right) \qquad \textbf{Eq. 2-27}$$

where $c' = 0$, no cohesion is assumed

A_p= pore pressure coefficient given as a function of the pore pressure response

(b) Robertson and Campanella (1983) - natural soils:

$$\tan\phi' = 0.1 + 0.38\log\left(\frac{q_c}{\sigma'_{vo}}\right) \qquad \textbf{Eq. 2-28}$$

East et al. (1988) in using this bearing capacity type formulation on the Homestake gold tailings dam found friction angles ranging between 20 and 34° and as low as 10°. East et al. (1988a) conclude that interpretation of cone results in this way is not sufficient to describe the strength of the material and stress the importance of relative density in controlling the behaviour of tailings.

(c) East and Ulrich (1989) - tailings in general:

$$\tan\phi' = 0.105 + 0.161\ln\left(\frac{q_c}{\sigma'_{vo}}\right) \qquad \textbf{Eq. 2-29}$$

Eq. 2-29 is a modification of Eq. 2-28, specifically adapted for use in tailings.

(d) Mlynarek et al. (1991) - non-cohesive tailings:

$$\phi' = 10(2a_2 + b_2 \cdot D_r) \qquad \textbf{Eq. 2-30}$$

where a_2 & b_2 = constants given as a function of friction ratio or tailings grade.

(e) Tschuschke et al. (1992) - copper tailings:

$$\tan\phi' = -1.547 + 1.574\gamma_d + 0.012w(1 - 0.083w) \qquad \textbf{Eq. 2-31}$$

where $$\frac{\gamma_w}{\gamma_d} = 1.04 - 0.113\frac{\log q_c}{Pa} + 0.025\frac{\log\sqrt{\sigma_v}}{Pa} \qquad \textbf{Eq. 2-32}$$

γ_d = effective unit weight of the tailings

w = moisture content

γ_w = unit weight of water

Pa = reference pressure (atmospheric)

σ_v = vertical overburden pressure

These equations were used by the authors to calculate the friction angle of tailings on partially saturated beach areas.

East et al. (1988) prefer the self-boring pressuremeter for determining effective friction angles at selected depths in tailings impoundments, and in applying the interpretation proposed by Robertson and Hughes (1986) with correction for looseness, found the friction angles in the Homestake gold tailings dam to vary between 30 and 40°.

The undrained shear strength parameter, c_u, is often used in the design of tailings dams for calculating the factor of safety against undrained slope instability. Undrained shear strength is usually derived from cone penetration data using a cone factor, N_{kt}, in the following equation,

$$c_u = \frac{q_e}{N_{kt}} \qquad \textbf{Eq. 2-33}$$

Values for the cone factor quoted in the literature for tailings are:

- Larson and Mitchell (1986) - uranium tailings, N_{kt} = 15 to 19
- East and Ransone (1988) – gold tailings, N_{kt} = 9 to 12
- East and Ulrich (1989) - tailings in general, N_{kt} = 10.4

- Mlynarek et al. (1994) – copper tailings, N_{kt} = 15.5±4.5

Ishihara et al. (1990) derived correlations for empirically estimating the residual strength of tailings dams and other slopes from cone data using a cone factor of 15 for silty sands. However, the scatter is great.

Deformation and stiffness parameters are usually related to cone penetration data in the form of Eq. 2-34 (Senneset et al., 1989).

$$M = \alpha \cdot q_c \qquad \textbf{Eq. 2-34}$$

where M = drained constrained secant modulus

α = constant

Mlynarek et al., (1995) found α to range between 1.9 and 4.6 as a function of grain size and in-situ stress level for a variety of tailings types, whereas Tschuschke et al. (1994) quote the value of α = 18.4 on average in copper pond tailings.

Assessment of liquefaction potential with the CPT is usually done by correlations with Standard Penetration Test (SPT) data. In assessing the liquefaction potential of a tailings dam, Ulrich and Valera (1995) found very low SPT blow counts typically ranging between 0 to 5 up to a depth of 10 m. Due to the insensitivity of the SPT in this range it was decided to use the cone penetration test, which is not as operator dependent as the SPT, does not require a borehole and gives a lot more information, much faster, even at great depth. The cone penetration data can be transformed into equivalent SPT numbers, which are then used to determine the liquefaction potential after Seed and De Alba (1986). Unfortunately the guidelines do not extend to low enough q_c values, and extrapolation is required when considering the data in tailings. However, the CPT gives additional information on the equilibrium pore pressure distribution and location of the water table, which can be used to calculate vertical effective stresses from overburden pressures and serve as guidelines to the possibility of pore pressure generation during a seismic event.

A number of papers have been published on the use of in-situ tests in tailings other than gold. Coal: Wahler and Associates (1973); Copper: Campanella et al. (1983), Campanella et al. (1984), Tschuschke et al. (1992), Tschuschke et al. (1993), Vidic et al. (1995), Tschuschke et al. (1994), Tschuschke et al. (1995); Uranium: Larson and Mitchell (1986).

2.5.4 Basic Engineering Properties of Tailings Deposits

A tailings impoundment consists of multiple layers of sediment formed by the processes of deposition, sedimentation and consolidation. The engineering characteristics of these layers

ultimately control the safety and serviceability of the structure as a function of the in-situ composition (particle properties) and state (density, stress level, stress history, etc.). The remainder of this chapter is dedicated to a review of the engineering properties of gold tailings deposits with the aim of defining composition and state .

For publications on the properties of tailings other than gold, reference can be made to: Uranium: Keshian and Rager (1988); Hard rock tailings: Aubertin et al. (1996), Aubertin et al. (1998).

Fundamental Particle Properties

The mineral constituents of tailings particles include quartz, chlorite, biotite/mica, talk, pyrite and arsenopyrite (Donaldson, 1965; Hamel & Gunderson, 1973), quartz being by far the most abundant mineral in the coarser grains (Mlynarek et al., 1995). Considering the mineral shapes of these constituent minerals it becomes clear why tailings particles are mainly angular in shape (Pettibone & Kealy, 1971):

- Quartz : Angular grains.
- Pyrite : Cubic grains.
- Mica : Platy shaped grains.
- Talc : Platy shaped grains.

A recurring theme in the published literature on tailings is the similarity in engineering properties between coarse and fine tailings grades. Ulrich and Valera (1995) ascribe this phenomenon to the absence of clay minerals in gold tailings, although it will be shown in this thesis that gold tailings can have significant amounts of clay minerals especially in the slimes.

Quoted values of the specific gravity of gold tailings particles are listed in Table 2-5

Table 2-5: Specific gravity of gold tailings.

Reference	G_s
Pettibone and Kealy (1971)	2.5 to 3.5
Hamel and Gunderson (1973)	3.1
East et al. (1988a)	3.02

The sands or coarser fraction of gold tailings range in shape from very angular to sub-angular with sharp edges (Mittal & Morgenstern, 1975; Lucia et al., 1981; Garga & McKay, 1984; Mlynarek et al., 1995). The fines are invariably angular, sometimes needle shaped, with very sharp edges and resemble shards of broken glass under the microscope (Hamel

& Gunderson, 1973). Papageorgiou et al. (1999) mention, in addition to the irregular shapes of the particles, also harsh surface textures.

Gradings and Atterberg Limits

The particle size gradings of gold tailings are generally limited to and uniformly distributed in the silt size range with small percentages, of the order of 10%, in the sand and clay sized ranges (Pettibone & Kealy, 1971; Van Zyl, 1993).

Figure 2-13 represents a summary of grading curves for gold tailings as found in the literature.

Gold tailings exhibit very little plasticity and no cohesiveness (McPhail & Wagner, 1989), and classify, based on their Atterberg limits, as low to high plasticity silts on the Casagrande chart, see Figure 2-14 (Carrier et al., 1983). Mlynarek et al. (1995) advises the use of the fall cone test to determine the liquid limit and plasticity properties of gold tailings. The Atterberg limits for gold tailings generally fall within the following ranges (Wagener et al., 1998):

- Liquid Limit : 23 - 43
- Plastic Limit : 22 - 35
- Plasticity Index : 1 - 8
- Linear Shrinkage : 2.7 - 4.7

Despite this Wates et al. (1999) quote a linear shrinkage of gold tailings of up to 22%.

Density

The density of the material on a tailings impoundment is controlled by both the properties of the slurry and the depositional conditions. Depending on the specific gravity of the solids the sediment in the pond of a tailings impoundment settles to a dry density of approximately 1000 kg/m^3 at a moisture content of 60%. On the beach above the water table the solids settle to a density of approximately 1450 kg/m^3 at a moisture content of 20 - 50%. There is usually an increase in density with depth in an impoundment, as consolidation takes effect, but with considerable scatter. Vick (1983) argues that the density state in a tailings impoundment is better described by in-situ void ratio than dry density; void ratios do not include the effect of specific gravity and are only a function of the tailings particle properties and stress level.

Quoted values of the densities of gold tailings deposits are listed in Table 2-6.

Table 2-6: In-situ densities and void ratios for gold tailings.

Reference	Description	Density (kg/m^3)	Void Ratio
Donaldson (1965)	Dry density sub-aerial	1750	
	Dry density sub-aqueous	900	
Blight (1969)	Void ratio after deposition		1.7
	After evaporation		1.25
	After sun drying		0.5
Hamel & Gunderson (1973)	Standard Proctor	1700	
	Modified Proctor	1860	
	Minimum dry density	1000	
Blight & Steffen (1979)	Void ratio		1.1 - 1.2
Blight (1981)	In-situ dry density	1835	
Vick (1983)	Tailings sands		0.6 - 0.9
	Low plasticity slimes		0.7 - 1.3
	High plasticity slimes		5 - 10
East et al. (1988a)	In-situ dry density	1340 - 1740	
	Average dry density	1650	
Van Zyl (1993)	In-situ dry density	1000 - 1450	

Permeability

Permeability, in general, is a function of the particle properties, density state and structure of a soil (Pettibone & Kealy, 1971). According to Kealy and Busch (1979) the spatial variation of permeabilities through a dam cross section, from embankment wall to decant pond, is by far the most significant factor in determining the location of the phreatic surface. Anisotropy in permeability and foundation permeability only have minor effects in controlling the location of the phreatic surface. Material is generally coarser towards the embankment wall as a function of hydraulic sorting processes, Section 2.5.2. The resulting increase in permeability towards the embankment helps lowering the phreatic surface. However, this may be counteracted by severe anisotropy in permeability (Blight et al., 1985). Permeability is dependent on the coarseness of the tailings, but McPhail and Wagner (1989) report a maximum permeability difference of only one order of magnitude or less between gold tailings sands and slimes.

The permeability of tailings, excluding the effects of structure, can be calculated by the well known empirical relationship proposed by Hazen in 1892,

$$k = c \cdot D_{10}^2 \qquad \textbf{Eq. 2-35}$$

where k = permeability in cm/s

D_{10} = particle diameter for 10% passing

c = constant varying between 1.0 and 1.5

Mittal and Morgenstern (1975), from laboratory studies, confirm the use of Eq. 2-35 with c = 1 for tailings sands at a relative density of about 40 to 50%. Blight et al. (1985) also recommends the use of this equation in tailings.

Other attempts at defining the mass permeability of tailings have been made by:

(a) Bates and Wayment (1967):

$$\ln(K_{20}) = 11.02 + 2.912\ln(e \cdot D_{10}) - 0.085\ln(e)\ln(CU) + 0.194e \cdot CU - 56.5D_{10}D_{50} \qquad \textbf{Eq. 2-36}$$

where K_{20} = permeability at 20°C in in/hr

e = void ratio

D_{10} = particle diameter for 10% passing

D_{50} = particle diameter for 50% passing

CU = coefficient of uniformity

This equation is reported to be conservative by Mittal and Morgenstern (1975), who recommend the use of Hazen's formula.

(b) Carrier et al. (1983):

$$k = \left(95.2G_s \frac{PI}{100}\right)^{-4.29} \frac{e^{4.29}}{1+e} \qquad \textbf{Eq. 2-37}$$

where k = permeability in m/s

G_s = specific gravity

PI = plasticity index as a percentage

e = void ratio

(c) Sherard et al. (1984; 1984a):

These authors propose an expression similar to Hazen with,

$$k = 0.35D_{15}^2$$

where k = permeability in cm/s

D_{15} = particle size for 15% passing

or using the characteristics of the beach profile,

$$k = a \cdot \exp(-bx)$$

where a & b = beach constants

x = horizontal distance from the discharge point.

Quoted values for the permeability of tailings in the literature are summarised in Table 2-7.

Table 2-7: Permeability values for gold tailings.

Reference	Description	Permeability (*m/yr*)
Blight (1980)	Range	1 - 50
Blight (1981)	General	3
Sully (1985)	For tailings sands	
	50 kPa effective stress	0.31
	100 kPa effective stress	0.23
	150 kPa effective stress	0.22
	200 kPa effective stress	0.21
	300 kPa effective stress	0.21
Aubertin et al. (1998)	Hard rock tailings	1.5 - 60

The depositional processes on a tailings impoundment result in a highly layered, and anisotropic profile, as mentioned previously. Measured anisotropies, k_h/k_v, in gold tailings range from 5 - 10 (Pettibone & Kealy, 1971), 10 (Kealy & Busch, 1979), 2 - 10 (Vick, 1983), 7 - 22 (Van der Berg, 1995), 25 (Wagener et al., 1998) and even as high as 100 at the beach pond interface (McPhail & Wagner 1989). McPhail and Wagner (1989) point out that desiccation cracks and their preferential filling with coarse material reduce the effects of layering and consequently the macro anisotropy to only some 1.5 to 3.

The literature gives conflicting reports on the reduction of permeability with depth and increasing stress levels. Sully (1985) showed little reduction in the permeabilities of undisturbed block samples of coarse gold tailings for stress levels ranging between 50 and 400 kPa, whereas McPhail and Wagner (1989) mention reductions in permeability by a factor of 5 to 10 as a function of compressibility.

Engineers have become increasingly aware of the importance of unsaturated flow above the phreatic surface in modelling the seepage regime in a tailings impoundment. Aubertin et al. (1998) studied the water-retention properties of hard rock tailings to estimate the unsaturated hydraulic conductivity and capillary rise of these materials. Plate extractor tests (ASTM D3152) and Tempe cells (ASTM D2325 & D3152) were used to find the moisture retention curve (MRC) on remoulded tailings specimens, densified to void ratios between 0.5 - 0.9. The MRC, characteristic of the hydraulic properties of unsaturated porous media, provides a relationship between volumetric water content, θ, and matric suction, ψ. Popular models for the MRC include those proposed by Brooks and Corey (1966) and Van Genuchten (1980), where model parameters are empirically related to the grading

characteristics and porosity of the material. Another model proposed by Kovacs (1981) has physical significance that is lacking in the others. Aubertin et al. found saturated permeabilities well predicted by the Kozeny-Carman equation (Chapuis & Montour, 1992). Air entry values (*AEV*), or the matric suction at which the largest pore space de-saturate, are equally well estimated using Eq. 2-38.

$$AEV = \frac{b}{e \cdot D_{10}} \qquad \textbf{Eq. 2-38}$$

where e = void ratio

D_{10} = particle size for 10% passing

b = constant ranging between 2.5 to 4 mm^2

2.5.5 Compressibility and Strength of Tailings

The compressibility and strength of tailings as a function of their composition and in-situ state, together with a knowledge of the seepage regime, will determine the stability, storage capacity, allowable rate-of-rise and other controlling factors in the design and operation of an impoundment. Compressibility and the change in compressibility with time as well as static and dynamic strength of gold tailings will be the subject of this section.

Compressibility

Tailings appear to be more compressible than similar natural soils, partly due to their grading characteristics, high angularity and loose depositional state, Vick (1983). Considering the very recent stress history of tailings sediments, many authors assume a normally consolidated state. However, when deposition is sub-aerial, desiccation suctions and capillary effects can build in some overconsolidation. Donaldson (1965) measured pre-consolidation pressures of up to 500 kPa in gold tailings using the method of Casagrande in the oedometer, as well as tensiometers. Blight (1969) reports desiccation suctions of 1 to 10 MPa in gold tailings, although 10 MPa would require an unrealistically small D_{10} of the order of 0.15 micron[3]. Donaldson found almost all of the material above the water table to be overconsolidated. Nevertheless, the increase in shear strength due to pore suctions is unreliable as a result of frequent re-wetting and an almost instantaneous release in suction following precipitation and seepage from subsequent depositions. The principal advantage of desiccation is the resulting increase in density and stiffness. The overconsolidation effect may also be destroyed with depth and overburden pressure as the dam rises. Under sub-aqueous deposition, in the pond, the state of the tailings can be expected to be normally

[3] Calculated assuming the effective pore diameter, d, is 20% of the effective grain size, D_{10}, which can support a capillary suction of $4T\cos(\alpha)/\rho_w d$, where, T, the surface tension is taken as 73 mN/m and, α, the contact angle as zero.

consolidated or even under-consolidated during the process of ongoing primary consolidation.

The coefficient of compressibility for gold tailings, as reported in the literature, is listed in Table 2-8. However, these values were derived from reconstituted normally consolidated laboratory samples and would not be applicable to material that has become overconsolidated due to desiccation suctions.

Table 2-8: Coefficient of Compressibility, C_c, of gold tailings.

Reference	Description	C_c
Blight & Steffen (1979)	Tailings slimes	0.35
Vick (1983)	Tailings sands	0.05 - 0.1
	Tailings slimes	0.2 - 0.3

Carrier et al. (1983) approximates the compressibility of tailings for low stress levels as a function of the overburden pressure by,

$$e = 17.7 G_s \frac{PI}{100} \cdot \sigma'^{-0.29}_v \qquad \text{Eq. 2-39}$$

where G_s = specific gravity of the particles

PI = plasticity index as a percentage

σ'_v = vertical effective overburden pressure

Consolidation Characteristics

Depositional processes and sedimentation are followed by primary and secondary consolidation, where primary consolidation is associated with the dissipation of excess pore pressures, and secondary consolidation or creep with viscous effects in the particle skeleton. Primary and secondary consolidation occur simultaneously until primary consolidation ceases with full dissipation of the excess pore pressures. Secondary consolidation is reported to be small and relatively insignificant in tailings and is attributed to continuing particle rearrangement, grain to grain slippage under the influence of constant load and continuing contact fracture propagation promoted by water, Vick (1983).

Blight and Steffen (1979) show that the coefficient of consolidation decreases with increased effective stress level and slightly with decreasing void ratio. Vick (1983) maintains that the consolidation behaviour of tailings can sometimes be dominated by permeability and at other times by compressibility.

Typical values of the coefficient of consolidation for gold tailings are listed in Table 2-9.

Table 2-9: Coefficients of consolidation, c_v, for gold tailings.

Reference	Description	c_v (m^2/yr)
Blight & Steffen (1979)	Tailings slimes	198
Blight (1980)	General	10 - 50
Blight (1981)	General	300
Vick (1983)	Tailings sands	$1.6x10^3$ - $0.3x10^6$
	Tailings slimes	0.3 - 30
Sully (1985)	For tailings sands as a function of effective stress	
	50 kPa	112
	100 kPa	67
	150 kPa	82
	200 kPa	68
	300 kPa	55
	400 kPa	81

Shear Strength - Static

Many factors influence the shear strength of a hydraulic fill including:

- Material properties, i.e. mineralogy, grading, particle shape and surface texture, etc.
- Processes of deposition, sedimentation and self-weight consolidation and its effect on stress level, density, fabric, etc.
- Construction control, i.e. rate-of-rise, desiccation and re-wetting cycles and its influence on stress level, pore pressure distribution, overconsolidation, etc.
- Other factors including flocculation vs. dispersion, oxidation leading to precipitation bonding, etc.

Natural remoulded sands, generally, exhibit no cohesion with angles of internal friction ranging between 30° and 40° as a function of relative density and stress level (Guerra, 1972). However, at low stress levels the friction angle can be as high as 48° as reported by Bica and Clayton (1998) for Leighton Buzzard sand. Mittal and Morgenstern (1975) believe that tailings should have slightly higher friction angles than natural sands due to the highly angular nature of tailings particles.

Vick (1983) describes the shear strength properties of tailings as cohesionless with rare exceptions, and an effective angle of internal friction, ϕ', ranging between 30° and 37°. The influence of various factors on ϕ' is summarised by him as:

- Very little dependence of ϕ' on grading, see also Van Zyl (1993) and McPhail and Wagner (1989).
- Density has a surprisingly small influence on ϕ', 3 - 5° for tailings sands.
- Overconsolidation also has a relatively small effect.
- Effective stress level is the most important parameter controlling ϕ', with the strength envelope curved at high stress levels as a result of particle crushing.

Kuerbis et al. (1988) studied the phenomenon of nearly constant friction angles between the tailings sands and slimes by adding natural silt fines to a tailings sand. Undrained triaxial compression and extension tests demonstrated that the angle of friction at phase transformation remained constant and independent of silt content or mode of deformation. The silt fines were simply occupying void spaces, whereas the sand skeleton was controlling the shear behaviour. The addition of silt fines, however, resulted in higher settled densities following specimen preparation, and also increased dilatency under shear.

Hamel and Gunderson (1973) performed a number of direct shear tests to determine the effect of level of saturation and density on the shear strength of Homestake gold tailings. A range from completely dry to fully saturated specimens was prepared by compaction to varying densities and subjected to direct shear in the shear box. Shear strength parameters for these specimens are listed in Table 2-10. The dry specimens (moisture content of 0.2 %) were compacted to 1344 kg/m^3, loose, and 1520 kg/m^3, dense; the wet specimen to 1372 kg/m^3, moisture content 17%; and the dense saturated specimen to 1512 kg/m^3, moisture content 34%. All results indicated contraction with no dilation during shear. The reduction in ϕ' with added moisture is explained by the lubricating effect of the water on the layer lattice (clay) minerals in the tailings mix. Hamel and Gunderson argue that the addition of water reduced the charge attraction between partially hydrated surface ions on the clay minerals thus reducing the angle of internal friction (see Lambe & Whitman, 1969). The high cohesion values are ascribed to aggregate interlock resulting from compaction, increased electrical attraction which varies with the square of the distance between charges and pore water suction as a result of partial saturation. Nevertheless, the reliability of such high cohesion measurements in direct shear should be questioned.

Mittal and Morgenstern (1975) found ϕ', at peak shear strength in the shear box, to be a function of normal stress and density up to a normal stress of 400 kPa using compacted specimens. Below 400 kPa, ϕ' reduces with increasing normal stress. Above 400 kPa, ϕ' becomes independent of normal stress until particle crushing effects become significant. However, they also found ϕ' for uncompacted loose specimens to be independent of both stress level and density. The dependency of ϕ' on stress level and density for the

compacted specimens is principally the result of overconsolidation built in by the high compaction stresses. Similar results were found by Vesic and Clough (1968) for loose and dense samples of Chattahoochee River sand tested at different stress levels in the triaxial apparatus. The overconsolidated state and high density lead to peak strength behaviour and dilation during shear. Nevertheless, cohesionless soils in general behave as though heavily overconsolidated due to soil structure (Poulos, 1988). Poulos warns against the use of peak strengths, which can be up to ten times the steady state or ultimate strength, in designing for static and seismic stability. If the material has been strained beyond the strain level at peak strength, it exists in a meta-stable strain softening state which can easily lead to failure or liquefaction.

Static shear strength parameters for gold tailings are summarised in Table 2-10.

Table 2-10: Static shear strength parameters for gold tailings.

Reference	Description	Test	c' (kPa)	ϕ' (°)
Donaldson (1965)	General	Triaxial	0	35
Hamel & Gunderson (1973)	Dense air-dry	Direct shear	79	38
	Loose air-dry		0	39
	Loose wet		100	28
	Dense saturated		11	24
Mittal & Morgenstern (1975)	Peak, loose	Direct shear	0	34
Blight & Steffen (1979)	Slimes		0	28 - 41
Blight (1981)	General		0	35
Vick (1983)	General			30 - 37
Sully (1985)	Average	Direct shear	5	33
Van Zyl (1993)	Sand & Slimes		0	35
Blight (1997)	Sand & Slimes	Both	0	29 - 35

Shear Strength - Dynamic or Seismic

Cyclic triaxial strength of soil is considered to be a function of relative density and stress level, grain characteristics, method of deposition, ageing effects and previous seismic history (Seed, 1976). Compared with natural soils, both the coarse sands and fine slimes of tailings are believed to have angular to sub-angular grain shapes and similar grain textures and hardness. In addition tailings gradings lie within a remarkably narrow range, mostly in the fine sand and silt size ranges. The stress history will depend on whether the material has been allowed to dry following deposition, in which case it may be heavily overconsolidated, and is not likely to include effects of any significance of seismic events. The most important

factor controlling cyclic strength in tailings, therefore, is the in-situ density (Garga & McKay, 1984). Density and seismic strength can be greatly improved by compaction during construction.

Garga and McKay (1984) performed a number of cyclic triaxial tests on undisturbed and reconstituted samples from 20 tailings and 13 non-tailings materials and concluded that:

- Reconstituted samples tend to have lower cyclic strengths than undisturbed samples (possibly the result of in-situ structure).
- Cyclic strength is sensitive to stress anisotropy.
- Cyclic strength decreases with increasing principal stress ratio.
- Materials in the fine sand range, such as tailings sands, exhibit the lowest cyclic strengths.

2.5.6 Liquefaction Potential of Tailings Deposits

Many incidents on tailings impoundments are claimed to be related to liquefaction. If failure is not caused by liquefaction, then liquefying of the mass mobilised by other types of failure can result in extensive damage as illustrated in Section 2.4.10.

Liquefaction is "the phenomenon wherein a saturated sand looses a large percentage of its shear resistance, due to monotonic or cyclic loading, and flows in a manner resembling a liquid until the shear stresses acting on the mass are as low as its residual shear resistance", Castro and Poulos (1977). Liquefaction in soils can result from either an unstable or contractile soil skeleton with collapse potential, or when effective stresses are annulled by positive pore pressure build-up, usually during cyclic loading. In the case of collapse potential (Sladen et al., 1985) the material state must lie in structurally permitted space, which will collapse to a more stable state on de-structuring. It is interesting to note that in studying the sedimentation-consolidation behaviour of natural sands, Schiffman et al. (1986) discovered that cohesionless sands and silts, deposited sub-aqueously at low to moderate relative densities (30 - 50%), may exhibit peak undrained shear strength behaviour. It must be assumed that this is a result of the particle arrangement or fabric under these conditions. Kramer and Seed (1988) found similar results on natural sand, where the peak behaviour and susceptibility to liquefaction was found to be a function of confining stress and the initial consolidation shear stress. Collapse is usually initiated by a trigger mechanism in the form of increased pore pressures due to a rise in the phreatic surface, increased shear stress due to a rise in the dam height, cyclic loading from seismic activity, loss of confining stress due to failure, etc. The work of Sasitharan et al. (1993) shows that liquefaction can follow either drained or undrained loading conditions, but that

the actual liquefaction event is undrained with a rapid loss of effective strength caused by positive pore pressure generation.

The potential for liquefaction in tailings is controlled by the level of saturation, density state, fines content and confinement stress levels (Troncoso, 1986). Liquefaction potential varies on a typical impoundment as a function of (Klohn et al., 1978):

(a) **Permeability zoning**: The permeable embankment leads through intermediate beach zones to the relatively impermeable pond (Finn, 1982). The intermediate and pond areas are more prone to liquefaction due to more extensive saturation and higher fines content. Singh and Chew (1988) found tailings with less than 20% silt sized content to behave similar to clean sands. However, for mixes with more than 60% silt, typical of gold tailings, the behaviour was controlled by the silt fraction, which is more susceptible to liquefaction due to the reduced permeability.

(b) **Saturation levels**: It is only under saturated conditions that liquefaction, as a result of pore pressure build-up, becomes a major concern (Klohn, 1980). However, Papageorgiou et al. (1999) warn that liquefaction as a result of structural collapse can be of importance in both partially and fully saturated soils. Use of internal drains, decant facilities and controlled rate-of-rise should prevent the phreatic surface from exiting on the downstream face of the embankment wall. In addition to improving static stability through the effective stresses, levels of saturation and hence liquefaction potential are also lowered if the phreatic surface is kept as low as possible in the embankment wall.

(c) **Deposition densities**: Uncompacted sands are most susceptible to liquefaction, however, in low to moderate seismic areas, compaction of the embankment material may not be required.

(d) **Fines content**: Lucia et al. (1981) allude to the fact that silt sized particles may form meta-stable honeycomb structures under sub-aqueous deposition. Similar observations have been made by Troncoso (1986), where the addition of fines to triaxial specimens led to collapse behaviour. In an extensive investigation of the effects of fines content on the liquefaction susceptibility of gold tailings, Papageorgiou et al. (1999) report the following:

- Increased fines content displaces the critical state line (CSL see Chapter 4) downwards in terms of void ratio at the same effective stress, thus increasing the density.[4]
- Addition of fines leads to a reduction in permeability, making undrained response more likely.
- More angular particles result in a steeper slope of the CSL, thus decreasing the stiffness.
- Increasing the fines content also results in a smaller range of densities attainable by a placement technique during specimen preparation.
- Higher densities are required to produce phase transfer dilation at failure, as the fines content increases.

The consequence of all these effects, on aggregate, is an increased potential for liquefaction with increasing fines content.

Seismic history and ageing are also important causes of evolution and changes in the static and dynamic stability of an impoundment structure (Troncoso, 1988).

Papageorgiou et al. (1997; 1999) investigated liquefaction of mine tailings in terms of steady state concepts. Loading conditions were identified as possible triggers of liquefaction ranging from dynamic events such as seismic shaking, piling vibrations and blasting shocks, to static loads from a sudden increase in surcharge, raise in the level of the phreatic surface or a sudden loss of confining stress on the embankment wall following liquefaction of the impounded slimes. In their 1997 paper Papageorgiou et al. report that cyclic triaxial tests on cyclone overflow (slimes), cyclone underflow (sands) and whole tailings specimens prepared using water pluviation techniques all resulted in stable dilatant behaviour. They attribute this behaviour to particle angularity, irregular particle shapes and harsh surface textures, and confirmed the observation with in-situ measurements indicating dilatant states not susceptible to collapse liquefaction. Subsequently, in 1999, using moist tamping techniques to reconstitute samples, the authors were able to induce contractile behaviour in the laboratory in fine and coarse grades, resulting in liquefaction under static load conditions. An instability trigger was identified on the stress path as a function of the effective stress state, which corresponds to the collapse potential of Sladen et al. (1985). In-situ void ratio's were measured and found to lie mostly above the steady state line developed from the moist-tamped fine specimens. The conclusion was made that the in-

[4] This argument is only valid as long as the fines are filling void spaces within a greater sand skeleton. As soon as the sand skeleton is disrupted addition of more fines will reduce the density and lift the CSL upwards as coarser particles start to float within a sea of fines.

situ material must be susceptible to liquefaction. However, no shear tests on undisturbed samples were presented to confirm this susceptibility to liquefaction.

Highter and Tobin (1980) use Bishop's Brittleness Index (Bishop 1967, 1973) to predict the liquefaction susceptibility and post rupture behaviour of garnet iron and zinc tailings. The brittleness index is calculated for drained loading as,

$$I_{B(Drained)} = \frac{\tau_f - \tau_r}{\tau_f} \cdot 100\% \qquad \textbf{Eq. 2-40}$$

where I_B = Brittleness Index

τ_f = shear stress at peak strength

τ_r = shear stress at residual strength

and for undrained loading as,

$$I_{B(Undrained)} = \frac{c_{uf} - c_{ur}}{c_{uf}} \cdot 100\% \qquad \textbf{Eq. 2-41}$$

where I_B = Brittleness Index

c_{uf} = peak undrained shear strength

c_{ur} = residual undrained shear strength.

Specimens were specially prepared with high brittleness values using wet tamping techniques, and showed pronounced peak and post peak reduction in shear stress. This behaviour is evident even at high confining pressures. Initial void ratio was found to be the most important parameter governing the undrained brittleness index with no brittleness if the void ratio is greater than 80% of the maximum void ratio, e_{max}.

There is an interesting dispute in the literature concerning the failures of the Nerlerk underwater sand berms in the Canadian Beaufort Sea up to 1985. These berms were constructed using sub-aqueous hydraulic deposition of clean sands. Some of the berms even failed under static monotonic load conditions. The failures are generally attributed to post peak contractile softening behaviour as a result of meta-stable collapsible structure following deposition (Sladen et al. 1985). Been et al. (1988) contest that the material will have a natural tendency towards a stable non-contractile state following deposition and if it proved to be contractile, then there must have been some agent interfering with sedimentation process such as,

- Partial saturation resulting in apparent cohesion.
- Deposition of sand with silt infill preventing a stable sand skeleton forming.
- High upward seepage gradients during deposition.

Been et al. (1987; 1988) maintain that none of the failures were caused by collapse of a contractile structure, but that they were due to strains in the foundation. They conclude that

flow slides may occur in dilatant sands initially below the critical state line, and that it has manifested during seismic failures and in the laboratory, where cyclic loading induces positive pore pressure build-up. Even with static loading dilatant sands usually contract first, before they dilate. This initial contraction or positive pore pressure response is more profound in mildly dilatant sands and a flow type failure may result providing a significant trigger mechanism. The trigger was provided, in the case of the Nerlerk berms, by the foundation settlements.

It therefore appears that the structure of hydraulically placed sands, and for that matter tailings, is not obvious and needs careful consideration of the in-situ composition and state. It has been mentioned that increased silt content may lead to a meta-stable structure and strain softening collapse in tailings. Vaid (1994) on the other hand was never able to induce liquefaction in a series of cyclic triaxial tests with various void ratios and silt contents. It seems that only when samples were prepared using wet tamping techniques that liquefaction in the laboratory was evident.

Publications on the liquefaction behaviour of tailings other than gold include: Copper: Scott et al. (1989); Bauxite (aluminium red muds): Poulos et al. (1985); Uranium: Dunbar et al. (1991); Zinc & Garnet: Highter & Vallee (1980).

Special mention should also be made of the CANLEX experiment, in progress, in Canada (Phillips & Byrne,1995; Konrad, 1997). CANLEX stands for Canadian Liquefaction Experiment and involves a large controlled field liquefaction event using oil sand tailings from Syncrude Canada and the Fraser River delta. The experiment is divided into three stages; stage one and two determine the in-situ state and stress-strain response of the material and stage three comprises a controlled liquefaction event. Both static and dynamic liquefaction will be studied and numerical predictions will be compared with field behaviour. The objectives of the CANLEX experiments are to:

- Obtain high quality undisturbed samples through freezing techniques.
- Calibrate and verify in-situ tests.
- Obtain a better understanding of liquefaction.
- Develop and evaluate liquefaction models.
- Investigate the effects of fines content, fabric, load direction, shape of the state boundary surface and triggering mechanisms on liquefaction behaviour.

2.6 CONCLUSIONS FROM THE LITERATURE

2.6.1 Summary of Conclusions from the Literature

The following list summarises the philosophies of design, construction and operation practised in the South African gold mining industry as well as relevant conclusions on the composition and state of gold tailings from a review of tailings literature.

(a) **Tailings production**:

- In the gold extraction process, mined ore is crushed and finely ground down by mechanical means, after which it is subjected to chemical treatments to dissolve, separate and precipitate the gold valuables. The by-product of this process is a fine rock flour slurried with process water, known as tailings.
- South African gold tailings slurries are generally flocculated and slightly alkaline when leaving the reduction plant.

(b) **Impoundment design, construction and operation**:

- For economic reasons, tailings dams are generally not designed with the same conservatism as conventional water-retention dams.
- South African gold tailings impoundments are almost exclusively designed and operated as perimeter ring dikes with the tailings embankment raised, up-stream, throughout the lifetime of the impoundment, using the daywall-nightpan paddock system. Deposition is sub-aerial by open ended pipe discharge or in some cases by spigotting or cycloning. The daywall is raised to provide adequate freeboard, but also to allow maximum time, three weeks on average, for evaporation and desiccation to improve the mechanical properties (especially the density) of the material. Rate-of-rise as a function of this commonly ranges between 1 and 3 m per year. The impoundment can be operated as one or more isolated compartments, each with its own delivery and decant facilities. Decant systems are almost always of the penstock type with internal drainage systems absent in all but the most recent developments. In addition to internal and surface drainage measures, ground level catchment paddocks are provided around the perimeter of the dam to intercept runoff from the side slopes of the impoundment.
- Construction of this kind relies heavily on densification through desiccation and to some extent on segregation to provide a competent embankment. Segregation is achieved either mechanically using hydro-cyclones or gravitationally along the flow path from the discharge point towards the pond area. Gold tailings do not segregate readily due to their uniform grading, and rely on the pulp density to assist segregation.

- Control of the phreatic surface from a design and operational point of view is the single most important factor controlling the stability and serviceability of a tailings impoundment. The controlled rate-of-rise and sequence of deposition should be tailored in relation to the post depositional properties of the tailings and any internal drainage facilities to ensure both adequate storage capacity and a safe structure.
- When selecting a failure criterion and design strength for static stability, careful consideration should be given to the drainage conditions prior to and during a potential failure, as well as to the strain history and stress-strain response of the material.
- Liquefaction of tailings results either from excessive pore pressure build-up during seismic shaking or from softening of a collapsible soil structure following static or dynamic loading. The fine, loose and uncompacted state of hydraulically placed tailings and the resulting low effective stress levels make tailings more susceptible to liquefaction than natural sands.
- In addition to construction related factors such as rate-of-rise and pond control, successful management of an active tailings impoundment requires a comprehensive monitoring program and continuous detailed analysis of all data, backed up by rapid remedial action on identifying possible problems.

(c) **Gold tailings slurries**:

- Gold tailings can be classified as a low plasticity, fine, hard and angular rock flour, slurried with process water in a flocculated slightly alkaline state together with soluble salts. The flocculated state of the slurry promotes low post sedimentation densities, as the material does not readily segregate.
- Pulp densities normally range between 25 and 50% (dry density of 300 to 750 kg/m^3) when delivered to the impoundment site.
- The rheology of a gold tailings slurry lies somewhere between a Bingham plastic and a Newtonian fluid with the shear stress of the slurry a function of viscosity and the rate of shear strain. The viscosity of a gold tailings slurry ranges between 2 and 7 times that of water. Shear strength only develops in the slurry at moisture contents below 30%, thus marking the change between slurry and sediment with the development of effective stresses.

(d) **Soil forming processes on an impoundment**:

- Depositional practices, variations in the mill product, and soil forming processes on the impoundment result in a highly layered profile with coarse and fine layers alternating over small depths.
- The soil forming process on a tailings impoundment includes simultaneous transportation of sediments, sedimentation, consolidation and evaporation. Transportation and sedimentation are followed by primary and secondary

consolidation, where primary consolidation is associated with the dissipation of excess pore pressures, and secondary consolidation or creep with viscous effects in the particle skeleton. Secondary consolidation in tailings is usually assumed to be negligible. If a deposit is exposed to sun-drying the effects of desiccation suctions will result in additional densification.

- The state of the material on a tailings impoundment is controlled by the properties of the slurry including particle size, shape and specific gravity, water content and viscosity, as well as deposition related flow conditions on the beach (sub-aerial) compared with those in the pond (sub-aqueous). Under sub-aqueous conditions the stress history and hindered settling result in a soft and normally consolidated state. Instantaneous sedimentation under sub-aerial conditions on the beach is preferably followed by drying, which can build in large pre-consolidation stresses and result in a relative dense, heavily overconsolidated, state. The principal advantage of such overconsolidation is the resulting increase in density and stiffness and not the temporary increase in effective stresses as a result of high pore water suctions.
- The geometry of the surface profile or beach profile on a gold tailings dam is largely a function of pulp density. The lower the pulp density the more effective the sorting processes and the steeper the beach. As the solids content of the slurry increases to a critical value mudflow commences and sorting processes no longer have an effect, resulting in a flattening of the beach slope. Being able to predict the beach slope or profile of an impoundment not only allows better management of the pond, but also improved estimates of storage volumes, freeboard and the settled physical properties of the tailings. The beach profile can be modelled using the Melent'ev master profile or a similar exponential function.

(e) **Engineering properties**:

- *Mineralogy*: Quartz is by far the most abundant mineral in gold tailings with small quantities of phyllosilicates as well as pyrites and other sulphides. Specific gravity ranges between 2.5 and 3.0. Oxidation of sulphide minerals in tailings can result in self cementing of the structure, or more importantly leaching of toxic substances. Oxidation can only take place in the presence of free oxygen and water or through anaerobic bacterial processes.
- *Grading*: Gold tailings gradings are generally limited to and uniformly distributed in the silt size range with small percentages of sand and clay sized particles. The particles throughout the gradings are angular to sub-angular with sharp edges and harsh surface textures.
- *Plasticity*: Gold tailings exhibit very little plasticity and no cohesiveness and classify, based on their Atterberg limits, as low to high plasticity silts on the Casagrande chart. Typical values of the liquid limit, plastic limit and plasticity index are: 33, 28 and 5%.

- *Density*: In-situ dry density of the slimes is close to 1000 kg/m^3 and for the sands range between 1250 and 1650 with an average of 1450 kg/m^3.
- *Permeability*: Permeability is usually estimated using Hazen's equation as a function of the grading properties, but more advanced formulations incorporate the density state as well. Permeability ranges between 0.5 and 50 m/yr, although there is usually only one order of magnitude difference between the permeabilities of the sands and slimes of a particular tailings product. The anisotropy ratio, k_h/k_v, is approximately 10, but can be as low as 2 and as high as 20. Desiccation cracks tend to reduce the anisotropy to about 3 on average. Permeability reductions of up to one order of magnitude or more can result from self-weight consolidation.
- *Compressibility*: Tailings appear to be more compressible than similar natural soils due to their grading characteristics, high angularity and loose depositional state. Compressibility and consolidation characteristics are significantly affected by grading, with tailings slimes reported to be three times more compressible and 6 orders of magnitude slower to consolidate than tailings sands.
- *Shear Strength*: The shear strength properties for tailings are, cohesionless with rare exceptions, and an effective angle of internal friction, ϕ', ranging between 30 and 40°. Apparent cohesion only develops under partially saturated conditions as a function pore water suction and electrical charge attraction between clay minerals, if present. Aggregate interlock following compaction can also induce some apparent cohesive strength. Apart from this, the internal fiction angle can be assumed largely independent of grading, density, overconsolidation and effective stress level up to the onset of particle crushing. Under dry or partially saturated conditions the friction angle may reduce somewhat with the addition of water due to lubricating effects.
- Tailings exhibit behaviour somewhere between that of a sand and a clay, depending on the composition and state of the material. This is especially troublesome in the interpretation of in-situ tests, where assumptions of fully drained or fully undrained shear cannot be relied on. The low density and low effective stress levels, which result from depositional processes as well as the cohesionless properties of the material make undisturbed sampling for laboratory testing practically impossible on a working impoundment. It is, therefore, extremely important in preparing reconstituted or remoulded laboratory samples to use techniques that simulate field behaviour and result in a composition and state representative of in-situ conditions.
- In triaxial shear, tailings require relatively large strains for failure and seldom dilate prior to failure. They exhibit no strain softening or strength reduction following peak shear strength. In low stress and high density states, typical of samples recovered from desiccated beaches, dilation does occur and strain softening may be a possibility as a result of the overconsolidated states of these specimens. In undrained shear, the coarser material is particularly prone to phase transfer dilation followed by strain

hardening at the critical state. Only specimens prepared by methods of wet-tamping show liquefaction potential as a result of structural collapse in triaxial shear.

(f) **Liquefaction**:

- Many incidents on tailings impoundments are ascribed to liquefaction. If failure is not caused by liquefaction in itself, liquefaction is said to be induced by other types of failure.
- Liquefaction, in general, can result from either an unstable or contractile soil skeleton with collapse potential, or when effective stresses are annulled by positive pore pressure build-up, usually during cyclic loading. Cyclic pore pressure build-up may well cause liquefaction in a tailings deposit during a seismic event, but collapsible structure has never been identified outside the laboratory. The potential for liquefaction in tailings is controlled by the level of saturation, density state, fines content and confinement stress levels.

2.6.2 Specific Issues Addressed in this Thesis

With respect to the above, this study aims to investigate the composition and state of gold tailings to advance the understanding of the engineering behaviour of this material. The following aspects will be addressed:

(a) **Composition**:

A comprehensive study will be made of the composition of gold tailings including mineralogical make-up, grading properties, particle characteristics and specific gravity. While the literature reports on some of these properties, very little if any evidence is given. It is vitally important that the fundamental properties of tailings be accurately defined before any attempt is made at studying the in-situ state and mechanical behaviour of this man-made material.

To determine the composition of the material, electron micrographs, x-ray techniques and standard soil mechanics laboratory tests will be employed as follows:

- *Mineralogy:* Energy Dispersive X-ray Spectrometry and X-ray Diffraction techniques will be employed to determine the elemental and mineralogical composition of the tailings. The mineralogy, especially the clay content, is fundamental to understanding the mechanical behaviour of tailings. This aspect has not been addressed sufficiently in tailings literature.
- *Specific Gravity*: During this standard soil mechanics test, special care will be taken to minimise potential errors resulting from poor experimental practice. Accurate measurements of specific gravity should give an indication of the importance of gravity sorting, as opposed to size sorting, in individual layers on an impoundment.

- *Grading*: Gradings will be determined using standard sieve and hydrometer tests, as well as visual observations on electron micrographs. The influence of standard preparation techniques and theoretical assumptions for the sieve and hydrometer tests will also be investigated. Of special interest is the flocculated nature of the tailings fines.
- *Particle Shape and Surface Texture*: A comprehensive set of micrographs will be prepared of the various size fractions of tailings particles to accurately determine particle size, shape and surface texture properties.

(b) **State**:

With a better understanding of the composition and fundamental properties of tailings the state and behaviour of the material will be investigated using reconstituted remoulded laboratory samples in conjunction with undisturbed field samples.

- *Compressibility*: The effect of composition on the compressibility properties of gold tailings will be examined. An attempt will also be made to predict density states using normalised compression curves and some composition related parameters.
- *Strength*: It is a well documented fact that the shear strength of a particular gold tailings is governed by a single effective stress parameter, ϕ', (typically 35°) irrespective of its grading. This observation will be verified and further investigated with the aim of improving shear strength interpretation of in-situ test data.
- *Structure*: The potential for interparticle bonding as a result of precipitating agents and the existence of collapsible fabric is mentioned in the literature. Electron micrographs of undisturbed samples and triaxial test data on undisturbed samples will be examined for evidence of bonding and fabric.

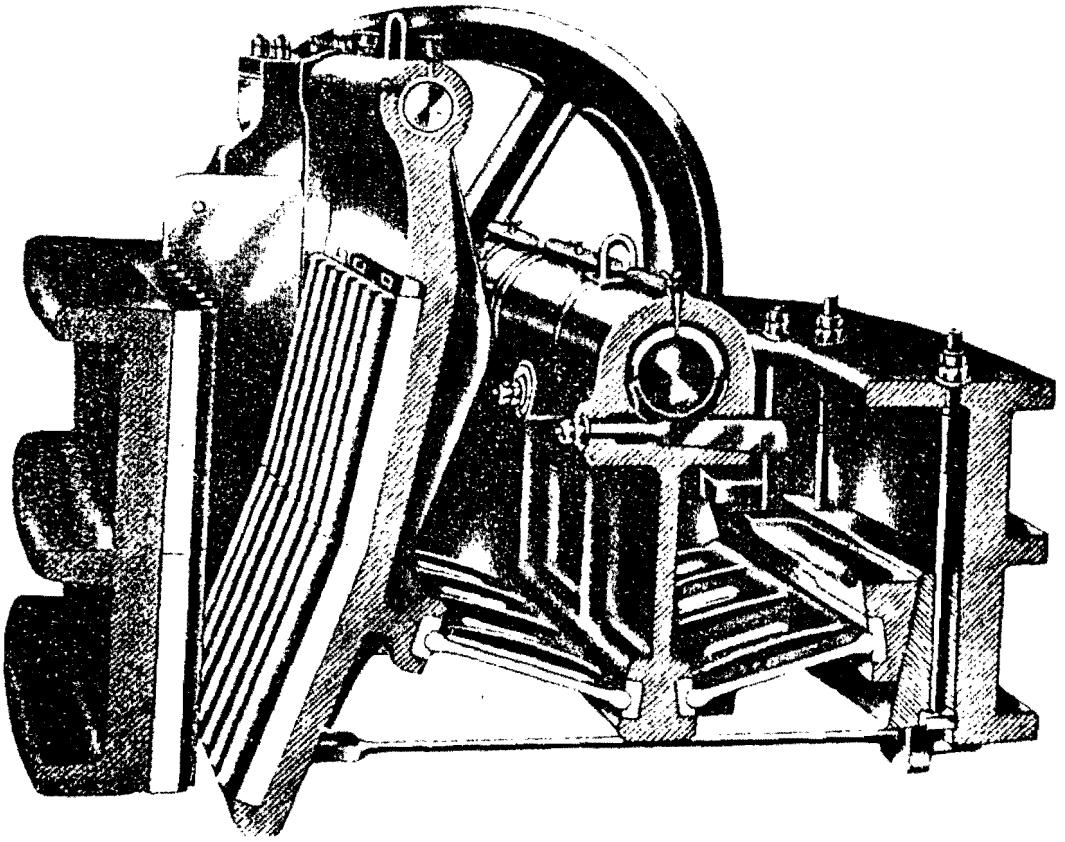

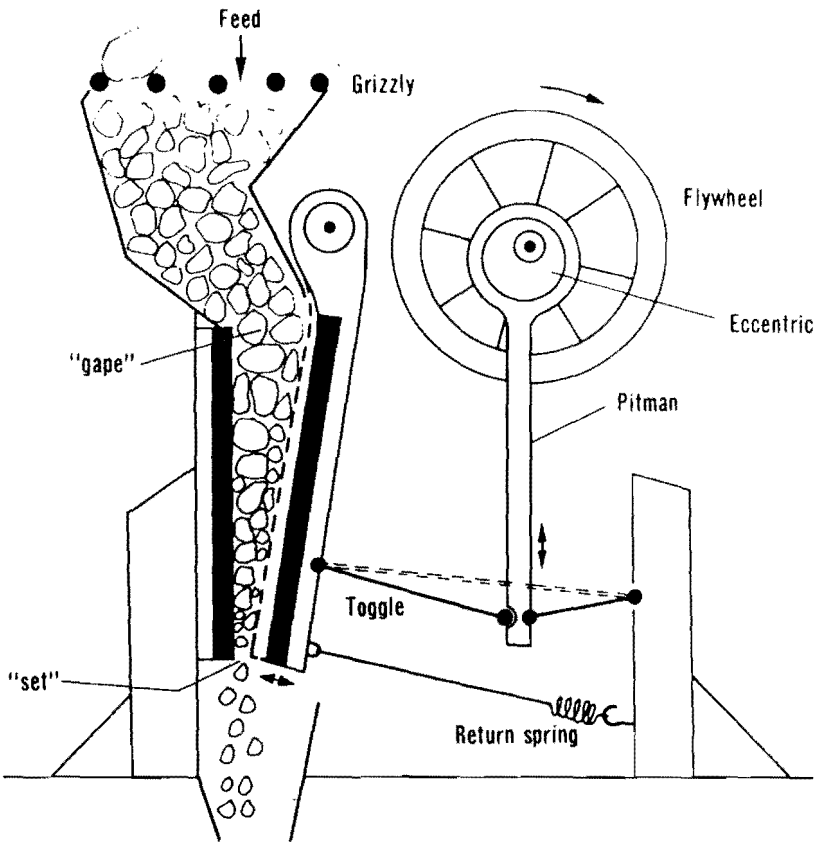

Figure 2-1: Jaw breakers (Wills, 1992; Gilchrist, 1989).

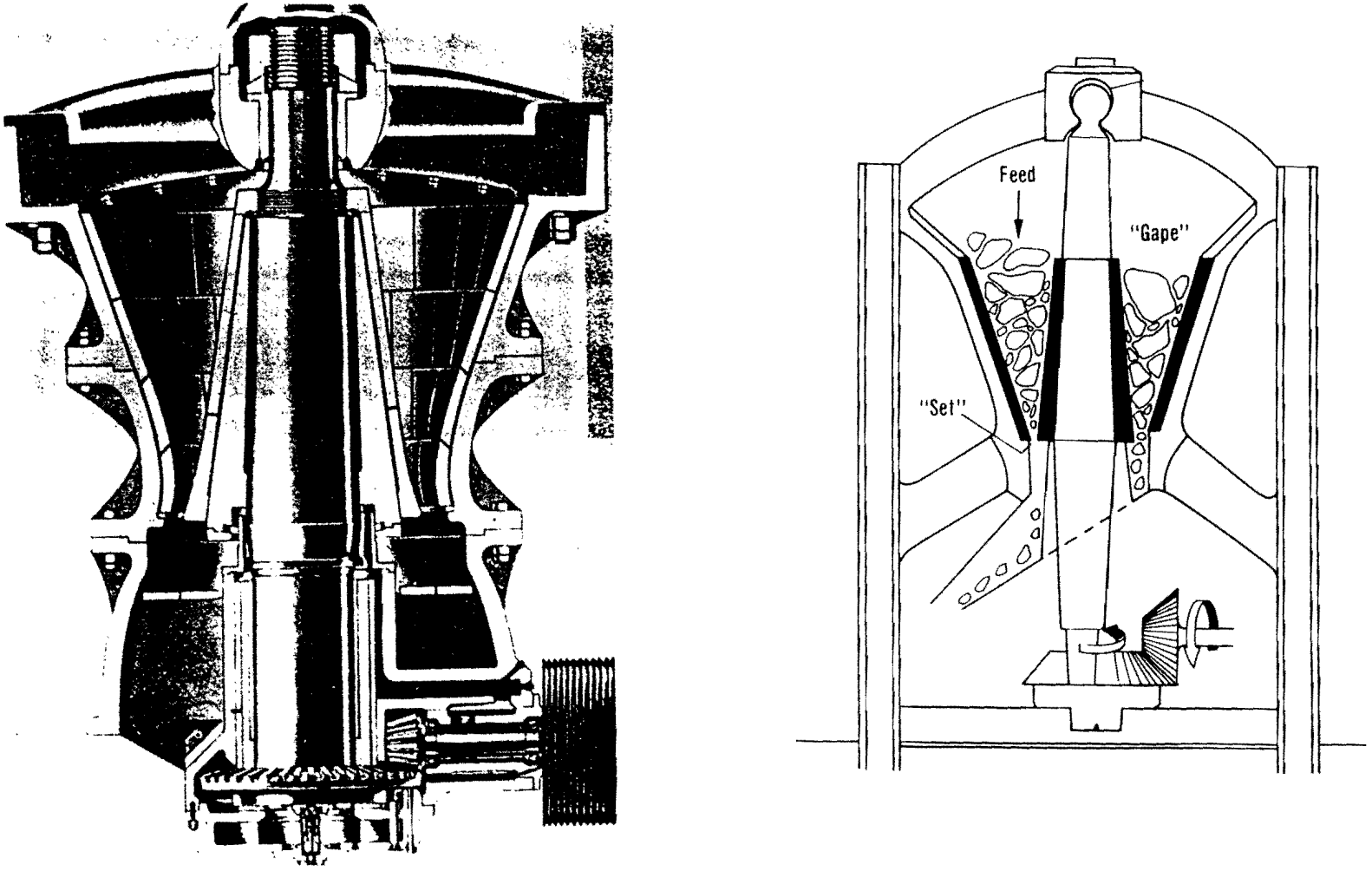

Figure 2-2: Gyratory cone breakers (Wills, 1992; Gilchrist, 1989).

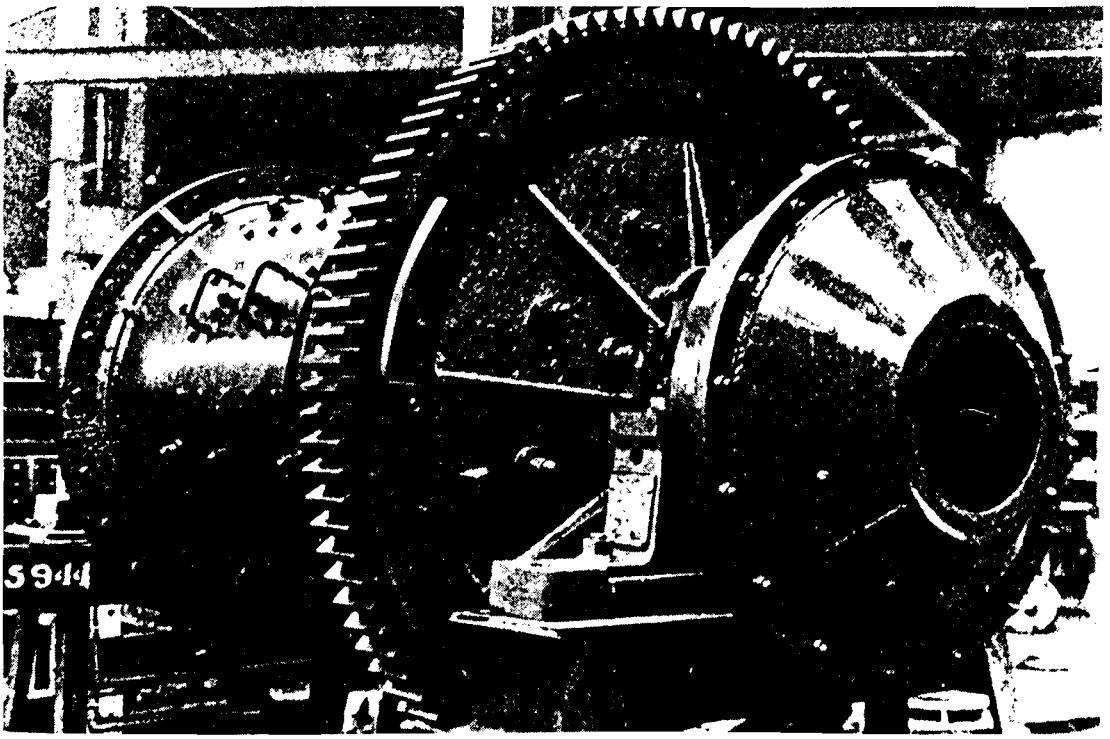

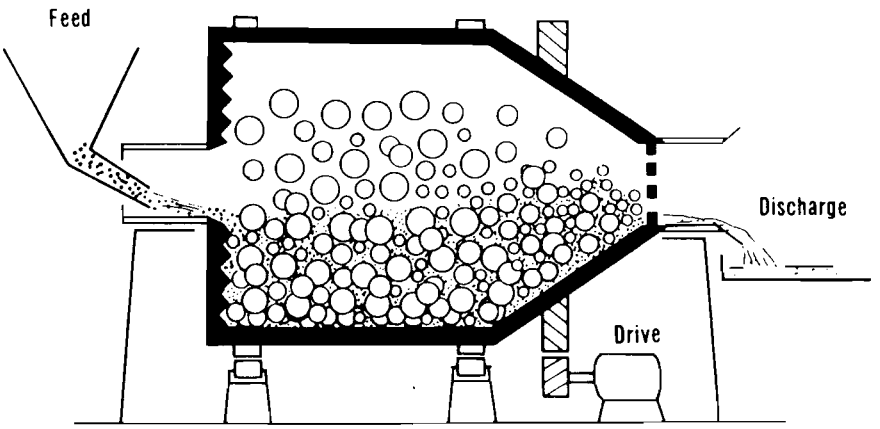

Figure 2-3: Ball Mills and Tube Mills (Wills, 1992; Gilchrist, 1989).

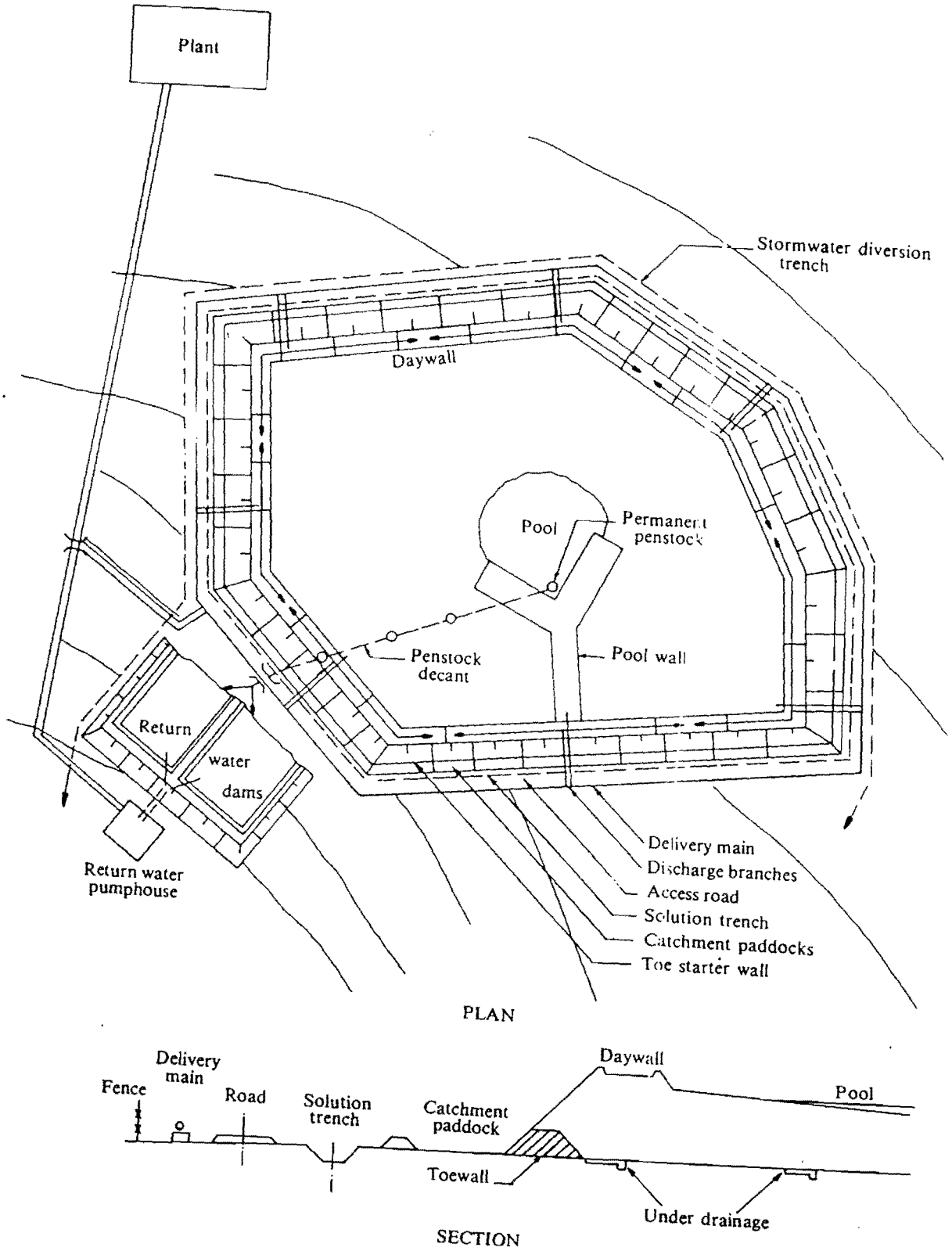

Figure 2-4: Main components of the tailings disposal system (McPhail & Wagner, 1989).

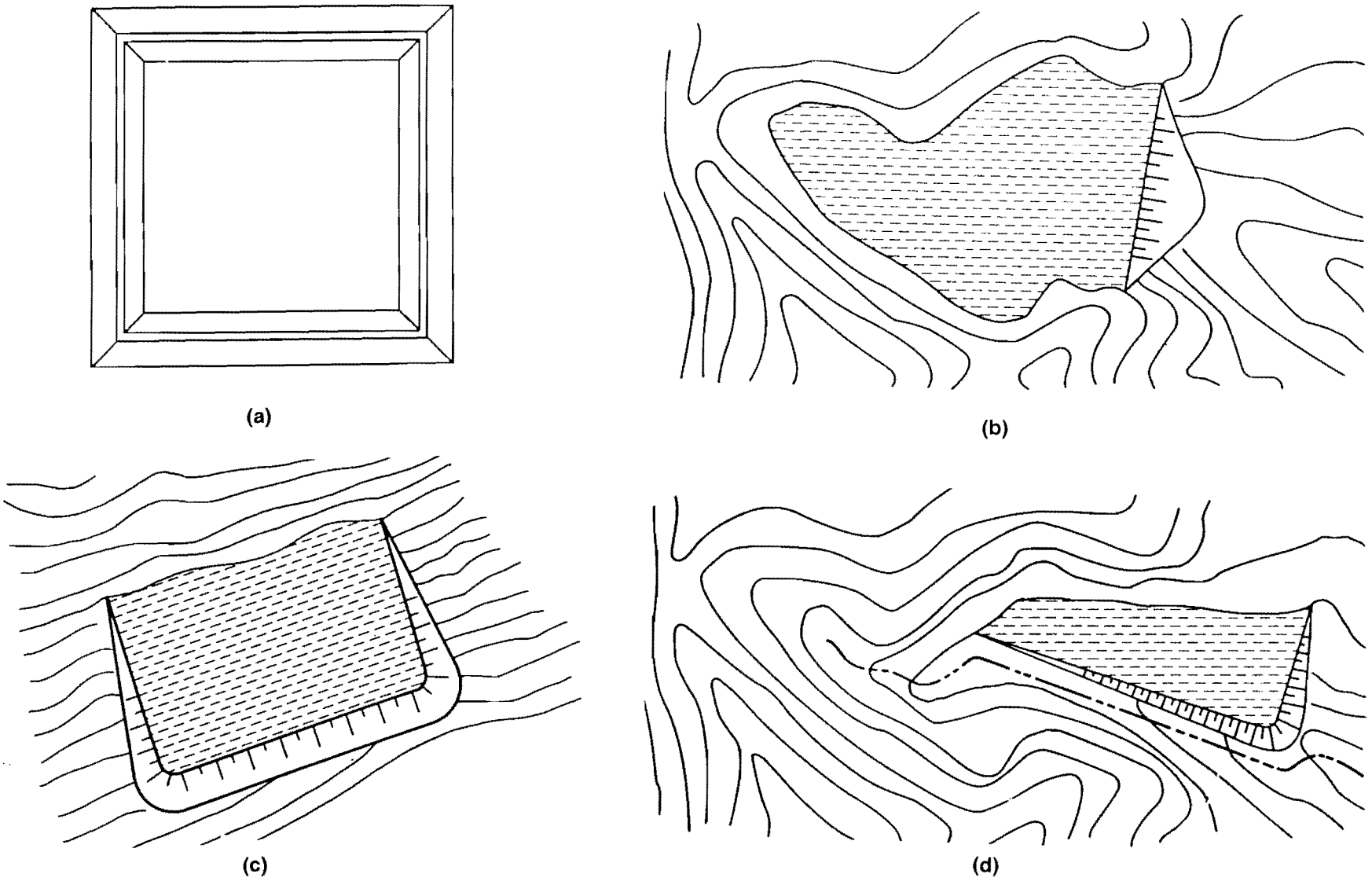

Figure 2-5: Basic impoundment layout designs: (a) ring dyke, (b) cross valley, (c) side-hill and (d) valley bottom or incised (Vick, 1983).

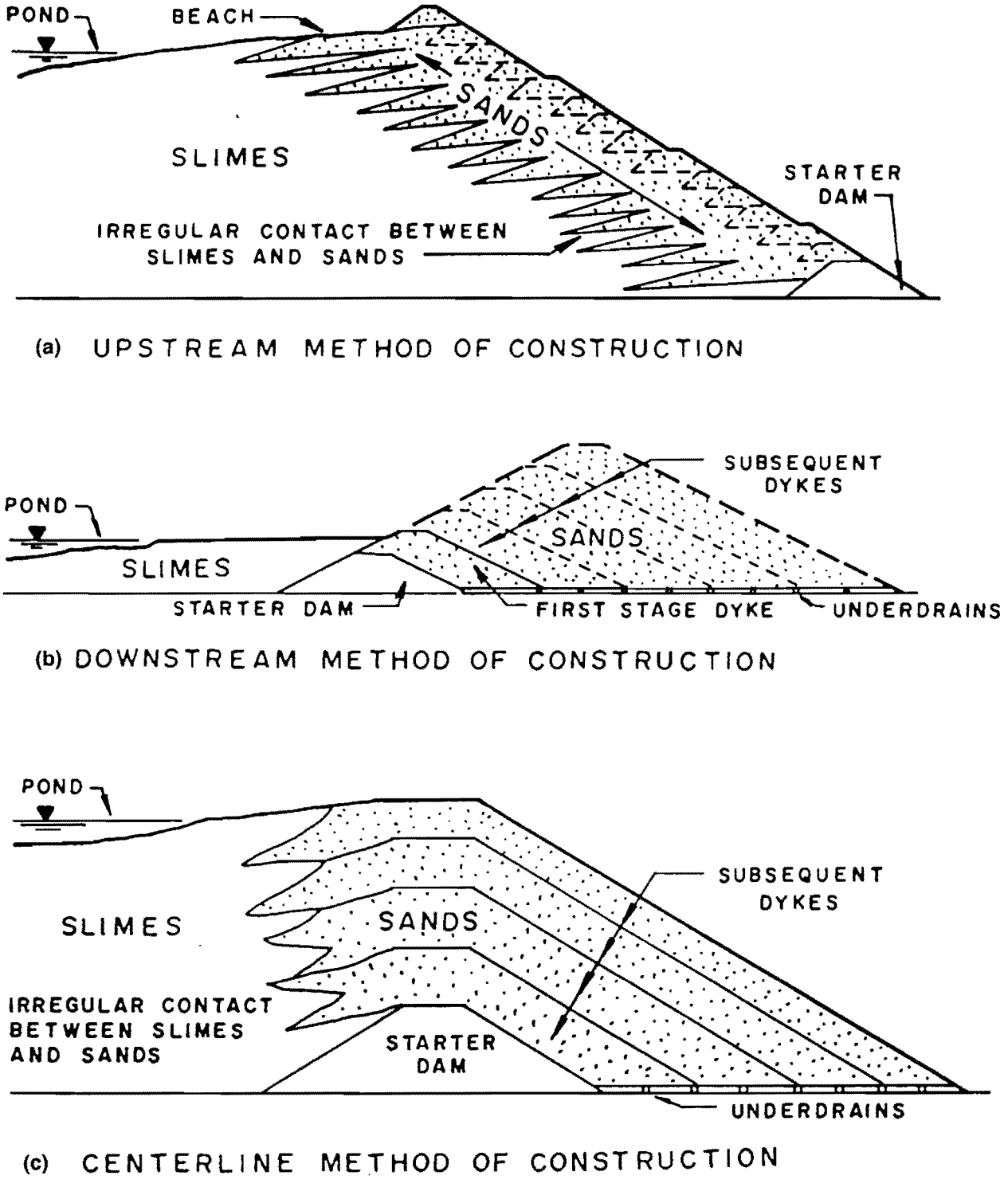

Figure 2-6: Embankment construction methods: (a) Upstream raised embankments, (b) Downstream raised embankments and (c) centreline raised embankments (Mittal & Morgenstern, 1977).

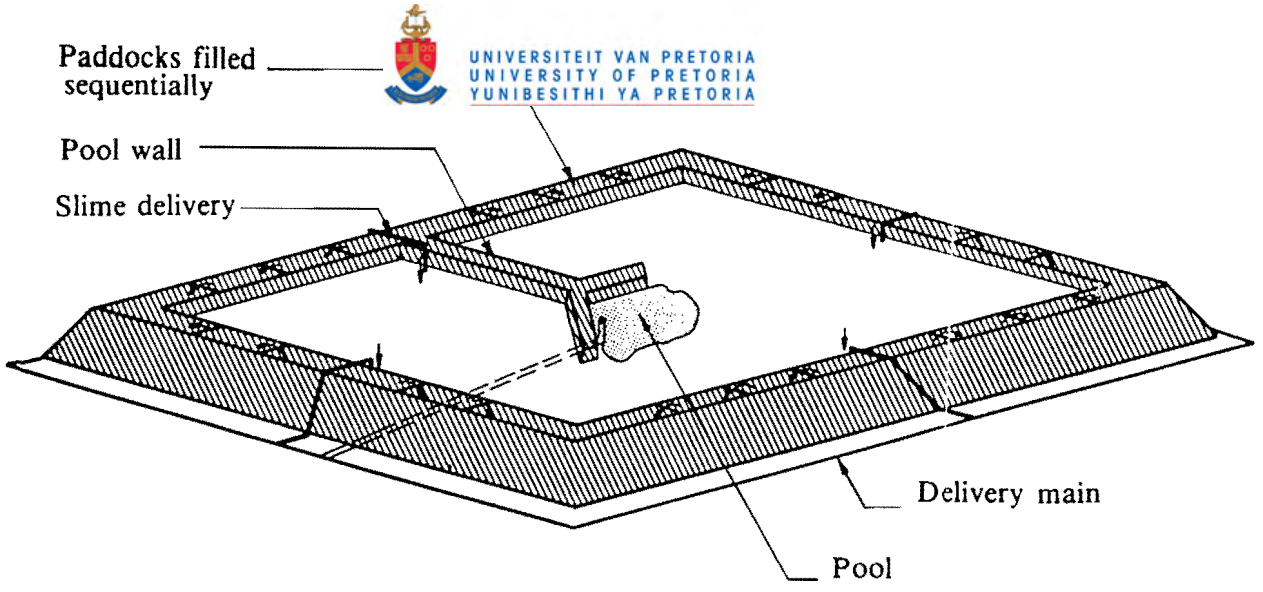

(a) Perspective view

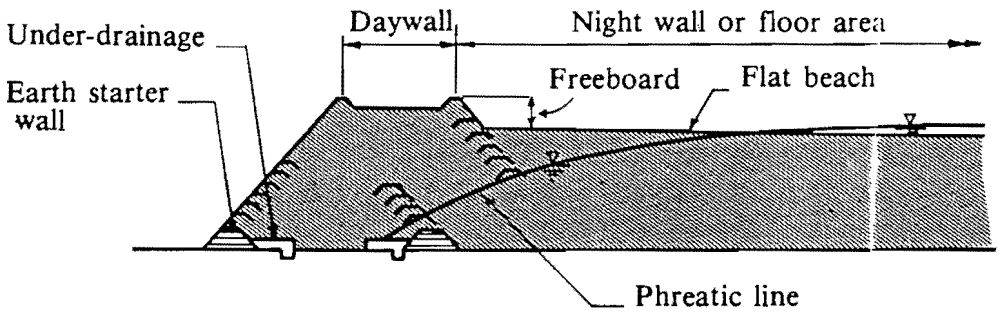

(b) Typical section

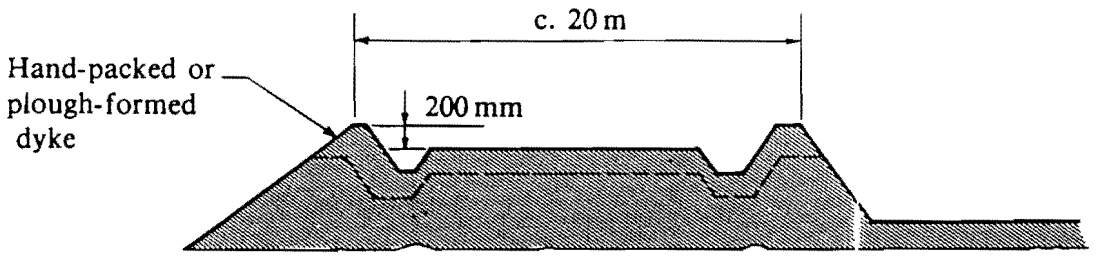

(c) Typical daywall section

Figure 2-7: Semi-dry paddock embankments (McPhail & Wagner, 1989).

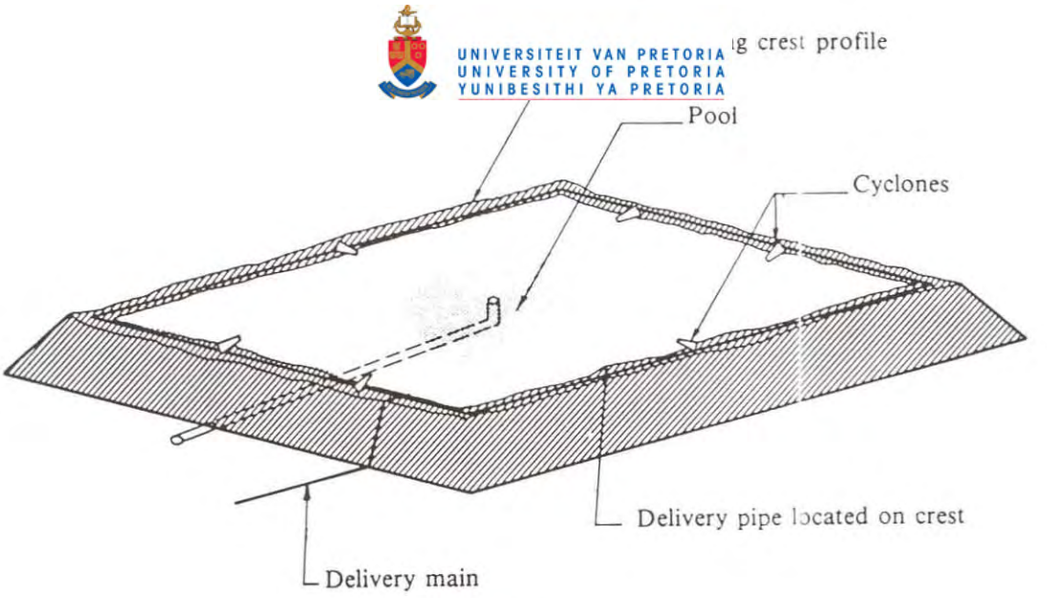

(a) Perspective view

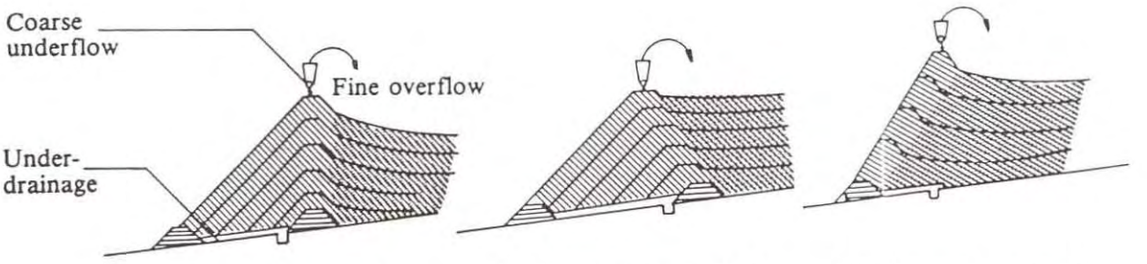

(b) Centreline method (c) Downstream method (d) Upstream method

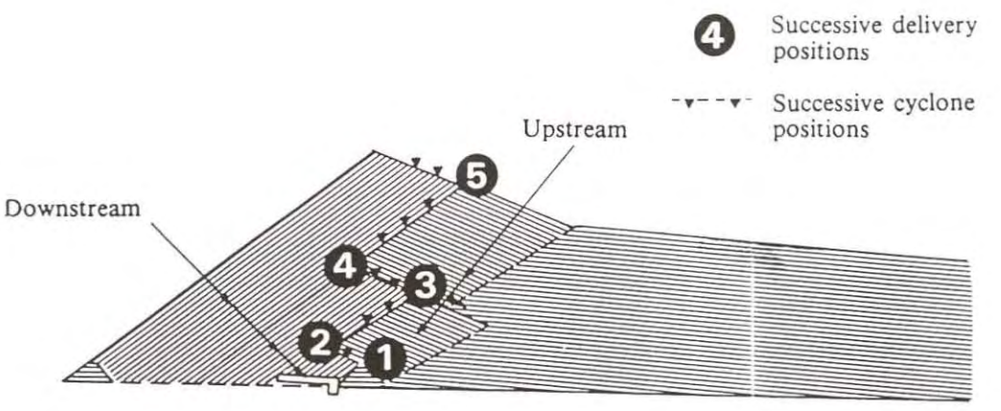

(e) Upstream/downstream method

Figure 2-8: Cyclone constructed embankments (McPhail & Wagner, 1989).

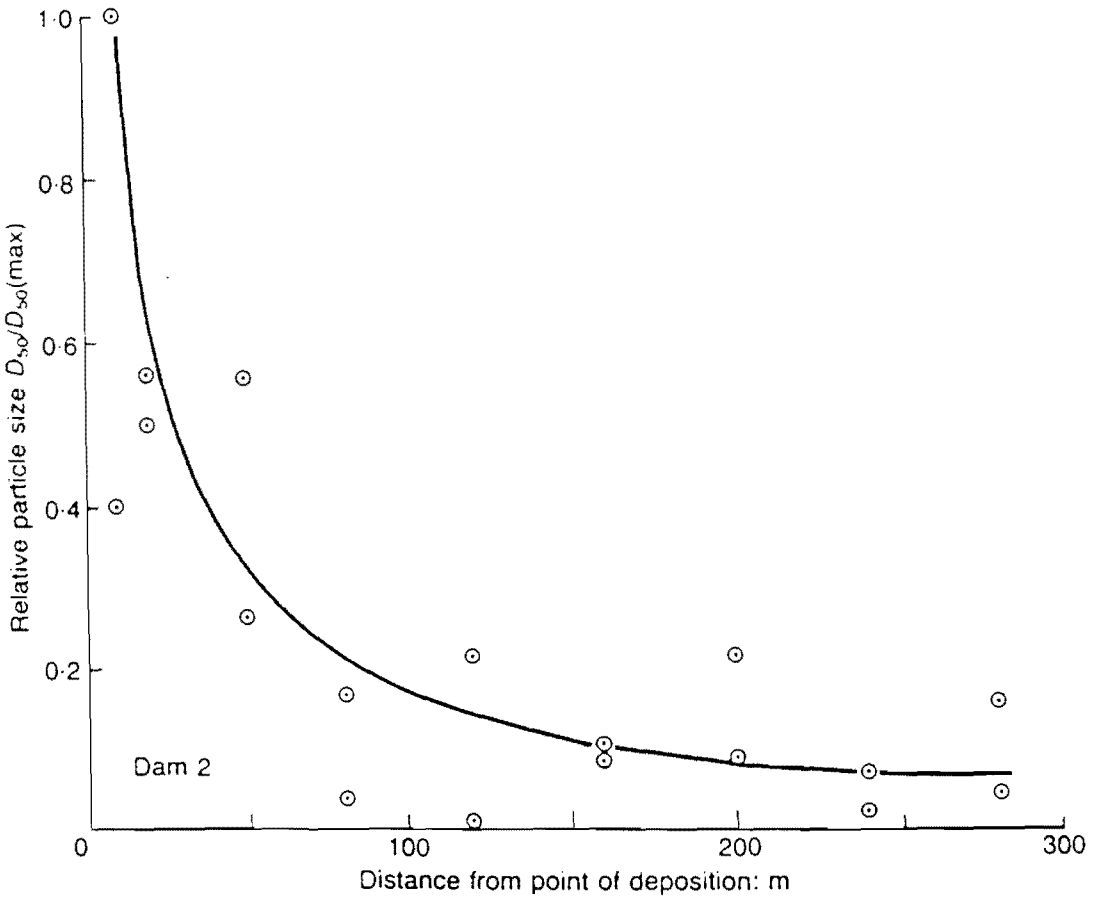

Figure 2-9: Particle size sorting observed on the beach of a diamond tailings dam (Blight & Bentel, 1983).

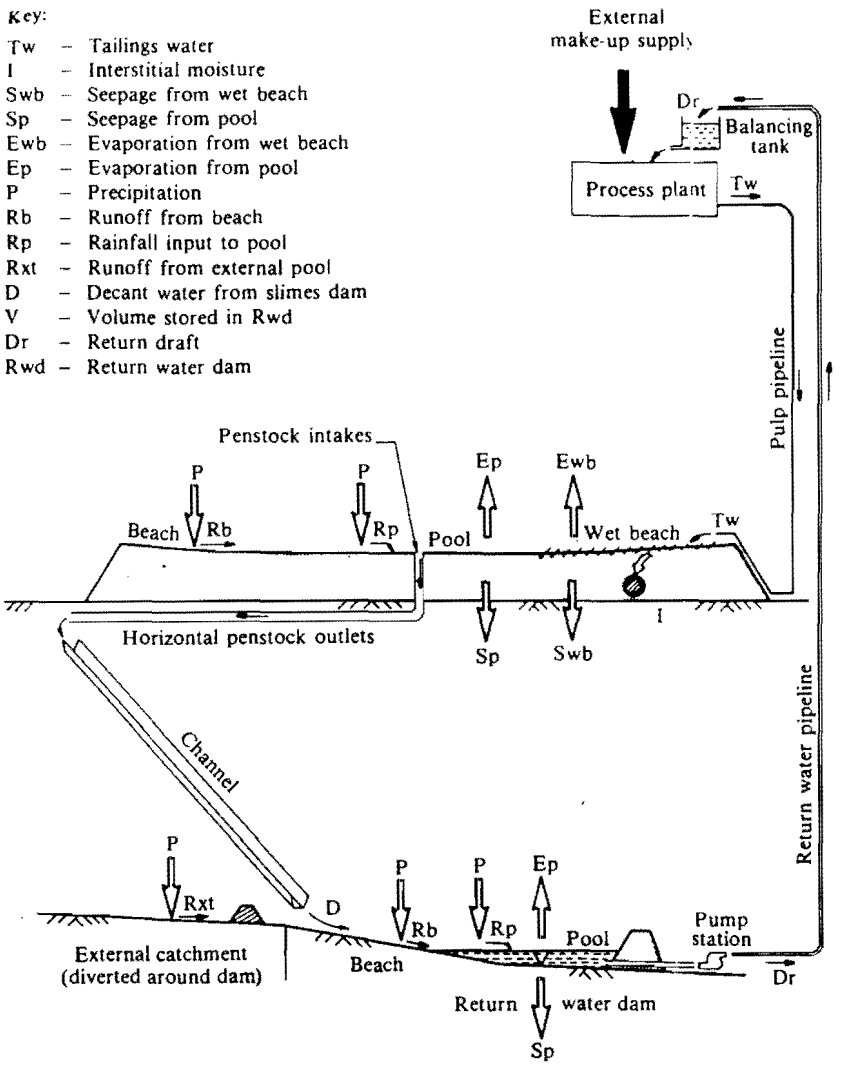

(a)

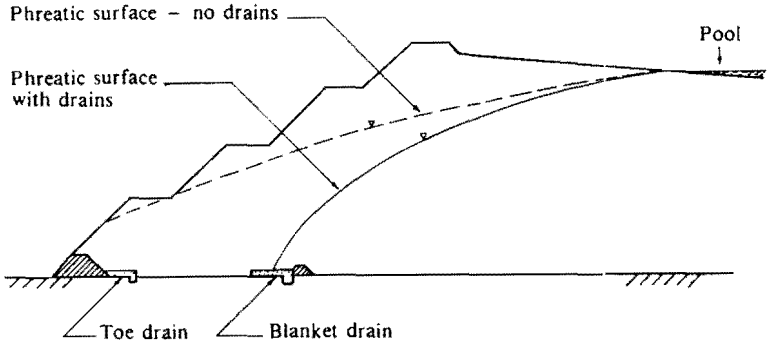

(b)

Figure 2-10: (a) Schematic of phreatic surface control in a typical tailings impoundment, (b) Influence of under wall drains on the position of the phreatic surface (McPhail & Wagner, 1989).

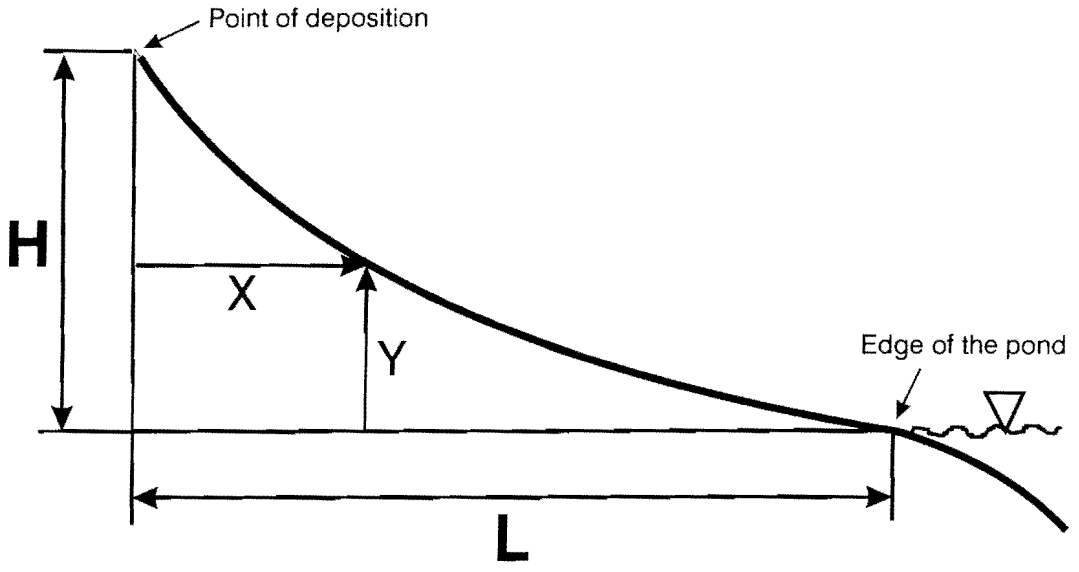

(a)

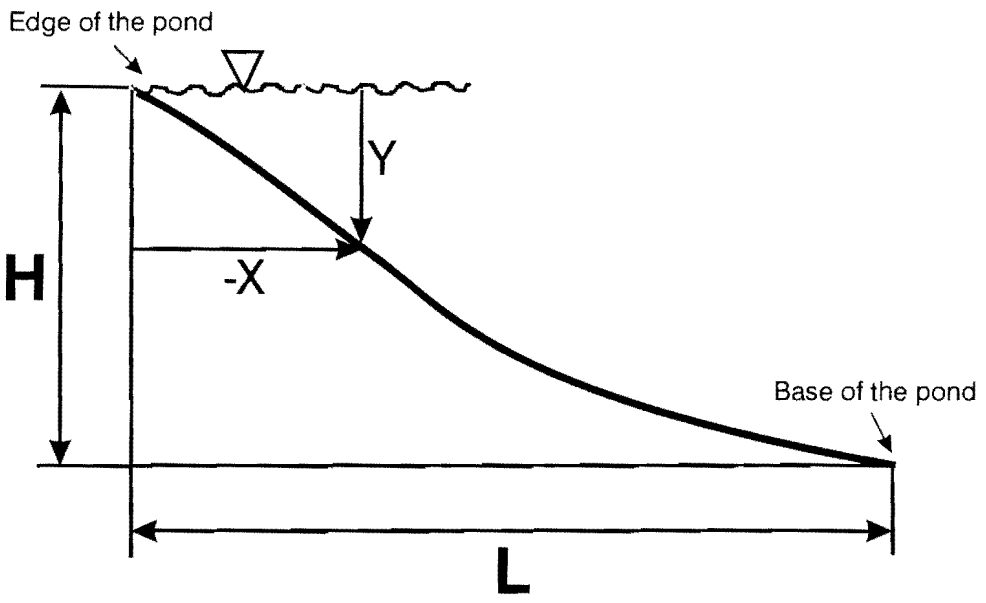

(b)

Figure 2-11: Schematic of the Melent'ev or Master Profile of tailings beaches for (a) sub-aerial deposition and (b) sub-aqueous deposition.

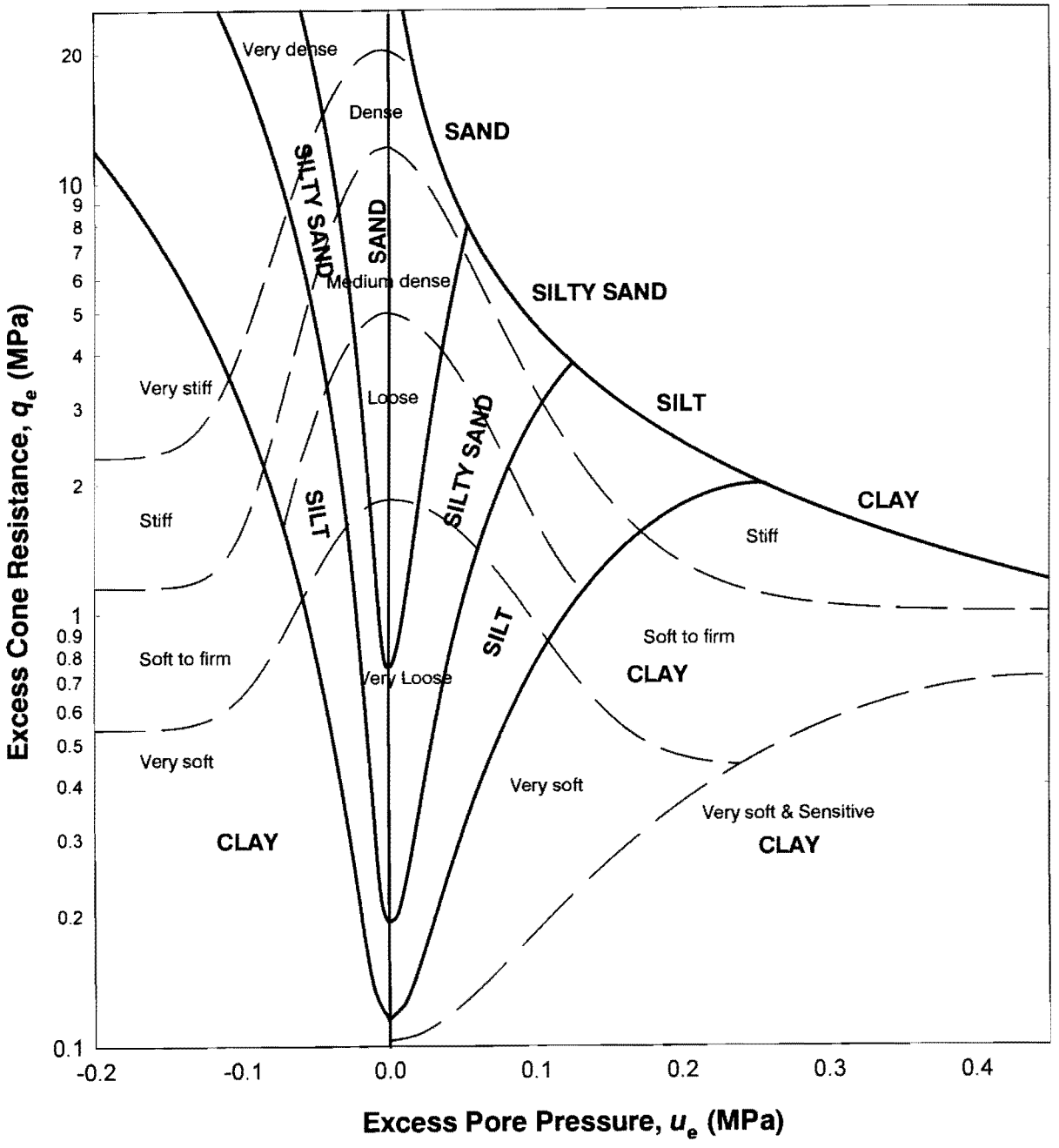

Figure 2-12: The Jones and Rust soil classification chart (Jones et al., 1981), modified by the author to emphasise the classification of soft soils.

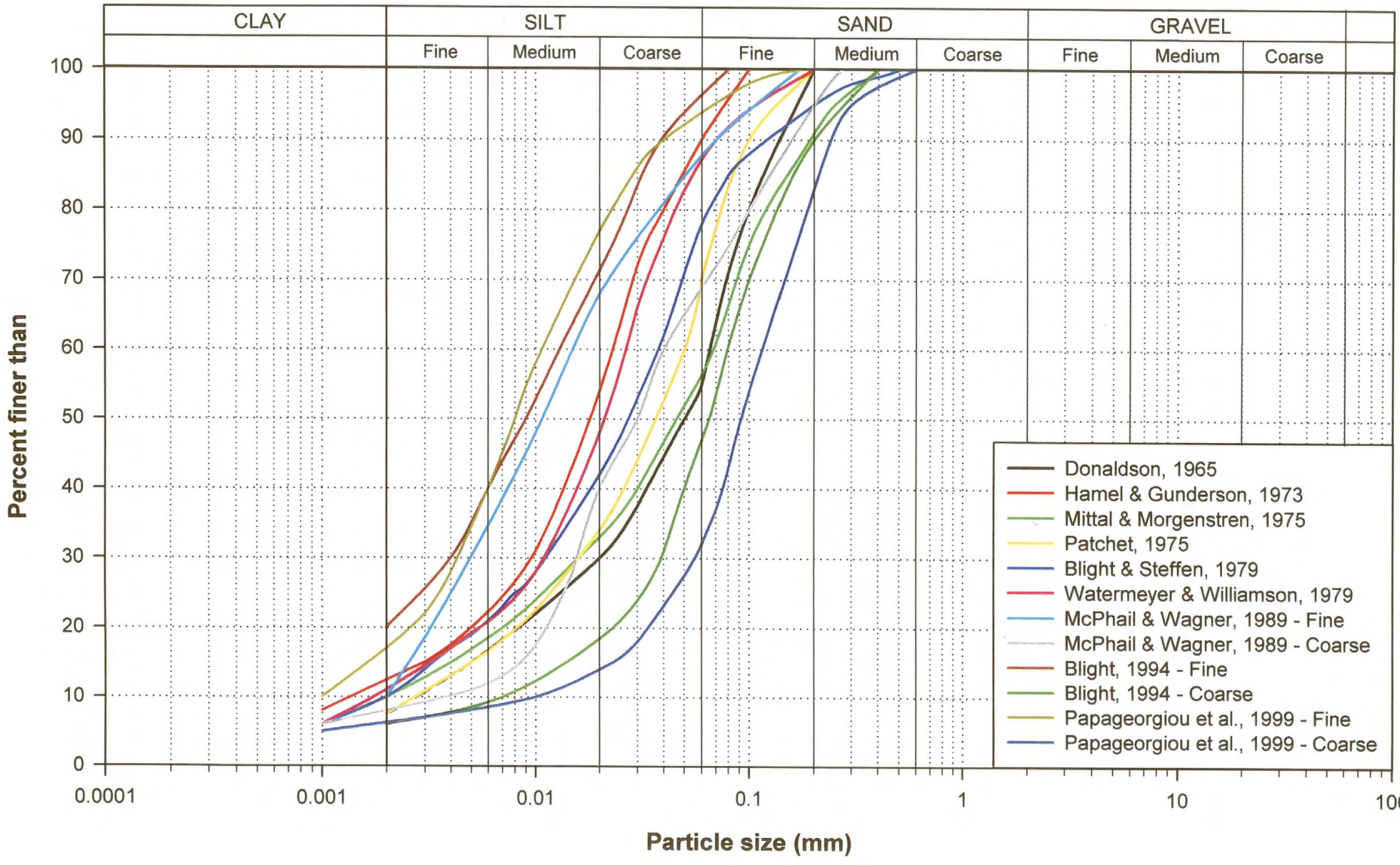

Figure 2-13: Grading curves for gold tailings.

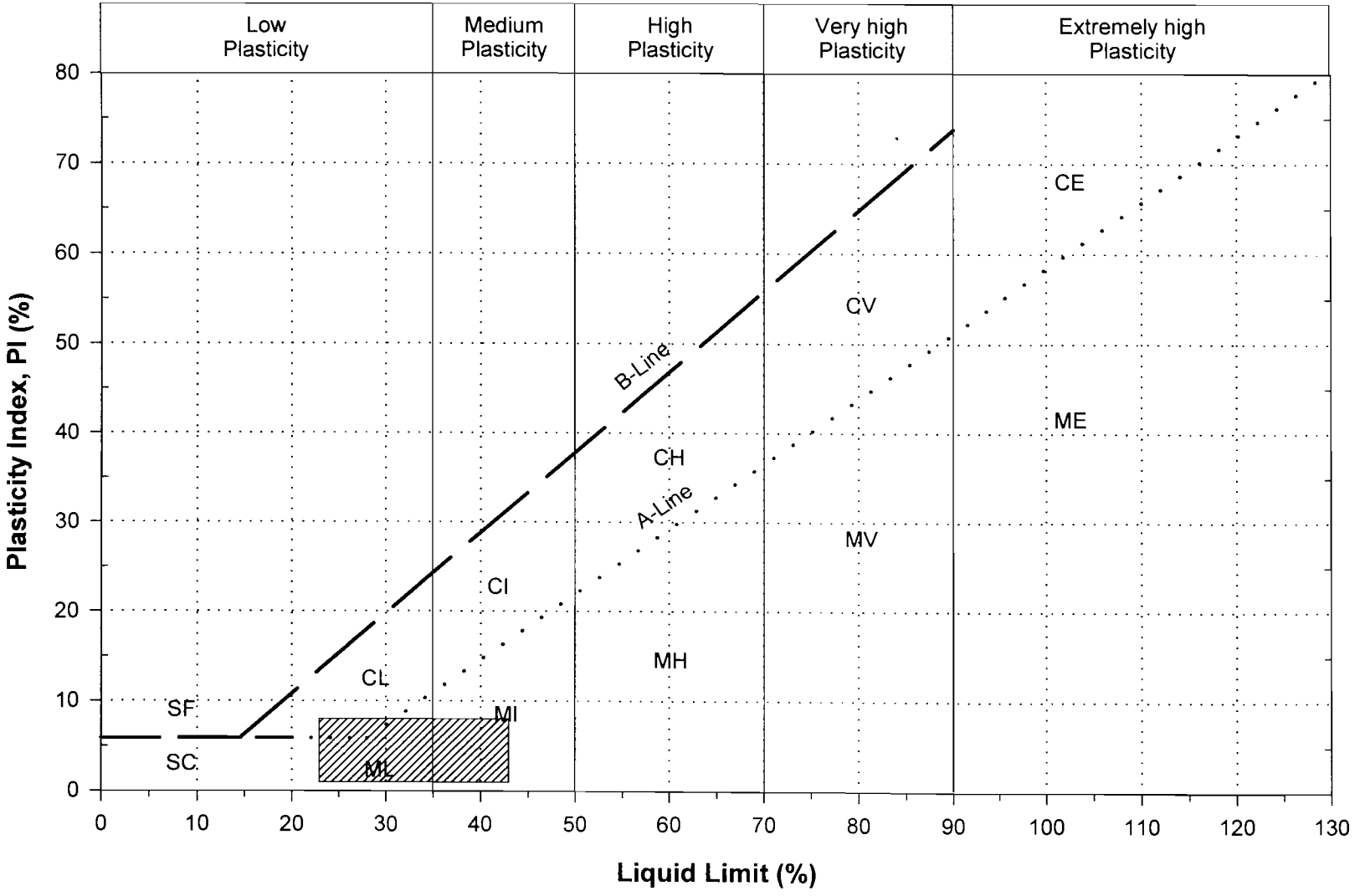

Figure 2-14: Casagrande classification of gold tailings.

CHAPTER 3

EXPERIMENTAL PROGRAM

3.1 INTRODUCTION

Chapter 3 presents the results of a programme of in-situ fields tests, standard laboratory soil tests, as well as electron microscope and x-ray diffraction work on typical South African gold tailings. All fieldwork was done at, and samples collected from, one of South Africa's foremost mining operations, Vaal River Operations in the Northwest Province. Two tailings dams were selected: Pay Dam, the oldest impoundment on the mine and Mizpah the most recent addition. The experimental programme focussed on examining the composition and state of the tailings. To this extent the following aspects have been addressed for the whole tailings mix, as well as assorted fine and coarse layer selections from both dams:

- *Fundamental particle properties:* Mineralogical make-up, features of the distribution of particle sizes as well as characteristics of particle shape and surface texture.
- *Compressibility:* Influence of composition on compressibility characteristics based on reconstituted remoulded laboratory samples.
- *Shear strength:* Influence of material composition and state on the shear strength properties and shear behaviour of tailings. Tests were performed on both reconstituted and undisturbed samples.
- *Undisturbed structure:* Although not a major focus of this study, evidence of structure including fabric and bonding has been explored.

Knowledge of the above not only leads to a better understanding of the in-situ state and expected engineering behaviour of tailings, but also to improved interpretation of site investigation data, especially from the piezocone.

Experimental work was basically limited to material collected from the pond areas of both dams. Special circumstances at these dams, reclamation at Pay Dam and delayed deposition at Mizpah, made it possible to perform field tests and collect samples from areas which are normally not accessible under operating conditions.

Test results are reported in this chapter with little or no additional analysis and interpretation. In the next chapter the data is further analysed, interpreted and discussed with the aim of defining the in-situ composition and state of a typical South African gold tailings.

3.2 SITE

Vaal River Operations, formally Vaal Reefs, is situated on the Vaal River bordering the Northwest Province and the Freestate Province between Potchefstroom and Klerksdorp. The nearest town, Orkney, is practically part of the mine. The mine operates mainly on the Vaal Reef of the Witwatersrand Complex. Vaal River Operations forms part of the Anglo Gold Corporation, which was formed in June 1998 through a merger of the gold operations, mineral rights division and exploration division of the greater Anglo American Corporation and its associated companies. Anglo Gold is the world's largest producer of gold, at 7.1 million ounces a year.

3.2.1 Mizpah

Mizpah, Figure 3-1a, is named after the farm Mizpah on which it is located, and is the latest addition to the mine's impoundment structures. The dam was commissioned in November 1993 and receives approximately 150,000 tons of tailings per month from the No. 8 Gold Plant, after the coarse fraction has been removed for backfill purposes, and from the No. 9 Gold Plant. The reduction plant is currently a conventional crusher and mill plant. After comminution, uranium is extracted by acid leach and gold by a carbon-in-pulp process. Leaching is followed by flotation for gold and pyrite extraction and removal of the coarse fraction from the tailings pulp. A metallurgical report for the month of March 1997 is reproduced in Table 3-1.

The dam is currently (March 2000) 15.3 m high with a planned final height of 60 m. The total surface area is approximately 165 Ha with ten deposition stations around the perimeter. The average rate of rise is 2.4 meters per year or approximately 200 mm per month, with one deposition cycle taking between 9 and 10 days.

At Mizpah a set of piezocone soundings was carried out through a cross-section of the dam on the south side. Five sounding locations were selected: on the daywall, on the upper beach, middle beach, lower beach and in the beach-pond interface (Figure 3-1b). Bulk samples for laboratory testing were also collected from the beach-pond interface. The operators of Mizpah interrupted deposition from the south side of the dam, station number five, and allowed the beach to dry to the extent that off-road vehicles could travel all the way to the beach-pond interface, see Figure 3-2. This allowed field tests to be performed and samples to be collected from the pond area.

Table 3-1: Mine Metallurgical Report for Mizpah Whole Tailings (March 1997)

Parent Rock	72% from Vaal Reef: "C"-reef, Mizpah Reef 28% from Vaal Reef: Zandpan Marker	
Metallurgical Process	*Washing & Screening* *Crushing:* Jaw & Cone Crushers *Milling:* Ball & Tube Mills *Uranium Extraction:* H_2SO_4 & MnO_2 leach; Counter Current Decantation *Gold Extraction:* Neutralising with CaO; CN-leach; Carbon-in-Pulp *Floatation* *Residue Disposal:* Pumped 2km to Mizpah slimes dam	
Relative Density of Pulp	1.250 - 1.350	
Grading	> 150µm < 150µm & > 75µm < 75µm	: 10% : 20% : 70%
Effluent Analysis	Total Dissolved Solids (TDS) Suspended Solids (SS) pH Total Alkalinity Conductivity Magnesium (Mg) Sodium (Na) Chlorine (Cl) Calcium (Ca) Iron (Fe) Manganese (Mn) Potassium (K) Nitrates (NO_3) Phosphates (PO_4)	: 3560 ppm : 30 ppm : 8.4 : 40 : 452 mS/m : 30 ppm : 468 ppm : 310 ppm : 640 ppm : <0.5 ppm : 0.8 ppm : 78 ppm : 42 ppm : <0.5 ppm

3.2.2 Pay Dam

The name of this dam, Figure 3-3a, was derived from the fact that it is located close to the original West Reduction Plant, and that the deposit is of a payable grade. The dam was originally started in the 1940's and has subsequently been expanded by the construction of the large West Complex comprising a number of separate compartments. Following the failure of the northern penstock in the 1970's a floating penstock was installed at this location. Since then an additional 10 m of fill has been deposited. Reclamation by hydro cannon or monitor, Figure 3-4, was started in 1994 and approximately 300,000 tons were reclaimed per month at a grade of 0.4 - 0.5 g/t, at the time of the investigation.

The reclamation of Pay Dam afforded the opportunity of gaining access to relatively undisturbed profiles of the deposit to a depth of at least 5 m. Two locations were selected: the site of the northern penstock, Figure 3-4, and a site in the upper beach, Figure 3-5, on the north side of the impoundment. See Figure 3-3b for the location of these sites.

3.3 IN-SITU PROFILES AND SAMPLING

3.3.1 Introduction

Reclamation with hydro cannon exposed near vertical faces of the pond and beach areas to a depth of approximately 5 m on Pay Dam, Figure 3-4. This rare opportunity was fully exploited for profiling and sampling purposes. Both bulk disturbed samples, and undisturbed block and tube samples were recovered from Pay Dam for the purposes of determining the composition and state by controlled laboratory testing. Great care was taken with sampling and transportation of the undisturbed samples to minimise disturbance.

3.3.2 In-situ Profiles at Pay Dam

Figure 3-6 shows the site of the penstock on Pay Dam as well as a 5 m exposed profile of the material deposited in the pond. Details of this profile, and a similar one in the upper beach area of Pay Dam, can be viewed in Figures 3.9 - 3.30 as summarised in Table 3-2. The profiles were described using the guidelines given by Jennings, Brink and Williams (1973), which are widely accepted in South Africa.

Table 3-2: Details of the in-situ profiles on Pay Dam - May 1999.

Site	Depth Interval	Photo	Profile
Penstock	Full	Figure 3-6	Figure 3-12
	0 - 1 m	Figure 3-7	Figure 3-13
	1 - 2 m	Figure 3-8	Figure 3-14
	2 - 3 m	Figure 3-9	Figure 3-15
	3 - 4 m	Figure 3-10	Figure 3-16
	4 - 5 m	Figure 3-11	Figure 3-17
Upper Beach	Full	Figure 3-18	Figure 3-24
	0 - 1 m	Figure 3-19	Figure 3-25
	1 - 2 m	Figure 3-20	Figure 3-26
	2 - 3 m	Figure 3-21	Figure 3-27
	3 - 4 m	Figure 3-22	Figure 3-28
	4 - 5 m	Figure 3-23	Figure 3-29
	5 - 6 m		Figure 3-30

3.3.3 Sampler Design

A stainless steel tube sampler was specifically designed and manufactured for the purpose of extracting undisturbed 75 mm tube samples for triaxial testing. The design and operation

of this sampler followed closely the guidelines of good quality undisturbed sampling proposed by Clayton et al. (1995) see Table 3-3.

Table 3-3: Good quality sampling practice after Clayton et al. (1995).

Clayton et al. (1995)	Tube Sampler Used
• Minimum sample size should be 5 to 10 times the maximum particle size.	• Inside diameter of the tube sampler is 75 mm, which is 375 times the maximum particle size of 200 μm sampled.
• The size of the sample should represent in-situ structure realistically.	• Samples were extracted from single deposited layers of thickness greater than the sample length and are, therefore, representative of the structure within a single layer.
• Disturbance prior to actual sampling should be minimised.	• Sampling pits were carefully excavated by hand prior to the sampling drive.
• To limit axial compressive and lateral shear distortion the sampler should have: Small area ratio Small cutting edge taper Minimal inside friction Length:Diameter ratio < 6	• For this tube sampler: Area ratio = 2.6% Cutting edge taper = 5° The inner sleeve is highly polished and the cutting edge slightly pinched Length:Diameter ratio = 3
• Disturbance during the driving of the sampler should be minimised.	• The sampler was steadily driven over a short length of approximately 200 mm. • The sampler is fitted with a vent (Klinger valve) to relieve pressure build-up on top of the sample during the driving action.
• Disturbance during extraction of a driven sampler should be minimised.	• The sampler with the sample was carefully dug out and severed from the base to eliminate disturbance caused by base suctions.
• Disturbance due to extrusion and specimen trimming should be minimised.	• Samples were extruded in the direction of the initial drive using a close fitting plunger immediately following extraction.
• Changes to the sample moisture should be limited, including: Moisture loss due to drying Migration of moisture Pore pressure migration Freezing or too high temperatures. Chemical reactions.	• Samples were immediately extruded after sampling and wrapped in three layers of cling film and tinfoil to preserve the moisture. • Samples were tested as soon as possible after sampling to minimise migration of pore water and pore pressures, as well as any chemical reactions. • Samples were only subjected to mild temperatures.
• Transportation disturbance should be minimised.	• Wrapped samples were carefully packed in buckets filled with loose tailings sand for support and transported with cushioning to damp shocks and vibrations.

The resulting sampler, Figure 3-31, consists of two parts, the top-cap and the sampling tube. The top-cap is fitted with a Klinger valve, which serves as a vent when driving the sampler slowly. The top-cap is also lined with a rubber mat to provide a good seal between the two parts when the sampler is extracted with the vent closed. However, for this investigation, the sampler was dug out rather than extracted to minimise disturbance. The sampling tube is 230 mm long with an inside diameter of 75 mm. Except for the top 30 mm the outside diameter is 76 mm resulting in a 1 mm wall thickness over the driving length. The top 30 mm section is 6.5 mm thick to provide support for the studs holding the top-cap. The cutting edge is tapered at 5°. Although no provision was made for inside clearance, the cutting edge is slightly pinched to a diameter of 74.75 mm as a result of the manufacturing process. The whole sampler was machined from a seamless stainless steel tube and was polished on the inside for smoothness.

3.3.4 Disturbed samples

Bulk samples were collected either directly from a discharge pipe, in order to be representative of the whole tailings slurry delivered, or by digging up material representative of a specific layer in the dam profile.

Mizpah:

- March 1997

  A bulk sample of the whole tailings slurry, delivered to the daywall through station number 1 on the north side of the dam, was collected directly from the discharge pipe. The total volume of solids was approximately 0.1 m^3.
- May 1999

  Samples were recovered from the surface of the beach-pond interface on Mizpah close to the piezocone sounding at this location. The top layer, approximately 150 mm deep, consisted of a very fine slurry of slimes, whereas the next layer, of more or less the same depth, consisted of a much coarser material. Bulk samples of both the fine and coarse layers were collected. The sampling location had been under water at the start of the week, on Monday, and by Friday when the samples were collected, the pond water had receded and exposed the site.

Pay Dam:

- May 1999

  Representative bulk samples of coarse and fine material were recovered at the location of the northern penstock in addition to the undisturbed samples noted in Section 3.3.5.

The coarser material was sampled at a depth of 2m, Figure 3-15, and the finer material at a depth of 4.3 m, Figure 3-17.

3.3.5 Undisturbed samples

Pay Dam:

A number of undisturbed block and tube samples were recovered from the site of the exposed penstock on Pay Dam in May 1999. These samples were selected to be representative of the finest and coarsest material deposited at this location.

(a) Block Samples - one per location:

- Coarse: 1.3 m below surface - Figure 3-14.
- Mixed: 1.8 m below surface - Figure 3-14.
- Coarse: 3 m below surface - Figure 3-15 and Figure 3-16.
- Fine: 4.7 m below surface - Figure 3-17.

(b) 75mm Tube Samples - four per location:

- Coarse: 2 m below surface - Figure 3-15.
- Coarse: 3 m below surface - Figure 3-15 and Figure 3-16.
- Fine: 4.3 m below Surface - Figure 3-17.
- Fine: 4.7 m below Surface - Figure 3-17.

Figure 3-32 and Figure 3-33 show the sampling of an undisturbed block at 4.7 m, followed by a tube sample at the same depth.

3.3.6 Summary of samples recovered at Vaal River Operations.

Table 3-4 summarises the particulars of the samples that were collected for the experimental work, together with the codes that will be used to refer to each in this document.

3.4 LABORATORY TESTS

3.4.1 Introduction

The results of a comprehensive range of basic indicator, compressibility and shear strength tests, as well as electron microscope work and x-ray diffraction tests, are presented in this section. In Chapter 4 these results are discussed and used to build a framework for the

Table 3-4: Summary of sample descriptions and codes.

Tailings Dam	Description	Location	Code
Mizpah	**Disturbed: Bulk Samples**		
	Whole Tailings	Daywall delivery station pipe	MPDWT
	Fine	Beach-pond interface, surface	MPDF
	Coarse	Beach-pond interface, just below fines	MPDC
Pay Dam	**Disturbed: Bulk Samples**		
	Coarse	2 m below surface next to penstock	PPNDC
	Fine	4.3 m below surface next to penstock	PPNDF
	Undisturbed: Block samples, 1 per location		
	Coarse	1.3 m below surface next to penstock	PPNBC1
		3 m below surface next to penstock	PPNBC2
	Mixed	1.8 m below surface next to penstock	PPNBM
	Fine	4.3 m below surface next to penstock	PPNBF
	Undisturbed: 75 mm Tube Samples, 4 per location		
	Coarse	2 m below surface next to penstock	PPNTC2
		3 m below surface next to penstock	PPNTC1
	Fine	4.3 m below surface next to penstock	PPNTF2
		4.3 m below surface next to penstock	PPNTF1

mechanical behaviour of gold tailings as a function of the in-situ composition and state. All tests were done according to the British Standard, BS 1377: 1990, *Methods of Testing Soils for Civil Engineering Purposes*, where applicable.

3.4.2 Basic Indicator Tests

Specific gravity, gradings and Atterberg limits were determined using representative specimens selected from the bulk samples recovered from Mizpah and Pay Dam. The words sample and specimen are used in the context of this thesis as:

- *Sample*: A selection of material extracted from an on-site location either in bulk or as an undisturbed portion.
- *Specimen*: A laboratory test specimen, which can be artificially prepared from a bulk sample or consists of a trimmed part of an undisturbed sample.

Specific Gravity

BS test procedure: *Density Bottle (Small Pyknometer - 500 ml) Method* (BS1377: Part 2:1990:8.3).

The density bottle test is not the preferred method in BS 1377. However, the test procedure was modified for the purposes of this study to ensure full saturation of the sample before the final measurements were taken. Regardless, it is still a major improvement over the South African Institute for Transport and Roads Research recommendations, as set out in TMH1 (1986) and widely used in South Africa. The value of the calculated specific gravity is extremely sensitive to small inaccuracies in the measurements, and every precaution was taken to enssure reliable results. If the specimen is not fully saturated a significant error may be incorporated into the final result. In order to aid saturation, de-aired water was added to the dry specimen and subjected to at least five cycles of stirring and vacuum. Following this, the whole pyknometer was placed in a vacuum desiccator and left overnight.

The first tests were performed with both distilled water and tailings water to verify that the use of distilled water does not affect results. All subsequent tests were, therefore, done using only distilled water (Table 3-5).

Table 3-5: Values of Specific Gravity for the tailings tested.

Tailings Dam	Description	Fluid used	G_s (Mg/m^3)			
			Individual Results			Avg.
Mizpah	Whole Tailings	Distilled water	2.736	2.737	2.738	2.74
		Tailings water[1]	2.737	2.738		2.74
	Pond Fines	Distilled water	2.750	2.758	2.752	2.75
	Pond Coarse	Distilled water	2.728	2.726	2.723	2.73
Pay Dam	Penstock Fines	Distilled water	2.742	2.746	2.736	2.74
	Penstock Coarse	Distilled water	2.728	2.739	2.735	2.73

From Table 3-5 it is evident that an average value of G_s = 2.74 should suffice in most cases.

Grading

BS test procedures: *Wet Sieving - Fine Non-Cohesive Soils* (BS1377: Part 2:1990:9.2) and *Hydrometer Analysis* (BS1377: Part 2:1990:9.5).

Pre-treatment procedures performed on the specimens before subjecting them to the sieve and hydrometer tests included:

[1] The density of the tailings bleed water was determined to be 1.0041 g/ml at 25°C

- *Removal of organic material* - Organic matter present, mainly wood fibres in the tailings, can be removed by chemical treatment. This is achieved by the addition of hydrogen peroxide which oxidises the organic matter.
- *Calcareous content test* - Acid treatment of calcareous compounds, although not called for in the BS code might sometimes be appropriate. Calcareous compounds can act as a cementing agent, preventing separation of individual grains. To check for calcareous compounds, a few drops of hydrochloric acid are added to a specimen of the material to be graded. Effervescence indicates the possible presence of these compounds. Hydrochloric acid showed no reaction with the tailings material and acid treatment was therefore not required.
- *Dispersion* - The soil must also be treated with a dispersant and thoroughly agitated to ensure the separation of discrete particles, especially in the silt and clay sized ranges. A stock solution of the standard dispersant, Calgon, was used. Calgon consists of 35 g sodium hexametaphosphate $(NaPO_3)_6$ and 7 g sodium carbonate (Na_2CO_3) to make a one litre solution with distilled water.

Parallel tests were carried out with and without pre-treatment on similar specimens to determine the effect of treatment on the test results. The details of these tests and the resulting gradings are available in Table 3-6 and Table 3-7 and will be discussed in Chapter 4.

Atterberg Limits

BS test procedures: *Liquid Limit - Cone Penetrometer Method* (BS1377: Part 2:1990:4.3), *Plastic Limit* (BS1377: Part 2:1990:5.3), *Shrinkage Limit - Alternative Method* (BS1377: Part 2:1990:6.4) and *Linear Shrinkage* (BS1377: Part 2:1990:6.5).

The cone penetrometer method is preferred over the Casagrande method for determining the liquid limit of tailings for the following reasons:

- It is less operator dependent.
- Results are more repetitive.
- Preparation and handling of the silty tailings is better suited to this method.

The standard plasticity chart or Casagrande A-line chart, Figure 3-45, classifies the tailings used in this study as follows:

- Mizpah whole tailings and pond coarse tailings as well as Pay Dam penstock coarse tailings, classify as low plasticity silt/clay right on the intersection of the A-line and the clay-silt boundary.
- Mizpah pond fines classify as intermediate plasticity silt.
- Pay Dam penstock fines classify as high plasticity silt.

Table 3-6: Grading curves.

Tailings Dam	Description	Figure	Pre-treatment
Mizpah	Whole Tailings	Figure 3-34	Dispersed Non-dispersed Tailings water as solution
	Pond Fines	Figure 3-35	Dispersed Non-dispersed Organic treated & dispersed Organic treated & non-dispersed
	Pond Coarse	Figure 3-36	Dispersed Non-dispersed Organic treated & dispersed Organic treated & non-dispersed
Pay Dam	Penstock Fines	Figure 3-37	Dispersed Non-dispersed Organic treated & dispersed Organic treated & non-dispersed
	Penstock Coarse	Figure 3-38	Dispersed Non-dispersed Organic treated & dispersed Organic treated & non-dispersed
Combined		Figure 3-39	Dispersed

Table 3-7: Summary of the grading properties of dispersed gold tailings from Vaal River Operations.

Tailings Dam	Description	D_{10} (μm)	D_{30} (μm)	D_{60} (μm)	D_{90} (μm)	[2]*CU*	[3]*CC*
Mizpah	Whole Tailings	2.0	10.0	55.0	125.0	27.5	0.91
	Pond Fines	1.5	4.5	16.0	55.0	10.7	0.84
	Pond Coarse	3.0	25.0	75.0	145.0	25.0	2.78
Pay Dam	Penstock Fines	1.7	3.2	8.3	41.0	4.9	0.75
	Penstock Coarse	2.0	9.0	43.0	115.0	21.5	0.94

[2] *CU* = Coefficient of Uniformity = D_{60}/D_{10}

[3] *CC* = Coefficient of Curvature = $D_{30}^2/D_{10}D_{60}$

The results of the Atterberg limit tests are summarised in Table 3-8.

Table 3-8: Atterberg Limits.

Tailings Dam	Description	LL		PL	PI
		(%)	Figure	(%)	(%)
Mizpah	Whole Tailings	29	Figure 3-40	22	7
	Pond Fines	43	Figure 3-41	32	11
	Pond Coarse	28	Figure 3-42	22	6
Pay Dam	Penstock Fines	56	Figure 3-43	39	17
	Penstock Coarse	29	Figure 3-44	22	7

Shrinkage tests on Mizpah whole tailings indicated a shrinkage limit of 22% resulting in a shrinkage ratio of 1.68. Linear shrinkage was measured at 2%.

3.4.3 Microscope and X-ray Analyses

It is often convenient to simplify soils to continuum media for analytical purposes. However, it is the properties at particle level that ultimately control its engineering behaviour. Fundamental particle properties which are of importance include: mineralogy, grain size distribution, shape and surface texture. The basic indicator tests give an indirect measure of the grain size distribution and the importance of the clay minerals in a soil, but give no direct information on any of the fundamental particle properties. For this reason it was decided to undertake a comprehensive study of the tailings under the Scanning Electron Microscope (SEM) and using x-ray analysis techniques. In addition to photo micrographs of the tailings particles and the undisturbed structure, x-ray emission and diffraction analysis provided a means of identifying the elemental and mineral compositions of the material through x-ray spectrography.

Scanning Electron Microscope Images

Vermeulen (2000) gives an overview of the SEM and its basic operation as well as specimen preparation techniques. A concentrated beam of electrons interacts with the specimen in a vacuum. By detecting back-scattered incident electrons or secondary electrons liberated from the specimen surface an image is formed representing the object. This image appears naturally illuminated by light and shadow to the human eye, and is readily interpreted. However, image quality on non-conductive specimens, such as tailings, suffers from charge

build-up on the surface of the specimen. To improve image quality the specimen may be coated with a thin coating of conductive material (gold, carbon, etc.), to eliminate charge build-up and interference with the electron imaging system. In this study the tailings specimens were sputter-coated with a very thin gold film for SEM imaging purposes.

Mizpah whole tailings were mainly used to study the fundamental properties of the particles throughout the size ranges. Specimens were selected from the fractions separated by wet sieving and from the hydrometer sedimentation cylinder. The level of the sediment in the cylinder was marked following each timed interval for reading the hydrometer. On completion of the test these layers were then carefully extracted and separated to provide specimens for the SEM work. The material subjected to the grading analysis had been pre-treated with standard dispersant and should represent the composition of the material in a segregated state. In addition to the whole tailings, undispersed specimens of Mizpah and Pay Dam fine and coarse samples were also imaged for comparison.

Undisturbed specimens, trimmed from the block samples collected from Pay Dam, were used to study the structure of the material in an undisturbed state. These specimens were dried in an oven at a maximum temperature of 35°C to simulate conditions which the material might have been subjected to during cycles of drying. For SEM work on fragile biological samples specialised techniques of flash freezing and freeze drying may be employed to preserve the undisturbed structure of the biological tissue. These techniques may be adapted for soil mechanics purposes, where weak bonding and fragile structure may be destroyed in drying the specimen. These methods are time consuming and highly specialised.

Specimens were mounted on the microscope stage using conductive double-sided carbon tape, which appears as a dark smooth background with regularly spaced pores. To further ensure conductivity of the otherwise non-conductive tailings particles, a thin coating of gold was applied by the sputter method. Five coatings, lasting 30 seconds each, were applied to minimise heating of the specimen. During the imaging process the beam of electrons was accelerated using a voltage of 15 kV in a relatively low vacuum of 10^{-4} torr. An image of the specimen surface was formed using a scintillator detector sensitive to low energy secondary electrons. The detector produces light when bombarded by accelerated electrons of a specific energy, and thus is able to differentiate between high energy back-scattered electrons and lower energy secondary electrons. Secondary electrons give a high definition of surface features as they can only escape from very near to the specimen surface.

SEM micrographs of the tailings considered in this study are catalogued in Table 3-9.

Table 3-9: Scanning Electron Micrographs.

Tailings Dam	Description		Figure
Mizpah	Whole Tailings	Dispersed and graded	Figure 3-46 to Figure 3-61
	Pond Fines	Undispersed, bulk	Figure 3-62
	Pond Coarse	Undispersed, bulk	Figure 3-63
Pay Dam	Penstock Fines	Undispersed, bulk	Figure 3-64
		Undisturbed	Figure 3-65
	Penstock Coarse	Undispersed, bulk	Figure 3-66
		Undisturbed	Figure 3-67

Energy Dispersive X-ray Spectrometry

As part of the SEM imaging process, energy dispersive x-ray spectrometry (EDS) may be performed for a qualitative and quantitative spectral analysis of elemental composition. One of the interactions of the incident electron beam with the specimen is the emission of characteristic x-rays as a result of transitions between energy levels in atoms ionised by the bombarding electrons. Elements are then identified by their characteristic spectrum lines, the amplitudes of which give an indication of the concentration. EDS is essentially a spot measurement, which can be applied to a single tailings particle. Spatial resolution, representing the smallest particle that can be analysed, is limited to about 1 μm due spreading of the electron beam within the specimen.

The specimens used for SEM imaging were also subjected to selective EDS analyses. The acceleration voltage was increased to 20 kV during spectrometry to comply with the calibration of the analytical system, which uses a silicon/lithium solid state detector. A detection time of 100 seconds was allowed for each reading resulting in approximately 20 seconds dead time in the detector, well within acceptable limits. It should be noted that all EDS spectra show a strong peak for the element gold due to the thin gold coating.

From a total of more than 100 EDS analyses that were performed on material from both Mizpah and Pay Dam, only four distinct spectra could be identified, see Table 3-10 and Figure 3-68. These are representative of:

- Smooth surfaced tailings sand: 93% silicon.
- Rough surfaced tailings sand: 64% silicon, 21% aluminium and 10% potassium.
- Flaky slimes: 75% silicon, 12% aluminium and 4% each of potassium and iron.
- Flocs of flaky slimes: 57% silicon, 17% aluminium, 13% iron and 6% potassium.

Table 3-10: Elemental composition of tailings particles by EDS.

Element	Percentages Detected														
	Smooth surfaced Sands			Rough surfaced Sands			Flaky Slimes			Slime flocs			Hydrometer Precipitate		
	Maximum	Average	Minimum	Maximum	Average	Minimum	Maximum	Average	Minimum	Maximum	Average	Minimum	Maximum	Average	Minimum
Na	1	0	1	1	0	1	2	1	1	1	1	1		43	
Mg	0	0	0	0	0	0	1	0	1	7	2	1		0	
Al	4	2	1	29	21	11	25	12	1	24	17	7		0	
Si	96	93	89	82	64	49	97	75	48	75	57	36		1	
P	0	0	0	0	0	0	3	1	1	1	0	1		15	
S	1	0	1	1	0	1	3	1	1	0	0	0		31	
K	2	1	1	17	10	1	8	4	1	11	6	1		0	
Ca	1	0	1	0	0	0	4	1	1	2	1	1		4	
Fe	1	0	1	4	2	1	7	4	1	34	13	3		1	
Other	3	2	1	4	2	1	3	2	1	4	3	2		4	

Table 3-10 and Figure 3-68 also show the results of EDS analyses on the precipitate that remains after drying the clear solution floating on top of the sediment in a hydrometer sedimentation test. It should be noted that the chemistry of this solution must have been influenced by the addition of a dispersing agent. The results indicate 43% sodium, 31% sulphur, 15% phosphor and 4% calcium.

X-ray Diffraction Analyses

Powder X-ray Diffraction (XRD) is one of the primary techniques used by mineralogists and solid state chemists to examine the physico-chemical make-up of unknown solids. According to the XRD technique a powdered sample is placed in a holder, and illuminated with x-rays of a fixed wave-length. The intensity of the reflected radiation is then recorded using a goniometer. The results are represented in a collection of single-phase X-ray powder diffraction patterns or spectra. Each crystalline solid or mineral has its unique characteristic X-ray powder pattern, which may be used as a "fingerprint" for its identification.

XRD tests were not performed by the author, but were done by the University of Pretoria, Mineral Sciences Division. Two series of tests were performed, the first on untreated specimens of each of the five different tailings samples studied, and the second on five

selected size fractions of the Mizpah whole tailings: 150 μm, 75 μm, 10 μm, 2μm and 1μm. The Mizpah whole tailings fractions were pre-treated with dispersant, subjected to sieve and hydrometer tests and subsequently dried. The results are summarised in Table 3-11.

Table 3-11: XRD results on Mizpah Whole Tailings.

Mizpah and Pay Dam Tailings					
Tailings Dam	**Description**	**Figure**			
Mizpah	Whole tailings	Figure 3-69			
	Pond fine tailings	Figure 3-70			
	Pond coarse tailings	Figure 3-71			
Pay Dam	Penstock fine tailings	Figure 3-72			
	Penstock coarse tailings	Figure 3-73			
Mizpah Whole Tailings: Separate Fractions					
Mineral	**150 μm**	**75 μm**	**10 μm**	**2 μm**	**1 μm**
	Figure 3-74	Figure 3-75	Figure 3-76	Figure 3-77	Figure 3-78

3.4.4 Densities

In-situ Densities:

Table 3-12, summarises the in-situ densities measured on two undisturbed tube samples recovered from the Pay Dam penstock area for this purpose. Table 3-13 gives additional information from measurements on the undisturbed tube samples that were used for triaxial testing in Section 3.4.5 and 3.4.6.

Table 3-12: In-situ densities at Pay Dam penstock from undisturbed tube samples.

Description		**PPNTF2**	**PPNTC2**
		Fine	**Coarse**
Depth below surface	m	4.3	2.0
Moisture content	%	53.9	19.6
Degree of saturation	%	99	61
Bulk density, ρ_{nat}	kg/m^3	1694	1742
Dry density, ρ_{dry}	kg/m^3	1101	1457
Void ratio		1.49	0.87
In-situ vertical stress, σ_v	kPa	71	34
Pore pressure from CPTU dissipation tests	kPa	-4	1
Vertical effective stress, σ'_v	kPa	75	33

Table 3-13: In-situ stresses and densities at Pay Dam penstock from triaxial specimens.

Description		PPNTF1			PPNTC1		
		Fine			Coarse		
Depth below surface	m	4.3			3.0		
Moisture content	%	52.7	56.6	50.4	18.2	20.5	17.2
Degree of saturation	%	100	100	98	64	69	62
Bulk density, ρ_{nat}	kg/m^3	1750	1743	1700	1819	1812	1821
Dry density, ρ_{dry}	kg/m^3	1146	1100	1138	1539	1503	1553
Void ratio		1.39	1.46	1.41	0.77	0.81	0.76
In-situ vertical stress, σ_v	kPa	71			51		
Pore pressure from CPTU	kPa	-4			-4		
Vertical effective stress, σ'_v	kPa	75			55		
Pre-consolidation pressure σ'_{vmax}	kPa	150			100		
Overconsolidation ratio, (R_o)		2			2		

Compaction Densities of Mizpah Whole Tailings.

BS test procedures: *"Light" Compaction Test (2.5 kg hammer method)* (BS1377: Part 4:1990:3.3), *"Heavy" Compaction Test (4.5 kg hammer method)* (BS1377: Part 4:1990:3.5) and *Maximum Density - Sands* (BS1377: Part 4:1990:4.2).

All compaction tests were performed on Mizpah whole tailings in an ASTM 4" mould with internal volume of 944 cm^3 and applied energies as set out in Table 3-14. These tests were done to investigate the possibility of preparing reconstituted triaxial test specimens using standard compaction methods.

Table 3-14: Compaction energies applied to Mizpah Whole Tailings.

Compaction	Hammer (*kg*)	Fall Height (*mm*)	Layers	Blows / Layer	Energy (*kJ/m^3*)
BS Light	2.49	305	3	25	592
2 x BS Light	2.49	305	3	46	1089
BS Heavy	4.54	457	5	25	2695
2 x BS Heavy	4.54	457	5	46	4959
Maximum	4.54	457	5	75	8085

Dry density and optimum moisture content plots are shown at the various compaction energies in Figure 3-79 and summarised in Table 3-15.

Table 3-15: Density tests on Mizpah whole tailings.

Compaction densities: Mizpah whole tailings			
	Maximum Dry Density (kg/m^3)	**Bulk Density (kg/m^3)**	**Opt. Moisture Content (%)**
BS Light	1710	2010	17
2 x BS Light	1745	2030	16
BS Heavy	1850	2090	14
2 x BS Heavy	1905	2150	13
Limiting densities: Mizpah whole tailings			
	Dry Density (kg/m^3)	**Void Ratio**	**Moisture Content (%)**
Minimum	867	2.156	80
Maximum	1945	0.407	12

From the densities listed in Table 3-15 it was concluded that standard compaction techniques could not be used to prepare reconstituted laboratory specimens for triaxial testing. The compaction dry densities were far too high compared with typical values measured in-situ, which range from 1000 to a maximum of 1500 kg/m^3. It was, therefore, decided to use sedimentation techniques to prepare specimens artificially for compression and shear testing. The low density states attained following sedimentation (minimum density of approximately 900 kg/m^3 in Table 3-15) are more representative of in-situ densities and of the processes by which deposits are formed on a tailings impoundment.

3.4.5 Compression and Consolidation

Isotropic Compression and Consolidation

Isotropic compression and consolidation tests were performed in 75 mm triaxial cells according to the guidelines given in BS1377:1990 Parts 5 and 6. Special consideration was given to the techniques of specimen preparation to simulate the field or in-situ conditions as closely as possible. To this end the following methods were employed:

(a) 75 mm undisturbed specimens from tube samples:

Very little preparation was needed, resulting in the minimum time of exposure and moisture loss due to drying.

- Samples were extruded in the field and wrapped with successive layers of cling film and tin foil before being transported to the laboratory.
- After unwrapping the samples in the laboratory, triaxial specimens were carefully trimmed to the required length, measured and placed into the cell, ready for testing.

(b) Reconstituted remoulded slurry specimens:

Specimens were prepared in the form of a slurry by sedimentation and consolidation of tailings from a aqueous solution. These specimens should be representative of in-situ states.

- A specimen was selected from a bulk sample of tailings at the in-situ moisture content.
- This material was then mixed with tap water to form an aqueous solution at a moisture content of at least 3 times the liquid limit of the tailings.
- The solution was placed under vacuum to get rid of as much air as possible and then allowed to settle and consolidate for 48 hours.
- After sedimentation the bleed water was decanted and the sample thoroughly mixed (remoulded). Typical moisture content and densities at this stage are summarised in Table 3-16. These values correspond to the minimum densities attainable by sedimentation methods, see Table 3-15.

Table 3-16: Moisture content and void ratio after sedimentation.

Tailings Dam	Description	*w* (%)	*e*	ρ_d (kN/m^3)
Mizpah	Whole Tailings	65	1.8	979
	Pond Fines	90	2.5	786
	Pond Coarse	50	1.4	1138
Pay Dam	Penstock Fines	135	3.7	583
	Penstock Coarse	75	2.1	881

The void ratios are less than half those predicted by Carrier et al. (1983), Section 2.5.2, for the end of sedimentation start of consolidation phase. It is likely that the samples have undergone some self-weight consolidation in the 48 hour rest period in addition to sedimentation.

- The triaxial cell was prepared by cleaning, flushing, etc. and fitted with a 75 mm split mould, membrane, bottom porous stone and base filter paper. Side drains were not used.
- The mould was filled with de-aired water to just above the level of the bottom porous stone, followed by the remoulded tailings slurry to fill the mould.

- A slight suction (5 kPa) was then applied through the bottom porous stone to induce a small effective stress in the specimen. This provides enough strength in the specimen to allow the cell to be assembled without causing liquefaction.
- Under these conditions the specimen was allowed to consolidate. More slurry had to be added in increments until the mould was filled to the intended height at the applied suction.
- At no stage was the specimen allowed to dry or de-saturate by maintaining a free water level over the specimen.
- The top-cap, porous stone and top filter paper were then placed and secured and the split mould removed.
- Before the cell was assembled the specimen was measured through the membrane taking account of membrane thickness, etc.
- After the cell had been filled with water the suction was removed and the B-value checked under a "bedding" pressure of 5 kPa. At this stage the moisture content and density had reduced by approximately one half of the initial values as indicated in Table 3-17.

Table 3-17: Moisture content and void ratio before testing.

Tailings Dam	Description	w (%)	e	ρ_d (kN/m^3)
Mizpah	Whole Tailings	35	0.9	1442
	Pond Fines	45	1.2	1250
	Pond Coarse	25	0.7	1606
Pay Dam	Penstock Fines	60	1.7	1015
	Penstock Coarse	30	0.8	1517

The void ratios of the reconstituted remoulded Pay Dam fine and coarse specimens were in reasonable agreement with the void ratios of the undisturbed samples collected from the dam. For the fine tailings the void ratios were: 1.5 in-situ and 1.7 reconstituted in the laboratory; for the coarse tailings: 0.9 in-situ and 0.8 reconstituted. The lower in-situ values are probably the result of light overconsolidation following desiccation, as well as the slightly higher effective stress level of approximately 30 to 70 kPa in-situ. From these comparisons it was concluded that the method of preparing the reconstituted specimens from a slurry resulted in fine and coarse specimens representative of in-situ densities.

Procedures adopted for carrying out consolidation stages in the triaxial apparatus were:

(a) Once the triaxial cell had been assembled, the back pressure was gradually increased to 300 kPa, while the cell pressure was maintained at 5 kPa above the back pressure. During this procedure the specimen was therefore subject to a 5 kPa effective isotropic consolidation pressure. With reconstituted specimens a B-value of 0.98 to 1.00 could easily be attained, but with the undisturbed tube samples, especially the coarser drier material, a B-value of 0.95 or more was considered sufficient.

(b) Saturation was followed by isotropic consolidation stages at 12.5, 25, 50, 100, 200 and 400 kPa effective stress. Pore pressures were measured at the base of the specimen and drainage allowed through the top-cap without the use of side drains. The volume of pore water draining to or from a specimen, against the back pressure, was measured using a volumetric burette marked in increments of 0.1 ml. Both filter paper and a porous stones were used to cap the specimen and prevent material loss and clogging of the drainage system during consolidation.

The above procedures resulted in an isotropic stress condition during consolidation, but with one-dimensional upwards flow of pore water.

Figure 3-80 shows the combined results of the triaxial compression tests. The results of the individual compression and consolidation tests on reconstituted and undisturbed specimens are referenced in Table 3-18.

Table 3-18: Results of isotropic compression tests.

Tailings Dam	Description	Preparation	Figures
Mizpah	Whole Tailings	Slurry	Figure 3-81 to Figure 3-84
	Pond Fine & Coarse	Slurry	Figure 3-85 to Figure 3-91
Pay Dam	Penstock Fine & Coarse	Slurry	Figure 3-92 to Figure 3-98
	Penstock Fine & Coarse	Undisturbed	Figure 3-99 to Figure 3-105

These results are analysed and discussed in Section 4.3.1 in the next chapter. It will be demonstrated that the compression behaviour of tailings, as a log-linear relationship, can be normalised and correlated to composition related properties such as the Atterberg limits. An interesting observation is the large amount of secondary compression that took place during the consolidation stages. This is contrary to what is normally assumed for gold tailings. The fast draining properties of the tailings can cause problems during consolidation. It is uncertain whether the drainage facilities of the triaxial apparatus did not restrict free-flow of the drainage water to some extent.

3.4.6 Shear strength

Undrained Triaxial Shear

Consolidated undrained compressive triaxial shear tests were performed on the tailings material, according to the guidelines given in BS1377:1990 Part 8, as follows:

(a) Specimen preparation and consolidation followed the procedures described in Section 3.4.5. For purposes of determining the compression and consolidation response of a sample, the full set of consolidation increments (12.5, 25, 50, 100, 200 and 400 kPa effective) were applied. Once this behaviour had been established for a particular sample, subsequent specimens were consolidated in a single stage to either 50 or 200 kPa effective. This resulted in a set of three undrained shear stress paths for each sample at stress levels of 50, 200 and 400 kPa.

(b) Following consolidation, each specimen was subjected to undrained compressive shear by closing the internal drainage valve and applying axial compressive force using the loading ram. The axial force on the loading ram was measured using an external load-ring. The measured force, the calculated cross-sectional area of the specimen and the applied cell pressure could then be used to determine the axial total vertical stress in the specimen. An attempt was made at compensating for the mechanical friction between the loading ram and the cell body by zeroing the load dial-gauge as the ram was pushed towards the top-cap without making contact with the specimen. A flat top-cap was used to eliminate problems of disturbance if the sample is not perfectly aligned with the loading ram (Baldi et al., 1988). Axial deformation was measured using a dial-gauge fixed between the load ring and the cell body, and excess pore pressures using an electronic transducer measuring at the base of the specimen.

(c) The rate of shear was fixed at 0.38 mm/min, consistent with the drainage properties of the material determined from consolidation data and resulted in approximately 15% shear strain per hour.

Results of the triaxial tests are summarised in Table 3-19 and discussed in Section 4.3.3 in the next chapter. It will be shown that a single effective strength parameter of $\phi' \approx 34°$ is sufficient to describe the shear strength of all the samples considered in this study. However, the undrained shear behaviour of fine and coarse samples are separated by the fact that the fine samples reach a steady failure state, while the coarse samples tend to dilate and strengthen in post failure states.

Table 3-19: Results of undrained triaxial compressive shear on tailings material.

Tailings Dam	Description	Figure
Mizpah	**Reconstituted Specimens - (MPDWT, MPDF & MPDC)**	
	Whole Tailings - Triaxial results	Figure 3-106
	Whole Tailings - Stress paths	Figure 3-107
	Whole Tailings - Mohr's circles	Figure 3-108
	Pond Fine Tailings - Triaxial results	Figure 3-109
	Pond Coarse Tailings - Triaxial results	Figure 3-110
	Combined Fine & Coarse Stress paths	Figure 3-111
	Combined Fine & Coarse Mohr's circles	Figure 3-112
Pay Dam	**Reconstituted Specimens - (PPNDF & PPNDC)**	
	Penstock Fine Tailings - Triaxial results	Figure 3-113
	Penstock Coarse Tailings - Triaxial results	Figure 3-114
	Combined Fine & Coarse Stress paths	Figure 3-115
	Combined Fine & Coarse Mohr's circles	Figure 3-116
	Undisturbed Specimens - (PPNTF1 & PPNTC1)	
	Penstock Fine Tailings - Triaxial results	Figure 3-117
	Penstock Coarse Tailings - Triaxial results	Figure 3-118
	Combined Fine & Coarse Stress paths	Figure 3-119
	Combined Fine & Coarse Mohr's circles	Figure 3-120

3.5 IN-SITU TESTS

3.5.1 Piezocone

Piezocone tests were conducted at both sites to obtain a measure of the in-situ state within each dam. The instrument used measures cone resistance, pore pressure and inclination with depth, and records the test data automatically in electronic format. The equipment and test procedure conform to the international reference test procedure, ISSMFE (1989), with the filter element placed immediately above the cone tip, commonly referred to as position-u_2.

Five soundings were made through a cross section of Mizpah Dam starting on the southern daywall and progressing down the beach to the beach-pond interface area, Figure 3-1b. Two soundings were made on Pay Dam, one on the beach and one next to the northern penstock where the bulk of the laboratory test samples were taken (Figure 3-3b).

Results of the piezocone soundings are summarised in Table 3-20 and discussed in Section 4.4.

Table 3-20: Summary of piezocone test results.

Description	Field Log	Pore pressure Dissipations	Ambient Pore pressure	Normalised Log	Identification Chart
Mizpah					
Daywall	Figure 3-121	Figure 3-122	Figure 3-123	Figure 3-124	Figure 3-125
Upper Beach	Figure 3-126	Figure 3-127	Figure 3-128	Figure 3-129	Figure 3-130
Middle Beach	Figure 3-131	Figure 3-132	Figure 3-133	Figure 3-134	Figure 3-135
Lower Beach	Figure 3-136	Figure 3-137	Figure 3-138	Figure 3-139	Figure 3-140
Pond	Figure 3-141	Figure 3-142	Figure 3-143	Figure 3-144	Figure 3-145
Pay Dam					
Beach	Figure 3-146	Figure 3-147	Figure 3-148	Figure 3-149	Figure 3-150
Penstock	Figure 3-151	Figure 3-152	Figure 3-153	Figure 3-154	Figure 3-155

The terms used in Table 3-20 are explained as follows:

- **Field log**: Raw field penetration data, including cone resistance and pore pressure. These values were taken directly from the electronic data acquisition system without any corrections or adjustments.
- **Pore pressure dissipations**: Results of pore pressure dissipation tests taken at stationary intervals during a sounding.
- **Ambient pore pressure**: The ambient or equilibrium in-situ pore pressure distribution based on the piezocone pore pressure dissipation data. This information is also used to determine the depth of the phreatic surface at the location of the sounding.
- **Normalised log**: A representation of the piezocone sounding normalised with respect to the effects of overburden pressure and the ambient pore pressure. For this purpose the field data have been corrected for: electronic drift in the sensors if applicable, extended length of the first rod carrying the instrumented cone as well as the offset in measurement depths between the cone tip and pore pressure element due to their physical separation.

Excess cone resistance: $q_e = q_c + \lambda \cdot u_t - \sigma_{vo}$ **Eq. 3-1**

Excess pore pressure: $u_e = u_t - u_o$ **Eq. 3-2**

where q_c = corrected cone resistance
λ = correction factor for unequal areas effect
u_t = measured pore pressure
u_o = ambient pore pressure

σ_{vo} = total vertical overburden pressure assuming γ_{sat} = 17.8 kN/m^3 below the water table and a bulk weight of γ_{nat} = 16.9 kN/m^3 above the water table

- **Identification chart**: Normalised penetration data represented on the Jones and Rust soils identification chart for classification purposes.

(a)

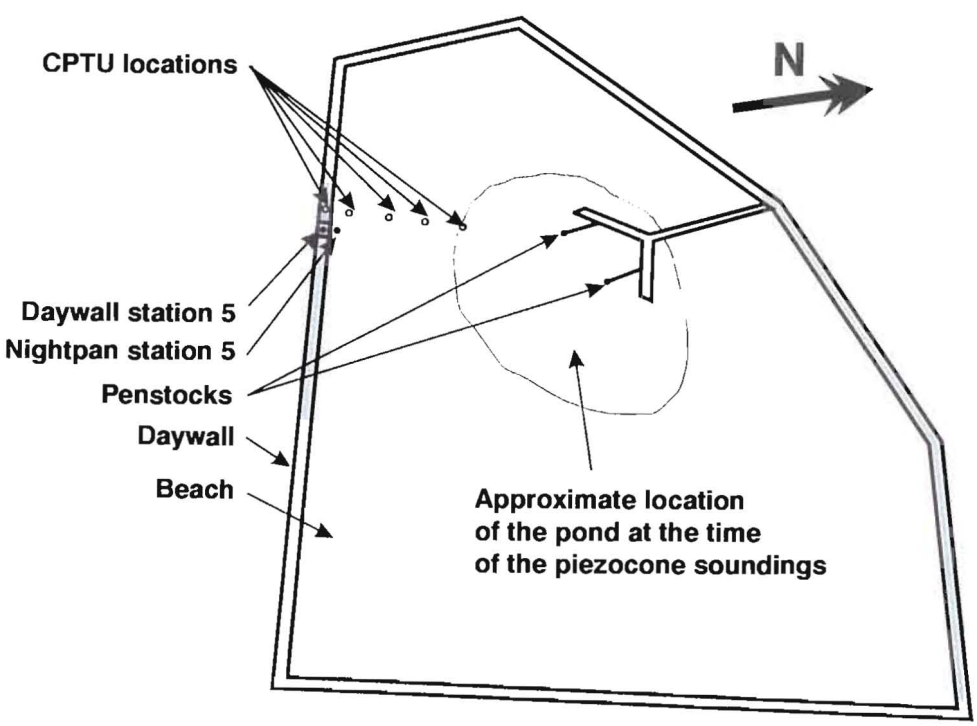

(b)

Figure 3-1: (a) Aerial photograph of Mizpah, (b) Diagram of In-situ test and sampling locations.

Figure 3-2: Transportation of equipment on the dried out beach of Mizpah.

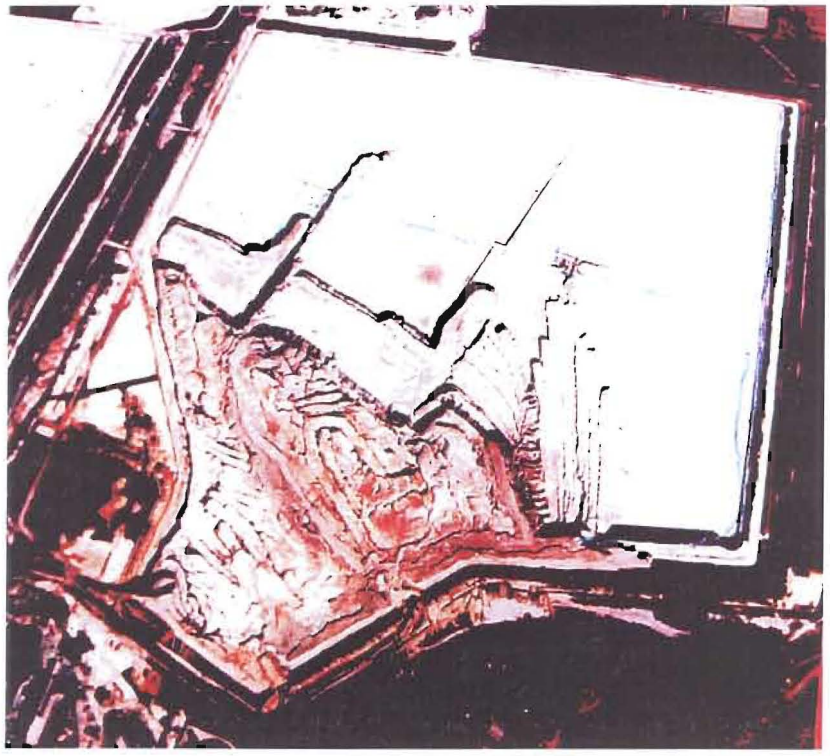

(a)

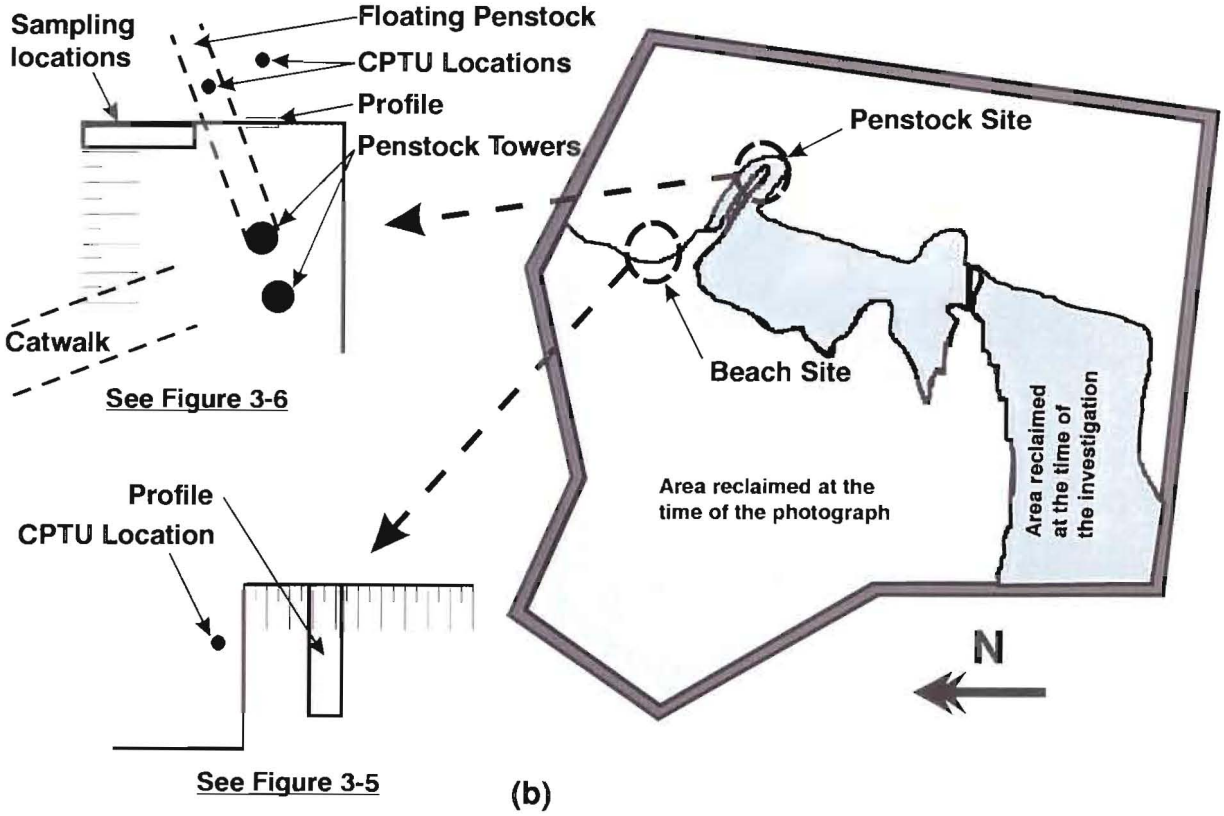

(b)

Figure 3-3: (a) Aerial photograph of Pay Dam, (b) Diagram of In-situ test and sampling locations.

Figure 3-4: Hydro-cannon or monitors used on Pay Dam.

Figure 3-5: Site of the upper beach exposed by reclamation on Pay Dam.

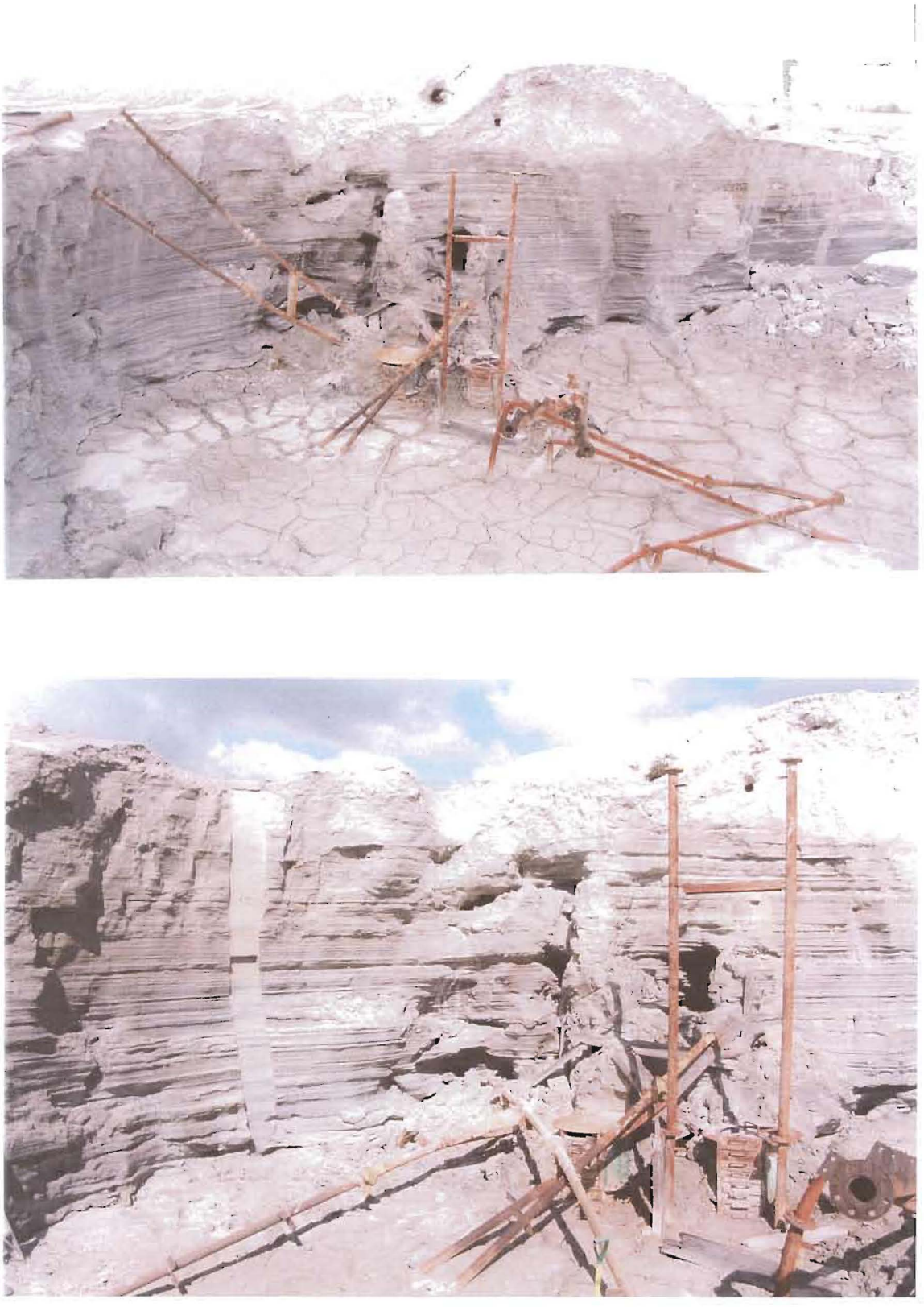

Figure 3-6: (a) Exposed northern penstock at Pay Dam.

Figure 3-6: (b) Pay Dam site showing a close-up of the 5 m profile and the sampling pits.

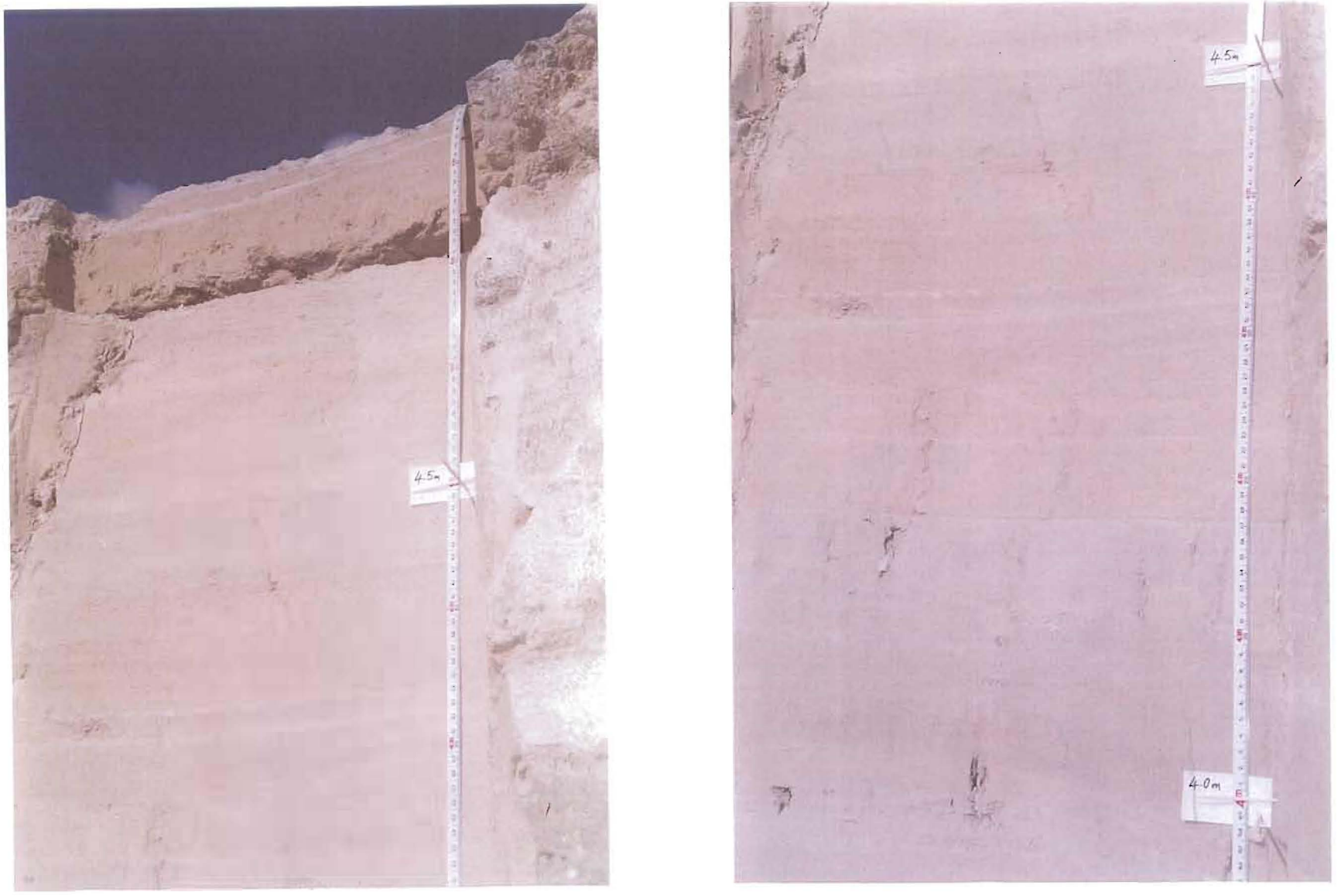

Figure 3-7: Pay Dam - Penstock: Photos of the profile from 0 to 1 m in depth.

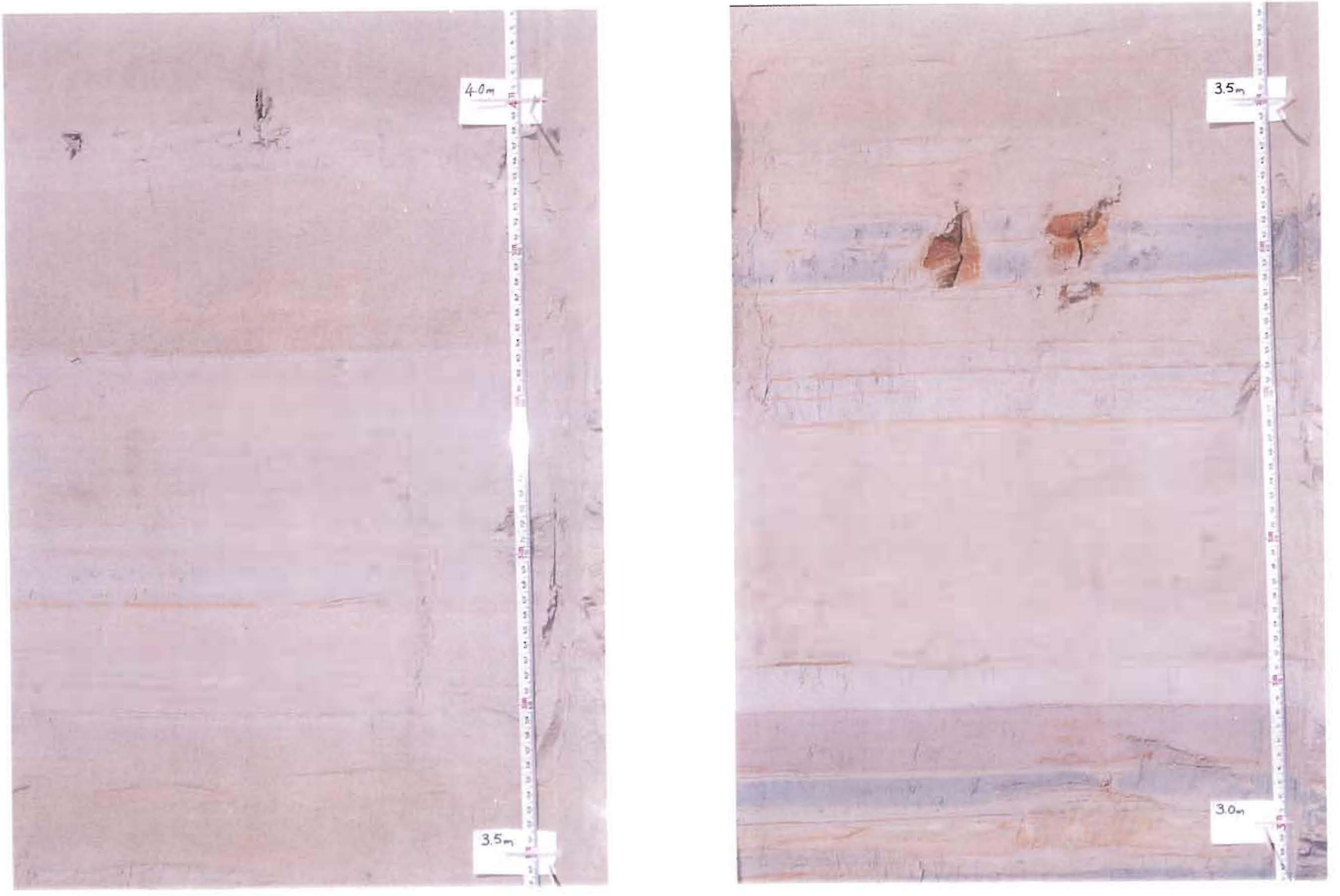

Figure 3-8: Pay Dam - Penstock: Photos of the profile from 1 to 2 m in depth.

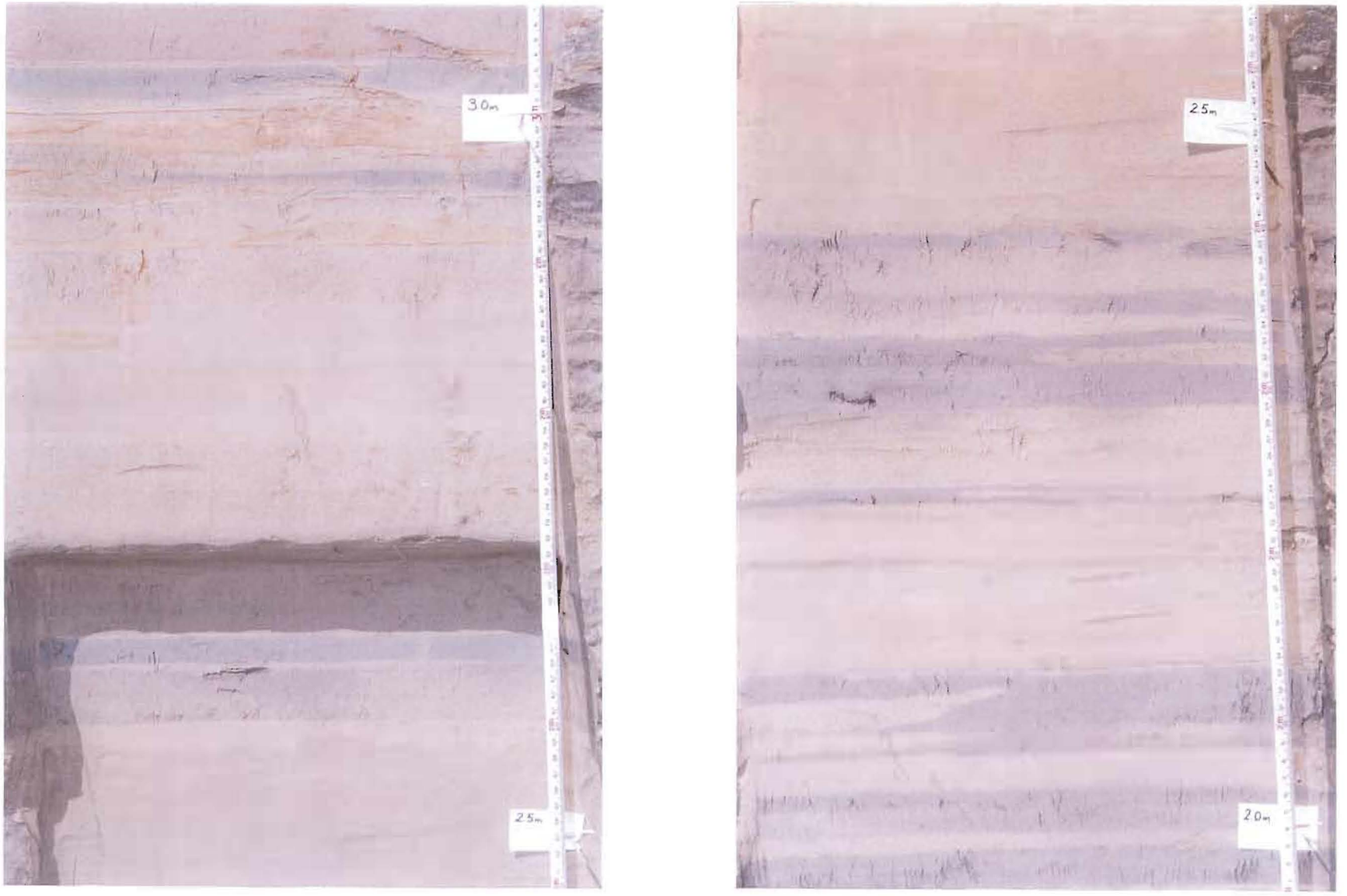

Figure 3-9: Pay Dam - Penstock: Photos of the profile from 2 to 3 m in depth.

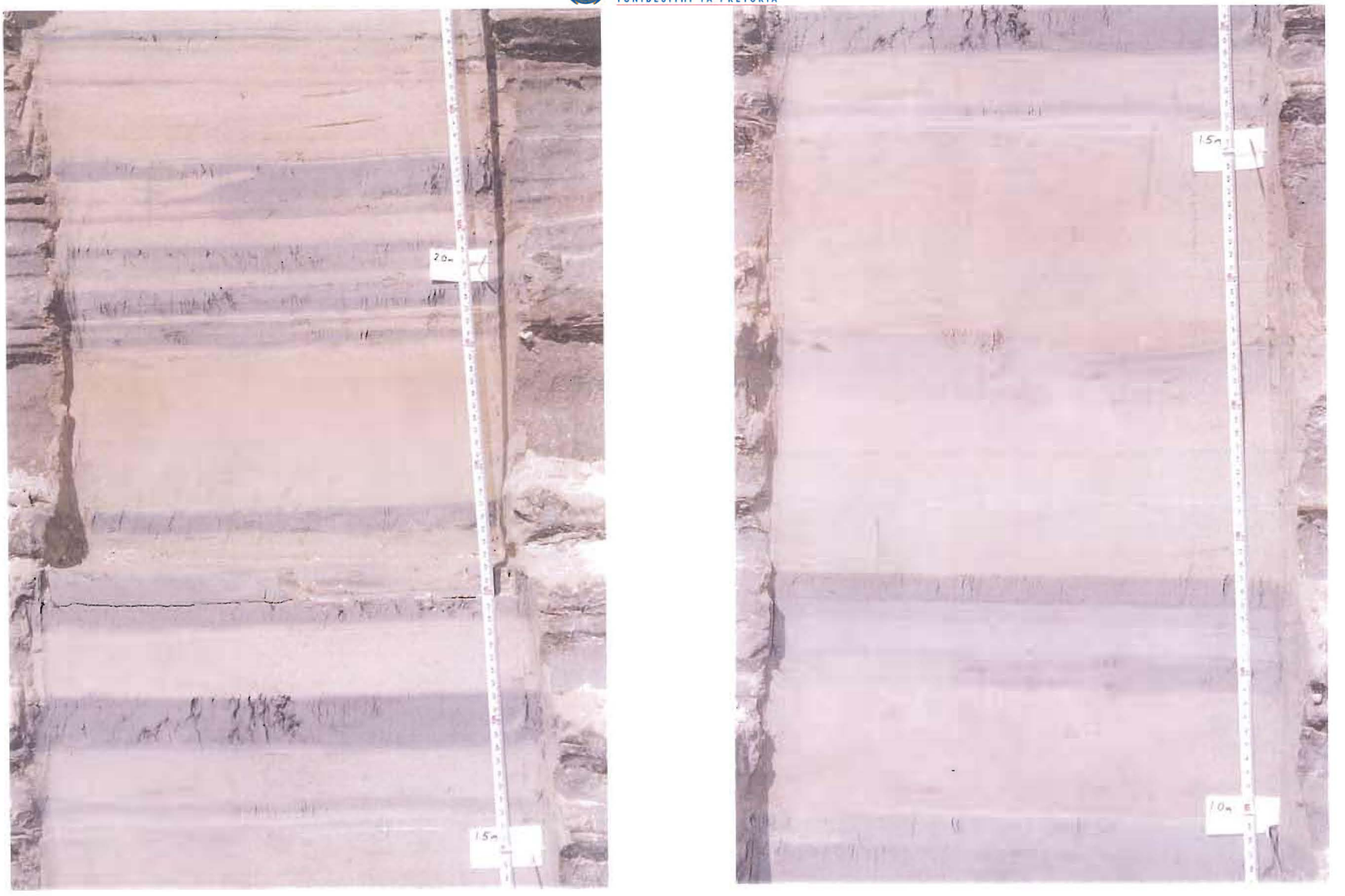

Figure 3-10: Pay Dam - Penstock: Photos of the profile from 3 to 4 m in depth.

Figure 3-11: Pay Dam - Penstock: Photos of the profile from 4 to 5 m in depth.

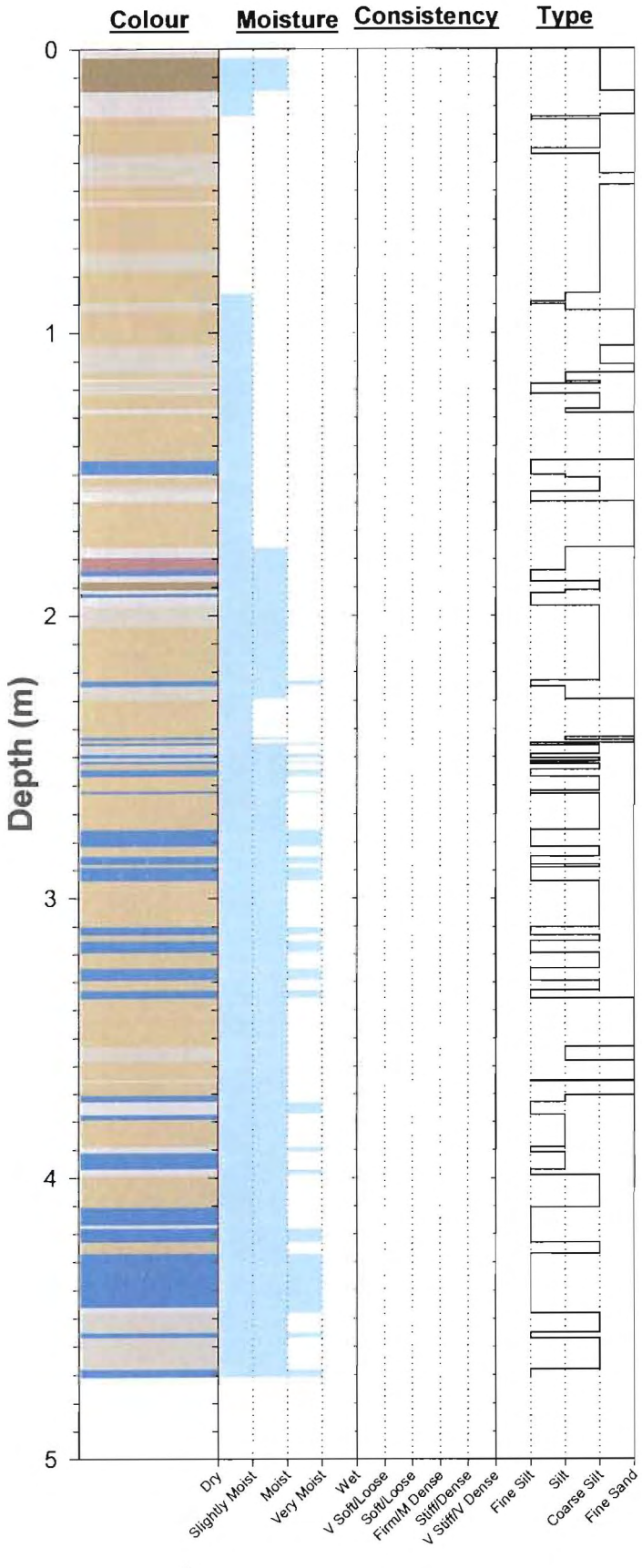

Figure 3-12: Pay Dam - Penstock: Full profile from 0 to 5 m in depth.

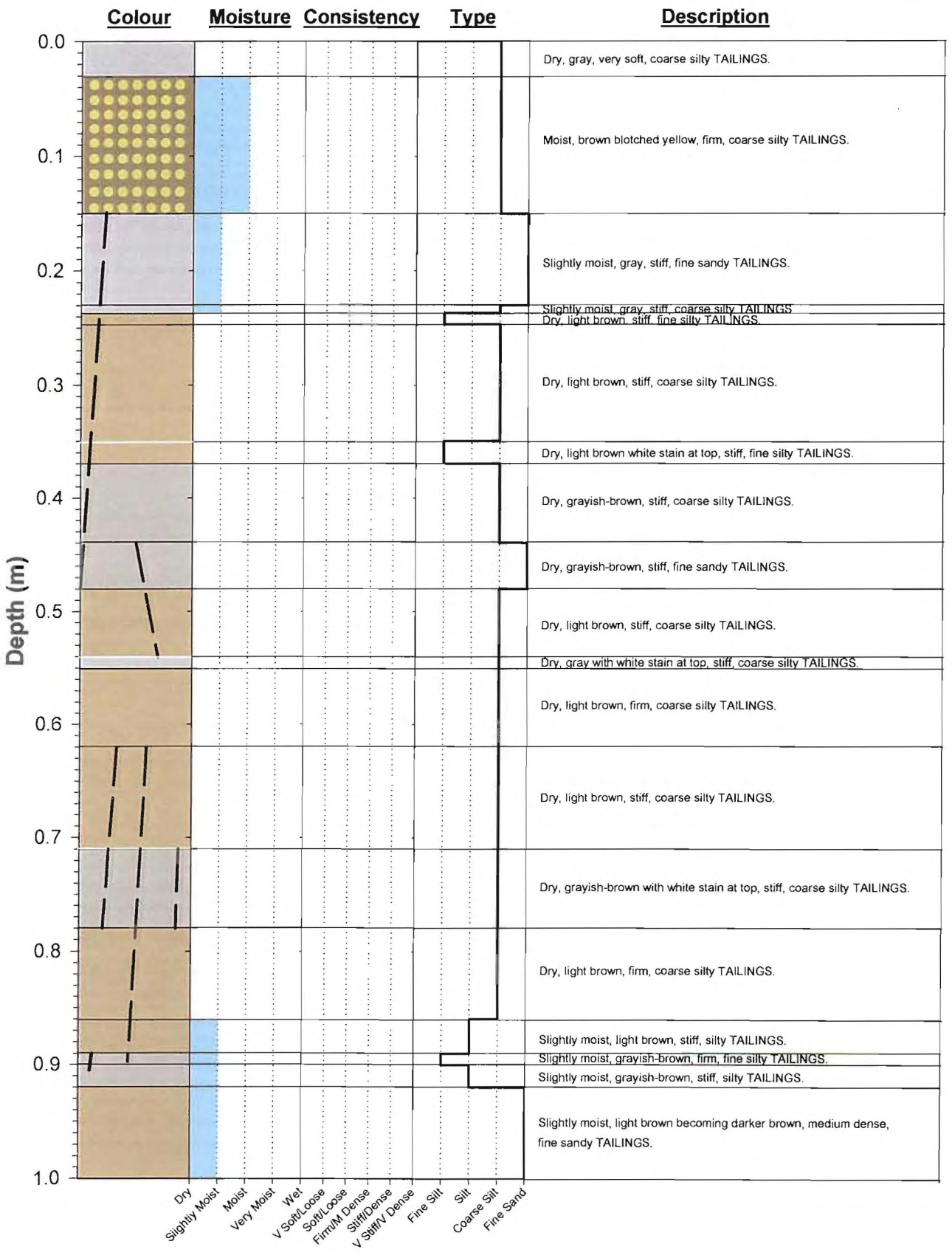

Figure 3-13: Pay Dam - Penstock: Profile from 0 to 1 m in depth.

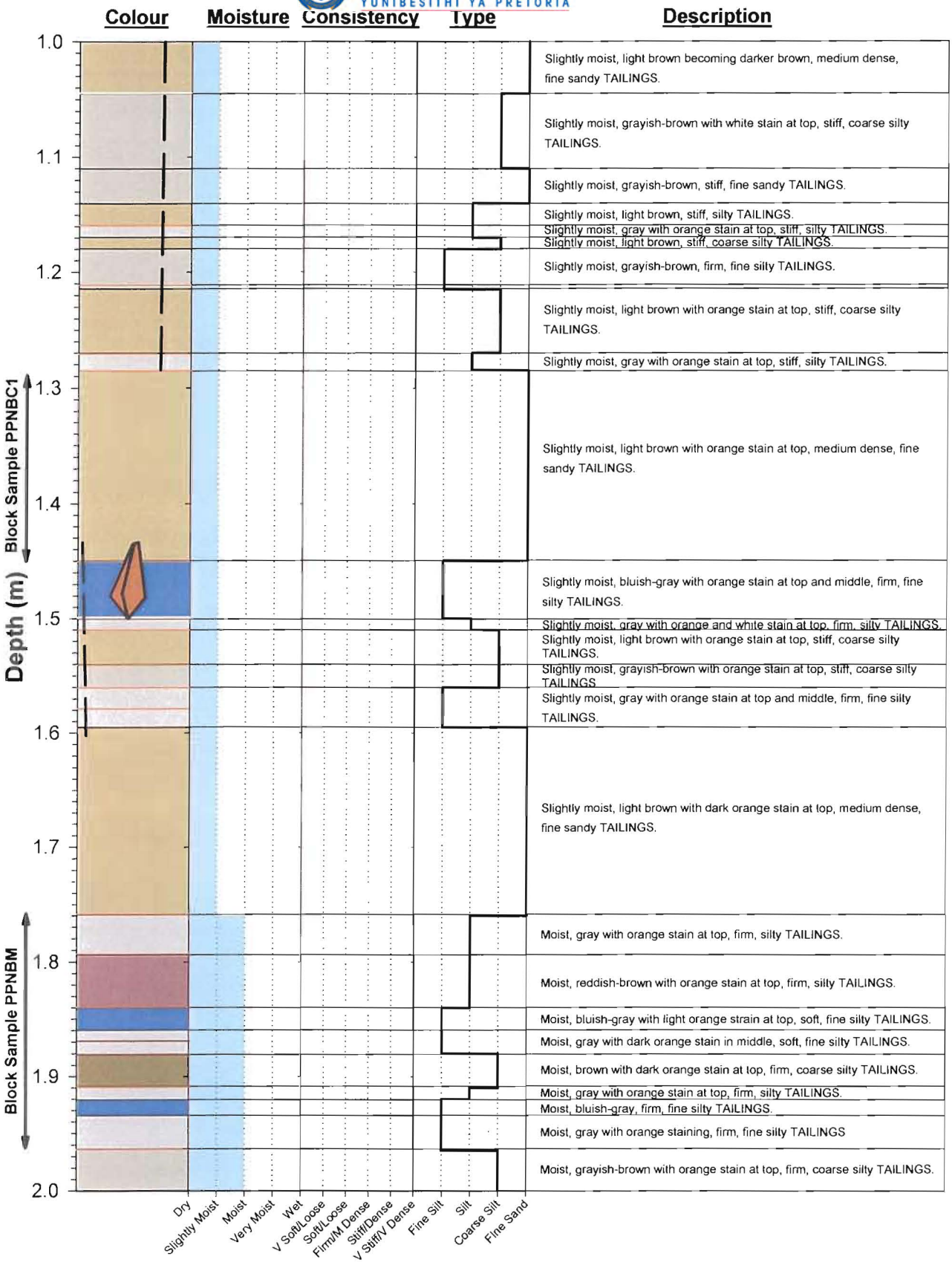

Figure 3-14: Pay Dam - Penstock: Profile from 1 to 2 m in depth.

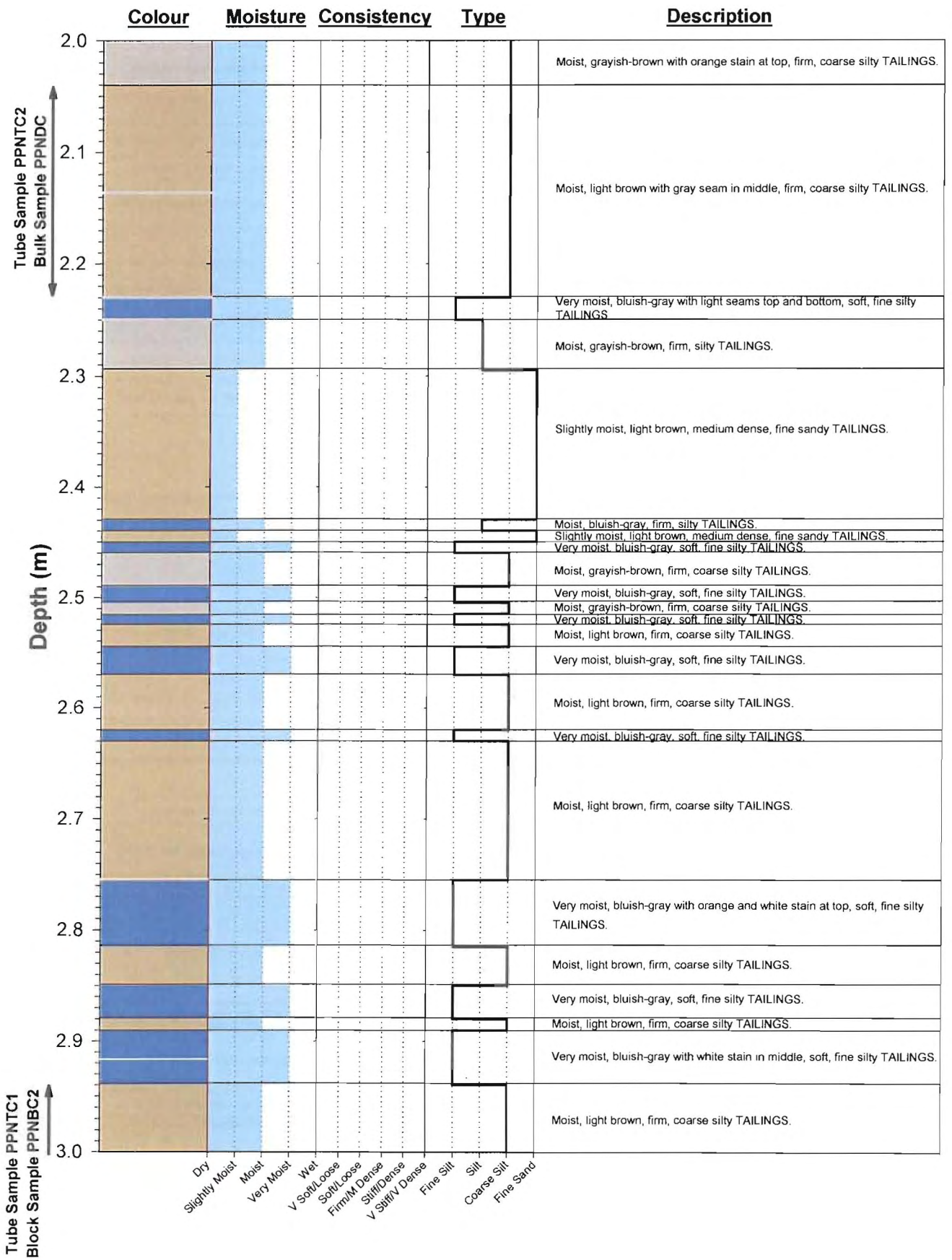

Figure 3-15: Pay Dam - Penstock: Profile from 2 to 3 m in depth.

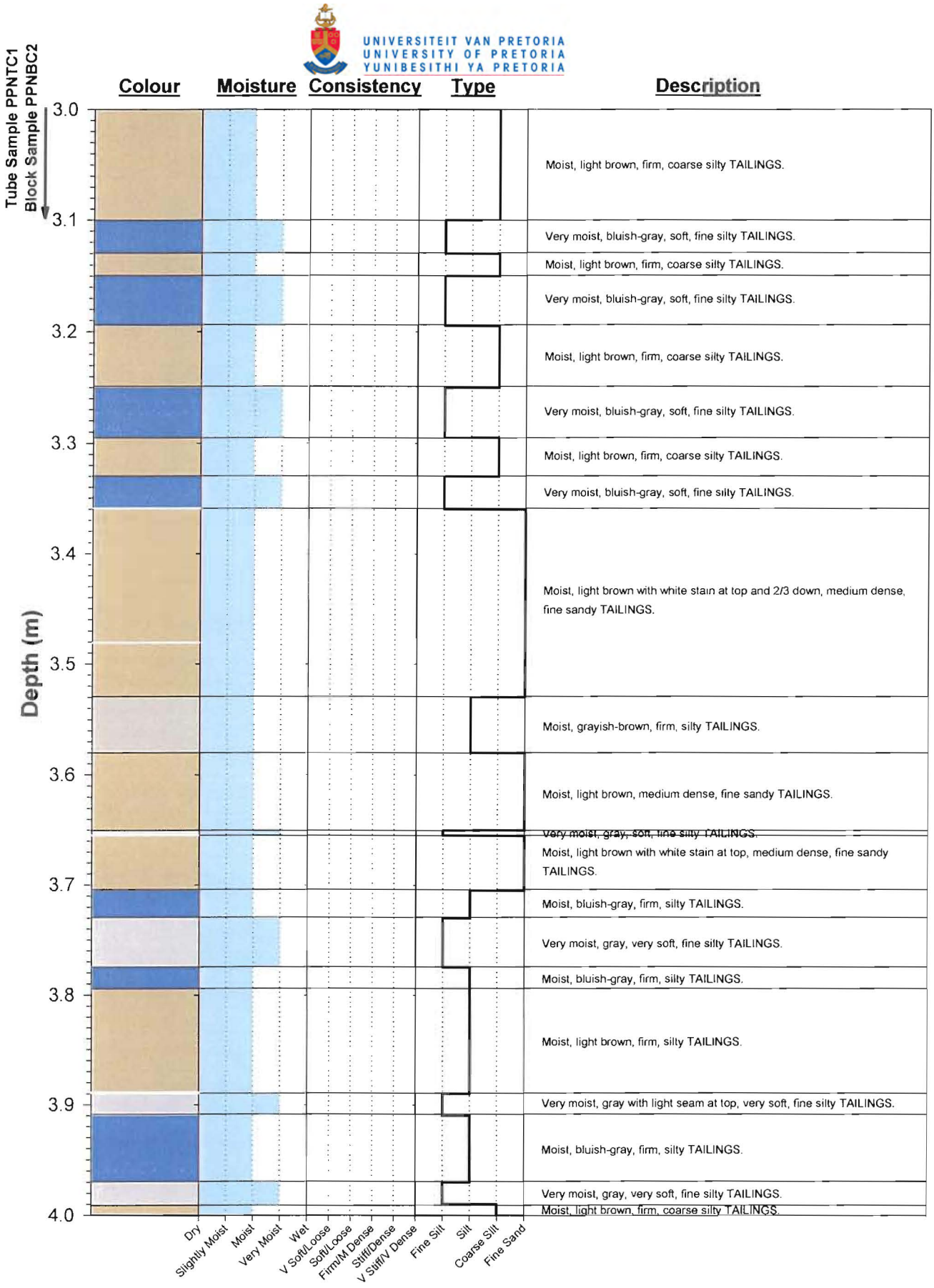

Figure 3-16: Pay Dam - Penstock: Profile from 3 to 4 m in depth.

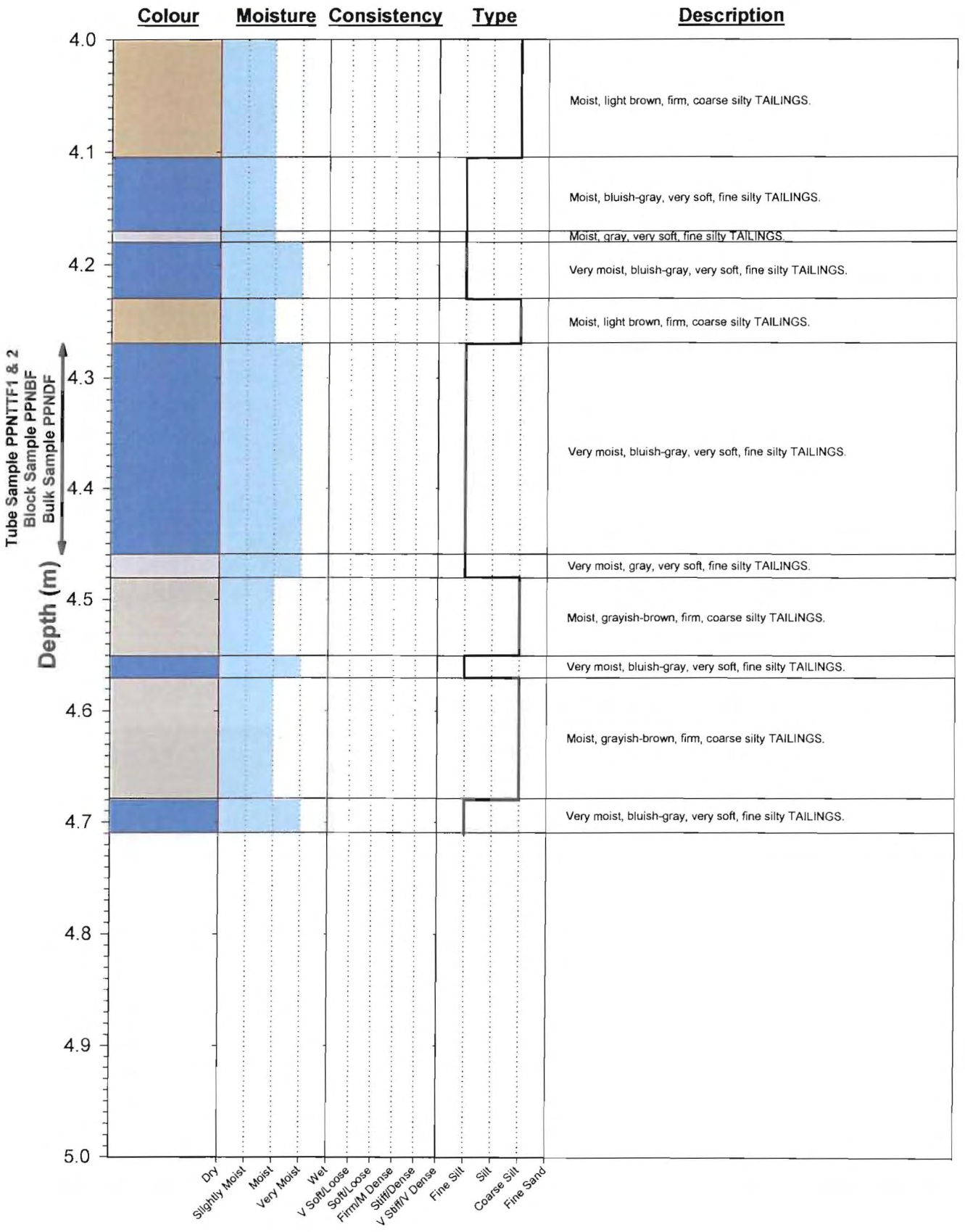

Figure 3-17: Pay Dam - Penstock: Profile from 4 to 5 m in depth.

Figure 3-18: Pay Dam - Upper Beach: Photos of the full profile from 0 to 5.5 m in depth.

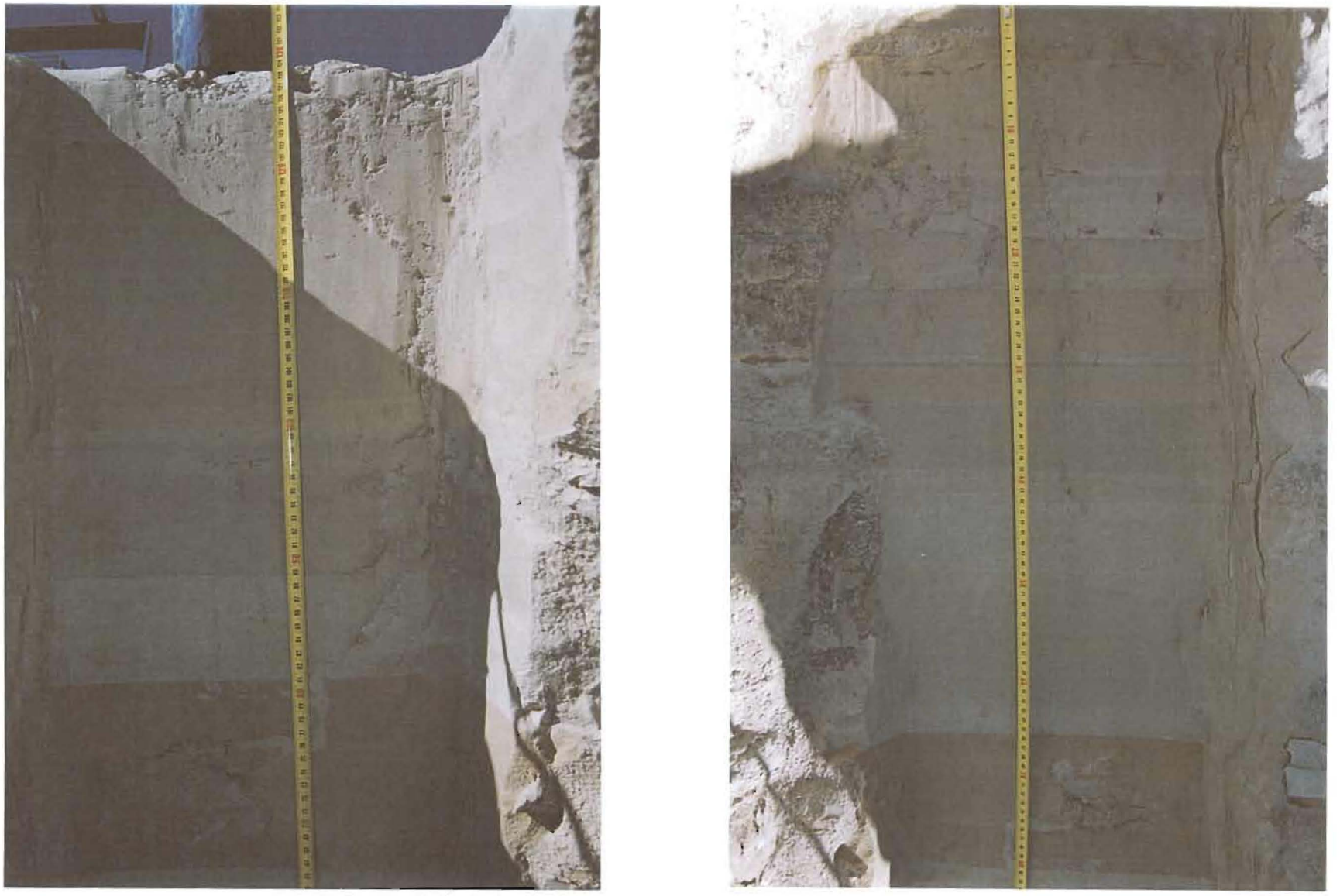

Figure 3-19: Pay Dam - Upper Beach: Photos of the profile from 0 to 1.3 m in depth.

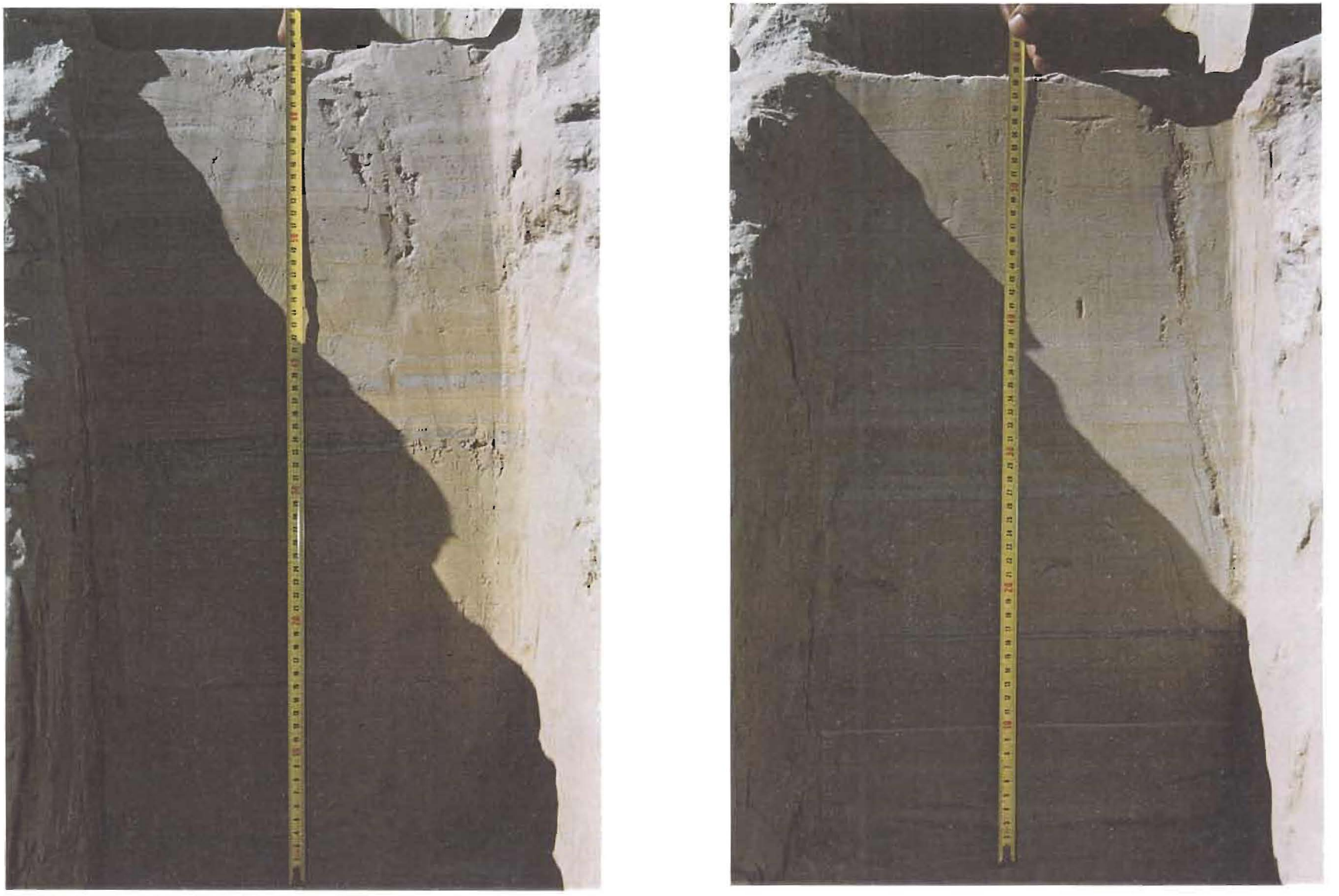

Figure 3-20: Pay Dam - Upper Beach: Photos of the profile from 1.3 to 2.6 m in depth.

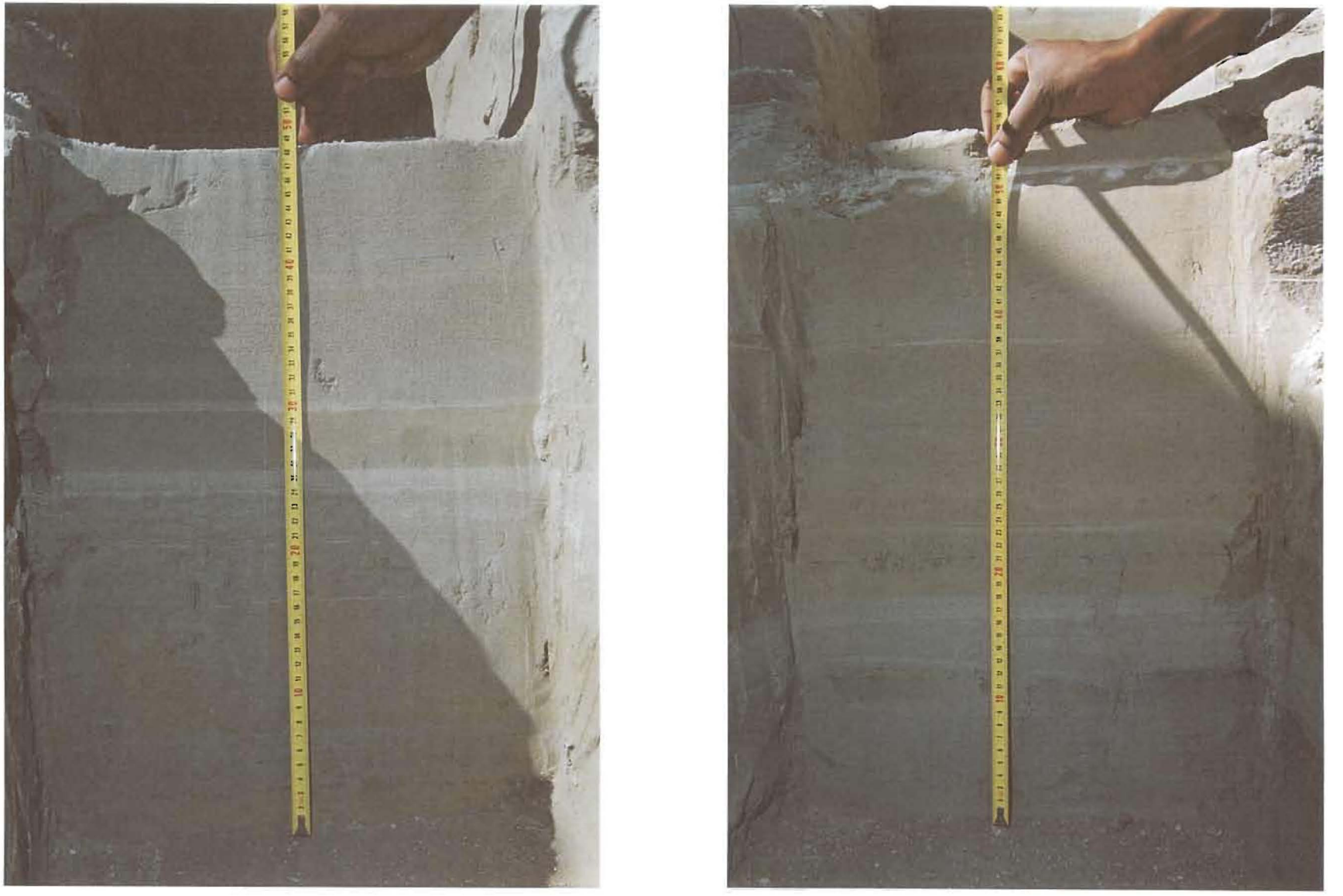

Figure 3-21: Pay Dam - Upper Beach: Photos of the profile from 2.6 to 3.6 m in depth.

Figure 3-22: Pay Dam - Upper Beach: Photos of the profile from 3.6 to 4.8 m in depth.

Figure 3-23: Pay Dam - Upper Beach: Photos of the profile from 4.8 to 5.5 m in depth.

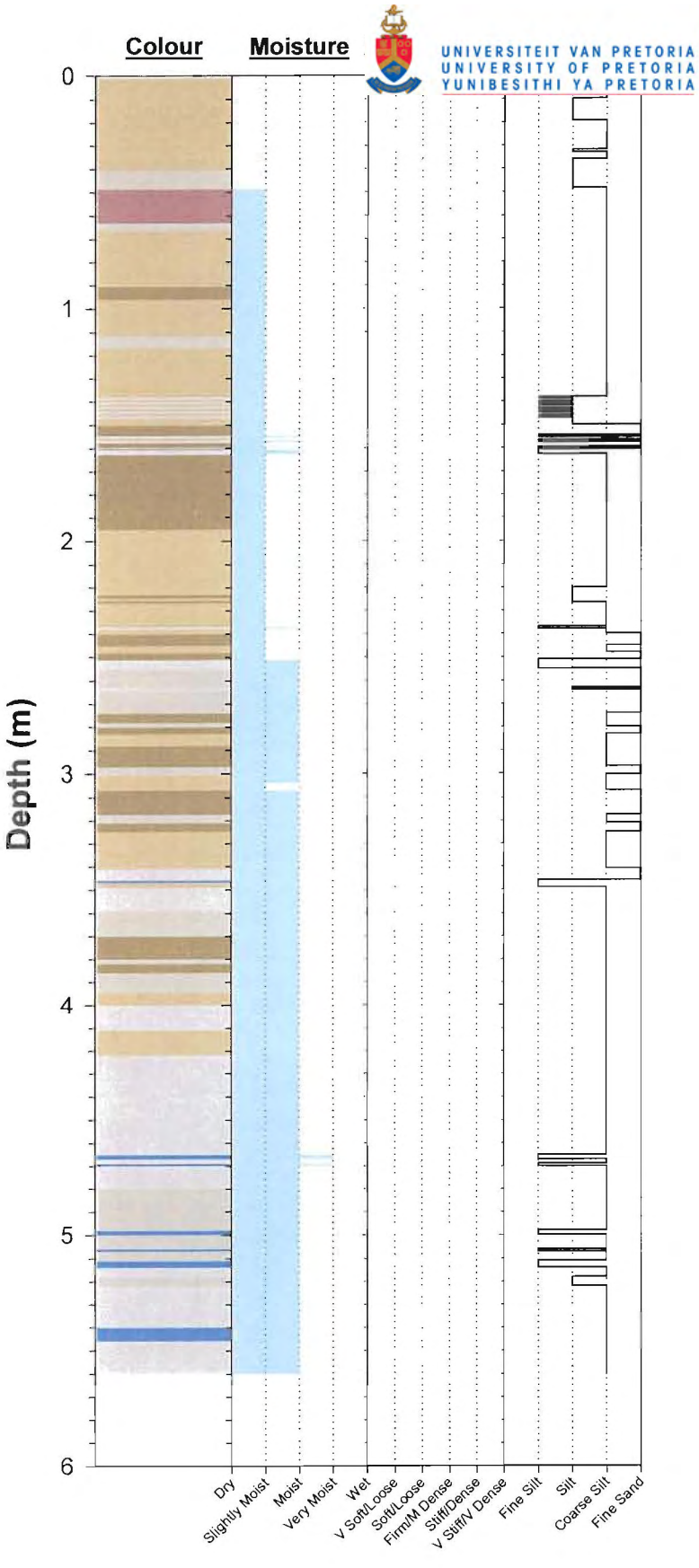

Figure 3-24: Pay Dam - Upper Beach: Full profile from 0 to 5.5 m in depth.

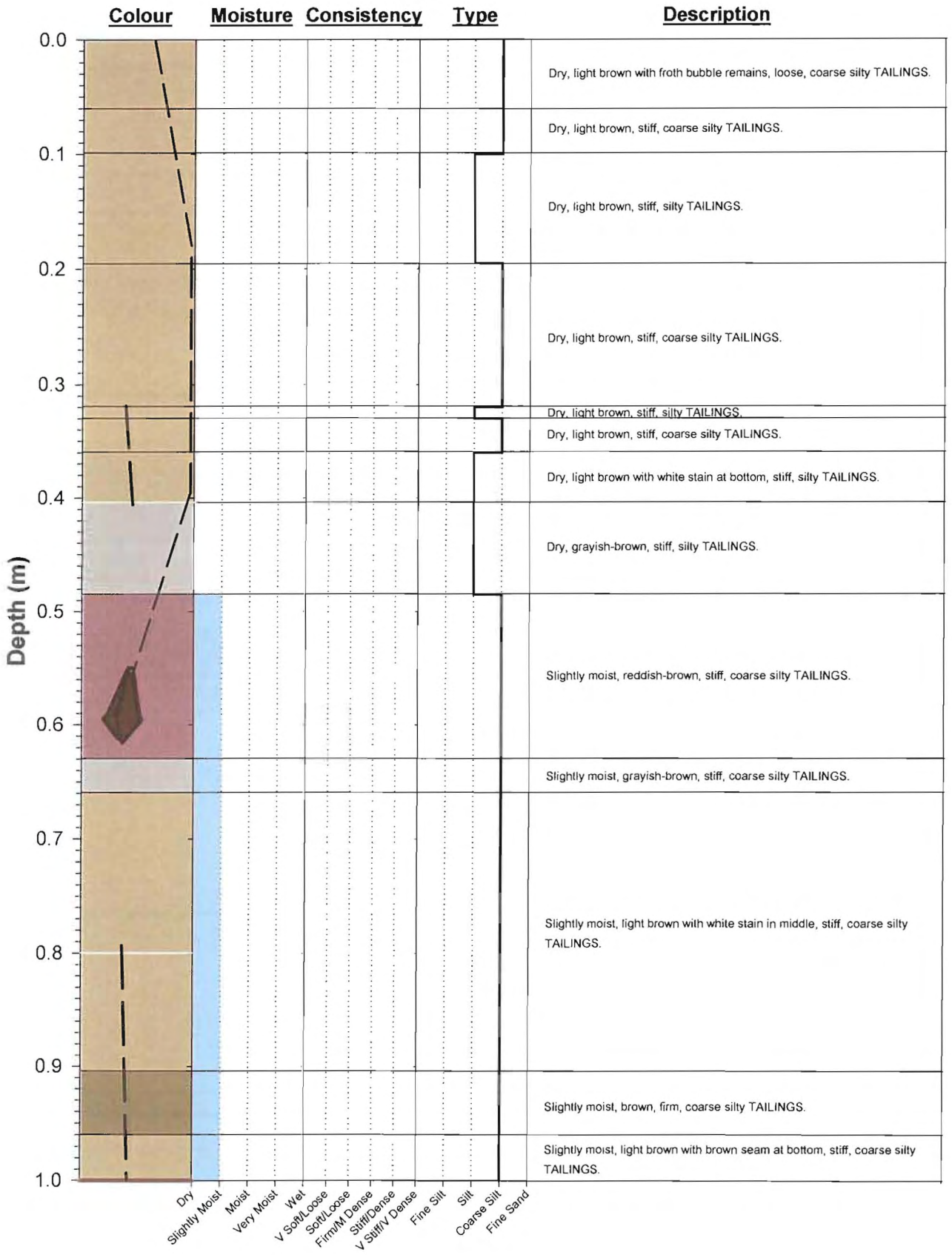

Figure 3-25: Pay Dam - Upper Beach: Profile from 0 to 1 m in depth.

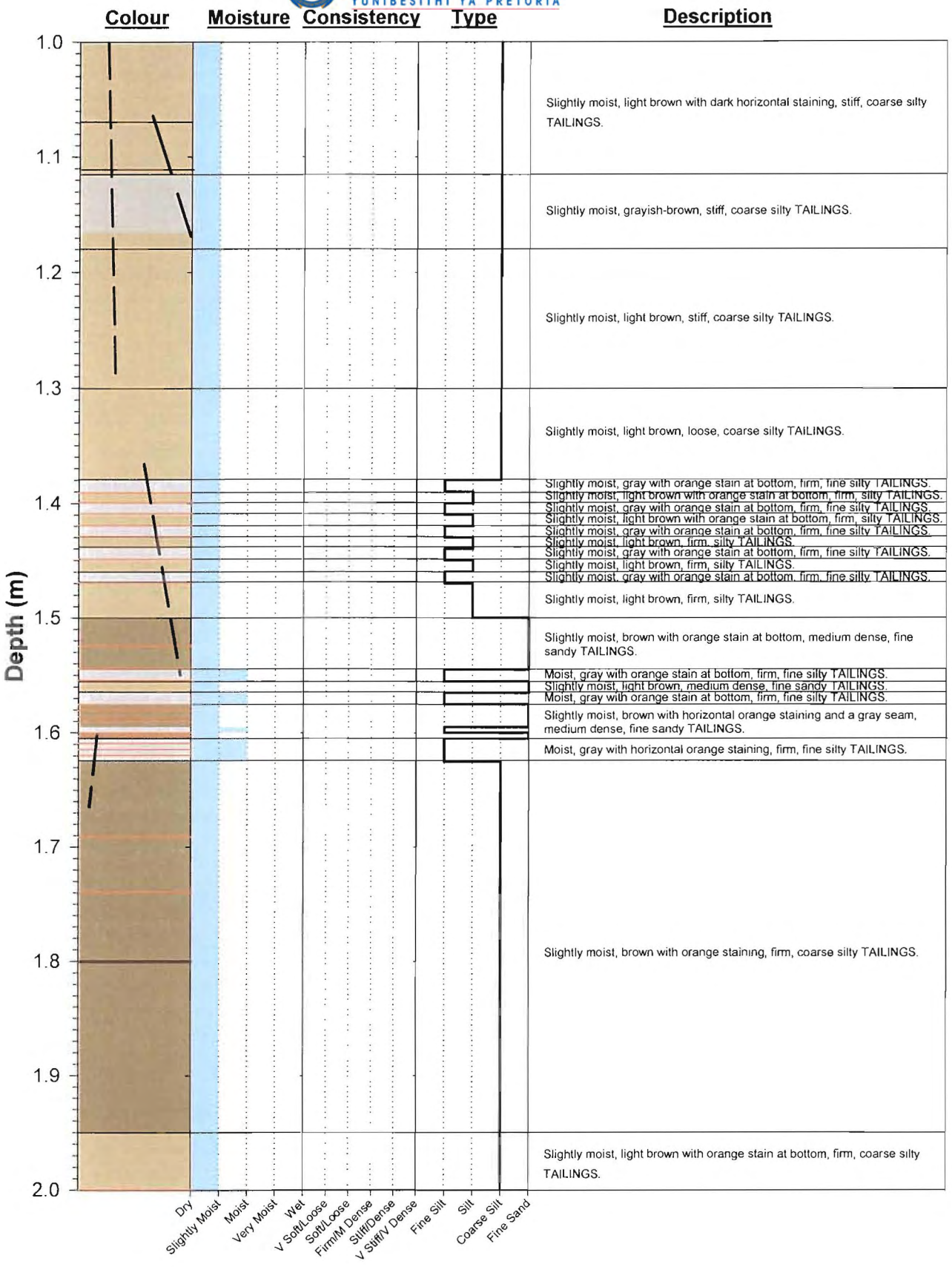

Figure 3-26: Pay Dam - Upper Beach: Profile from 1 to 2 m in depth.

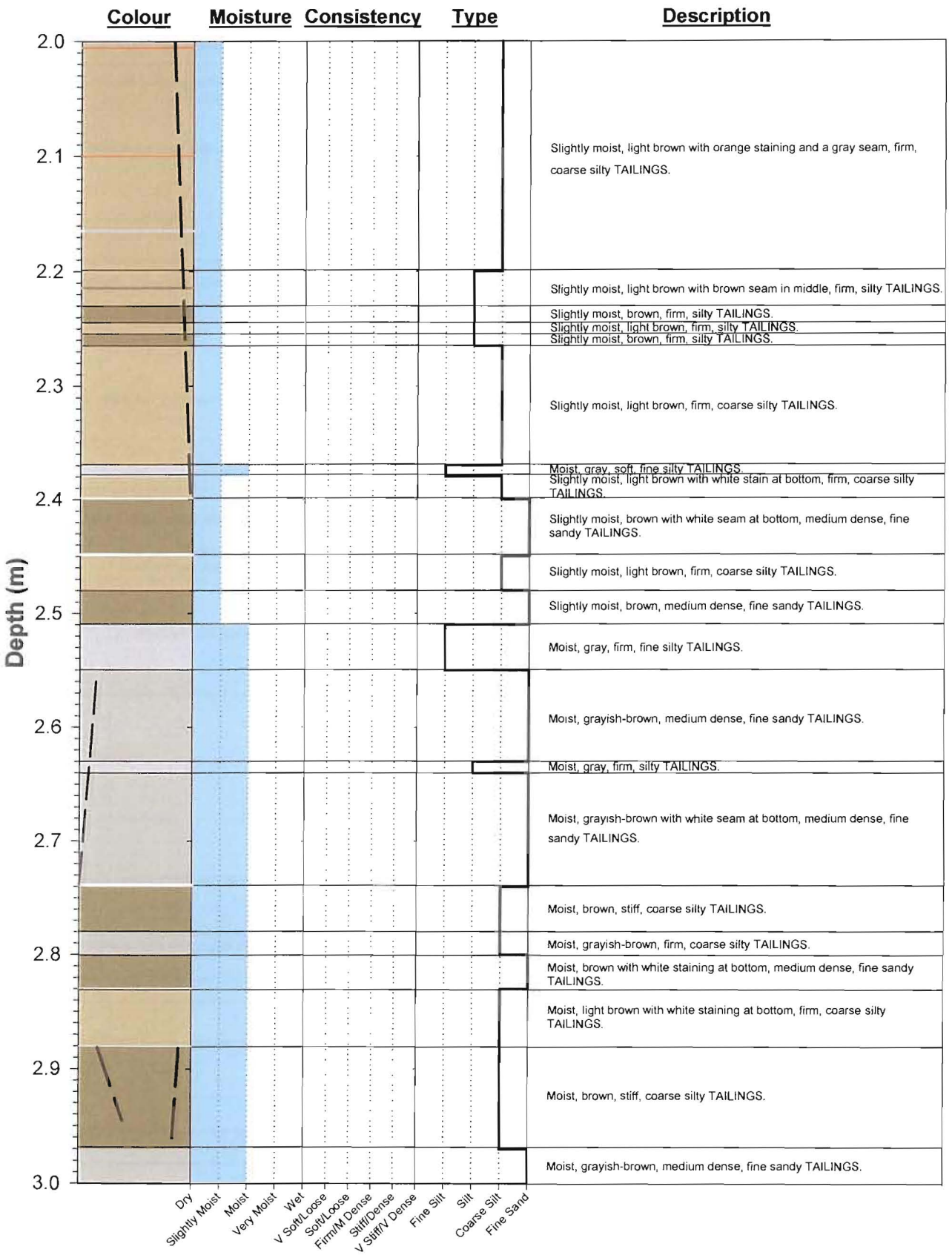

Figure 3-27: Pay Dam - Upper Beach: Profile from 2 to 3 m in depth.

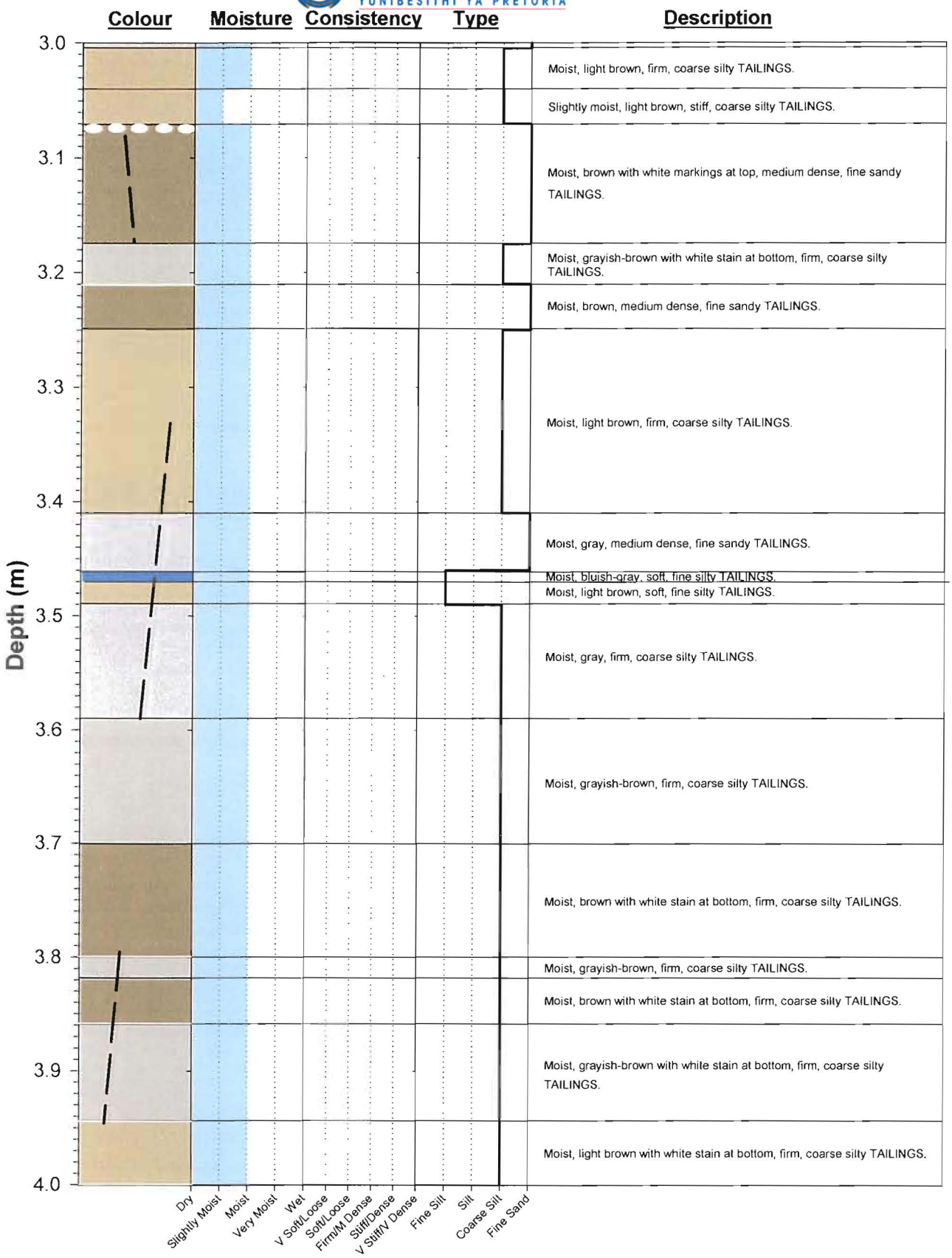

Figure 3-28: Pay Dam - Upper Beach: Profile from 3 to 4 m in depth.

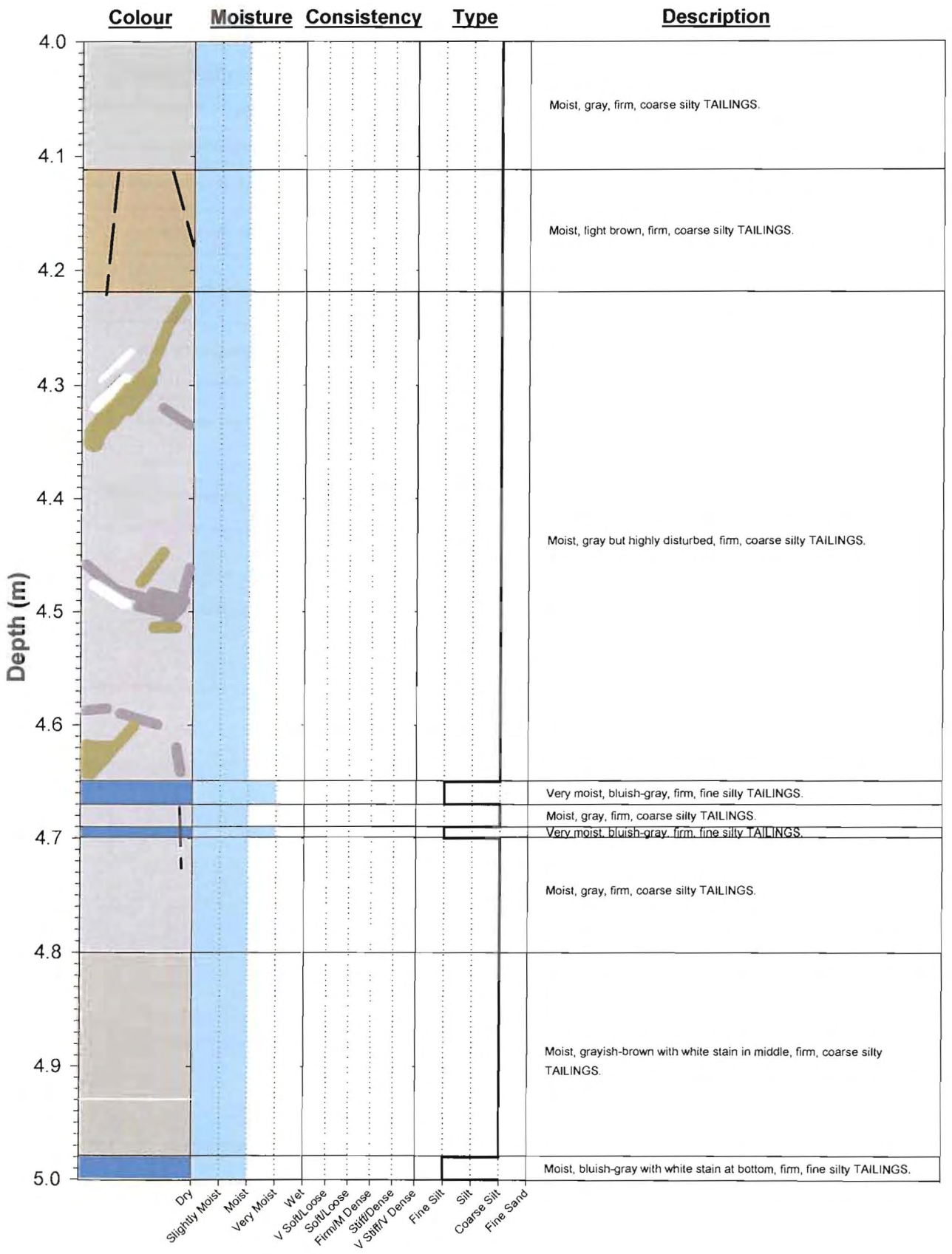

Figure 3-29: Pay Dam - Upper Beach: Profile from 4 to 5 m in depth.

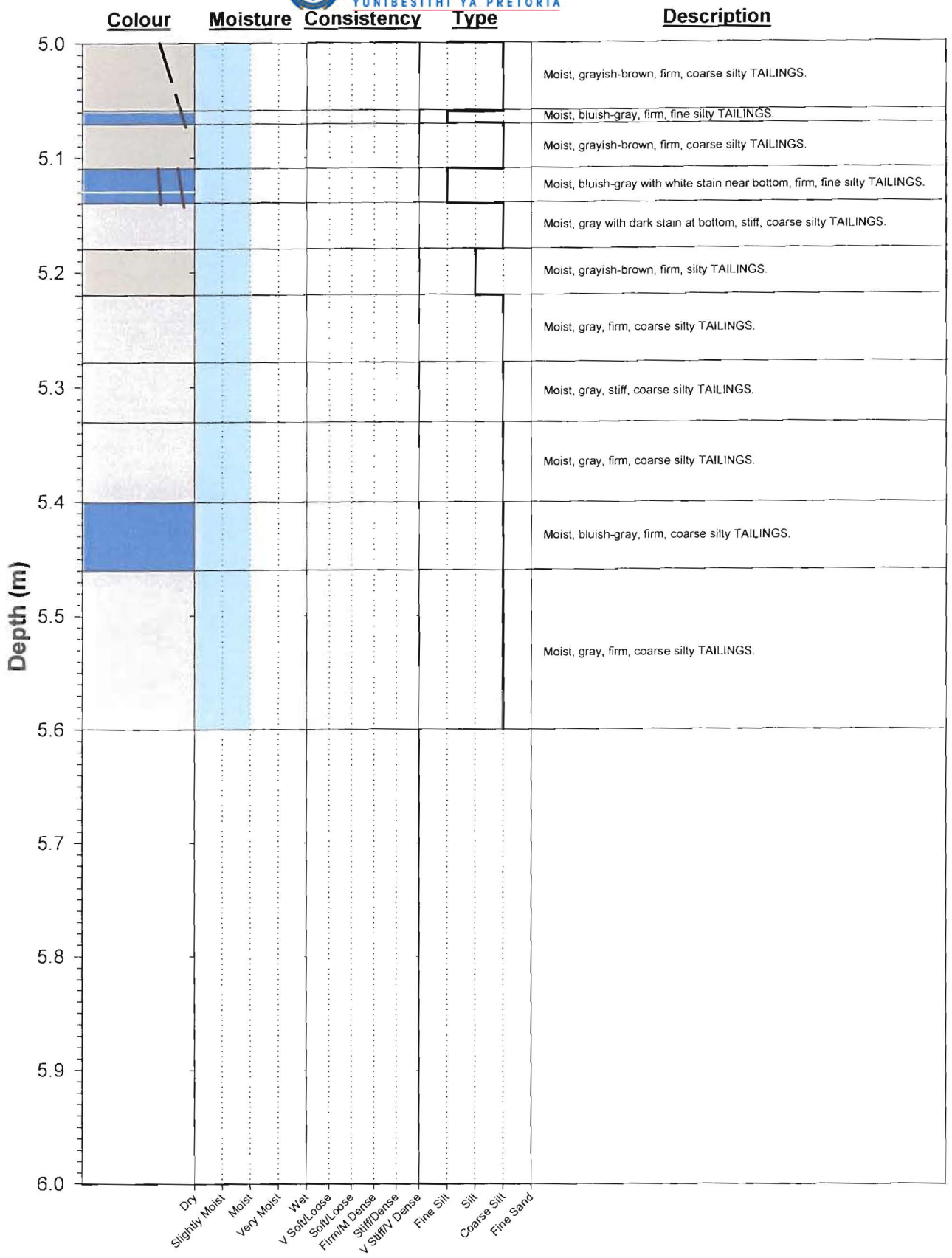

Figure 3-30: Pay Dam - Upper Beach: Profile from 5 to 6 m in depth.

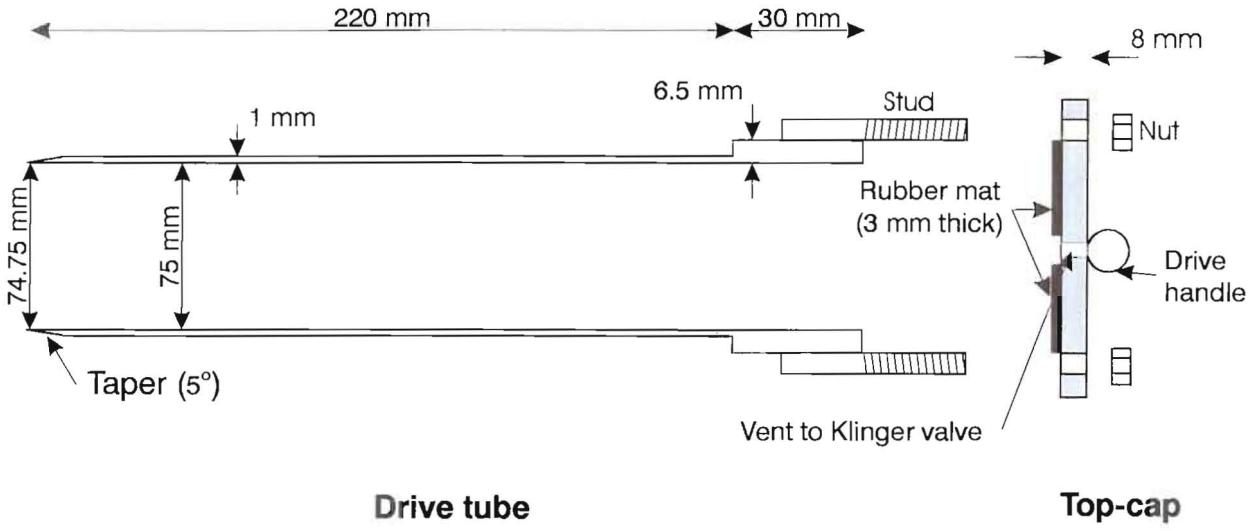

Figure 3-31: Stainless steel 75 mm diameter tube sampler.

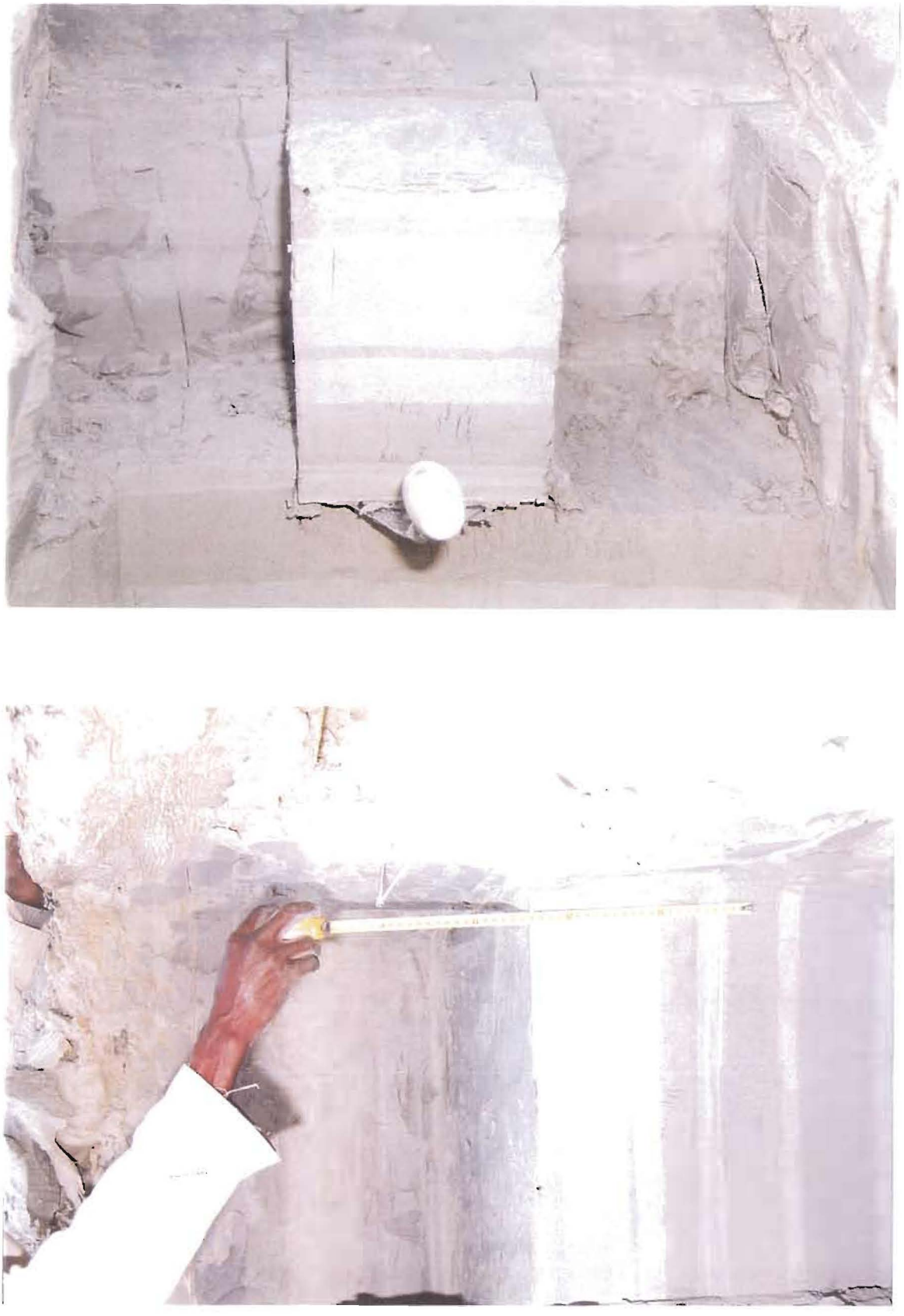

Figure 3-32: Sampling of Block Sample No. PPNBF at a depth of 4.3 m at the Pay Dam penstock.

Figure 3-33: Sampling of Tube Sample No. PPNTF1 at a depth of 4.3 m at the Pay Dam penstock.

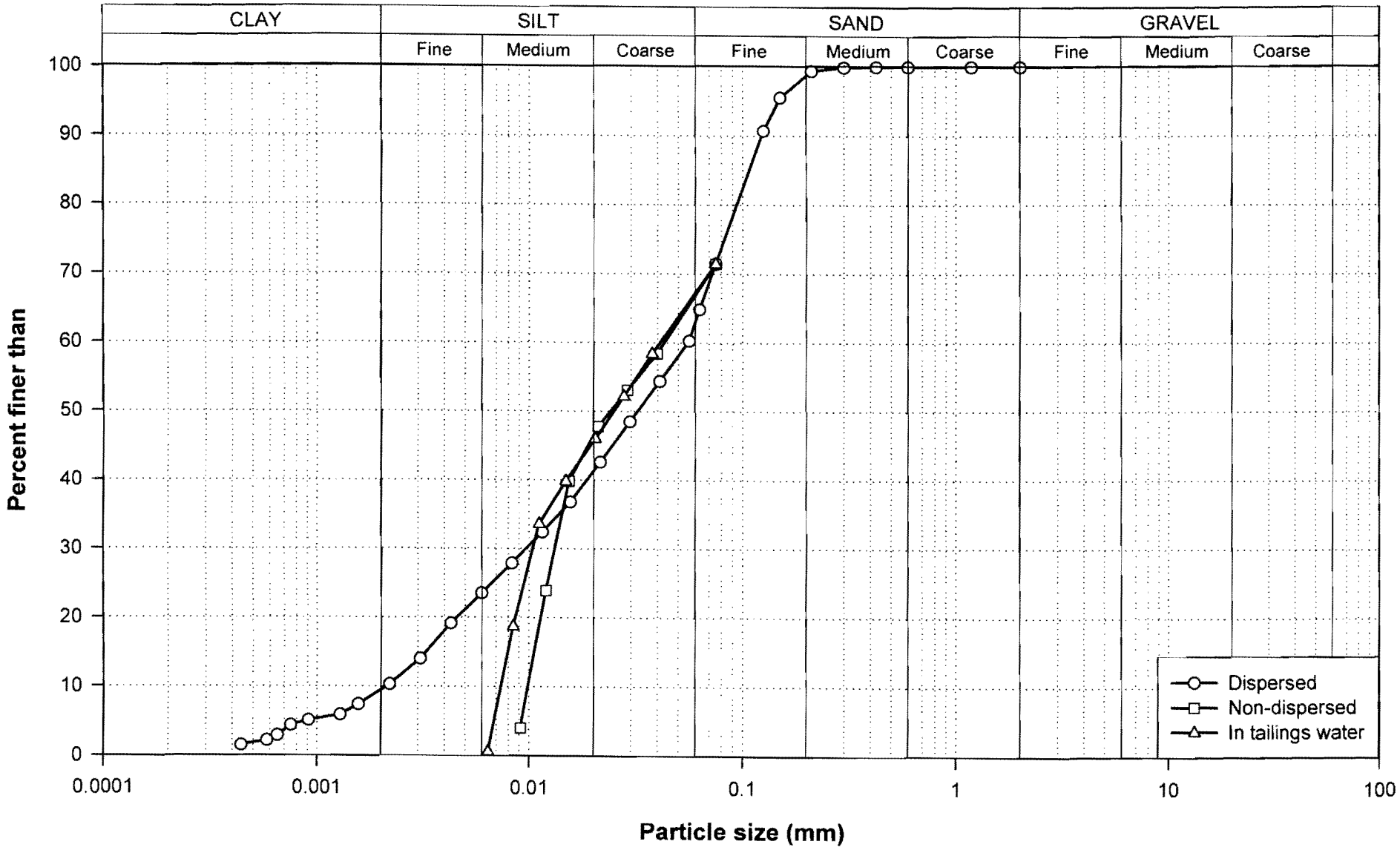

Figure 3-34: Grading curves for Mizpah Whole Tailings.

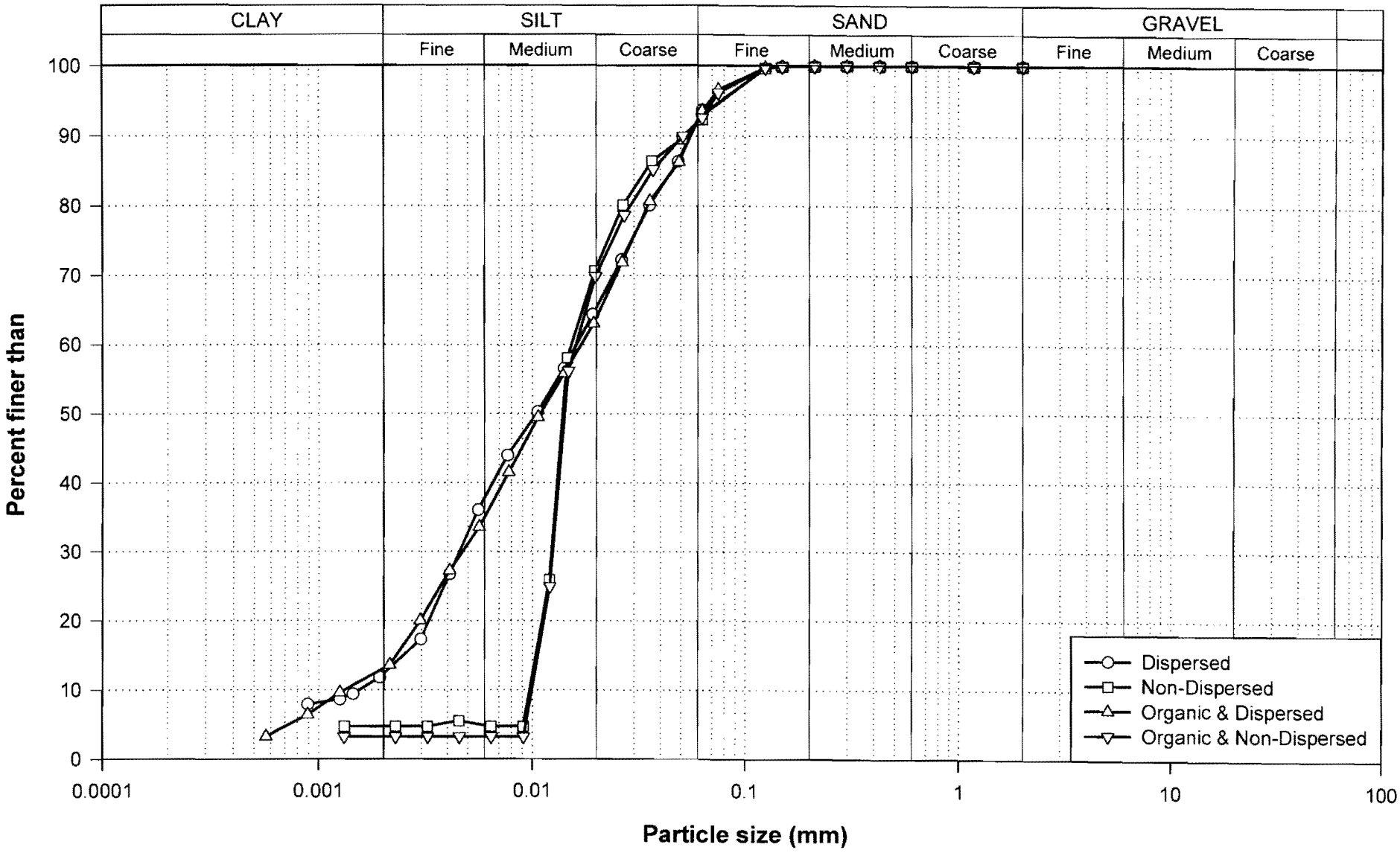

Figure 3-35: Grading curves for Mizpah Pond Fine Tailings.

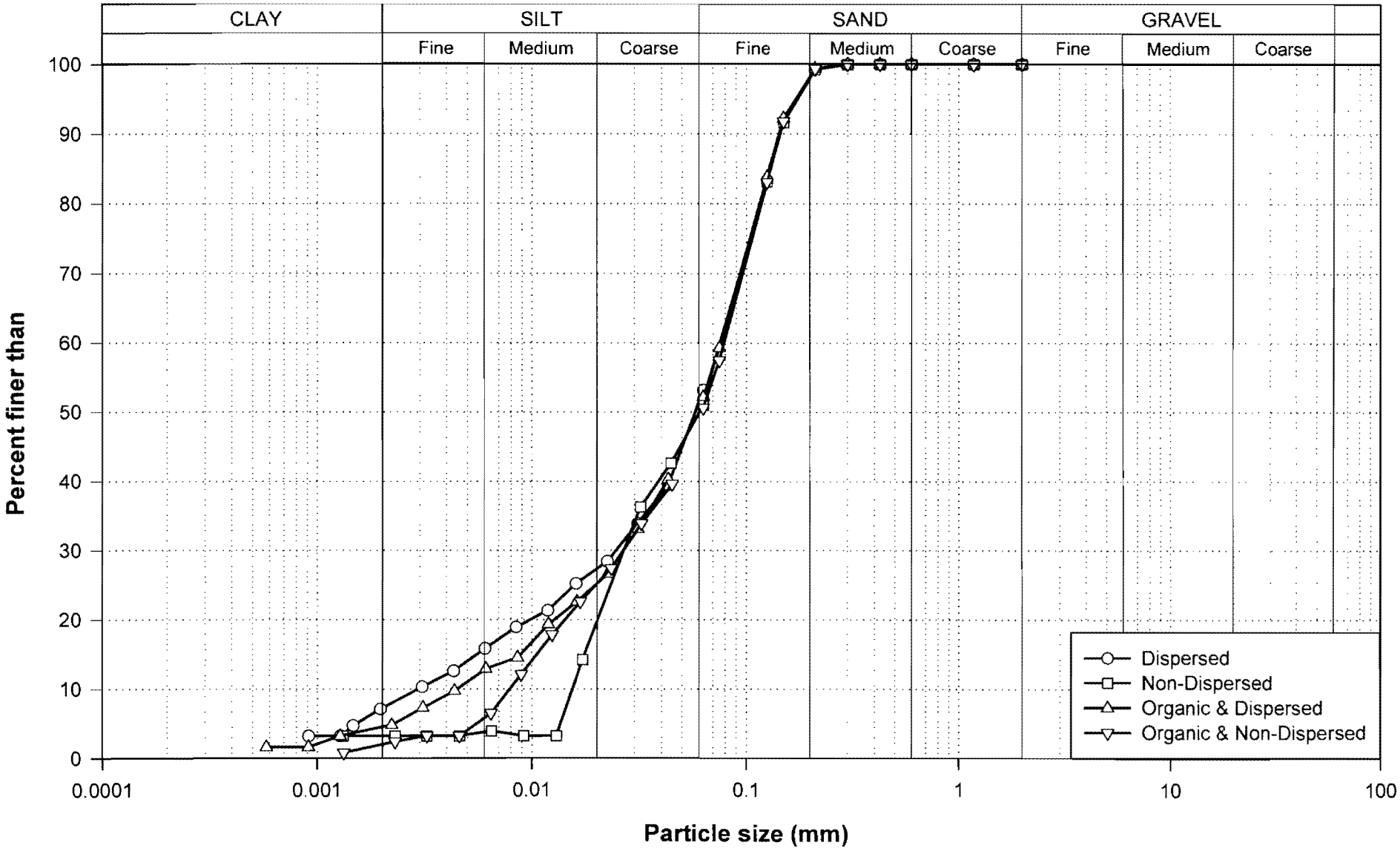

Figure 3-36: Grading curves for Mizpah Pond Coarse Tailings.

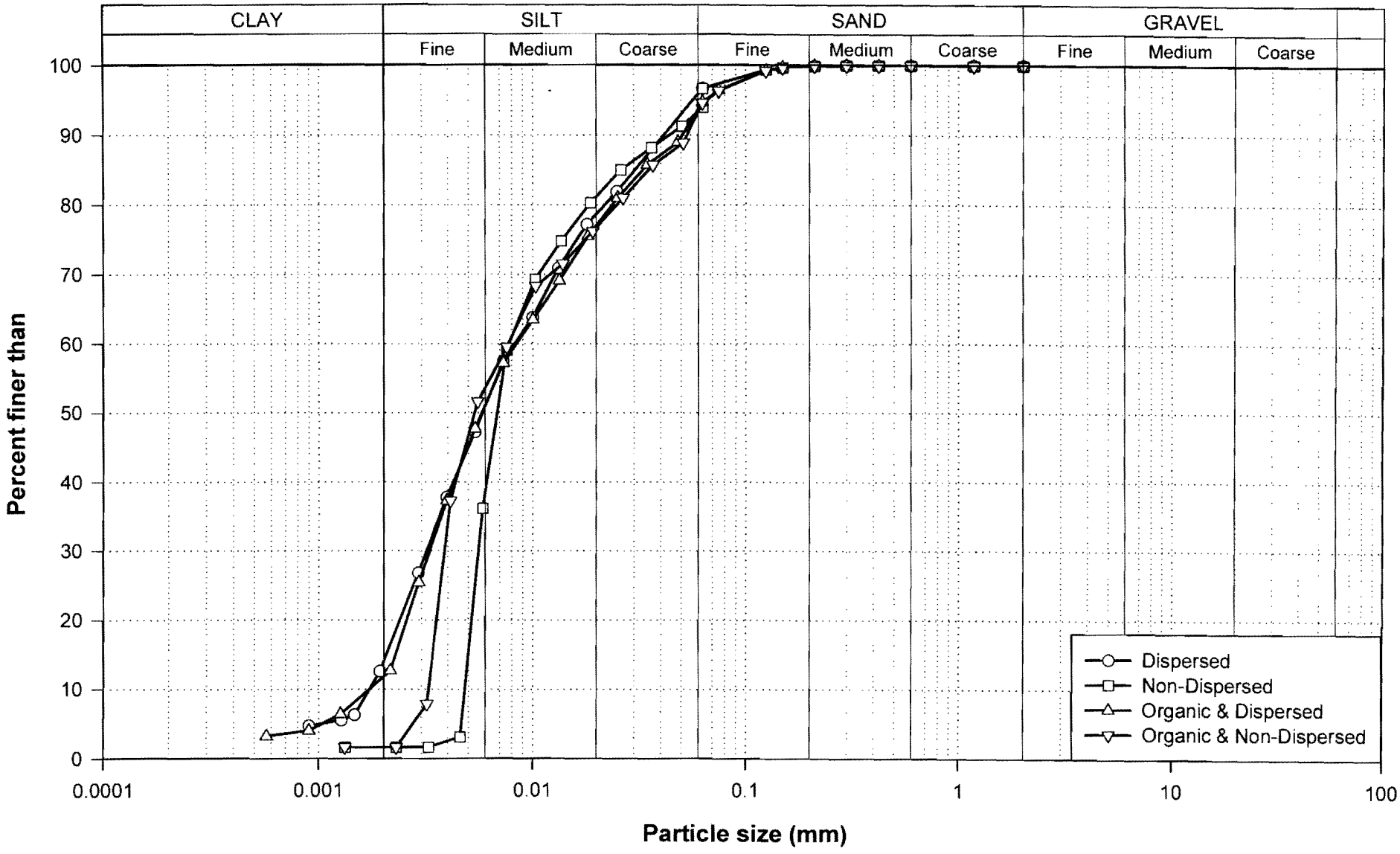

Figure 3-37: Grading curves for Pay Dam Penstock Fine Tailings.

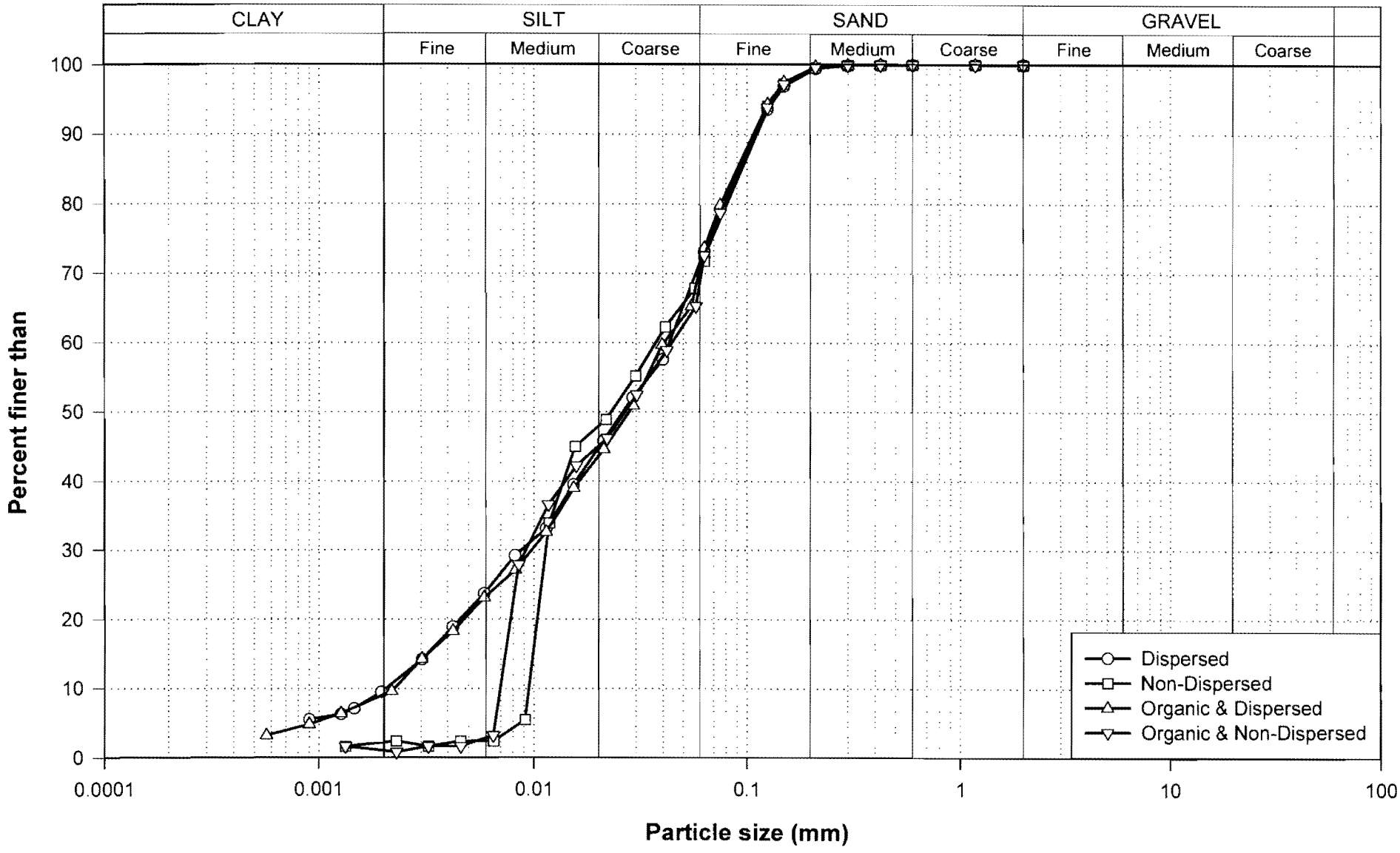

Figure 3-38: Grading curves for Pay Dam Penstock Coarse Tailings.

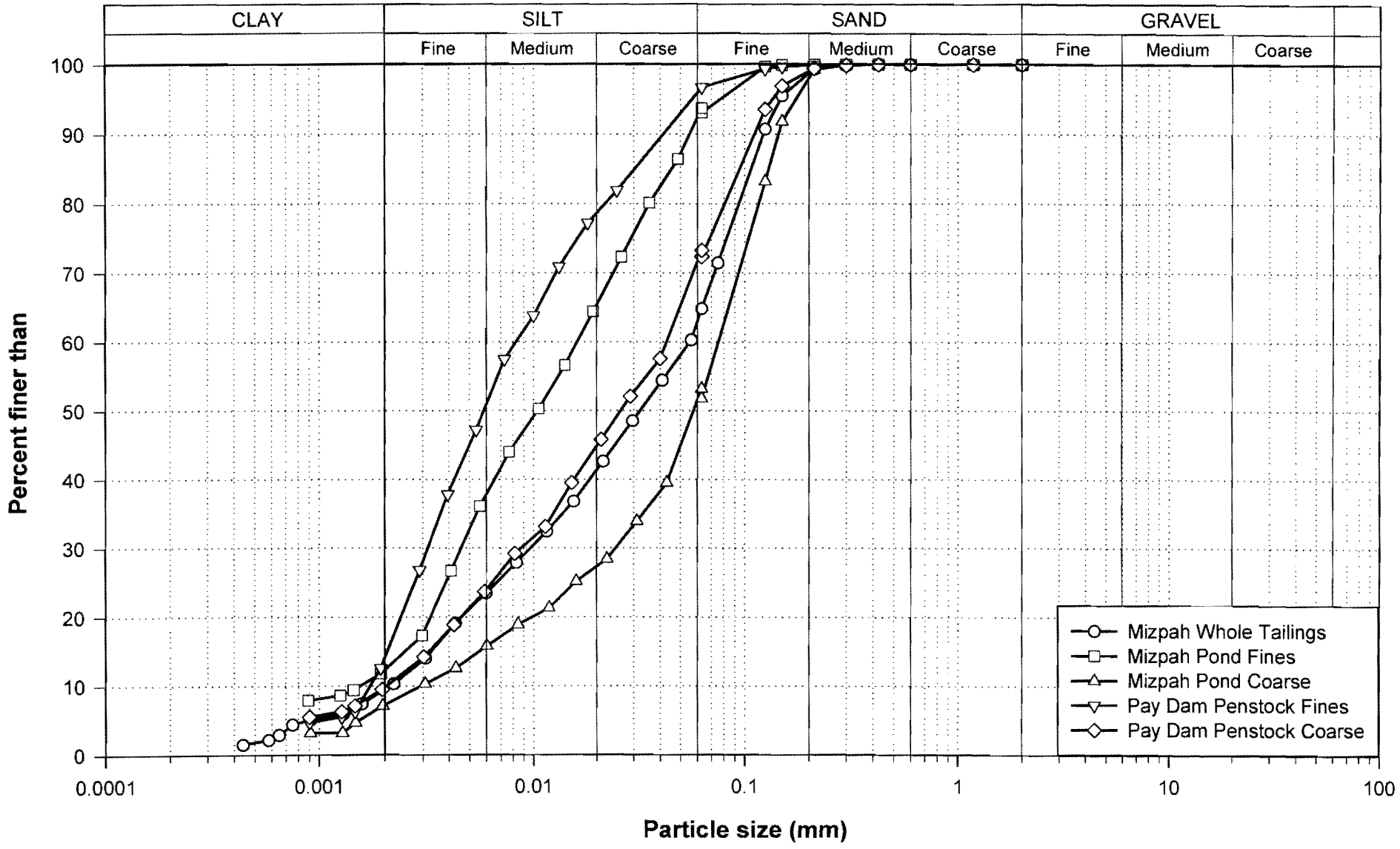

Figure 3-39: Grading curves of dispersed tailings combined.

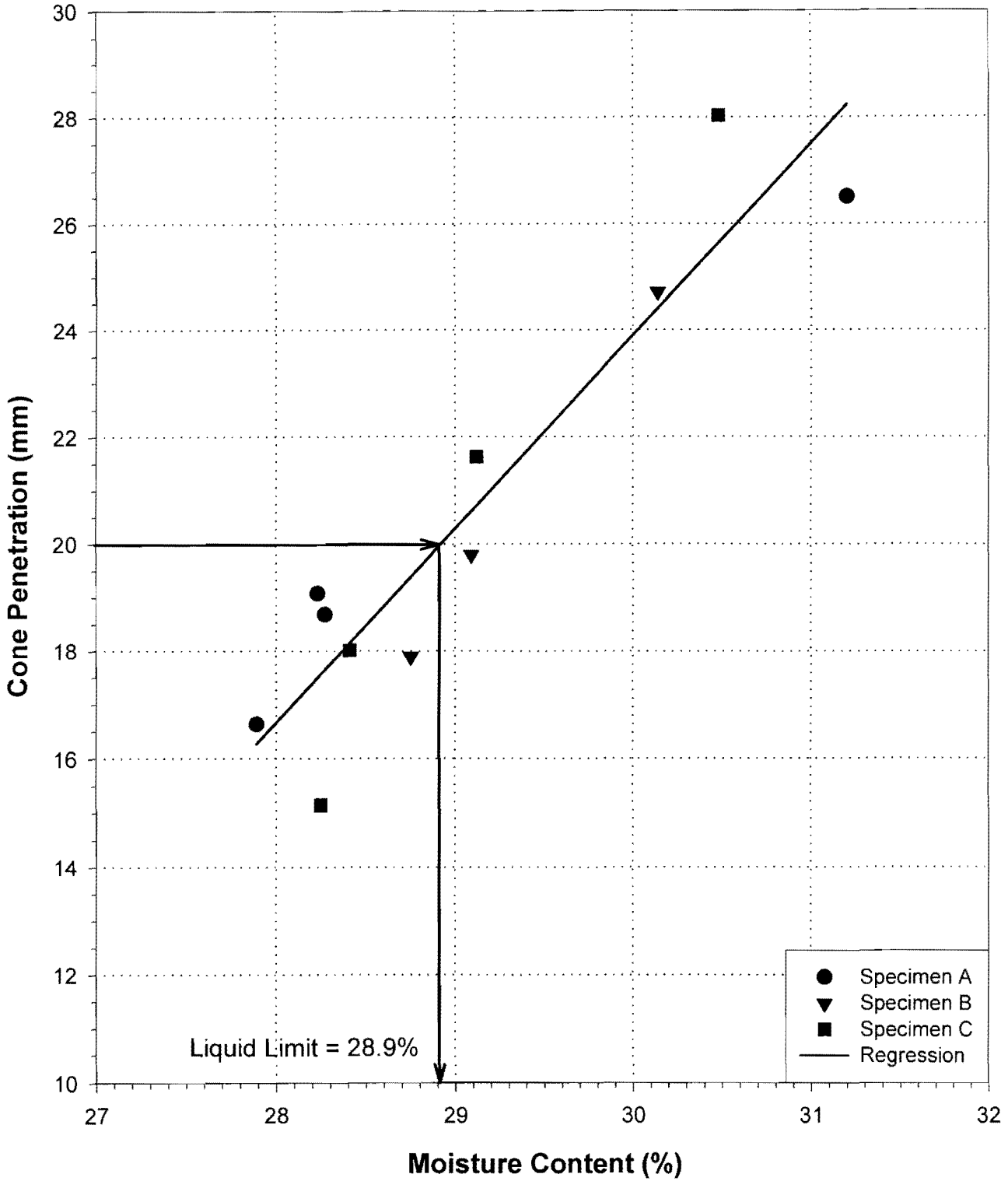

Figure 3-40: Liquid Limit by fall cone test: Mizpah Whole Tailings.

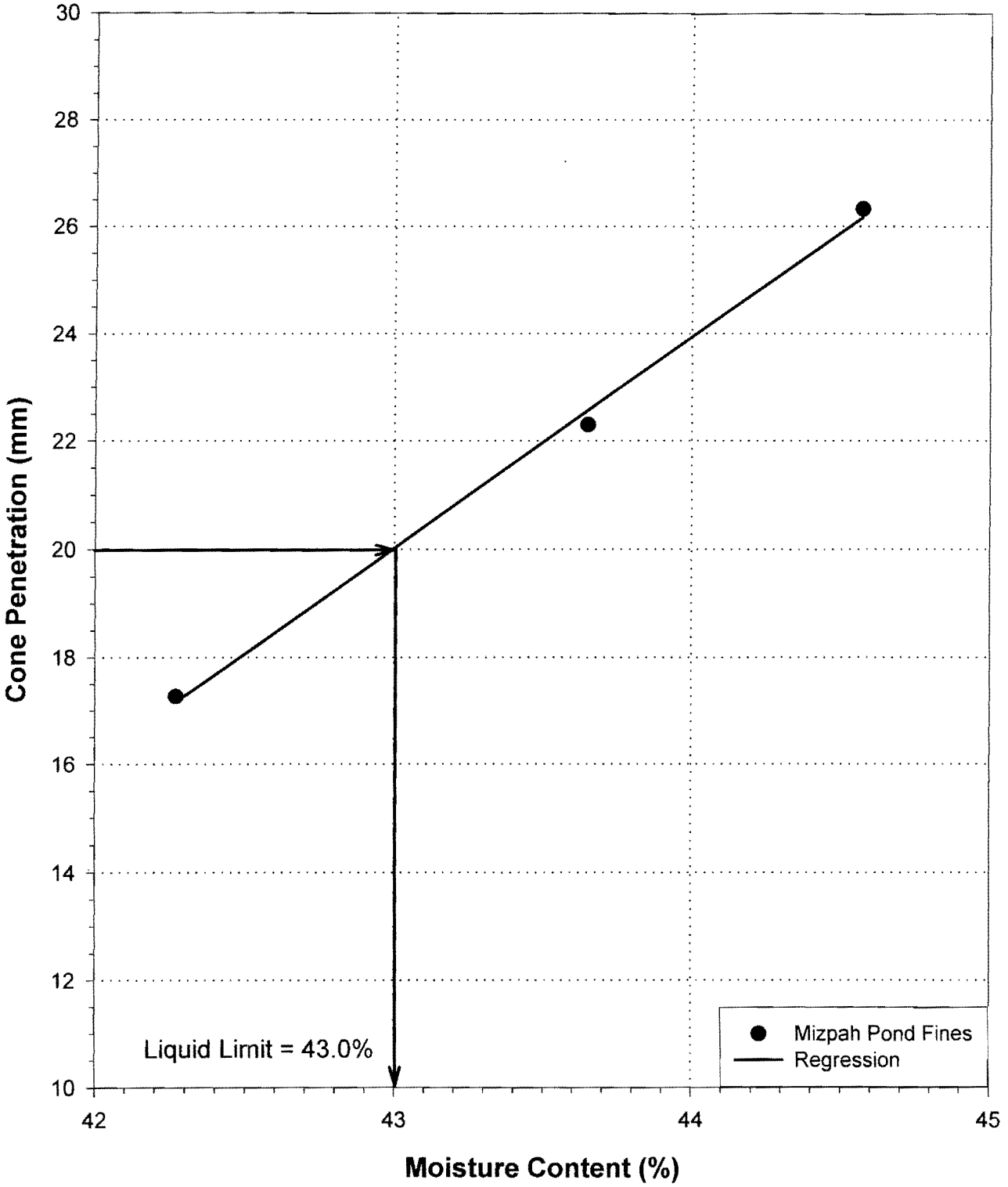

Figure 3-41: Liquid Limit by fall cone test: Mizpah Pond Fine Tailings.

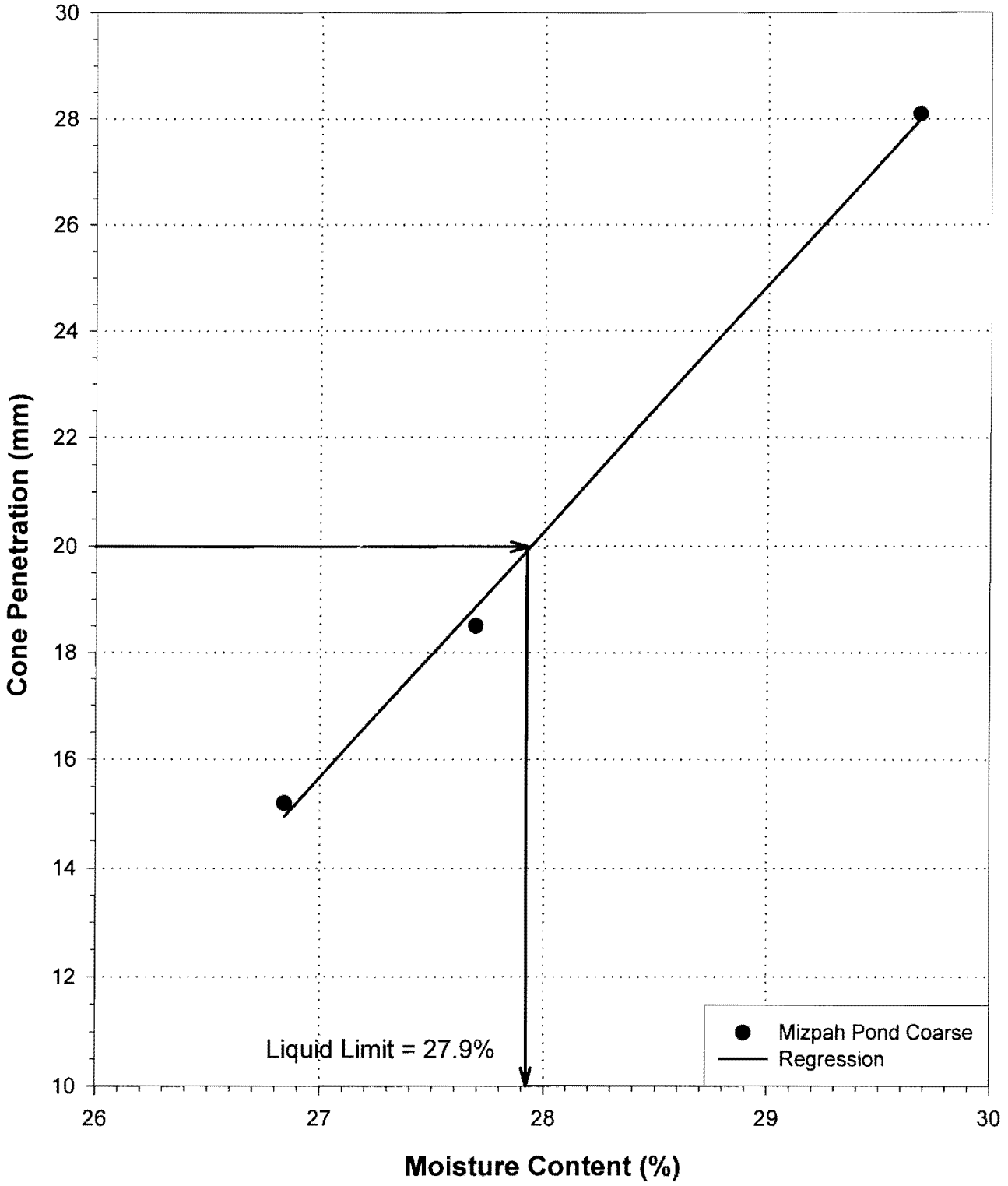

Figure 3-42: Liquid Limit by fall cone test: Mizpah Pond Coarse Tailings.

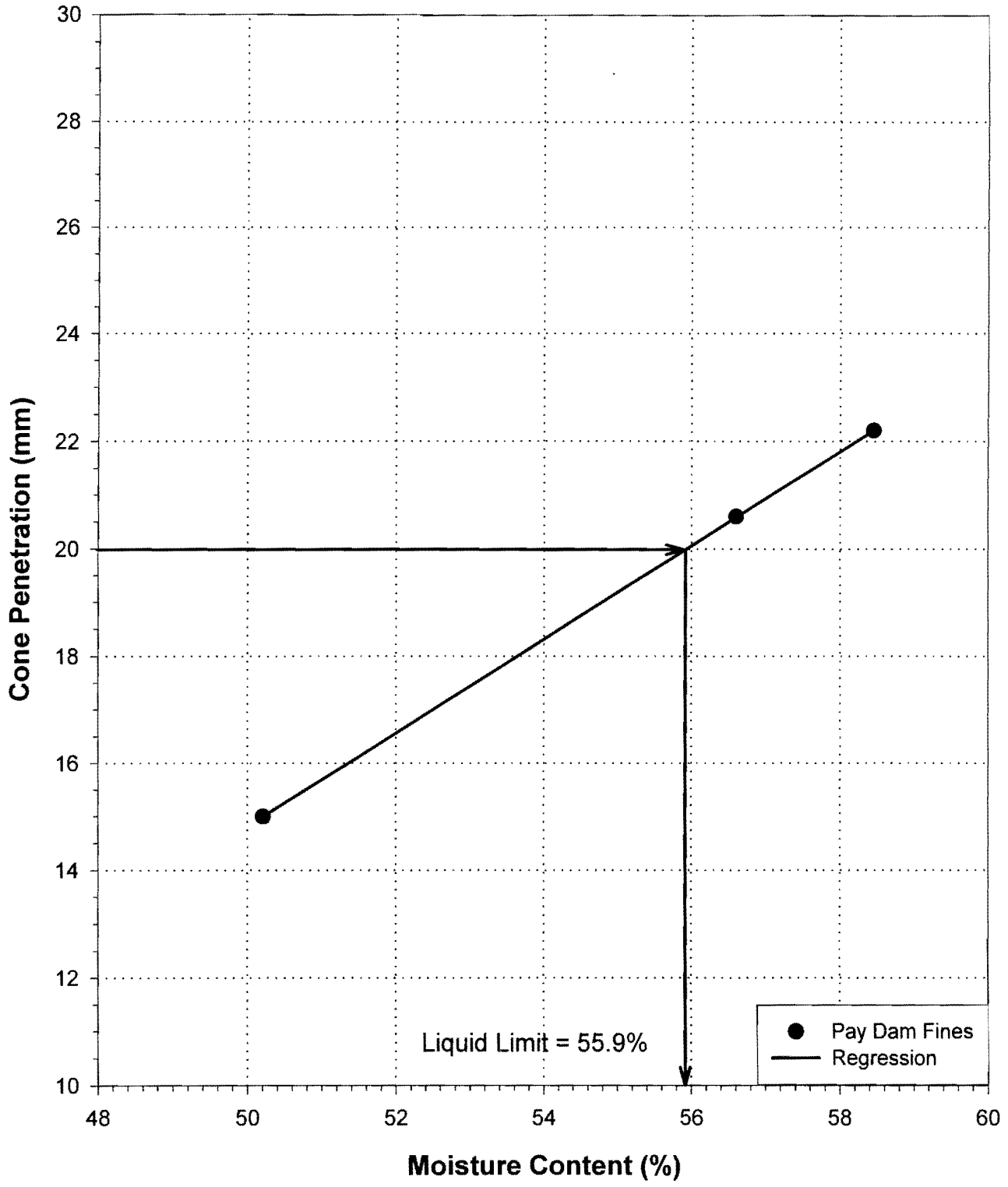

Figure 3-43: Liquid Limit by fall cone test: Pay Dam Penstock Fine Tailings.

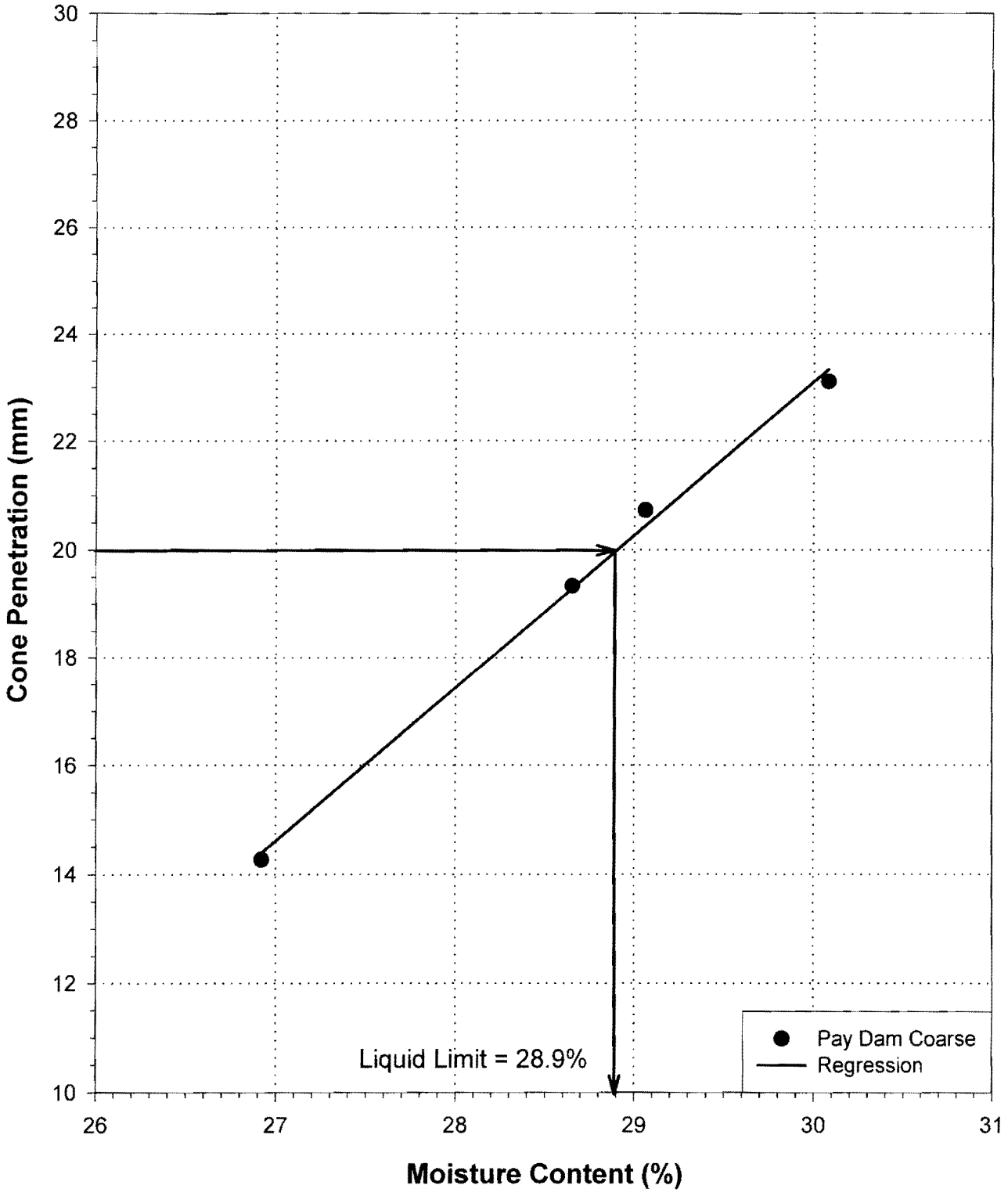

Figure 3-44: Liquid Limit by fall cone test: Pay Dam Penstock Coarse Tailings.

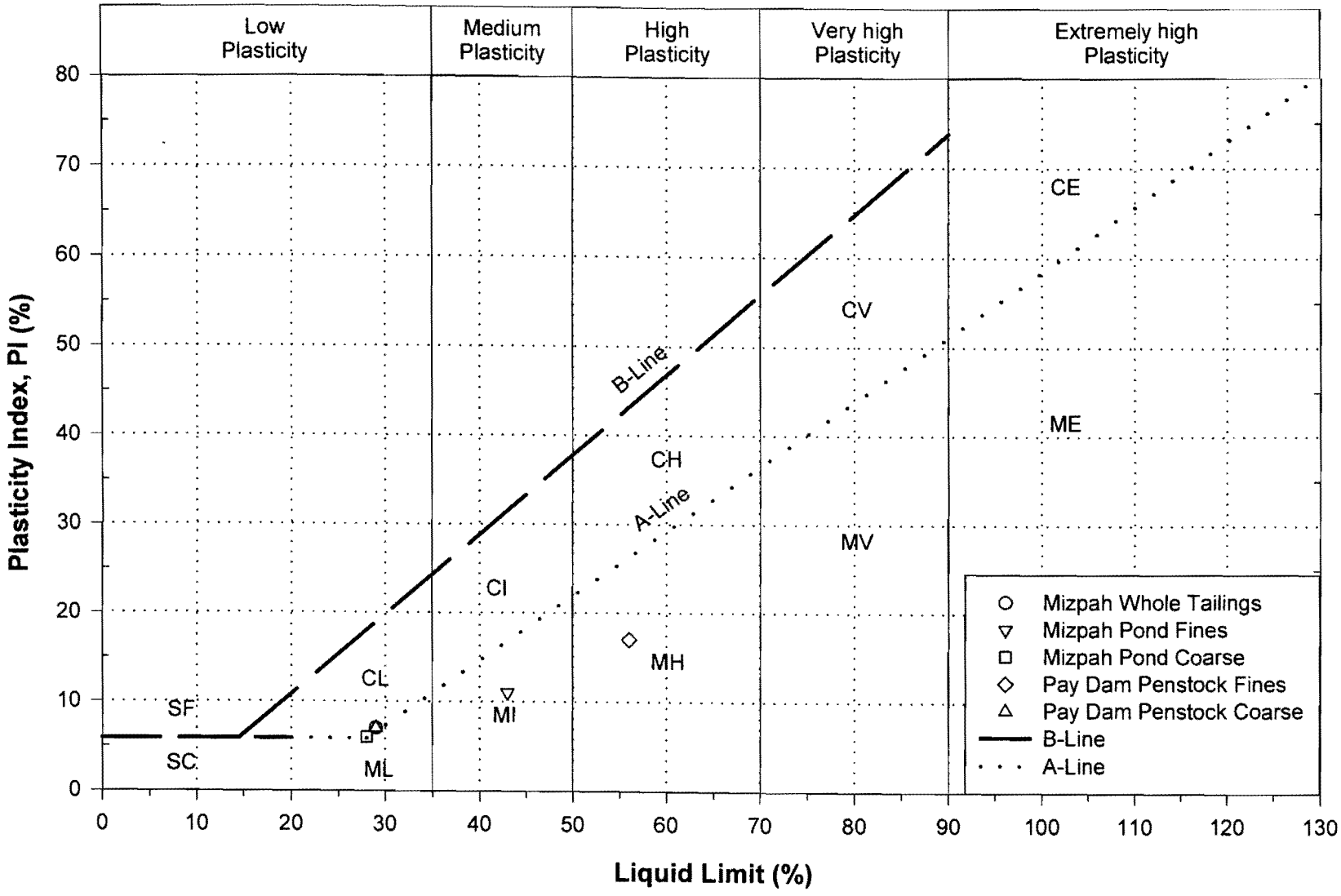

Figure 3-45: Plasticity chart classification of Mizpah and Pay Dam tailings.

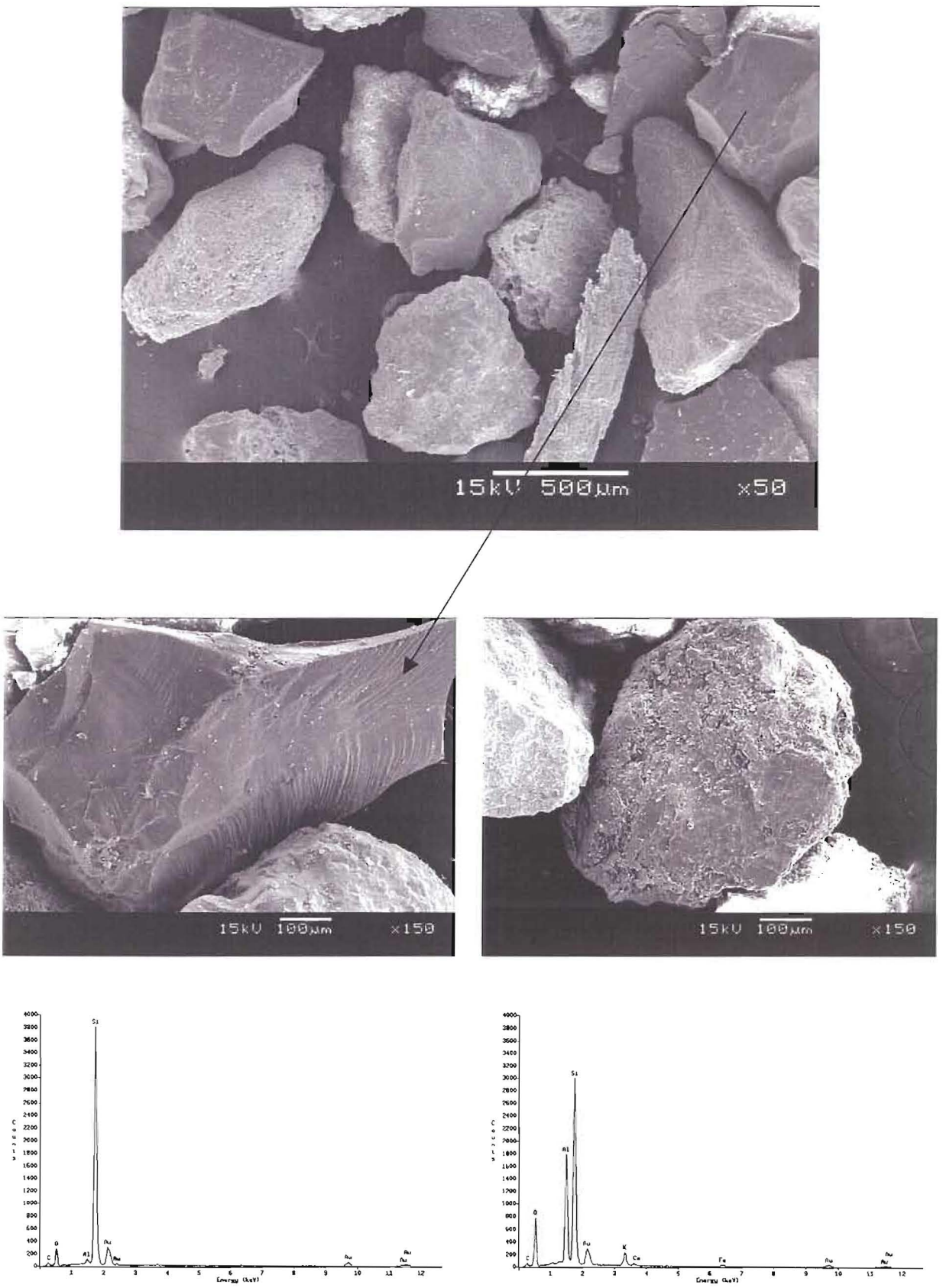

Figure 3-46: Mizpah Whole Tailings, dispersed and retained on the 425 µm sieve.

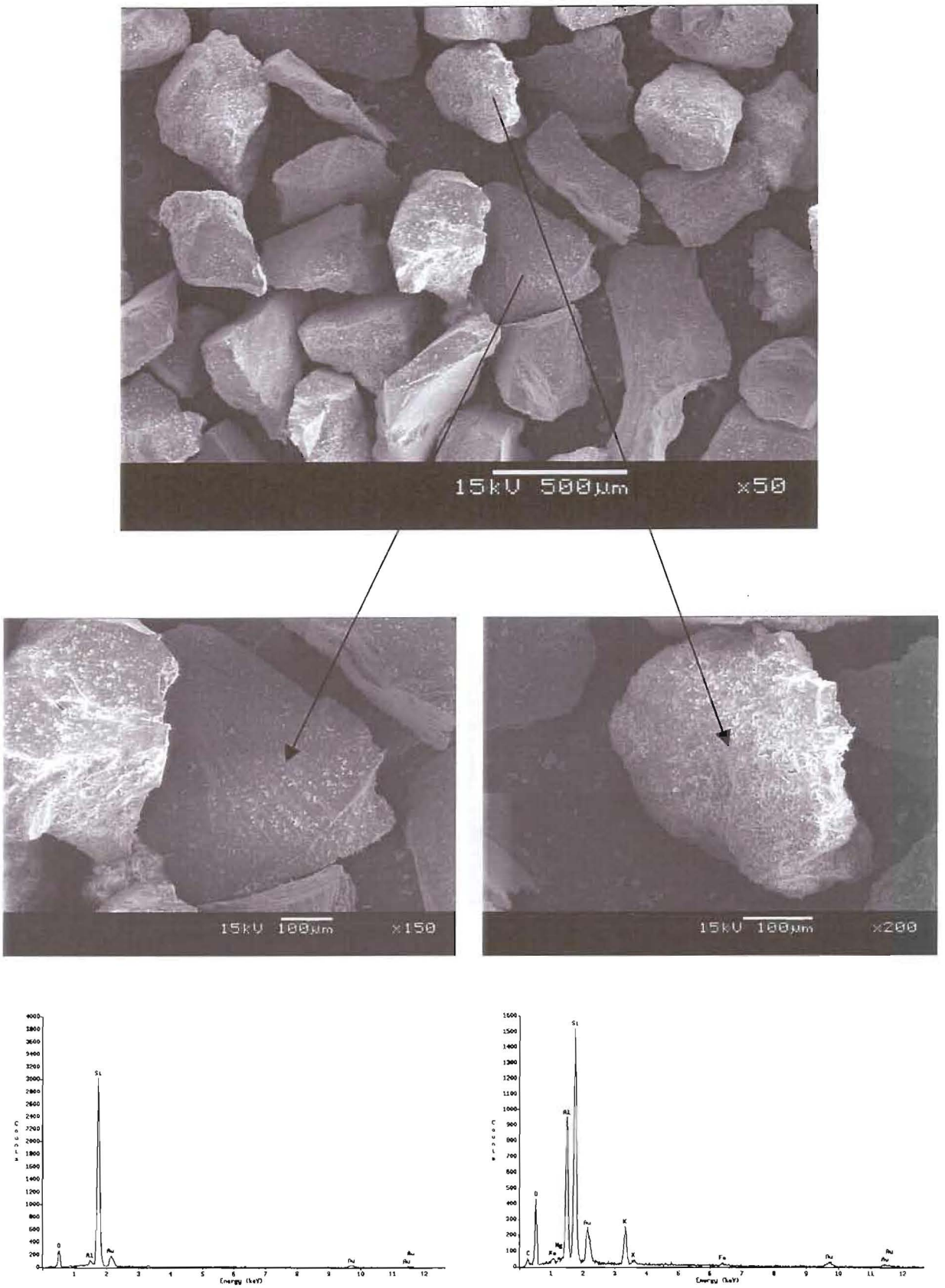

Figure 3-47: Mizpah Whole Tailings, dispersed and retained on the 300 µm sieve.

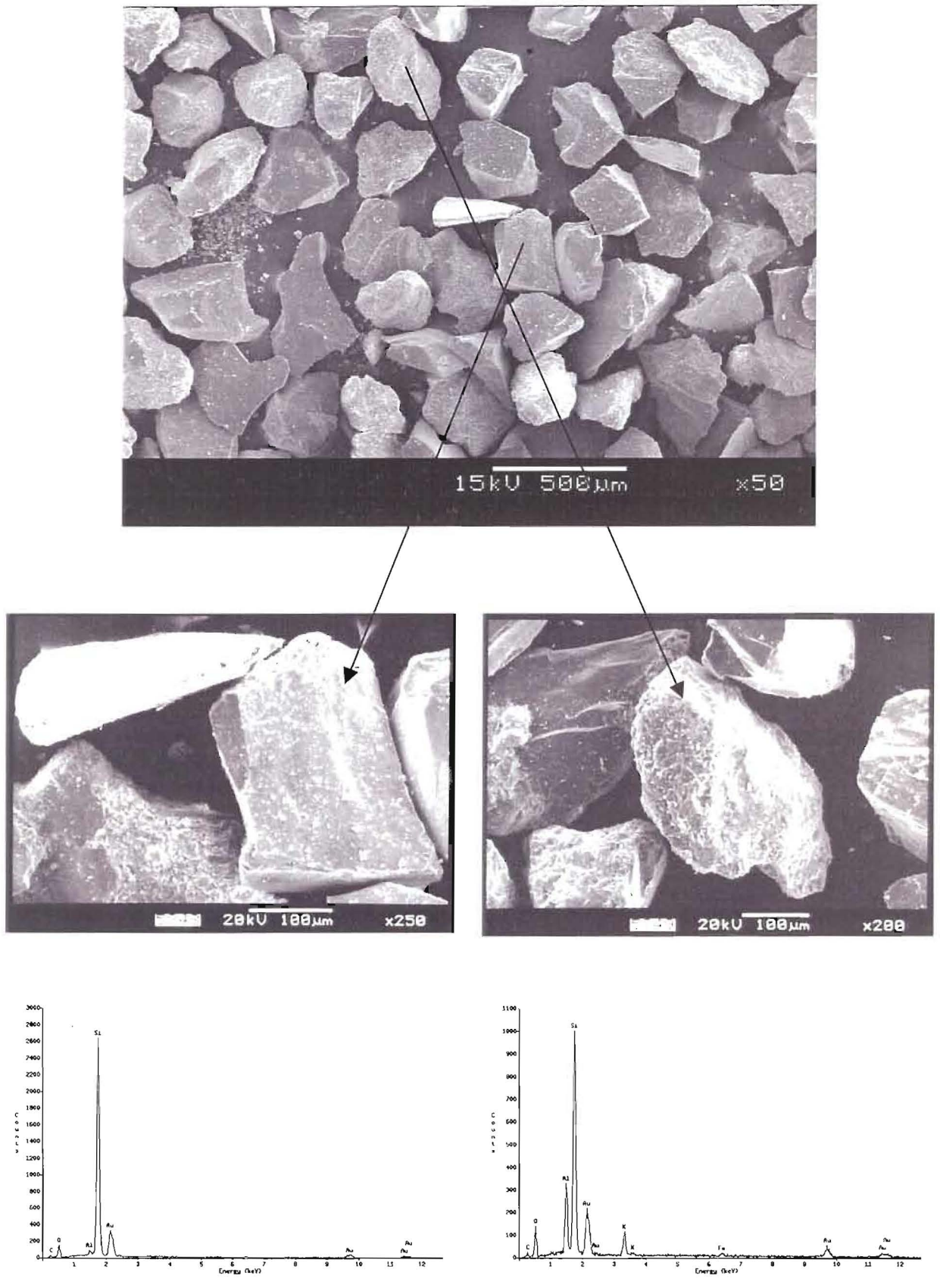

Figure 3-48: Mizpah Whole Tailings, dispersed and retained on the 212 µm sieve.

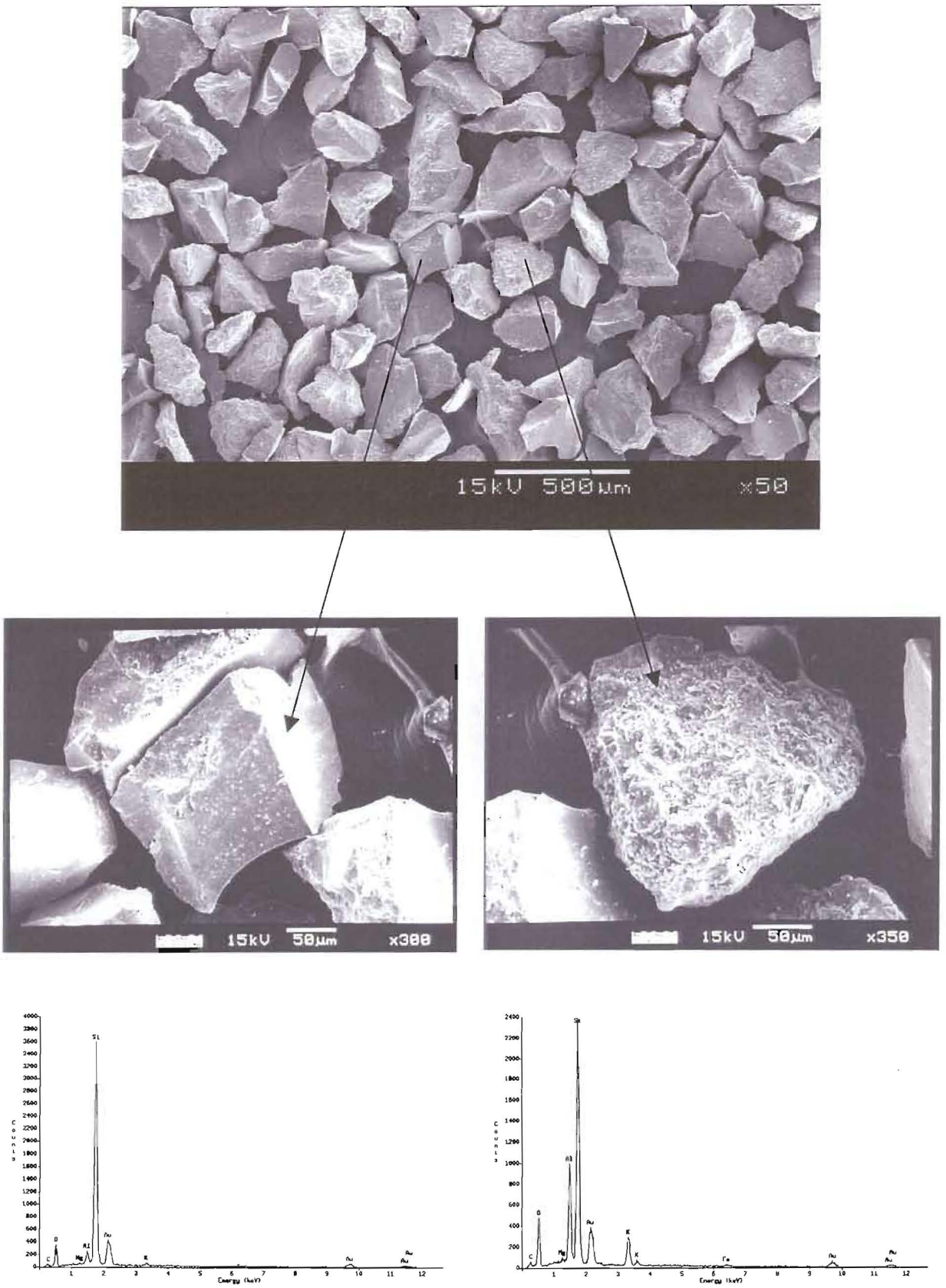

Figure 3-49: Mizpah Whole Tailings, dispersed and retained on the 150 µm sieve.

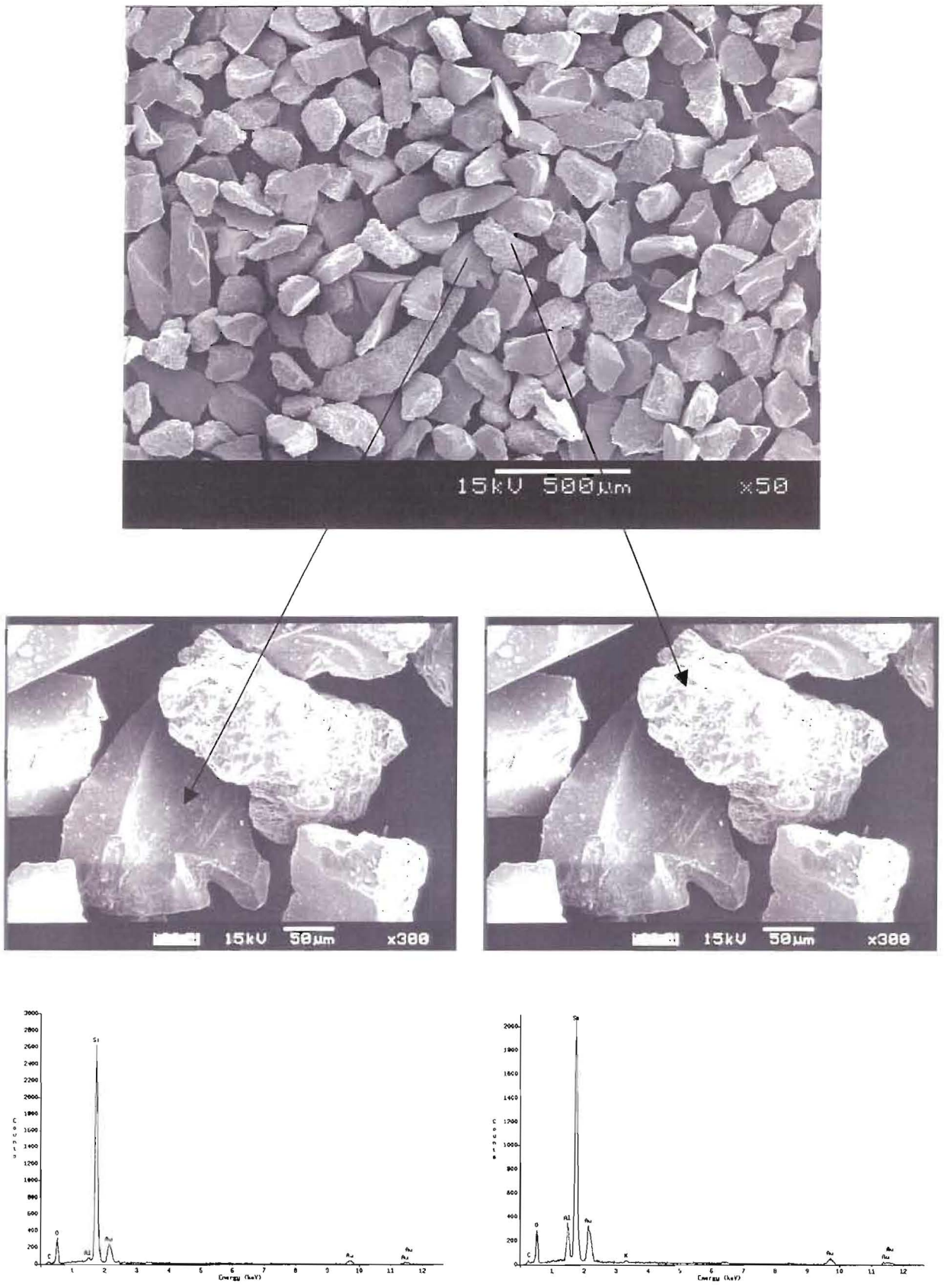

Figure 3-50: Mizpah Whole Tailings, dispersed and retained on the 125 µm sieve.

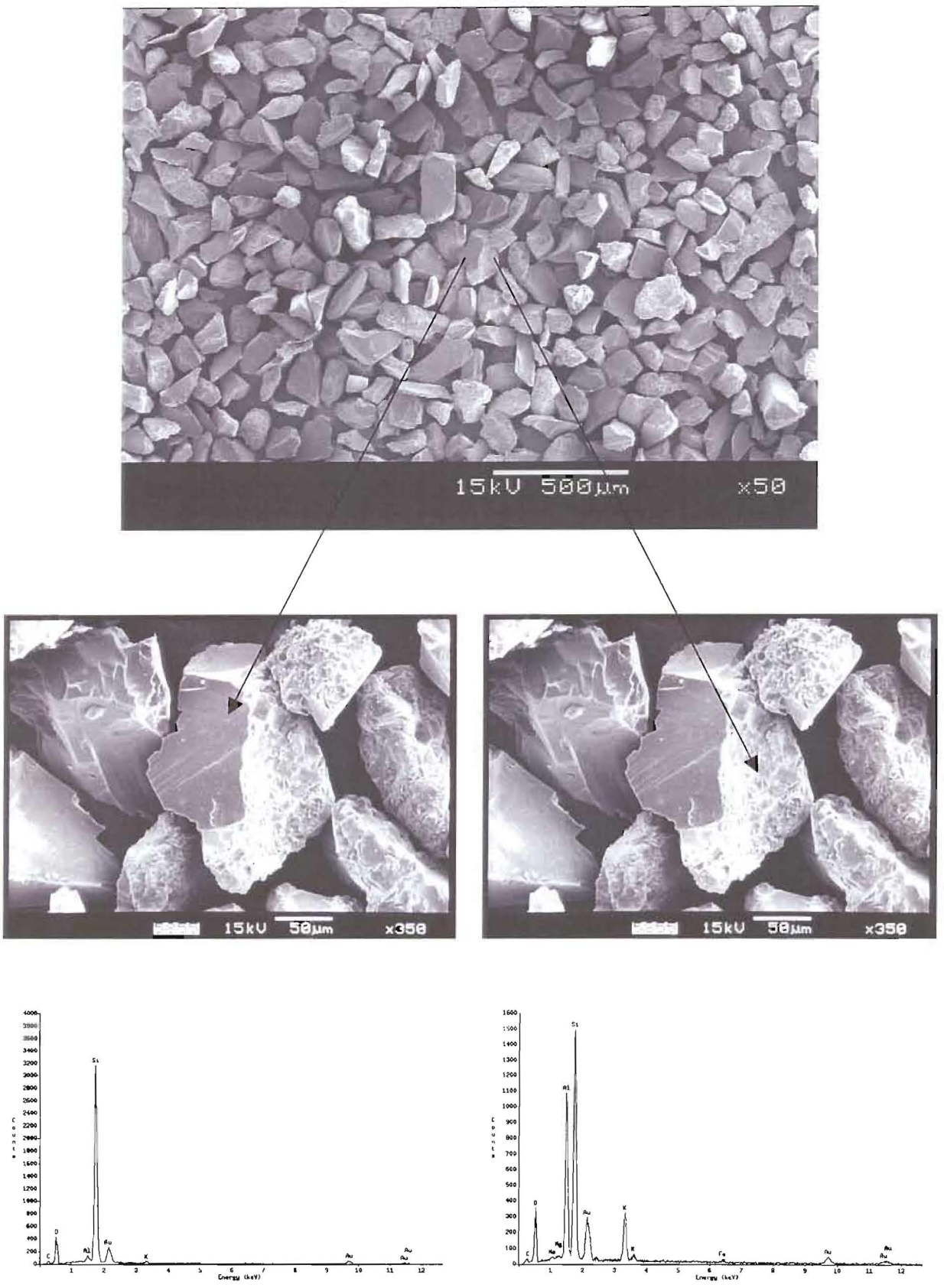

Figure 3-51: Mizpah Whole Tailings, dispersed and retained on the 75 µm sieve.

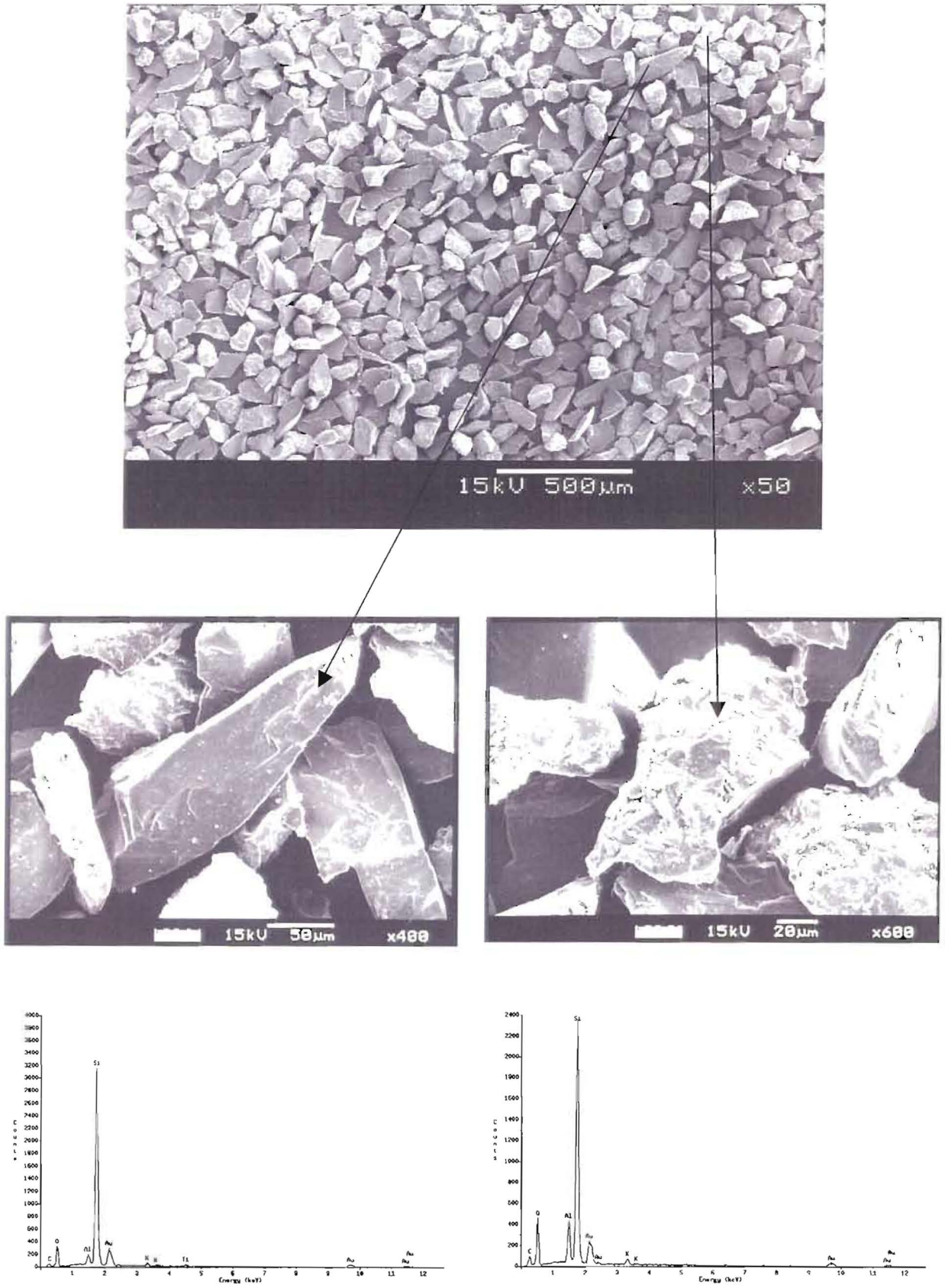

Figure 3-52: Mizpah Whole Tailings, dispersed and retained on the 63 µm sieve.

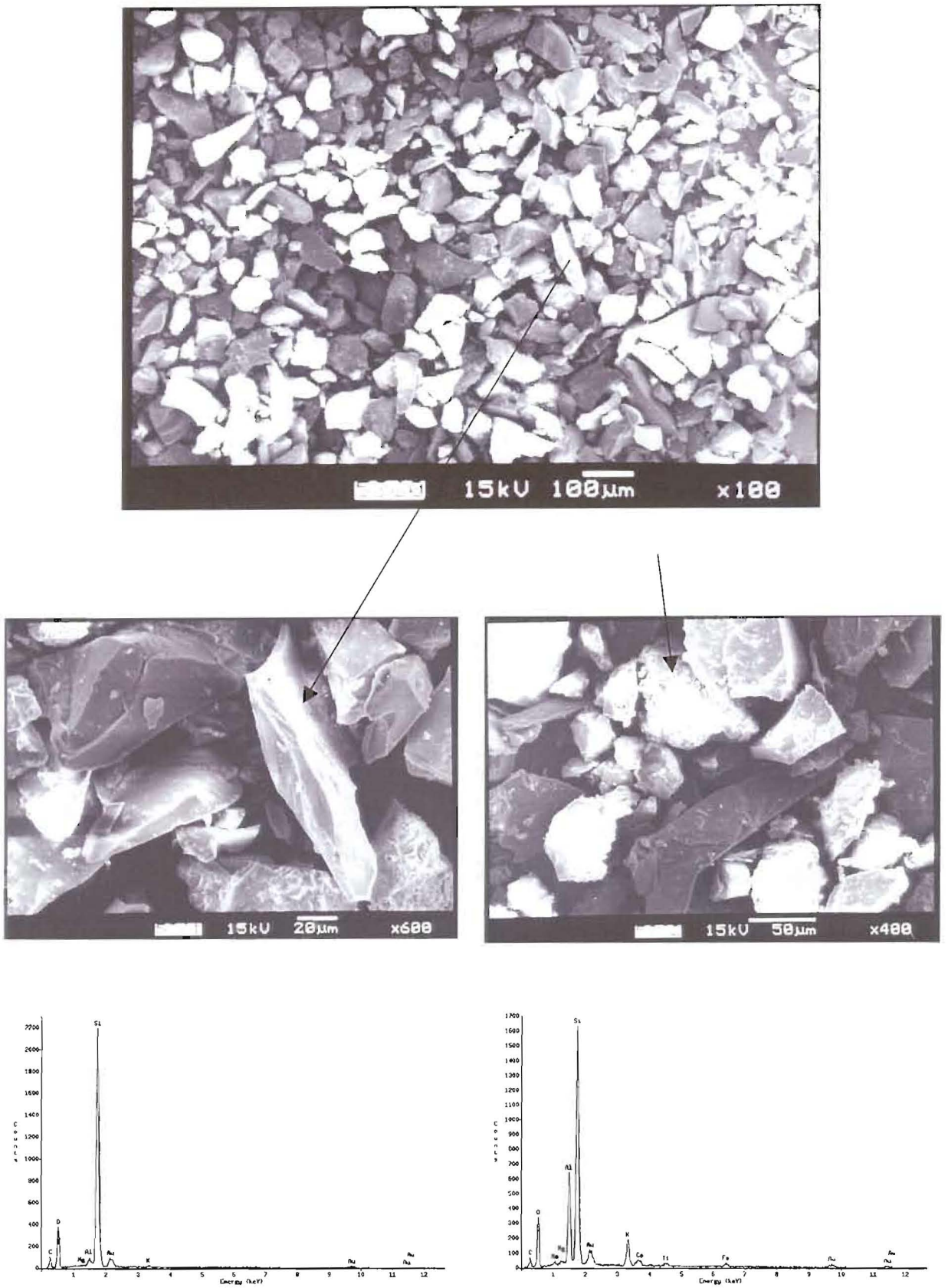

Figure 3-53: Mizpah Whole Tailings, dispersed and settled after 4 minutes or >20 µm.

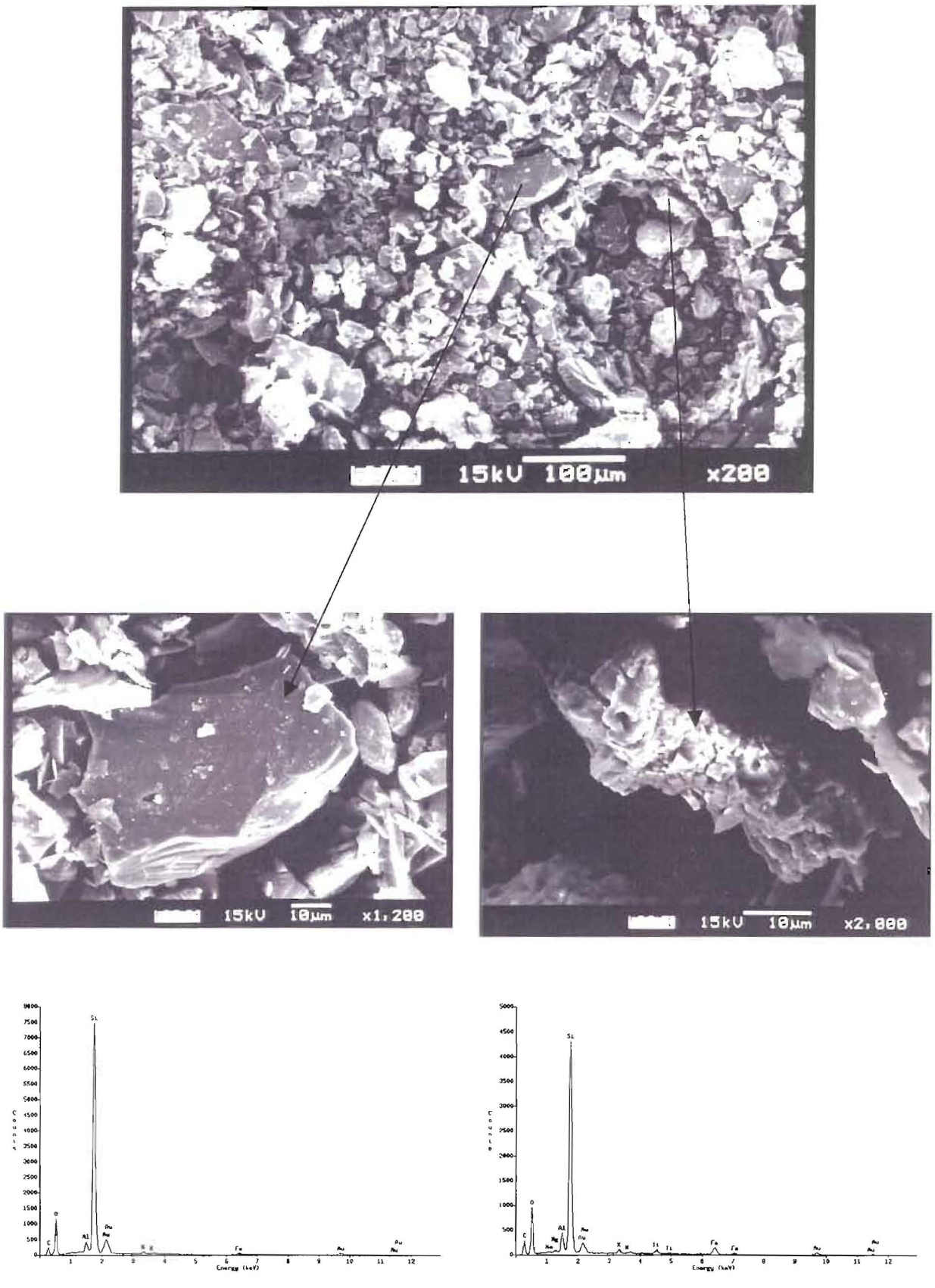

Figure 3-54: Mizpah Whole Tailings, dispersed and settled after 15 minutes or >10 µm.

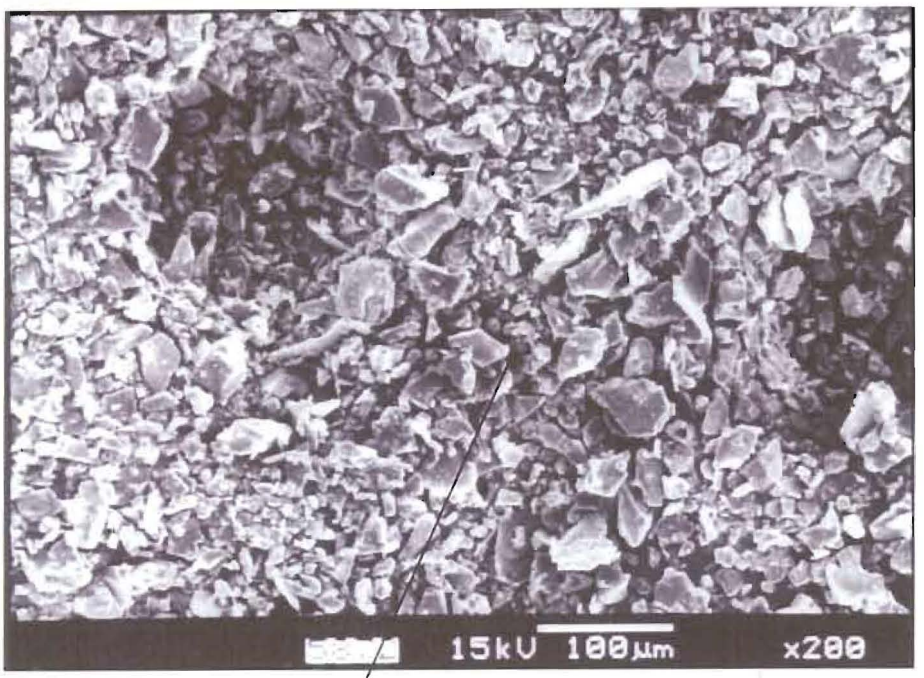

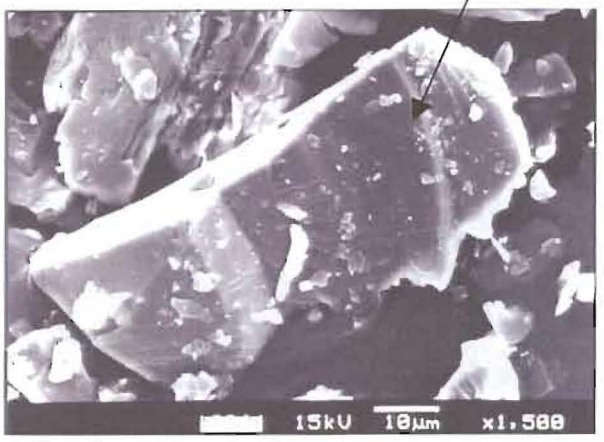

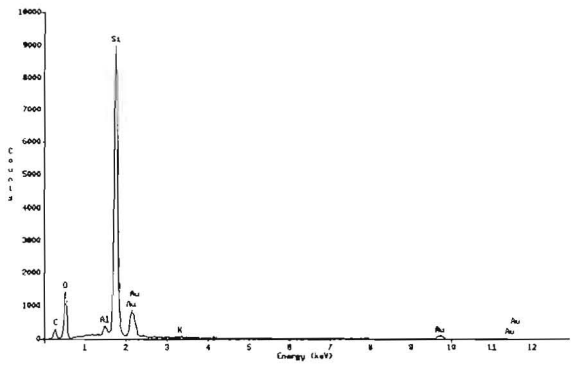

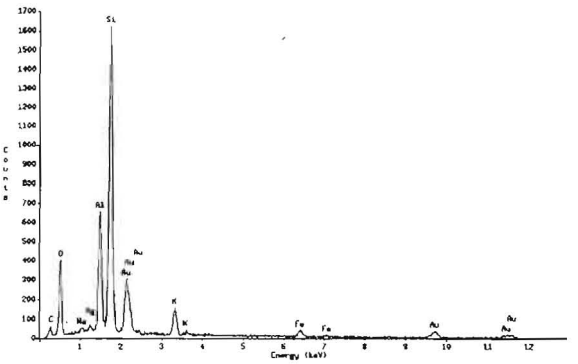

Figure 3-55: Mizpah Whole Tailings, dispersed and settled after 30 minutes or >8 µm.

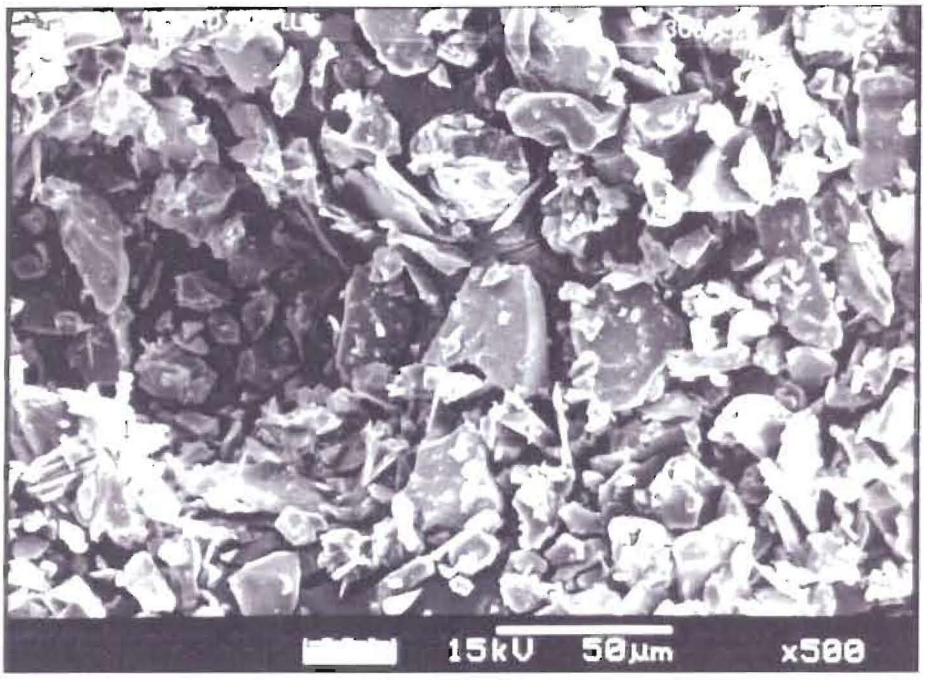

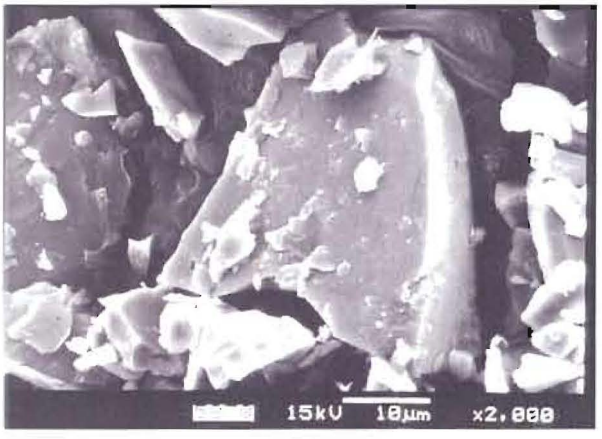

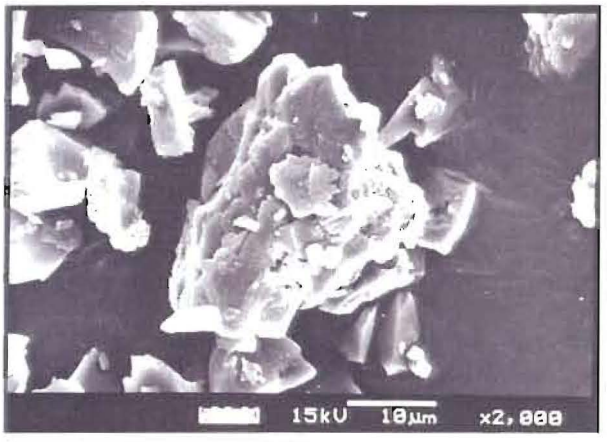

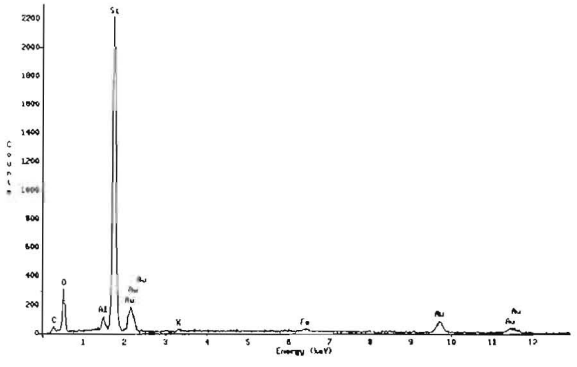

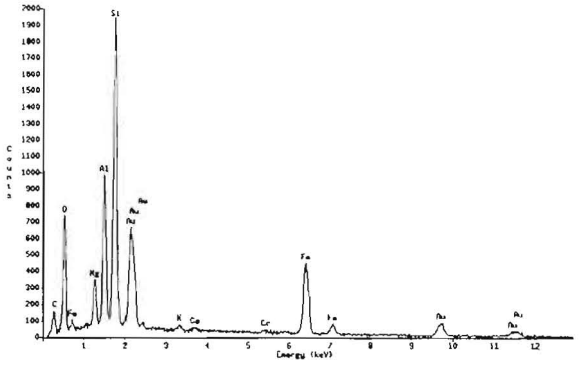

Figure 3-56: Mizpah Whole Tailings, dispersed and settled after 1 hour or >6 µm.

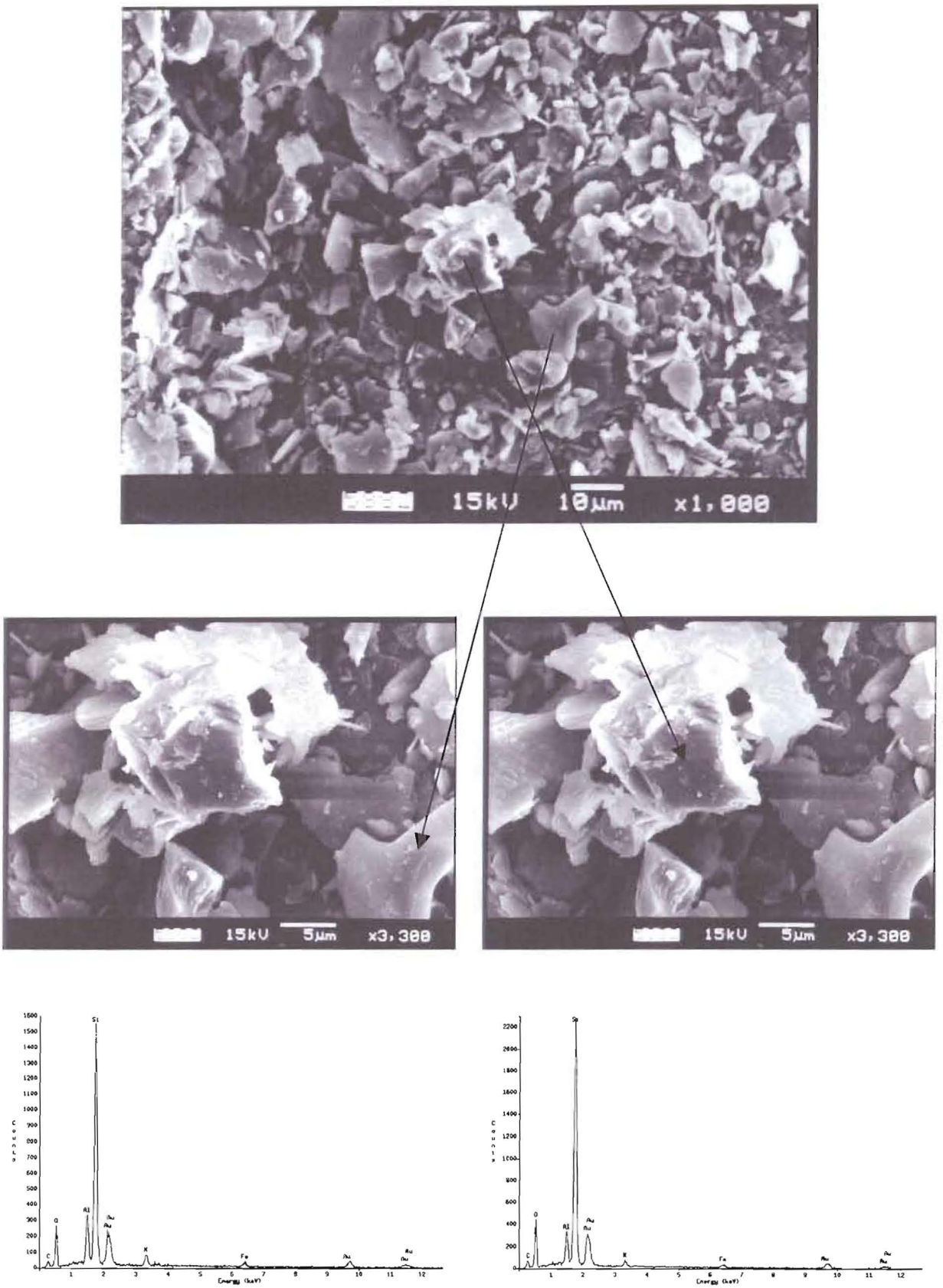

Figure 3-57: Mizpah Whole Tailings, dispersed and settled after 4 hour or >3 µm.

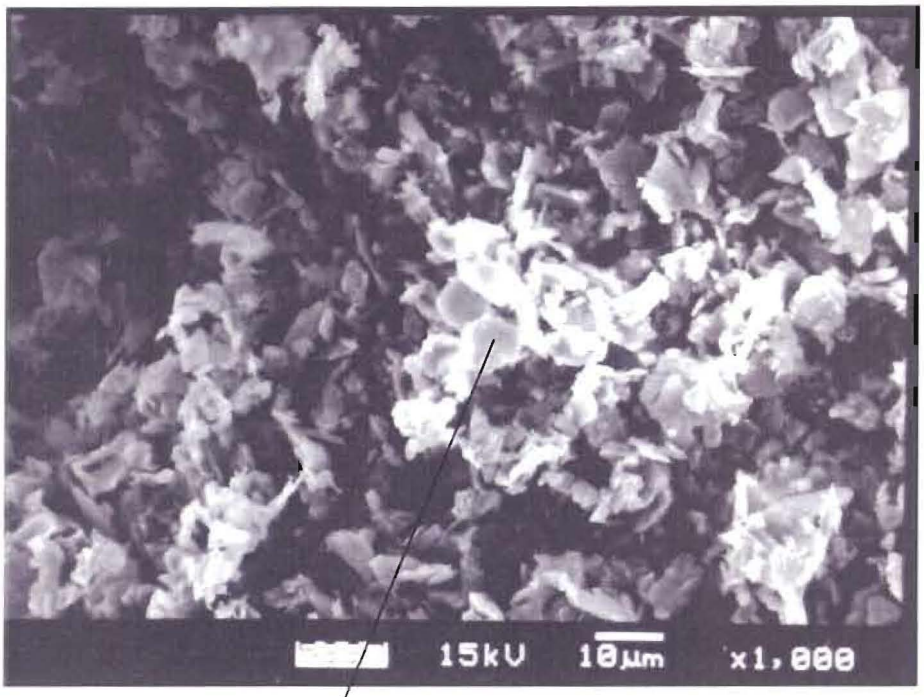

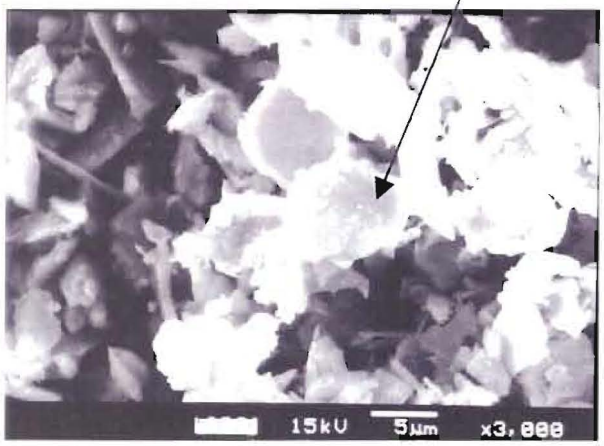

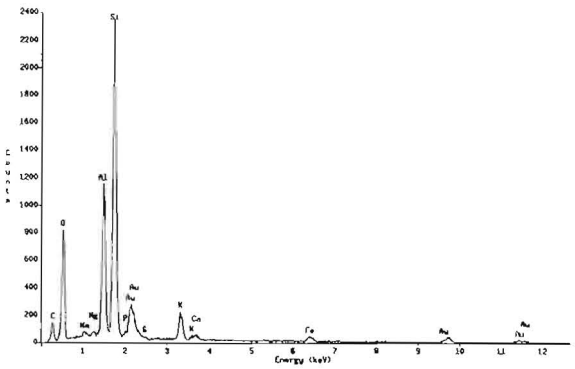

Figure 3-58: Mizpah Whole Tailings, dispersed and settled after 8 hours or >2 µm.

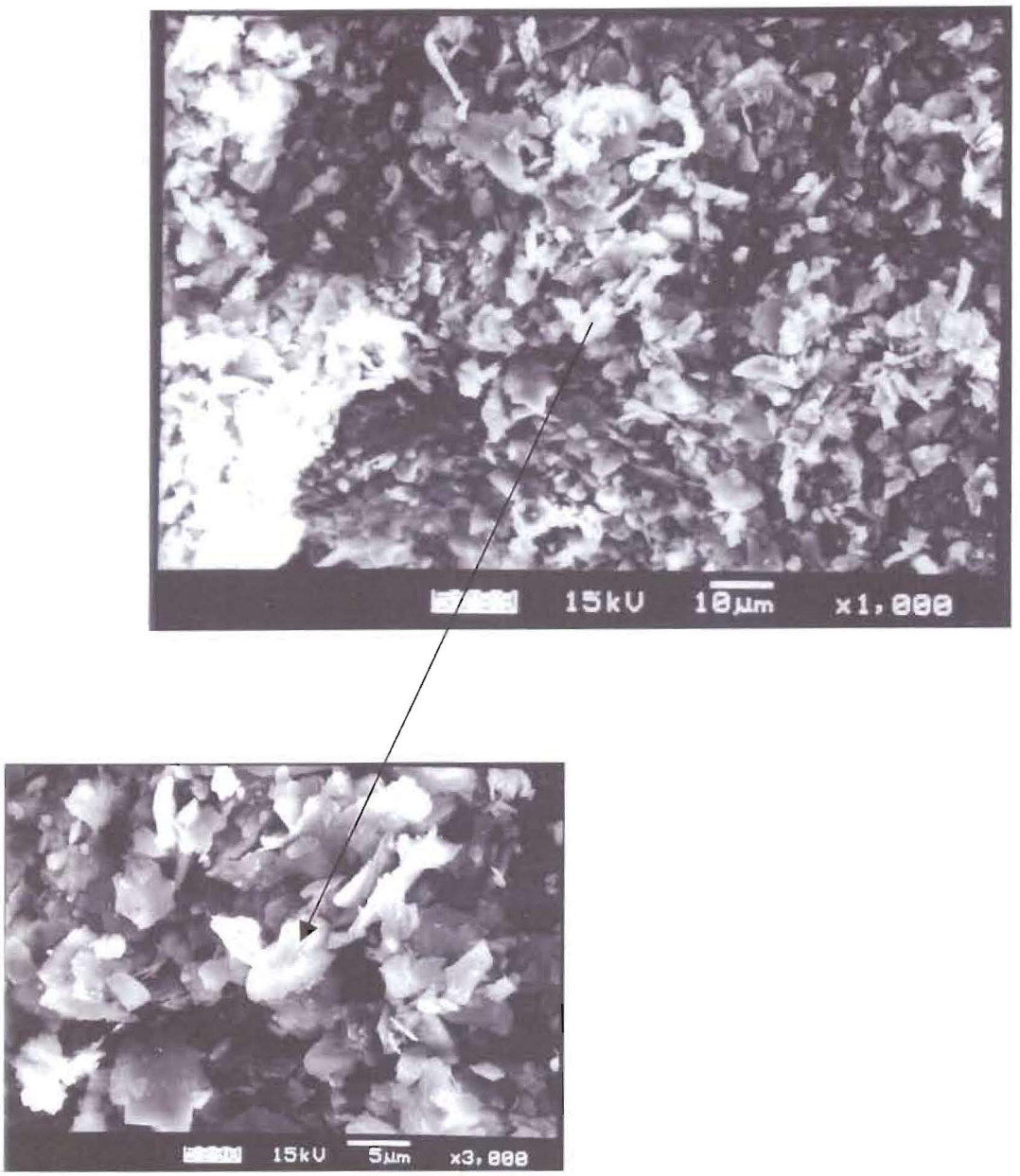

Figure 3-59: Mizpah Whole Tailings, dispersed and settled after 16 hours or >1.5 µm.

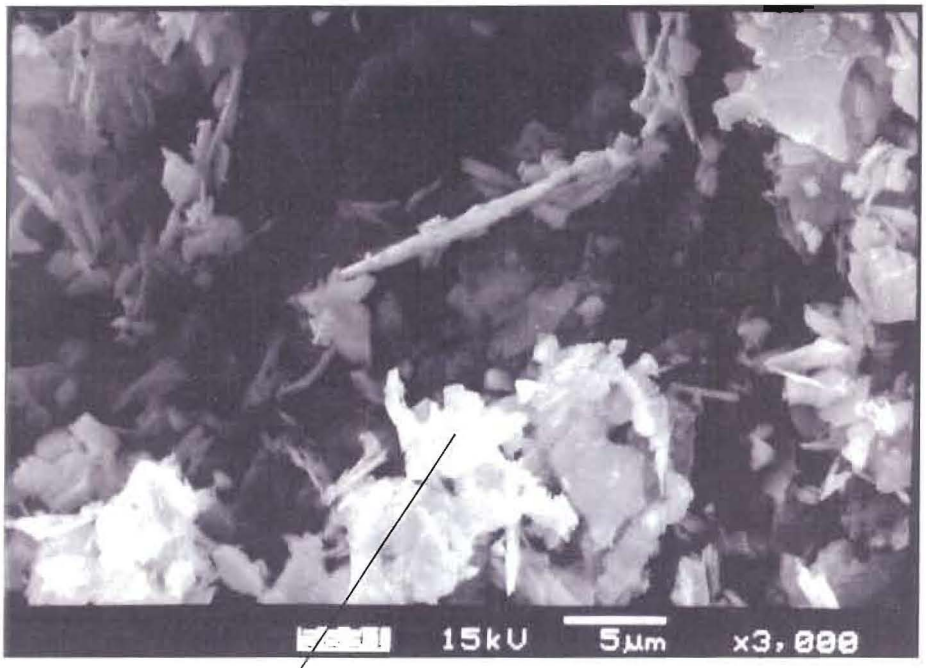

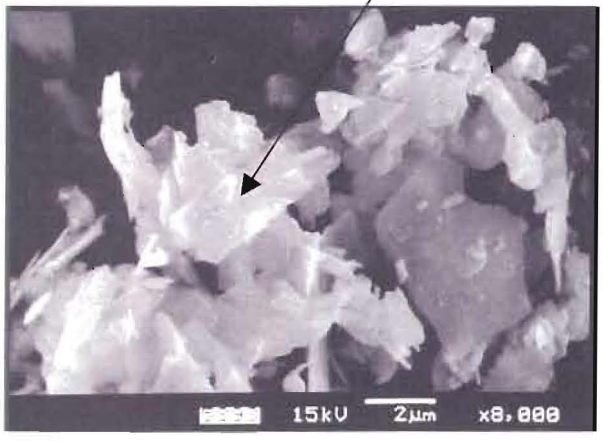

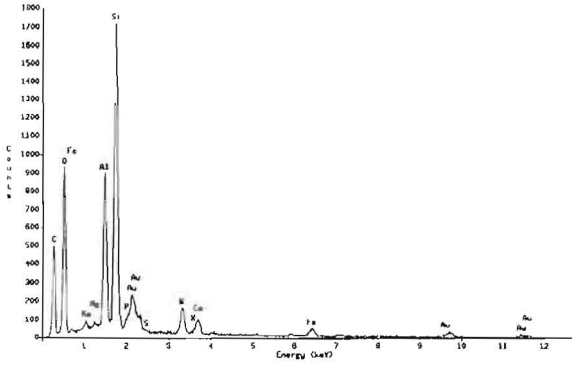

Figure 3-60: Mizpah Whole Tailings, dispersed and settled after 24 hours or >1.25 µm.

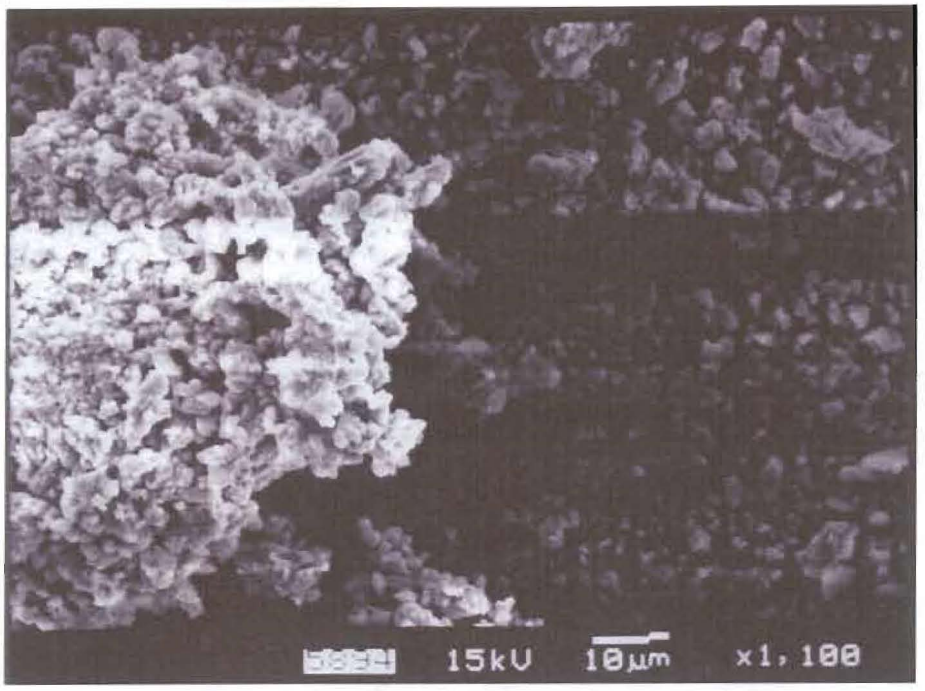

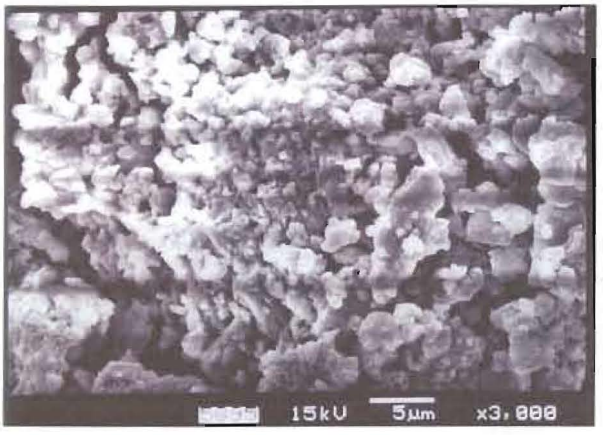

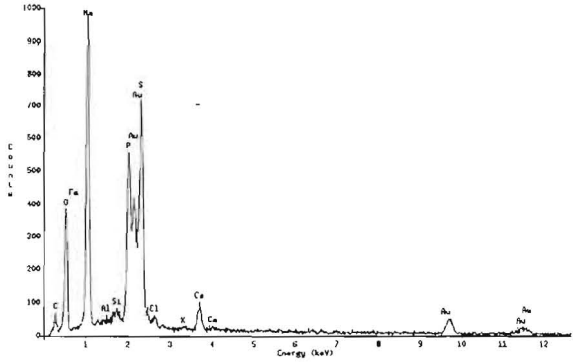

Figure 3-61: Mizpah Whole Tailings, dispersed effluent in sedimentation cylinder.

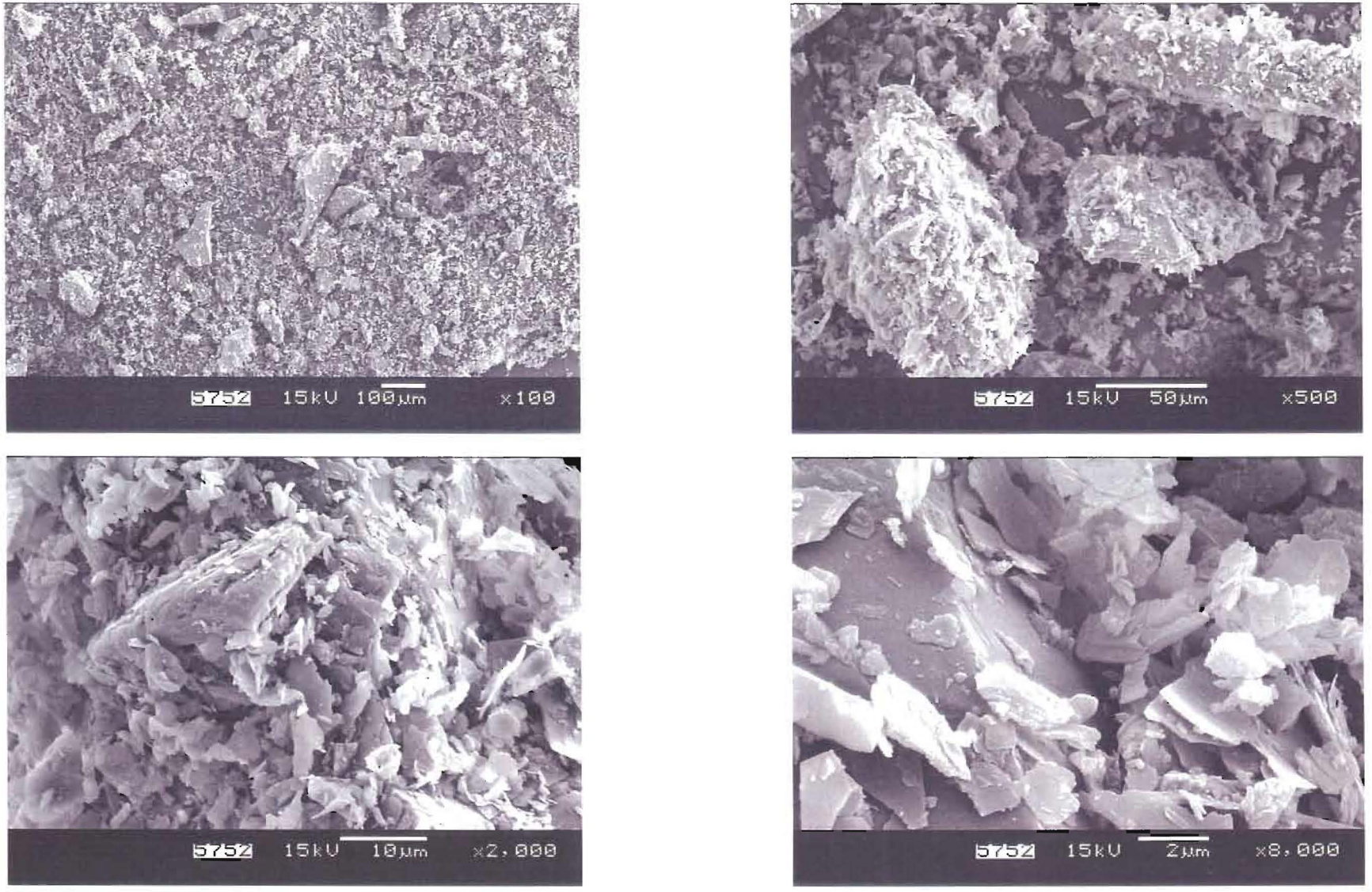

Figure 3-62: Mizpah Pond Fine Tailings, undispersed bulk specimen.

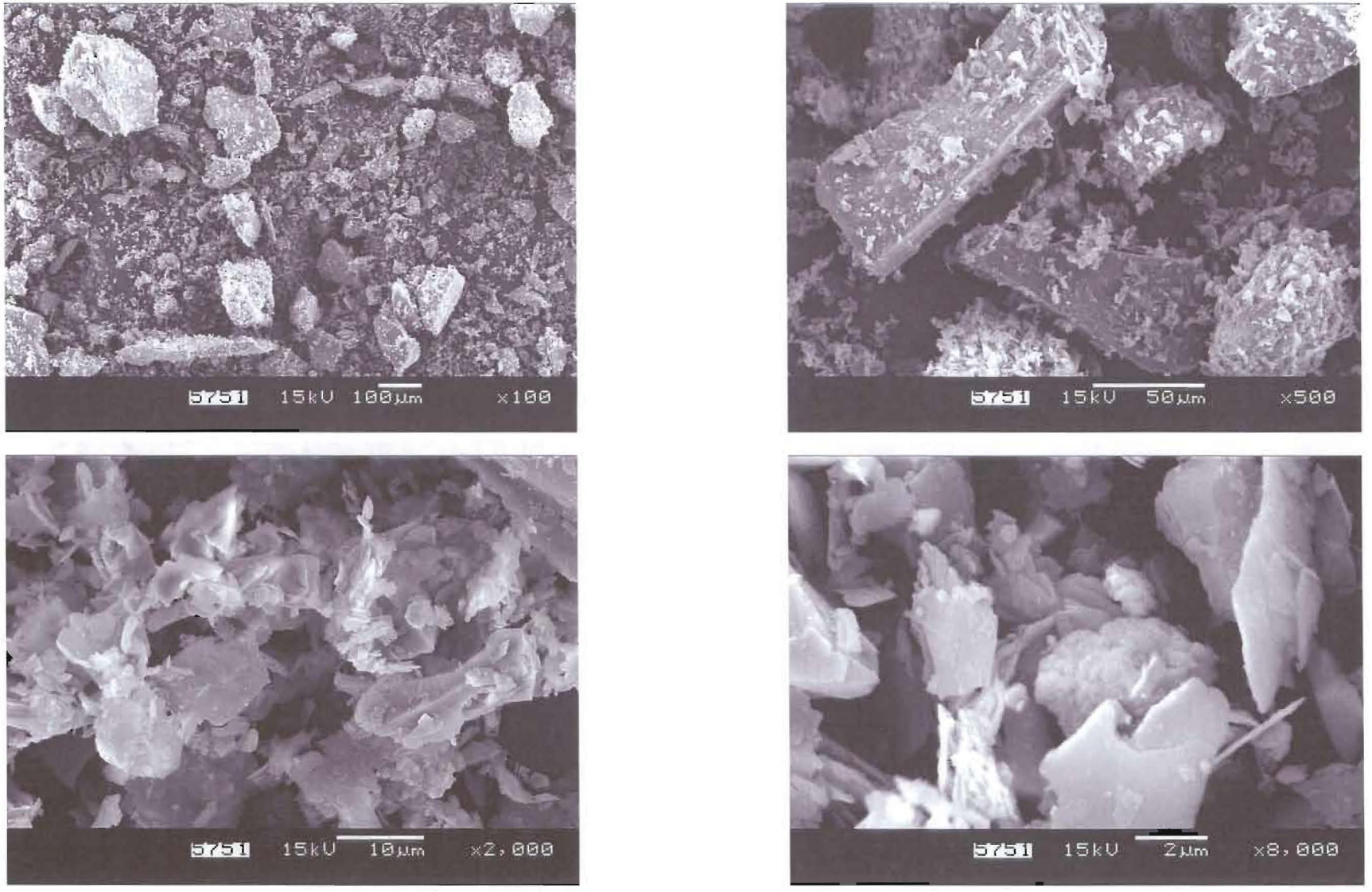

Figure 3-63: Mizpah Pond Coarse Tailings, undispersed bulk specimen.

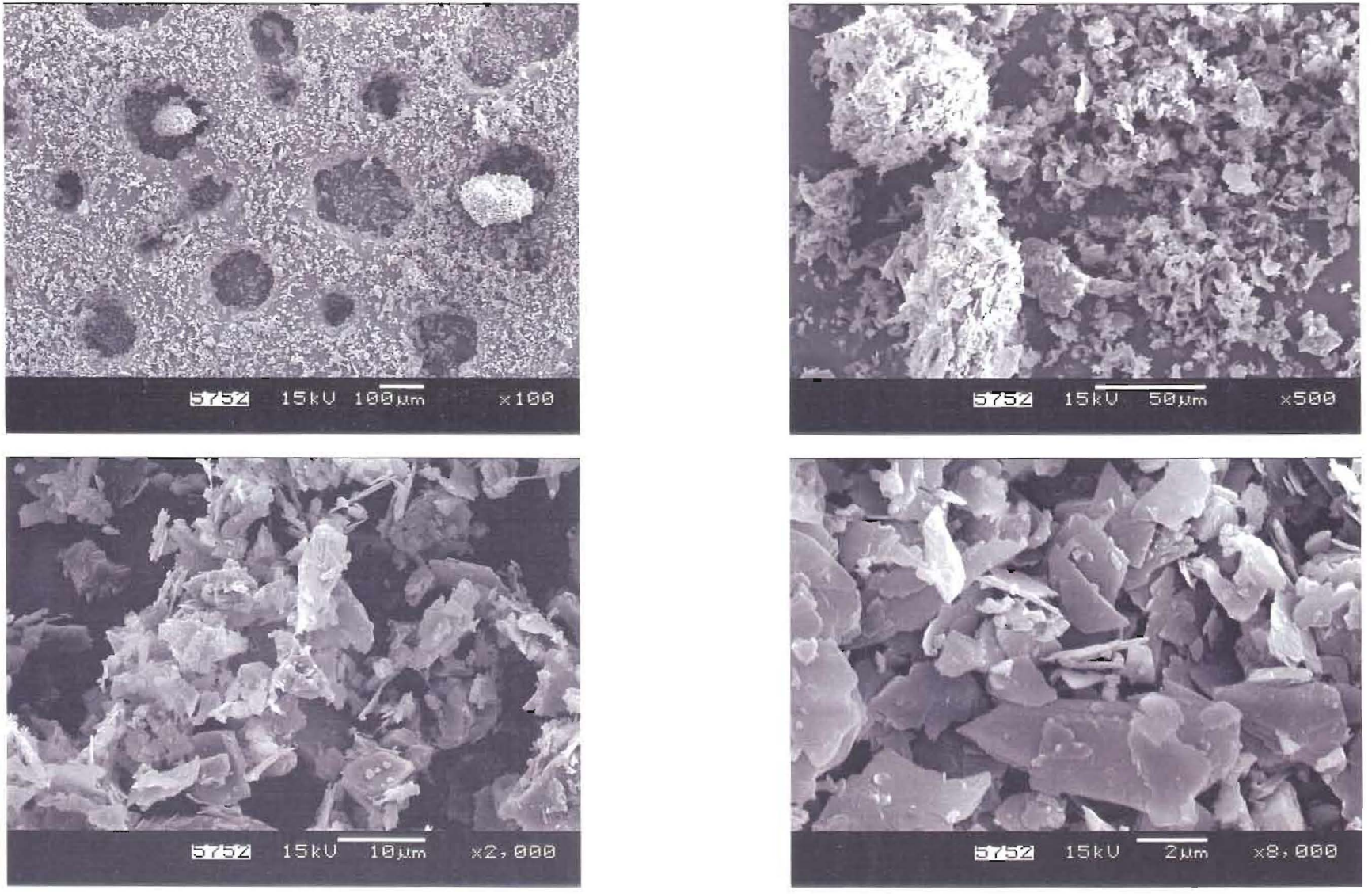

Figure 3-64: Pay Dam Penstock Fine Tailings, undispersed bulk specimen.

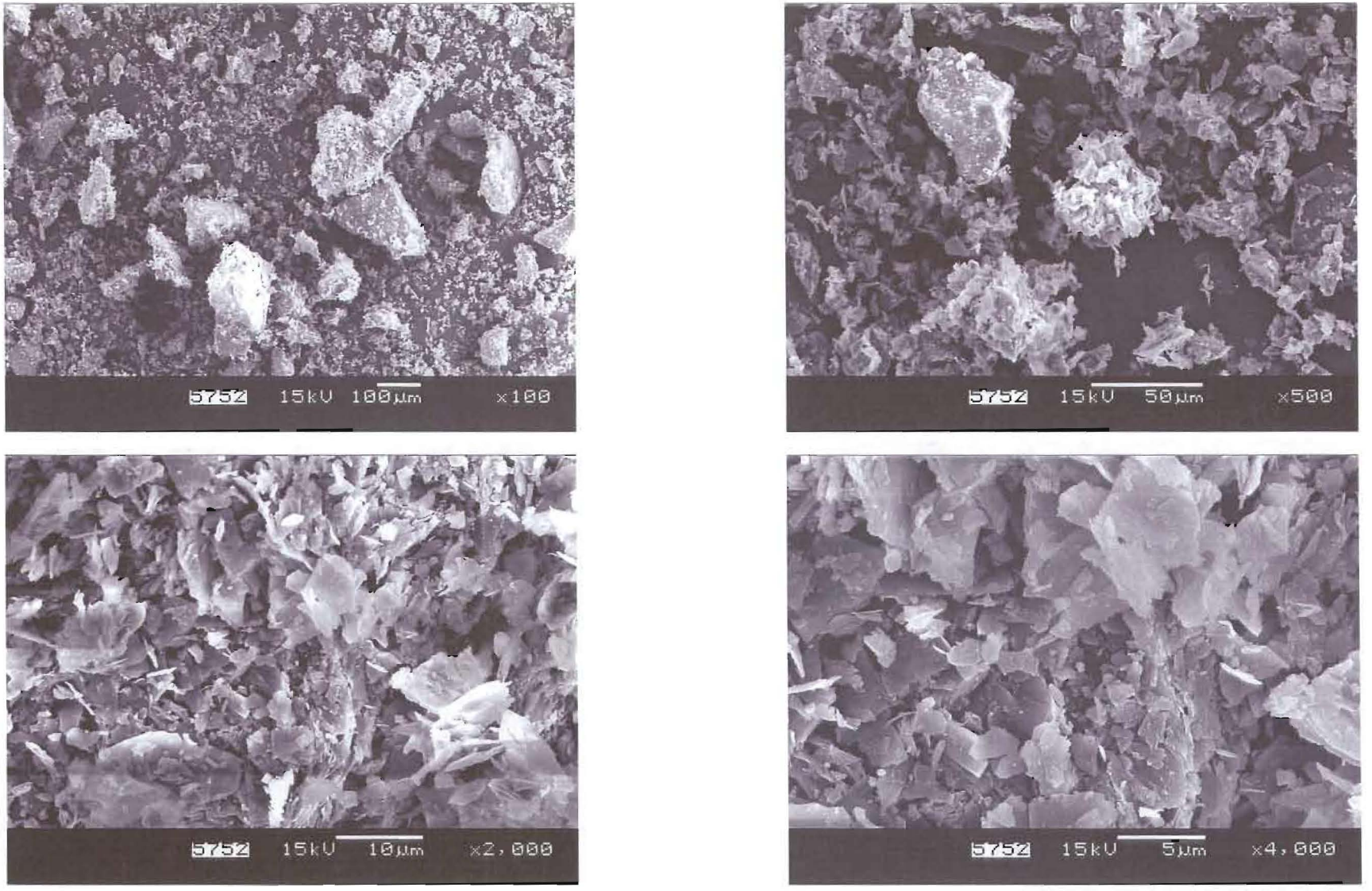

Figure 3-65: Pay Dam Penstock Coarse Tailings, undispersed bulk specimen.

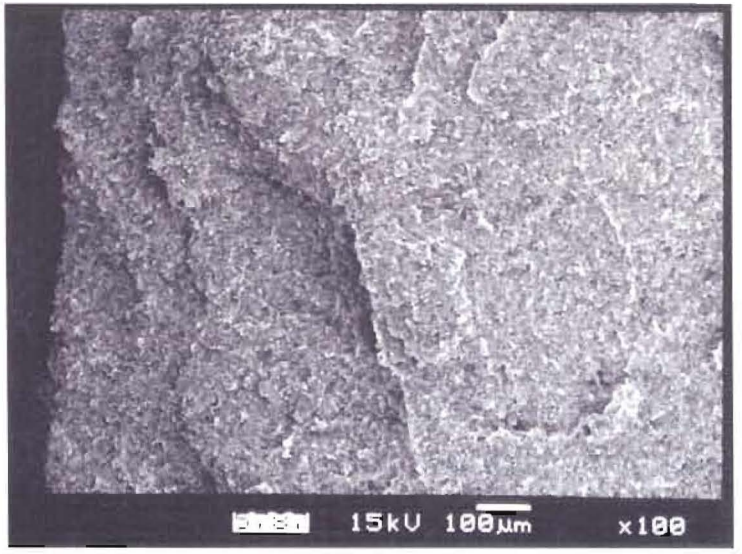

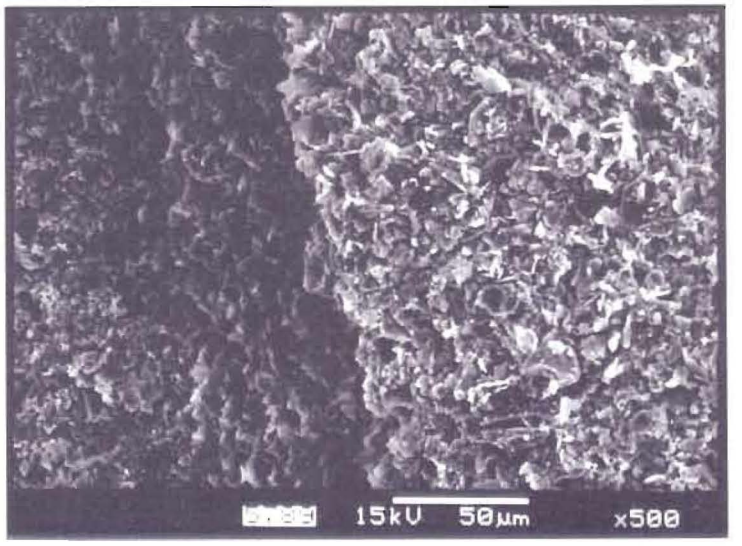

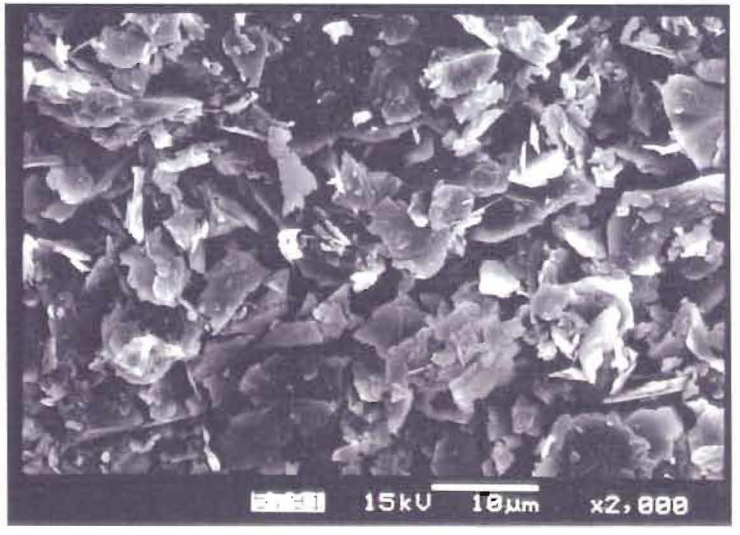

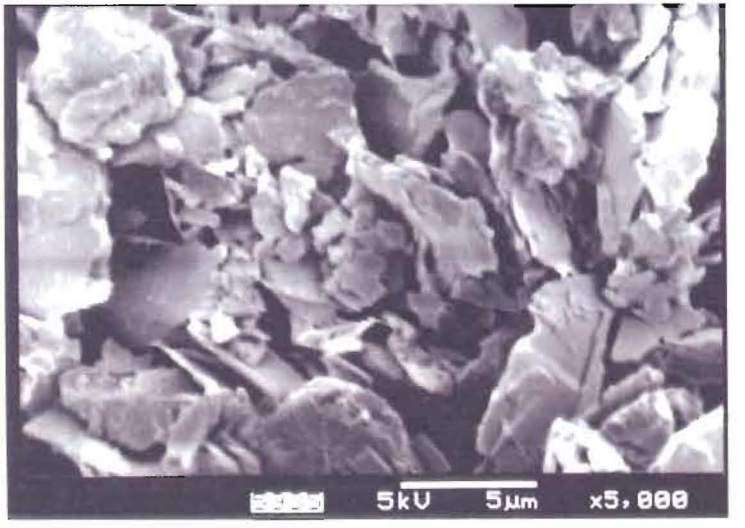

Figure 3-66: Pay Dam Penstock Fine Tailings, undisturbed specimen.

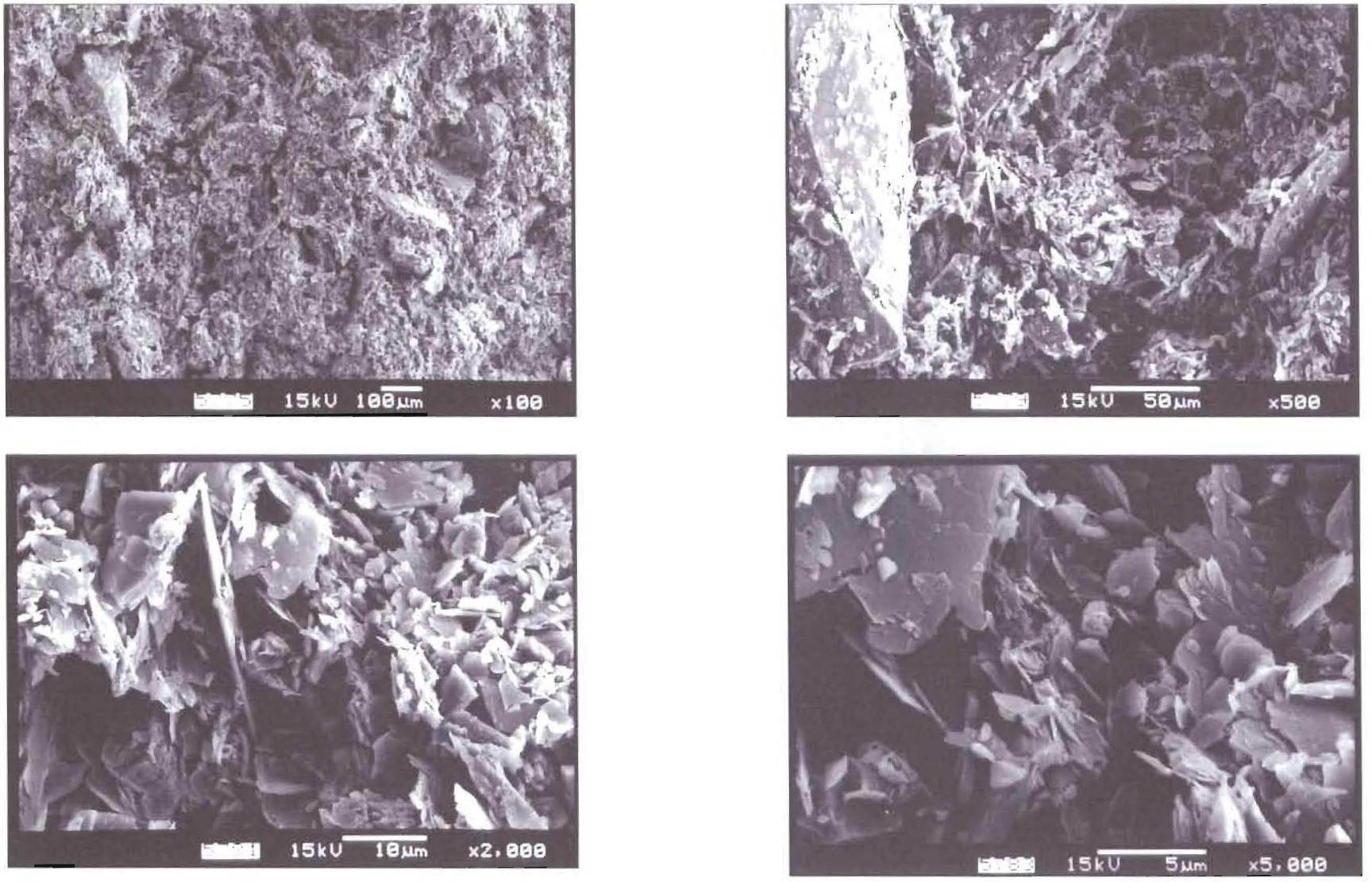

Figure 3-67: Pay Dam Penstock Coarse Tailings, undisturbed specimen.

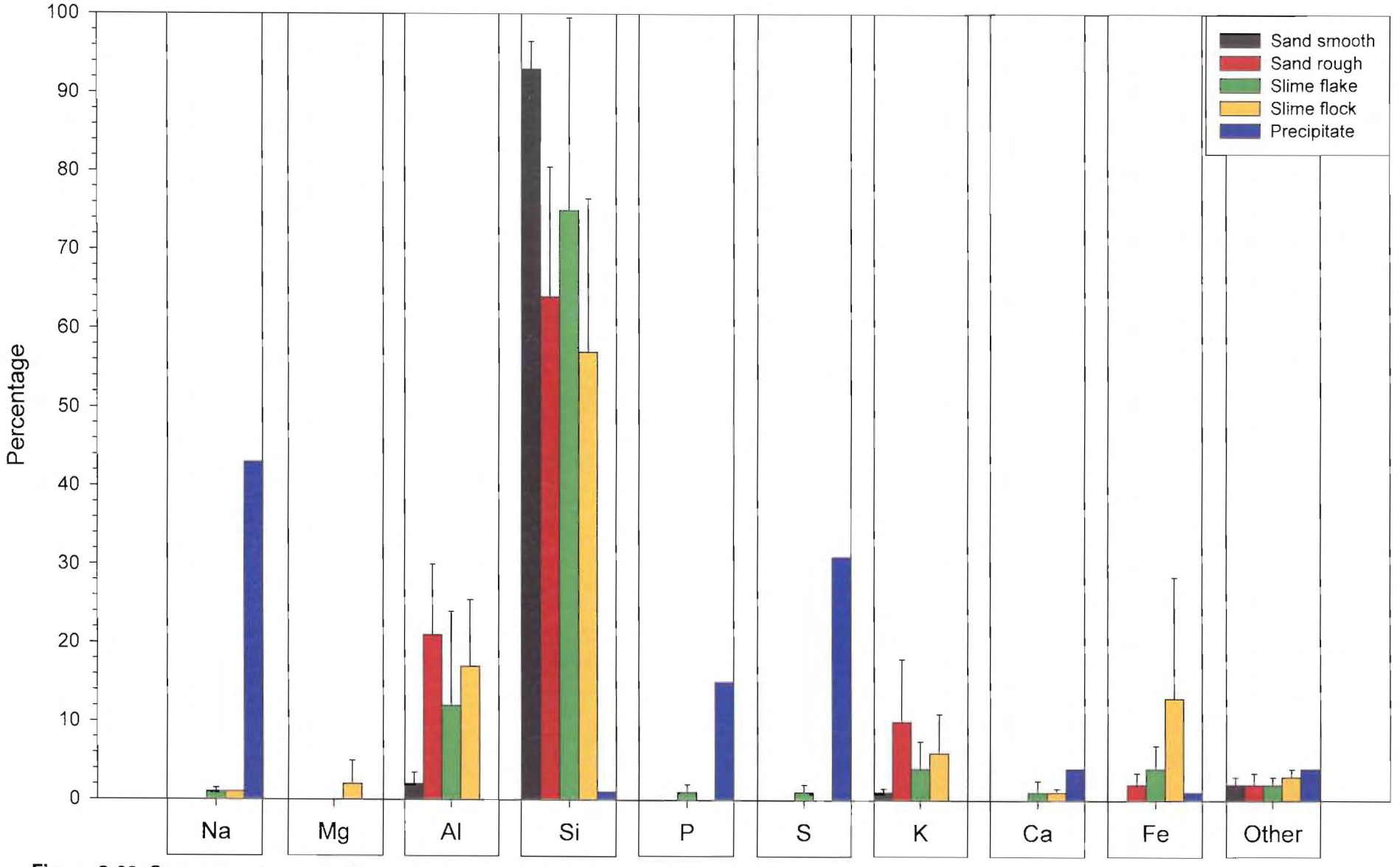

Figure 3-68: Summary of energy dispersive x-ray spectrometry on Mizpah whole tailings.

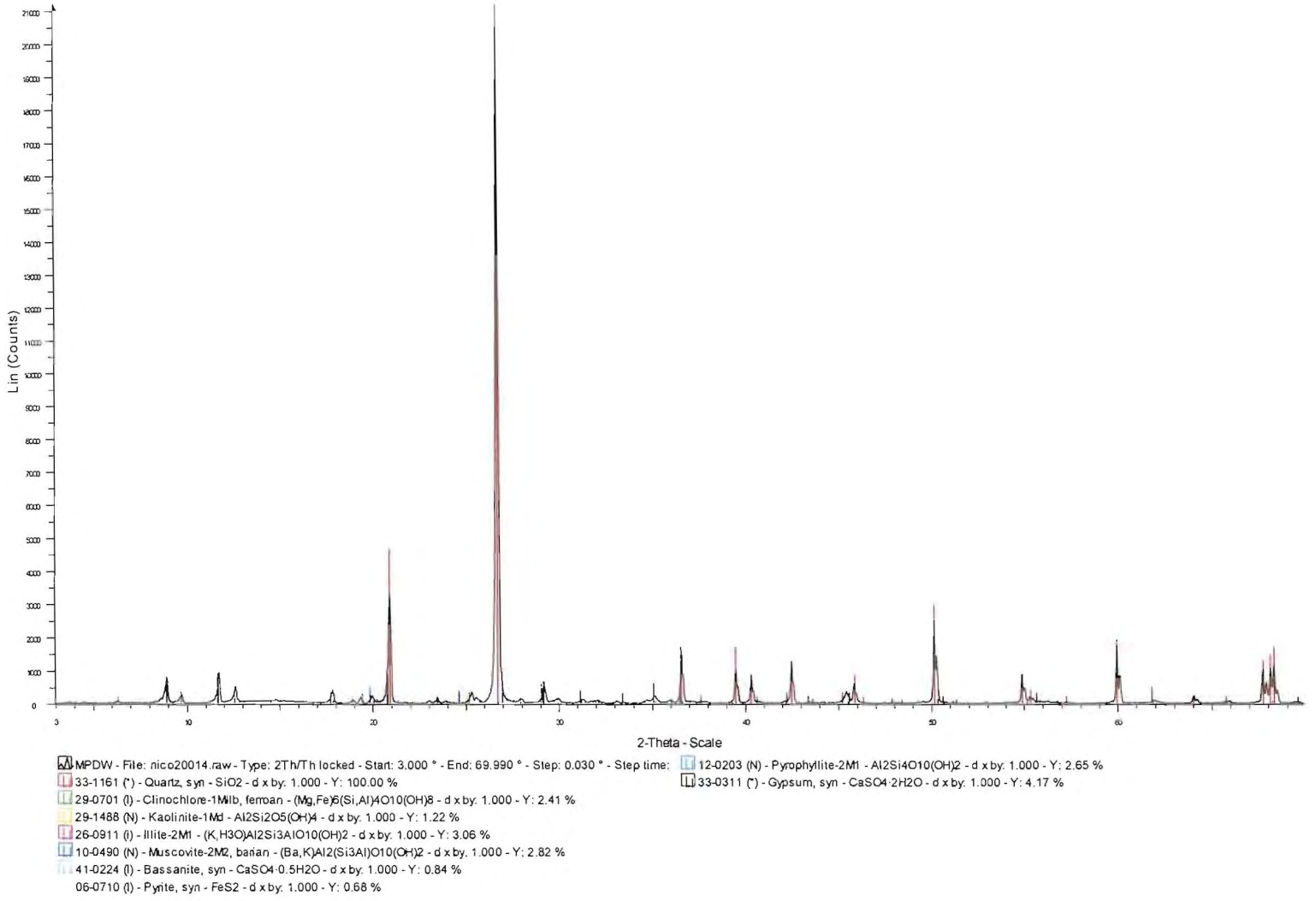

Figure 3-69: XRD spectrograph: Mizpah Whole Tailings.

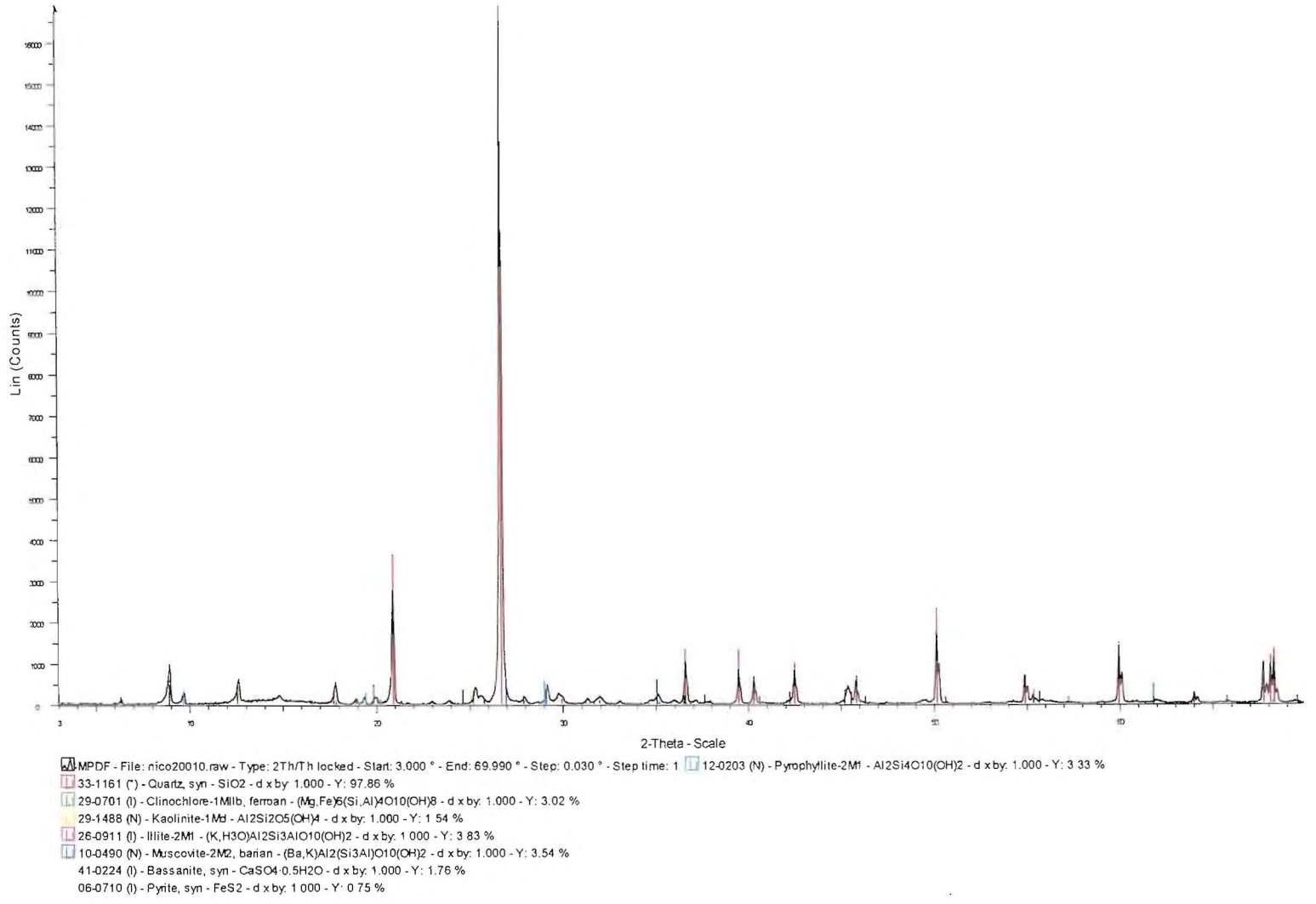

Figure 3-70: XRD spectrograph: Mizpah Pond Fine Tailings.

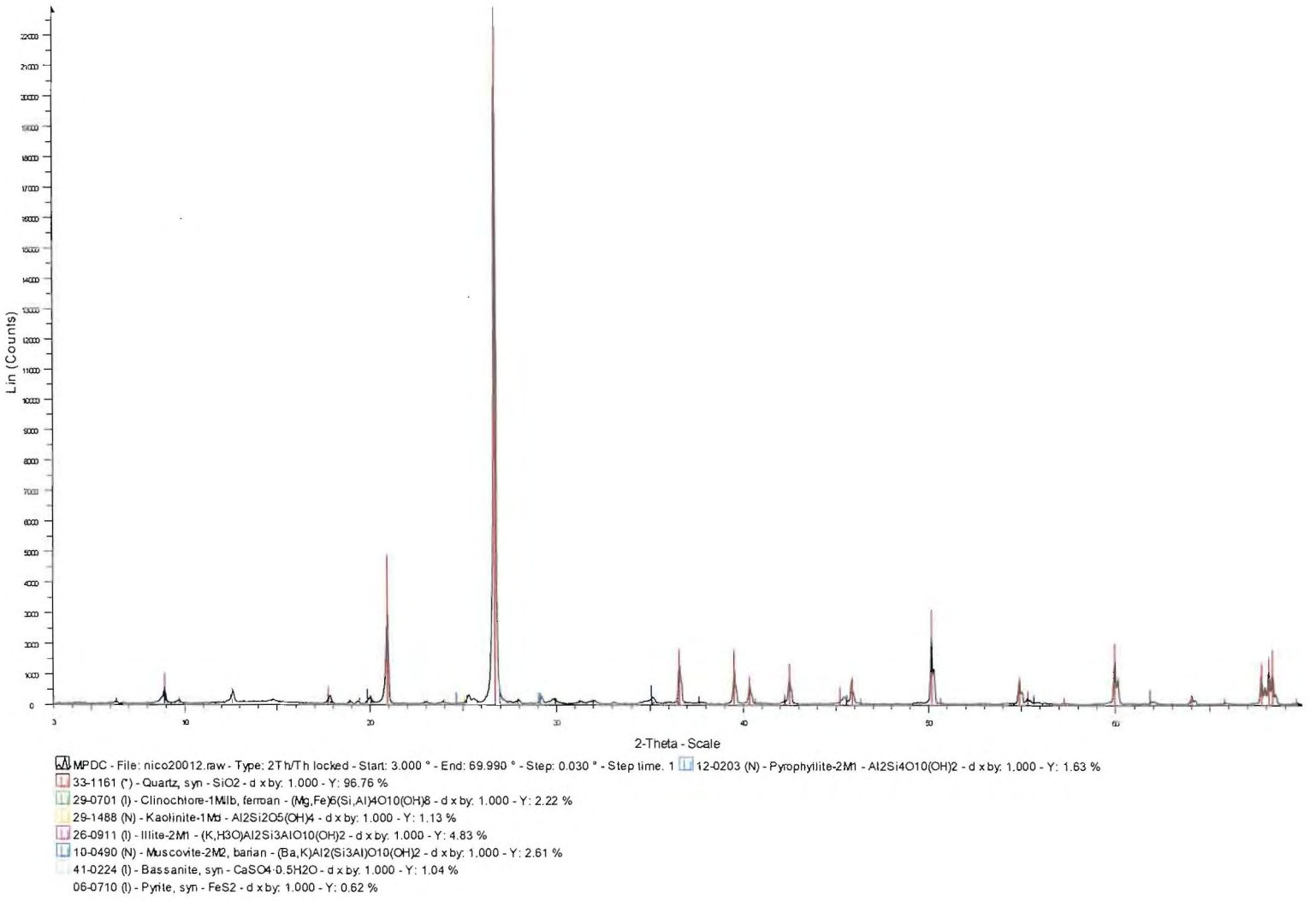

Figure 3-71: XRD spectrograph: Mizpah Pond Coarse Tailings.

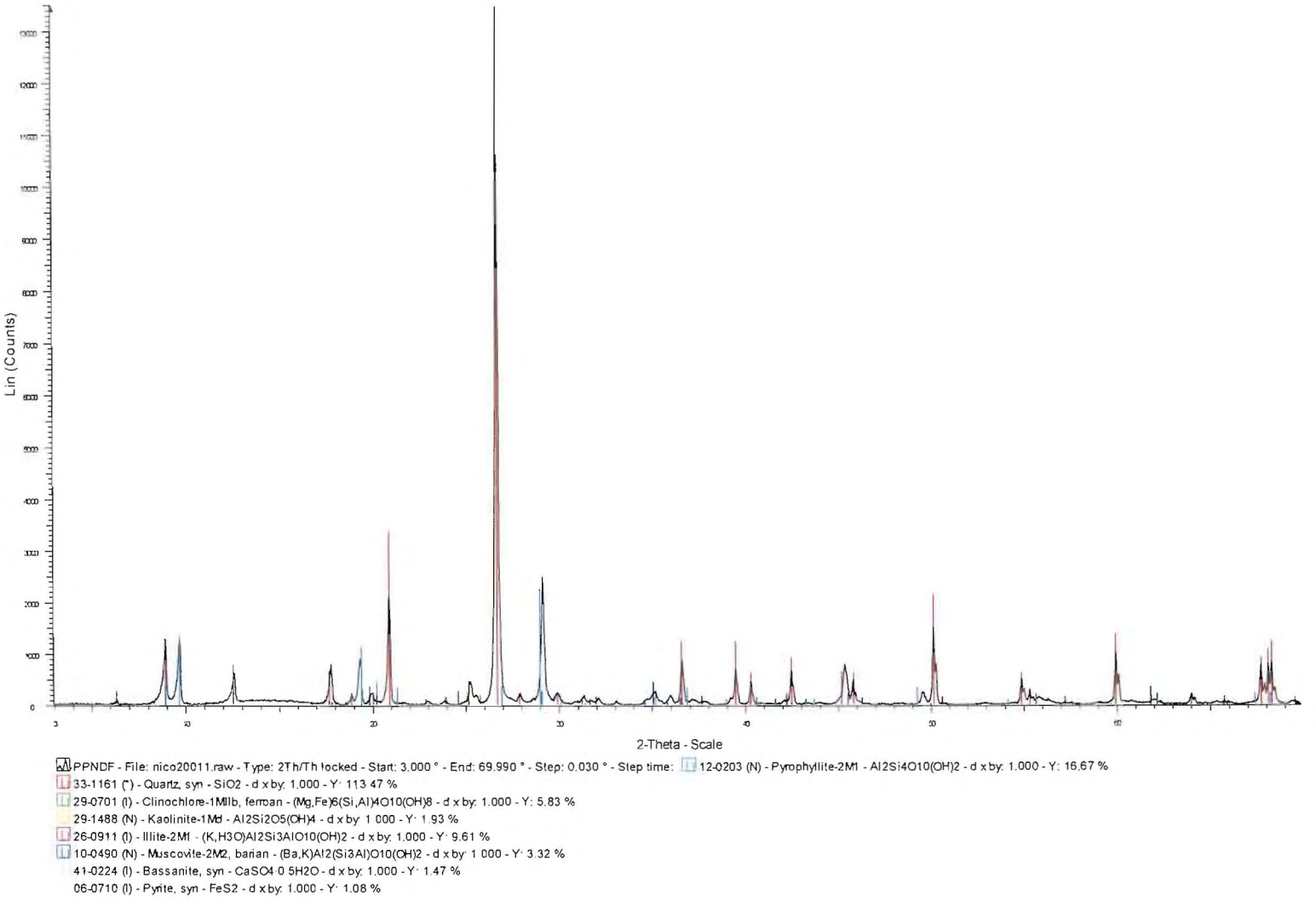

Figure 3-72: XRD spectrograph: Pay Dam Penstock Fine Tailings.

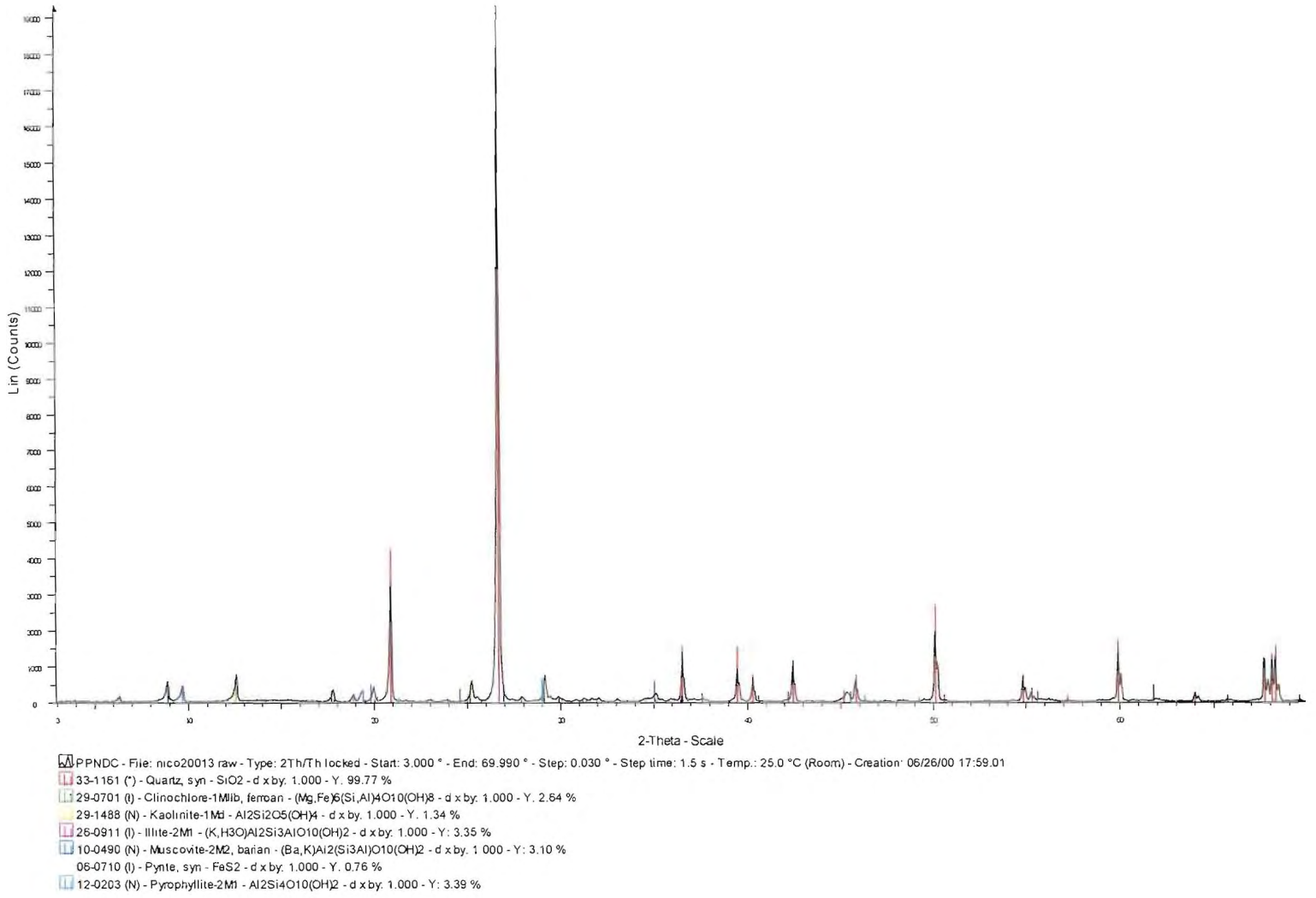

Figure 3-73: XRD spectrograph: Pay Dam Penstock Coarse Tailings.

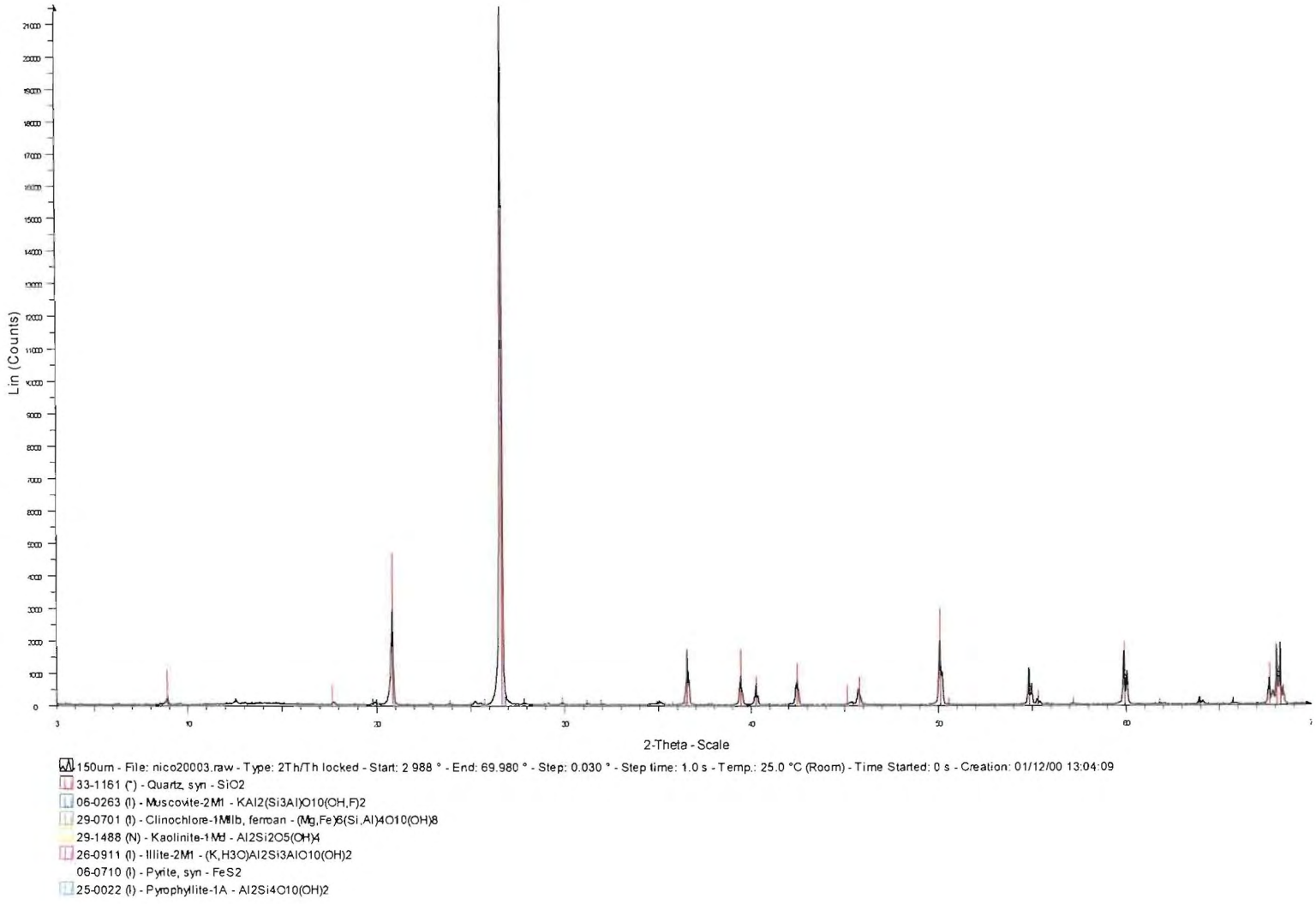

Figure 3-74: XRD spectrograph of Mizpah whole tailings 150 μm fraction.

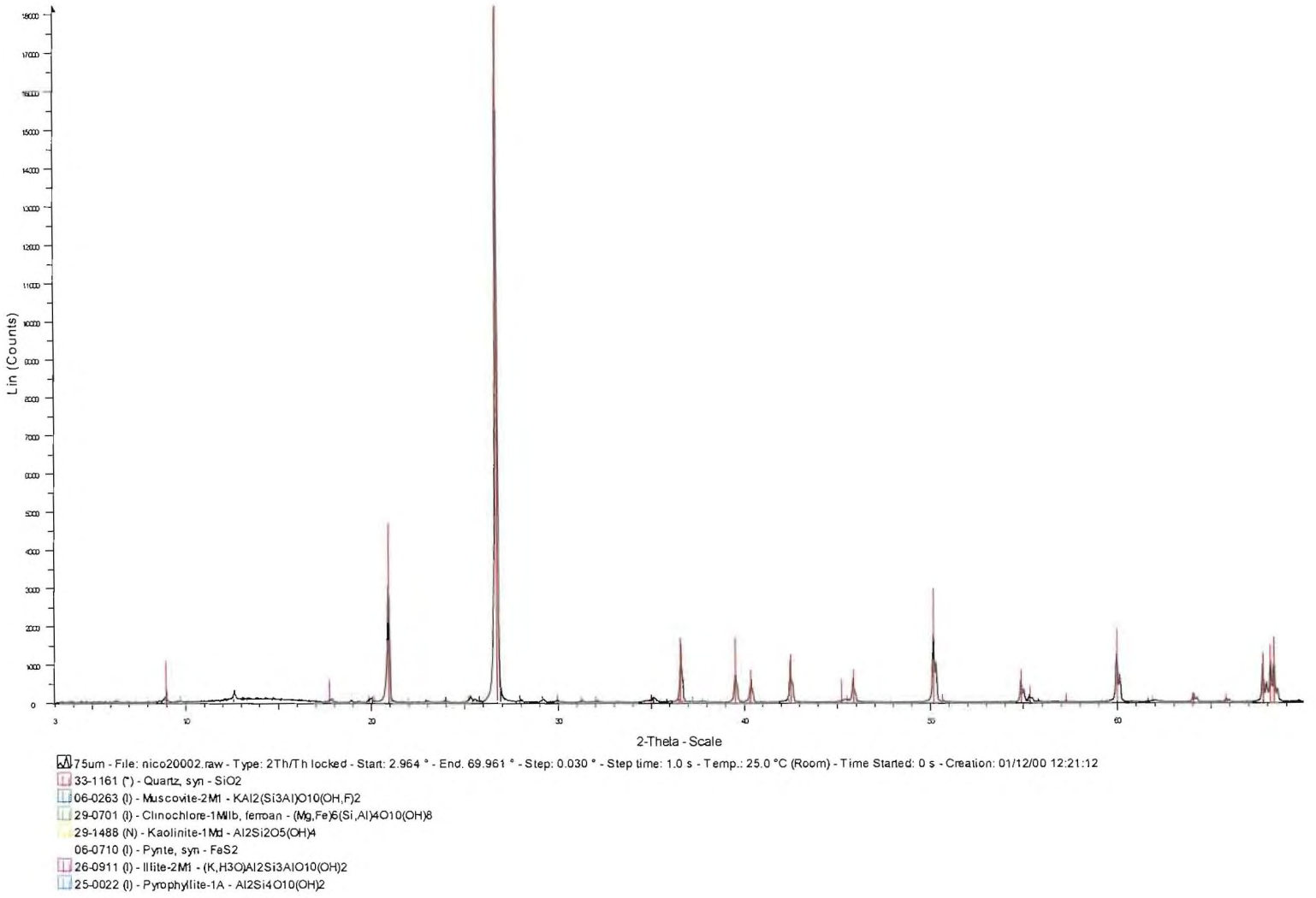

Figure 3-75: XRD spectrograph of Mizpah whole tailings 75 μm fraction.

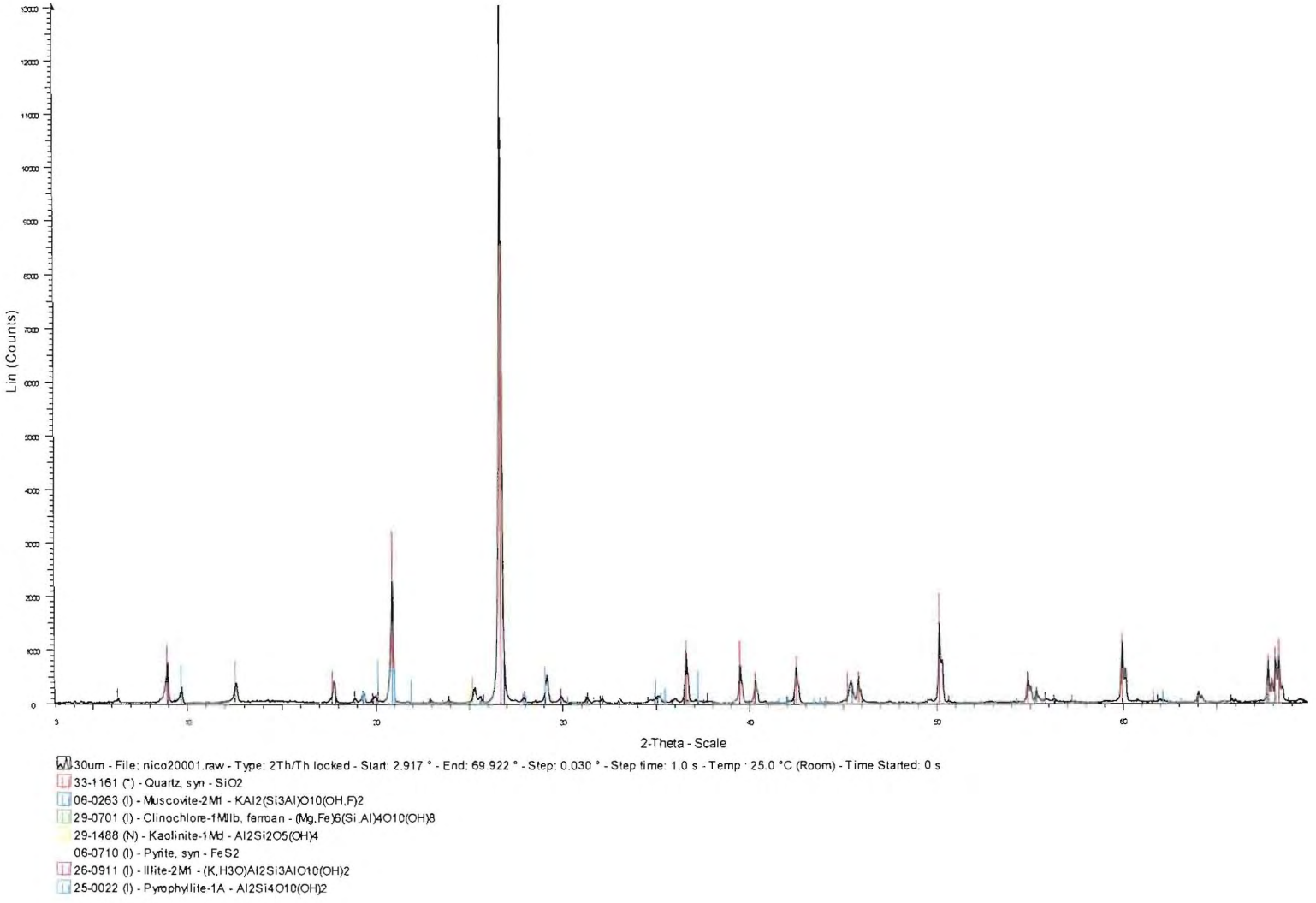

Figure 3-76: XRD spectrograph of Mizpah whole tailings 10 μm fraction.

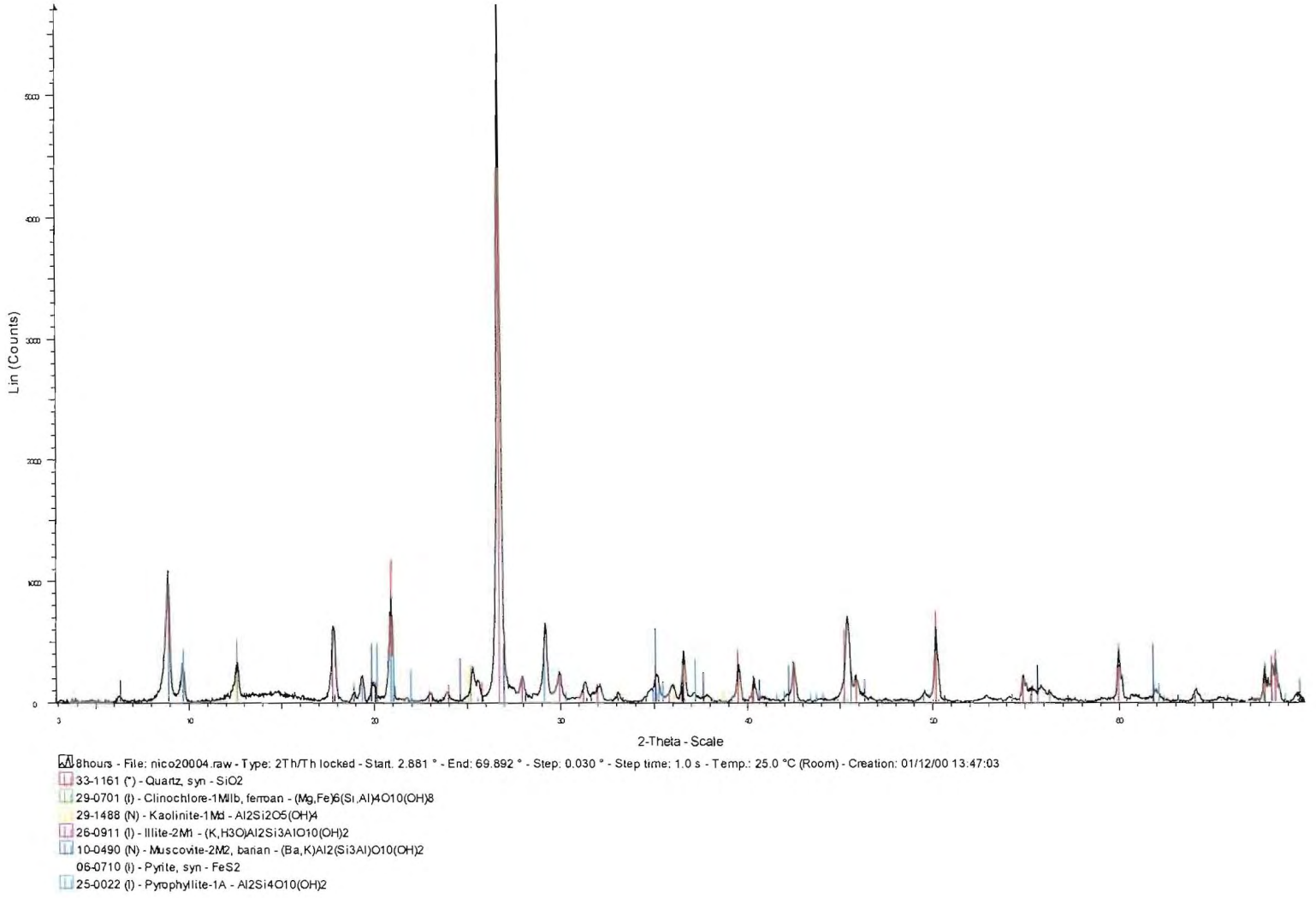

Figure 3-77: XRD spectrograph of Mizpah whole tailings 2 μm fraction.

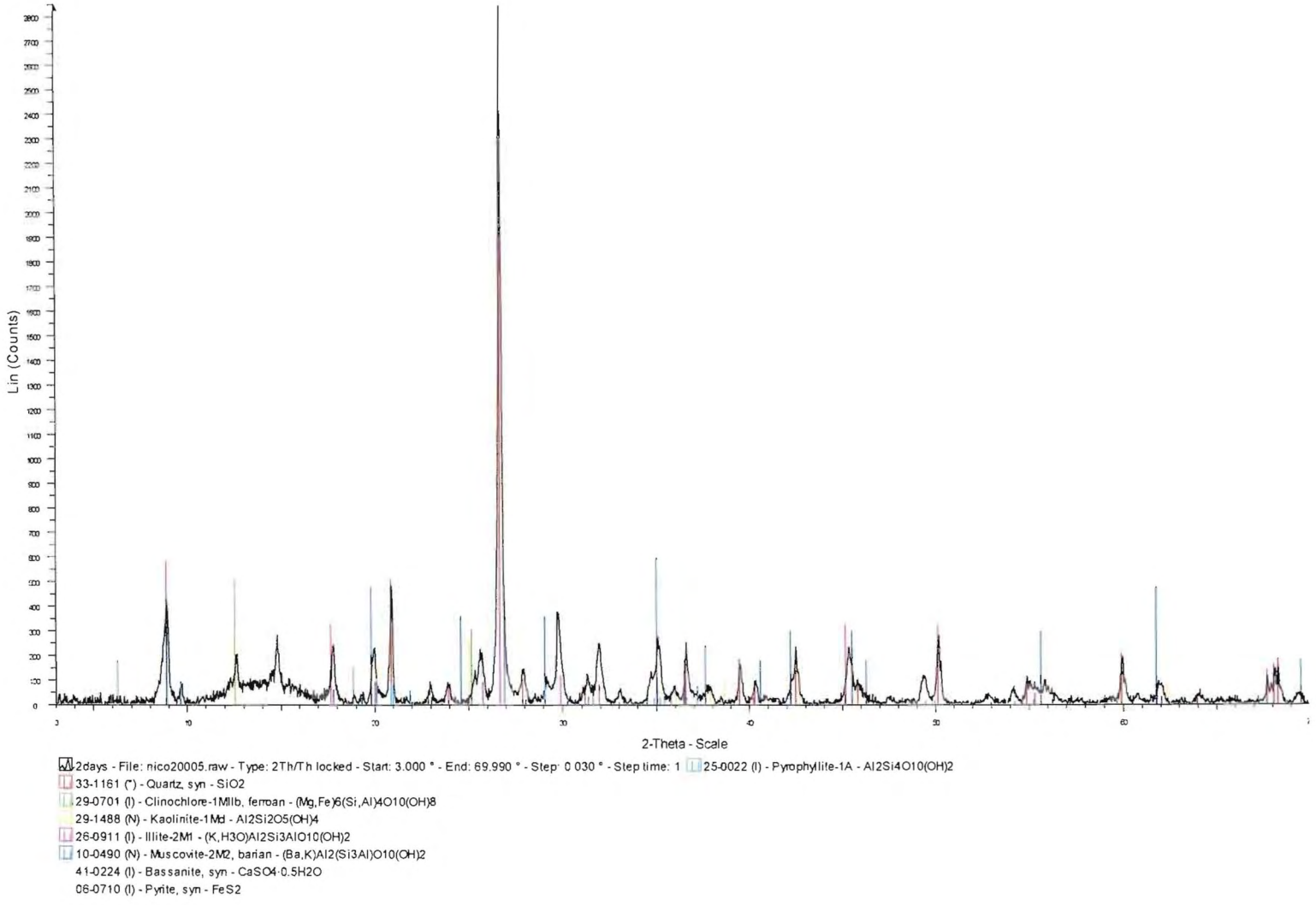

Figure 3-78: XRD spectrograph of Mizpah whole tailings 1 μm fraction.

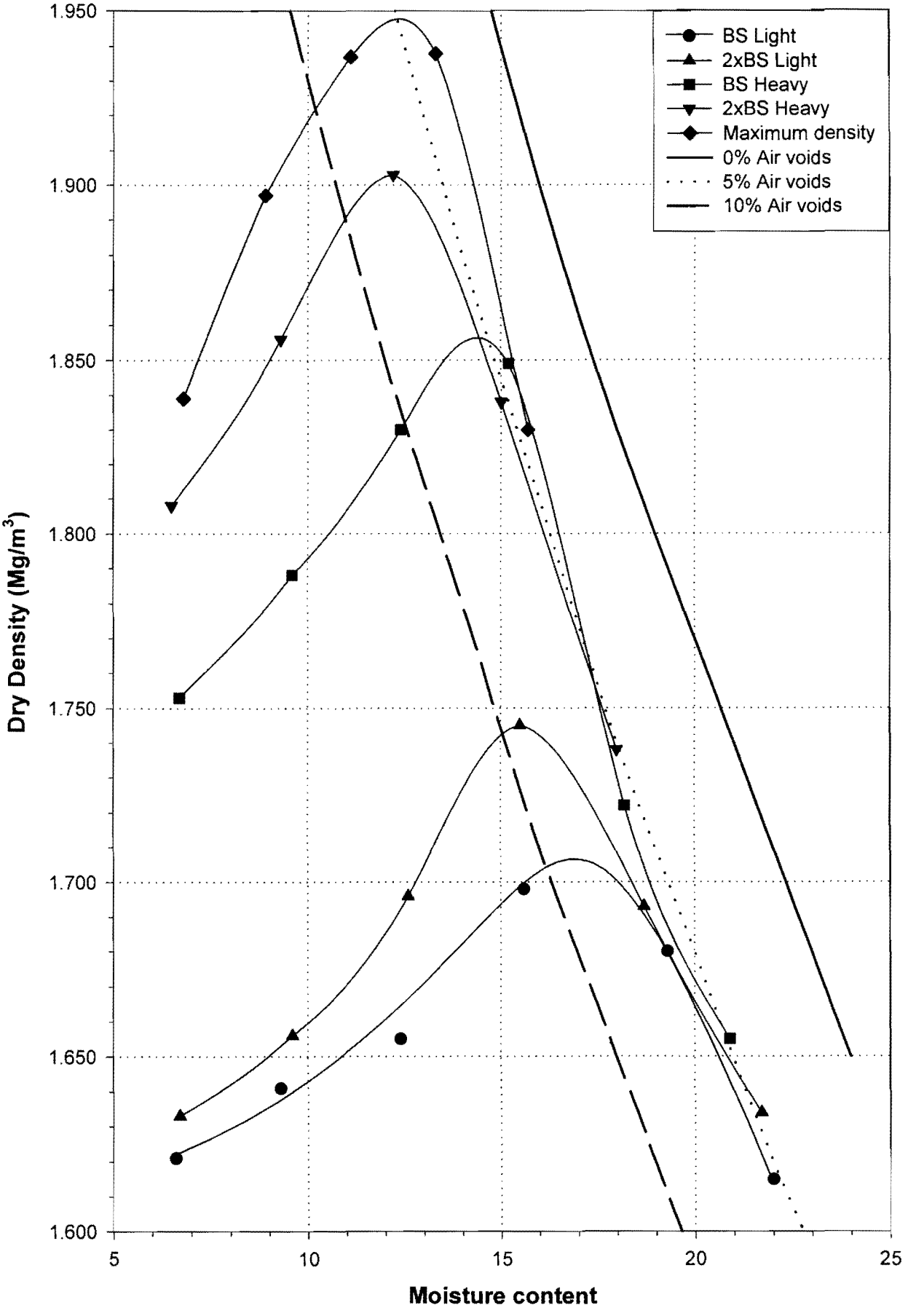

Figure 3-79: Compaction curves for Mizpah Whole Tailings.

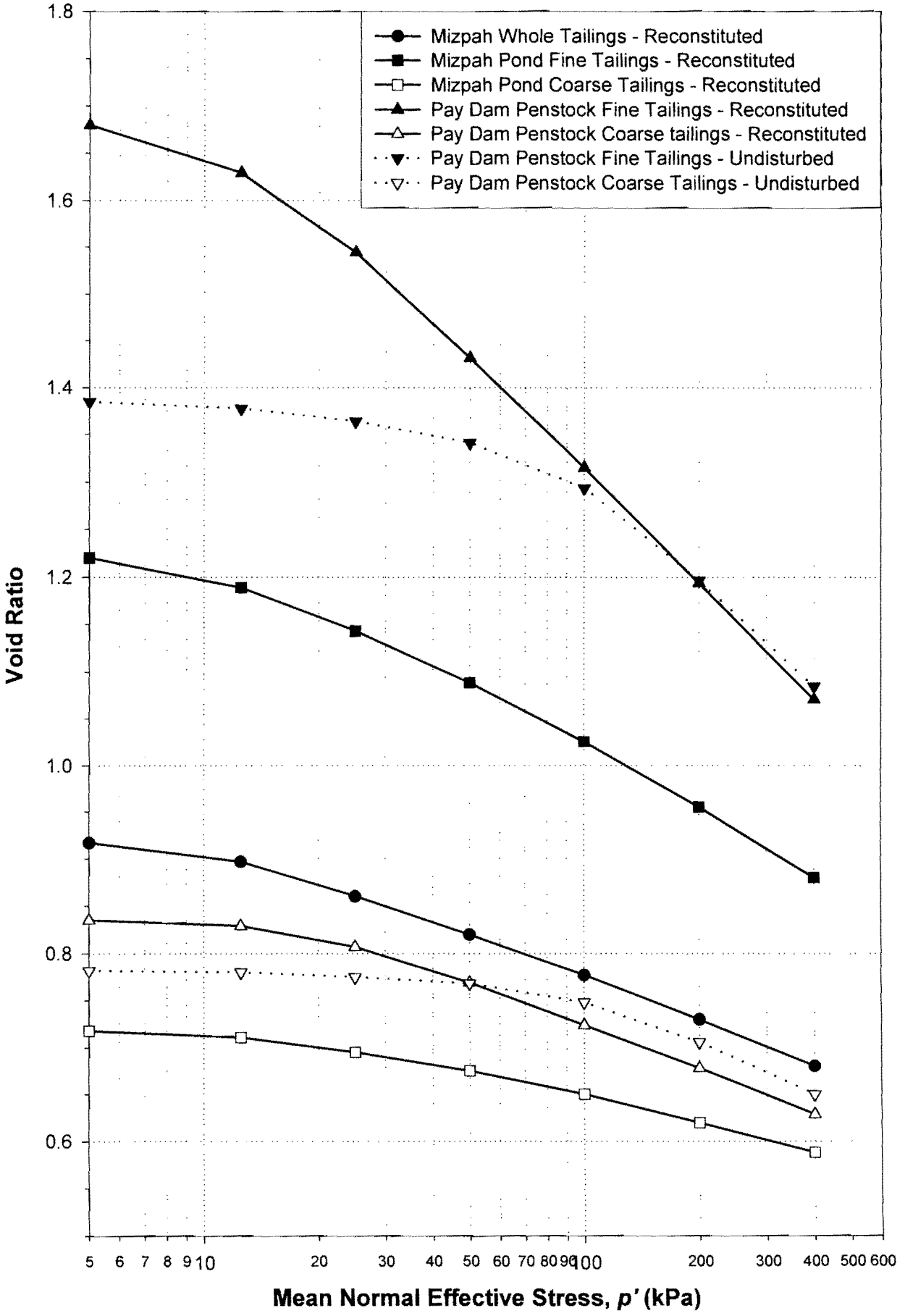

Figure 3-80: Isotropic compression: Combined results for Mizpah and Pay Dam.

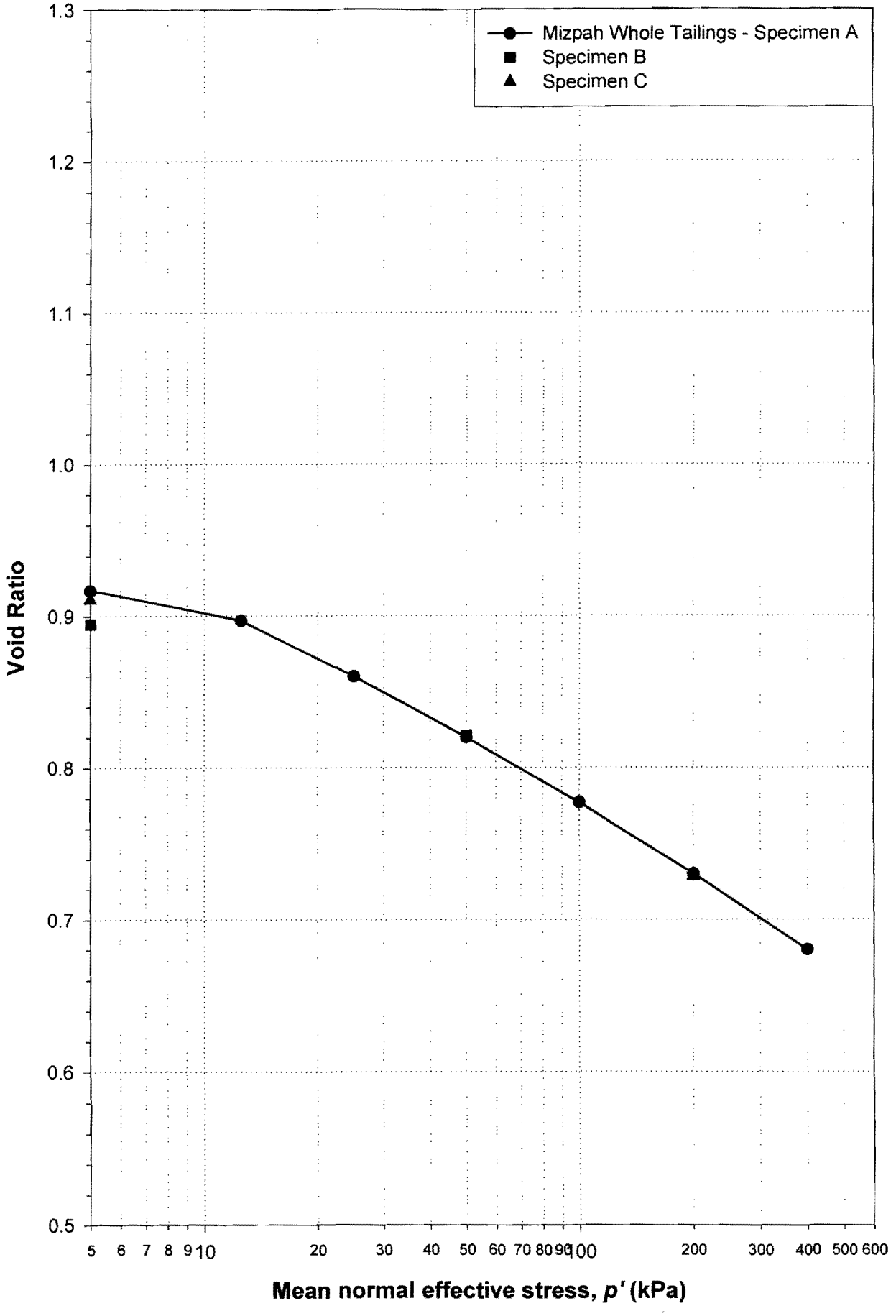

Figure 3-81: Reconstituted Mizpah Whole Tailings: Isotropic compression.

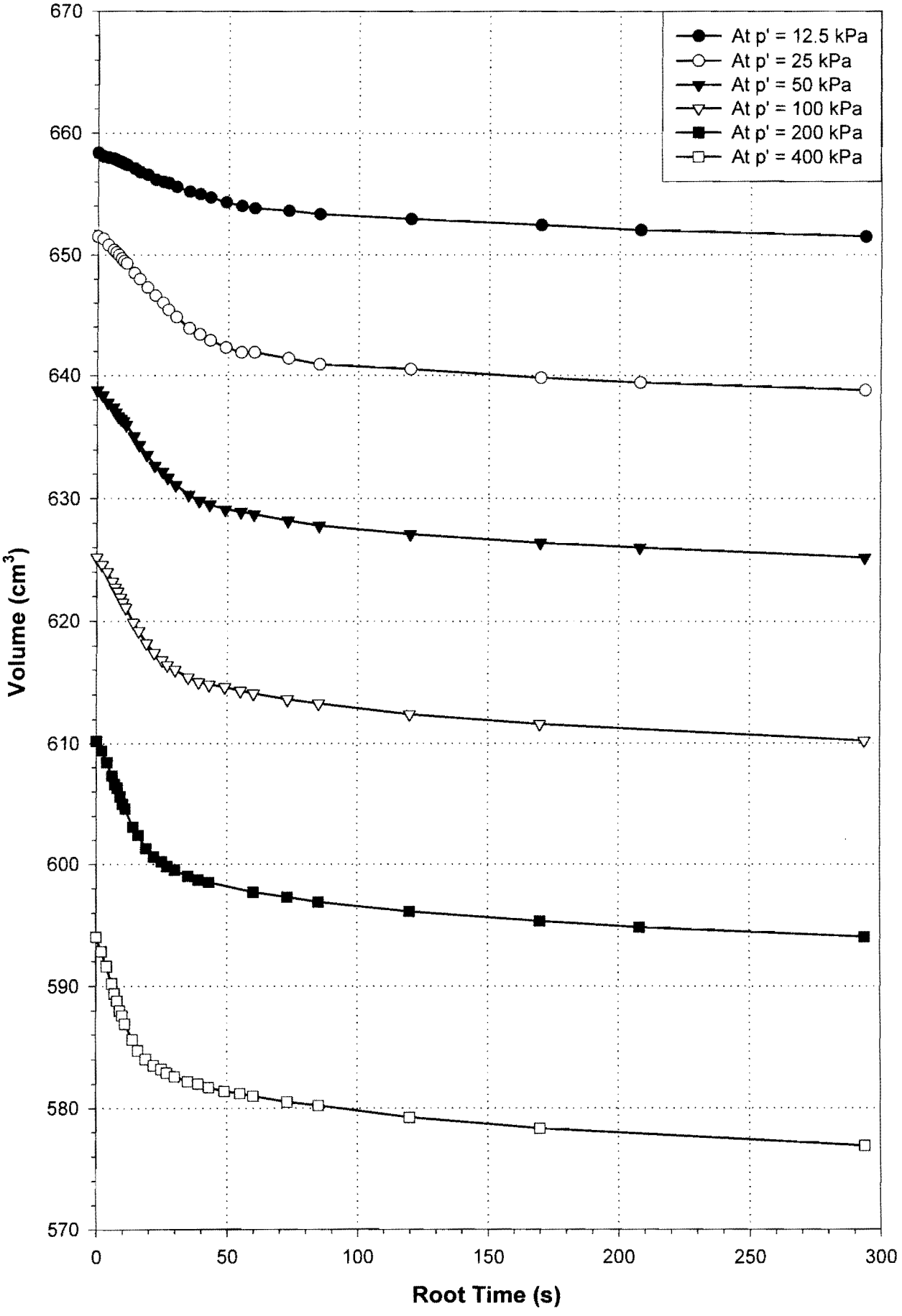

Figure 3-82: Reconstituted Mizpah Whole Tailings: Volumetric consolidation.

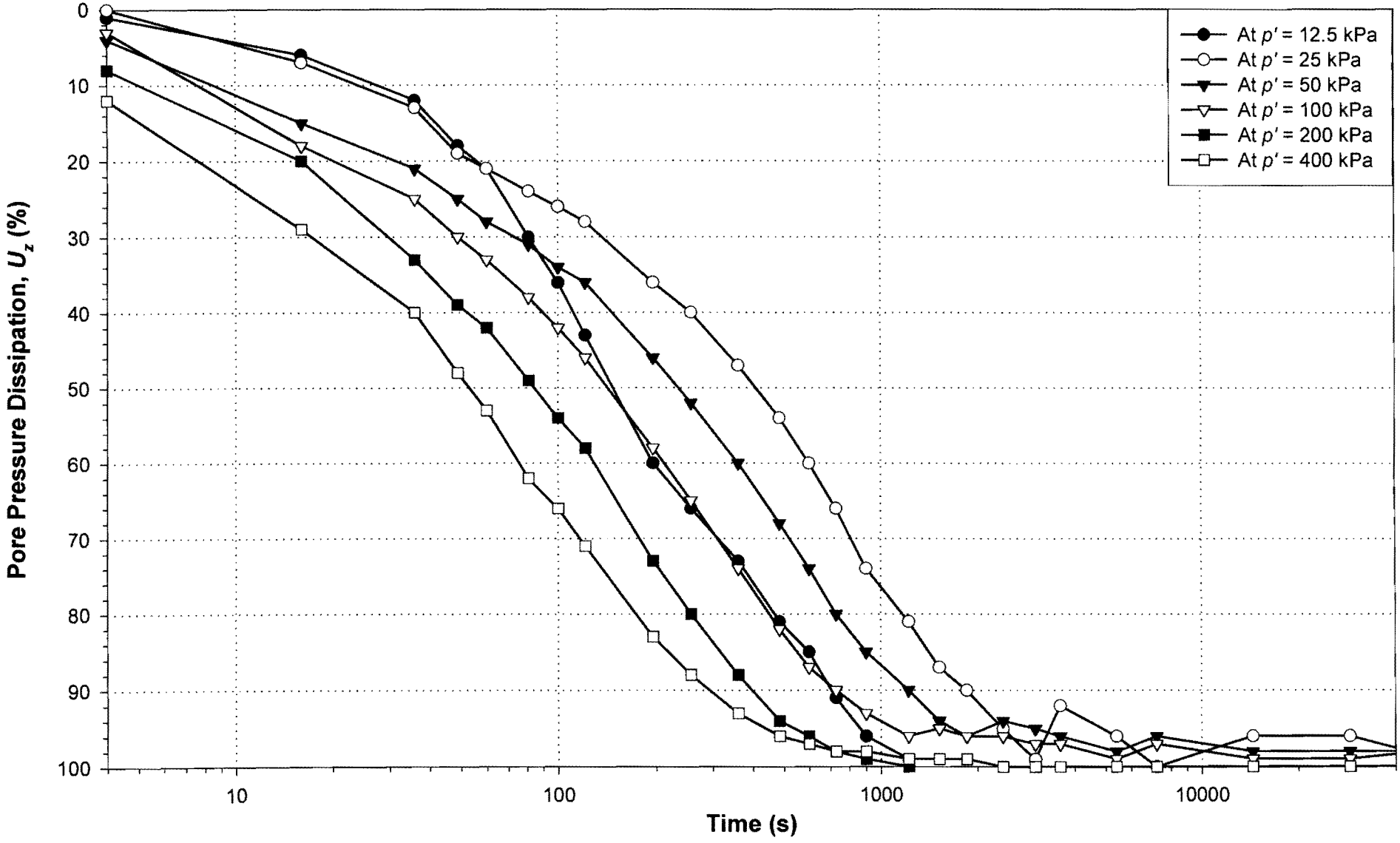

Figure 3-83: Reconstituted Mizpah Whole Tailings: Pore pressure dissipation.

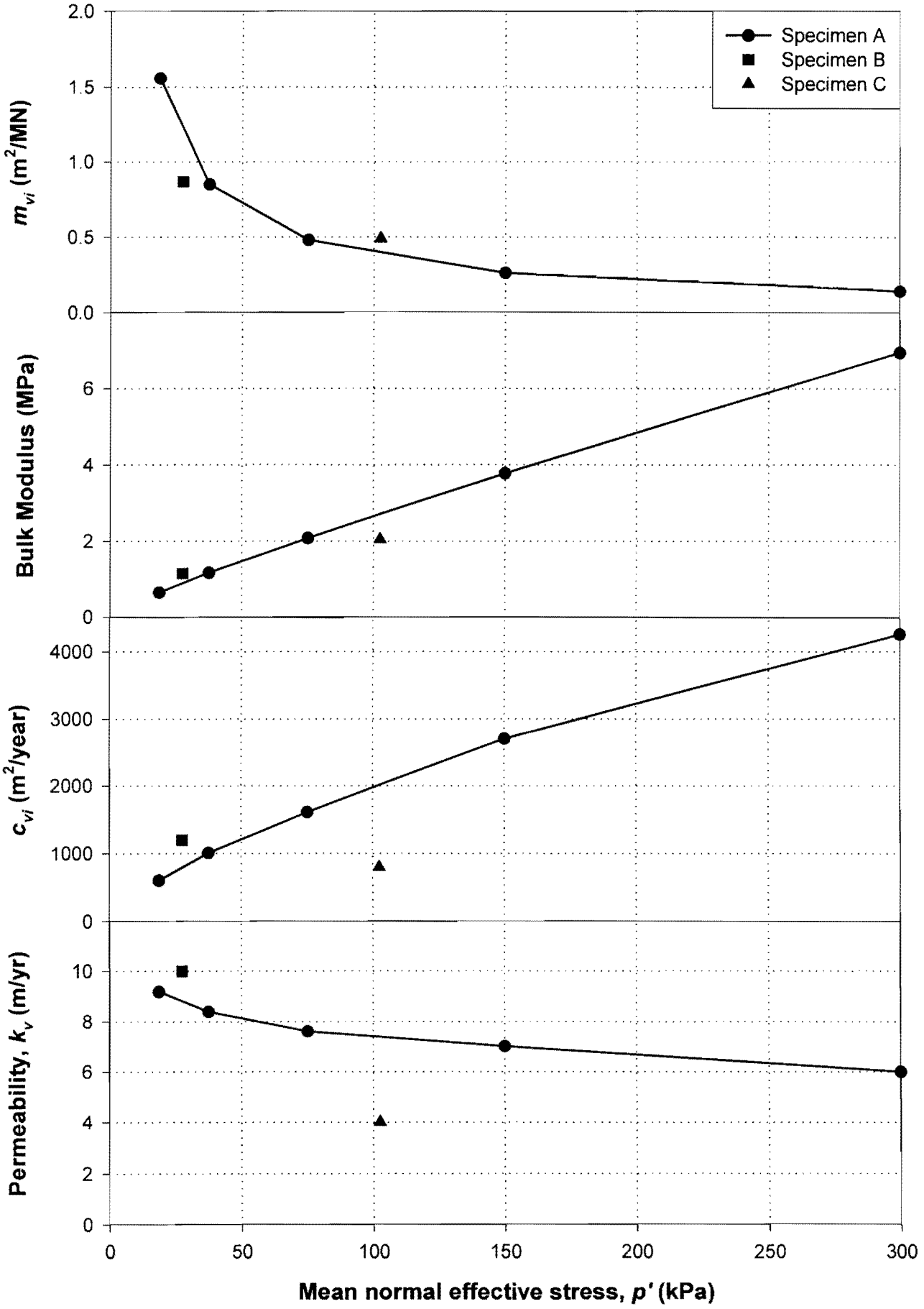

Figure 3-84: Reconstituted Mizpah Whole Tailings: Consolidation parameters.

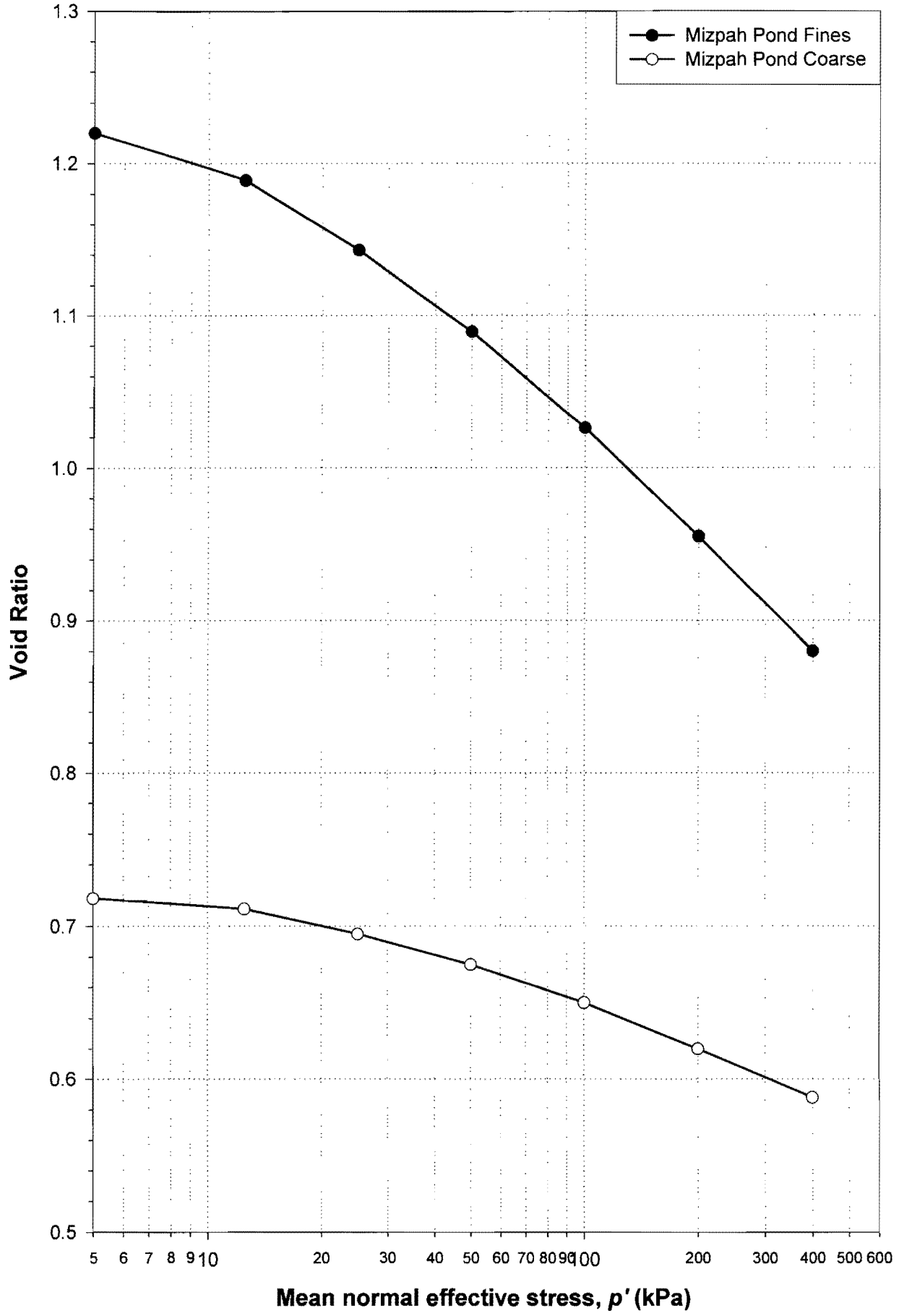

Figure 3-85: Reconstituted Mizpah Pond Tailings: Isotropic compression.

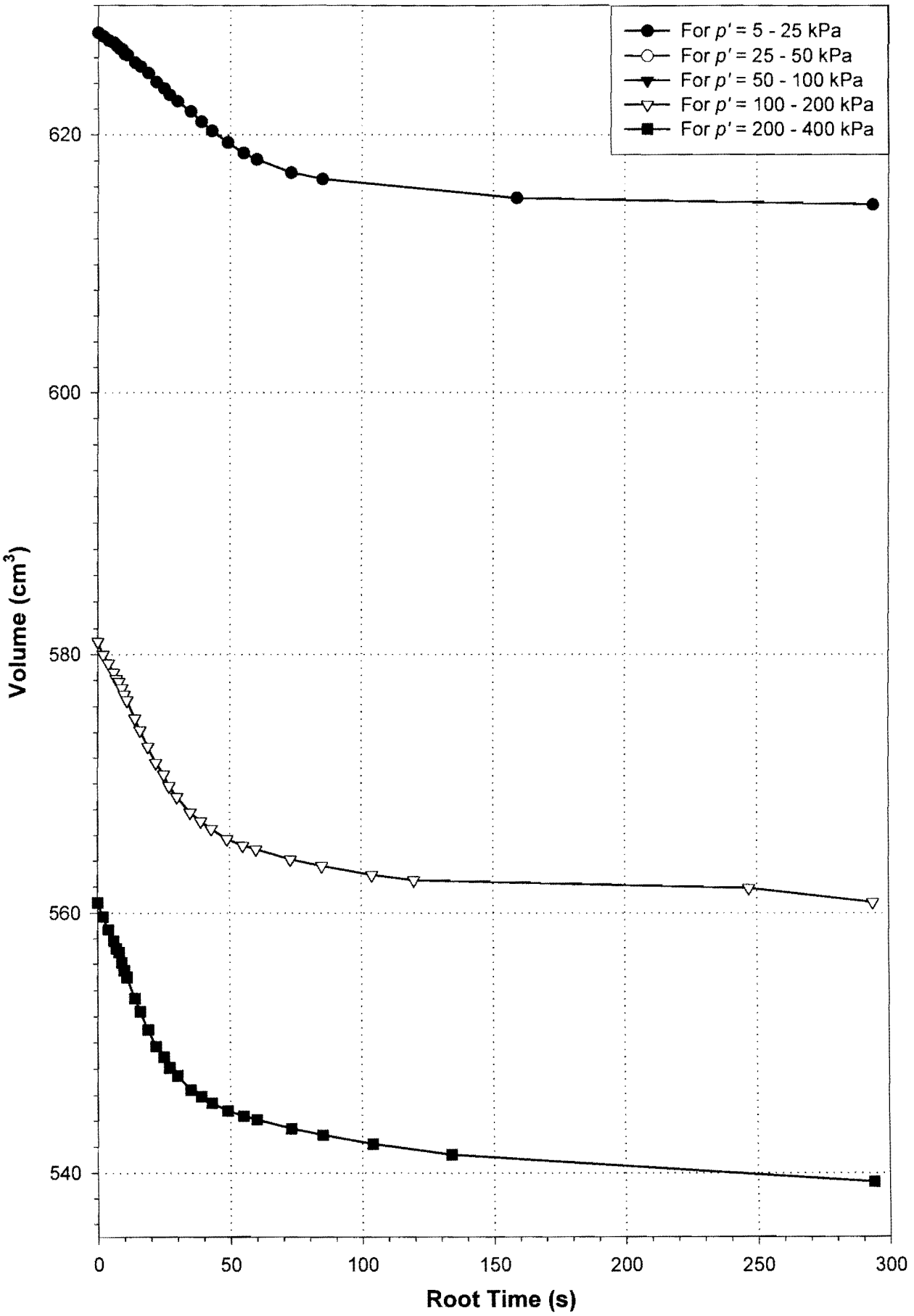

Figure 3-86: Reconstituted Mizpah Pond Fine: Volumetric consolidation.

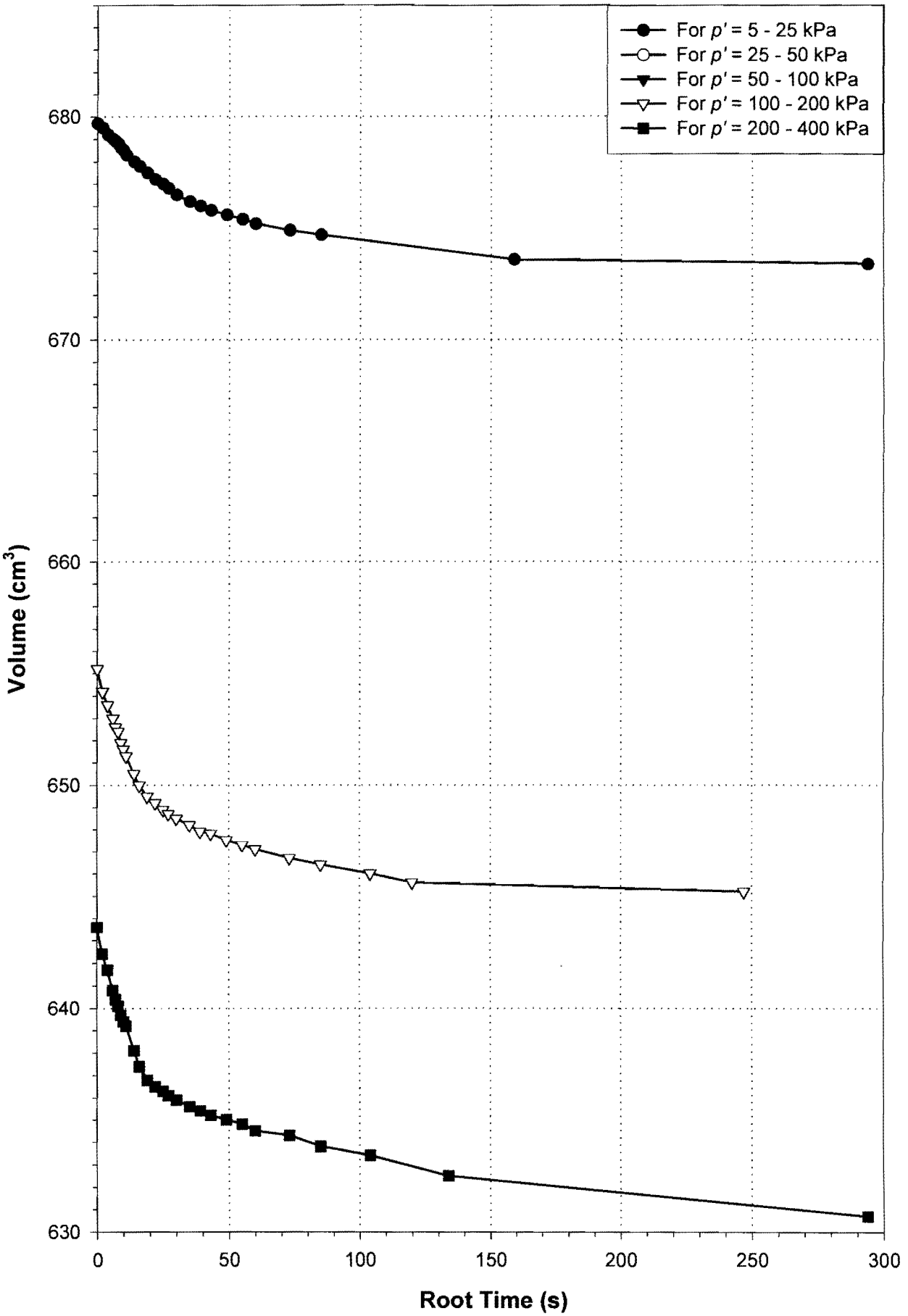

Figure 3-87: Reconstituted Mizpah Pond Coarse: Volumetric consolidation.

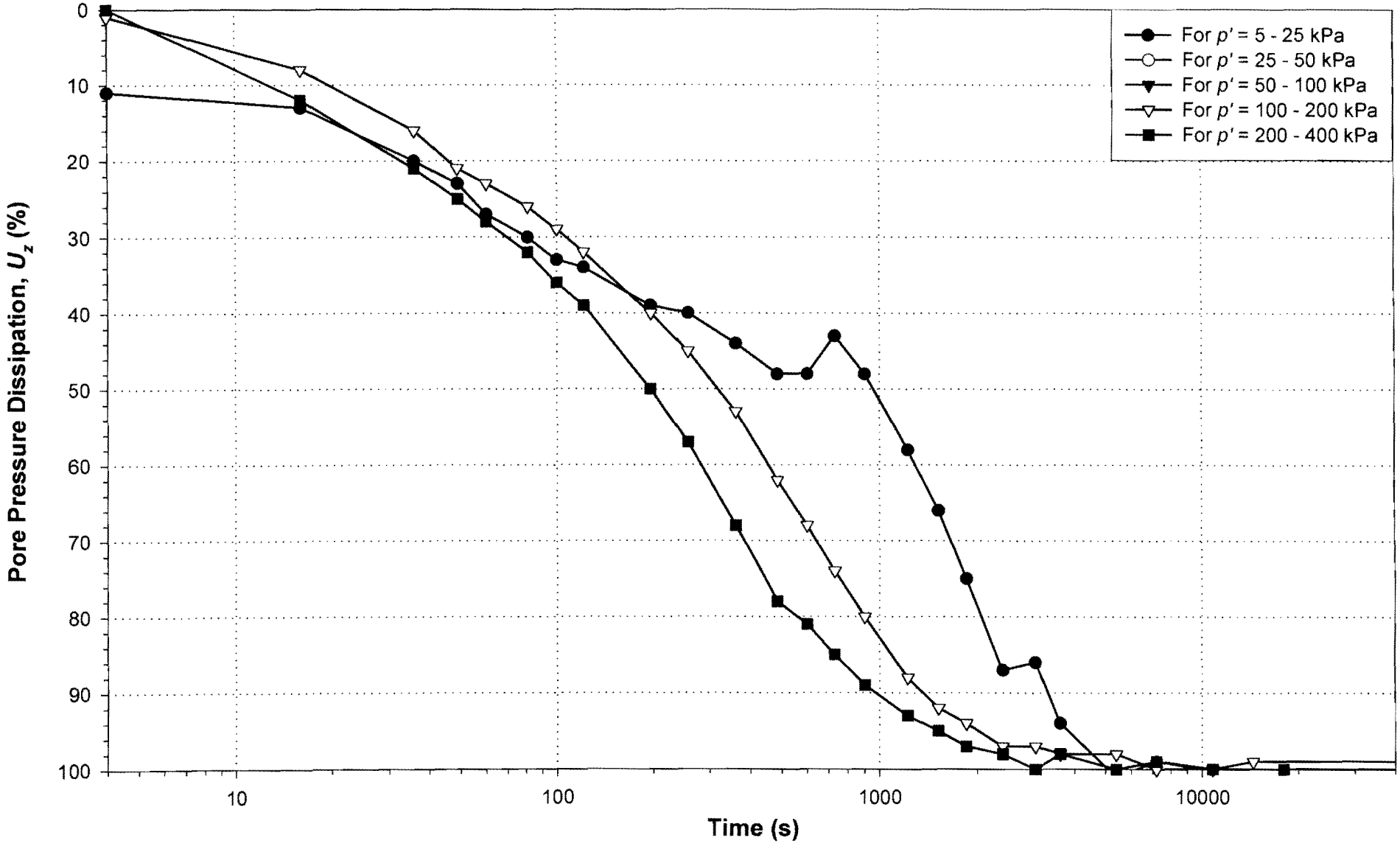

Figure 3-88: Reconstituted Mizpah Pond Fine: Pore pressure dissipation.

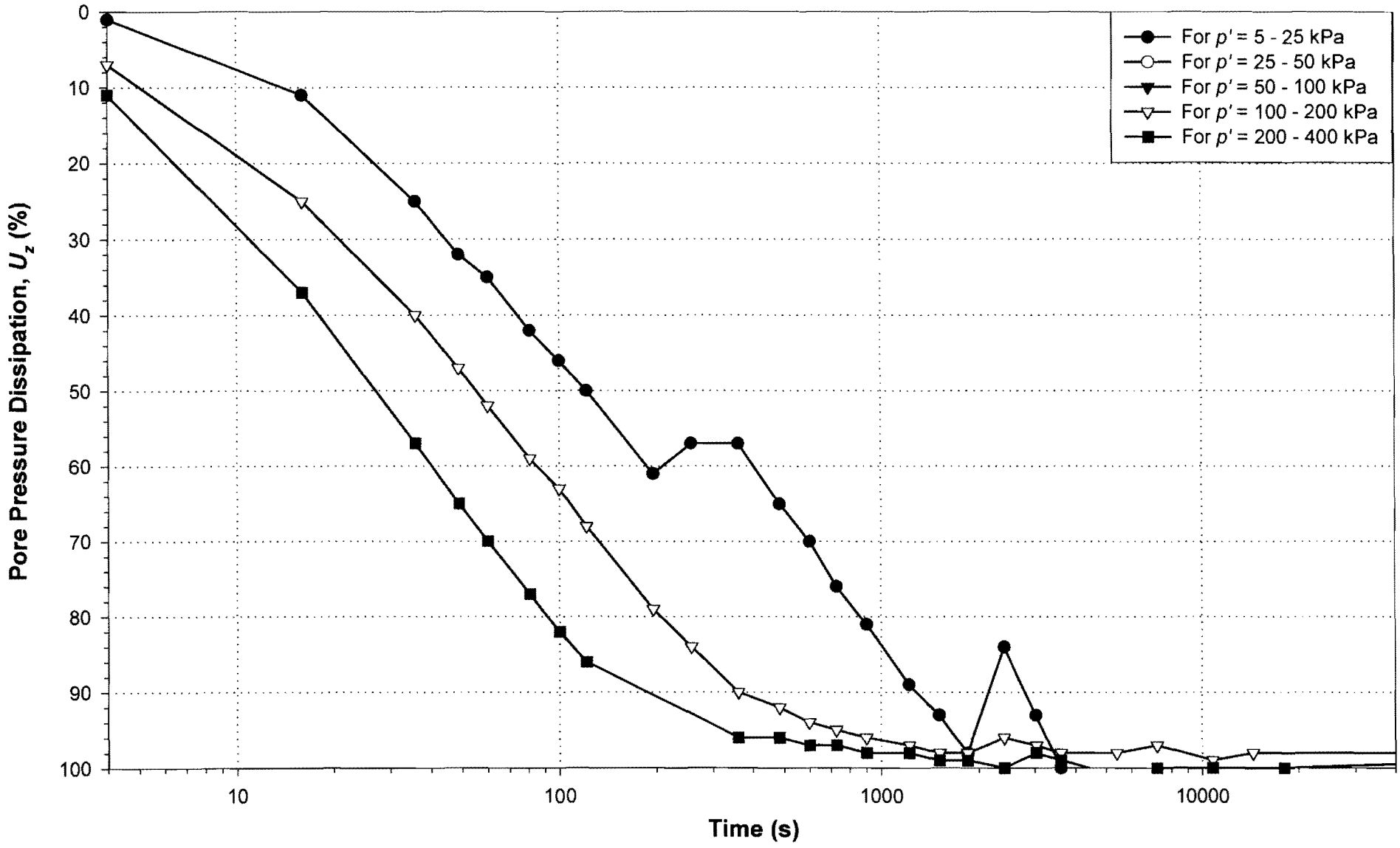

Figure 3-89: Reconstituted Mizpah Pond Coarse: Pore pressure dissipation.

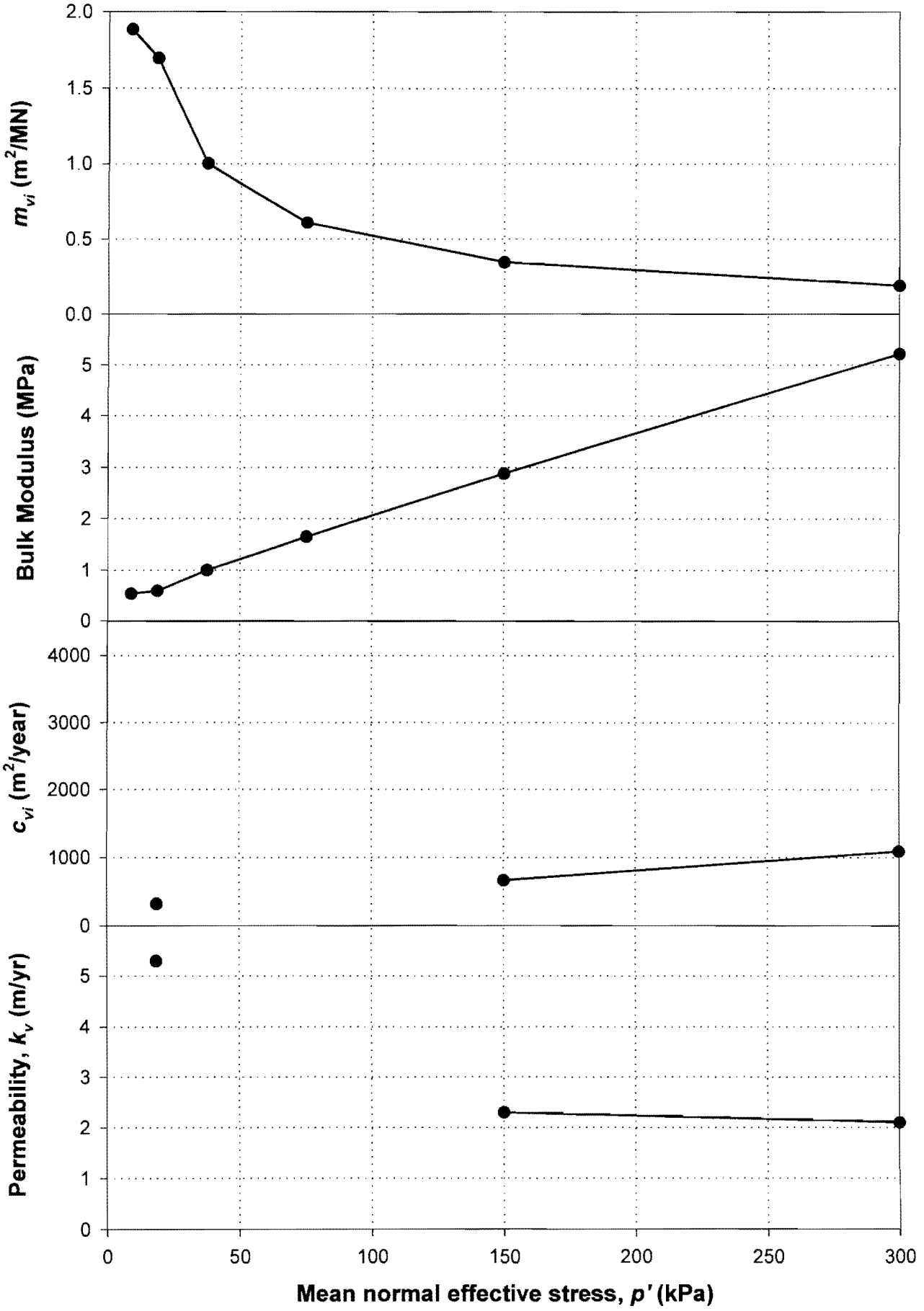

Figure 3-90: Reconstituted Mizpah Pond Fine: Consolidation parameters.

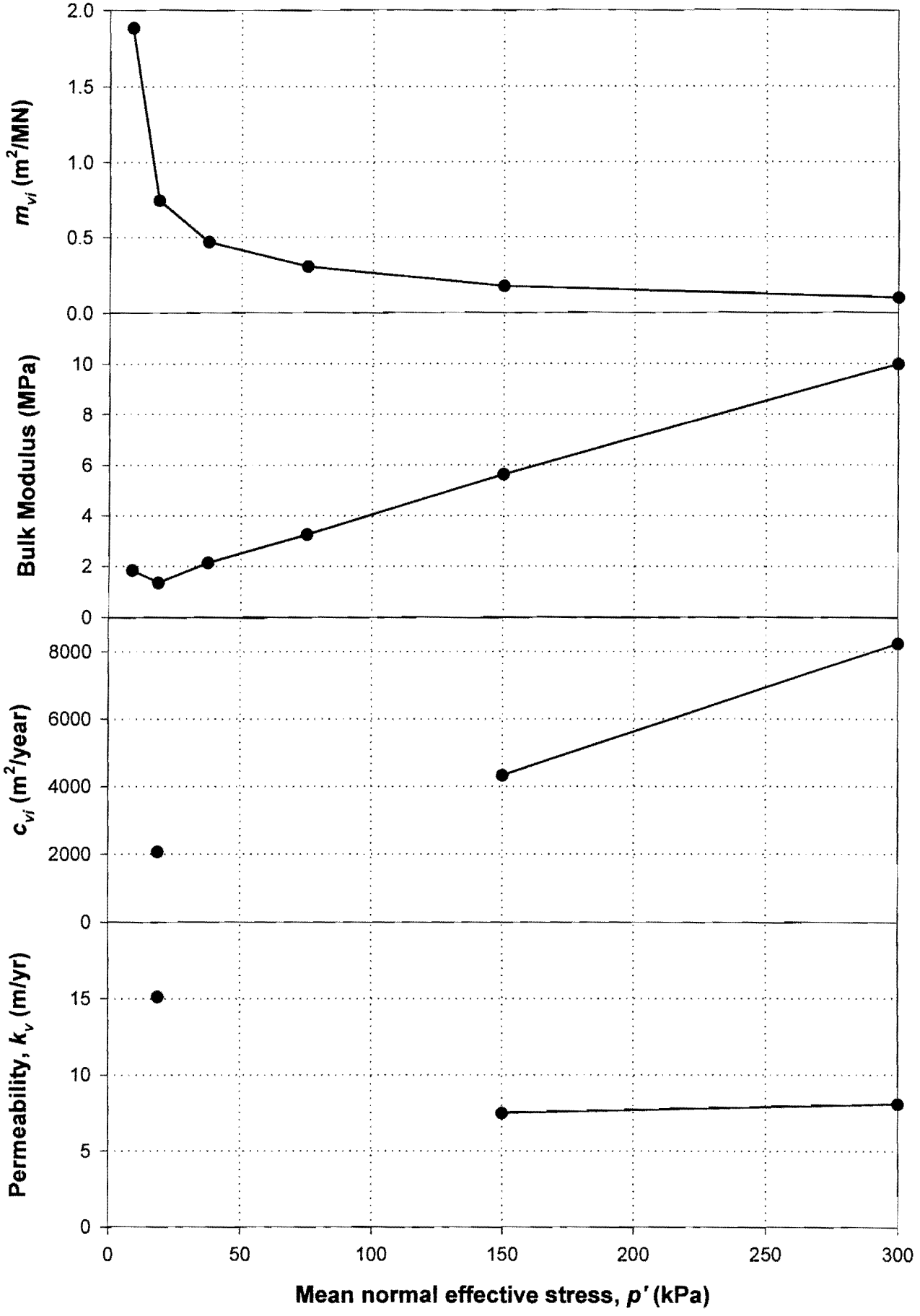

Figure 3-91: Reconstituted Mizpah Pond Coarse: Consolidation parameters.

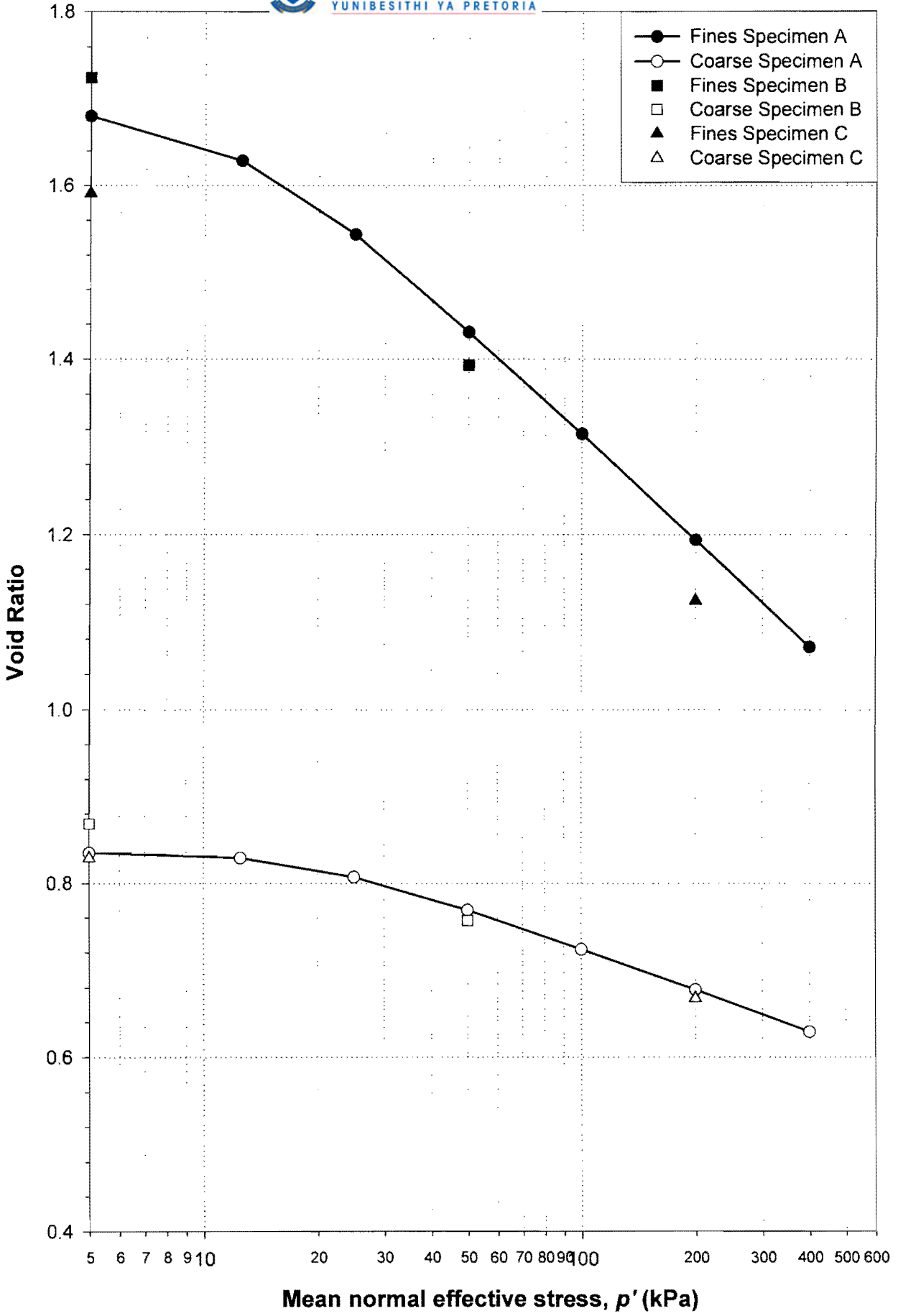

Figure 3-92: Reconstituted Pay Dam Penstock Tailings: Isotropic compression.

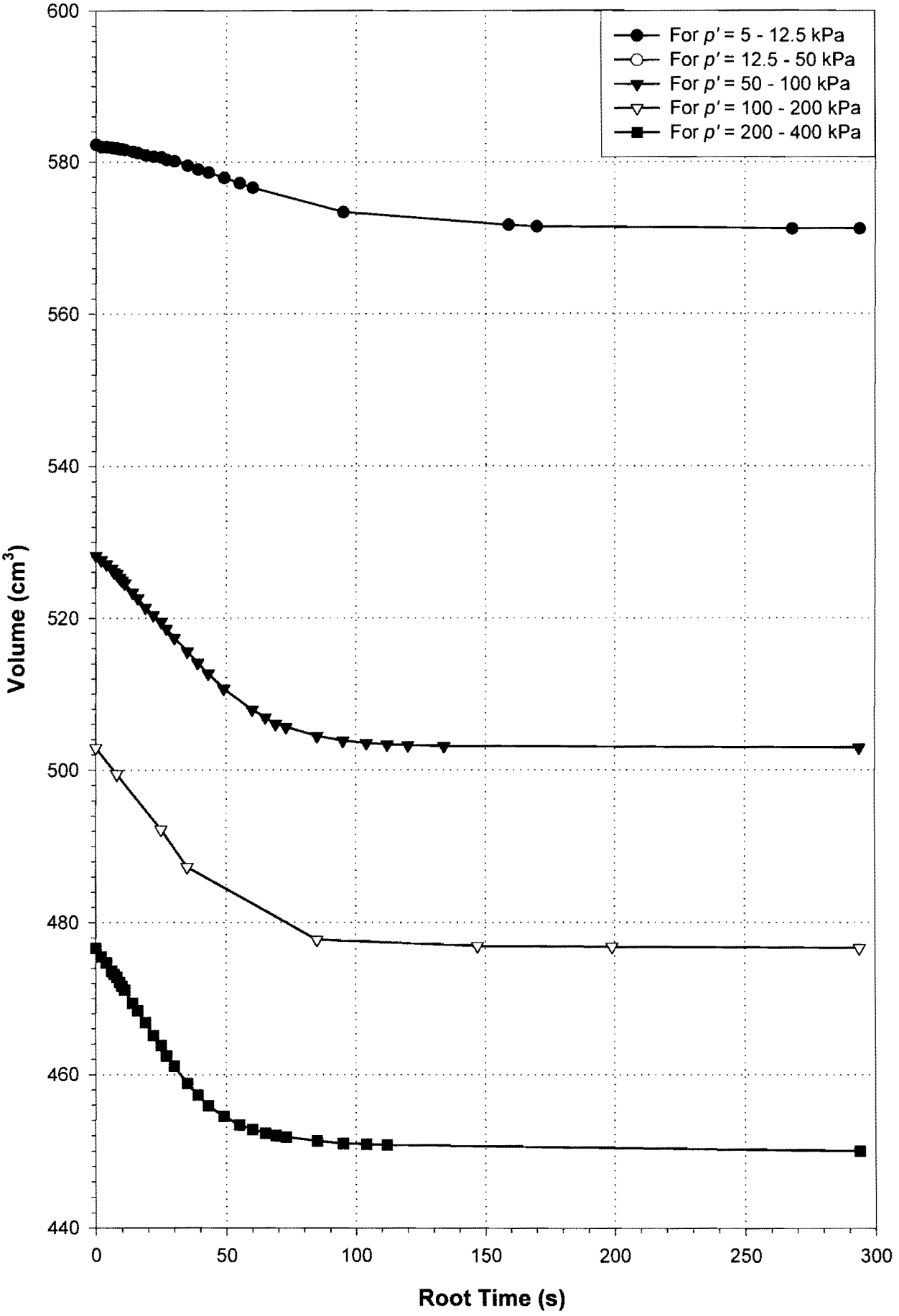

Figure 3-93: Reconstituted Pay Dam Penstock Fine: Volumetric consolidation.

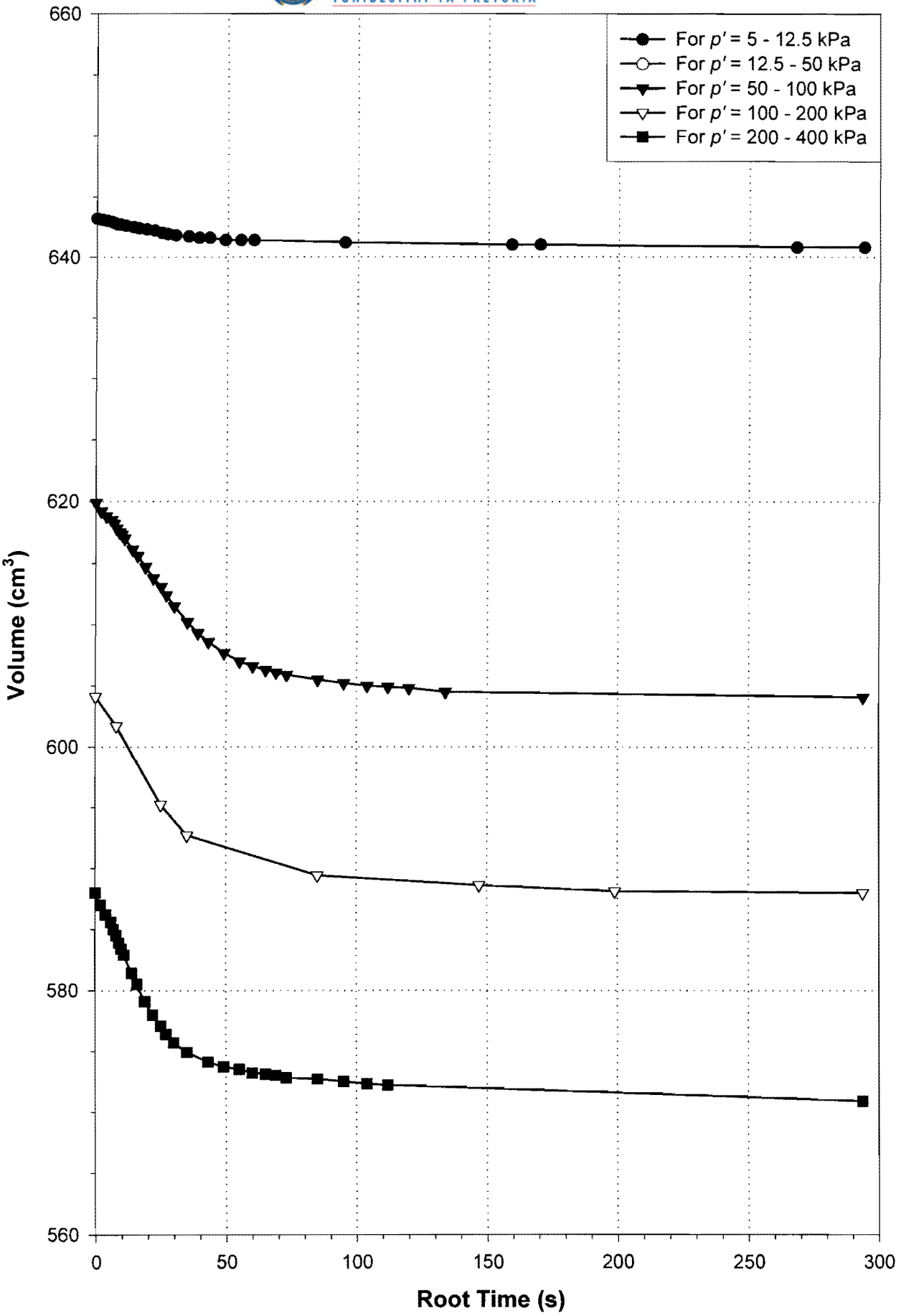

Figure 3-94: Reconstituted Pay Dam Penstock Coarse: Volumetric consolidation.

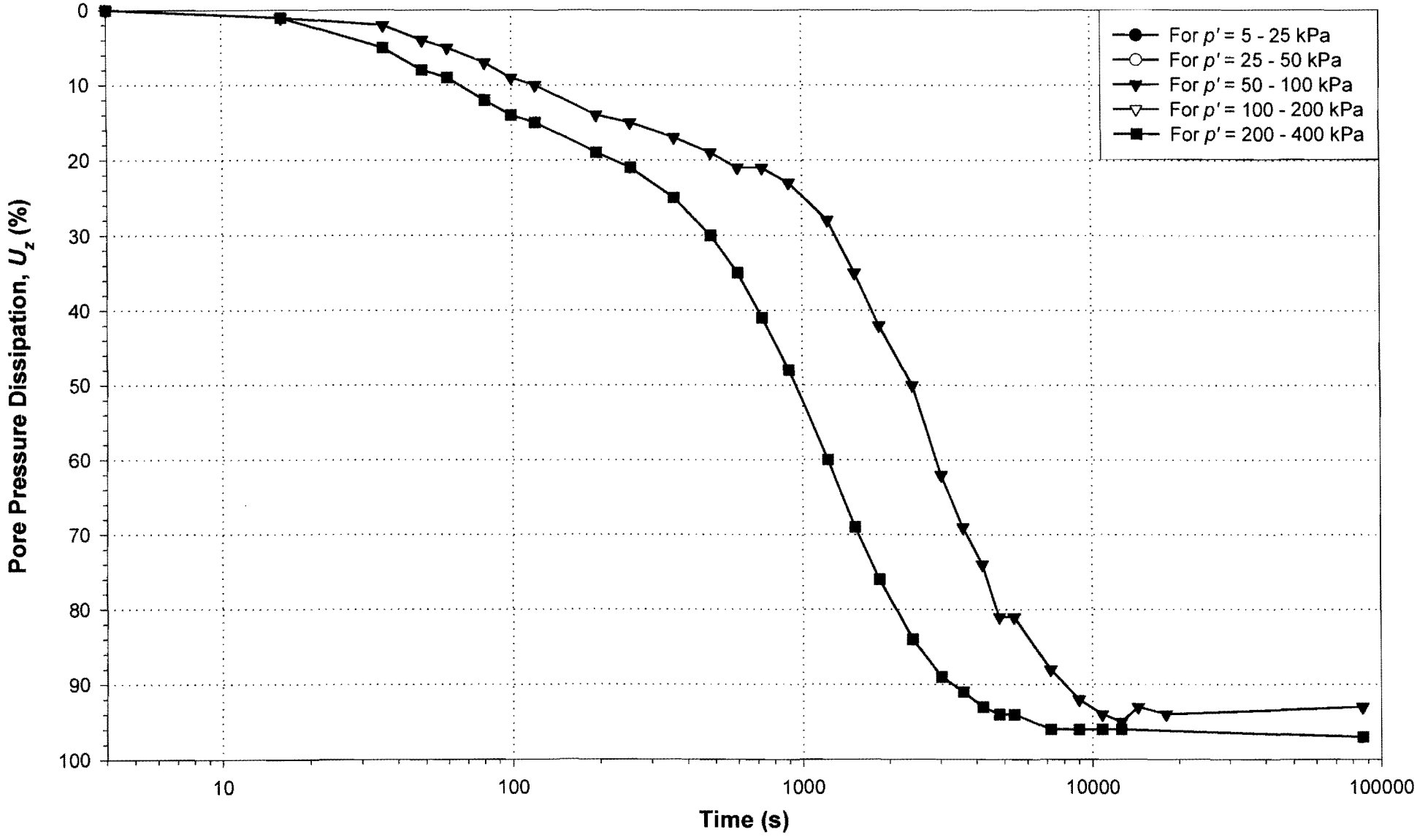

Figure 3-95: Reconstituted Pay Dam Penstock Fine: Pore pressure dissipation.

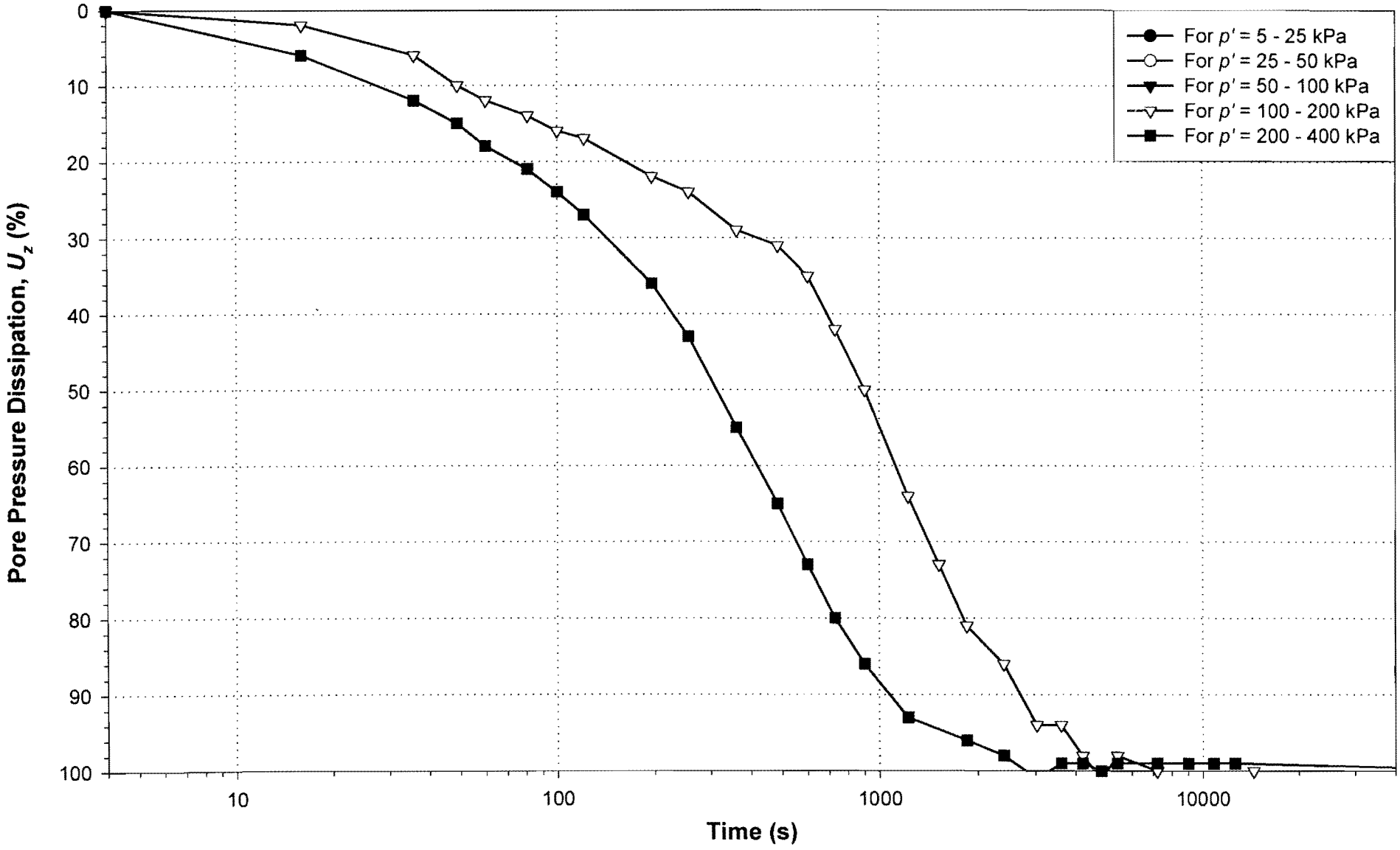

Figure 3-96: Reconstituted Pay Dam Penstock Coarse: Pore pressure dissipation.

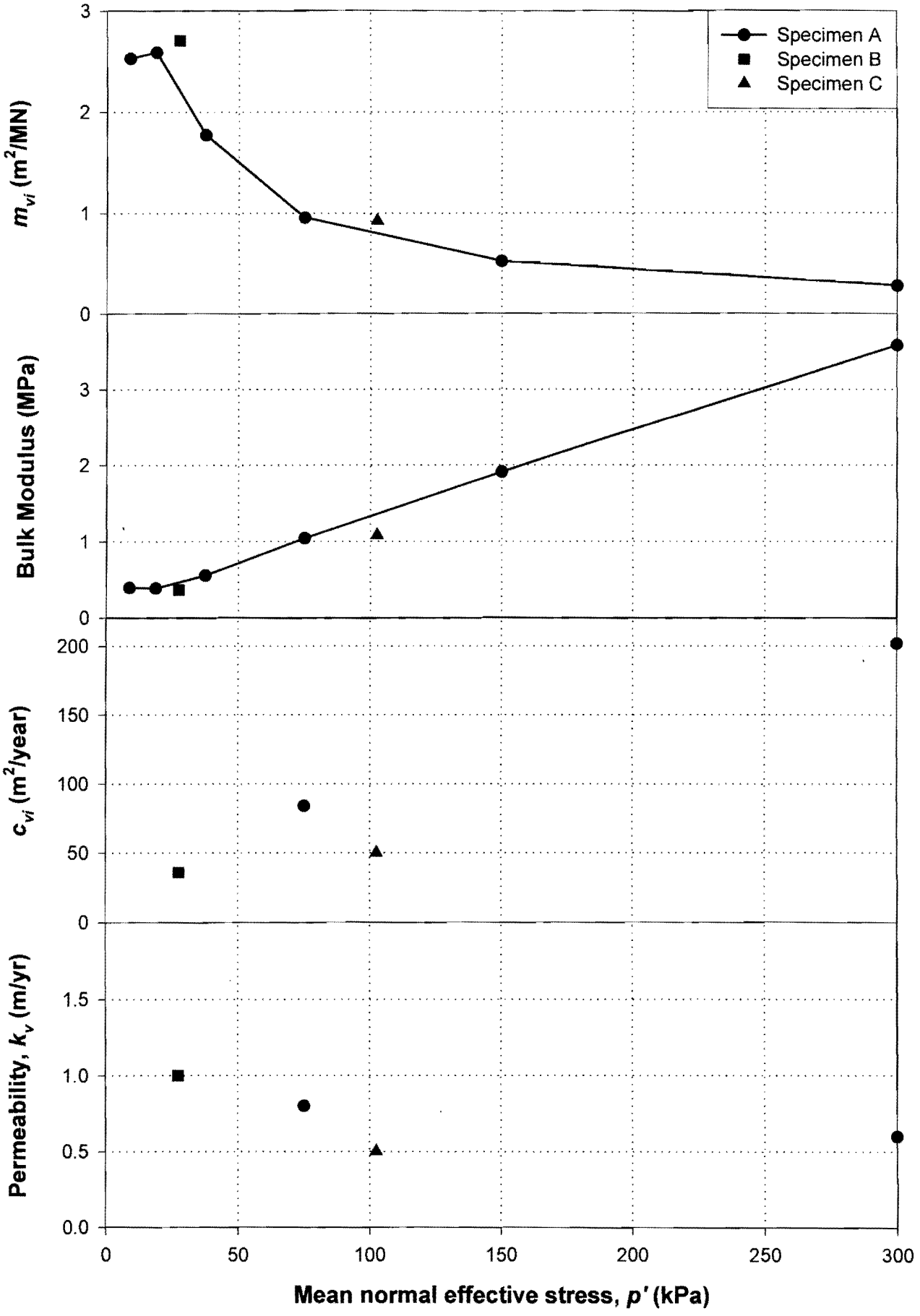

Figure 3-97: Reconstituted Pay Dam Penstock Fine: Consolidation parameters.

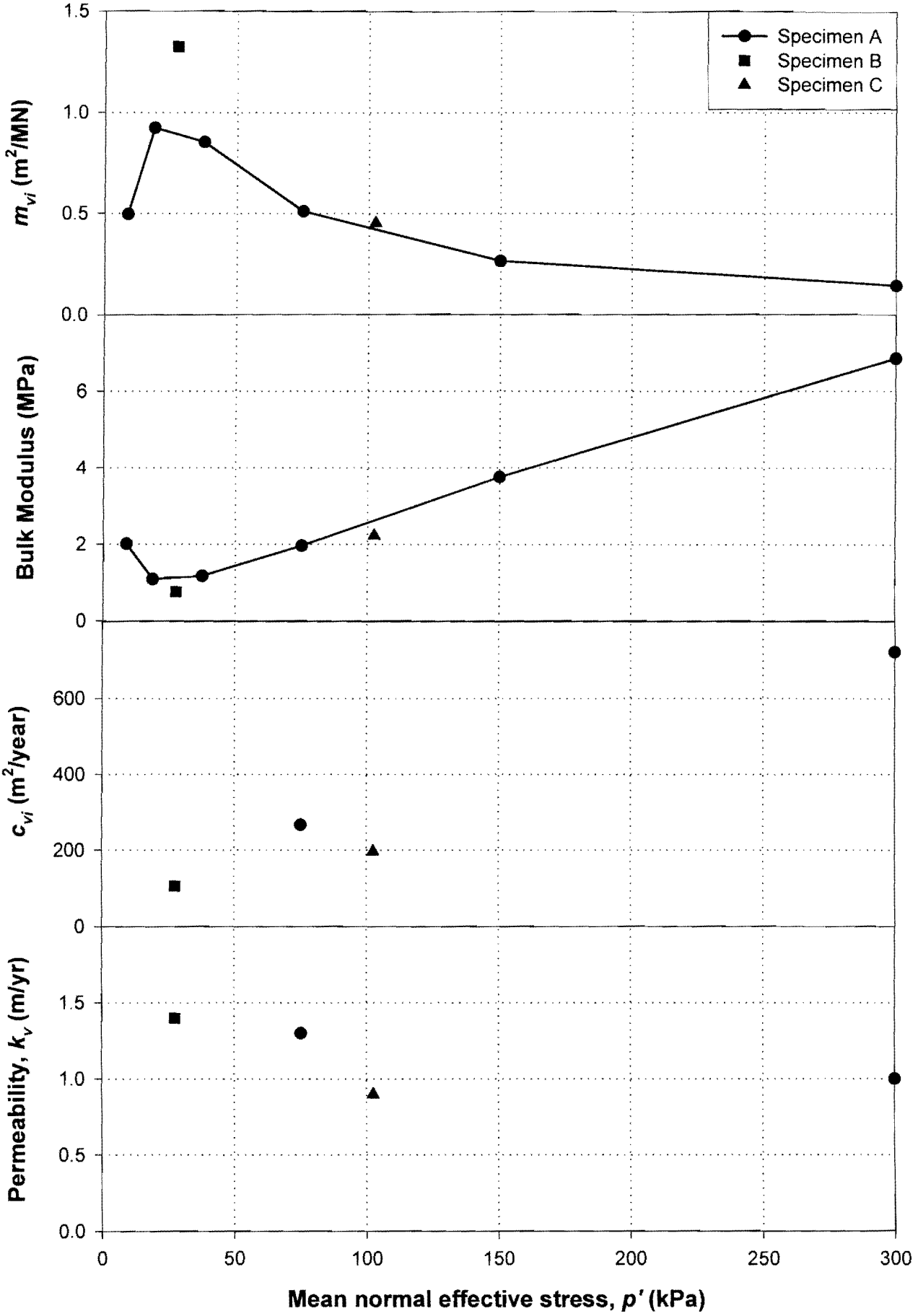

Figure 3-98: Reconstituted Pay Dam Penstock Coarse: Consolidation parameters.

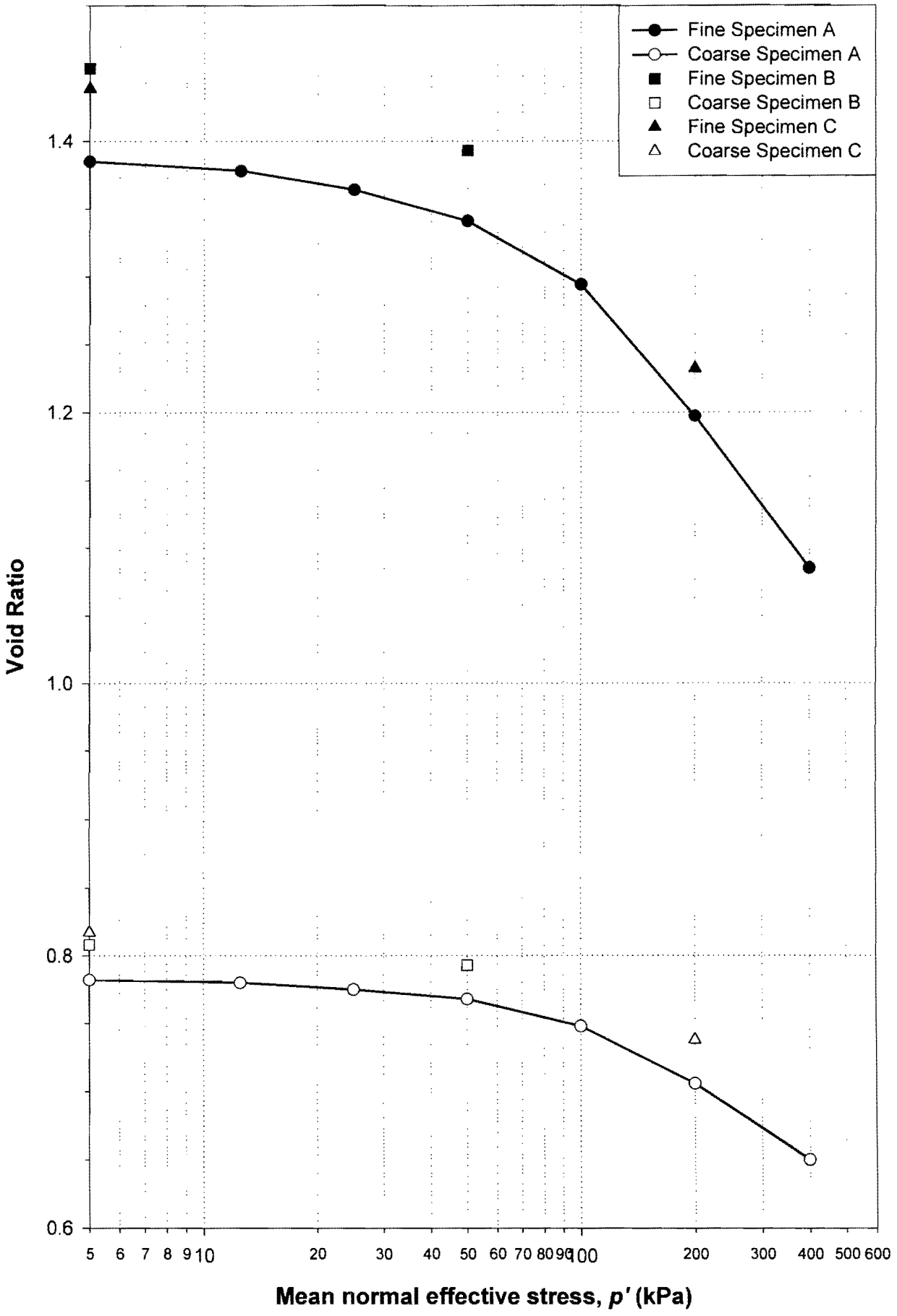

Figure 3-99: Undisturbed Pay Dam Penstock Tailings: Isotropic compression.

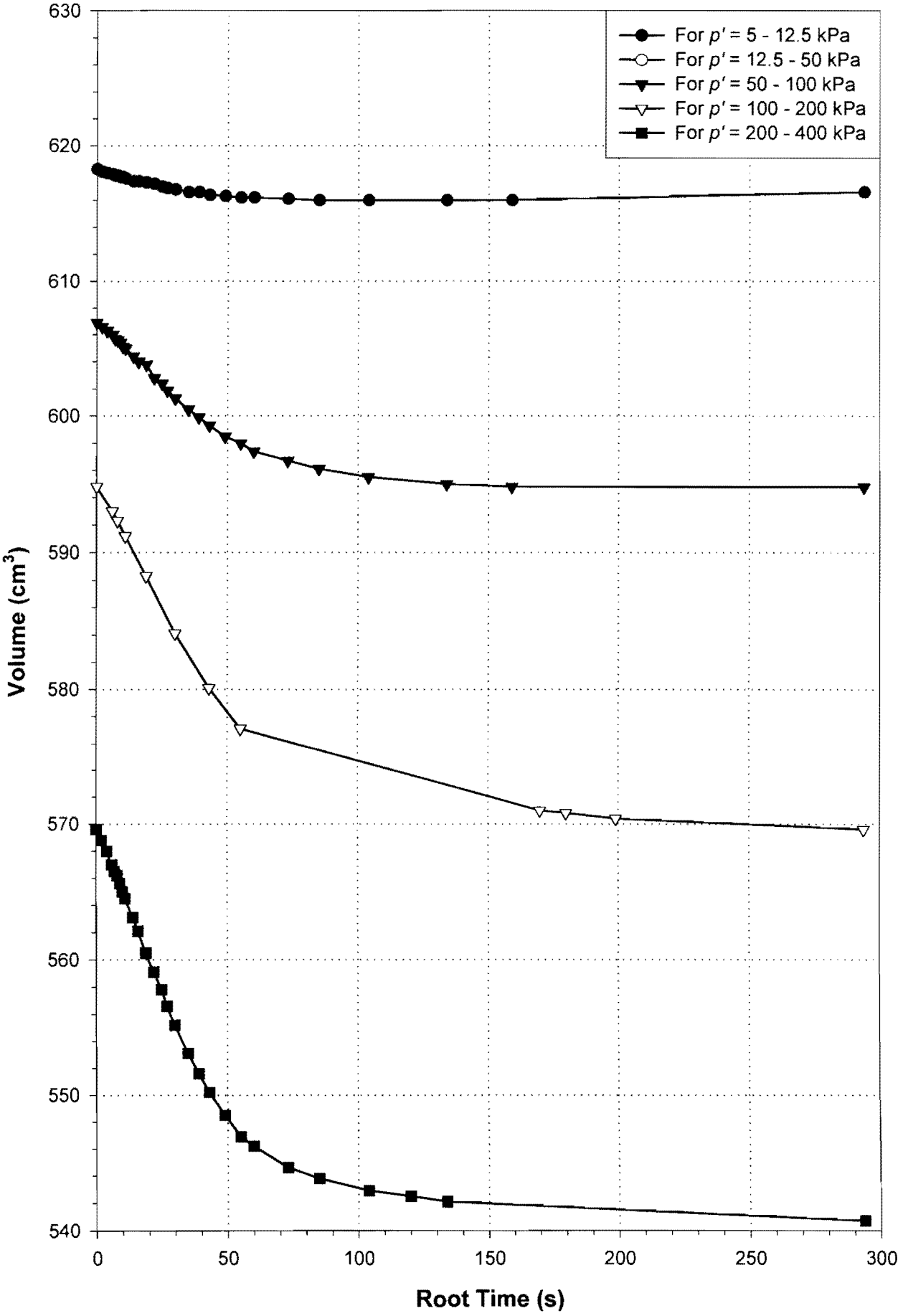

Figure 3-100: Undisturbed Pay Dam Penstock Fine: Volumetric consolidation.

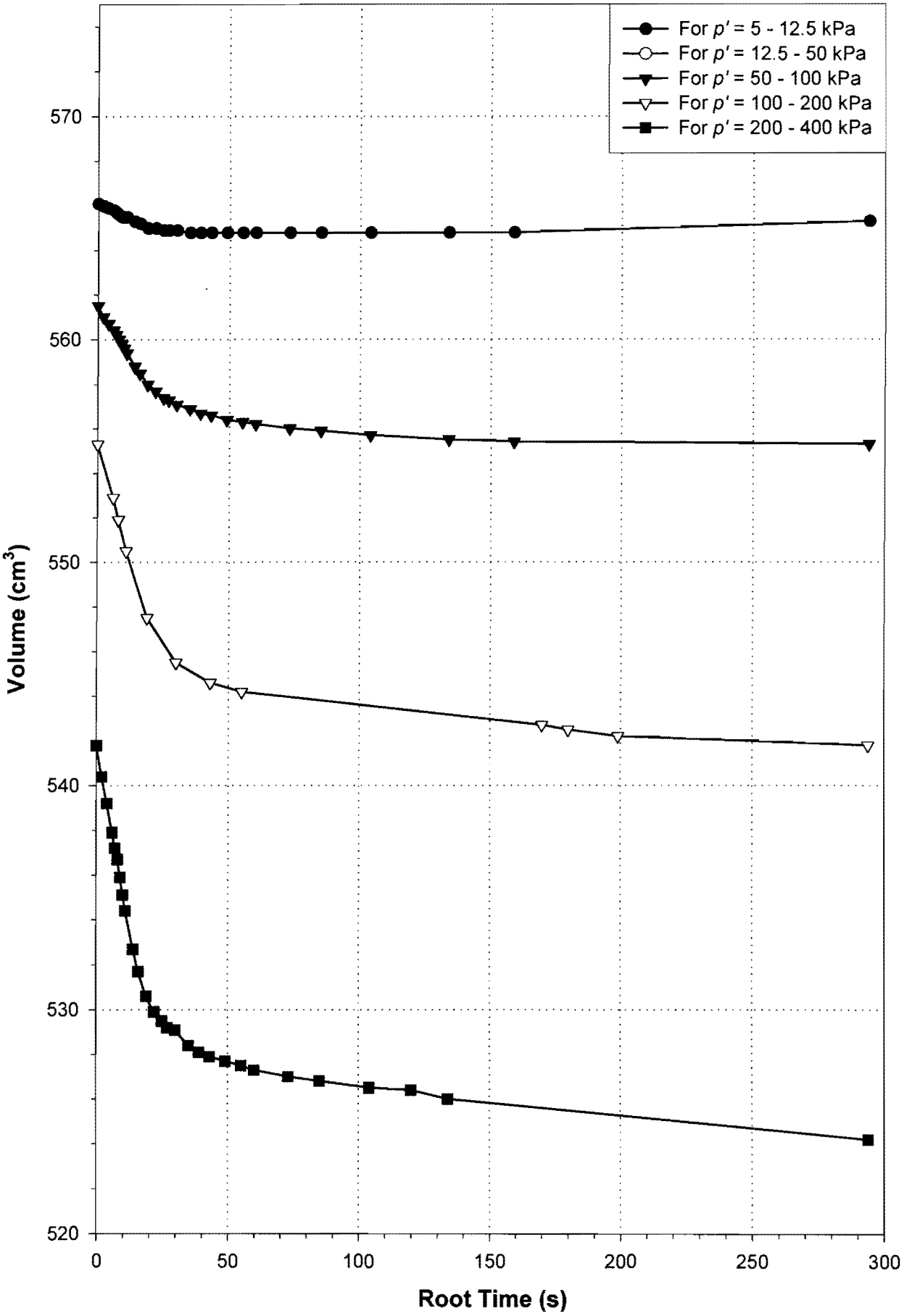

Figure 3-101: Undisturbed Pay Dam Penstock Coarse: Volumetric consolidation.

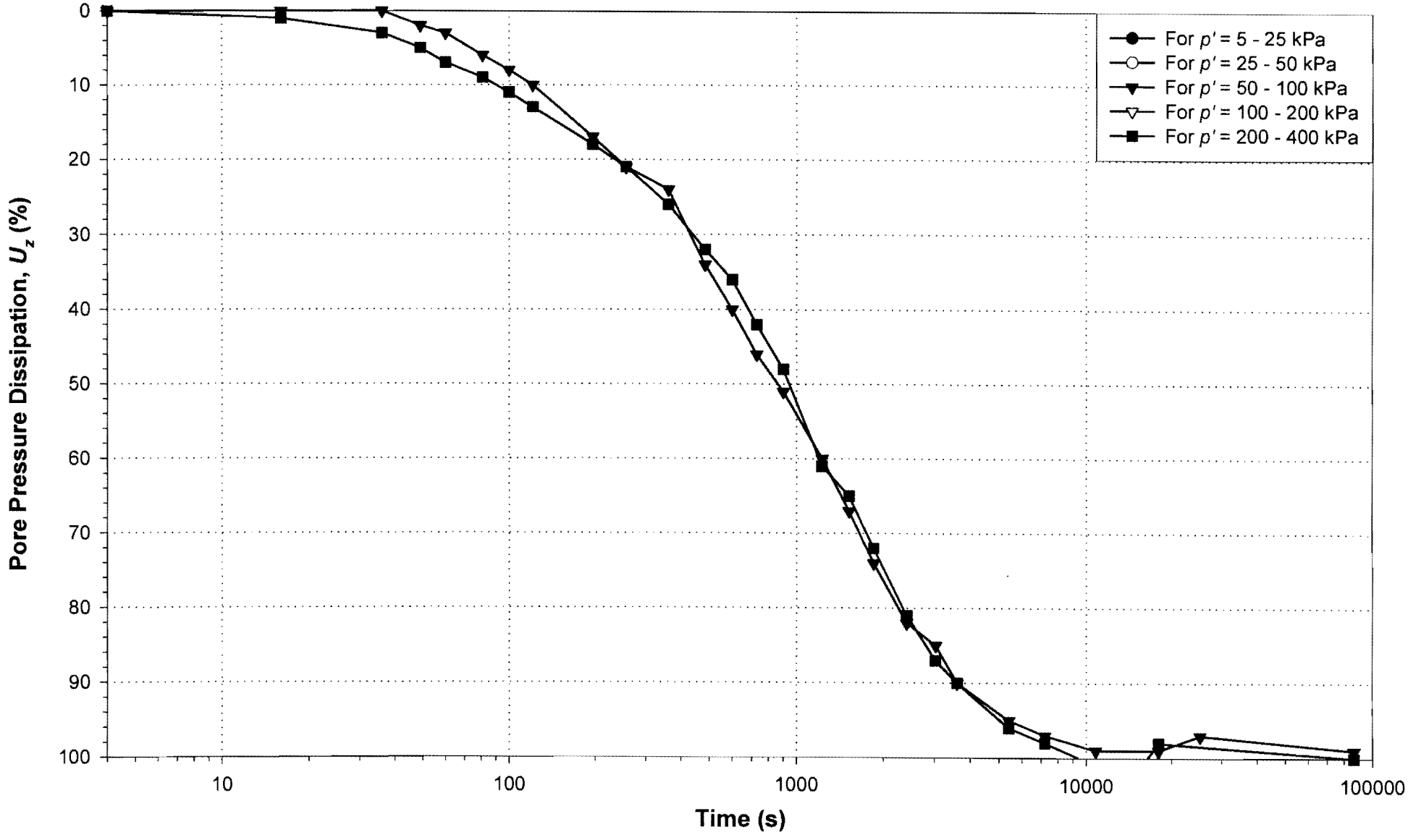

Figure 3-102: Undisturbed Pay Dam Penstock Fine: Pore pressure dissipation.

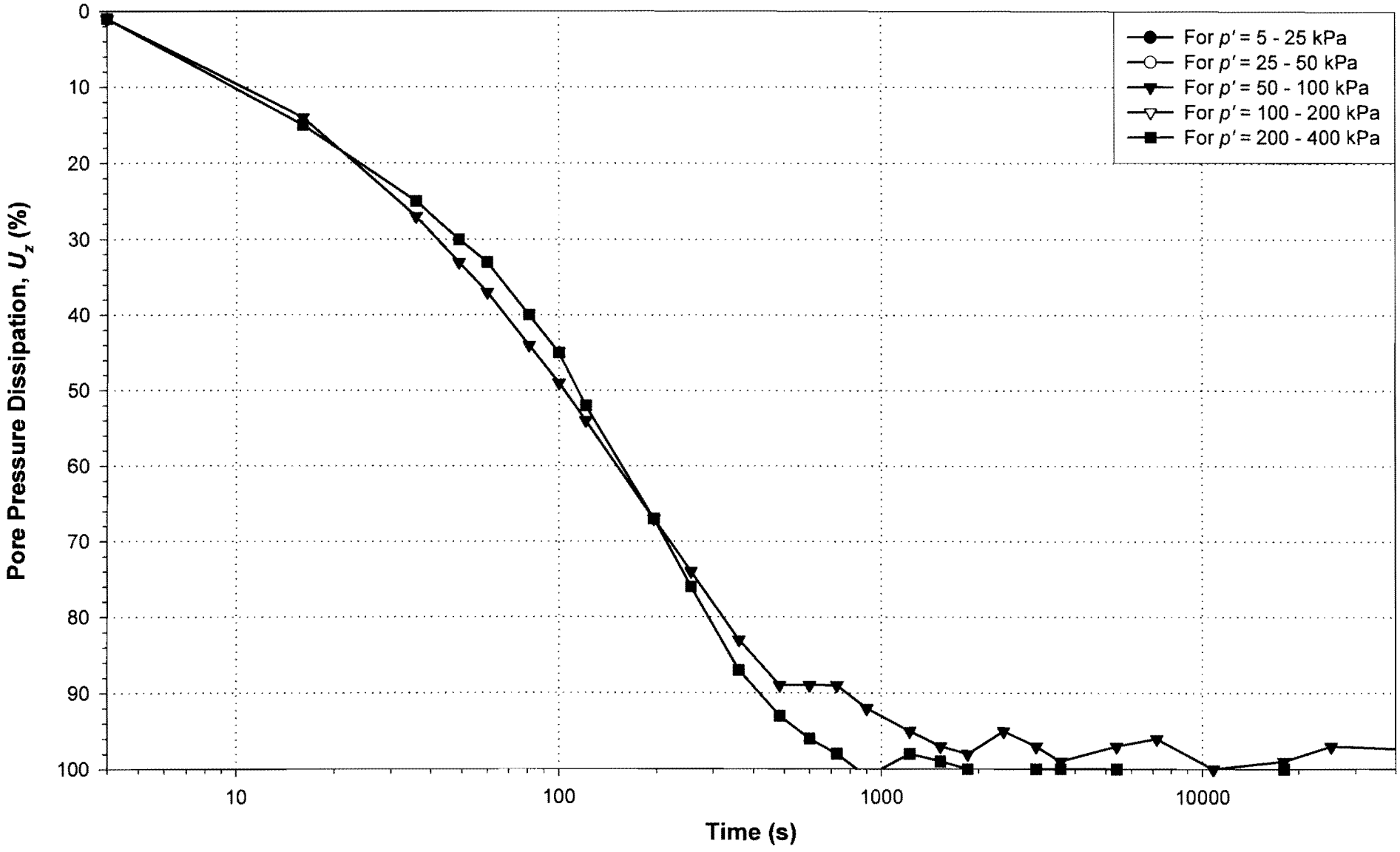

Figure 3-103: Undisturbed Pay Dam Penstock Coarse: Pore pressure dissipation.

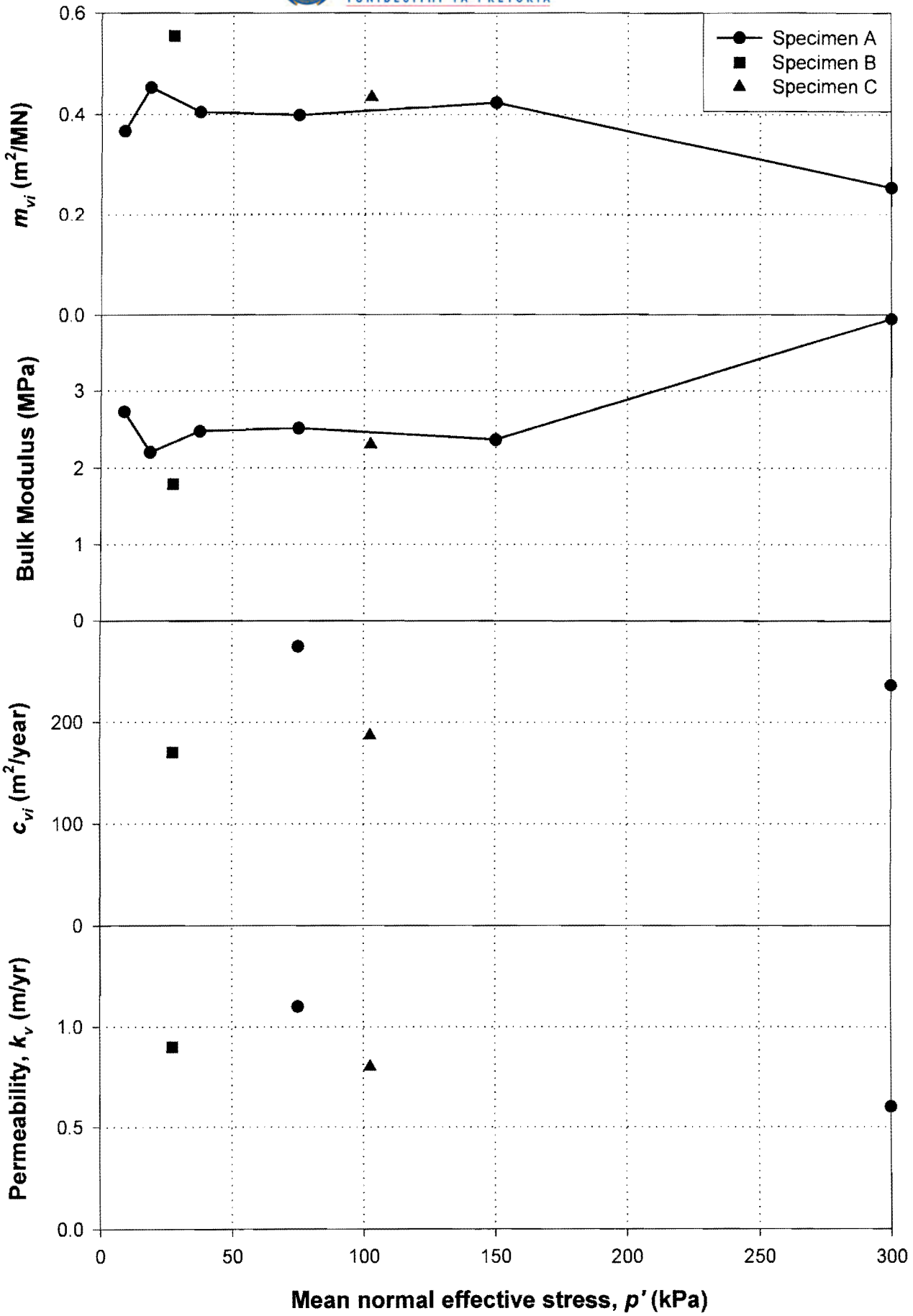

Figure 3-104: Undisturbed Pay Dam Penstock Fine: Consolidation parameters.

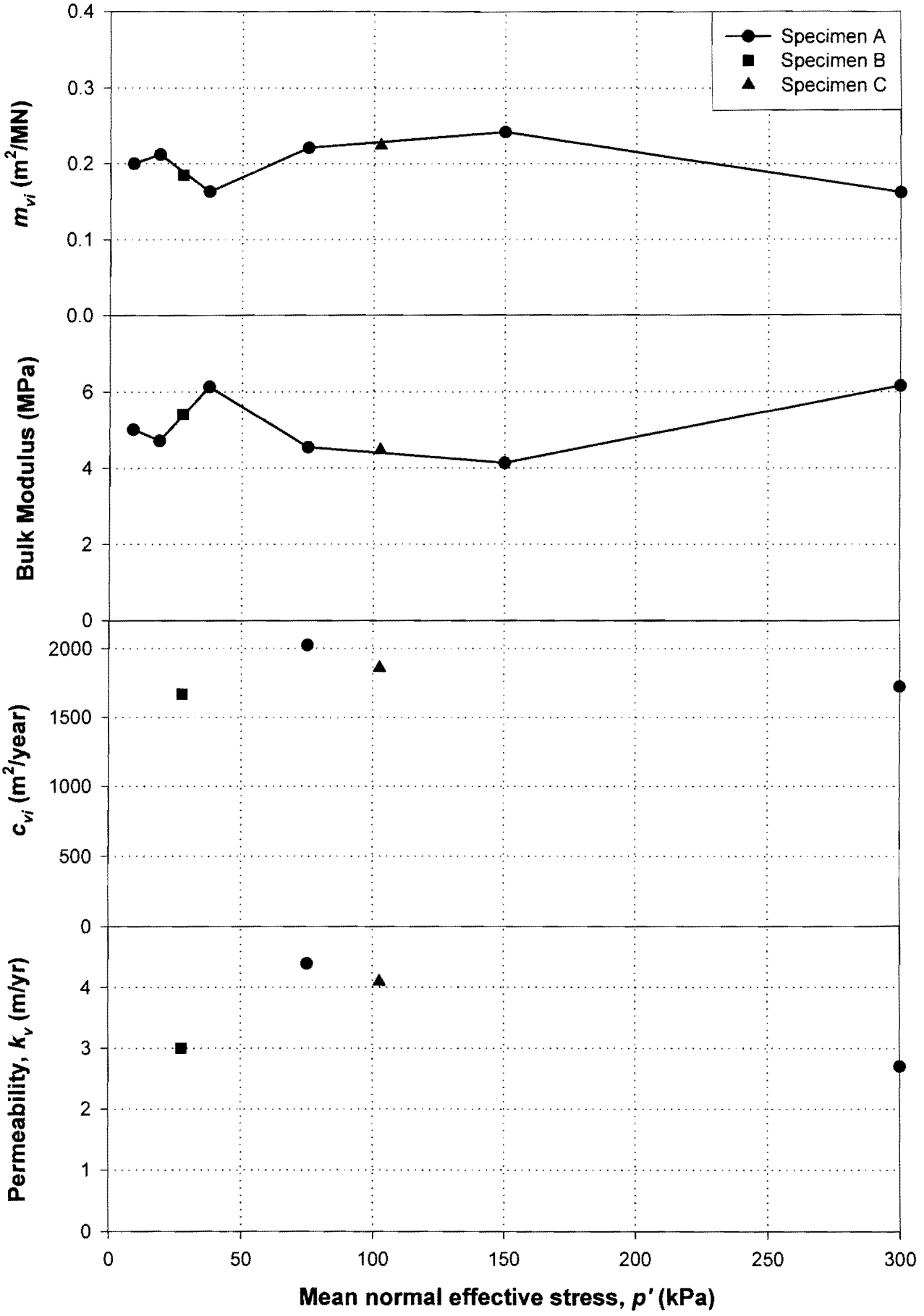

Figure 3-105: Undisturbed Pay Dam Penstock Coarse: Consolidation parameters.

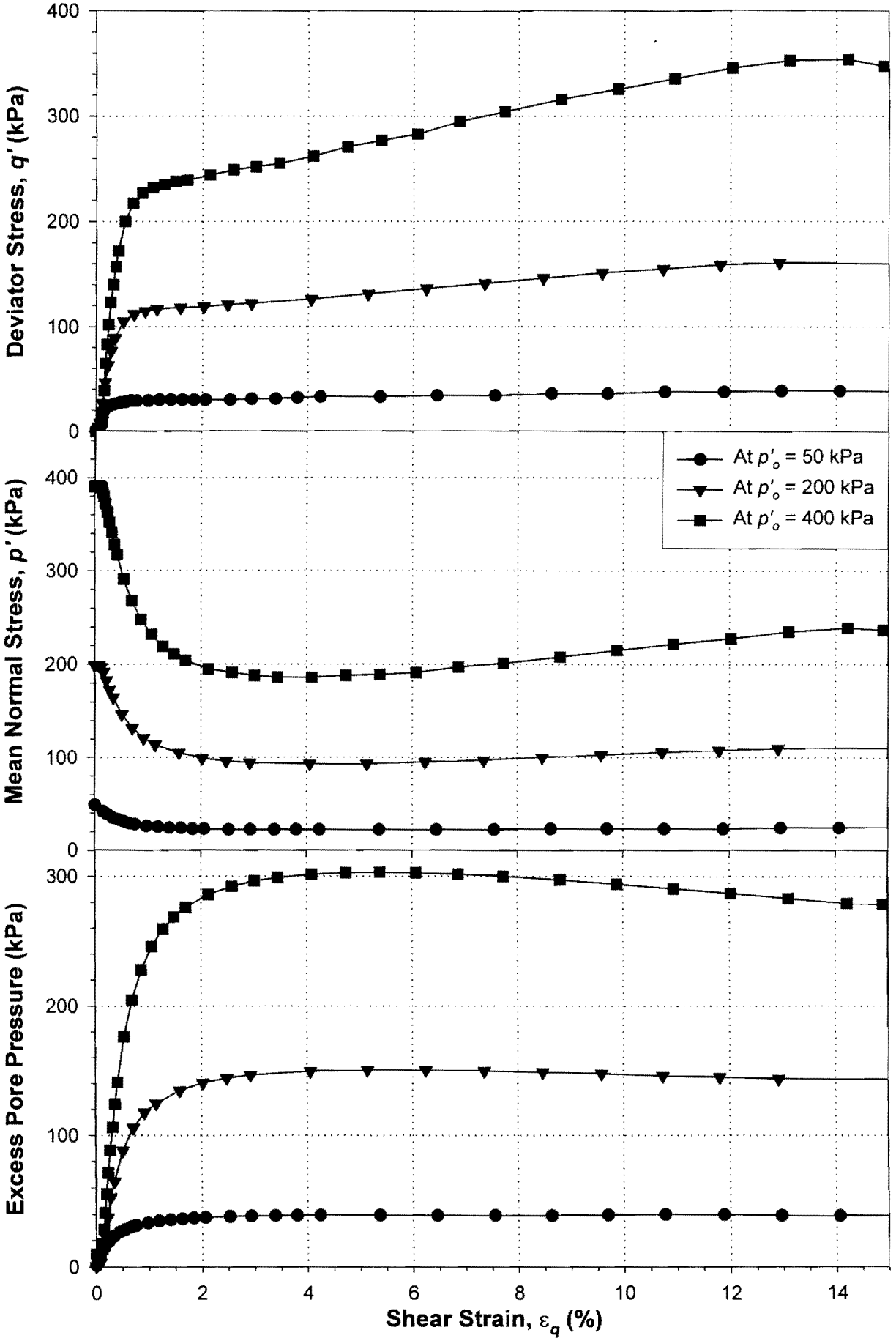

Figure 3-106: Mizpah Whole Tailings: Undrained triaxial shear.

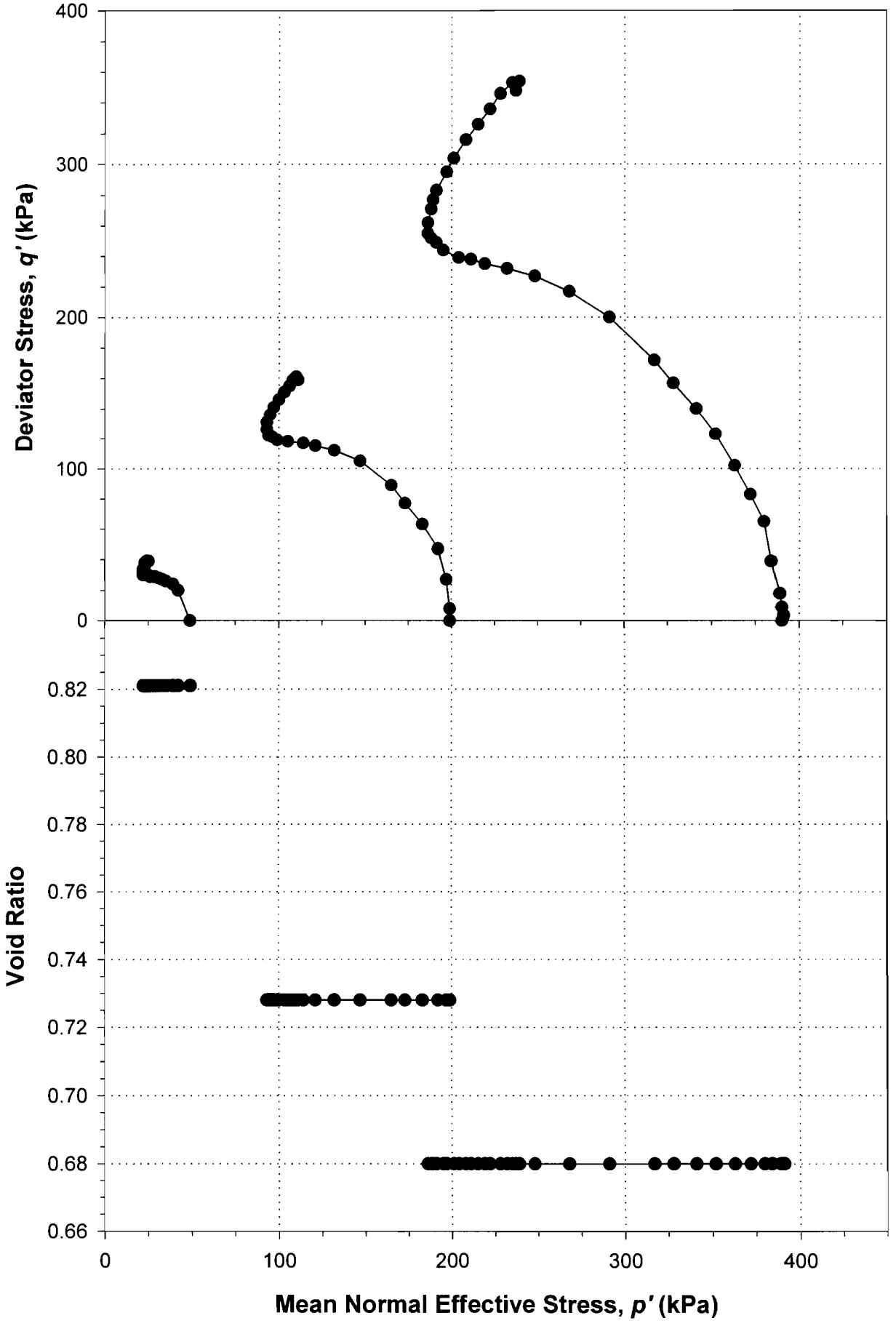

Figure 3-107: Undrained triaxial stress paths for reconstituted Mizpah whole tailings.

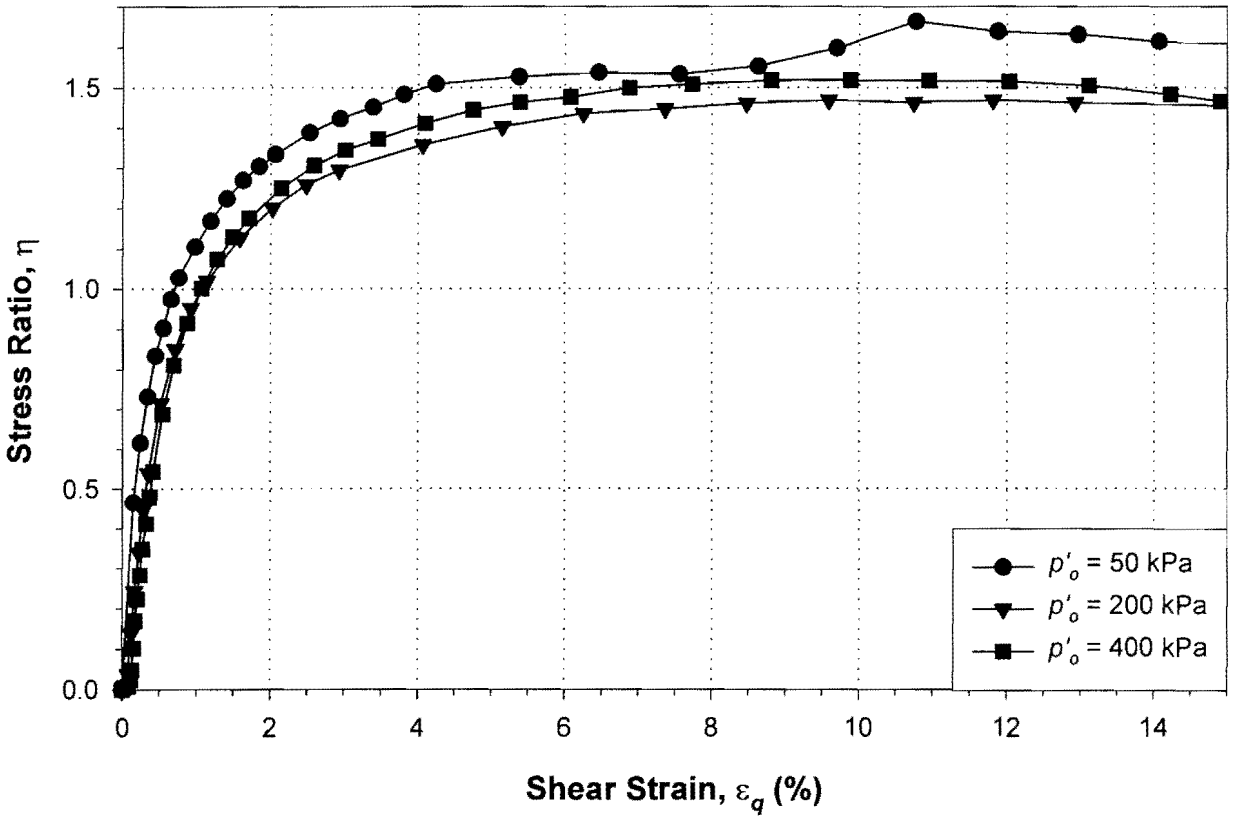

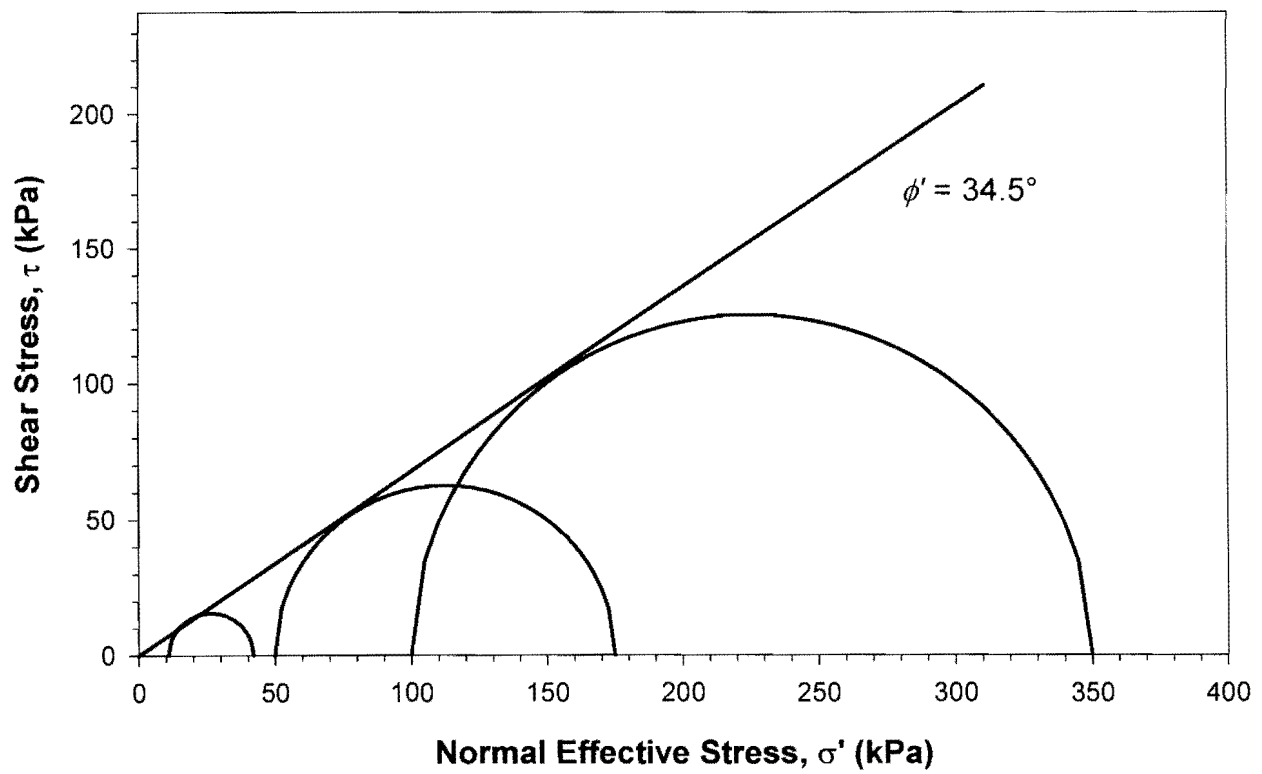

Figure 3-108: Undrained triaxial Mohr's Circles at failure for reconstituted Mizpah whole tailings.

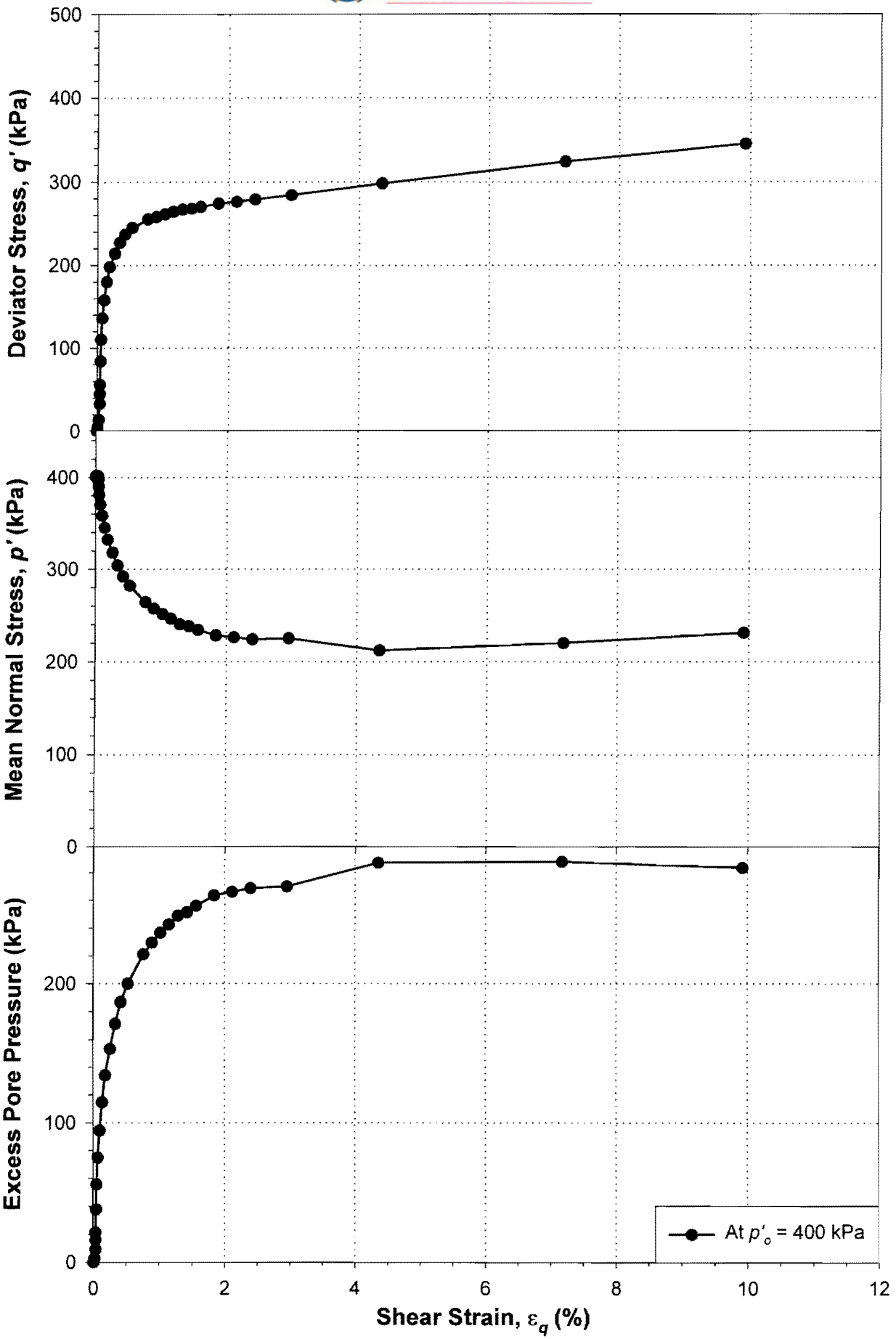

Figure 3-109: Mizpah Pond Fine: Undrained triaxial shear.

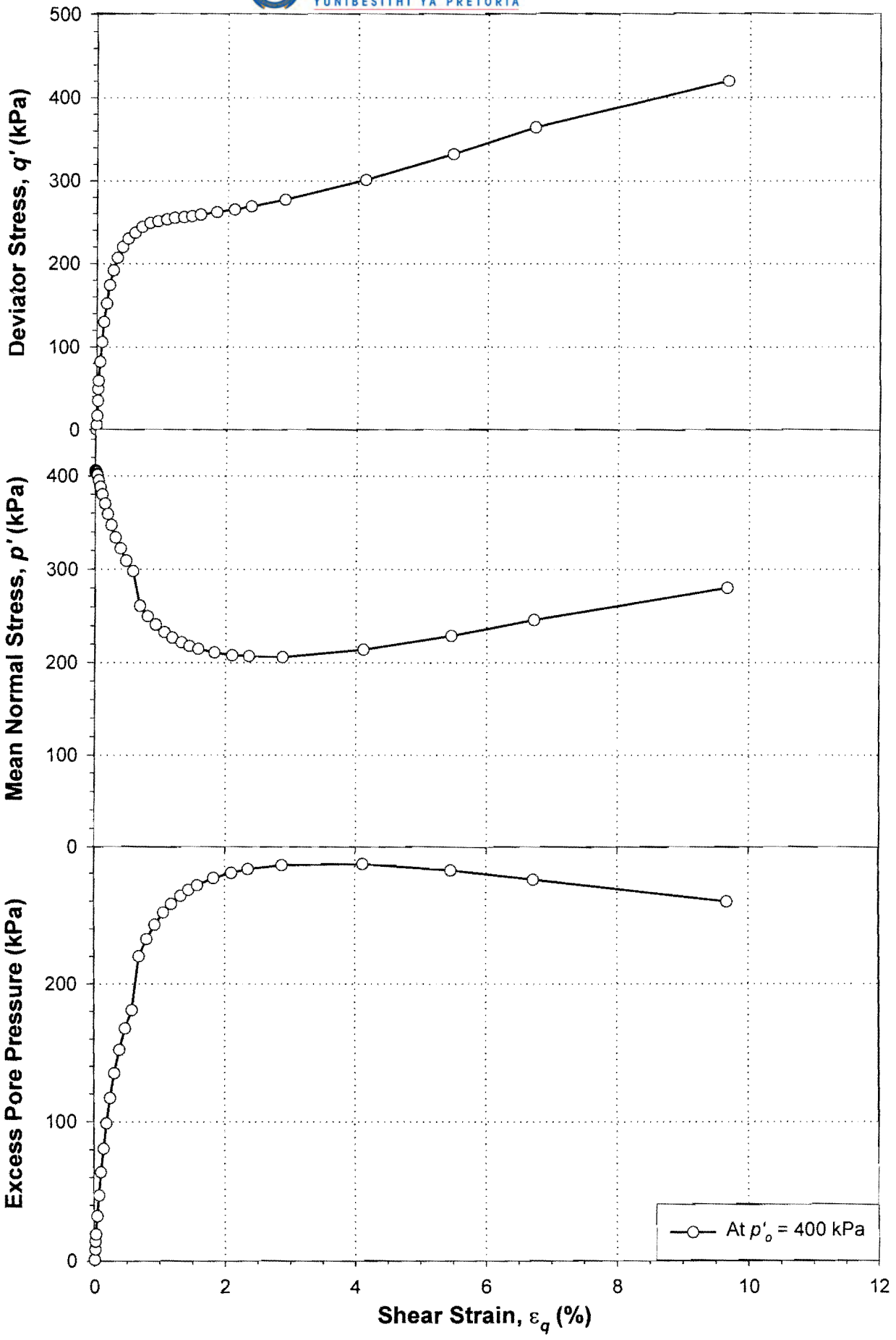

Figure 3-110: Mizpah Pond Coarse: Undrained triaxial shear.

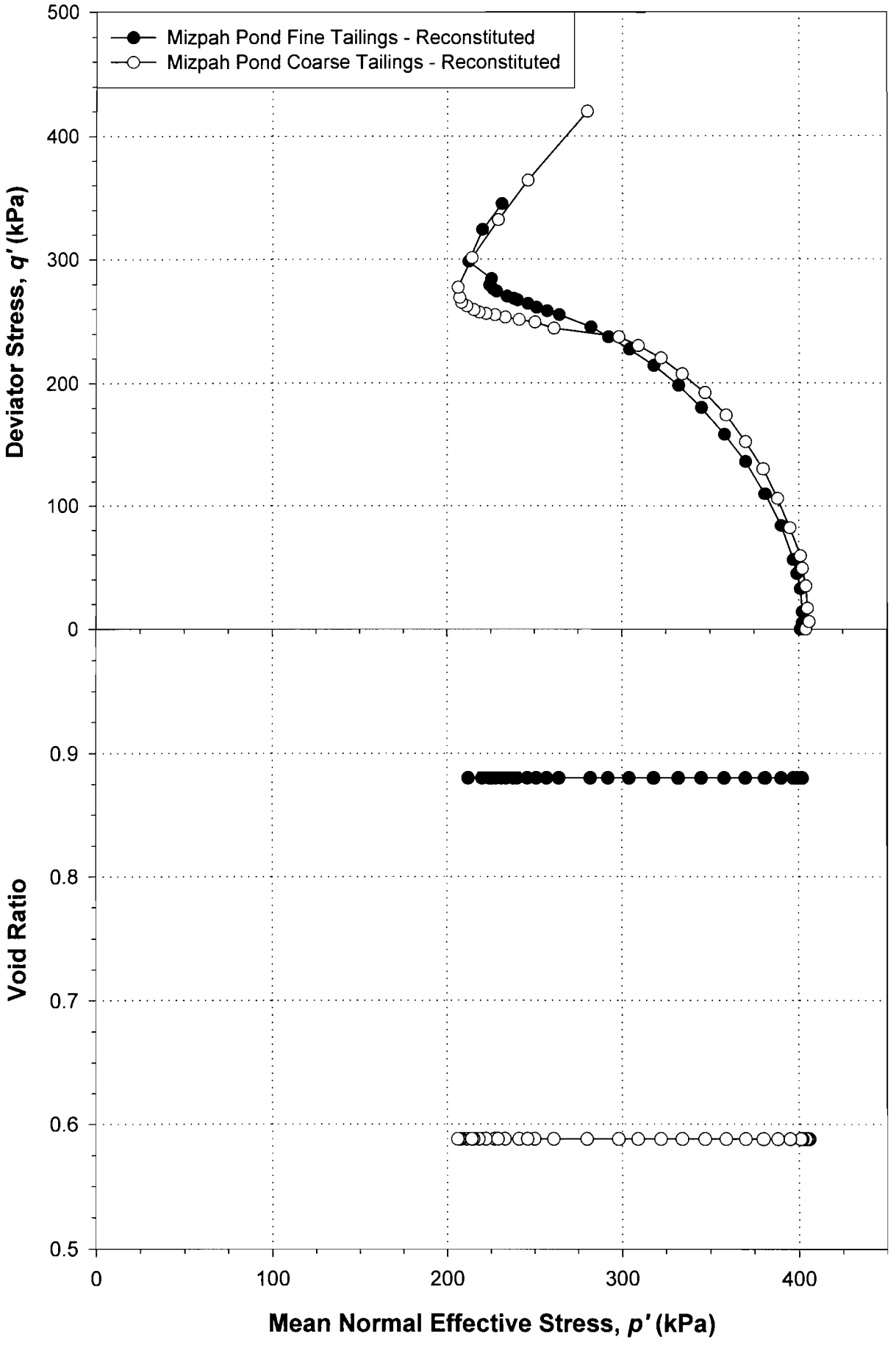

Figure 3-111: Undrained triaxial stress paths for reconstituted Mizpah pond tailings.

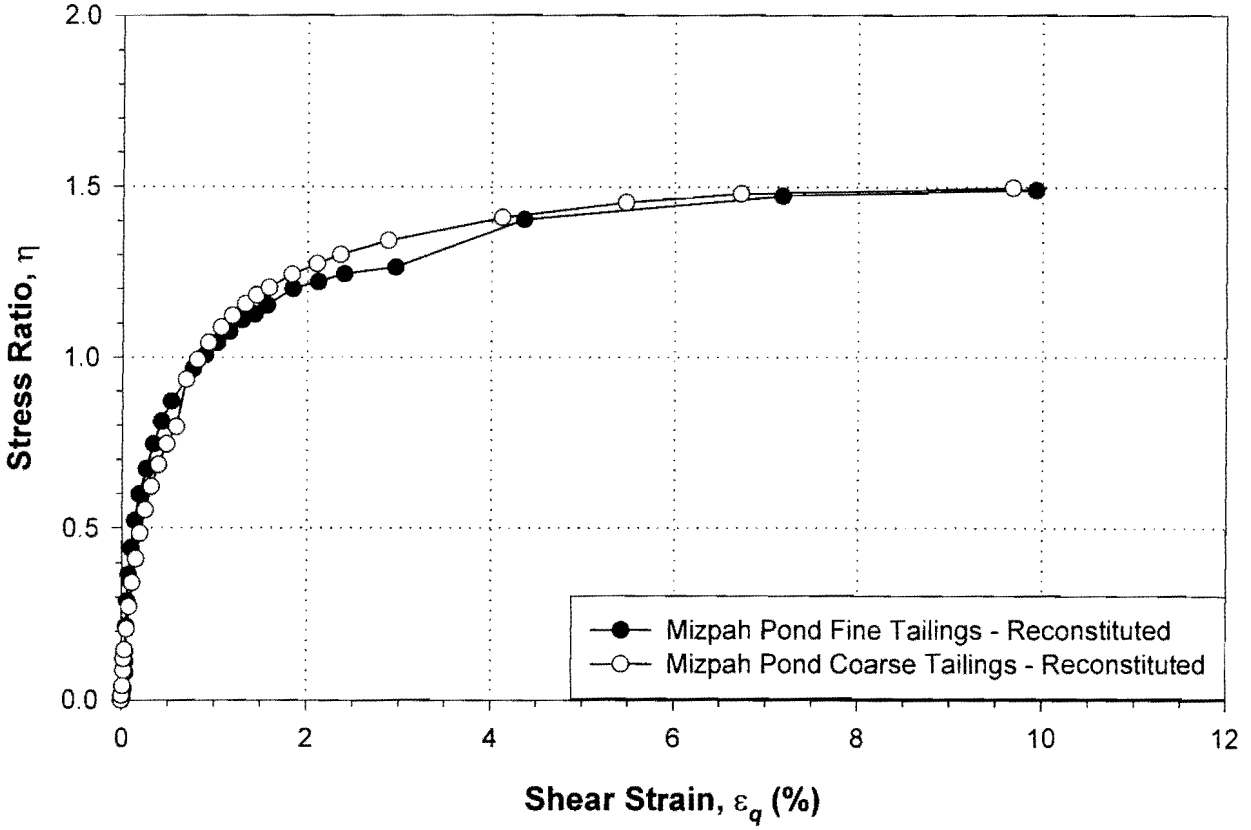

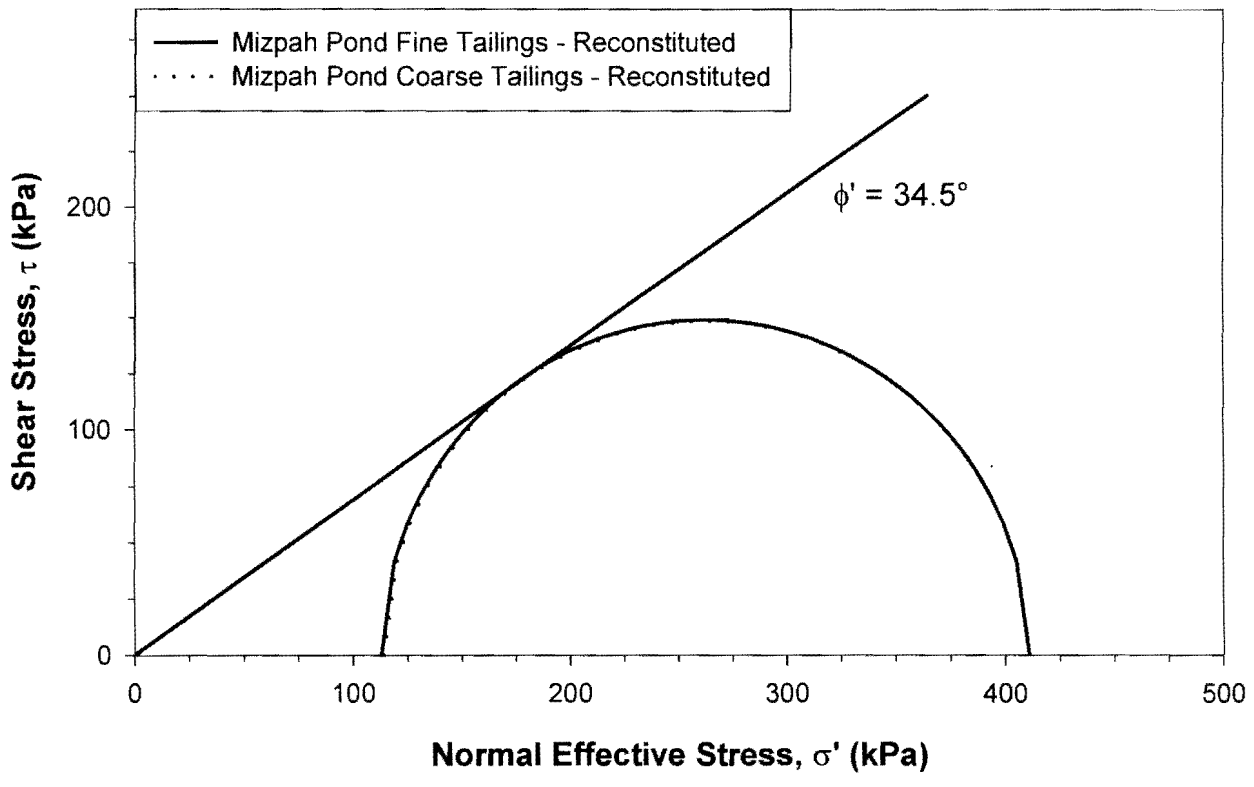

Figure 3-112: Undrained triaxial Mohr's Circles at failure for reconstituted Mizpah pond tailings.

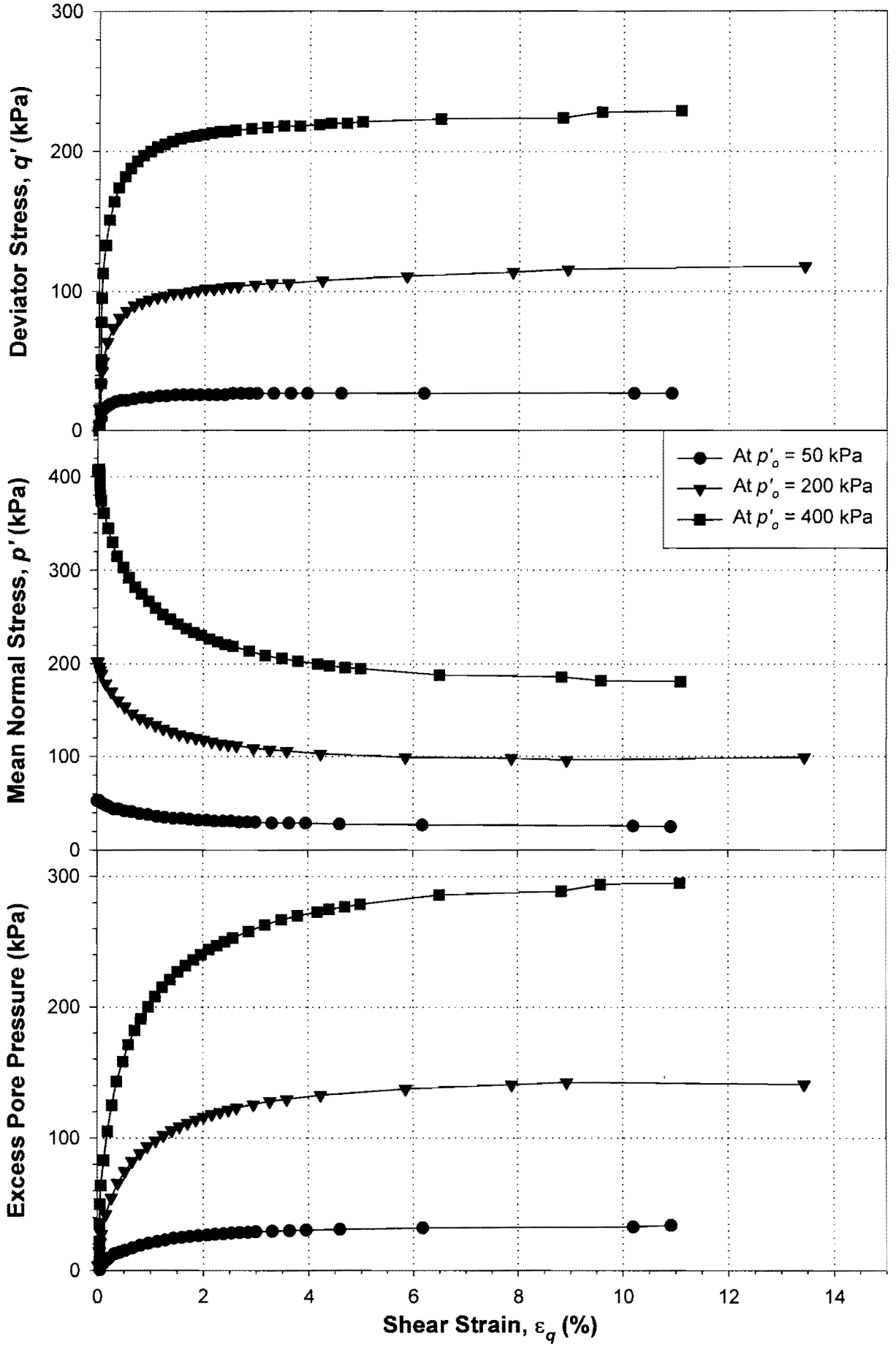

Figure 3-113: Reconstituted Pay Dam Fine Tailings: Undrained triaxial shear.

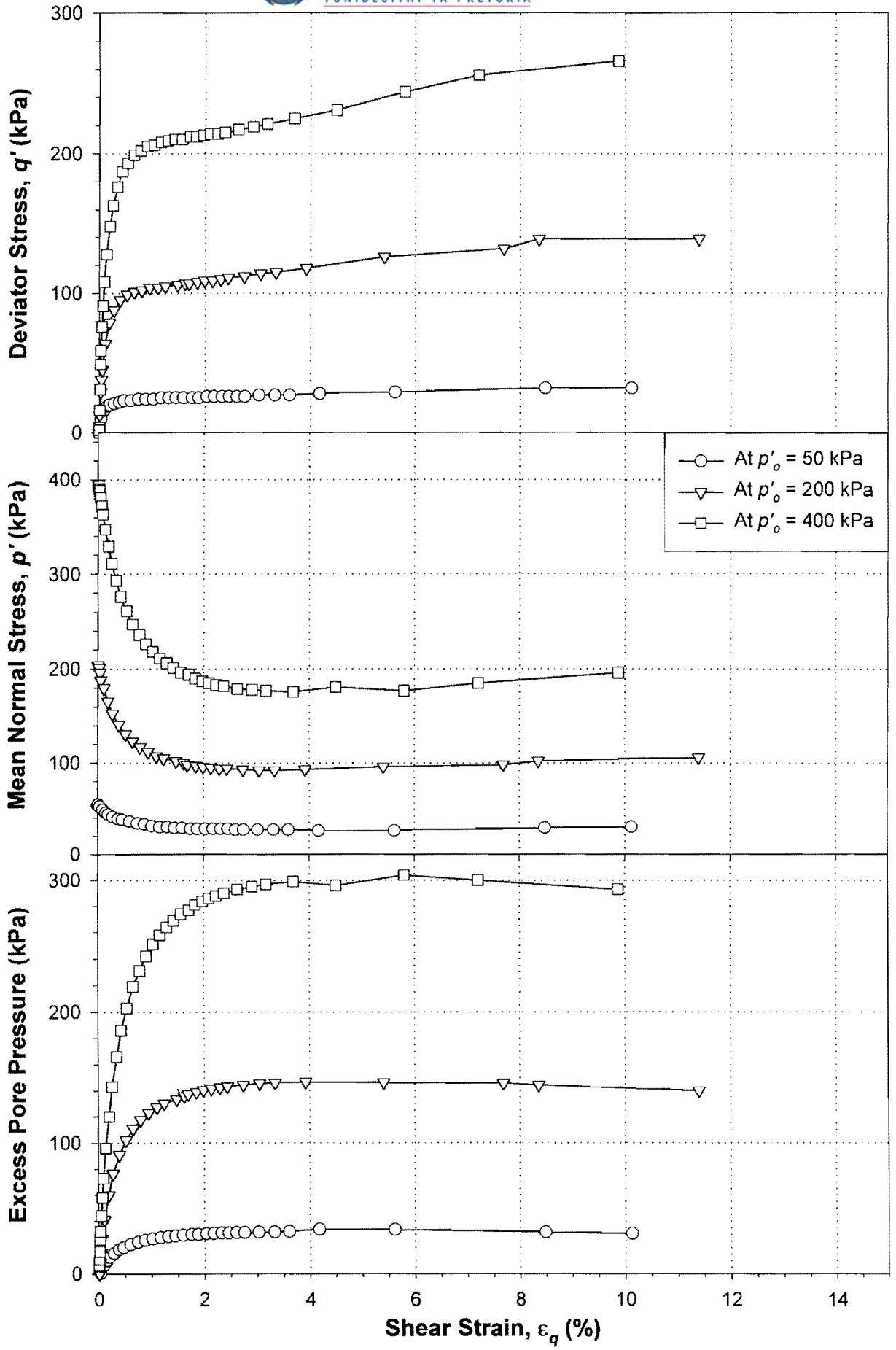

Figure 3-114: Reconstituted Pay Dam Coarse Tailings: Undrained triaxial shear.

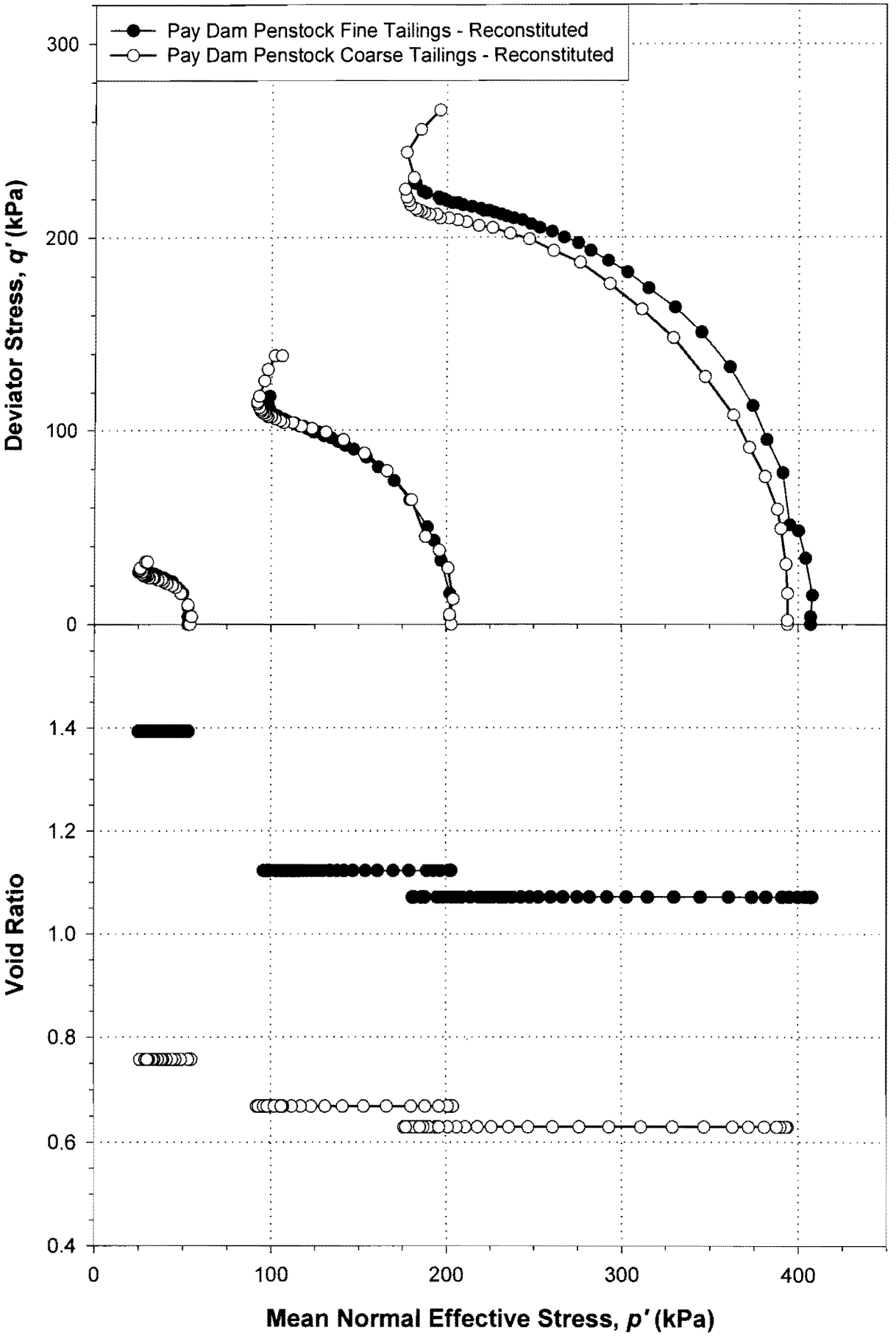

Figure 3-115: Undrained triaxial stress paths for reconstituted Pay Dam tailings.

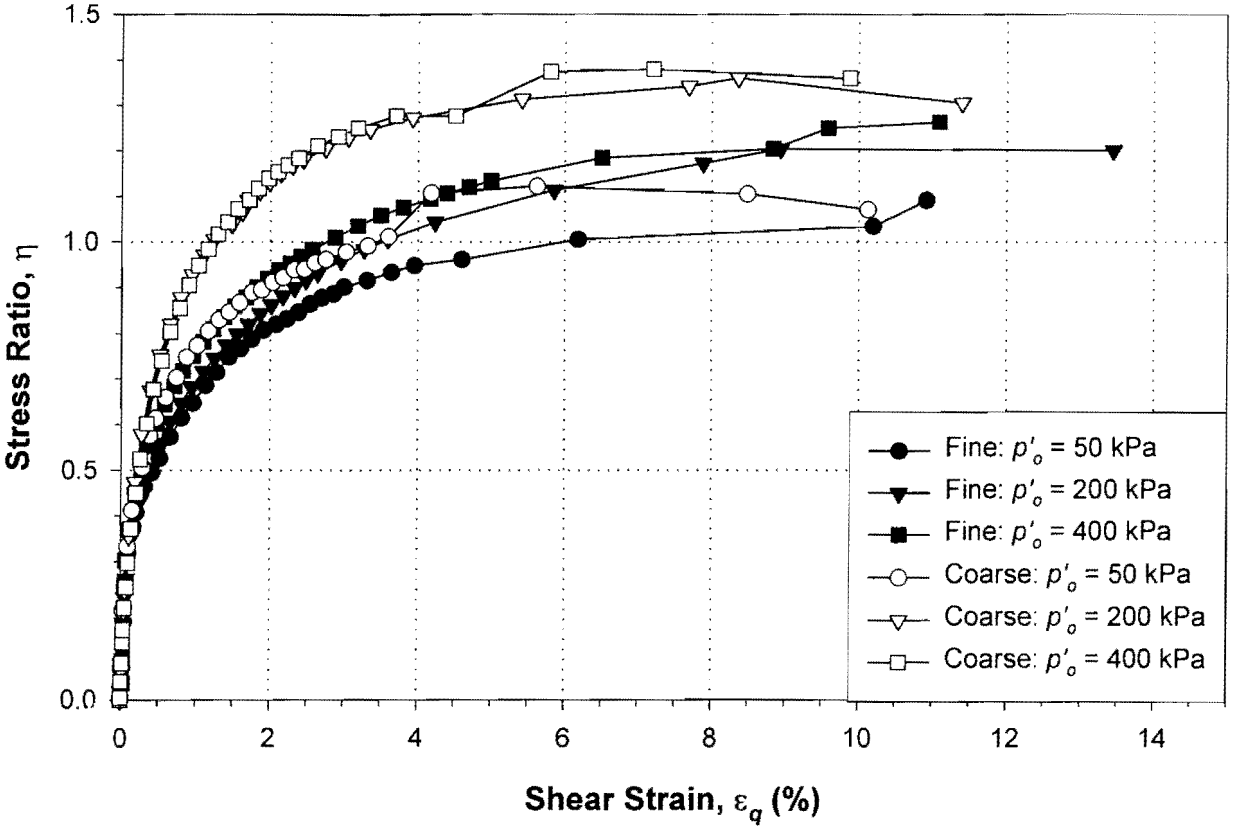

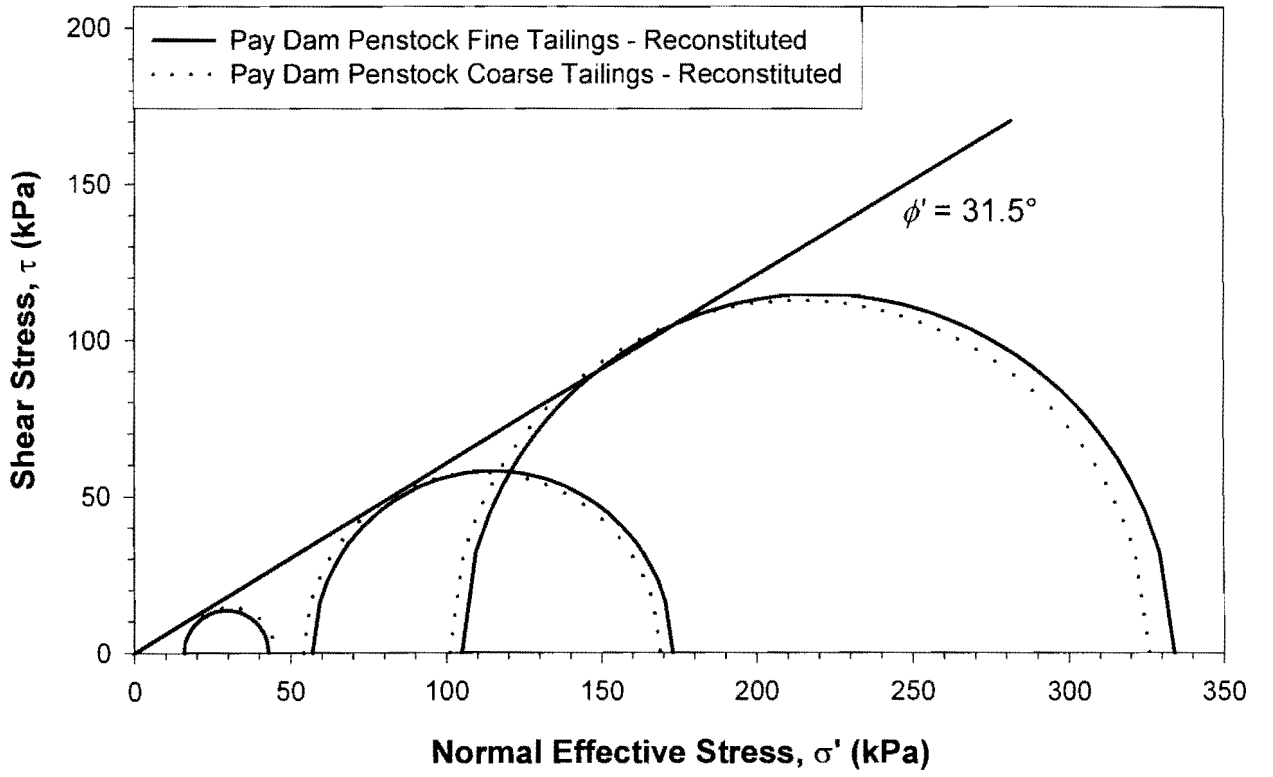

Figure 3-116: Undrained triaxial Mohr's Circles at failure for reconstituted Pay Dam tailings.

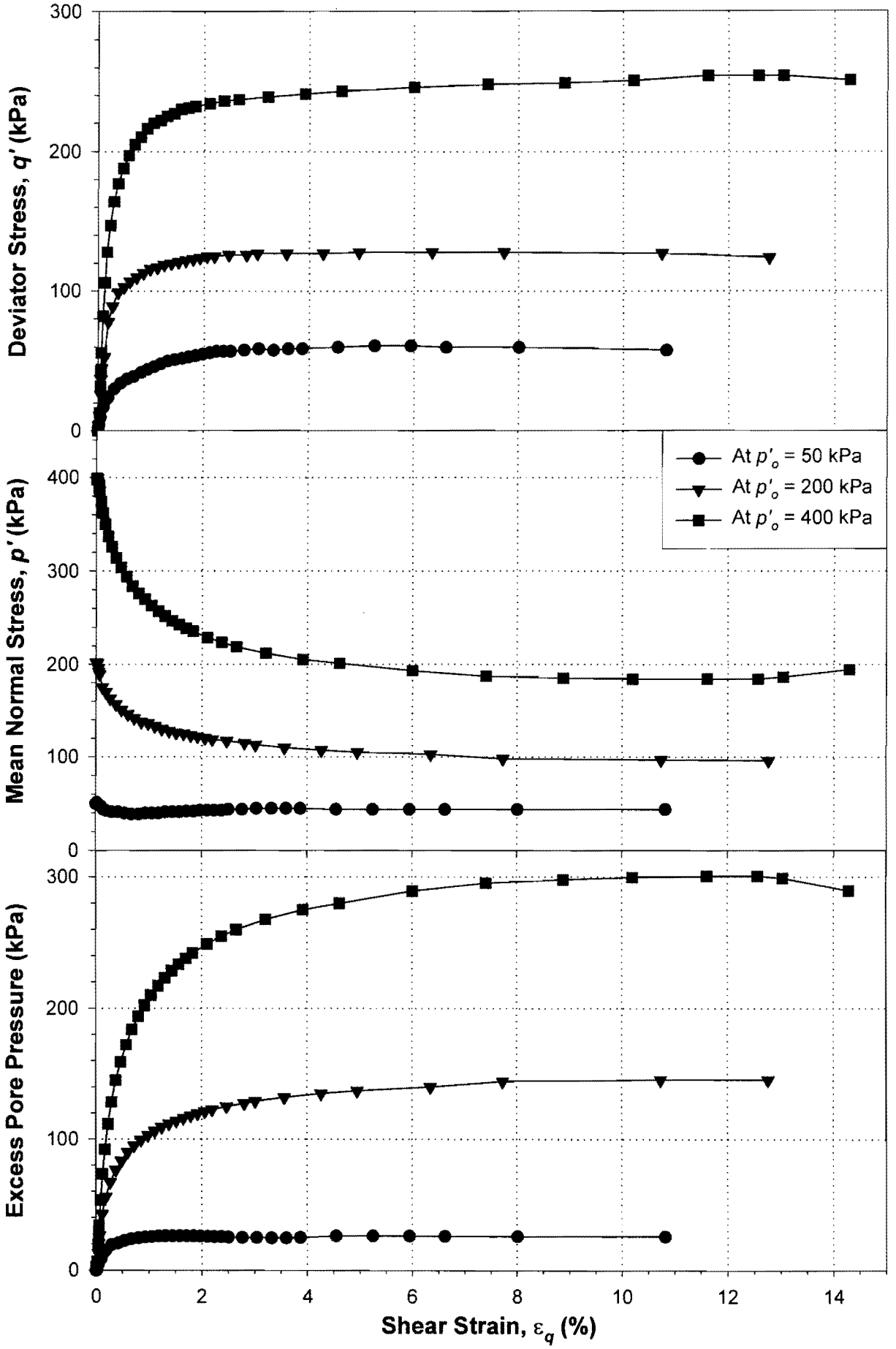

Figure 3-117: Undisturbed Pay Dam Fine Tailings: Undrained triaxial shear..

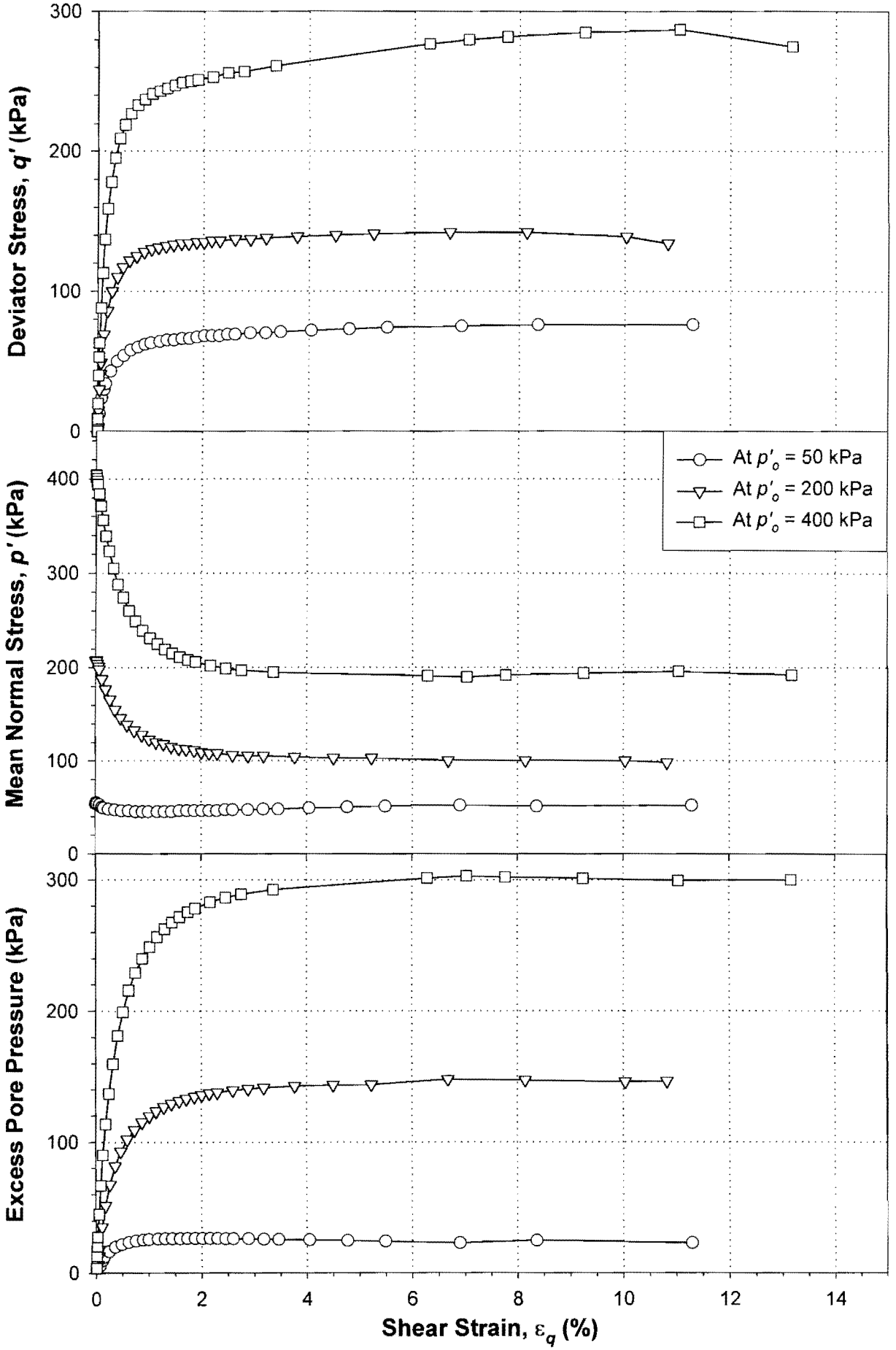

Figure 3-118: Undisturbed Pay Dam Coarse Tailings: Undrained triaxial shear..

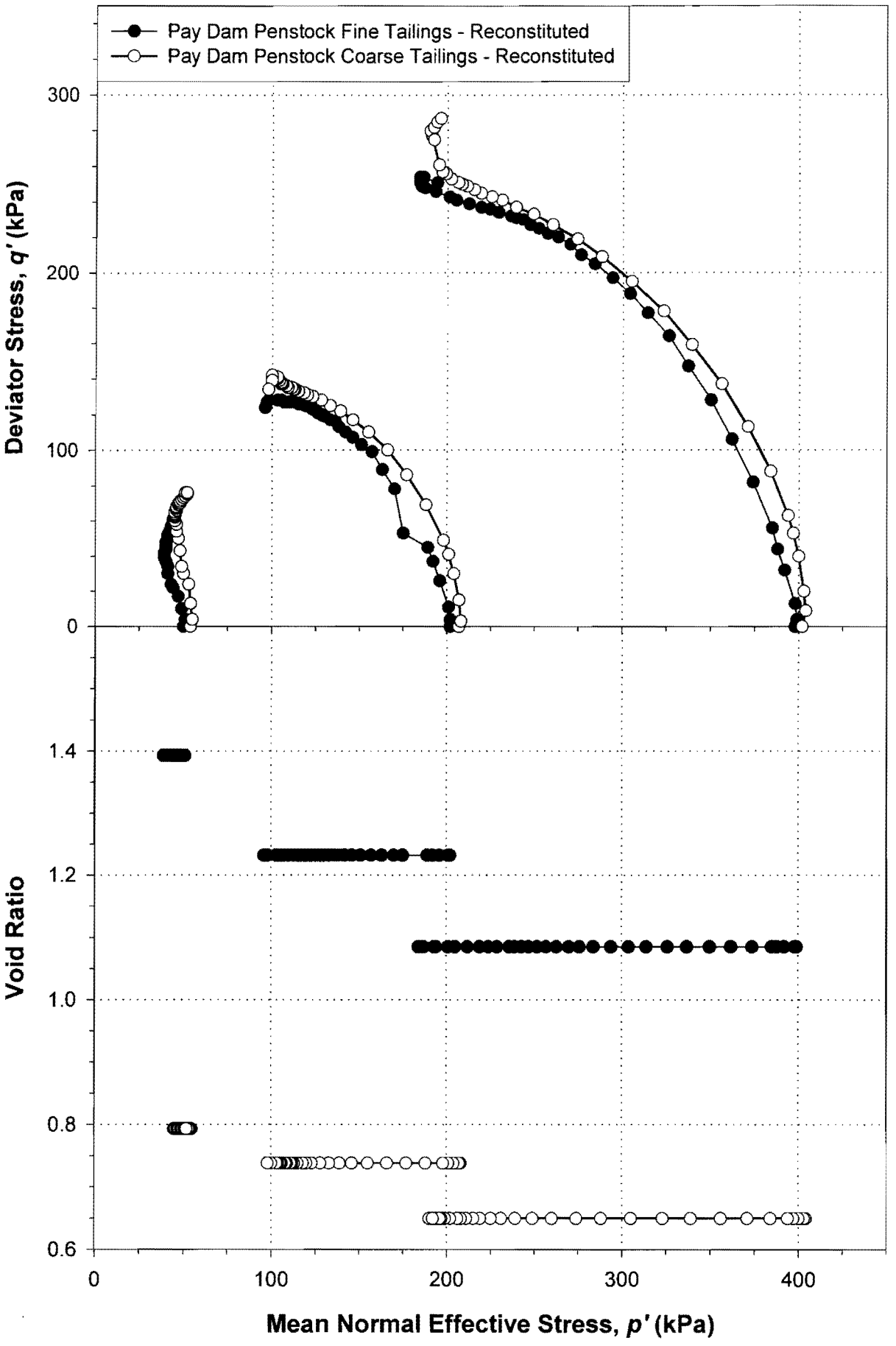

Figure 3-119: Undrained triaxial stress paths for undisturbed Pay Dam tailings.

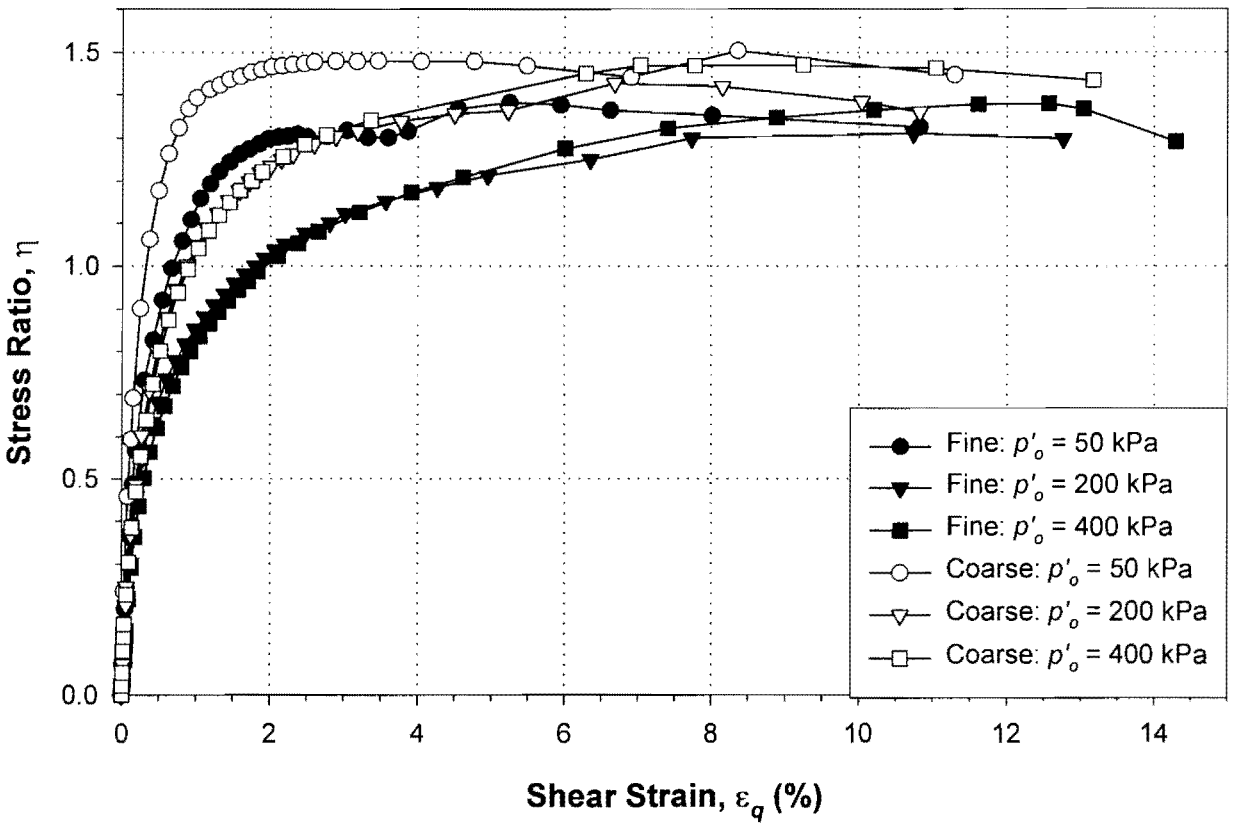

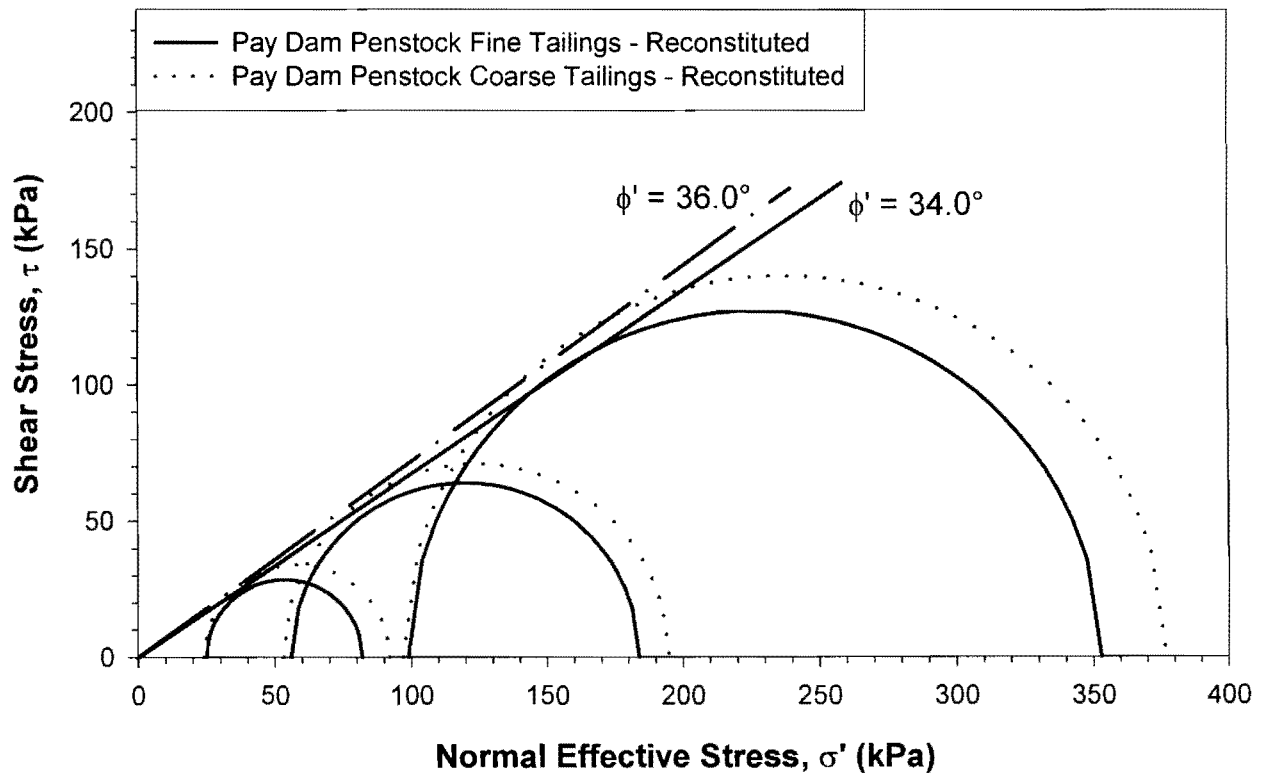

Figure 3-120: Undrained triaxial Mohr's Circles at failure for undisturbed Pay Dam tailings.

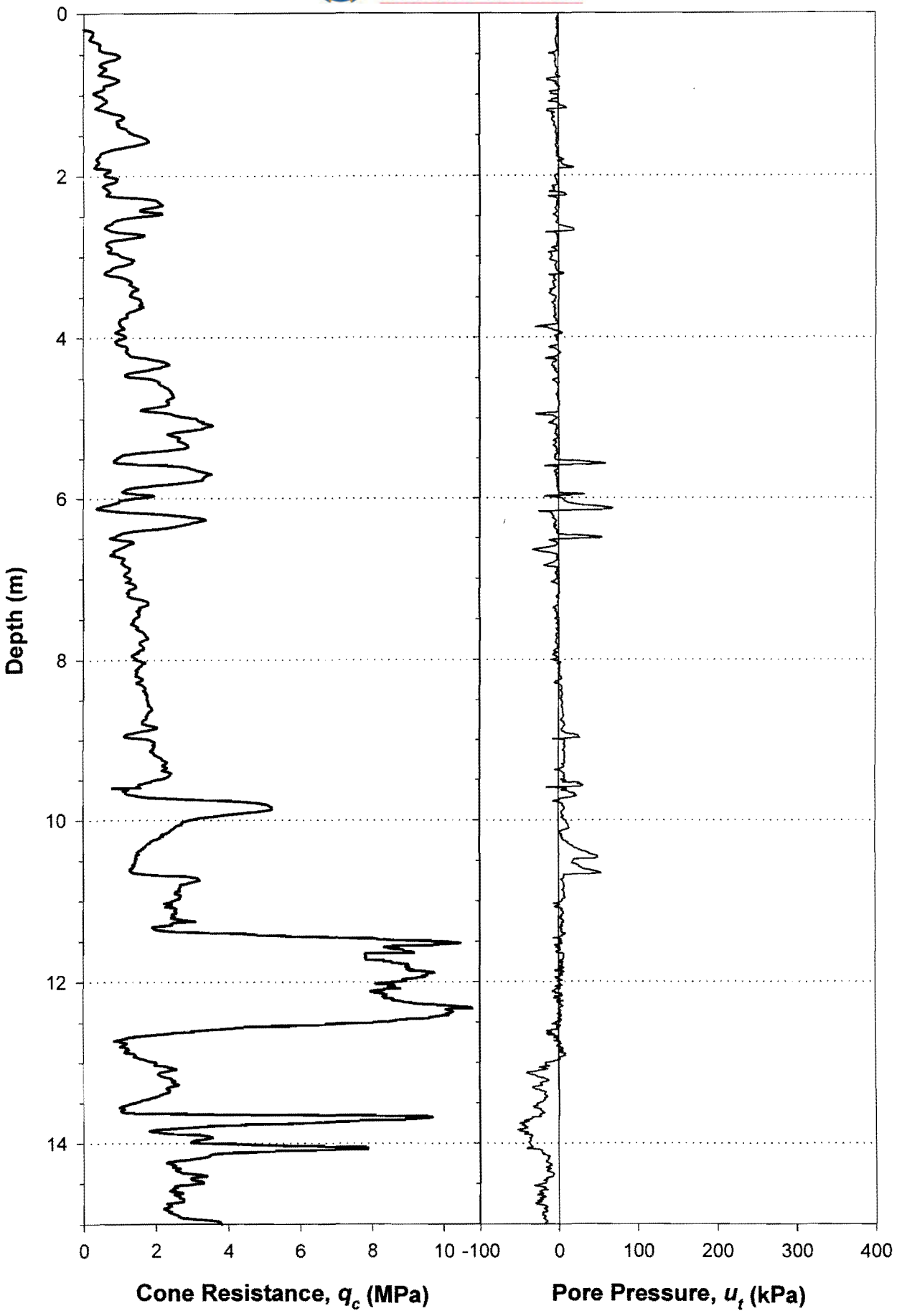

Figure 3-121: Piezocone field log: Mizpah - Daywall.

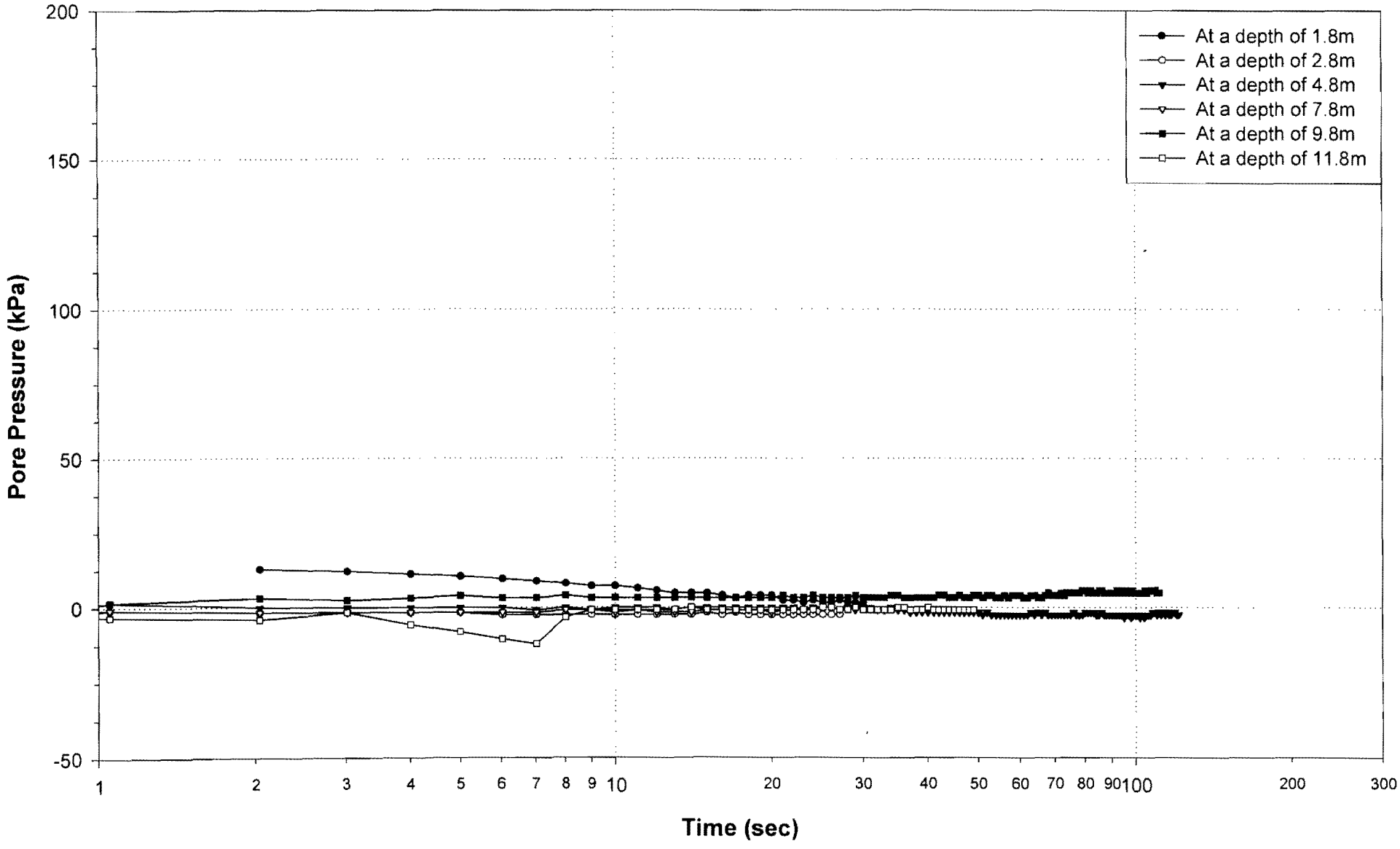

Figure 3-122: Piezocone dissipation data: Mizpah - Daywall.

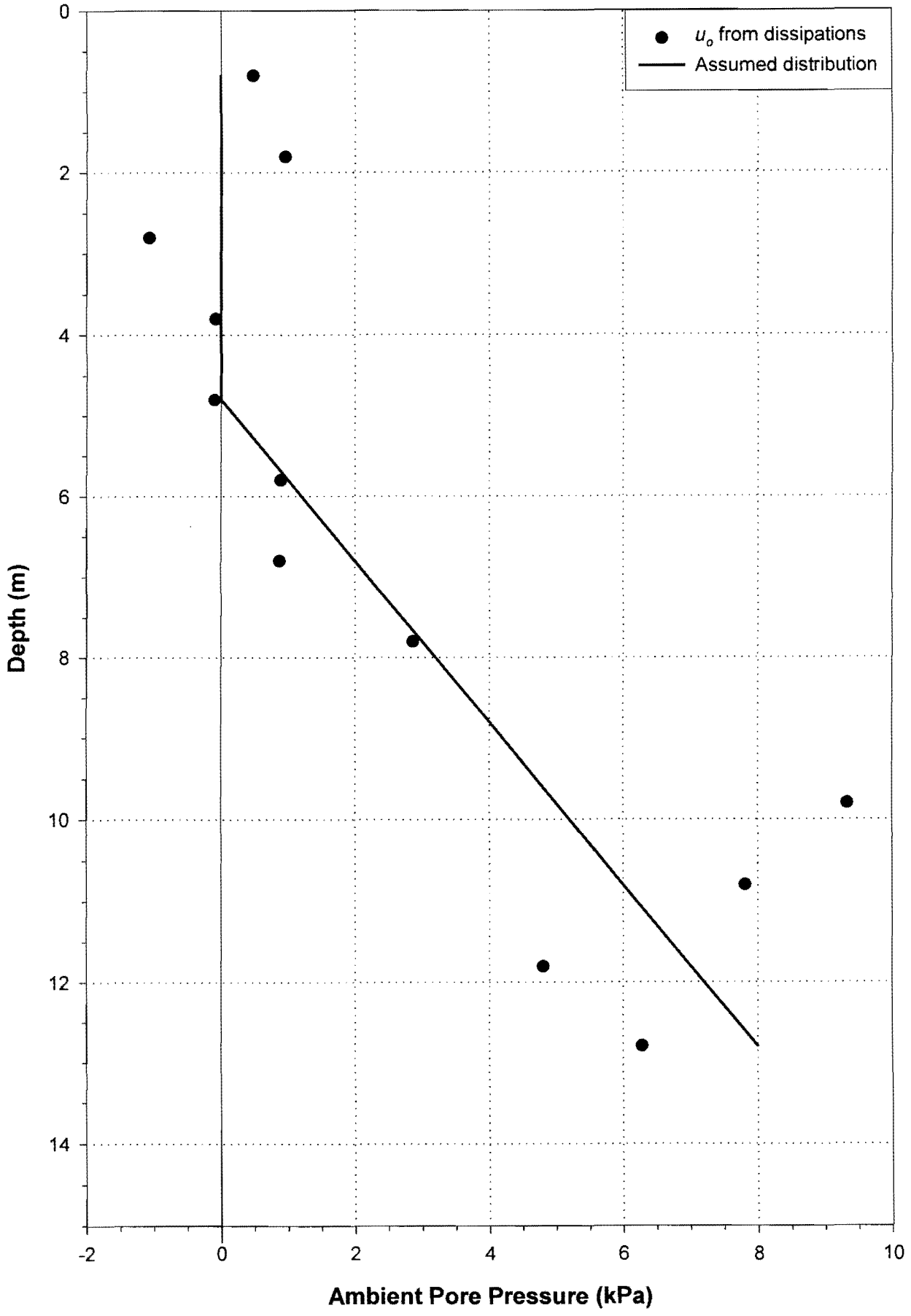

Figure 3-123: Ambient pore pressure distribution: Mizpah - Daywall.

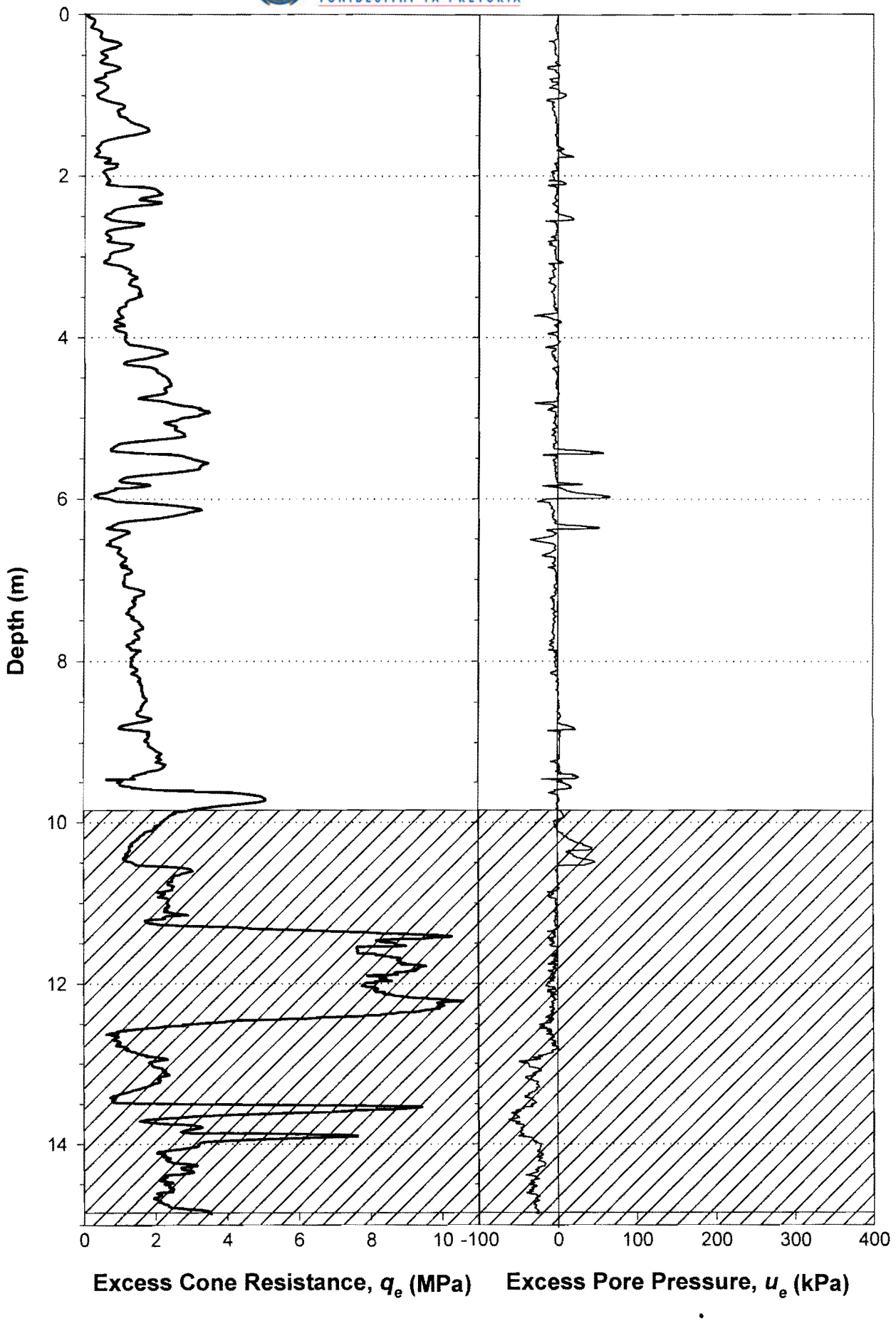

Figure 3-124: Normalised piezocone log: Mizpah - Daywall.

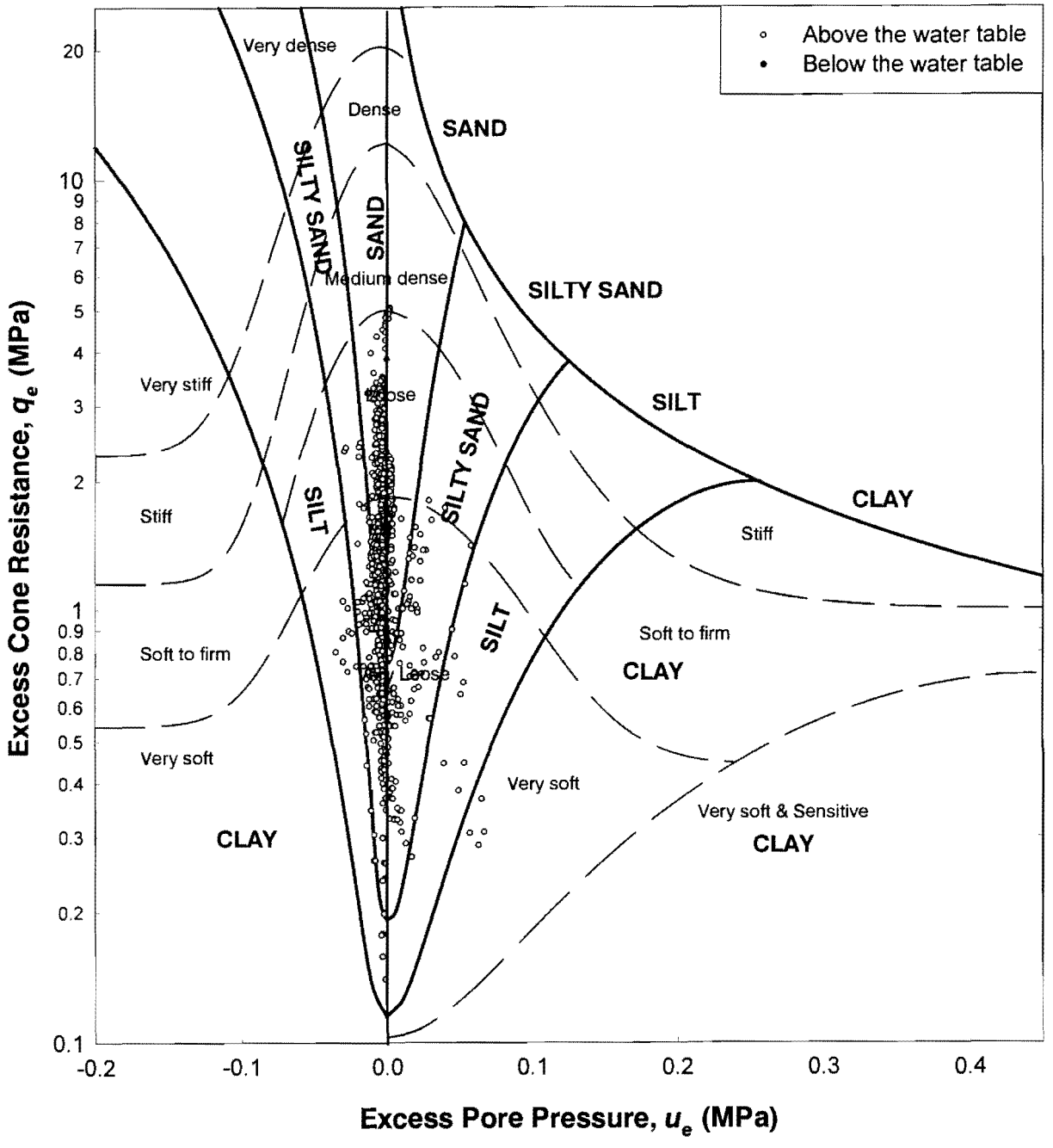

Figure 3-125: Piezocone soils identification chart: Mizpah - Daywall.

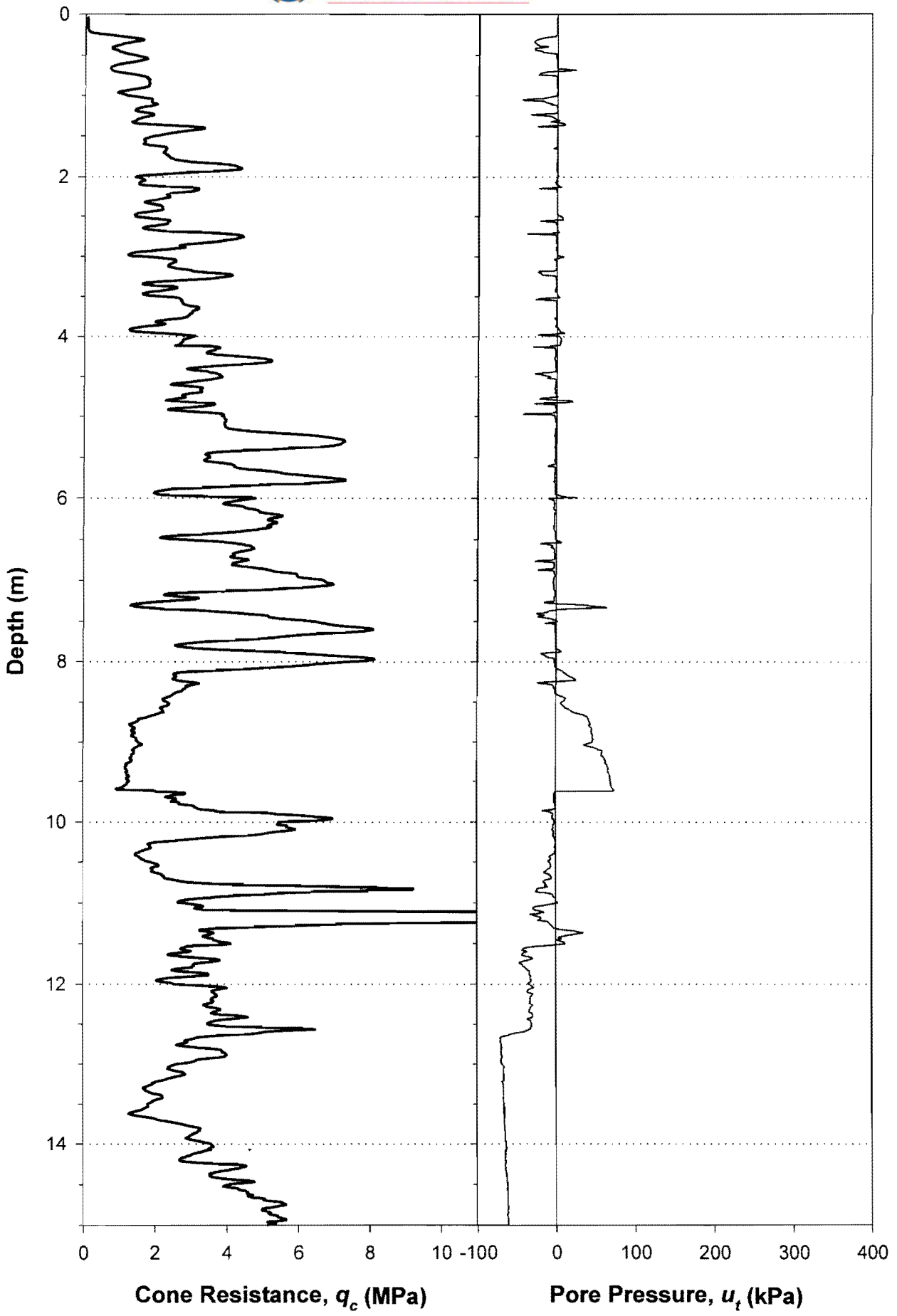

Figure 3-126: Piezocone field log: Mizpah - Upper Beach.

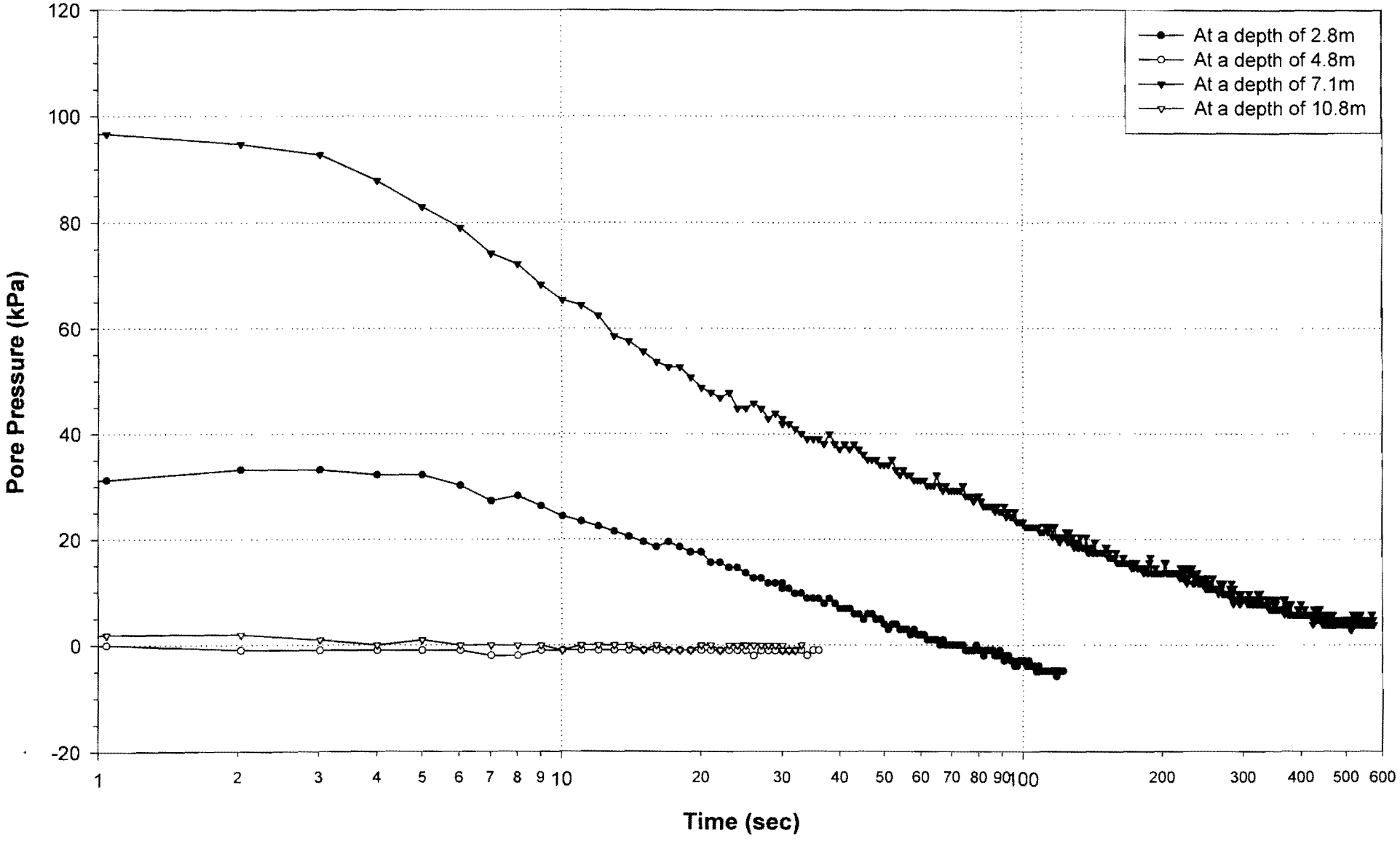

Figure 3-127: Piezocone dissipation data: Mizpah - Upper Beach.

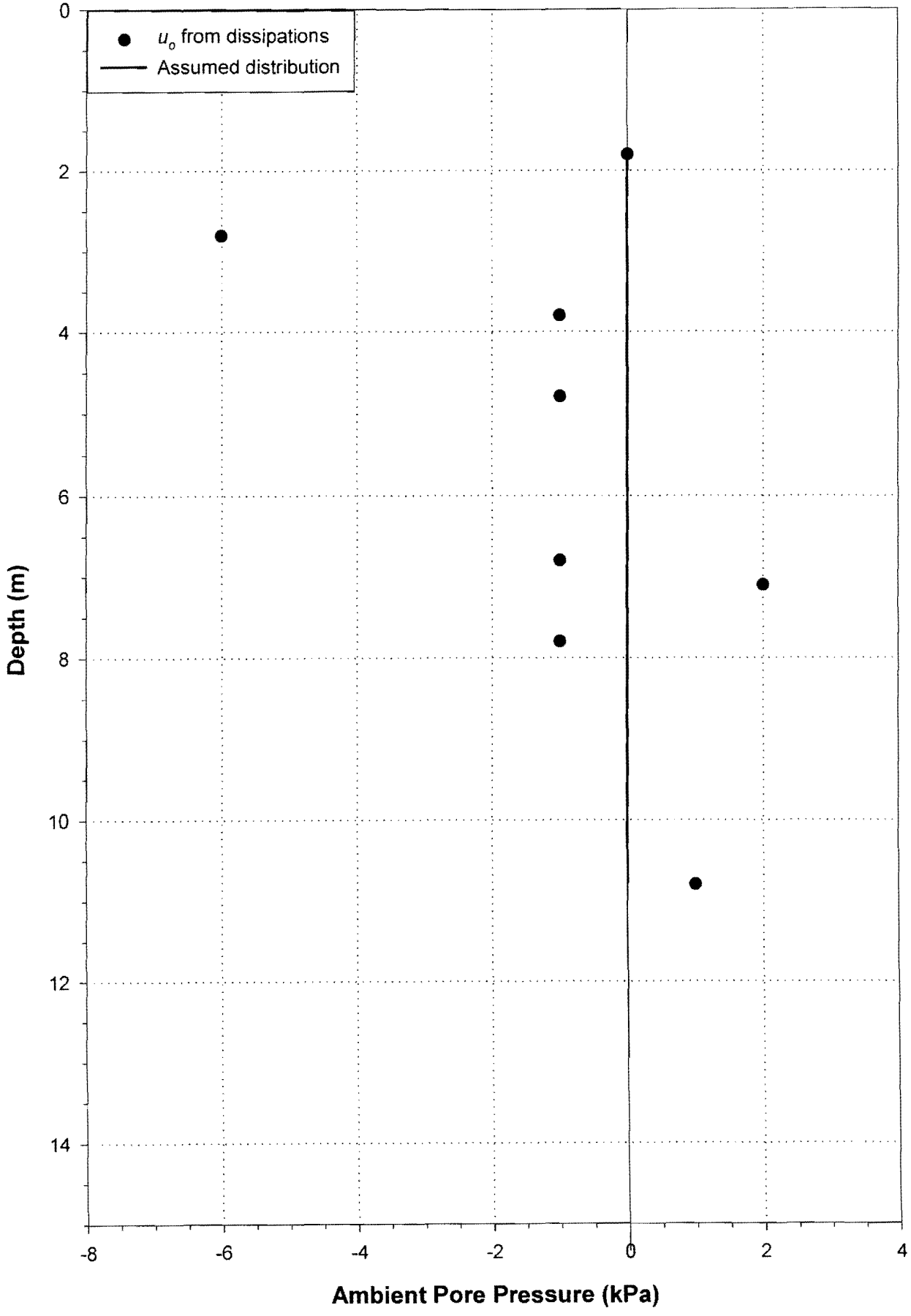

Figure 3-128: Ambient pore pressure distribution: Mizpah - Upper Beach.

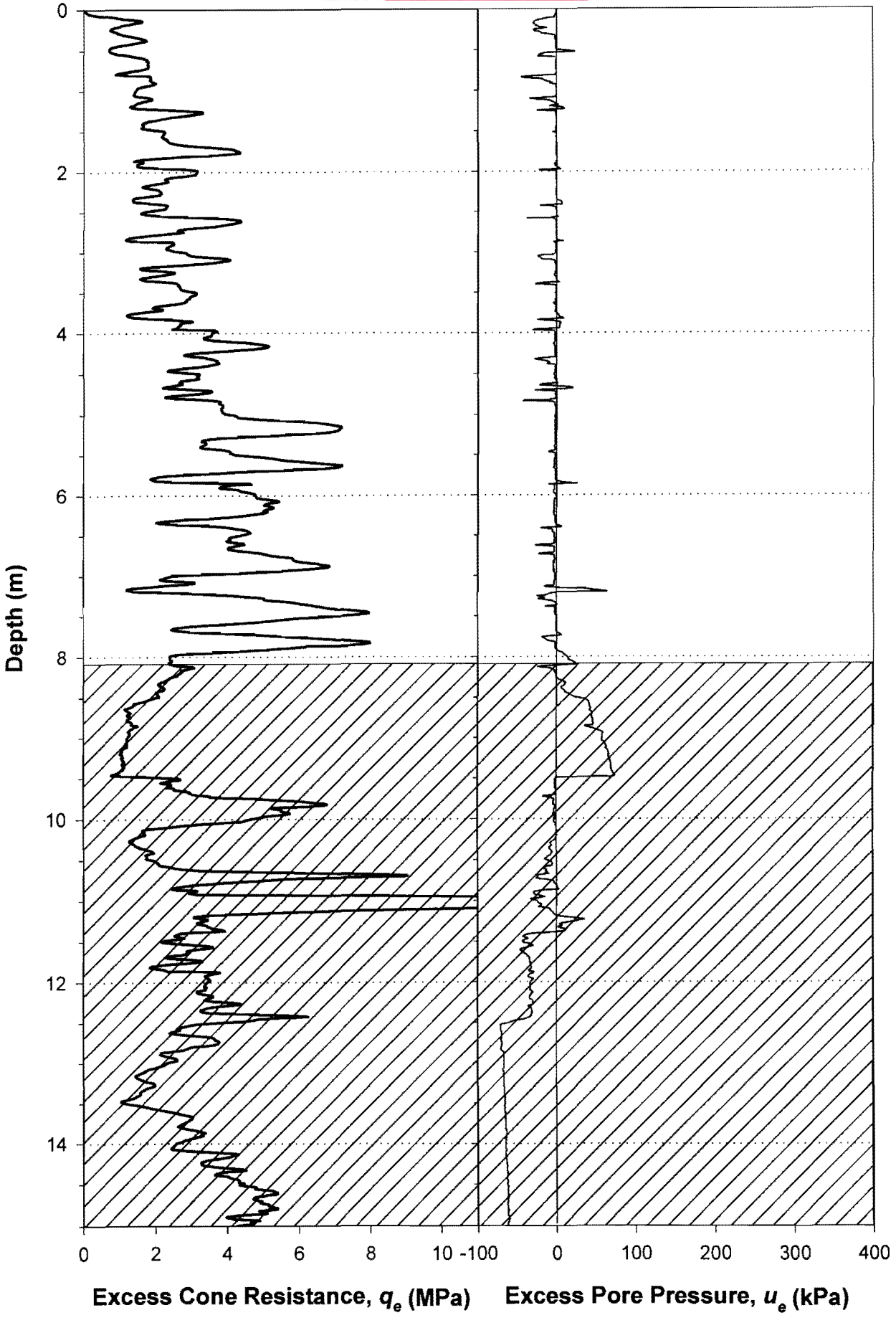

Figure 3-129: Normalised piezocone log: Mizpah - Upper Beach.

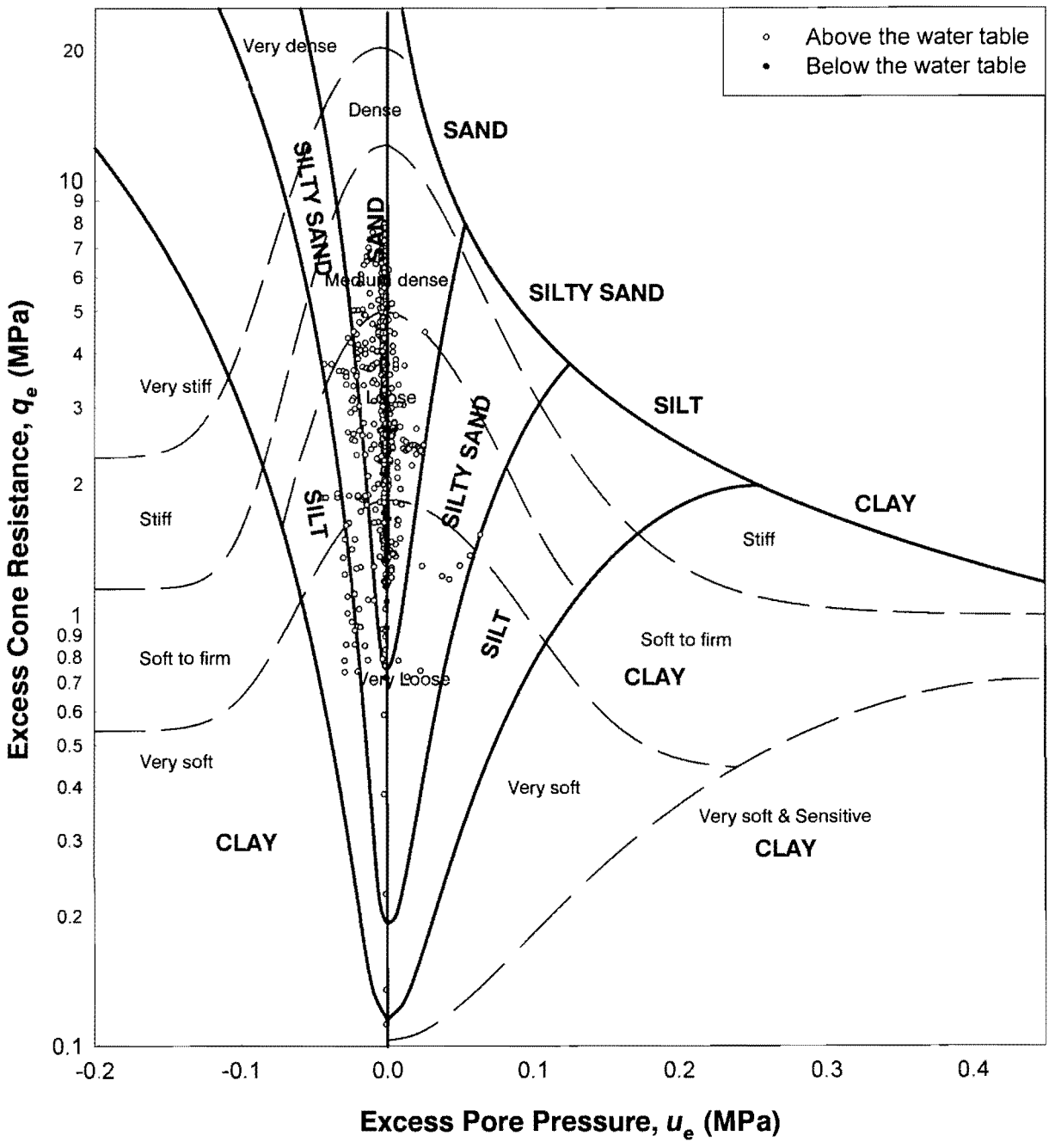

Figure 3-130: Piezocone soils identification chart: Mizpah - Upper Beach.

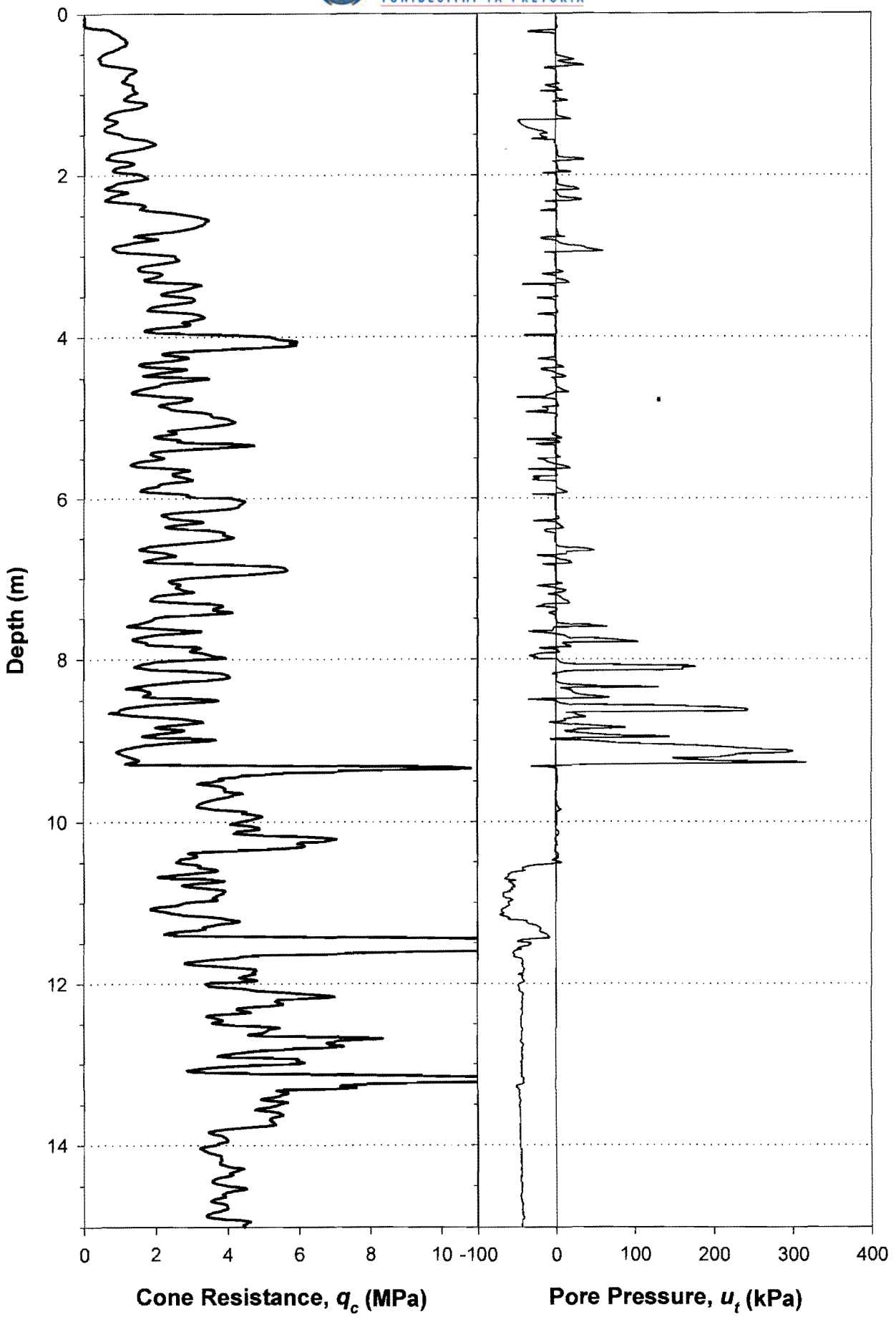

Figure 3-131: Piezocone field log: Mizpah - Middle Beach.

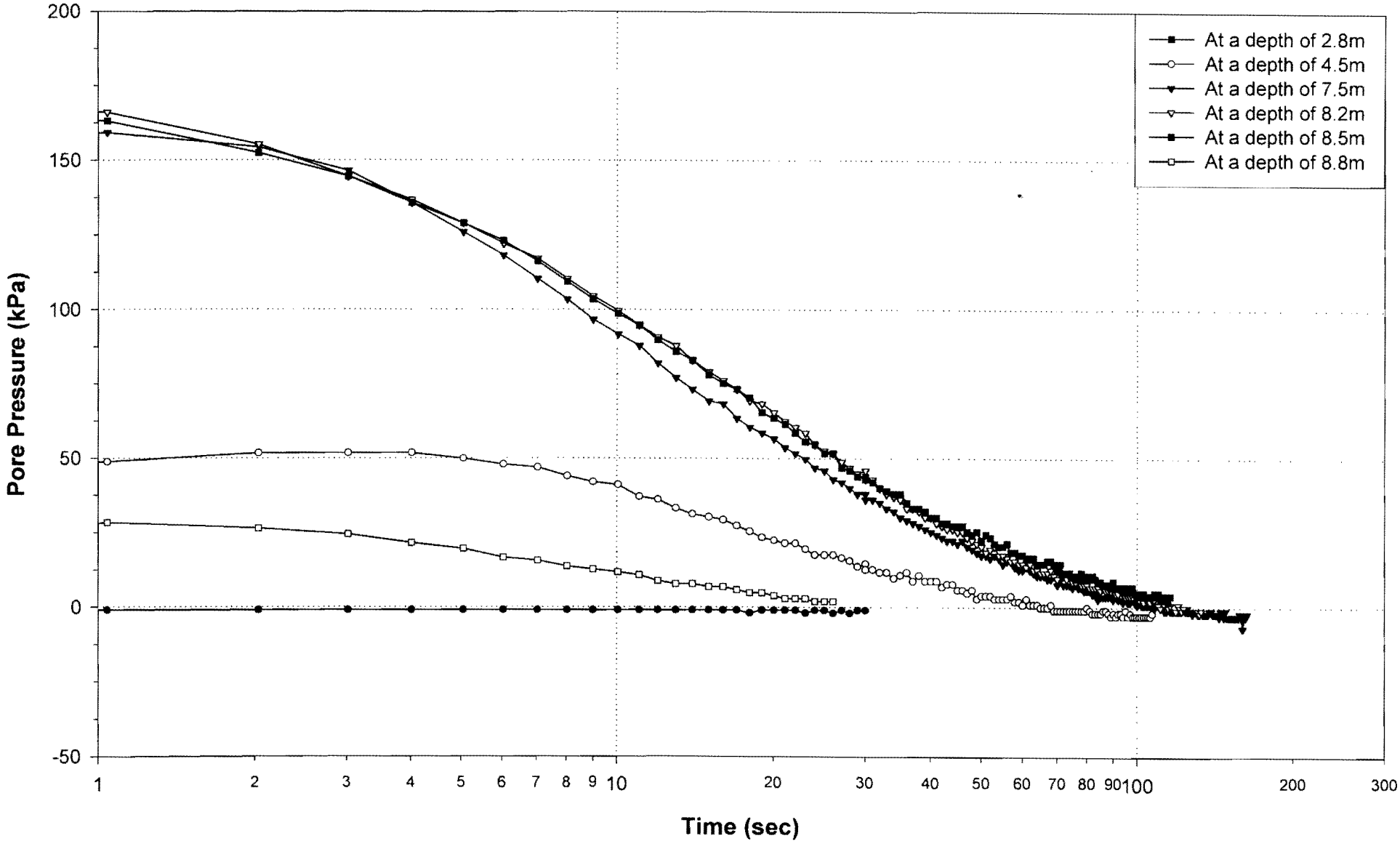

Figure 3-132: Piezocone dissipation data: Mizpah - Middle Beach.

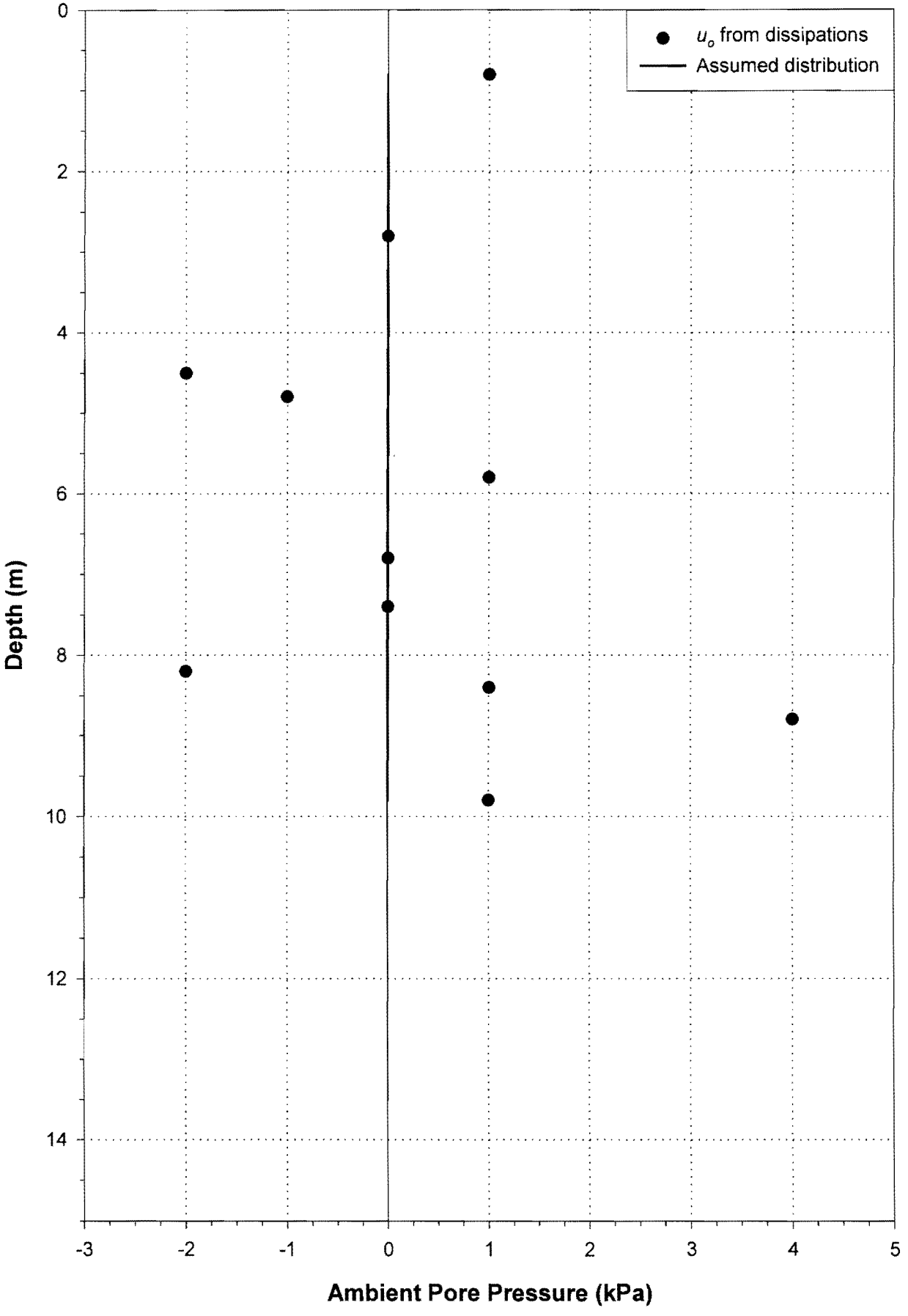

Figure 3-133: Ambient pore pressure distribution: Mizpah - Middle Beach.

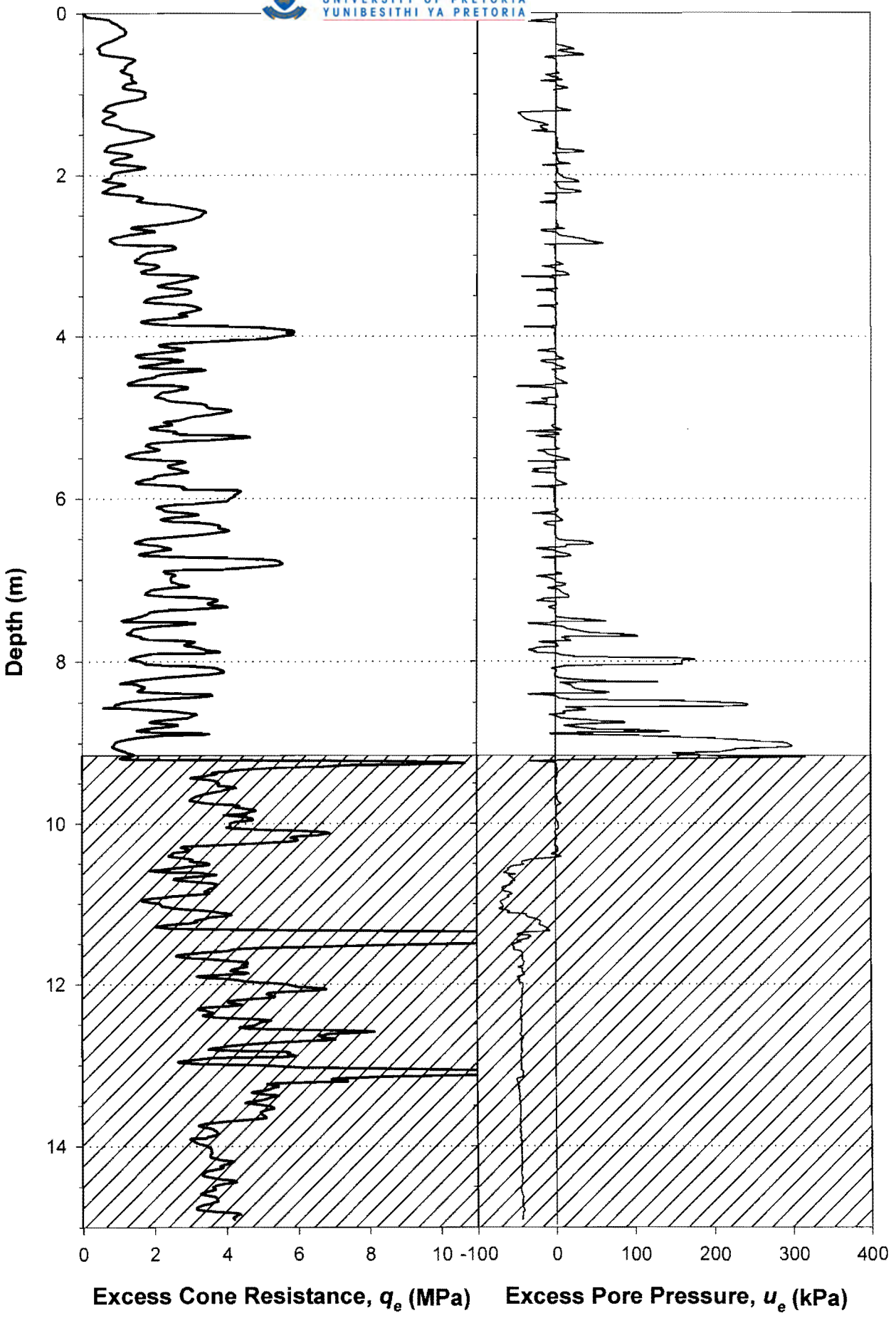

Figure 3-134: Normalised piezocone log: Mizpah - Middle Beach.

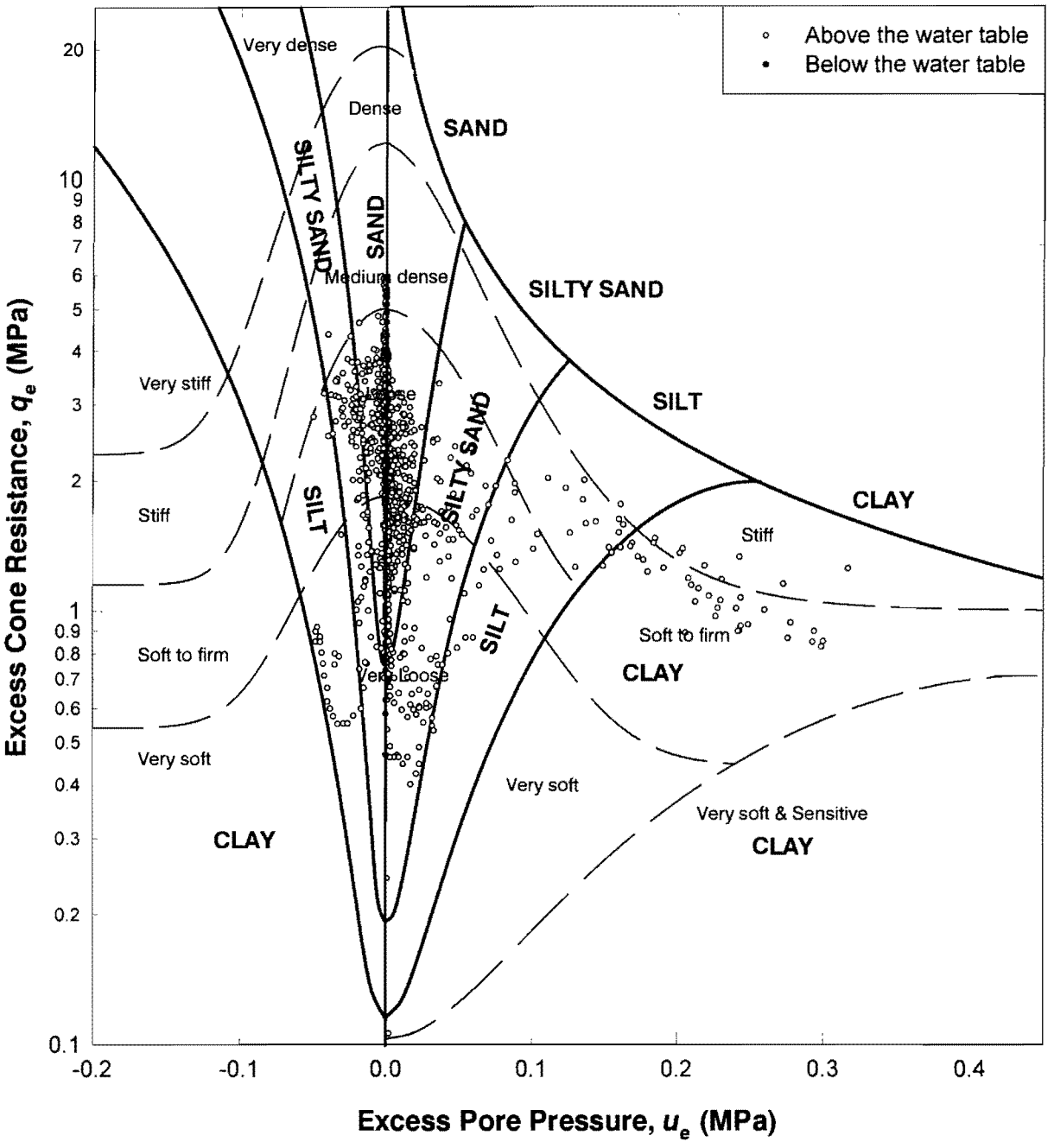

Figure 3-135: Piezocone soils identification chart: Mizpah - Middle Beach.

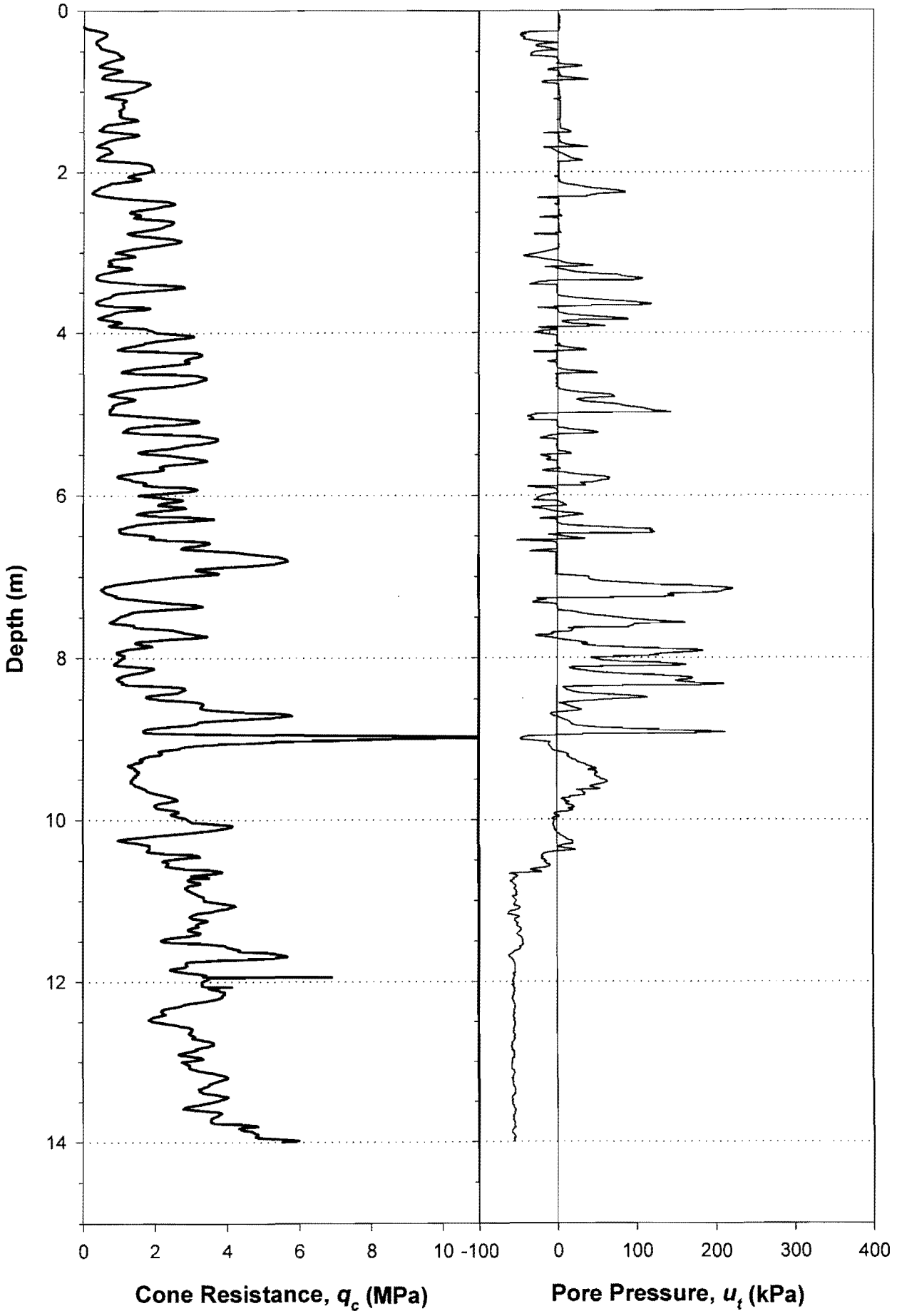

Figure 3-136: Piezocone field log: Mizpah - Lower Beach.

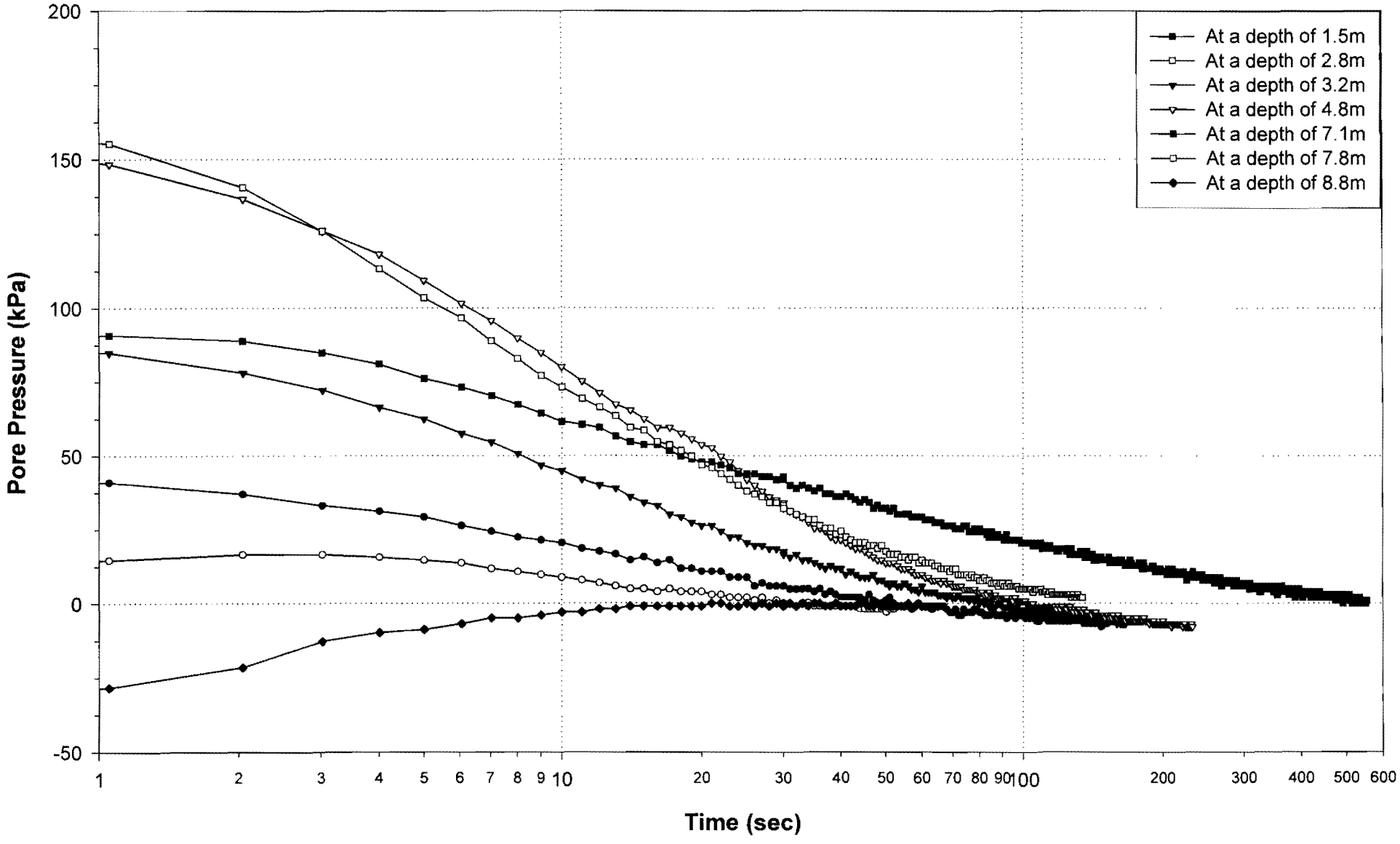

Figure 3-137: Piezocone dissipation data: Mizpah - Lower Beach.

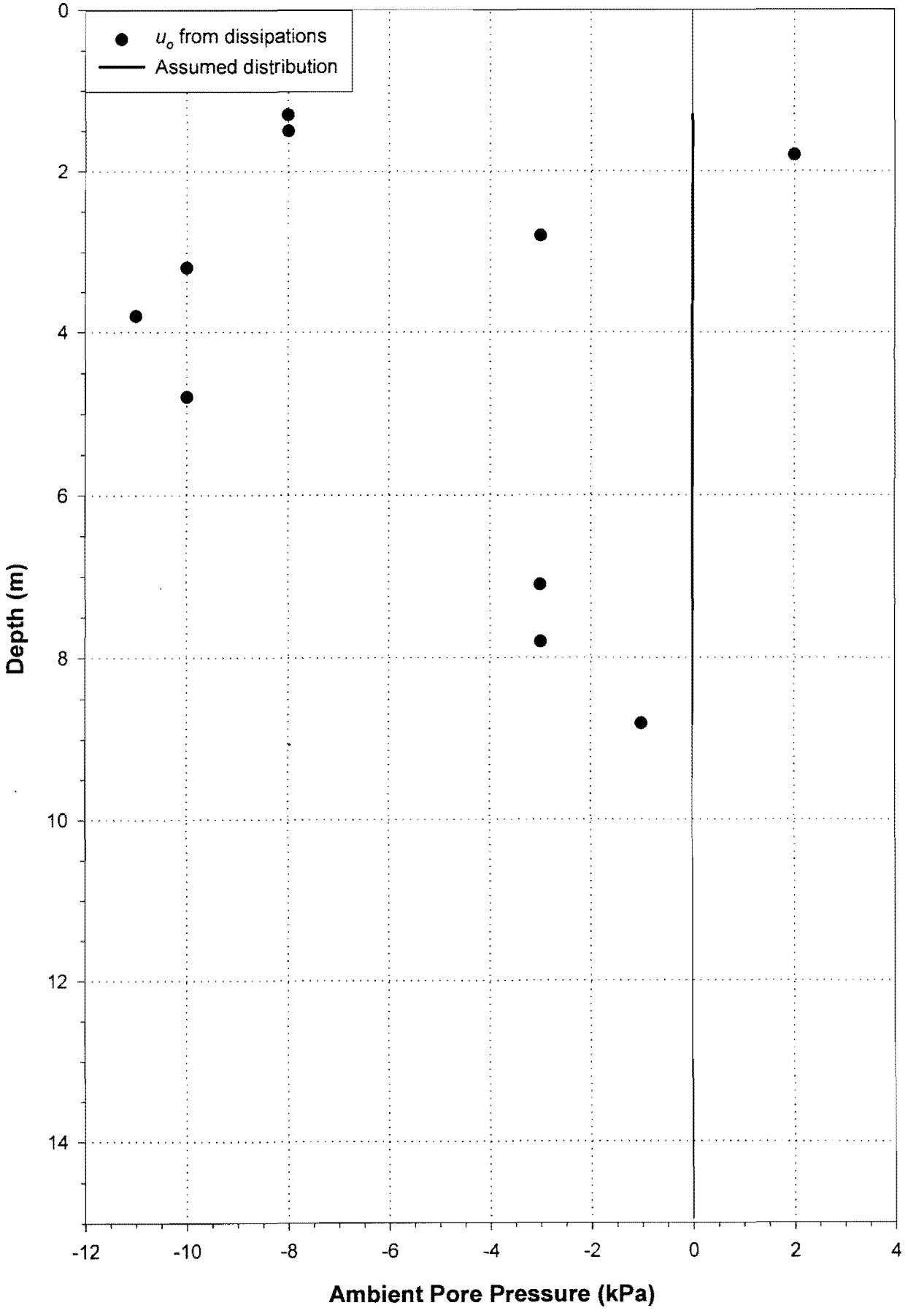

Figure 3-138: Ambient pore pressure distribution: Mizpah - Lower Beach.

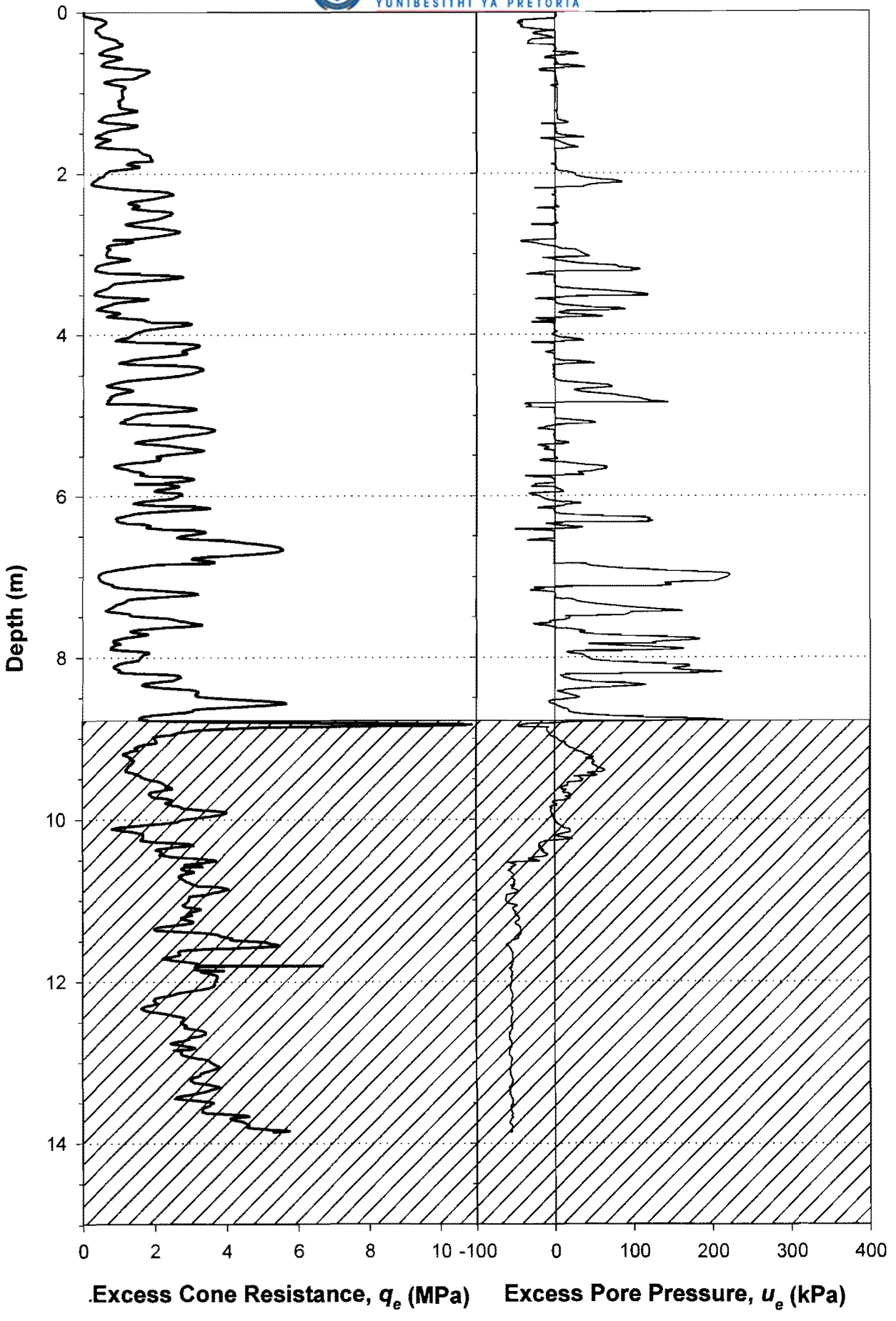

Figure 3-139: Normalised piezocone log: Mizpah - Lower Beach.

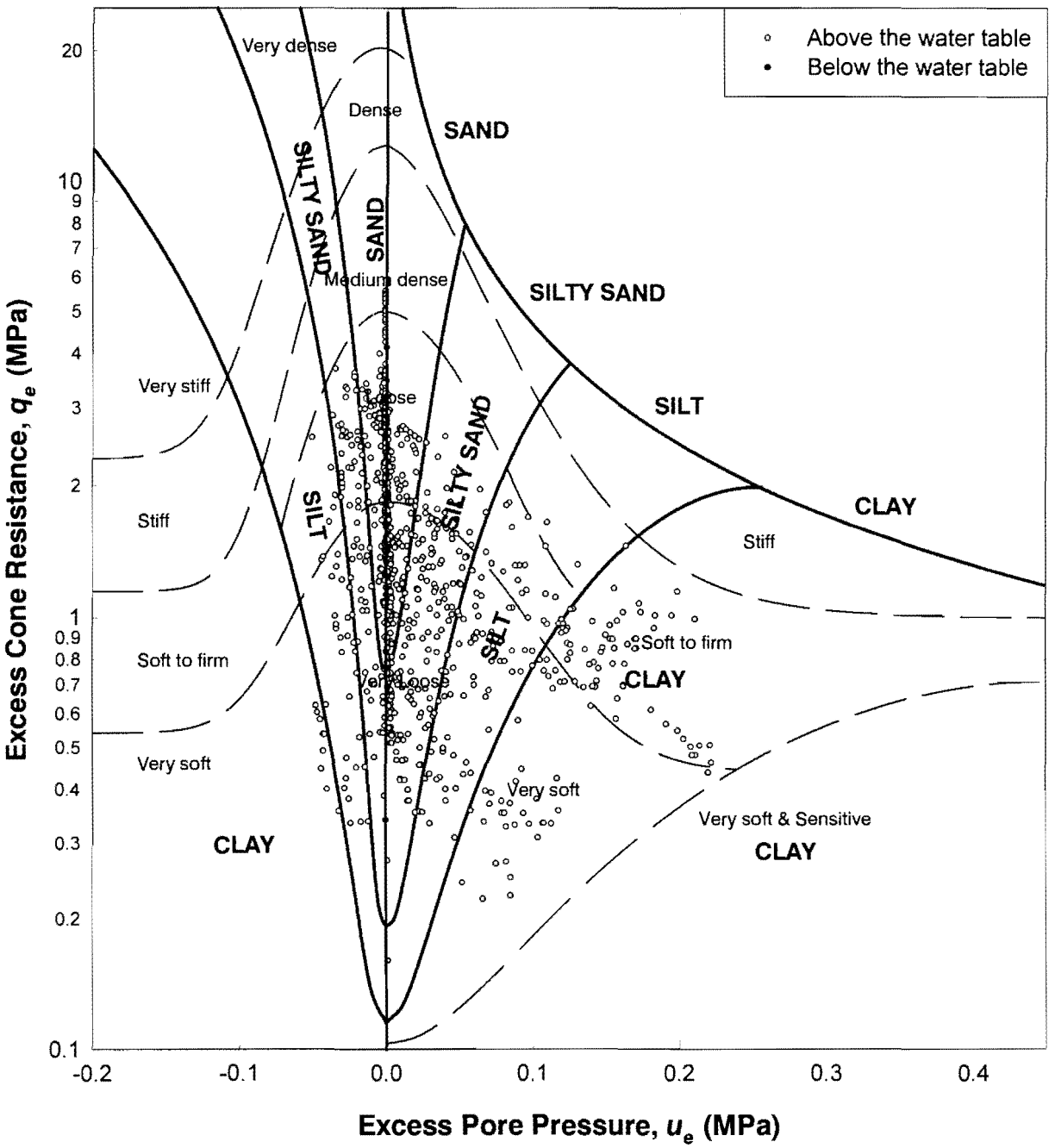

Figure 3-140: Piezocone soils identification chart: Mizpah - Lower Beach.

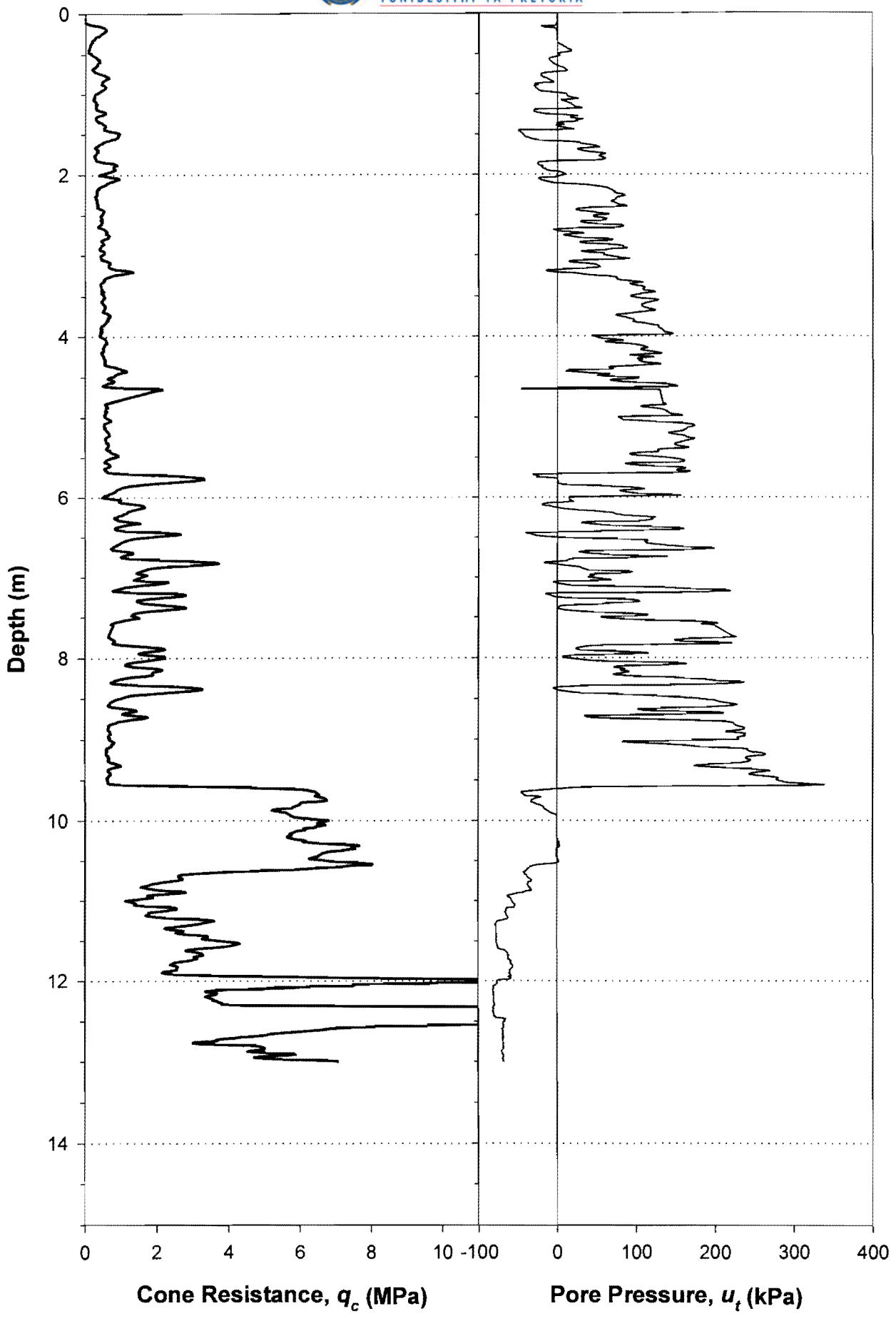

Figure 3-141: Piezocone field log: Mizpah - Beach Pond Interface.

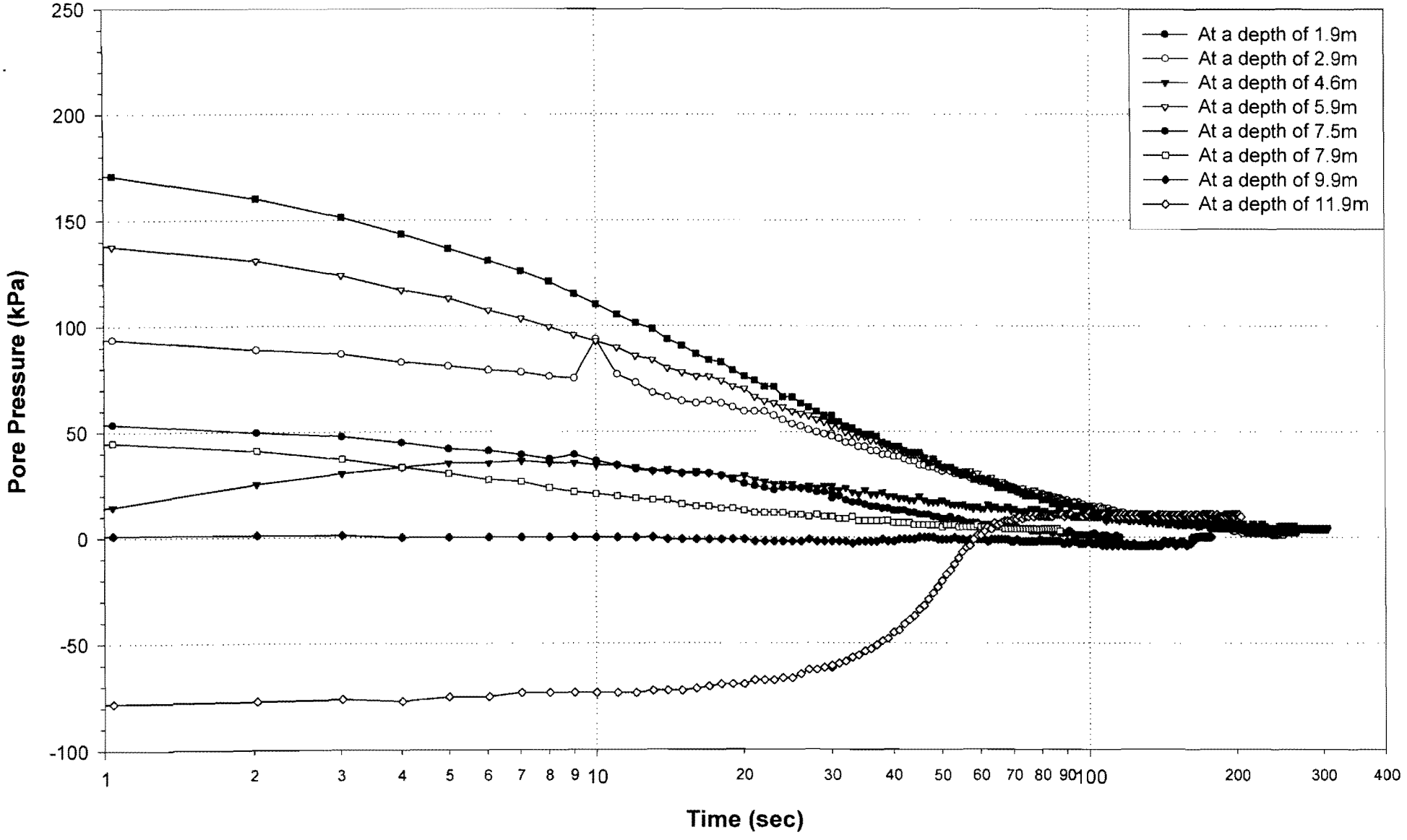

Figure 3-142: Piezocone dissipation data: Mizpah - Beach Pond Interface.

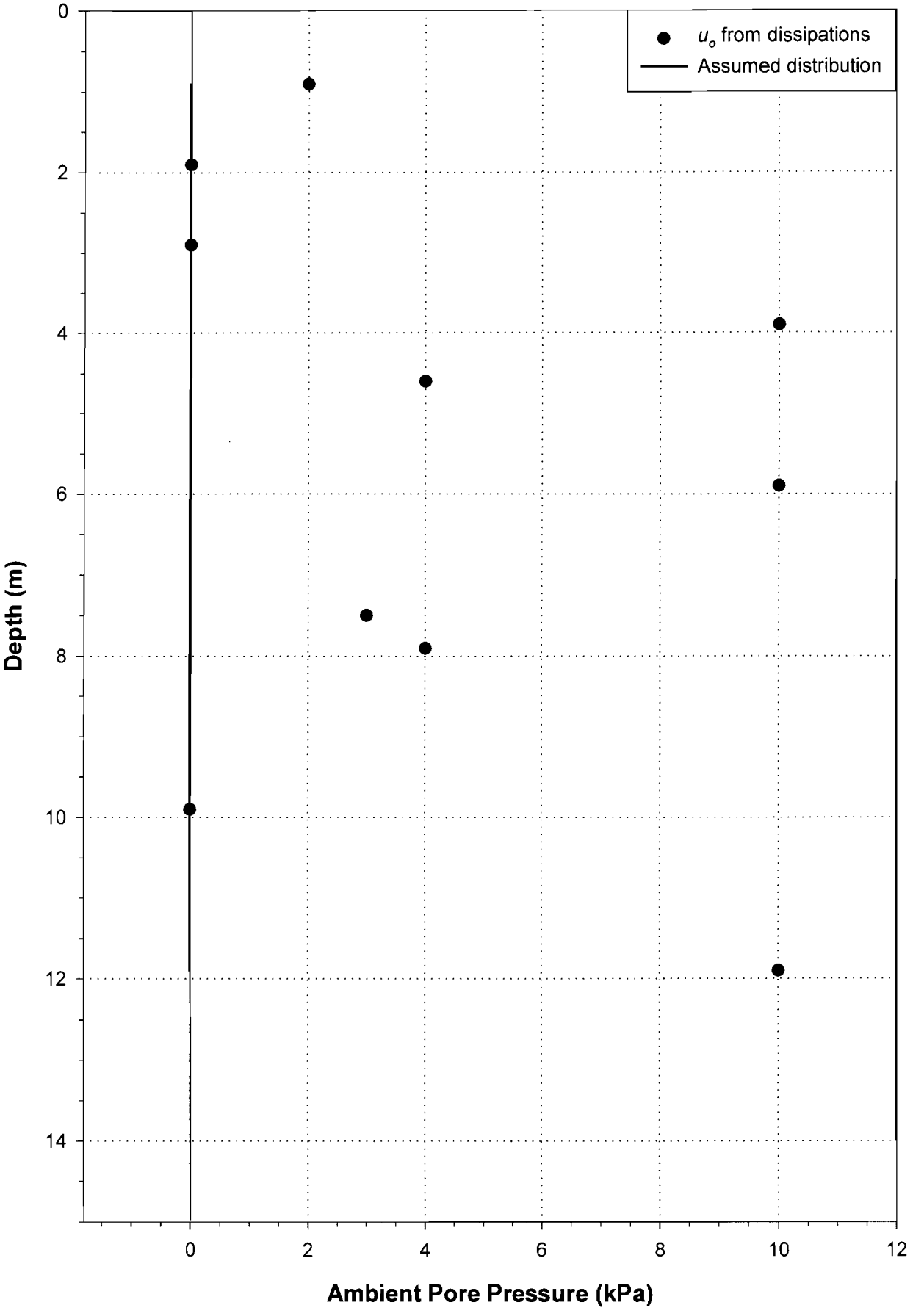

Figure 3-143: Ambient pore pressure distribution: Mizpah - Beach Pond Interface.

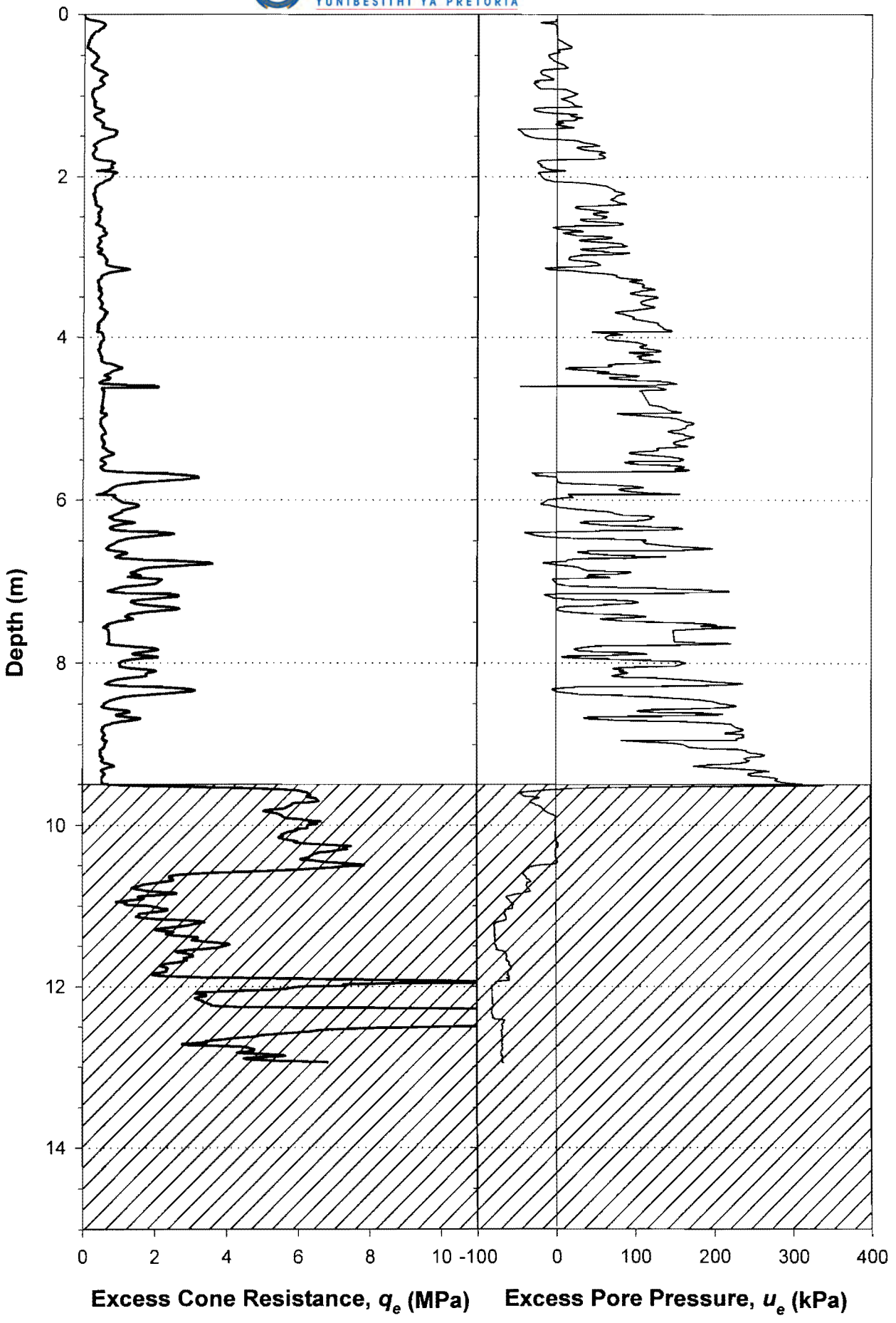

Figure 3-144: Normalised piezocone log: Mizpah - Beach Pond Interface.

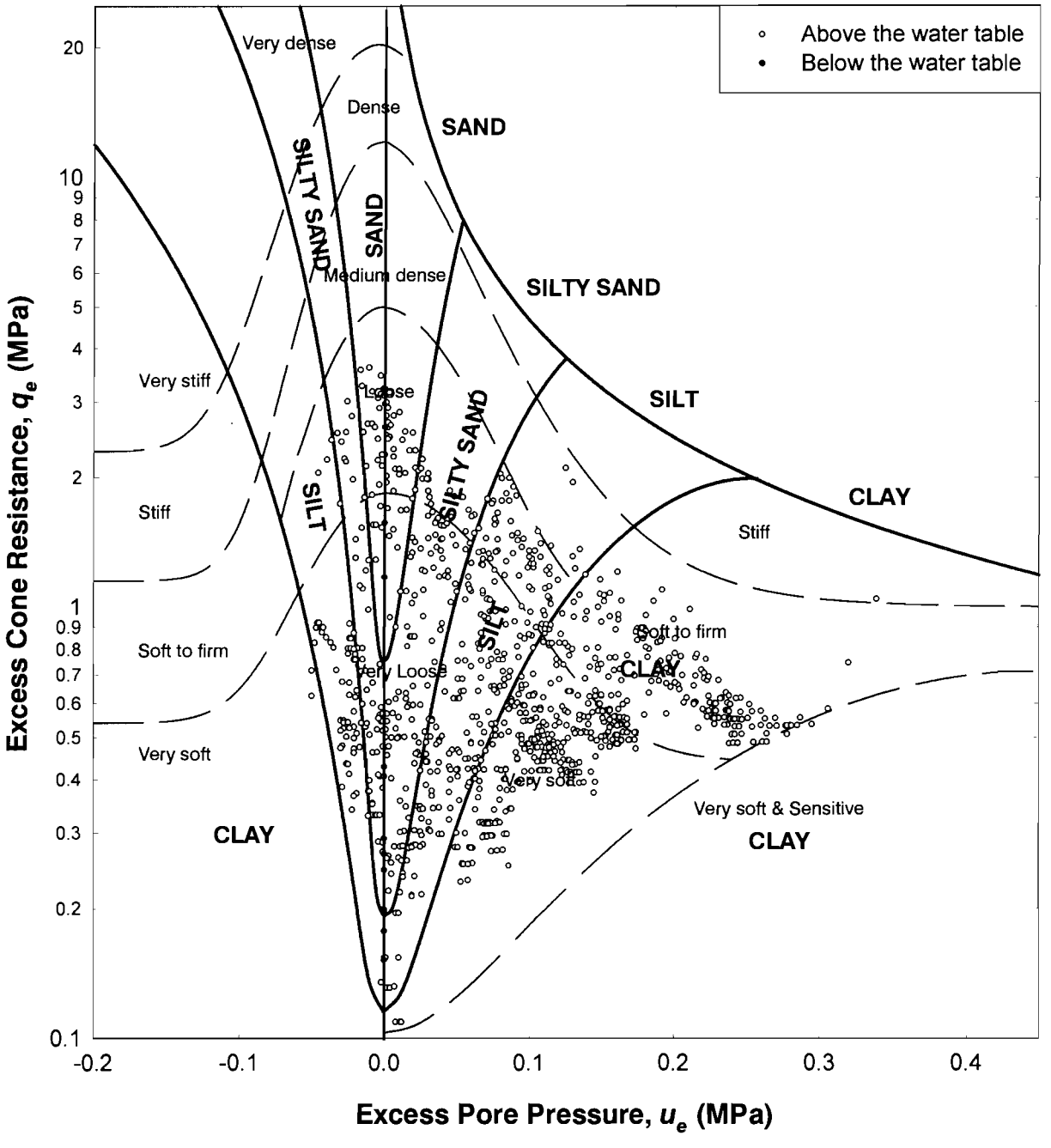

Figure 3-145: Piezocone soils identification chart: Mizpah - Beach Pond Interface.

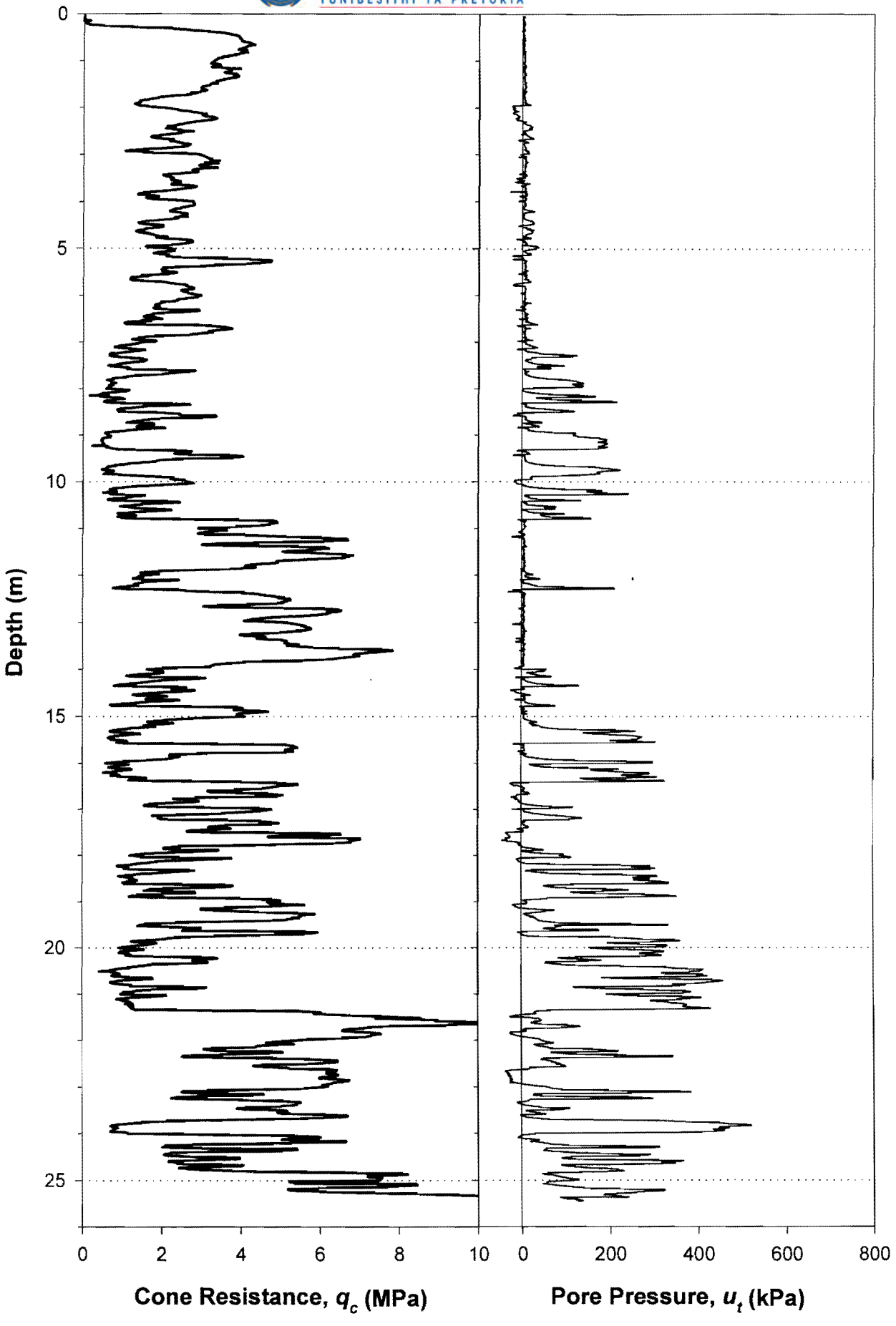

Figure 3-146: Piezocone field log: Pay Dam - Beach.

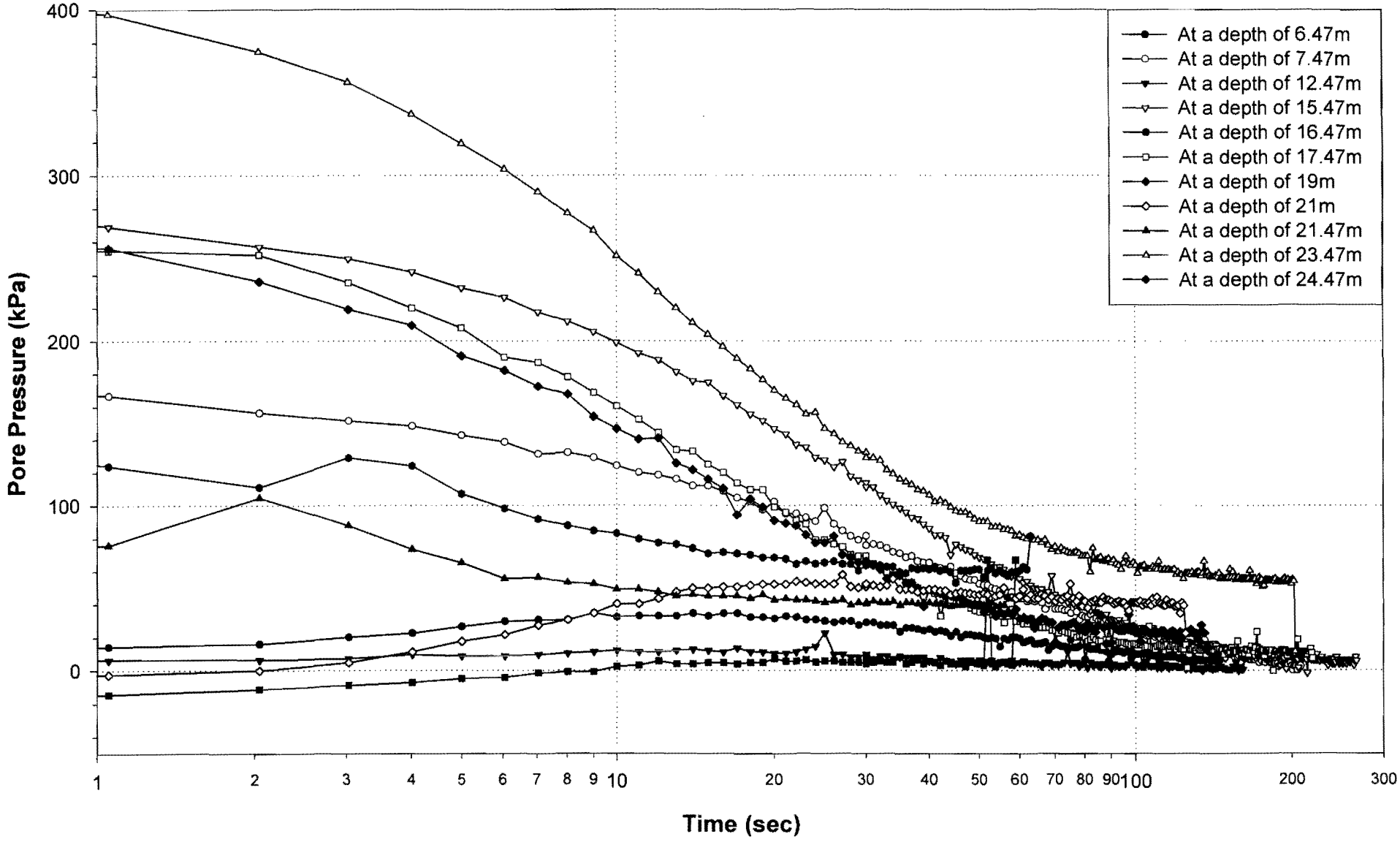

Figure 3-147: Piezocone dissipation data: Pay Dam - Beach.

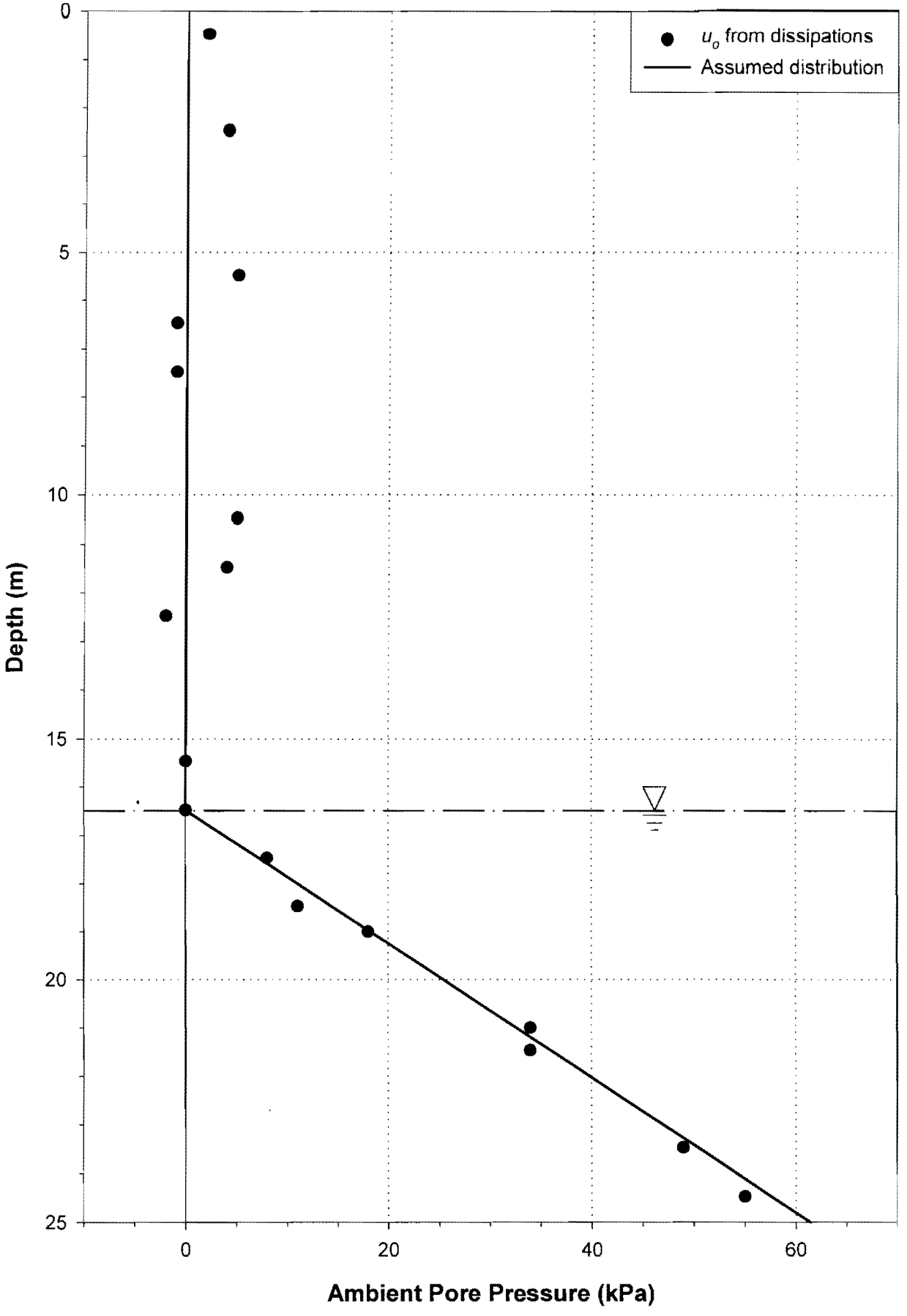

Figure 3-148: Ambient pore pressure distribution: Pay Dam - Beach.

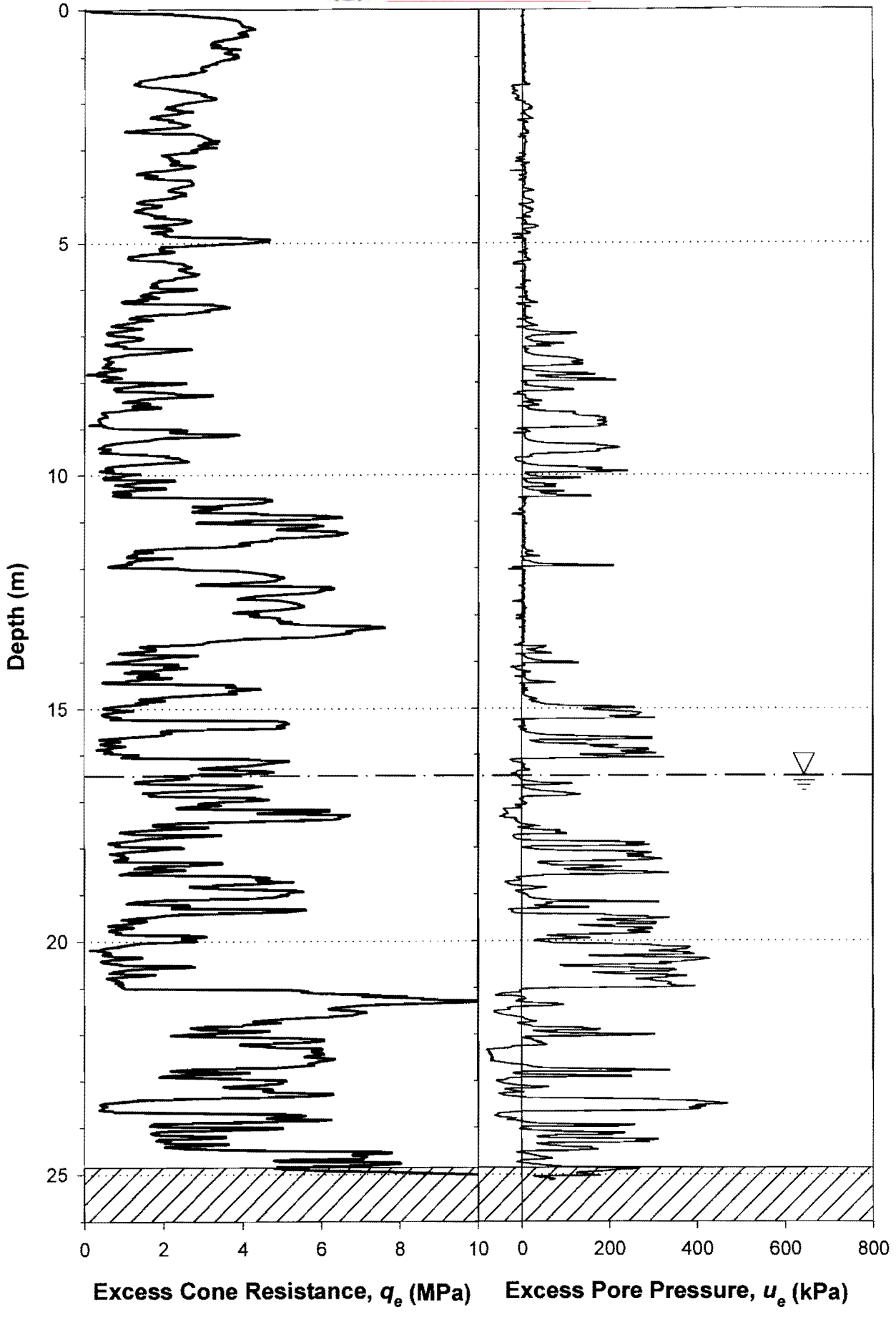

Figure 3-149: Normalised piezocone log: Pay Dam - Beach.

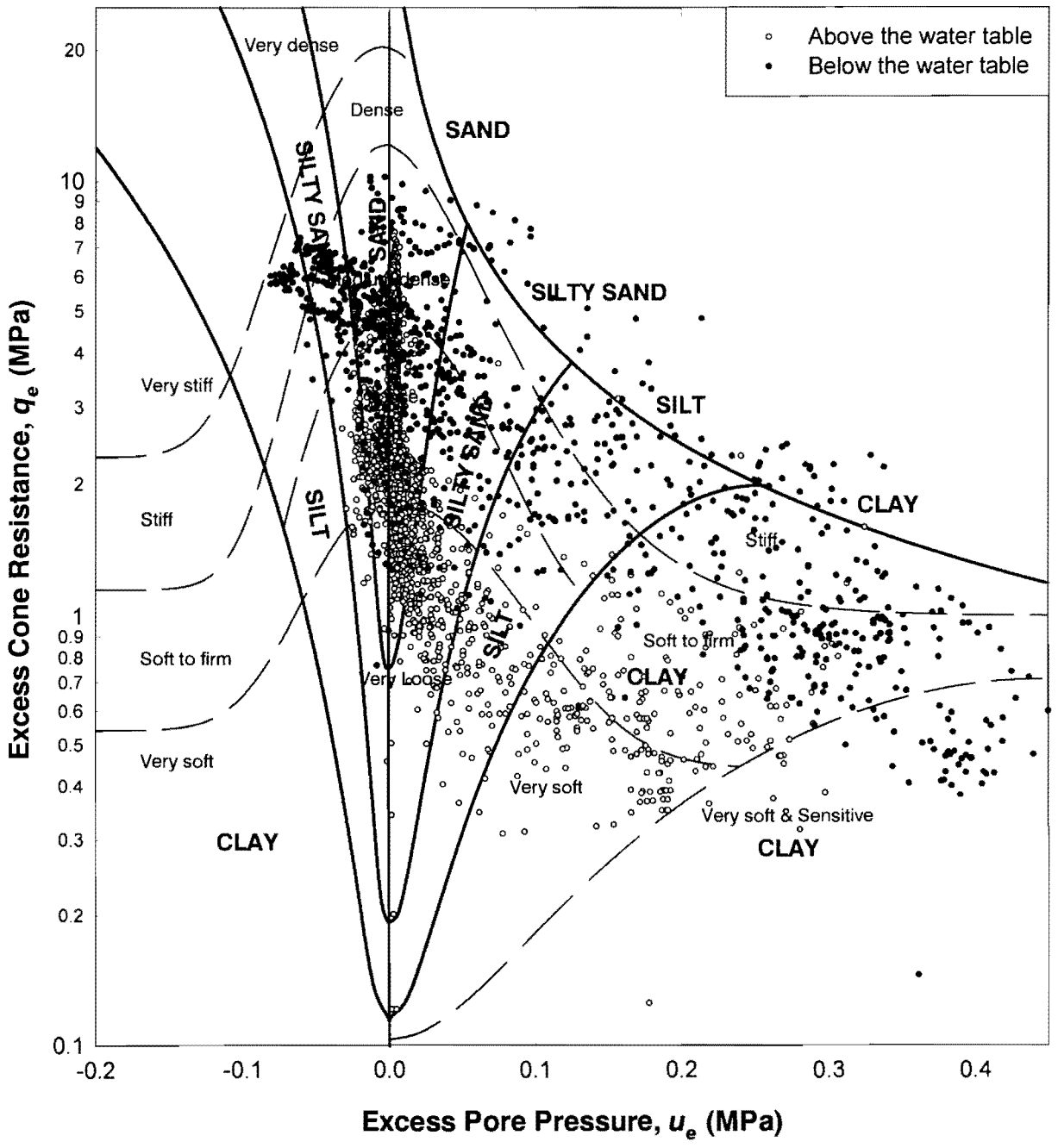

Figure 3-150: Piezocone soils identification chart: Pay Dam - Beach.

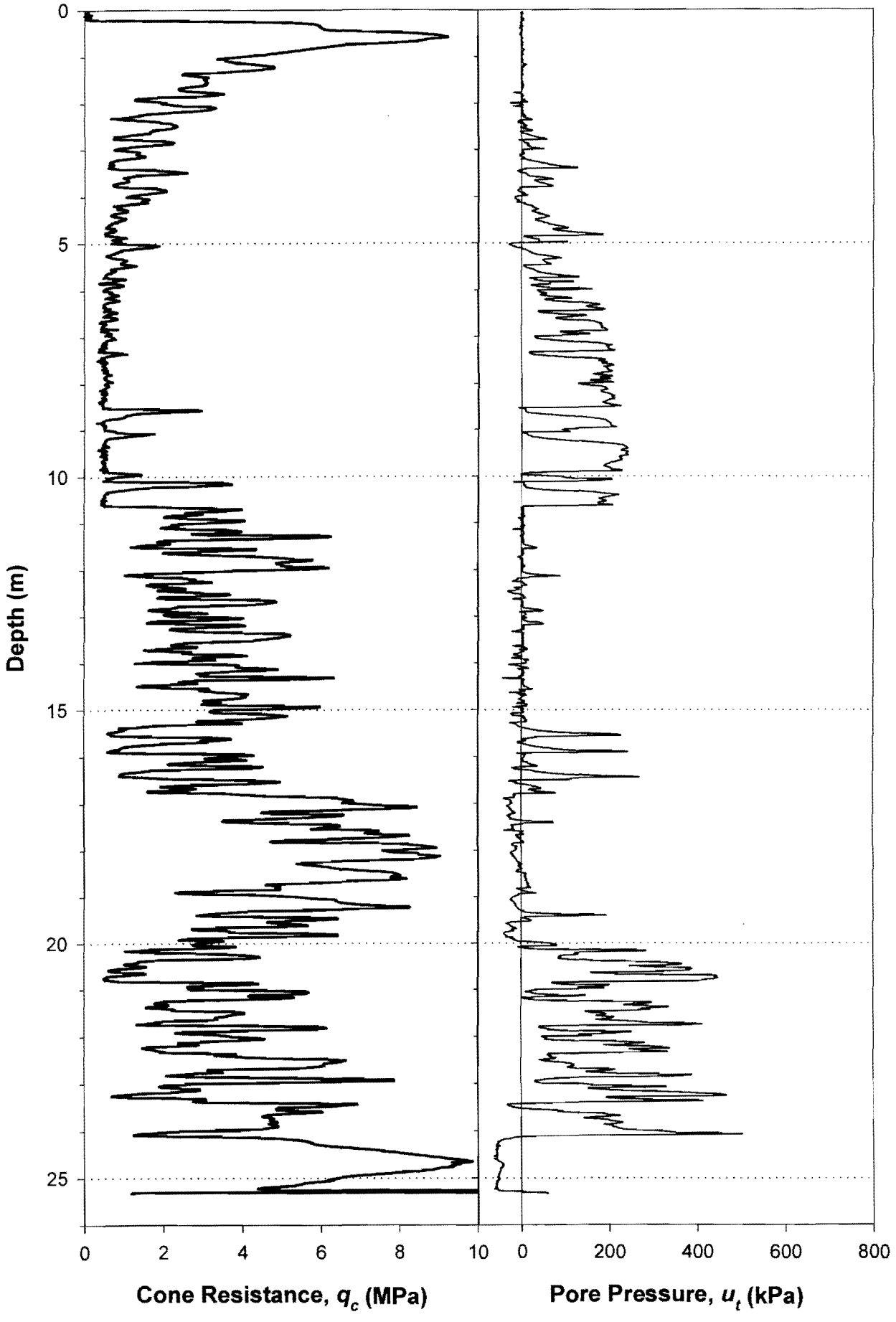

Figure 3-151: Piezocone field log: Pay Dam - Penstock.

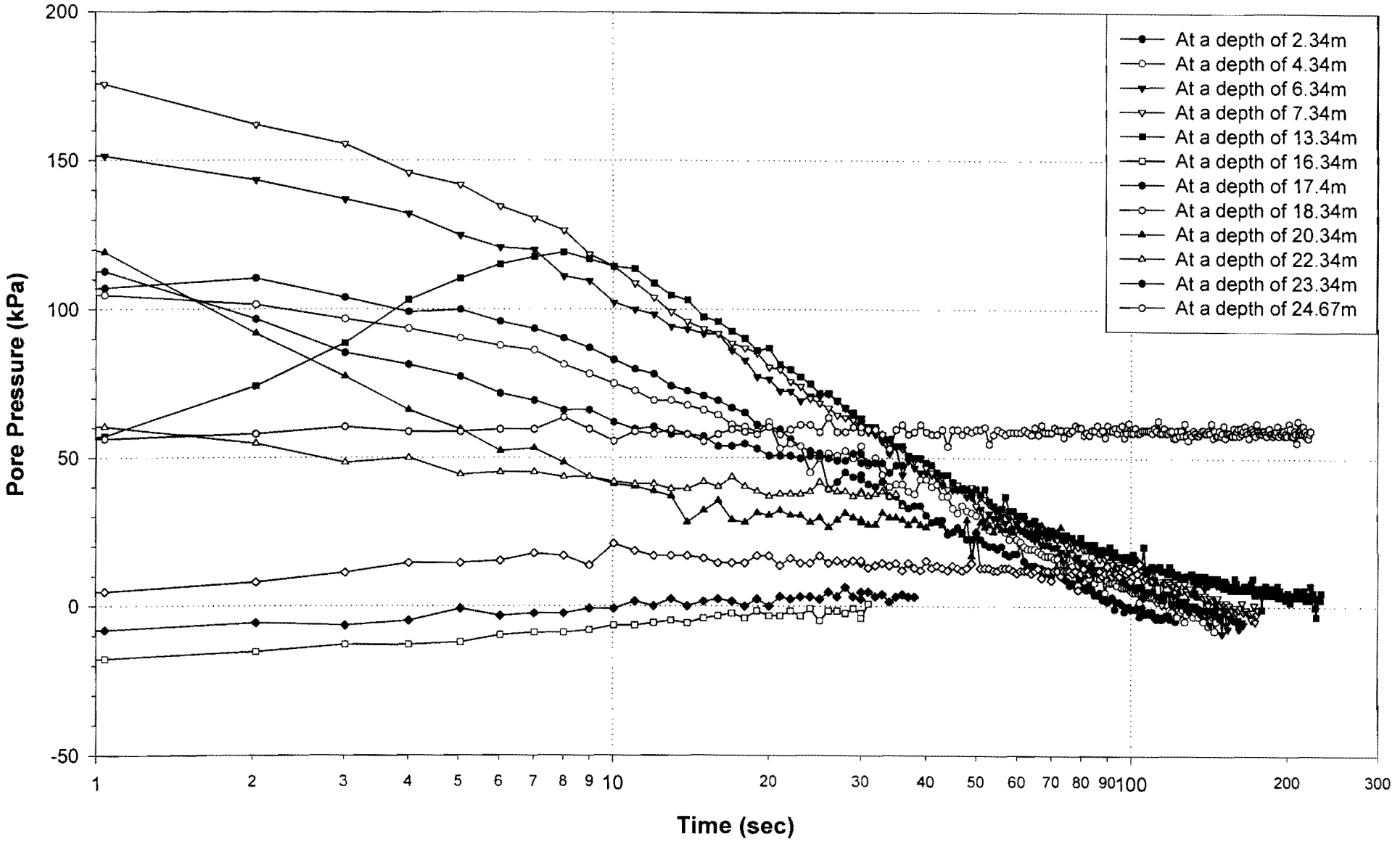

Figure 3-152: Piezocone dissipation data: Pay Dam - Penstock.

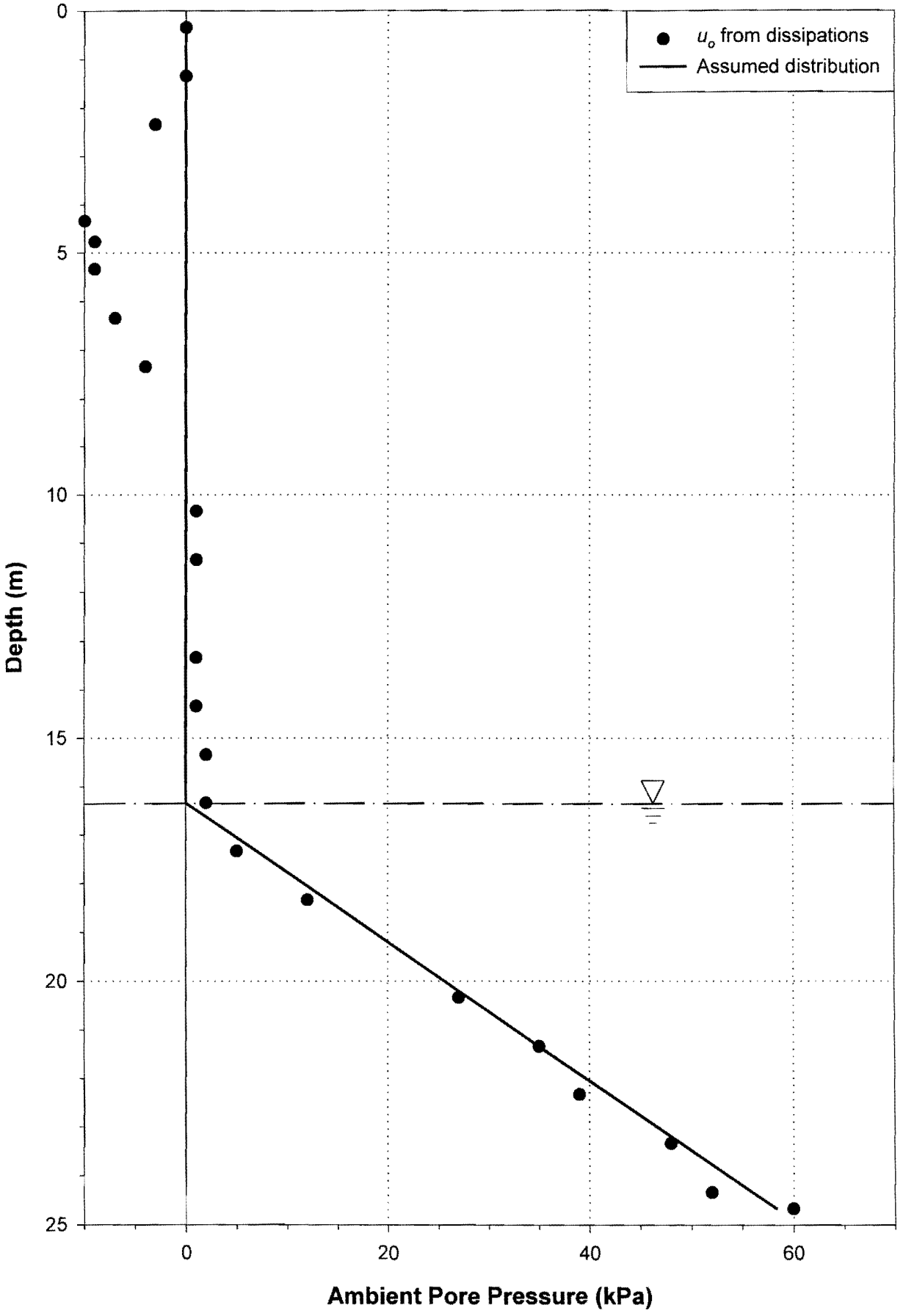

Figure 3-153: Ambient pore pressure distribution: Pay Dam - Penstock.

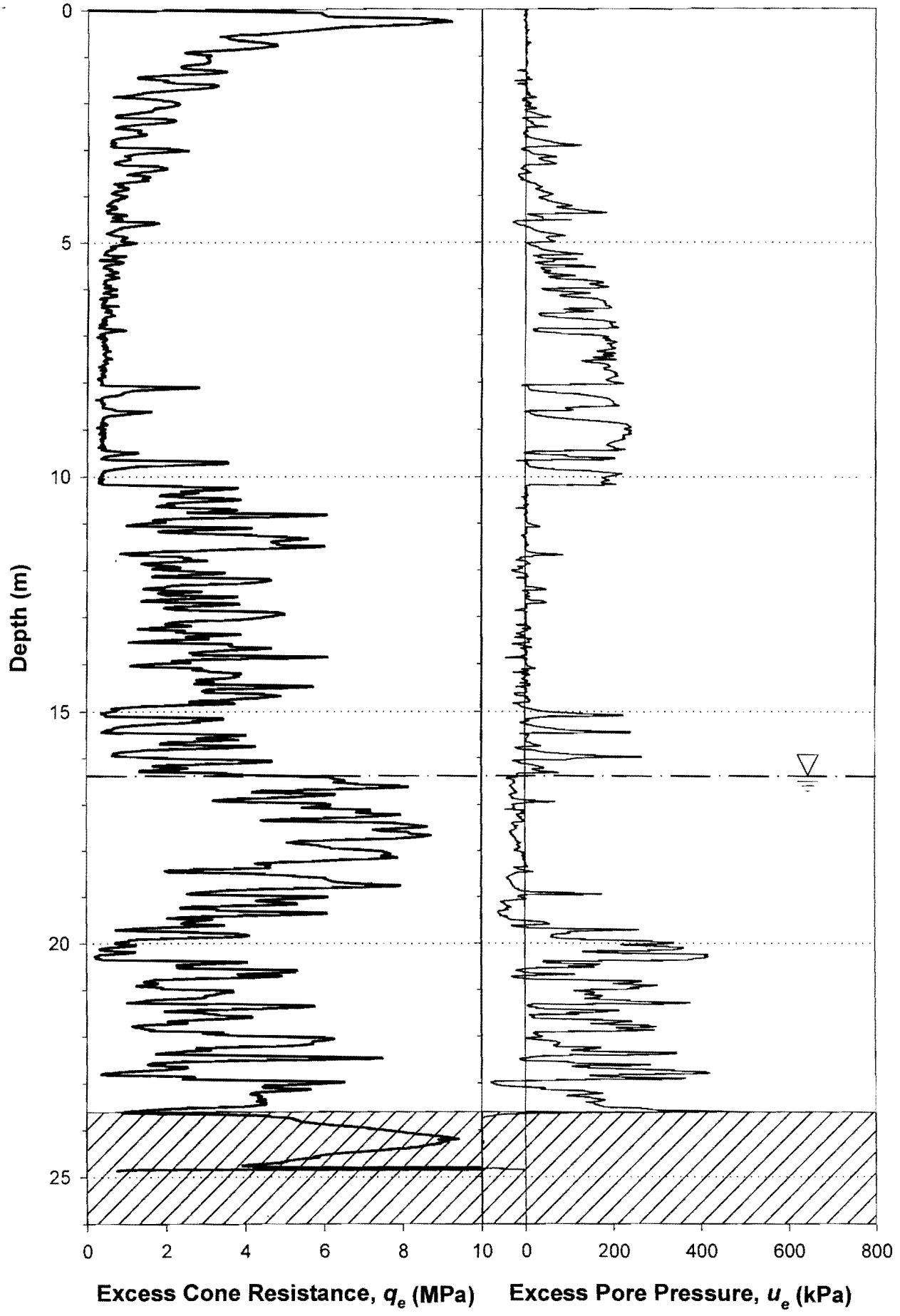

Figure 3-154: Normalised piezocone log: Pay Dam - Penstock.

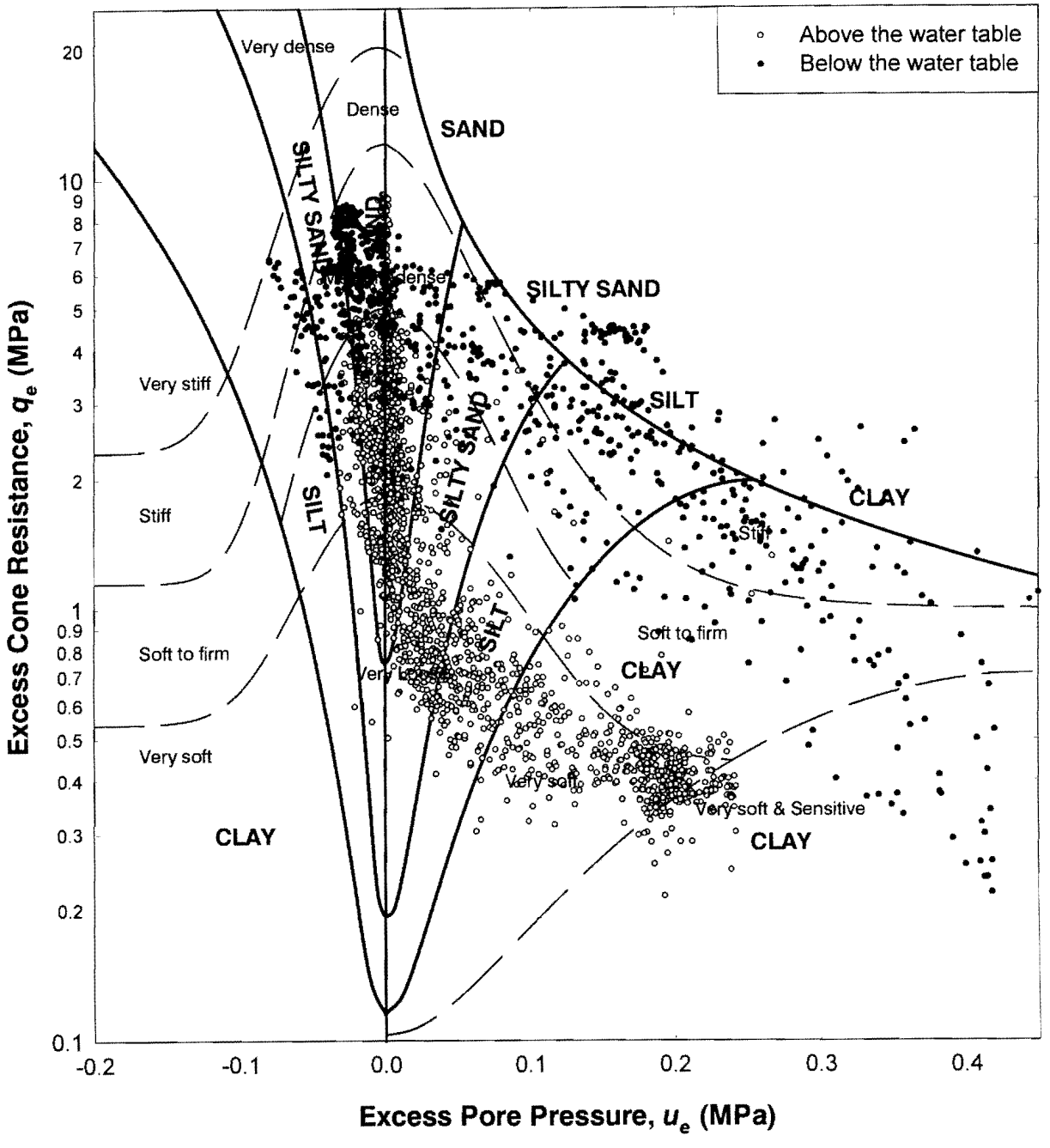

Figure 3-155: Piezocone soils identification chart: Pay Dam - Penstock.

CHAPTER 4

DISCUSSION

4.1 INTRODUCTION

The purpose of Chapter 4 is to analyse, interpret and discuss the experimental results from Chapter 3 against the literature background of Chapter 2.

The mechanical behaviour of particulate materials is controlled by the composition and state of the material, which are functions of the fundamental properties of the particles, the properties and state of interstitial fluids and the state of the packing arrangement, including density and structure. The composition and state of gold tailings are discussed here, based on the results from controlled laboratory experiments on reconstituted as well as undisturbed samples. The discussion leads to a working model of the condition of gold tailings in an impoundment and can be used as a guide to the geotechnical behaviour of this man-made soil.

The piezocone is already established as an important site investigation tool for the characterisation of tailings impoundments. It gives excellent results in defining the stratigraphy and seepage regime in a dam. However, it has not found favour in characterising strength and stiffness properties as yet. This chapter concludes with a re-evaluation of the interpretation of piezocone data in tailings. The ability of this tool to delineate the highly layered and variable tailings profile and to establish an accurate representation of seepage conditions is confirmed. In addition, the cone penetration data in a typical tailings profile are justified with respect to strength characteristics and shear behaviour. This will significantly extend the usefulness of piezocone data in tailings.

4.2 COMPOSITION

The solid phase of a soil plays a major part in determining its engineering behaviour. The most important soil solids are: minerals and products of organic synthesis and decay. Minerals are naturally occurring chemical compounds of definite composition and crystal structure. Tailings solids consist mainly of rock-forming minerals that have been liberated by mechanical and chemical processes in the reduction works, rather than the more natural processes of disintegration and decomposition.

The composition of gold tailings solids is discussed in the following sections in the context of the fundamental properties of the particles based on visual observations and x-ray spectrometry. The natural lighting effect on scanning electron micrographs, and the fact that the size fractions had been separated prior to imaging greatly facilitated interpretation. Energy dispersive x-ray spectrometry (EDS) and x-ray diffraction (XRD) techniques are used to identify the elemental and mineralogical composition of the material. It should be noted that quantitative information on the mineralogy is not as reliable as the qualitative information and should be regarded only as an estimate of the abundance of the various constituents.

4.2.1 Mineralogy

Particle mineralogy is derived from x-ray analyses: EDS spectrometry in the electron microscope for the elemental composition and XRD for the mineral composition. It should be noted that EDS targets are very small areas on the specimen, usually a particle and essentially gives a spot reading. XRD, however, illuminates a comparatively large area on a powdered specimen and therefore gives an estimate of the average mineralogy.

Energy Dispersive X-ray Spectrometry in the SEM

The original EDS spectra in Chapter 3 all show peak counts for carbon (C), oxygen (O) and gold (Au), which might be misleading to interpretation for the following reasons:

- Carbon is picked up from the pure carbon sticker used to mount a specimen onto the microscope stage without losing conductivity.
- X-ray emission can only take place from a solid phase and any oxygen detected must be from chemically bound oxygen, for example in the quartz as SiO_2 or from oxides of many of the metallic elements such as aluminium and iron.
- The gold peak originates from the thin coating of gold used to ensure a conductive surface and to enhance the imaging process.

The abundance of these elements has been ignored when quoting percentages of elements detected using EDS.

Some particles appear overexposed in the micrographs, this happens when a particle is loose or does not make good conductive contact with the microscope stage and becomes charged on its surface during imaging.

EDS is essentially a spot measurement and as such could only be applied to individual particles imaged under the SEM. For the purpose of discussion and in keeping with the

classification of EDS data in Chapter 3, tailings particles are divided into sands and slimes with the following distinctions:

(a) *Tailings sands*

- Particles larger than 63 μm.
- Typically either smooth surfaced or rough surfaced bulky grains.

(b) *Tailings slimes*

- Particles smaller than 63 μm
- Exist predominantly as flaky or plate-like particles, either loose or aggregated into flocs.

The results of energy dispersive x-ray spectrometry on the Mizpah whole tailings sample are summarised in Table 4-1.

Table 4-1: Elemental composition of Mizpah whole tailings particles by EDS.

Element	Average Percentages Detected[1]				
	Smooth surfaced Sands	Rough surfaced Sands	Flaky Slimes	Slime Flocs	Hydrometer Precipitate
Na			1	1	43
Mg				2	
Al	2	21	12	17	
Si	93	64	75	57	1
P			1		15
S			1		31
K	1	10	4	6	
Ca			1	1	4
Fe		2	4	13	1
Other	2	2	2	3	4

Table 4-1 shows very high percentages of sodium, phosphor and sulphur detected in the precipitate, in other words in solution in the tailings water. However, it must be considered that the specimen was dispersed using Calgon ($NaPO_3$ and Na_2CO_3), which would have contributed to the abundance of some of these elements. The last column in Table 4-1 can be compared with the effluent analysis in Table 3-1 from Chapter 3, which confirms the high concentrations of sodium, calcium and chlorine in the tailings effluent.

[1] Note that individual columns do not add up to 100% because the numbers represent average percentages of each element detected in more than 100 individual EDS analyses.

Powder X-ray Diffraction

X-ray diffraction is probably the most reliable method for the identification of clay and other minerals and provides information on both the minerals and their abundance in a specimen. Table 4-2 summarises the properties of the main minerals identified with XRD in the tailings.

The silicates are the largest, and by far the most complicated class of minerals. Approximately 30% of all minerals are silicates and some geologists estimate that 90% of the earth's crust consists of silicates.

Tectosilicates are also known as "Framework Silicates" because their structure is composed of interconnected silica tetrahedrons going outward in all directions forming an intricate framework. In this subclass all the oxygens are shared with other tetrahedrons giving a silicon to oxygen ratio of 1:2. In the near pure crystalline state of only silicon and oxygen the mineral is quartz (SiO_2). Quartz is the most common earth mineral. It is hard and tough with no cleavage and resists mechanical weathering better than any other important rock mineral. It will be seen in the discussion that follows that the composition of tailings is also dominated by quartz. In fact, tailings sands consist almost exclusively of quartz grains. Quartz is slightly soluble in a basic environment.

In the Phyllosilicate subclass, rings of tetrahedrons are linked through shared oxygens to other rings in a two dimensional plane which produces a sheet-like structure. The typical crystal habit of this subclass is flat, platy, book-like and displays good basal cleavage. Typically, the sheets are then connected to each other by layers of cat-ions. Cat-ion layers are weakly bonded and often have water molecules and other neutral atoms or molecules trapped between the sheets. These complex aluminium and magnesium silicates are extremely fine grained, with large surface areas per unit mass. Probably all of them have definite crystal structures that include large numbers of atoms arranged in complex three-dimensional patterns and are electrically charged. Mica is a large group with nearly 30 members recognised, but only a few of which are common. Those few however make up a large percentage of the most common rock types found in the earth's crust. Micas often contain iron and magnesium in addition to potassium. Mica flakes are soft and resilient, with pronounced cleavage. They split easily and break to form still smaller, thinner flakes. The Chlorite group is often associated with the clay group due to the flat flakiness of the breakage particles. Muscovite, pyrophyllite, illite, clinochlore and kaolinite are all phyllosilicates with clay-like properties. When these minerals are present in a soil, they can radically change its mechanical behaviour. Although tailings are normally not thought of as clay-like materials, it will be shown that there are fairly high concentrations of phyllosilicates in the fines. These

Table 4-2: Properties of the principal minerals that are present in tailings.

Mineral	Formula	Classification	Habits	G_s	Mohs Hardness
Quartz	SiO_2	*Class:* Silicates *Subclass:* Tectosilicates *Group:* Quartz	*Crystalline:* Coarse - Occurs as well-formed coarse sized crystals. Fine - Occurs as well-formed fine sized crystals.	2.63	7
Muscovite - Barian	$(Ba,K)Al_2(Si_3Al)O_{10}(OH)_2$	*Class:* Silicates *Subclass:* Phyllosilicates *Group:* Mica	*Massive:* Lamellar - Distinctly foliated fine-grained forms. Foliated - Two dimensional platy forms. Micaceous - Platy texture with "flexible" plates.	2.82	2 - 2.5
Pyrophyllite	$Al_2Si_4O_{10}(OH)_2$	*Class:* Silicates *Subclass:* Phyllosilicates *Group:* Pyrophyllite-talc	Earthy - Dull, clay-like texture with no visible crystalline affinities.	2.84	1.5 - 2
Illite	$(K,H_3O)Al_2Si_3AlO_{10}(OH)_2$	*Class:* Silicates *Subclass:* Phyllosilicates *Group:* Mica		2.75	1 - 2
Clinochlore	$(Mg,Fe)_6(Si,Al)_4O_{10}(OH)_8$	*Class:* Silicates *Subclass:* Phyllosilicates *Group:* Chlorite	*Massive:* Fibrous - Distinctly fibrous fine-grained forms. Pseudo hexagonal - Crystals show a hexagonal outline. Granular - Generally occurs as anhedral to subhedral crystals in matrix.	2.65	2 - 2.5

Kaolinite	$Al_2Si_2O_5(OH)_4$	*Class:* *Subclass:* *Group:*	Silicates Phyllosilicates Kaolinites	Earthy - Dull, clay-like texture with no visible crystalline affinities.	2.60	1.5 - 2
Gypsum	$CaSO_4{\cdot}2H_2O$	*Class:*	Sulphates	*Tabular:* Form dimensions are thin in one direction. *Crystalline:* Occurs as well-formed coarse sized crystals. *Massive:* Distinctly fibrous fine-grained forms.	2.30	2
Pyrite	FeS_2	*Class:* *Group:*	Sulphides Pyrite	*Striated:* Faces have parallel lines (e.g. plagioclase). *Druse:* Crystal growth in a cavity which results in numerous crystal tipped surfaces. *Stalactitic:* Shaped like pendant columns as stalactites or stalagmites.	5.01	6.5

will surely be affected by electrical surface charges and other similar effects associated with clays.

The members of the Sulphide Mineral Class form an economically important class of minerals. Most major ores of important metals such as copper, lead and silver are sulphides. Strong generalities exist in this class. The majority of sulphides are metallic, opaque, generally sectile, soft to average in hardness and possess high densities. The Pyrite Group is composed of minerals with a similar isometric structure and related chemistry. It is named after its most common member, pyrite, which is often associated with gold in South African ores. The significance of pyrite in the tailings mix, is the high density of this mineral, of the order of 5 Mg/m^3, and the fact that it reduces to sulphuric acid and iron oxides following oxidation. The oxidation of the sulphide minerals is clearly evident as the yellowish coloration on exposed surfaces on gold tailings impoundments. Changes in pH as a result of the sulphuric acid can lead to precipitation of agents such as silica, but also to a solution of heavy minerals that can cause serious pollution problems.

Contrary to the Mizpah whole tailings specimen used for the EDS work in the previous section (Table 4-1), none of the XRD specimens were treated with a dispersant. Gypsum ($CaSO_4 \cdot 2H_2O$) identified in the Mizpah whole tailings (delivery slurry) and not in the other samples, is probably the result of precipitation of gypsum from solution when the sample was dried. Gypsum was not detected in the samples recovered from the pond areas on the dam probably because it was either siphoned of with the return water or leached out without opportunity to precipitate. Analysis of the hydrometer precipitate in Table 4-1 confirms the presence of Ca and S in the delivery slurry, because these are not found in the dispersing agent.

Discussion

The results of the EDS and XRD analyses are used in this section to determine the mineralogical composition of the tailings samples considered in this study. Although EDS data are quantitative with respect to the elements identified, XRD data are not intended to be quantitative. Nevertheless, in the discussion that follows the XRD data are quantitatively analysed, in an approximate way, and compared with the EDS results. The abundance of minerals in the XRD spectrographs was estimated by adding all the peak counts, percentage-wise, of a specific mineral. The results are summarised in Table 4-3.

Table 4-3 represents the mineralogical composition of the tailings, including that of the dispersed whole tailings sample. To compare these results with the EDS data on the Mizpah

Table 4-3: Approximate mineral percentages from XRD results.

Approximate percentages identified with XRD					
All samples: non-dispersed.					
Sample[2]	**Mizpah Whole**	**Mizpah Fine**	**Mizpah Coarse**	**Pay Dam Fine**	**Pay Dam Coarse**
Quartz	69	75	83	59	79
Muscovite	8	9	8	7	9
Pyrophyllite	5	4	1	17	5
Illite	6	6	5	11	3
Clinochlore	2	3	2	3	3
Kaolinite	2	2	1	3	1
Gypsum	7				
Pyrite				1	
Mizpah whole tailings: separated fractions and dispersed.					
	150 μm (*Sand*)	**75 μm (*Sand*)**	**10 μm (*Slime*)**	**2 μm (*Slime*)**	**1 μm (*Slime*)**
Quartz	90	89	72	43	27
Muscovite			9	21	31
Pyrophyllite			1	4	9
Illite	10	8	9	19	15
Clinochlore		1	4	7	9
Kaolinite		1	3	4	7
Pyrite			1	2	1

whole tailings sample in Table 4-1, the XRD minerals for the sand (150 & 75 μm) and slime (8, 2 & 1 μm) fractions have to be broken down into their constituent elements. This is shown in Table 4-4, where the Mizpah whole tailings minerals are represented by their characteristic elements (Mg, Al, Si, S, K, & Fe) as follows:

- Quartz SiO_2 Si = 1
- Muscovite $KAl_2(Si_3Al)O_{10}(OH,F)_2$ K : Al : Si : F = 1 : 3 : 3 : 2
- Pyrophyllite $Al_2Si_4O_{10}(OH)_2$ Al : Si = 2 : 4
- Illite $(K,H_3O)Al_2Si_3AlO_{10}(OH)_2$ K : Al : Si = 1 : 3 : 3
- Clinochlore $(Mg,Fe)_6(Si,Al)_4O_{10}(OH)_8$ Mg : Fe : Si : Al = 6 : 6 : 4 : 4
- Kaolinite $Al_2Si_2O_5(OH)_4$ Al : Si = 2 : 2
- Pyrite FeS_2 Fe : S = 1 : 2

[2] The terms fine and coarse should not be confused with tailings sands and tailings slimes. The coarsest sample studied contained more than 50% slimes and the finest sample close to 5% sand.

Table 4-4: Mizpah Whole tailings: XRD mineral identification and breakdown of characteristic elements.

Mineral composition: Sand (avg. of 150 & 75 μm) and Slime (avg. of 8, 2 & 1 μm).							
	Quartz	Illite	Clinochlore	Kaolinite	Muscovite	Pyrite	Pyrophyllite
Sand	89	9	1	1			
Slime	47	14	7	5	20	1	6
Ratios of characteristic elements for each mineral from the chemical formulae.							
Mg			0.3				
Al		0.43	0.2	0.5	0.43		0.33
Si	1.0	0.43	0.2	0.5	0.43		0.67
S						0.67	
K		0.14			0.14		
Ca							
Fe			0.3			0.33	
Percentages of characteristic elements in the separate sand and slime fractions.							
Sand:							
Mg			0.15				
Al		3.86	0.10	0.25			
Si	89.00	3.86	0.10	0.25			
S							
K		1.29					
Ca							
Fe			0.15				
Sum	**89.0**	**9.0**	**0.5**	**0.5**	**0.0**	**0.0**	**0.0**
Slime:							
Mg			2.10				
Al		6.00	1.40	2.5	8.57		2.00
Si	47.00	6.00	1.40	2.5	8.57		4.00
S						0.67	
K		2.00			2.86		
Ca							
Fe			2.10			0.33	
Sum	**43.0**	**14.0**	**7.0**	**5.0**	**20.0**	**1.0**	**5.0**

Once the minerals in the sand and slime fractions have been broken down into their constituent elements, a direct comparison can be made with the EDS data, as shown in Table 4-5.

Table 4-5: Comparison of XRD and EDS mineral composition of Mizpah whole tailings.

Element	SAND			SLIME		
	EDS		XRD	EDS		XRD
	Smooth	Rough		Flake	Flock	
Mg					2	2
Al	2	21	4	12	17	20
Si	93	64	93	75	57	70
S				1		1
K	1	10	1	4	6	5
Ca				1	1	
Fe		2		4	13	2
Other	4	3		3	4	
Sum	**100**	**100**	**98**	**100**	**100**	**100**

Table 4-5 demonstrates good agreement between the XRD and EDS mineral compositions of the dispersed tailings sands and slimes. Based on these results the mineralogical composition of the gold tailings sands and slimes is as follows:

- *Tailings sands:*

  90% quartz and 5 to 10% illite, with illite mainly detected on rough surfaced particles. It might be conjectured that the rough surfaced particles are pyrophyllite, which would also register silicon and aluminium on the EDS. However, the powder XRD did not detect any pyrophyllite in the 150 and 75 μm Mizpah whole tailings specimens. It is, therefore, concluded that the clay mineral in the sands was illite.

- *Tailings slimes:*

  50% quartz, 20% muscovite, 15% illite, and approximately 5% each of clinochlore, kaolinite, pyrophyllite.

These percentages, although approximate, give insight into the mineralogy of a typical gold tailings. The coarse particles are basically pure quartz except for a small percentage of illite clay, most probably attached to the quartz grains. The slimes, although predominantly quartz, have increasing amounts of pyrophyllite, muscovite and illite, as well as traces of kaolinite, and pyrite. The muscovite could actually be seen glittering in the slimes when held in a bright light.

Thus, referring to the XRD results on the five tailings samples examined, the mineralogy of gold tailings, i.e. delivery slurry as well as fine and coarse deposited layers can be summarised as:

- Quartz (%)[3]: 83 - 75 - 59
- Muscovite (%): 9 - 8 - 7
- Pyrophyllite (%): 17 - 5 - 1
- Illite[4] (%): 11 - 5 - 3
- Small percentages of Clinochlore, Kaolinite and Pyrite.

These percentages are also in good agreement with the composition of the Witwatersrand gold reef according to Stanley (1987); Table 2-1 from Chapter 2 reproduced here as Table 4-6.

Table 4-6: Mineral composition of a typical Witwatersrand gold reef.

Mineral	Abundance
Quartz (SiO_2), primary and secondary	70 - 90 %
Muscovite and other phyllosilicates	10 - 30 %
Pyrites	3 - 4 %
Other sulphides	1 - 2 %
Grains of primary minerals	1 - 2 %
Uraniferous Kerogen	1 %
Gold	~ 45 ppm in the Vaal Reef

4.2.2 Specific Gravity

Table 4-7: Specific gravity of the tailings samples.

Tailings Dam	Description	G_s
Mizpah	Whole tailings	2.74
	Pond fine	2.75
	Pond coarse	2.73
Pay Dam	Penstock fine	2.74
	Penstock coarse	2.73

Table 4-7 shows a very interesting feature of the different tailings samples considered: they have almost exactly the same specific gravity of 2.74 Mg/m^3. This observation suggests that soil-forming processes on a gold tailings impoundment are possibly driven by gravity - at least in the pond areas and in the delivery pulp. The delivery pulp contains specific percentages of quartz, muscovite, pyrophyllite, illite and traces of other minerals with their

[3] The percentages give the full range based on the XRD results and an average value for the 5 samples tested.

[4] Compared with the separated sands and slimes there appears to be a deficiency in illite in the whole samples, however, most of the illite was detected in sand and slime particles larger than 150 μm and smaller than 2 μm. In the full gradings the bulk of the material lies between these sizes with much less illite detected, refer to Table 4-3.

respective densities, but with an overall specific gravity of 2.74. It is speculated here that soil-forming processes on the impoundment will sort these fractions gravitationally, rather than according to size, so that the mixtures of minerals in deposited layers, whether fine or coarse, result in a specific gravity of 2.74 Mg/m^3 for each layer.

4.2.3 Grading

Grading analyses were performed using standard wet-sieve and hydrometer methods. It will be illustrated that the properties of the tailings particles affect the results and produce grading curves which are consistently finer than estimates of particle dimensions based on the electron micrographs.

Effects of Pre-treatment Procedures:

In order to judge the effects of different pre-treatment procedures on the grading distributions, parallel tests were performed with non-treated specimens as a reference. Conclusions from these tests are subsequently discussed:

(a) *Calcareous compounds*

A simple test for calcareous matter, using hydrochloric acid, was performed on the samples as suggested in Chapter 3. None of the samples recovered from the dams showed any response, indicating the absence of carbonate compounds. It is concluded that carbonate bonding does not occur in tailings deposits.

(b) *Dispersion*

Treatment with the standard dispersing agent, Calgon, altered the gradings significantly throughout. With dispersant the gradings are fairly uniformly distributed in the fine sand and silt size ranges with approximately 10% finer than 2 μm. Without dispersant none of the gradings identified any material finer than medium silt sized particles, approximately 10 μm. There are two possible explanations for this behaviour:

- Tailings exist in a flocculated state on leaving the reduction plant, wherein most of the finer material is aggregated into flocs no less than 10 μm in diameter. These flocs are broken down into their individual constituents by the dispersing agent and can be detected in the hydrometer sedimentation test.
- Alternatively the fine flaky slimes attach themselves to the bulky sand and coarse silt particles in the undispersed state. The slimes essentially blanket the coarser particles and settle out together with them. On dispersion the flakes are detached from the coarser particles and individually measured during sedimentation.

Evidence on the electron micrographs, suggests that a combination of both these effects is responsible for the flocculated nature of untreated gold tailings. Figure 4-1 demonstrates an example of each effect on micrographs of untreated (undispersed) tailings from this study.

(c) *Organic matter*

The British standard provides for the removal of organic matter by oxidation using hydrogen peroxide. Organic removal was considered for this study due to the occurrence of wood fibres in the tailings. Tramp pieces of wood are processed with the mined ore, and end up as fine fibres in the tailings. Reaction of the oxidising agent with the samples were highly dependent on the age of the tailings. Fresh tailings produced a violent and rapid reaction, whereas older tailings resulted in a slow and subdued reaction. The fresh tailings were sampled directly from the discharge pipe or from surface deposits and the older material at depth below the surface of a deposit. The author is of the opinion that the hydrogen peroxide not only oxidises organic material, but also sulphide minerals such as pyrite. Visual observation after organic treatment showed that there were still some wooden fibres left, although, much reduced. For these reasons it is not recommended to use organic pre-treatment on tailings. Nevertheless, organic treatment on undispersed tailings result in grading curves somewhere between fully dispersed and non-dispersed gradings as illustrated in Table 4-8.

Table 4-8: Effects of organic treatment on fresh and older tailings specimens.

Tailings Dam	Description	Age (Depth of sampling)	Result
Mizpah	Pond Fines	Surface	Violent reaction No change in grading
	Pond Coarse	Surface	Violent reaction Intermediate grading
Pay Dam	Penstock Fines	4.3 m below surface	Mild reaction Intermediate grading
	Penstock Coarse	2.0 m below surface	Moderate reaction Intermediate grading

Fully Dispersed Gradings

The gradings performed on all samples in this study indicated very little, less than 2% per mass, coarser than 200 μm (limit of fine sand) and generally of the order of 10% smaller then 2 μm (clay sized). The remaining material was distributed in the silt and fine sand size ranges as summarised in Table 4-9.

Table 4-9: Summary of dispersed grading properties of gold tailings.

Tailings Dam	Description	Median Particle Size D_{50}		*CU*	*CC*
		(μm)	Description		
Mizpah	Whole Tailings	30	Coarse silt	28	0.9
	Pond Fines	10	Medium silt	11	0.8
	Pond Coarse	60	Coarse silt	25	2.8
Pay Dam	Penstock Fines	6	Fine Silt	5	0.8
	Penstock Coarse	25	Coarse silt	22	0.9

The gradings in Table 4-9, although representative of the pond areas of tailings dams, almost cover the full range of published gradings in Figure 2-11. The Coefficient of Uniformity (*CU*) is less than 36 throughout, which is the value for the "Ideal" Fuller Curve (Fuller & Thompson, 1907). The Fuller curve describes the uniformity properties of spherical particles for the densest possible state of packing; the largest particles barely touch each other, while there are enough intermediate-size particles to occupy the voids between the largest without holding them apart, smaller particles subsequently occupy voids between intermediate-sizes, etc. A sample of spherical particles with *CU* less than 36 has an abundance of fines so that the coarser particles cannot all be in contact and it is less dense than the optimum density. If *CU* is greater than 36, the voids between coarser particles are not fully occupied by the fines; the density is therefore also lower than the optimum density. It is interesting to note that:

- *CU* < 36: Addition of a small amount of fines will result in a less dense packing arrangement as the ideal structure, *CU* = 36, is further disrupted.
- *CU* > 36: Addition of a small amount of fines will result in a more dense packing arrangement, until void spaces between the coarser particles are filled (*CU* = 36).

The fine graded specimens in this study all have an abundance of fines, which tend to coat and push the coarser particles apart. The behaviour of these materials should, therefore, be governed by the fines fraction. The coarser grades, especially the whole tailings mix, are much closer to, but still less than the Fuller value (22, 25 and 28 compared with 36). It could, therefore, be argued that all of the samples shown in Table 4-9 will generally reduce in stiffness as their fines content increases. The soil structure of these tailings is controlled

by the fines rather than by a skeleton of coarser particles as suggested by the following evidence:

- Coefficients of Uniformity are less than 36 throughout. Although tailings particles are far from spherical, it is assumed that the basic principals stated in the previous paragraph still hold.
- All the gradings have more than 50% passing 63 μm, and of the order of 10% passing 2 μm, where the fines contain significant amounts of clay minerals. Thus, even the coarser samples contain more than 50% slimes.
- Micrographs of undisturbed samples shown in Chapter 3 show an abundance of fines so that the coarser bulky grains are always covered and displaced by these.
- In Section 4.3.3 it will be proved that the shear strength of all samples studied is unaffected by grading. This is consistent with a soil structure that is controlled by the fines.

Soils of this nature would have their compression curves displaced towards higher void ratios in e:logp' space with the addition of more fines. This is confirmed in Section 4.3.1, where samples have elevated and more steep compression curves with increasing fines content. As the compression curves are raised they also become more steep, thus reducing the bulk stiffness of the sample.

Sieve and Hydrometer Grading vs. "Visual" Grading

A "visual"-grading was derived from dispersed Mizpah whole tailings based on the electron micrographs presented in Chapter 3. SEM specimens were collected for this purpose from the sieve and hydrometer sedimentation tests. During the sedimentation test the sediment level was marked for each timed reading of the hydrometer. When the test had been completed, representative specimens were carefully extracted from each of these layers. Each specimen, representative of a specific size fraction, was then imaged under the SEM. The average diameter of the particles on each micrograph was subsequently measured, and applied to the mass fraction represented by the specimen photographed. For example, the fraction retained on the 150 μm sieve, with a measured diameter of approximately 200 μm, represents 4% of the total mass of the sample, 95.5% having passed this sieve the other 0.5% retained by sieves with a larger aperture. This process was greatly simplified by the fact that the original sample was already separated into size fractions by the sieve and sedimentation tests.

Figure 4-2 compares the grading determined from sieve and hydrometer tests to that derived from the SEM micrographs. The SEM "visual" grading, although approximate, is consistently coarser than the grading predicted by sieve and hydrometer tests. The reasons for this are two-fold:

- Test sieves in the sand-size range all have square apertures, where the sieve size measures the side length of an aperture. For a 150 μm sieve the diagonal across the square opening would be 212 μm thus allowing a flat or elongated particle of about 210 μm to pass through the sieve. The result is that the 4.5% mass fraction smaller than 150 μm, according to the sieve analysis, is actually representative of particles smaller than approximately 200 μm, due to the flattened nature of these particles.
- The hydrometer sedimentation test is interpreted using Stokes' Law after Sir George Stokes (1891), which among other things calculates the terminal velocity of the particles assuming small spheres. Electron micrographs of the particles smaller than 63 μm clearly show that these are plate-like and flat and would have a much reduced terminal velocity compared with a spherical particle of the same mass. Hence the "visual" coarser grading compared with the grading calculated using Stokes' theory.

4.2.4 Particle Shape

The shape of soil particles is as important as their size-range in determining the engineering behaviour of the material.

Tailings sands are bulky particles. The smooth surfaced grains imaged on SEM micrographs are highly angular to angular and generally flattened, sometimes elongated with sharp edges. Rough-surfaced sand particles are more rounded and can be sub-angular to sub-rounded. These observations are consistent with the products of rock crushing and grinding; the initial product is angular, but becomes sub-angular as the sharpest edges are smoothed by subsequent action.

Angularity has a profound influence on engineering behaviour. Under load, angular corners can break and crush, but particles tend to resist shear displacement. More rounded particles are less resistant to displacement, but less likely to crush. Soils composed of angular bulky grains are capable of supporting heavy static loads with little deformation. However, vibration and shock cause loose arrangements of angular bulky grains to be displaced easily. Such behaviour may be expected from clean tailings sands, which in addition should be non-plastic. Angularity also has the effect of increasing the angle of internal friction, ϕ (Mittal & Morgenstern, 1975).

Tailings slime particles are generally flaky grains consisting of disintegrated mica, clay and quartz minerals with very sharp edges. The slimes contain some silt-sized quartz particles. These small but bulky grains have similar properties to the smooth surfaced sands. Compared with the bulky sands, the slimes should be more compressible and behave like an intermediate plasticity clay. The fine sample collected from the Pay Dam penstock site

consisted of at least 90% slimes and had a PI of 17%. The slimes particles will be much more susceptible to surface and electromagnetic forces than the body force of gravity, which is the predominant force acting on the sand particles. The fact that the slimes can be flocculated is evidence of the effects of the surface forces.

4.2.5 Surface Texture

Inspection of the electron micrographs presented in Chapter 3 reveals the coarser or sand tailings particles to exist either with smooth or rough and irregular surfaces. The surfaces on the smooth sands appear to be the result of splitting and breaking of larger particles in the crushing and grinding processes of comminution. These surfaces show the typical concave geometry of pure quartz when broken. On the other hand, sand particles with irregular surfaces may have formed by fines attaching themselves to the particles and/or as a result of shattering and chipping of the particle surface rather than splitting during the reduction process. Evidence from EDS spectrometry on the rough surfaced particles indicates that there are at least some clayey minerals (illite) present on these otherwise pure quartz particles.

Individual particles of tailings slimes smaller than 63 μm have very smooth and flat surfaces. However, even dispersed there were some agglomerations and flocs of these flakes, which as a whole present a rough and irregular surface.

4.2.6 Summary of composition

The composition of gold tailings, as determined from the samples considered in this study, is summarised in Table 4-10. Although the terms sand and slime are used to distinguish between the coarser bulky tailings particles and the fines, there is no definite size separation between the two. For the tailings samples studied in this project the properties of the particles gradually change from sands to slimes in the fine sand to coarse silt-size ranges.

4.3 STATE

4.3.1 Normalised Compression Behaviour

Background

The idea of normalising the compression behaviour of a soil and linking it to commonly used geotechnical parameters such as the Atterberg limits is not a new one. Such

Table 4-10: Summary of fundamental particle properties of gold tailings.

Property	Tailings Sands	Tailings Slimes
Mineralogy	+90 % Quartz up to 10 % Illite	45 % Quartz 20 % Muscovite 15 % Illite 20 % Pyrophyllite, Kaolin & Clinochlore
	The mineralogy of gold tailings consists almost entirely of Tectosilicates and sheet-like Phyllosilicates. The coarser particles are mostly pure silica quartz, but as the fineness increases more and more mica-clay minerals are present. In the case of Mizpah dam the virgin slurry delivered contained some 40% tailings sand and 60% slime. Depositional conditions and sorting processes on the impoundment will result in deposited layers with a coarser composition - more sand less slime, or finer composition - less sand, more slime. Typically at the beach pond interface coarser layers contain 50% sand and slime, whereas the finer layers have 10% sand and 90% slime.	
Grading	The grading of gold tailings is highly dependent on whether a dispersing agent is used or not. *Dispersed:* Uniformly distributed in the fine sand and silt size ranges with approximately 2% coarser than 200 μm and 10% finer than 2 μm. *Non-dispersed:* Fines either flocculated (> 10 μm) or attached to coarser particles.	
Particle shape	Bulky but flattened.	Some silt sized particles similar to the sands, but mostly thin plate-like flakes, with high aspect ratios and large specific areas.
	Highly angular to sub-rounded.	Naturally flocculated.
Particle surface texture	Ranges from smooth to rough.	

normalising techniques and empirical correlations have been published for natural clay sediments for example by Schofield and Wroth (1968) and by Burland (1990).

To clarify the terms and definitions used in this discussion a brief review of critical state soil modelling will be given. For a more detailed treatment of the subject reference should be

made to: Schofield and Wroth (1968), Atkinson and Bransby (1978) and Muir Wood (1990). Roscoe, Schofield and Wroth developed Critical State Soil Mechanics (CSSM) at Cambridge University in the 1950's to model soil behaviour theoretically. Critical state by definition implies an ultimate failure state, where a soil mass is deforming in shear strain at constant shear strength, volume and effective stresses. The steady state, later defined by Casagrande (1969), differs from the critical state in that the failing mass, in addition, has to deform at constant velocity after particle orientation has reached a statically steady state condition and after all particle breakage if any is complete. There is some uncertainty in the literature about whether the critical state (CS) and steady state (SS) describe different conditions in a failing soil mass; Poulos et al. (1985), Poorooshasb (1989) and Ishihara in his 1993 Rankine lecture propose that both define the same ultimate state, but Castro (1969) and Alarcon-Guzman et al. (1988) disagree. Nevertheless, the term critical state will be used hereafter to indicate a state of ultimate failure.

In the theory of CSSM a set of invariant and fundamental soil parameters are used, which is entirely dependent on soil composition and independent of soil state and loading conditions. These parameters can, therefore, be derived from simple laboratory tests on reconstituted samples. The effects of soil state and the loading conditions are then modelled mathematically using well known constitutive relationships for soils including linear elastic theory, Cam-Clay (Schofield & Wroth, 1968), Modified Cam-Clay (Roscoe & Burland, 1968), Nor-Sand (Jefferies, 1993), etc.

Critical state stress paths are usually represented in two-dimensional invariant space consisting of a *Stress Plane* (q' vs. p') and a *Compression Plane* (e vs. p' or $\ln p'$) with,

- q', the deviator stress, equal to $(\sigma'_1 - \sigma'_3)$ or $\frac{3}{\sqrt{2}}\tau'_{oct}$ for the triaxial test (τ_{oct} = effective octahedral shear stress).
- p', the mean normal effective or isotropic stress, equal to the effective octahedral normal stress, σ_{oct} or $\frac{1}{3}(\sigma'_1 + 2\sigma'_3)$ for the triaxial test.
- e, the void ratio, is a measure of the density state[5].

Two reference soil states can be represented as logarithmic functions on these planes, i.e. the isotropic normally consolidated state or line (NCL) and the critical state failure line (CSL). These lines are functions of the following fundamental critical state parameters:

- λ – slope of the isotropic NCL in the compression plane.
- κ – slope of an isotropic rebound curve or swelling line (SL) in the compression plane.
- N – intercept of the NCL on the compression plane at p' = 1 kPa.

[5] Some researchers prefer using specific volume as a normalised density parameter, where specific volume is the volume of a sample containing a unit volume of soil solids. However, numerically specific volume is equal to 1 + e.

- M – slope of the CSL in the stress plane, measures frictional properties of the material.
- Γ – Similar to N, locates the CSL in the compression plane at $p' = 1$ kPa.

Using these parameters the NCL and CSL become:

NCL: $e = N - \lambda \ln p'$ and $q' = 0$ **Eq. 4-1**

CSL: $e = \Gamma - \lambda \ln p'$ and $q' = M \cdot p'$ **Eq. 4-2**

Schofield and Wroth (1969) noted that when the experimental log-linear CSL's of five different clays were extrapolated in the compression plane they appeared to converge at a focus point, Ω, with $e_\Omega = 0.25$ and $p'_\Omega = 10.3$ MPa, see Figure 4-3a. Such an extrapolation is certainly practically unjustified because of particle fracture and degradation at high pressure as well as the fact that the CSL must become asymptotic to the stress axis at zero void ratio. However, this geometric extrapolation allows some interesting analyses to be carried out, assuming that both the NCL and CSL's are theoretically parallel. Schofield and Wroth showed that points on the CSL corresponding to the liquid limit (LL) and the plastic limit (PL) of each individual clay tend to gather around the mean normal effective stresses of $p' = 5.5$ kPa and 550 kPa respectively; in other words $p'_{PL} \approx 100.p'_{LL}$. When the failure data are re-plotted as Liquidity Index, I_L vs. $\ln p'$, all CSL's collapse into a unique normalised line through the Ω-focus (Figure 4-3b), with the equation:

$$I_L = 1.371 - 0.217 \ln(p') \quad \textbf{Eq. 4-3}$$

where

$$I_L = \frac{w - PL}{LL - PL} \quad \textbf{Eq. 4-4}$$

w = moisture content
LL = liquid limit
PL = plastic limit

Thus, for any one soil,

$$e_{PL} - e_\Omega = \lambda \ln \frac{p'_\Omega}{p'_{PL}} \quad \textbf{Eq. 4-5}$$

Substituting the co-ordinates of Ω and $p'_{LL} = 551.6$ kPa into Eq. 4-5,

$$e_{PL} - 0.25 = \lambda \ln \frac{10342}{551.6} = 2.93\lambda \quad \textbf{Eq. 4-6}$$

or

$$\lambda = 0.341(e_{PL} - 0.25) \quad \textbf{Eq. 4-7}$$

Assuming G_s = 2.7 results in an approximate relation with the *PL* of

$$\lambda = 9.2 \cdot 10^{-3}(PL - 9.26) \qquad \textbf{Eq. 4-8}$$

Using the same arguments it can also be proved that,

$$\lambda = 3.6 \cdot 10^{-3}(LL - 9.26) \qquad \textbf{Eq. 4-9}$$

According to Schofield and Wroth, the better correlation with experimental results were obtained with Eq. 4-8.

The value of, λ, i.e. the slope of the CSL, is theoretically also the slope of the NCL as shown in Eqs. 4-1 and 4-2. If a similar focus to the Ω-point exists for normal compression, the properties of this focus together with Eqs. 4-8 and 4-9 could be used to reconstruct the compression behaviour of a clay.

Burland explored the normalised compression behaviour of natural clays. He proposed using the Void Index, I_v, as a normalising parameter for one-dimensional compression behaviour with,

$$I_v = \frac{e - e_{100}}{e_{100} - e_{1000}} \qquad \textbf{Eq. 4-10}$$

where e = void ratio

e_{100} = void ratio at σ'_{vo} = 100 kPa

e_{1000} = void ratio at σ'_{vo} = 1000 kPa

The void index serves as a measure of the compactness of a reconstituted clay and collapses e : $\log\sigma'_{vo}$ curves for different clays onto a single line called the Intrinsic Compression Line (ICL), Figure 4-4. This unique ICL confirms the assumption that the compression behaviour of a clay is truly log-linear as suggested by Eq. 4-1. The sign of the void index can be linked to the state of the material as follows: a "+" void index indicates a compact sediment and a "-" void index, a loose sediment. The intrinsic constants of compressibility, e_{100} and e_{1000}, can be linked to the critical state compressibility, λ, and clearly has a close analogy to the Liquidity Index.

Burland compared the intrinsic ICL to the Sedimentation Compression Line (SCL), representing the normalised in-situ state of a clay, to illustrate the effect of in-situ structure. The SCL consistently lies above the ICL for normally consolidated clays; a measure of the enhanced resistance of a naturally deposited clay over a reconstituted one resulting from differences in fabric and bonding (i.e. structure). The influence of structure on the compressibility or stiffness of clays was first recognised by Terzaghi (1941) and later

confirmed by Skempton (1944). At pressures in excess of 1000 kPa the ICL and SCL tend to converge as the natural material is de-structured.

The ICL for three natural clays covering a wide range of liquid limits and pressures was found to be represented with sufficient accuracy by the following equation:

$$I_v = 2.45 - 1.285 \log \sigma'_v + 0.015 \left(\log \sigma'_v\right)^3 \qquad \textbf{Eq. 4-11}$$

where σ'_v = vertical effective pressure in kPa

It was also found that for soils lying above the A-Line on the Casagrande chart, I_v could be correlated to the void ratio at liquid limit using:

$$I_v = \frac{e - 0.109 - 0.679 e_{LL} + 0.089 (e_{LL})^2 - 0.016 (e_{LL})^3}{0.256 e_{LL} - 0.04} \qquad \textbf{Eq. 4-12}$$

where e_{LL} = void ratio at the liquid limit

or by substituting $G_s = 2.7$ as Schofield and Wroth did,

$$I_v = \frac{e - 0.109 + 0.018 LL - 64.9 \cdot 10^{-6} LL^2 + 0.315 \cdot 10^{-6} LL^3}{0.007 LL - 0.04} \qquad \textbf{Eq. 4-13}$$

Eq. 4-13 only holds for clays with $26 < LL < 160$. Statistical analysis has shown that equally good correlations are achieved using plasticity index for high plasticity clays, but that errors become significant in low plasticity clays. According to Burland the normalisation did not fit soils lying below the A-Line on the Casagrande chart well.

Normalising the Compression Behaviour of Gold Tailings

In the previous section two methods of normalising the compression behaviour of natural clays were reviewed. These methods employ either the liquidity index or the void index, and propose simple correlations with the liquid and plastic limit through which the compression behaviour of a clay may be modelled. The question remains whether similar techniques can be applied to silty materials, such as tailings, which generally lie below the A-Line on the Casagrande chart. If successful, information on the state of density and bulk stiffness in a tailings profile, will be extremely useful, for example in calculating storage volumes, etc.

Figure 4-5 reproduces the compression data of the five tailings samples considered in this study, the properties of which are summarised in Table 4-11. In Figure 4-6 the compression data is geometrically extrapolated in a similar fashion to the extrapolation of the CSL by Schofield and Wroth. The equations for these extrapolated lines are, in fact, the normal consolidation lines for each sample, expressed in terms of the parameters λ and N

Table 4-11: Atterberg limits and critical state compression parameters for Mizpah and Pay Dam tailings.

Description	LL	e_{LL}	p'_{LL}	PL	e_{PL}	p'_{PL}	PI	CU	λ	N
Mizpah										
Whole tailings	29	0.790	71	22	0.600	1350	7	27.5	0.066	1.082
Pond Fine	43	1.183	14	32	0.880	400	11	10.7	0.1053	1.512
Pond Coarse	28	0.764	5	22	0.601	320	6	25	0.0447	0.856
Pay Dam										
Penstock Fine	56	1.534	27	39	1.069	400	17	4.9	0.1760	2.126
Coarse	29	0.792	35	22	0.601	600	7	21.5	0.0685	1.040

as given in Table 4-11. There is some convergence of the extrapolated NCL's to an unique focus point, at Ω_{NCL} = (20 000 ; 0.41). Also shown on Figure 4-6 is the location of the liquid and plastic limits of each tailings sample. The liquid limits are rather loosely scattered around a mean normal effective stress of 20 kPa, and the plastic limits around 430 kPa. Normalisation using the liquidity index relies on the uniqueness of these pressures.

Using the Ω_{NCL}-focus together with the 20 kPa and 430 kPa liquid limit and plastic limit stresses, the compression curves of the tailings should be normalised in the Liquidity Index, I_L (Schofield & Wroth, 1968). Alternatively the method proposed by Burland (1990), using the Void Index, I_V, can be used, which relies on the log-linear relationship of the compression curves. The application of these two techniques on the tailings samples are summarised in Table 4-12. The poor fit of the test data to the normalised lines at low stresses is due to sample preparation disturbance and bedding effects.

Table 4-12: Normalisation of compression data.

Normalisation		Equation of normalised line	Figure
Liquidity Index	$I_L = \frac{w - PL}{LL - PL}$	$I_L = 2 - \ln(p')/3$ $w = 100e/G_s$	Figure 4-7
Void Index (e_{100} & e_{1000})	$I_V = \frac{e - e_{100}}{e_{100} - e_{1000}}$	$I_V = 2 - \ln p'/2.303$	Figure 4-9
Void Index (N & λ)	$I_v = \frac{e - N}{\lambda}$	$I_v = -\ln p'$	Figure 4-11

The I_L- normalisation shows some scatter of the data around the normalised NCL with equation:

$$I_L = 2 - \ln(p')/3 \qquad \textbf{Eq. 4-14}$$

The significance of the constants in this equation can be explained as follows:

- The slope of the line, 1/3, indicates that the confinement stress at plastic limit is three natural log-cycles larger than at the liquid limit for gold tailings, i.e. or $p'_{PL} = 20p'_{LL}$. Schofield and Wroth (1968) found $p'_{PL} = 100p'_{LL}$ for natural clays.
- The intercept, 2, calibrates the normalised NCL so that the liquidity index is equal to zero at the liquid limit and 1 at the plastic limit.

The scatter is a result of the fact that the plastic limit and especially the liquid limit states are not closely gathered around the confinement stresses of p'_{LL} = 20 kPa and p'_{PL} = 430 kPa. Nevertheless, Figure 4-8 illustrates the use of Eqs. 4-4 and 4-14 for predicting the compression of the tailings studied. These equations fit both the Pay Dam and Mizpah fine tailings data quite well, but an error, in void ratio, of up to 0.08 results for the low plasticity coarse samples and the whole tailings mix.

Normalisation using the void index after Burland (1990), Figure 4-9 and Figure 4-11, results in a much better fit compared with the liquidity index, Figure 4-7. The normalisation can be done either by expressing I_V in terms of e_{100} and e_{1000} (as was done by Burland for one-dimensional compression), or by expressing I_V in terms of the critical state parameters N and λ, which is more appropriate for isotropic compression. The success of the I_V-normalisation confirms the log-linear nature of the compression behaviour of the tailings and does not include the effects of the Atterberg limits as does the I_L-normalisation.

The equations of the normalised lines in Figure 4-9 and Figure 4-11 are:

$$I_v = f(e_{100} \,\&\, e_{1000}): \qquad I_V = 2 - \ln p'/2.303 \qquad \textbf{Eq. 4-15}$$

$$I_v = f(N \,\&\, \lambda): \qquad I_V = -\ln p' \qquad \textbf{Eq. 4-16}$$

To predict the compression behaviour using Eqs. 4-15 and 4-16, correlations have to be found between the e_{100}, e_{1000}, N and λ, and the Atterberg limits for example. Figure 4-10 and Figure 4-12 use the following equations to this effect:

- In terms of e_{100} and e_{1000}

$$e_{100} = 0.647 \ln\left(\frac{LL - PL}{2.24}\right) \qquad \textbf{Eq. 4-17}$$

$$e_{1000} = 0.53 \ln\left(\frac{LL}{10}\right) \qquad \textbf{Eq. 4-18}$$

- In terms of N and λ

$$\lambda = \frac{PI - 1.44}{88.5} \qquad \textbf{Eq. 4-19}$$

$$N = \frac{PI + 2.3}{9} \qquad \textbf{Eq. 4-20}$$

Eqs. 4-17 and 4-18, Figure 4-10, predict the compression data of the tailings as a function of the Atterberg limits to an accuracy of 0.02 in void ratio, ignoring the effects of sample disturbance at low stress levels. It is concluded, therefore, that the density and stiffness of in-situ tailings can be accurately predicted as a function of the confinement stress and some fundamental parameters, such as the Atterberg limits. For these predictions, the normalisation technique proposed by Burland is recommended together with the equations above.

Influence of Composition on Tailings Compression

For the range of stresses considered in this study, 20 to 500 kPa, comparison between fine and coarse tailings samples indicates that in virgin compression:

Mizpah pond tailings: $e_{fine} \approx 1.5 \cdot e_{coarse}$ **Eq. 4-21**

Pay Dam penstock tailings: $e_{fine} \approx 2 \cdot e_{coarse}$ **Eq. 4-22**

These ratios are for reconstituted samples under controlled laboratory isotropic load conditions. Measurements on undisturbed samples from two locations at the Pay Dam penstock are shown in Table 4-13.

Stress levels in Table 4-13 are based on the measured unit weight of the material. Pre-consolidation pressures in the order of 100 to 150 kPa were estimated by comparing triaxial consolidation tests on reconstituted specimens with tests on undisturbed specimens (Figure 3-80, Chapter 3). The source of these pressures is most likely pore water suctions as a result of previous desiccation of the deposit. Unfortunately, suctions could not be measured directly at the time of this investigation to verify these values. In addition to suction effects, the processes of reclamation and sampling would have altered the in-situ stress state. Thus, void ratios quoted in Table 3-12 and Table 4-13 are based on direct measurements on undisturbed samples in the laboratory, but the stresses could well be as high as 150 kPa due to suctions or even lower than quoted values as a result of stress relief. However, data points representing the values in Table 4-13 plot close to the reconstituted compression curves from triaxial tests as shown in Figure 4-13.

Table 4-13: In-situ void ratios at Pay Dam penstock from undisturbed samples.

Pay Dam		Fine			Coarse		
1. Undisturbed samples for triaxial tests.							
Depth below surface	m	4.3			3.0		
Void ratio		1.39	1.46	1.41	0.77	0.81	0.76
Average void ratio		1.42			0.78		
Vertical effective stress σ'_v	kPa	75			55		
Overconsolidation ratio (measured)		2			2		
[6] $K_o = 0.44 + 0.2(PI/100)$		0.47			0.51		
$p' = \sigma'_v(1+2K_o)/3$	kPa	49			37		
$e_{fine} : e_{coarse}$		1.8					
2. Independent set of undisturbed samples.							
Depth below surface	m	4.3			2.0		
Degree of saturation	%	99			61		
Void ratio		1.488			0.873		
Vertical effective stress σ'_v	kPa	75			33		
$p' = \sigma'_v(1+2K_o)/3$	kPa	49			22		
$e_{fine} : e_{coarse}$		1.7					

An interesting feature of Figure 4-13 is that, irrespective of stress level, the void ratios of the fine samples are nearly twice that of the coarse samples. It is concluded that layers of coarse and fine material in a tailings profile, will vary significantly in density or void ratio following soil-forming processes and consolidation. Section 4.3.3, however, will show that they have exactly the same undrained shear strength.

In Section 4.2.3 is was illustrated that the tailings considered in this study are structurally dominated by a matrix of fines or slimes. In fact, the finest sample (90% slimes, PI = 17) contained up to 40% clay minerals and the coarsest sample (50% slimes, PI = 6) at least 10% clay minerals (Table 4-3). The fine sample can be expected to have low bulk density (1 Mg/m^3 in-situ) and high compressibility due to its high slimes content. If a small percentage of tailings sand (quartz grains > 63 μm) is added to this sample[7], the density will increase slightly. An added bulky grain occupies its volume in the sample with a density of 2.63 Mg/m^3, in the fines matrix with a density of approximately 1 Mg/m^3. At some stage, with the

[6] The recommendations of Massarsch (1979) were strictly for normally consolidated clays but are used here as a rough estimate.

[7] Adding coarse particles, is the opposite of what was discussed in Section 4.2.3, however, the basic principles still apply.

addition of more sand, a maximum density will be reached, where fines fill the voids between coarser particles. At this stage, however the sands may still be coated with a thin layer of fines, in which case the mechanical behaviour may yet be influenced by the fines. With the addition of more sand, the density will decrease again with a lack of fines to completely fill void spaces between the coarse particles. The mechanical behaviour of such a sample, however, still depends on whether there is clean contact between coarse particles or a coating of fines. At the extreme end of adding more sand, both the density and mechanical behaviour of the sample will be controlled by the sand fraction. Tailings collected from the pond areas are more dense and less compressible the coarser they are, and vice versa. In this material the fines control both the structure (density) and mechanical behaviour (compressibility and shear strength).

4.3.2 Properties of Gold Tailings as a Function of the Density State

This section briefly discusses some relevant properties of gold tailings as a function of the reconstituted normally consolidated density state. Combined figures of stiffness and consolidation data, measured during the triaxial compression tests, are summarised in Table 4-14.

Table 4-14: Results of isotropic compression tests (stress levels: 5 - 500 kPa).

Description	Parameter	Units	Figure
Stiffness			
Coefficient of Compressibility	m_{vi}	m^2/MN	Figure 4-14
Bulk Stiffness	K	MPa	Figure 4-15
Drainage Properties			
Coefficient of Consolidation	c_{vi}	m^2/year	Figure 4-16

Stiffness

The bulk stiffness of a specimen can be expressed either through the Coefficient of Compressibility, m_{vi}, or its inverse, the Bulk Modulus, K. These parameters are calculated for each increment of compression loading and are dependent on the magnitude of the stress increment over which they are calculated. In this study load increments were doubled each time.

The Coefficient of Compressibility can be calculated from the compression data using,

$$m_{vi} = \frac{1000\delta e}{(1+e_o)\delta p'} \qquad \textbf{Eq. 4-23}$$

where m_{vi} = coefficient of compressibility in m^2/MN or 1/MPa

e_o = void ratio at the start of an increment

δe = incremental change in void ratio

$\delta p'$ = incremental change in mean normal effective stress in kPa

The Bulk Modulus is then simply the inverse of the coefficient of compressibility, or

$$K = \frac{1}{m_{vi}} \qquad \textbf{Eq. 4-24}$$

To determine the nature of the change in stiffness with increased confinement pressure, care should be taken with the measured initial values at very low stress levels. The void ratio measurements at the start of a compression test were found to lie consistently below the theoretical normal consolidation line. This is especially apparent on the Void Index normalised plots, Figure 4-7 and Figure 4-9. The slightly overconsolidated state of the specimens was probably the result of slight disturbances during specimen preparation at such high void ratios and the granular nature of the silty tailings.

Figure 4-17 and Figure 4-18 re-plots the experimental stiffness data as symbols, and compare these to curves of stiffness, based on the NCL's of the respective samples. Note the deviation of the measured points at low stress. The shape of the normally consolidated stiffness curves suggests that stiffness increases proportionally to the isotropic confinement stress as,

$$m_{vi} = \frac{A}{p'} \quad \text{or} \quad K = \frac{p'}{A} \qquad \textbf{Eq. 4-25}$$

where A = a curve fitting constant.

Best fit values for A with respect to the NCL-data are:

- Mizpah whole tailings $A = 39$
- Mizpah pond fine tailings $A = 55$
- Mizpah pond coarse tailings $A = 28$
- Pay Dam penstock fine tailings $A = 79$
- Pay Dam penstock coarse tailings $A = 42$

Empirical correlations between A and fundamental parameters such as the Atterberg limits may be sought. However, the stiffness parameters can just as well be calculated from the slope of NCL, which in itself is a function of the Atterberg limits.

Loading conditions in a tailings impoundment are often assumed to be one-dimensional for material in the pond area, or when overburden pressures overcome desiccation effects with depth in the beach and daywall areas. The Constrained Modulus, appropriate for one-dimensional load conditions, can be expressed as a function of the Bulk Modulus and Poisson's ratio, see Eq. 4-29.

For one-dimensional loading,

$$m_v = \frac{1}{M} \qquad \textbf{Eq. 4-26}$$

where m_v = coefficient of compressibility for one-dimensional loading

M = constrained modulus not to be confused with, M, the CSSM parameter

From the theory of elasticity,

$$\frac{m_{vi}}{m_v} = \frac{E'(1-\nu')}{(1+\nu')(1-2\nu')} \cdot \frac{3(1-2\nu')}{E'} \qquad \textbf{Eq. 4-27}$$

where E' = Young's Modulus for of effective stresses

ν' = Poisson's ratio for effective stresses

Thus,

$$\frac{M}{K} = \frac{3(1-\nu')}{1+\nu'} \qquad \textbf{Eq. 4-28}$$

or assuming $\nu' = 0.33$,

$$M = \frac{3K}{2} \qquad \textbf{Eq. 4-29}$$

Drainage Properties

An attempt was made at determining the drainage characteristics of the tailings during triaxial consolidation stages. Rust (1996) illustrated that piezocone pore pressure dissipation data in tailings did not fit well with consolidation theory derived for clay materials. It will be shown here that even under well controlled conditions in the triaxial apparatus, tailings consolidation deviates significantly from standard one-dimensional consolidation theory. However, by fitting theoretical curve data to tailings consolidation data at 50% pore pressure dissipation a fair estimate of the consolidation characteristics can be made.

Consolidation is the process by which pore water is dissipated through the porous skeleton of a soil following a change in the state of effective stress. Theories of consolidation fall into two main categories. The first, associated with the names of Terzaghi (1923) and Rendulic (1936) are known as unlinked approaches, where it is assumed that the total stress remains constant everywhere so that consolidation strains are caused only by the change of pore water volume. The second is the coupled Biot theory, in which the continuing interaction between soil skeleton and pore water is included in the formulation. This leads, in general, to more complex equations for solution (Biot, 1941).

Biot's equation governing general three-dimensional pore pressure variation can be written as (Gibson & Lumb, 1953),

$$c \cdot \nabla^2 u_e = \frac{\partial u_e}{\partial t} - \frac{1}{3}\frac{\partial \sigma_{kk}}{\partial t} \qquad \textbf{Eq. 4-30}$$

where c = a constant

u_e = excess pore pressure

t = time

σ_{kk} = sum of the total normal stresses

$\nabla^2 = \frac{\partial^2}{\partial x^2} + \frac{\partial^2}{\partial y^2} + \frac{\partial^2}{\partial z^2}$ is the LaPlacian operator

The corresponding Terzaghi-Rendulic equation is,

$$c \cdot \nabla^2 u_e = \frac{\partial u_e}{\partial t} \qquad \textbf{Eq. 4-31}$$

Biot's theory reduces to the Terzaghi equation when:

- The mean normal total stress is time independent.
- The displacement field is irrotational (Sills, 1975), for example during a constant load isotropic triaxial one-dimensional consolidation cycle.

The theory of small strain one-dimensional consolidation as proposed by Terzaghi in 1923 relies on a number of key assumptions:

- The soil is considered to be homogeneous, isotropic and fully saturated.
- The principal of effective stress is valid.
- Darcy's law is valid.
- Soil grains and pore water are incompressible.
- Displacements of the soil and flow of pore water are one-dimensional.
- The coefficients of compressibility, m_v, and consolidation, c_v, remain constant.

- The self weight of the material is ignored.
- Only infinitely small strains are considered.

Under these assumptions Eq. 4-31 can be written as,

$$c_v \frac{\partial^2 u_e}{\partial z^2} = \frac{\partial u_e}{\partial t} \qquad \textbf{Eq. 4-32}$$

where c_v = coefficient of vertical consolidation

z = depth in the dissipating layer

Eq. 4-32 may be solved analytically for appropriate boundary conditions by the method of separation of variables as described in detail by Taylor (1948). The solution emerges as a Fourier series giving the local degree of consolidation at a depth of z and time t, $U_t(z)$ by:

$$U_t(z) = 1 - \sum_{m=0}^{\infty}\left[\frac{2}{M}\sin(M \cdot Z)EXP\left(-M^2 \cdot T_v\right)\right] \qquad \textbf{Eq. 4-33}$$

where $M = \frac{1}{2}\pi(2m+1)$

$Z = z/H$

$T_v = c_v \cdot t/H^2$

H = length of the shortest drainage path.

Eq. 4-33 was subsequently used as a theoretical model of one-dimensional[8] triaxial consolidation. There are two recognised methods, based on Eq. 4-33, for calculating the coefficient of consolidation from consolidation stages in the triaxial: the square-root-of-time method and the logarithm-of-time method.

Taylor's square-root-of-time method (1948), requires an estimate for the time to the end of consolidation (at least 95% dissipation of excess pore pressure), or t_{100} from the volume change vs. square-root-of-time curve, Figure 4-19a. The value of c_{vi} can then be calculated from

$$c_{vi} = \frac{\pi D^2}{\lambda \cdot t_{100}} \qquad \textbf{Eq. 4-34}$$

where c_{vi} = coefficient of triaxial isotropic consolidation

D = specimen diameter

λ = constant depending on drainage boundary conditions

[8] During consolidation in the triaxial pore pressures were measured at the base with drainage taking place vertically upwards (no side drains) through the top cap to the volume change burette and a back pressure system.

For vertical drainage from the top of the specimen only, and for a specimen height to diameter ratio of L/D = 2, λ = 1 (Head, 1984 Vol.3).

The second method uses the theoretical time factors, T_{50} = 0.379 and T_{90} = 1.031, for pore pressure dissipation measured at the base of a specimen, draining through the top only, as illustrated by curve B on Figure 4-19b. The value of c_{vi} may be calculated from either of the following equations,

$$c_{vi} = \frac{T_{50} \cdot H^2}{t_{50}} \qquad \textbf{Eq. 4-35}$$

or

$$c_{vi} = \frac{T_{90} \cdot H^2}{t_{90}} \qquad \textbf{Eq. 4-36}$$

where t_{50} = time for 50% dissipation of excess pore pressures measured at the base
t_{90} = time for 90% dissipation of excess pore pressures measured at the base

Figure 4-20 compares pore pressure dissipation rates measured at the base of triaxial specimens, under approximately 300 kPa isotropic confinement pressure, to theoretical consolidation curves. The theoretical curves were derived using the following procedures:

- **Best Fit**: Equation 4-33 was solved for c_{vi} by numerical iteration, until the least squares error between the measured data and the theoretical curve was a minimum.
- t_{50}: The time for 50% dissipation of the base excess pore pressures was used together with T_{50} = 0.379 (appropriate for the triaxial boundary conditions) to calculate c_{vi}.
- t_{100}: The time for 100% consolidation was estimated using volume change vs. square-root-of-time data, and c_{vi} calculated with Eq. 4-34.

The shape of the tailings dissipation curves on Figure 4-20 deviates significantly from the shape of the theoretical curves. The tailings consolidate more quickly early on as remarked by Rust (1996), but is slower to consolidate near the end, compared with theoretical predictions. Consequently, the method using t_{100} to balance the measured data with the theoretical curves, gives inaccurate estimates of the coefficient of consolidation. This is clearly shown by the values of $c_{vi(t100)}$ at the bottom of Figure 4-20. However, the t_{50} method, which balances the two curves near the middle, results in as good an estimate of c_{vi} as can be expected, see values of $c_{vi(t50)}$ at the bottom of Figure 4-20. Reasons for the tailings consolidation curves to deviate from the shape of the theoretical curves include:

- The fast draining nature of silty tailings compared with the slow draining clays for which the original assumptions were made. For example Darcy's law is only valid under laminar flow conditions, etc.

- Close inspection of the consolidation curves presented in Chapter 3 shows a significant proportion of creep during the consolidation process. Volume changes were taking place up to 24 hours, whereas the excess pore pressures dissipated within about an hour. Creep within the soil skeleton invalidates the incompressible medium assumption.
- The permeability of especially the coarse samples are relatively high compared with the permeability of the triaxial drainage system including the porous stone, filter paper and top-cap drainage lead. Inertia of the measurement equipment may have had an influence on the rate of pore pressure dissipation and volume change.

The best fit procedure was subsequently used in Figure 4-21 to calculate values of the coefficient of consolidation for the tailings shown in Figure 4-16.

Rowe (1959) proposed a method of adjusting the coefficient of consolidation under isotropic load, c_{vi}, to give equivalent values for one-dimensional loading, c_v, for clays using a multiplying factor

$$f_{cv} = \frac{1}{1 - B(1 - A)(1 - K_o)} \qquad \textbf{Eq. 4-37}$$

where A & B = the Skempton (1954) pore pressure parameters
K_o = coefficient of earth pressure at rest

For normally consolidated clays, the pore pressure parameter A is likely to lie between 0.5 and 1 (Head, 1984 Vol. 3); according to Bishop and Henkel (1962) $A = 0.47$ for a sandy clay and $A = 0.08$ for a loose sand. K_o is approximately 0.5 for the range of plasticities measured in tailings, according to the work of Massarsch (1979). If B is close to unity and taking A as 0.3, $f_{cv} \approx 1.5$. Using this relationship together with the stiffness values from Eq. 4-29, the vertical permeability can be calculated using,

$$k_v = c_v \cdot m_v \cdot \gamma_w \qquad \textbf{Eq. 4-38}$$

Permeabilities for the tailings calculated using Eq. 4-38, are represented as the solid lines in Figure 4-22. This figure shows a rapid initial reduction of 2 to 3 times the permeability up to a confinement stress of 100 kPa approximately, but thereafter, becomes fairly constant at the following approximate values:

- Mizpah Whole Tailings 10 m/year
- Mizpah Pond Fine 5 m/year
- Mizpah Pond Coarse 15 m/year
- Pay Dam Penstock Fine 1.5 m/year

- Pay Dam Penstock Coarse 2.5 m/year

Tailings literature seem to agree that permeability can best be predicted using Hazen's formula or

$$k = c \cdot D_{10}^2 \qquad \textbf{Eq. 4-39}$$

Using the permeabilities in Figure 4-22 together with the effective particle diameters of the respective samples, D_{10}, Hazen's constant becomes 1.45. Mittal and Morgenstern (1975) proposed a value of 1 for tailings sands. Hazen's formula would under predict permeabilities at low stress levels by a factor of up to 3 or 4 compared with the values in Figure 4-22.

4.3.3 Shear Strength of Gold Tailings

It has been shown, for samples recovered from the pond areas of impoundments, that there are significant differences in:

- *Composition*: Between typical fine and coarse deposited layers there are significant differences in grading, especially in the median particle size or D_{50}, but not as much in the upper and lower limits of D_{10} and D_{90}. Different grades consist of varying percentages of bulky tailings sands and plate-like fines or slimes. The fundamental properties of these sands and slimes differ significantly with respect to mineralogy, particle shape and surface texture.
- *Compressibility State*: The density, compressibility and consolidation properties of tailings are highly dependent on grade, but seems to be controlled by the slimes fraction

It does, however, appear that the specific gravity remains constant for different grades recovered from the same location. A study of the literature on gold tailings shear behaviour in Chapter 2 also indicated that the shear strength properties of gold tailings are independent of grade, with zero effective cohesion and an effective angle of internal friction, ϕ', of 34° on average. The discussion that follows will show that not only the strength parameters, but also the absolute undrained shear strength, are independent of tailings grade.

Table 4-15 summarises the relevant shear and critical state parameters of the five gold tailings samples studied. The parameters were derived using best fit procedures on the undrained triaxial shear data of Chapter 3. The final selection of the failure state was based on a combination of the following aspects:

- Shape of the triaxial tests paths including deviator stress (q'), mean normal effective stress (p') and excess pore pressure (u_e) response with shear strain (ε_q).

Table 4-15: Stress paths and properties derived from undrained triaxial shear.

Dam	Description	[9]λ	N	Γ	M	ϕ'	Figure
Mizpah	**Reconstituted - (Whole tailings, delivery pulp)**						
	Whole Tailings	0.066	1.082	1.025	1.400	34.5	Figure 4-23 Figure 4-24
	Reconstituted - (Pond fine and coarse layers)						
	Pond Fines	0.105	1.512	1.442	1.400	34.5	Figure 4-25
	Pond Coarse	0.045	0.856	0.826	1.350	34.5	Figure 4-26
Pay Dam	**Reconstituted - (Pond fine and coarse layers)**						
	Penstock Fines	0.176	2.126	1.990	1.270	31.5	Figure 4-27
	Penstock Coarse	0.068	1.040	0.980	1.270	31.5	Figure 4-28
	Undisturbed - (Pond fine and coarse layers)						
	Penstock Fines	0.162	2.053	1.935	1.370	34.0	Figure 4-29
	Penstock Coarse	0.080	1.134	1.070	1.460	36.0	Figure 4-30

- Maximum stress ratio, $\eta = q'/p'$.
- Goodness of fit of the failure envelope to the Mohr's circles of failure using the following relationship between M and ϕ':

$$M = \frac{6\sin\phi'}{3 - \sin\phi'} \qquad \textbf{Eq. 4-40}$$

Eq. 4-40 holds for triaxial compression on purely frictional materials (Atkinson & Bransby, 1978).

Some observations on the behaviour of the tailings during undrained triaxial shear are listed below:

(a) Referring to Figures 4-23, 4-25 and 4-27 the stress paths for reconstituted specimens were all characteristic of normally consolidated strain hardening behaviour to failure. The mean normal effective stress decreased with increasing deviator stress resulting in the characteristic ellipse-shaped stress paths often used in CSSM.

(b) Only the undisturbed specimens at low confinement stress (p' = 50 kPa) showed lightly overconsolidated behaviour, confirming the assumption of a pre-consolidation stress of approximately 150 kPa for the in-situ material. This is clearly shown on Figure 4-29,

[9] The critical state parameters are given in terms of void ratio in the compression plane.

where both the fine and coarse specimens, but especially the coarse specimen, show near vertical stress paths to the CSL in the stress plane.

(c) No structural collapse or strain softening was evident in either reconstituted specimens prepared from a slurry, or in the undisturbed specimens. In other words, in Figures 4-23, 4-25, 4-27 and 4-29, there are no cases where the deviator stress increased up to a certain level, and then decreased with continued shear.

(d) Except for the Pay Dam fine tailings (fine specimens in Figures 4-27 and 4-29), which are the finest material of all, stress paths displayed phase transfer dilation at failure (Ishihara et al., 1975) and strain hardened with continued post failure shear. Post failure dilatency was especially prominent in the coarser grades shown in Figures 4-23 and 4-25. Pay Dam fine tailings reached an ultimate state or critical state at failure with no change in effective stress or pore pressure with continued shear.

(e) In each case where two specimens of different grades, but originating from the same sampling location, were tested, the stress paths were almost exactly the same in the stress plane. This observation holds for both reconstituted (Figures 4-25, 4-27) and undisturbed (Figure 4-29) samples. As a result, layers of fine and coarse composition from the same location had the same undrained shear strength, which is adequately described by a single effective shear strength parameter of $M \approx 1.36$ or $\phi' \approx 34°$. Collectively the variation in ϕ' was between $34 \pm 2°$ - a remarkable fact, considering the variations in grading, density, stiffness etc.

The observation of approximately constant undrained shear strength for fine and coarse samples can be explained with respect to differences in void ratio and drainage properties. The method of preparing specimens from a slurry at constant virgin confinement stress, results in widely different densities or void ratios for the fine and coarse samples respectively. For example at a confinement stress of 5 kPa the finer tailings exist at a void ratio of 1.7 compared with 0.8 for coarse tailings - a factor of two difference. These diverse density states exist throughout the consolidation stages and during undrained shear. Similar states were also measured on the undisturbed samples, with void ratios in the fine tailings approximately 1.5 compared with 0.8 in the coarse tailings, a ratio of nearly 1.9 (Table 4-13). If new specimens were to be prepared, where fine and coarse tailings have the same density at the same confinement pressure, it would only be possible by pre-consolidating the fine tailings. In this case the fine specimen would be much stronger than the coarse specimen. This principal is also well illustrated by the State Boundary Surfaces (SBS's) for the Pay Dam penstock fine and coarse tailings. Figure 4-31 shows the SBS's assuming Cam-Clay as a behavioural model and using the parameters derived in Table

4-15. The use of Cam-Clay theory is only for illustrative purposes, other behavioural models could just as well have been used. On the stress plane (q' vs. p' - Figure 4-32), there is hardly any difference between the two SBS's and CSL's, hence the similar shear strengths at any given confinement stress. However, in the compression plane (e vs. p' - Figure 4-32) there are major differences between the fine and coarse sample densities. In preparing the graphs, void ratios were chosen to correspond with the values measured during the triaxial consolidation tests, which are representative of void ratios and densities under confinement pressures of 50 up to 400 kPa. It is theoretically possible to overlap the two SBS's on the compression plane, either at extremely high confinement pressures in the fine tailings, or extremely low densities in the coarse tailings. However neither of these would be practically feasible.

Although the undrained shear strength of tailings appear to be independent of grade following similar soil-forming histories, field loading conditions are not necessarily fully drained (no build-up of excess pore pressure) or fully undrained (no change in pore water volume). Under field loading the higher permeability coarse layers could mobilise greater partially drained shear strengths compared with the lower permeability finer grades. In the extreme, the coarse material will mobilise the full drained shear strength, whereas the fine material will mobilise the much lower undrained shear strength, depending on the rate of shear. In fact, Eq. 4-45 indicates that the drained shear strength would be almost three times as high as the undrained shear strength, provided the same initial isotropic confinement stress.

The stress paths in Figures 4-25, 4-27 and 4-29 show that,

$$q'_{f(undrained)} \approx 0.65 p'_o \qquad \textbf{Eq. 4-41}$$

From the equation of the CSL,

$$q'_f = \mathrm{M} \cdot p'_f \qquad \textbf{Eq. 4-42}$$

and restrictions of drained triaxial compression,

$$q'_f = 3\left(p'_f - p'_o\right) \qquad \textbf{Eq. 4-43}$$

it can be shown that,

$$q'_{f(drained)} \approx 1.85 p'_o \qquad \textbf{Eq. 4-44}$$

Eq. 4-41 and Eq. 4-44 can be combined to show that,

$$q'_{f(drained)} \approx 2.85 q'_{f(undrained)} \qquad \textbf{Eq. 4-45}$$

Another source of differing shear strengths between fine and coarse tailings results from their respective post critical state stress paths. Under controlled undrained shear, fine tailings reach an ultimate critical state at constant strength with continued shear strain. On the other hand, coarse tailings are likely to undergo phase transfer dilation after reaching the critical state and mobilise greater shear strengths with continued dilation, even under fully undrained loading.

It is concluded that following similar sub-aqueous sedimentation-consolidation histories, tailings of different grades will exist in an impoundment at varying density states, but so that their specific gravity and undrained shear strengths are virtually the same. However, the quick draining properties of the coarser material coupled with post failure stress-dilatency can result in higher strengths being mobilised in these materials. No tests were performed on undisturbed samples from the daywall or beach areas to confirm these observations for sub-aerial deposition. However, isotropic suction from desiccation should not alter the state of the material apart from increasing the density and stress level in both the fine and coarse layers.

It has to be emphasised here that the samples were all collected from the pond areas of impoundments, representing a selection of fine and coarse layers from these sites. Evidence from electron micrographs and behaviour of these samples under laboratory test conditions suggest that state was controlled by the fine slimes rather than the coarse sands. With higher fines content, densities were lower and the material was more compressible, and vice versa.

4.3.4 Structure

It has not been a principal objective of this study to define the structure of deposited tailings. However, based on visual observations of undisturbed specimens under the electron microscope and the results of a number of laboratory tests, some general remarks are in order.

A packing of uniform spheres can range in void ratio between e_{max} = 0.9 and e_{min} = 0.35, which are typical of the limiting void ratios in cohesionless, single grained, rounded sands (Sowers, 1979). Soils with angular bulky grains usually have a somewhat smaller range with e_{max} = 0.85 to e_{min} = 0.45. Flattened or elongated particles do not form simple cohesionless

structures, slabs may bridge voids resulting in an open high void ratio packing, or be wedged tightly and parallel in a stable mass with low void ratio. In such materials the maximum and minimum void ratios probably have little significance. Flaky particles, such as clay minerals, may similarly form either an open haphazard packing or an oriented dense fabric, depending on the nature of the forces between the particles and the soil-forming environment.

With an heterogeneous arrangement of bulky grains and flaky fines such as tailings, the packing arrangement or fabric would be highly dependent on the amount and orientation of the fines. If there is a deficiency of fines the structure may be dominated by a skeleton of bulky particles and the fines will only serve to fill voids between these grains. On the other hand even with a deficiency of fines the mechanical behaviour can still be determined by layers of fines between the coarse particles. Nevertheless, with addition of fines the void ratio will decrease as more and more fines are filling the voids within the skeleton, resulting in a lowering of the normal consolidation and critical state lines in the compression plane. This is clearly illustrated by Papageorgiou et al. (1999) who found the steady state line for a coarse sandy tailings to lie above samples of the same material with some addition of fines. Such a coarse structure, dominated by the bulky tailings sands, can only be expected to exist on the upper beaches of an impoundment or when using cyclone underflow for embankment construction. At some stage, as the fines content increases, the bulky grains will be pushed apart and start to float in a "sea of fines". As soon as this happens the density reduces with increasing fines, resulting in higher void ratios and a raising of the normal consolidation and critical state lines in the compression plane. Tailings considered in this study show a deficiency of bulky particles, even for the coarser samples, so that the structure is determined and controlled by the randomly orientated fines rather than the bulky sands. This is entirely consistent with the measured high void ratios, the fact that the state lines of the fine samples are located above that of the coarse samples and with visual evidence from electron micrographs of undisturbed specimens.

According to Sowers (1979) a honeycomb structure can develop when cohesionless fine sand or silt particles settle in still water. Because of their small size they settle slowly and wedge between each other without having the opportunity to roll into more stable positions.

Schiffman et al. (1986) found that cohesionless sands and silts, deposited sub-aqueously at low to moderate relative densities, exhibit peak undrained shear strength behaviour consistent with a meta-stable structure. Similar observations have also been made by Lucia et al. (1981) and Troncoso (1986) on tailings and silty sand hydraulic fill, respectively. Such a meta-stable structure can also develop when damp, fine sand is dumped into a fill or pile without densification or when a specimen is prepared by wet-tamping techniques.

Papageorgiou et al. (1999) succeeded in inducing liquefaction behaviour in tailings only by using wet tamping techniques to prepare triaxial specimens. The honeycomb structure is usually able to support static loads by arching, with little distortion before de-structuring commences. Upon de-structuring under compression, shear or dynamic loading, the meta-stable structure may collapse with excessive deformation and possibly liquefaction.

It is possible for tailings to form with an open meta-stable structure when settling in the still pond of an impoundment. Undisturbed samples recovered from the Pay Dam penstock area did not indicate structurally permitted states under consolidation, or collapse during undrained shear. However, these samples were subject to the effects of drying prior to sampling, resulting in a lightly overconsolidated state, which could have destroyed any structure. Material on the beach and daywall areas cannot be expected to exist with an open structure as flow across the beach allows for horizontal movement and rolling of particles into a stable packing. In addition, the effects of desiccation on sub-aerial beaches result in an overconsolidated state.

It is a well known fact that gold tailings slurries are flocculated when leaving the reduction works. The degree of flocculation depends on the concentration and nature of the fines in the tailings. Inter-particle forces between the fine particles in a flock produce strong bonds trapping considerable free water in the structure with resulting high void ratios. Although a flocculated sediment is highly compressible under static loading the strong inter-particle bonds are able to resist displacement under vibration loading.

A number of potential bonding agents are present in the tailings particles and process water including silica, metal oxides and calcium carbonate. However, no evidence of cementation bonding by such elements could be found on the micrographs of undisturbed samples or detected during consolidation and shear of undisturbed triaxial specimens. The tailings behave rather like a loose but stable material that strain hardens to failure. On reaching the critical state the material may be subject to phase transfer dilation depending on the concentration of fines.

Precipitation on exposed surfaces often results in the formation of a white crystalline surface crust. This crust is so localised in nature that it constitutes only a thin surface skin, without influencing the strength of the material. However, it may affect the evaporation potential from the surface and possibly serve as a discontinuity in permeability.

4.4 CHARACTERISATION BY PIEZOCONE

Piezocone soundings were performed at both sampling locations, Pay Dam as well as at the Mizpah cross-section. The results of these soundings are correlated in this section with the findings of the laboratory test program to evaluate existing interpretation procedures and to extend these methods where applicable. The piezocone has enjoyed worldwide recognition as a valuable characterisation tool in tailings, especially for defining the tailings profile and establishing the internal seepage regime. The discussion will show that piezocone penetration data can also be used to estimate the state of strength and stiffness in a tailings impoundment.

Figure 4-33 and Figure 4-34 summarise the piezocone test results on Mizpah and Pay Dam. A phreatic surface or water table was only encountered on the Pay Dam at a depth of approximately 16.4 m below surface. The ambient pore pressure build-up below the water table was approximately 7 kPa per meter depth, indicating a slight vertical downwards seepage gradient. This is consistent with seepage losses from an adjacent, active, tailings impoundment, which has been a source of many problems for the mine.

4.4.1 Soils Identification

Throughout the development of the piezocone a number of soils identification systems have been proposed. Probably the best known of these include the Jones and Rust identification chart, Figure 4-35a (Jones & Rust, 1982; 1983), and the Robertson and Campanella charts, Figure 4-36 (Robertson, 1990). Both these systems provide similar results and are based on normalised data resulting from cone resistance, sleeve friction and pore pressure measurements under saturated conditions. They are designed for the pore pressure sensor located directly behind the cone tip. The Jones and Rust system has been modified slightly by the author by extending the material definitions in the soft to very soft clay ranges in accordance with the Robertson and Campanella system, Figure 4-35b. This modified Jones and Rust system will be used to compare the piezocone derived profiles with actual profiles.

The exposed profiles at the Pay Dam beach and penstock sites provided excellent opportunities to evaluate the performance of the piezocone soils identification system. However, these sites have been exposed to drying, and although layers of the finer tailings are saturated (S = 99% - Table 4-13), the coarse layers are not (S = 61% - Table 4-13).

Figure 4-37 and Figure 4-39 illustrate direct comparisons between the in-situ profiles and piezocone penetration data for both sites on Pay Dam, together with the profiles derived

using the modified Jones and Rust identification system, Figure 4-35b. For the purpose of tailings identification the soil descriptions have been changed from clay, silt, silty-sand and sand to fine silt, silt, coarse silt and fine sand, which are more practical descriptions for tailings. Figure 4-38 and Figure 4-40 show the penetration data represented on the identification chart itself.

Due to the stiffness of the system, the piezocone pore pressure sensor is able to react instantly to the different pore pressure responses in fine and coarse layers (Lunne et al., 1997). In the first meter or so on Figure 4-37 and Figure 4-39 the penetrometer moved through material that is dry to slightly moist and subsequently registered very little pore pressure response. Penetration through such dry material can lead to de-saturation of the pore pressure filter element. However, by using glycerine to saturate the piezocone filter element, the problem of de-saturation was eliminated. As the in-situ moisture content increased with depth, and thus the level of saturation[10], fine layers started to generate positive excess pore pressure and coarse layers, either no response or negative excess pore pressure.

Due to thin individual layers in the profiles, the measured cone resistances and pore pressures are not likely to be fully developed. Both measurements are influenced by a finite zone of material above and below the sensors, the size of which ranges between 2 or 3 to 10 and even 20 cone diameters, depending on material stiffness (Lunne et al., 1997). As the probe nears a coarse stiff layer from within a fine soft layer, for example, the tip resistance will "feel" the stiffness of the coarse layer before it enters and continues sensing the soft layer, once it has penetrated the coarse layer for some depth. Cone resistance is much more prone to these effects than pore pressure, because of the small localised filter element and quick reaction time of the pore pressure measuring system. Ideally a layer should be thick enough so that a measurement develops its full potential, indicated by a plateau or constant value near mid depth, which gradually changes as the next layer is approached. With the highly layered tailings profile, neither cone resistance or pore pressure measurements have the opportunity to fully develop. This is especially evident in the very sharp drop-off in excess pore pressure at depths of 2.3, 2.5, 2.9, 3.1, 3.3, 4.4 and 4.5 meters in Figure 4-37.

With such a highly layered profile as well as the fact that measurements were taken, in this case, mostly above the phreatic surface, it is surprising how well the soils identification chart predicts the field profiles in Figure 4-37 and Figure 4-39. The piezocone, therefore, should

[10] Note that for both these holes the water table is located below 16m, however at approximately 4 m below surface the fine layers are 99% saturated and the coarse layers 60% saturated.

be considered an effective tool for the in-situ stratification of tailings profiles, given that rapid continuous profiles can be extracted at small cost compared with methods of sampling.

4.4.2 Pore Pressure Dissipation

The piezocone today is recognised as probably the most reliable site investigation tool for determining the in-situ seepage regime in a tailings impoundment (Rust et al., 1984; East et al., 1988a; Van der Berg, 1995; Rust et al., 1995; Rust, 1996; Wagener et al., 1997). A full discussion of its use in this regard does not fall within the scope of this thesis. However, some comments will be made regarding estimates of the in-situ coefficient of consolidation based on pore pressure dissipation tests.

Torstensson (1975) concluded that, based on the theories of cavity expansion, the coefficient of consolidation should be interpreted at 50% dissipation using the following equation,

$$c = \frac{T_{50} \cdot r_o^2}{t_{50}} \qquad \textbf{Eq. 4-46}$$

where c = coefficient of consolidation
T_{50} = normalised time factor for 50% dissipation of excess pore pressures
r_o = cone diameter
t_{50} = time for 50% dissipation of excess pore pressures.

The value of the time factor T_{50}, is derived from theoretical solutions to the consolidation problem, similar to Eq. 4-33, and is dependent on the rigidity index of the material or

$$T_v = f\left(I_r = \frac{G}{s_u}\right) \qquad \textbf{Eq. 4-47}$$

where I_r = rigidity index
G = shear stiffness
s_u = undrained shear strength.

Rust (1996) suggested using a value of T_{50} = 3.74 based on the work of Randolph and Wroth (1979) for cavity expansion solutions to consolidation around driven piles. This value is appropriate for the filter element located directly behind the cone tip and for a rigidity index of I_r = 100, which he believed to be typical for tailings in general.

Piezocone dissipation tests, and hence estimates of the coefficient of consolidation in a tailings impoundment, are practically possible only in layers of the finest tailings. Dissipation

of excess pore pressure is so quick in the coarser layers that dissipation tests can not be recorded.

Since pore pressure dissipation is assumed to be horizontal or normal to the axis of the penetrometer in a layer of infinite extent, solution to Eq. 4-46 gives an estimate of the horizontal coefficient of consolidation or c_h. However, in a highly layered tailings profile, with thin successive layers of differing drainage properties, drainage paths may deviate significantly from horizontal. For example, if the penetrometer is stopped for a dissipation test within a layer of fine tailings, but near the interface with a coarse layer, then dissipation can be predominantly vertical in the direction of the coarse layer. Similarly, where discontinuities in the layering exists such as pre-existing surface cracks, drainage patterns may also be altered. These conditions could lead to misinterpretation of in-situ c_v values from piezocone dissipation tests.

Figure 4-41 shows estimates of the coefficient of consolidation based on piezocone dissipation data from Mizpah and Pay Dam. Also shown are the results of the triaxial consolidation tests with respect to the vertical coefficient of consolidation or c_v on reconstituted fine and coarse tailings from the same dams. The piezocone data lies well within the boundaries defined by the triaxial data on fine and coarse tailings from both dams. However, in-situ values, which are representative of the finer tailings only, are consistently higher than laboratory estimates on the same material. The reason for this lies probably in the fact that drainage boundary conditions around the penetrometer are much more complicated than suggested by the assumptions of cavity expansion theory. It is quite possible that there is a significant percentage of vertical drainage given the thin layer thickness and proximity to coarser free draining layers.

4.4.3 Shear Strength and Stiffness

Soil strength interpretation of cone resistance is usually expressed in the form of Eq. 4-48.

$$q_c = N_c \cdot s_u + \sigma_o \qquad \textbf{Eq. 4-48}$$

where q_c = measured cone resistance
N_c = a theoretical cone factor similar to bearing capacity factors
s_u = undrained shear strength based on triaxial data
σ_o = in-situ total confinement pressure, either σ_{vo}, σ_{ho} or σ_{mean} (p'_o)

Theoretical Solutions: Cavity Expansion Theory

According to Lunne et al. (1997) theoretical solutions for N_c can be grouped under the following classes:

- Classical bearing capacity theory: Terzaghi (1943).
- Cavity expansion theory: Spherical - Meyerhof (1951) or Cylindrical - Baligh (1975).
- Cavity expansion theory combined with conservation of energy: Vesic (1975).
- Analytical and numerical modelling using linear and non-linear stress-strain theories: Ladanyi (1967).
- Strain path theory: Baligh (1985).

In fine grained soils, penetration is generally assumed undrained or constant volume. Theoretical solutions for undrained penetration based on cavity expansion theory take the generalised form of,

$$N_c = \frac{4}{3}\left[1 + \ln\left(\frac{\text{Stiffness}}{\text{Strength}}\right)\right] + \text{Constant} \qquad \textbf{Eq. 4-49}$$

In this equation the stiffness to strength ratio or Rigidity Index, I_r, can be expressed as

$$I_r = \frac{G_u}{s_u} \qquad \textbf{Eq. 4-50}$$

where G_u = undrained shear stiffness

Values for the constant in Eq.4-49 vary for cylindrical and spherical cavity expansion theory, as well as on the choice of the stress-strain constitutive relationship. Typically the constant ranges between 1 and 10.

Teh (1987) improved the basic model using an elastic perfectly plastic strain path approach, and showed that undrained penetration is influenced by material shear strength (s_u), in-situ stress state (σ'_{vo} & K_o), relative stiffness ($I_r = G_u/s_u$) and cone roughness (α), so that,

$$N_c = 0.19 + 2.64\ln(I_r) - \frac{\sigma'_{vo}}{s_u}(1 - K_o) + 2\alpha \qquad \textbf{Eq. 4-51}$$

where α = roughness coefficient , rough (1), smooth (0), but 0.5 is commonly used.

In view of the fact that an undrained response is only likely under saturated conditions, the cavity expansion method was subsequently assessed using CPTU data from the Pay Dam penstock and Mizpah beach-pond interface locations. The purpose of this exercise was to determine how sensitive cone resistance is to differences in stiffness (rigidity Index) between fine and coarse layers in an impoundment. In other words, could the upper and lower bound cone values in a typical tailings profile (Figure 4-33 & Figure 4-34) be credited

to differences in stiffness between fine and coarse layers. A key feature of this exercise was the assumption of a constant effective angle of friction, $\phi' = 34°$, as was established with the undrained triaxial shear tests on reconstituted and undisturbed fine as well as coarse tailings samples from both locations.

The procedure was developed around the following arguments and assumptions:

(a) The first step was to select a range of mean normal effective confinement pressures, p'_o, representative of in-situ conditions in a typical tailings impoundment, in this case 0 to 400 kPa.

(b) Corresponding in-situ void ratios were then calculated using the normalisation technique proposed by Burland (1990) as set out in Section 4.3.1 of this chapter. To this extent

$$e = I_v \cdot (e_{100} - e_{1000}) + e_{100} \qquad \textbf{Eq. 4-52}$$

where I_v = void index so that

$$I_v = 2 - \frac{\ln(p'_o)}{2.303} \qquad \textbf{Eq. 4-53}$$

e_{100} & e_{1000} = void ratios at 100 and 1000 kPa confinement pressures

$$e_{100} = 0.647 \ln\left(\frac{PI}{2.24}\right) \qquad \textbf{Eq. 4-54}$$

$$e_{1000} = 0.53 \ln\left(\frac{LL}{10}\right) \qquad \textbf{Eq. 4-55}$$

(c) Assuming saturated conditions, the unit weight of the tailings was calculated using

$$\gamma_{sat} = \frac{G_s + e}{1 + e}\gamma_w \qquad \textbf{Eq. 4-56}$$

(d) It was then assumed that sedimentation in a large pool under self-weight loading results in a normally consolidated one-dimensional stress state so that the effective overburden pressure is given by

$$\sigma'_{vo} = \frac{3p'_o}{1 + 2K_o} \qquad \textbf{Eq. 4-57}$$

where K_o = coefficient of earth pressure at rest

K_o can be estimated using either the relationship proposed by Jaky (1944) or Massarsch (1979)

Jaky: $K_o = 1 - \sin(\phi')$ **Eq. 4-58**

Massarsch: $K_o = 0.44 + 0.2\frac{PI}{100}$ **Eq. 4-59**

Both these formulations resulted in approximately the same value of K_o = 0.45.

(e) To calculate the total overburden pressure the ambient pore pressure distribution, u_o, was taken from CPTU dissipation data and used in the equation,

$$\sigma_{vo} = \sigma'_{vo} + u_o$$ **Eq. 4-60**

In the case of Pay Dam a phreatic surface was encountered at a depth of 16.4m, but no free water table existed in the Mizpah profiles.

(f) It then became possible to calculate the depth, h, corresponding to each initial p'_o increment through,

$$h = \frac{\sigma_{vo}}{\gamma_{sat}}$$ **Eq. 4-61**

(g) The undrained shear strength at each depth increment was calculated assuming constant effective shear strength, ϕ' = 34°, together with the observation made in Section 4.3.3 that

$$q'_{f(undrained)} \approx 0.65 p'_o$$ **Eq. 4-62**

or

$$s_u = \tfrac{1}{2} q'_f = 0.325 p'_o$$ **Eq. 4-63**

(h) In Section 4.3.1 it was shown that the bulk stiffness of the tailings can be expressed as a function of the confinement stress with

$$K' = \frac{p'_o}{A}$$ **Eq. 4-64**

The values for A depend on the grading properties of the material and range between 40 and 80.

(i) The undrained shear stiffness was estimated from the theory of elasticity as

$$G_u = G' = \frac{3K'}{2}\frac{(1-2\nu')}{(1+\nu')}$$ **Eq. 4-65**

where ν = Poisson's ratio, assumed to be 0.33 for the tailings.

(j) Finally it was possible to calculate an equivalent value for the Rigidity Index

$$I_r = \frac{G_u}{s_u} \qquad \textbf{Eq. 4-66}$$

The above procedure was repeated first using material properties for the fine tailings, and then for the coarse tailings, but with constant strength parameters ($c' = 0$; $\phi' = 34°$) in both cases. Fitting predicted cone resistance values to the original CPTU data for both the Mizpah and Pay Dam sites resulted in,

$$N_c = \frac{4}{3}\left[1 + \ln(I_r)\right] + 10 \qquad \textbf{Eq. 4-67}$$

A direct comparison of Eq. 4-67 with the CPTU data is shown in Figure 4-42.

The cavity expansion method was used to study the stiffness dependency (strength assumed constant) of cone resistance in tailings. This was done in an attempt to account for the large differences in measured cone resistance, that typically follow upper and lower bound trends with depth in tailings. The stiffness ratios calculated for the tailings were very low compared with the suggested value of I_r = 100 by Rust (1996). For the fine tailings I_r ranged between 15 and 20 and in the coarse tailings it doubled to 30 to 40. Cavity expansion theory showed that cone resistance is little affected by the difference in stiffness between fine and coarse tailings. Even increasing I_r an order of magnitude, as was done on Figure 4-42, still did not make a significant difference. Cavity expansion theory predicted the lower bound penetration resistances in tailings well, but failed to account for the upper bound measurements as shown in Figure 4-42.

Effective Stress Interpretation

An effective stress method has been developed by Senneset et al. (1982; 1988), Senneset and Janbu (1985) and Sandven et al. (1988). In this method an empirical bearing capacity formula in terms of effective stress can be expressed as,

$$q_c - \sigma_{vo} = N_m\left(\sigma'_{vo} + a\right) \qquad \textbf{Eq. 4-68}$$

where σ_{vo} = total vertical overburden pressure

σ'_{vo} = effective vertical overburden pressure

a = attraction coefficient

N_m = a bearing capacity factor for cone penetration so that,

$$N_m = \frac{N_q - 1}{1 + N_u \cdot B_q} \qquad \textbf{Eq. 4-69}$$

N_q = bearing capacity factor so that,

$$N_q = \tan^2\left(45 + \frac{\phi'}{2}\right)\exp[(\pi - 2\beta)\tan\phi'] \qquad \textbf{Eq. 4-70}$$

β = angle of plastification

N_u = bearing capacity factor, or,

$$N_u \approx 6\tan\phi'(1 - \tan\phi') \qquad \textbf{Eq. 4-71}$$

B_q = normalised excess pore pressure generated or,

$$B_q = \frac{u_e}{q_c - \sigma_{vo}} \qquad \textbf{Eq. 4-72}$$

u_e = excess pore pressure measured immediately behind the cone with,

$$u_e = u_t - u_o \qquad \textbf{Eq. 4-73}$$

u_t = measured pore pressure

u_o = ambient pore pressure from dissipation data

The attraction coefficient is aimed at modelling the effects of overconsolidation, desiccation, cementation or any such attractive forces between particles. An estimate of the soil attraction value can be made based on the shape of the q_t vs. σ'_{vo} plot, from triaxial tests or from general experience. Typical values according to Senneset et al. (1989) are:

- 0-10 for soft clays and silts as well as loose sands,
- 10-20 for medium stiff clay/silt and medium dense sand,
- 20-50 for stiff clays/silt and dense sand,
- >50 for hard, stiff and overconsolidated or cemented soils.

The angle of plastification, β, expresses an idealised geometry for the generated failure zones around the advancing cone, and according to Senneset et al. (1990), is difficult to assess, both experimentally and theoretically. However, Senneset and his co-workers argue that β depends on soil properties such as compressibility and stress history, plasticity and sensitivity. Sandven et al. (1988) presented values of β found from experimental correlations between laboratory determined tan(ϕ) and CPTU values, as shown in Table 4-16.

The effective stress method is associated with large degrees of uncertainties and should be viewed as highly empirical and approximate. Nevertheless, ignoring the effects of surface

Table 4-16: Tentative values of the angle of plastification in various soil types after Sandven et al. (1988).

Soil Type	Tentative β-value
Dense sands, overconsolidated silts, high plasticity clays, stiff overconsolidated clays.	-20° to -10°
Medium sands and silts, sensitive clays, soft clays.	-5° to +5°
Loose silts, clayey silts	+10° to +20°

desiccation, $a = 0$, and using an angle of plastification of 20° in the fine tailings and 10° in the coarse tailings, the method was compared with field data in Figure 4-43. The normalised pore pressure parameter, B_q, was found to be in the order of 0.4 for the fine tailings and zero in the coarse tailings, and should account to some degree for drainage conditions.

Maximum measured cone resistances in the coarser layers were well predicted by this method, which serves as a type of upper boundary. Measurements in the fine tailings layers were overestimated and must be influenced by the fact that layer thickness does not allow full development of excess pore pressures, as well as the low absolute stiffness ratios in these materials.

State Parameter Approach

Been and Jefferies (1985) suggested that the state parameter, ψ, correlated well with large strain engineering parameters from triaxial tests. The state parameter defines the vertical separation of the current state of void ratio to the equivalent critical state void ratio, at the same mean normal effective stress. Been et al. (1986; 1987) developed a procedure for estimating the state parameter in sand from cone penetration tests based on calibration chamber tests. The procedure as adopted here is:

- Define the steady state or critical state line for the material based on laboratory triaxial tests - refer to Table 4-15.
- Normalised state parameters, m and κ are then determined from Figure 4-44 as a function of the slope of the steady state line, or λ_{ss}, see Table 4-17.

Table 4-17: Normalised state parameters for Mizpah and Pay Dam tailings.

Tailings Dam	Description	λ_{ss}	m	κ
Mizpah	Pond fine tailings	0.105	10.46	14.19
	Pond coarse tailings	0.045	11.19	22.90
Pay Dam	Penstock fine tailings	0.170	10.04	12.02
	Penstock coarse tailings	0.075	10.75	16.51

- The state parameter follows from the void ratio at depth minus the equivalent steady state void ratio or

$$\psi = e - e_{ss} \qquad \textbf{Eq. 4-74}$$

where e = current void ratio

e_{ss} = the equivalent void ratio on the steady state line

- The relationship between the measured cone resistance and the state parameter follows from,

$$\frac{q_c - p_o}{p_o'} = \kappa \cdot \exp(-m \cdot \psi) \qquad \textbf{Eq. 4-75}$$

The result of the state parameter approach as a predictive tool in gold tailings is illustrated in Figure 4-45.

The state parameter approach relies on empirical correlations with the compressibility of the material and is not directly influenced by differences in strength. It should therefore be able to differentiate between the more compressible fine tailings compared with the stiffer coarse tailings. As with cavity expansion, measurements in the soft fine tailings were well predicted. In the coarser layers the state parameter gave a better response as a function of the reduced state parameter values in these layers, but still could not account for the upper bound measurements.

Using the known properties of the fine and coarse tailings, the state parameter for isotropic normally consolidated fine tailings range between +0.07 and +0.15 and for the coarse tailings between +0.02 and +0.1. The full range, therefore, lies approximately between +0.02 and +1.5. If the state parameter is calculated directly from field measurements using Eq. 4-75 and average values for κ and m as in Figure 4-46 are taken, the state parameter lies between 0.0 and +0.2 indicative of contractile normal to lightly overconsolidated states. However, in many of the coarser layers the state parameter was negative, indicating dilative states.

Conclusions

The preceding discussion applies well known strength interpretation methods to CPTU data in tailings with varying degrees of success. However, these results can be interpreted with regard to the composition and state of this material in a typical impoundment:

- Sub-aqueous deposition leads to the formation of a loose/soft normally consolidated sediment. This type of material should contract during drained shear or generate positive excess pore pressures during undrained shear, and is not expected to exhibit peak-strength behaviour in the absence of collapsible structure. Desiccation under sub-aqueous conditions can build in some overconsolidation on the beach areas, but limited evidence from this study suggests pre-consolidation pressures in the order of 150 to 200 kPa that will soon be destroyed with saturation and overburden loading.
- Layers of the finest composition of tailings, are expected to shear in an undrained manner during cone penetration at the standard rate of 2 cm/s. Bugno and McNeilson (1984) proposed that an undrained response is likely for material with permeability below 3 m/yr and that a fully drained response can be expected when the permeability exceeds 3000 m/yr. The fine tailings ranged in permeability between 1.5 and 15 m/yr suggesting undrained penetration. The quick and positive response in pore pressure during penetration through these layers, Figure 4-33 and Figure 4-34, strengthens this assumption. Under these conditions cavity expansion theory and the state parameters approach are able to predict penetration resistance as a function of strength and stiffness with sufficient accuracy for practical purposes.
- Layers of a coarser composition can allow considerable dissipation of excess pore pressure with permeabilities between 5 and 20 m/yr, and generate a much higher partially drained shear strength during penetration. The virtual absence of excess pore pressure in these layers, Figure 4-33 and Figure 4-34, is evidence to this fact. In some coarse layers negative excess pore pressures are measured - evidence of dilation. Dilation in granular soils results typically from an "overconsolidated" or dry-of-critical state, or more likely in this case, phase transfer dilation once the stress path reaches the critical state. Undrained triaxial shear of the coarser tailings all show contractile behaviour until the equivalent critical state strength is reached. With continued shear, phase transfer dilation becomes prominent in the coarse tailings. With the large strain field imposed by an advancing cone such dilation would increase the measured cone resistance and generate negative excess pore pressures. The effective stress approach with its B_q-parameter accounts to some extent for this dilatency.

It is concluded, therefore, that penetration resistance in a typical saturated tailings deposit is governed, in fine layers, chiefly by undrained strength and stiffness, but in coarse layers, more by stress dilatency and partial drainage. Lower bound cone resistances are well predicted by cavity expansion and state parameter methods based on the strength and stiffness properties of these layers. The difference between lower and upper bound measurements serves as an indication of the variance in fine and coarse layers in the tailings profile and the effects of partial saturation, partial drainage and post failure stress-dilatency in the coarser layers.

Figure 4-33 is duplicated as Figure 4-47 with the lower and upper bound measurements highlighted. Of these boundaries the lines of minimum cone resistance are fairly constant throughout the cross-section. At a depth of 10 m the minimum cone resistance is approximately 1 MPa for the daywall, lower beach and beach-pond interface locations. These measurements are consistent with the properties of the fine tailings examined in this study and would be well represented by a cavity expansion or state parameter model. At the middle beach and upper beach locations the minimum resistance increases to 2 and 3 MPa respectively at 10 m depth. Probable reasons for this increase include higher stiffness as a result of densification due to desiccation, and a general increase in the coarseness of the material deposited in these areas under sub-aerial conditions. Both these properties would also increase the effects of partial drainage and phase transfer dilation, thus increasing upper bound cone resistances as well. Throughout the cross section the profiles remain highly layered with a mixture of "weak" and "strong" layers of fine and coarse composition.

Figure 4-47 shows a gradual decrease in cone resistance from the upper beach to the pond area, consistent with a general decrease in grade towards the decant facilities. However, penetration resistances measured at the daywall location are comparable to the measurements at the beach-pond interface, rather than at the upper beach locations. This results from paddock system of daywall construction. The whole tailings slurry delivered is used to fill the daywall paddies along flow paths parallel to the wall. At a central low point between two discharge stations, the slurry passes through the daywall into the night area. The idea is that the coarser material will be deposited on the daywall and that the fines will decant to the nightpan. Figure 4-47 suggests that a significant amount of fines, comparable to the pond areas is deposited on the daywall and that the wall itself must be less competent than the upper beach, with respect to both strength and permeability.

The results of this study indicate that materials deposited sub-aqueously in a tailings impoundment can be expected to exist in a contractile normal consolidated state without any collapsible structure, but rather with the potential to dilate post critical state, especially in the coarser material. The question remains why large scale liquefaction has been observed to occur during some failures of gold tailings impoundments, notably during the Merriespruit disaster. Possible mechanisms for this can include the following:

- Loose saturated and uncompacted tailings can generate excess pore pressure during cycles of stress reversal. The effects become cumulative during a seismic event and can initiate liquefaction (Vick, 1983). However, the high permeability of coarse tailings should prevent undrained conditions during cyclic loading so that excess pore pressures dissipate as fast as they are generated. Coarse tailings should, therefore, have very low liquefaction susceptibility.

- Dilative overconsolidated coarse tailings can be contractile at very low strains, similar to overconsolidated sands as shown by Vesic and Clough (1968). This initial contractile state can generate small positive excess pore pressures if not fully drained. Following Been et al. (1987; 1988) a flow type failure may be the result under static load provided a significant trigger mechanism, such as a slope instability.
- Collapsible fabric can also result in a liquefaction type failure as was illustrated by Papageorgiou et al. (1997; 1999) on triaxial specimens prepared by wet-tamping techniques.

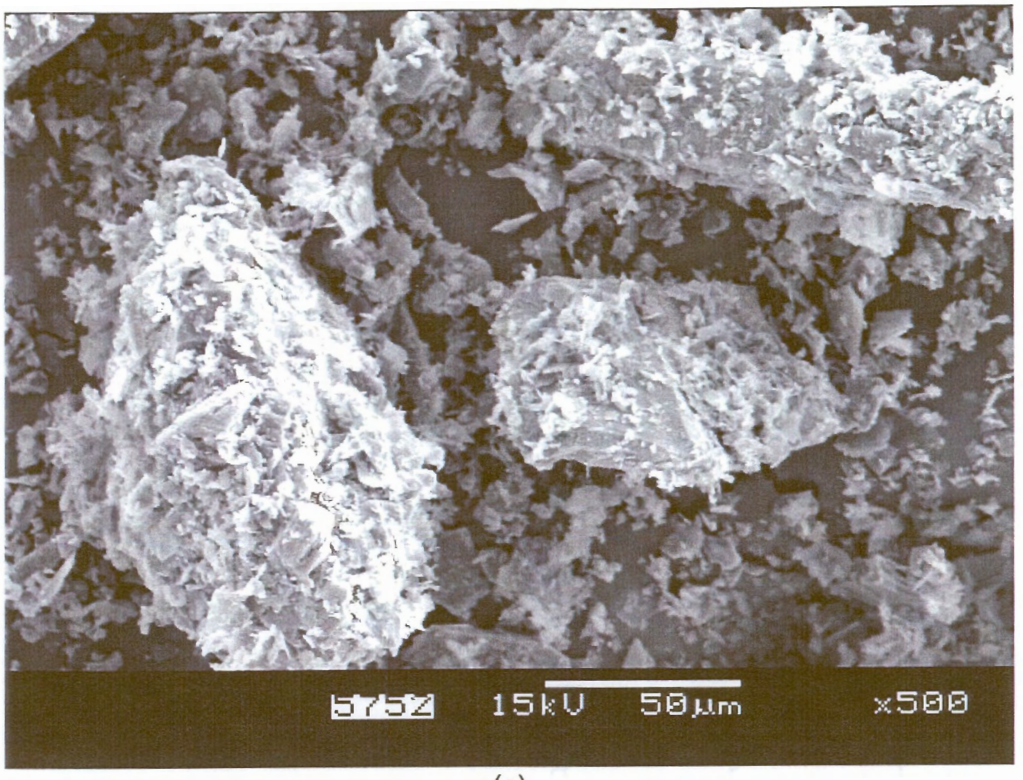

(a)

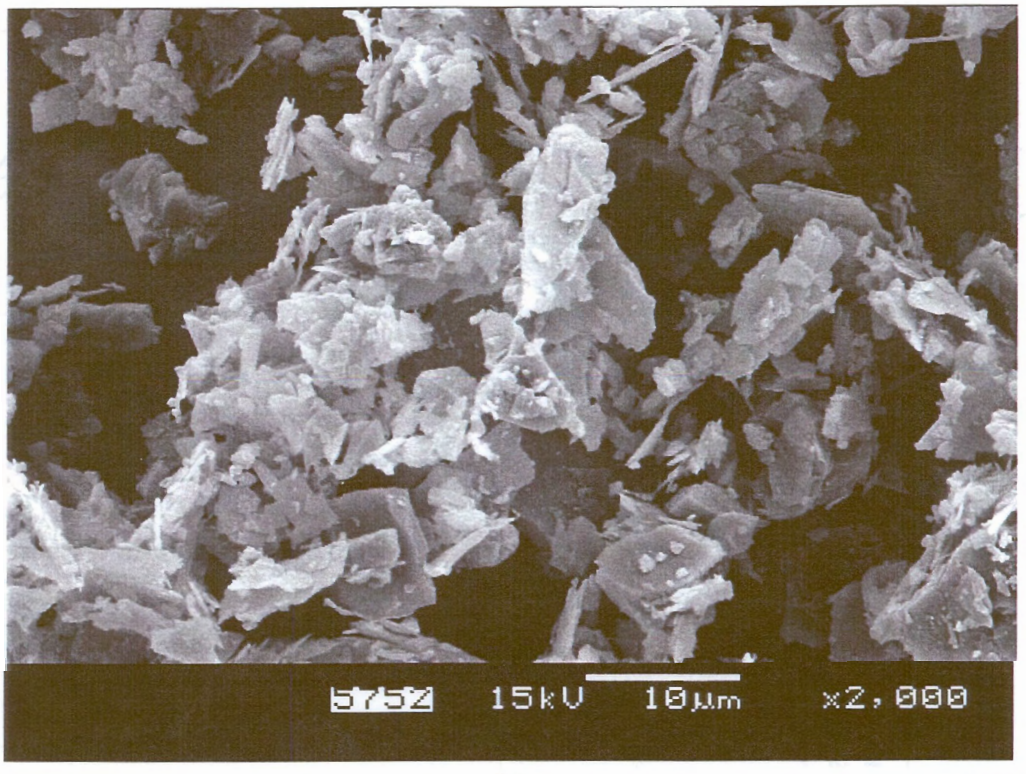

(b)

Figure 4-1: Evidence of flocculation of the flaky slimes (a) onto coarser sand grains, and (b) into flocs of slimes.

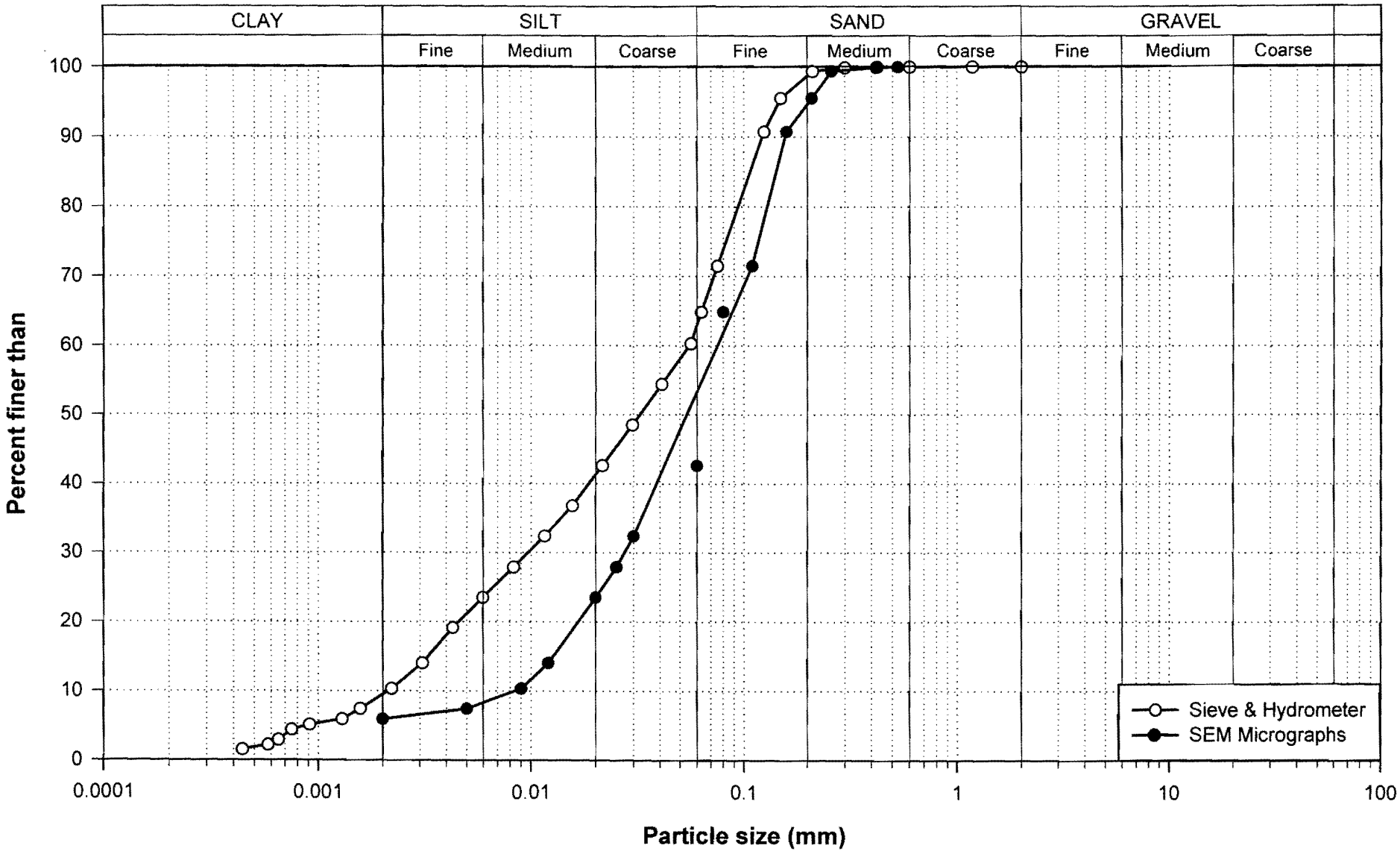

Figure 4-2: Mizpah Whole Tailings: Grading by sieve and sedimentation tests compared with the grading derived from SEM micrographs.

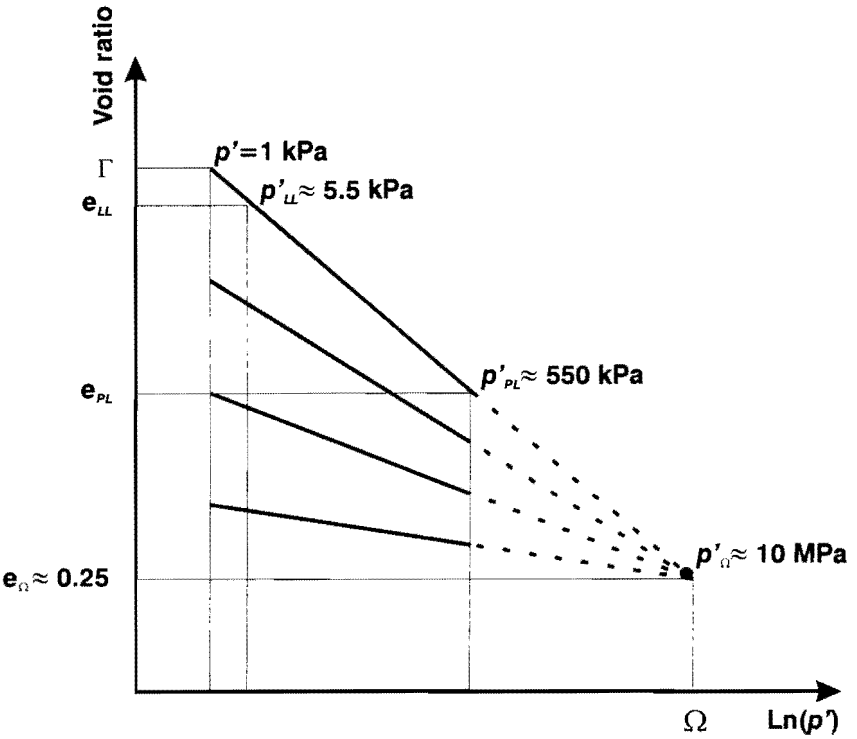

(a)

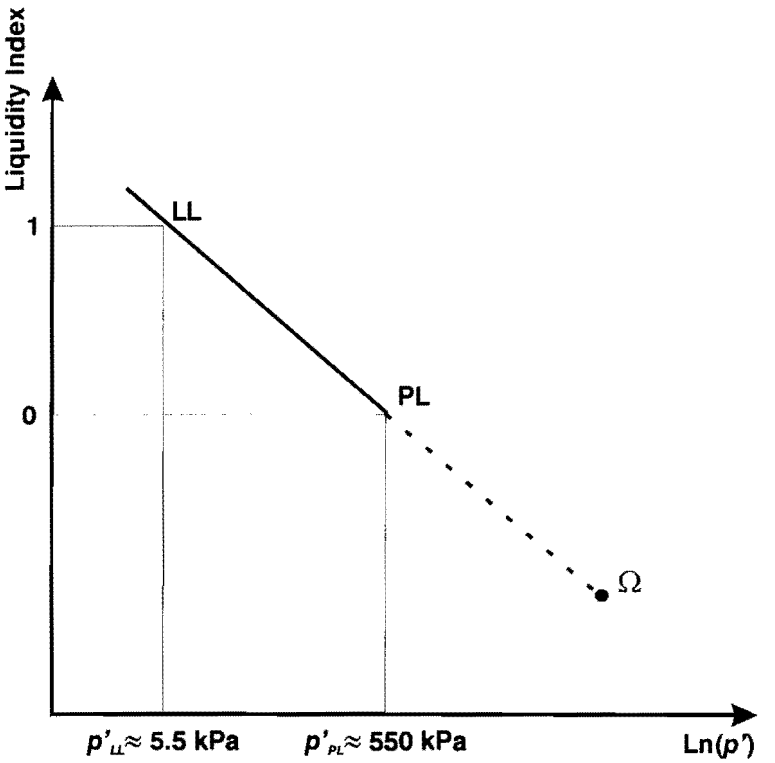

(b)

Figure 4-3: (a) Idealised family of Critical State Lines, (b) Normalised Critical State Line (Schofield & Wroth, 1968).

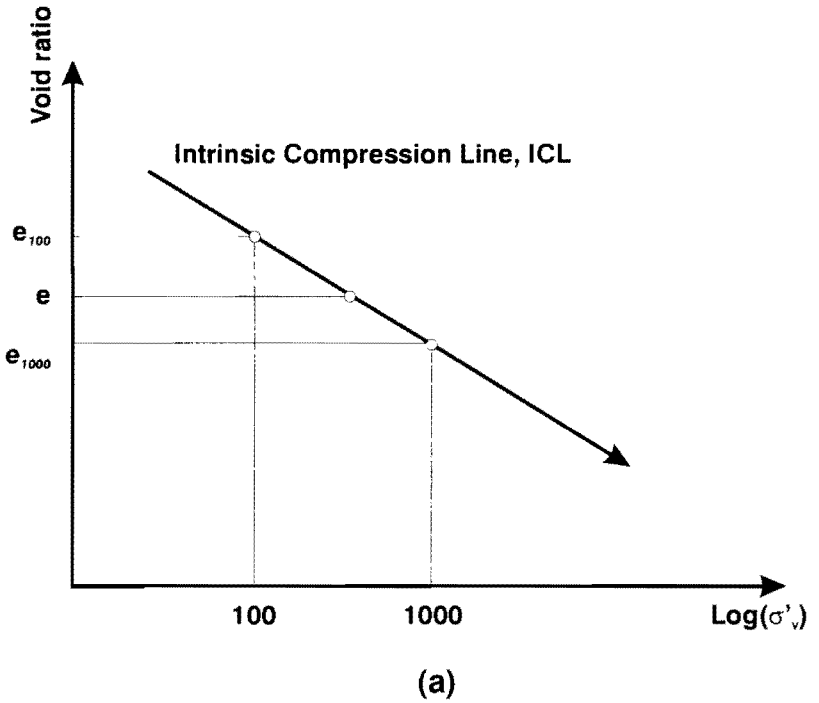

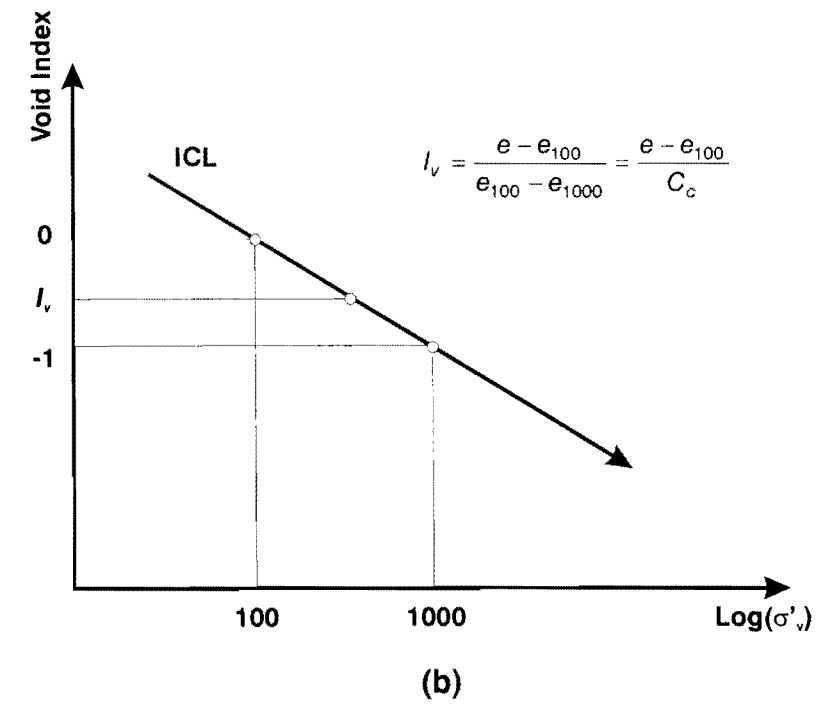

Figure 4-4: Use of the Void Index, I_v, to normalise compression data (Burland, 1990).

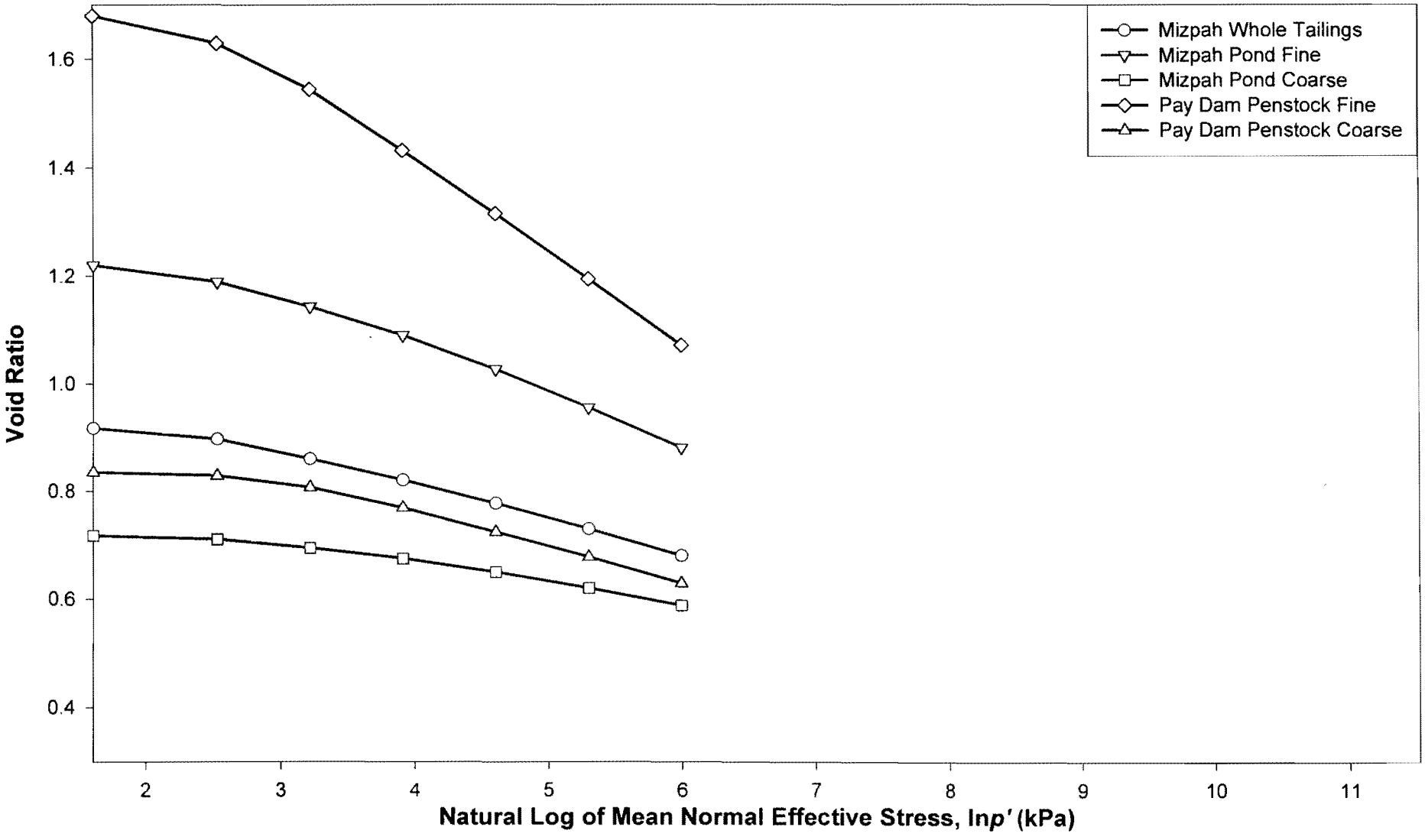

Figure 4-5: Isotropic compression behaviour of the tailings considered in this study.

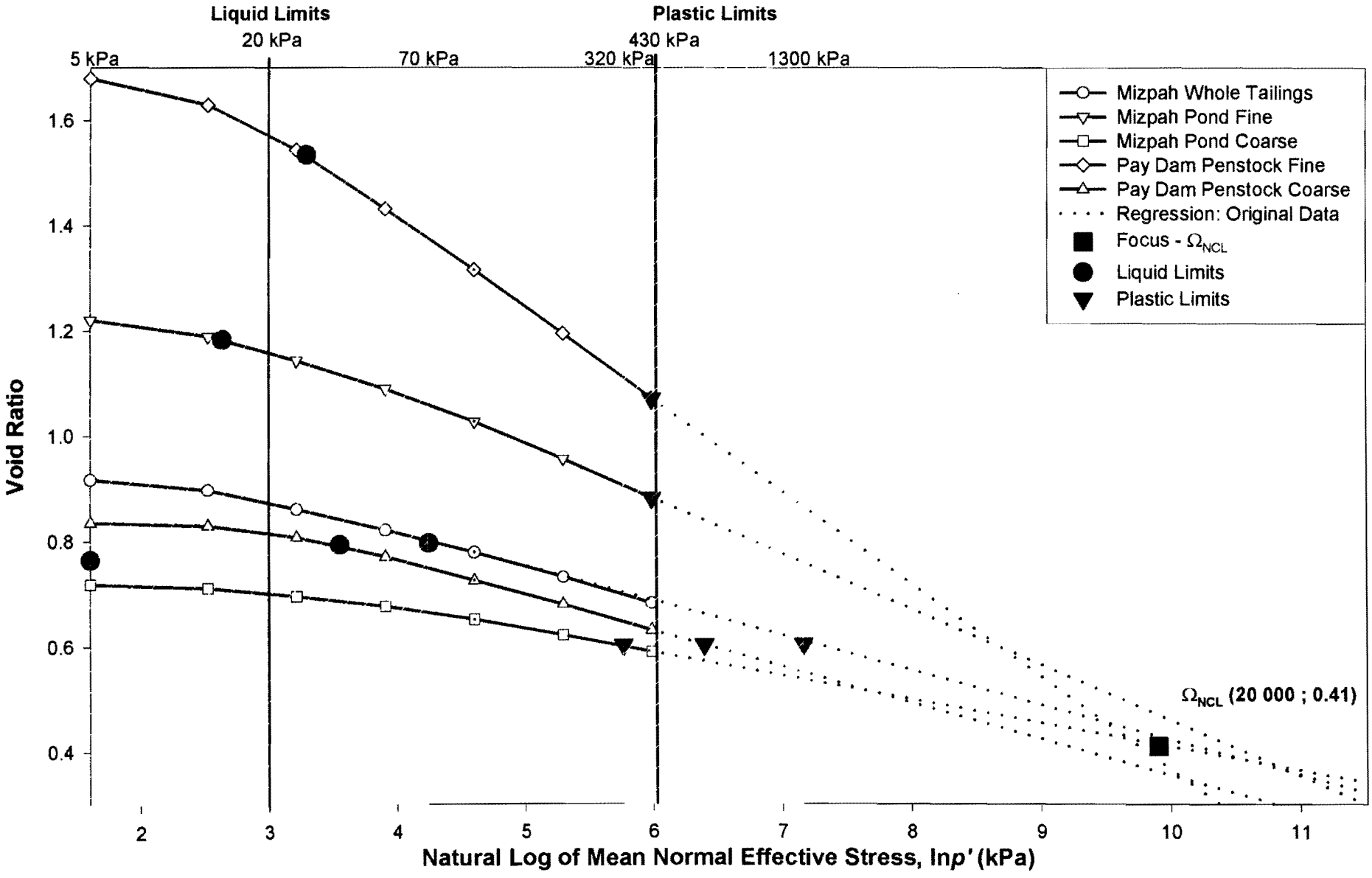

Figure 4-6: Geometric extrapolation of the compression data.

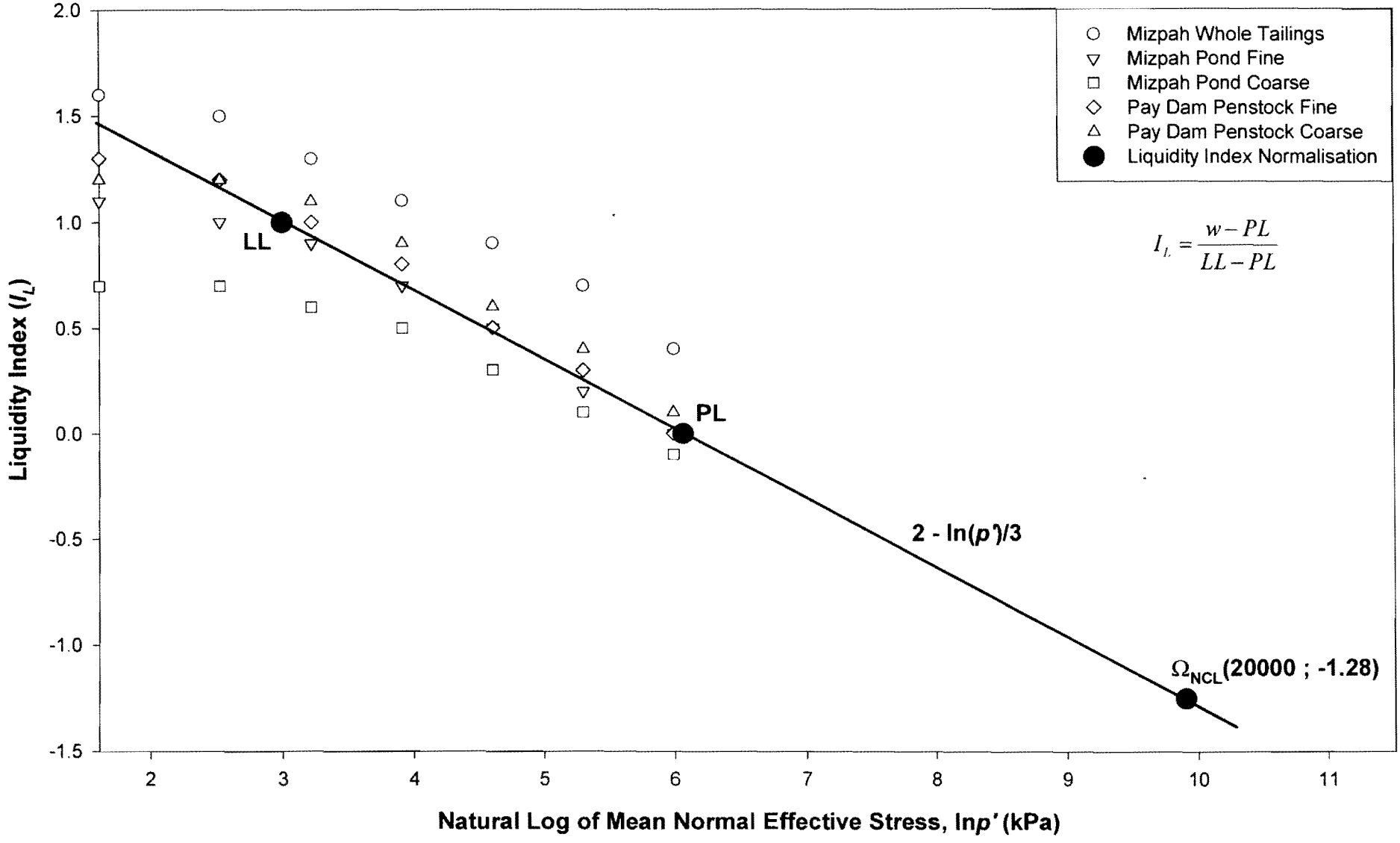

Figure 4-7: Isotropic compression data normalised with the Liquidity Index after Schofield & Wroth (1968).

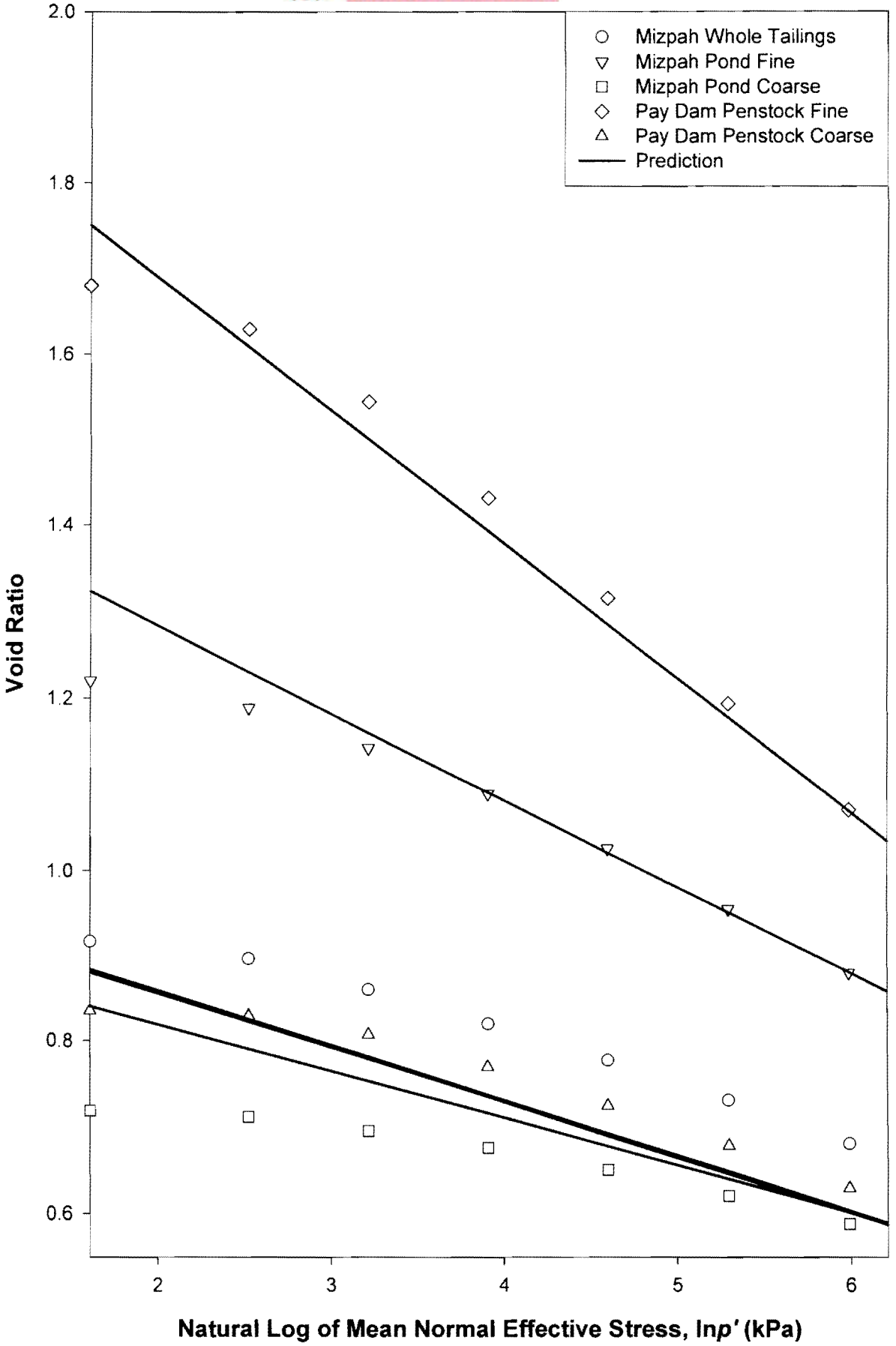

Figure 4-8: Predicting the compression behaviour of gold tailings using I_L and the Atterberg limits.

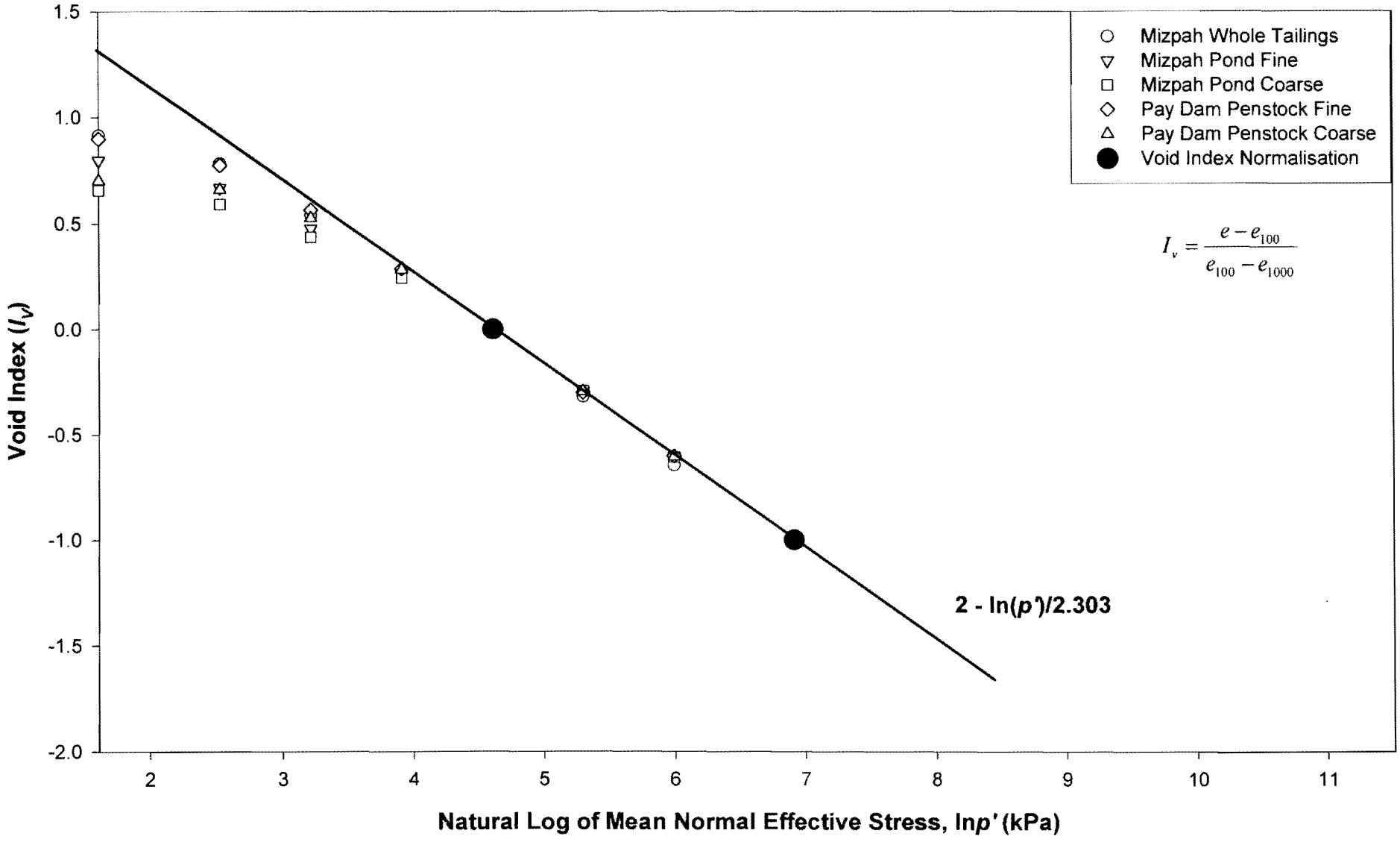

Figure 4-9: Isotropic compression data normalised with the Void Index after Burland (1990).

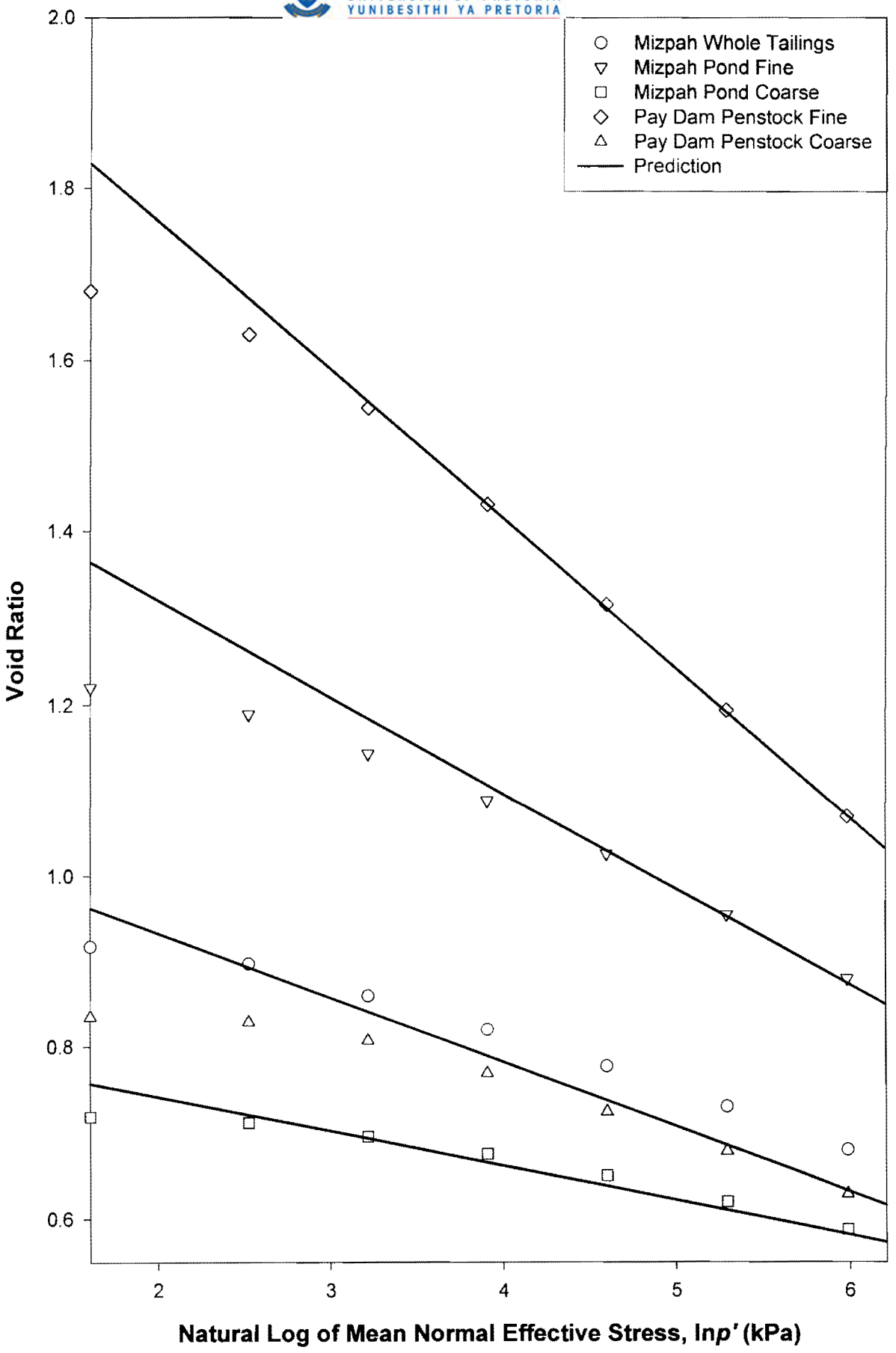

Figure 4-10: Predicting the compression behaviour of gold tailings using I_v and the Atterberg limits.

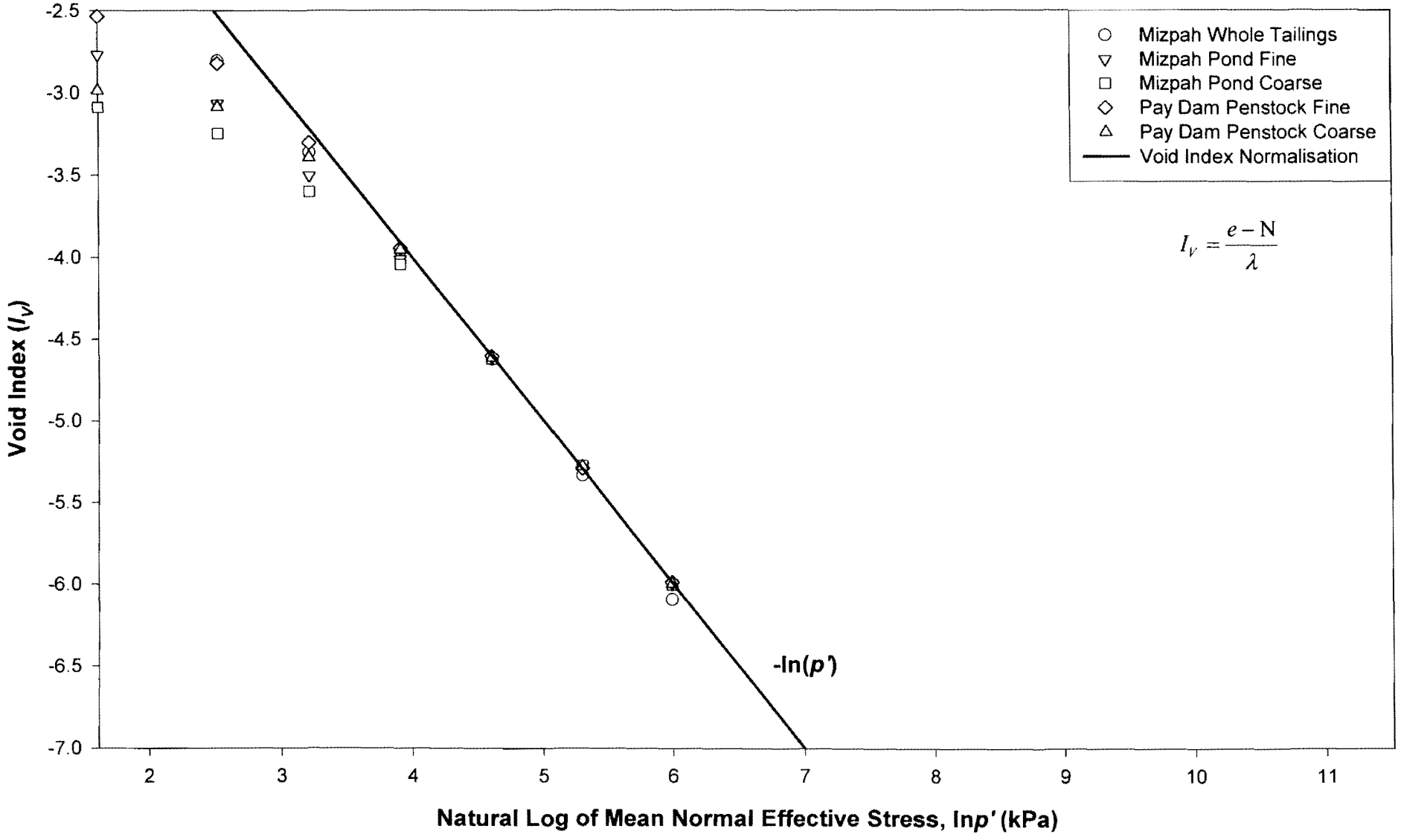

Figure 4-11: Isotropic compression data normalised with the Void Index in terms of critical state parameters.

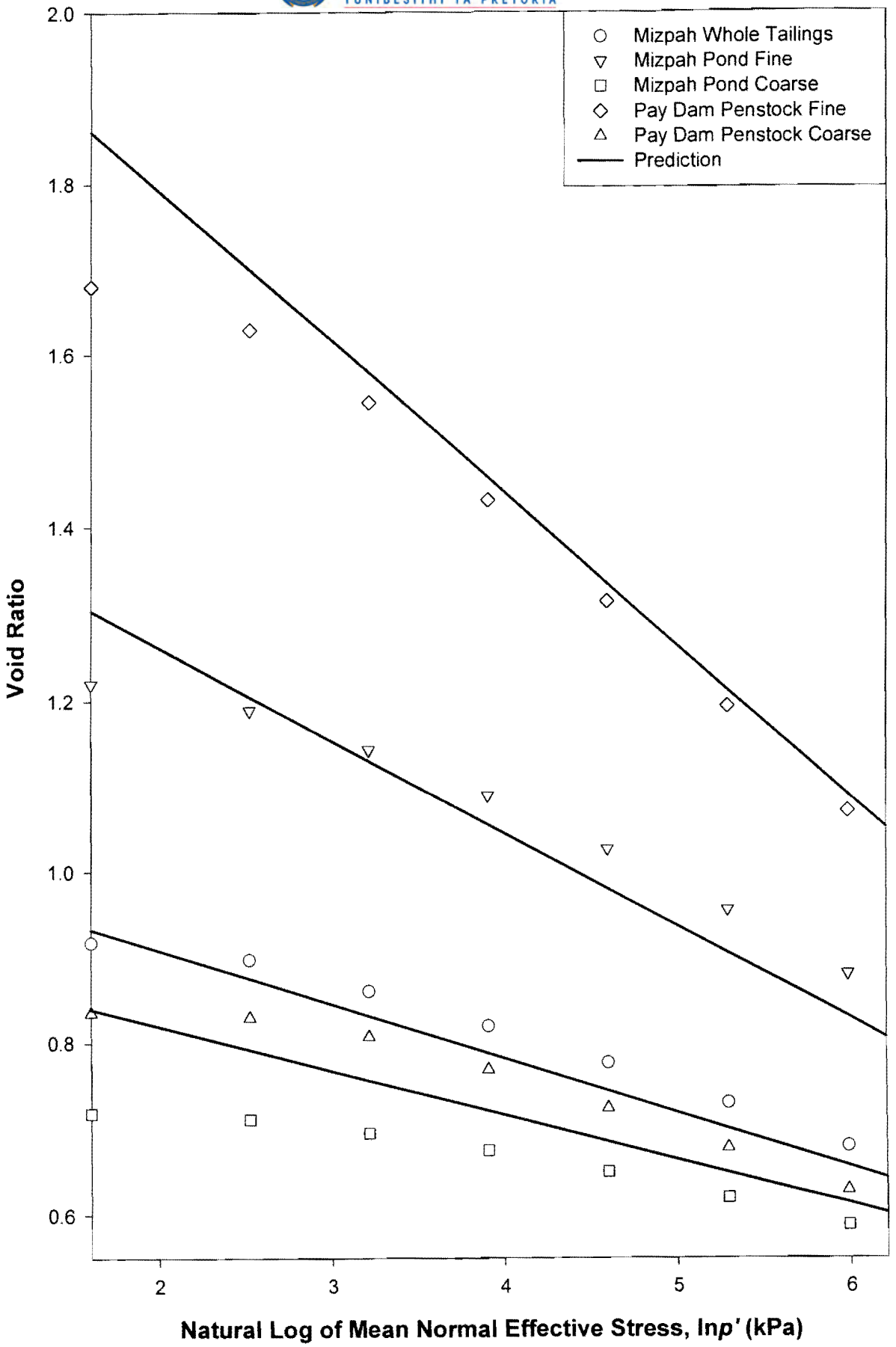

Figure 4-12: Predicting the compression behaviour of gold tailings using empirical correlations between CSSM-parameters and the Atterberg limits.

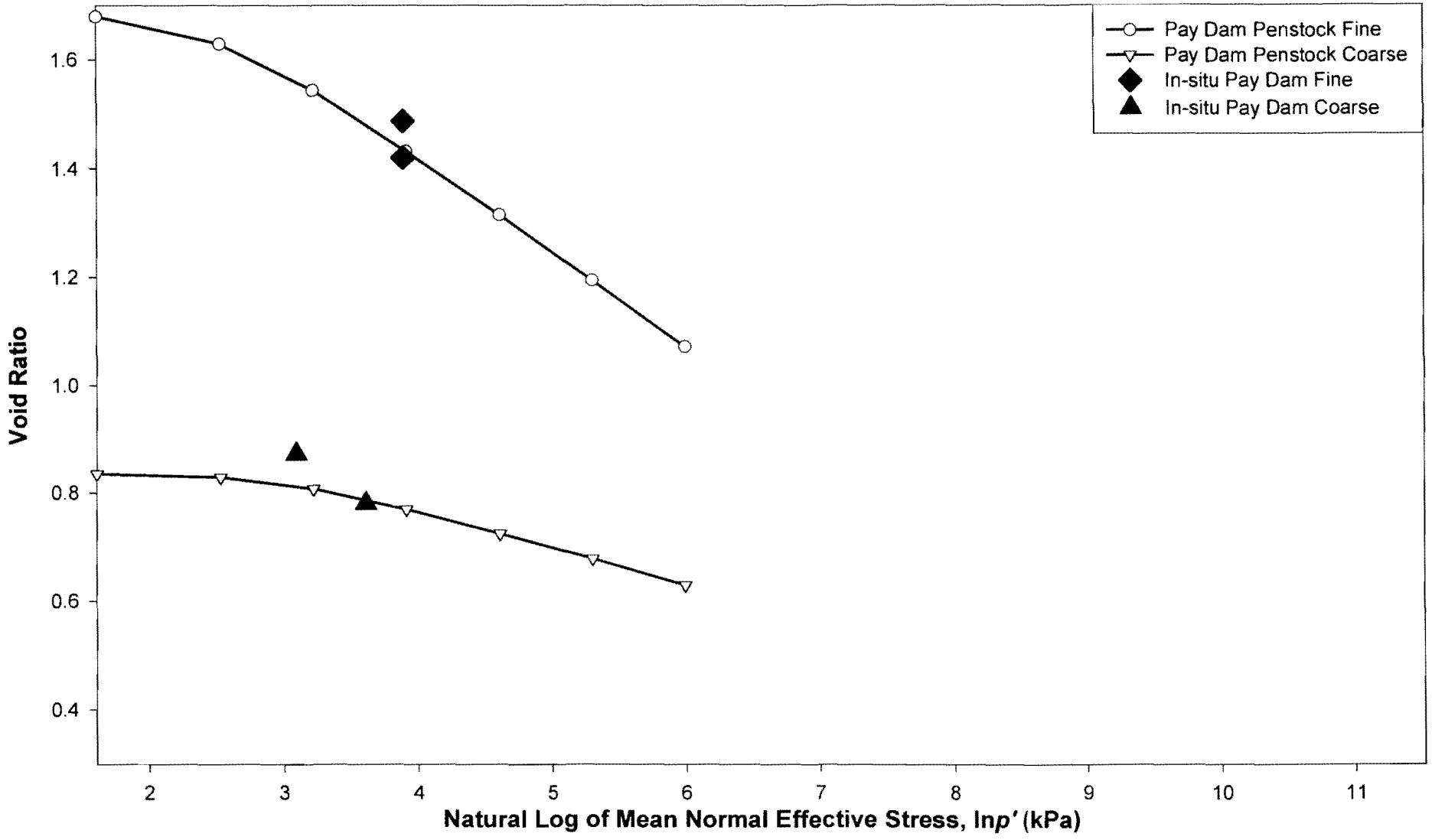

Figure 4-13: In-situ undisturbed void ratio's compared with reconstituted compression curves.

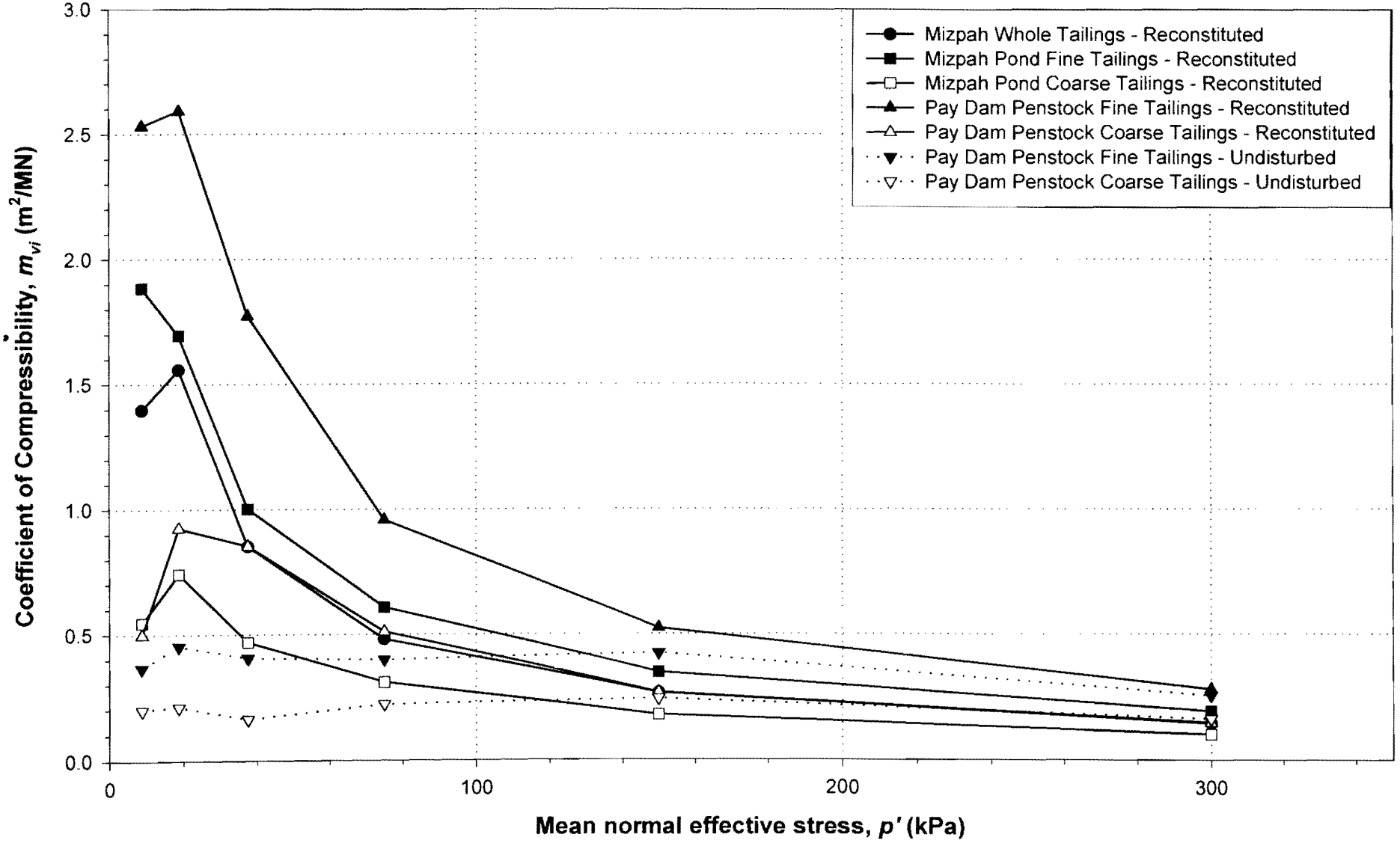

Figure 4-14: Gold Tailings: Coefficient of Compressibility data.

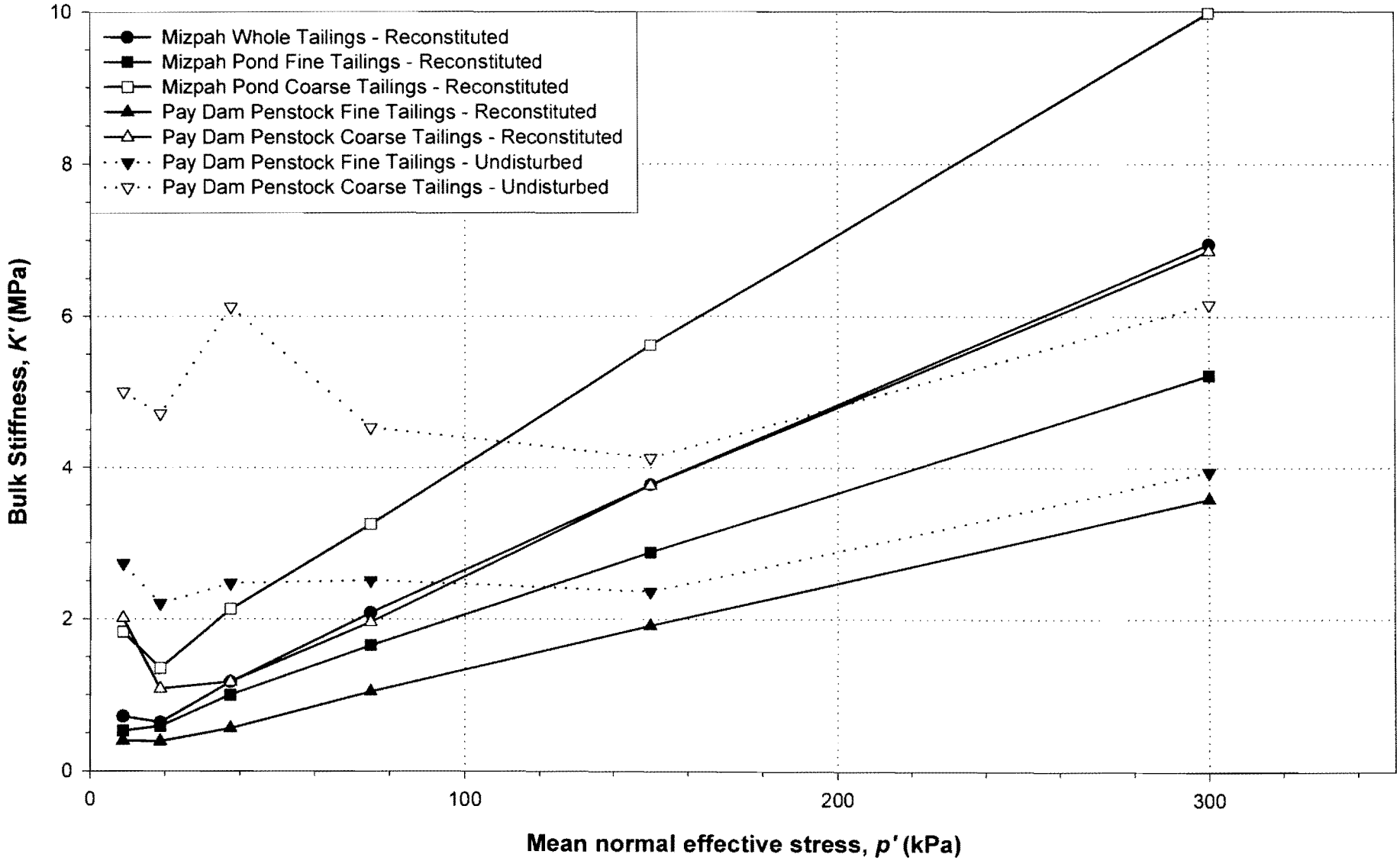

Figure 4-15: Gold Tailings: Bulk Stiffness data.

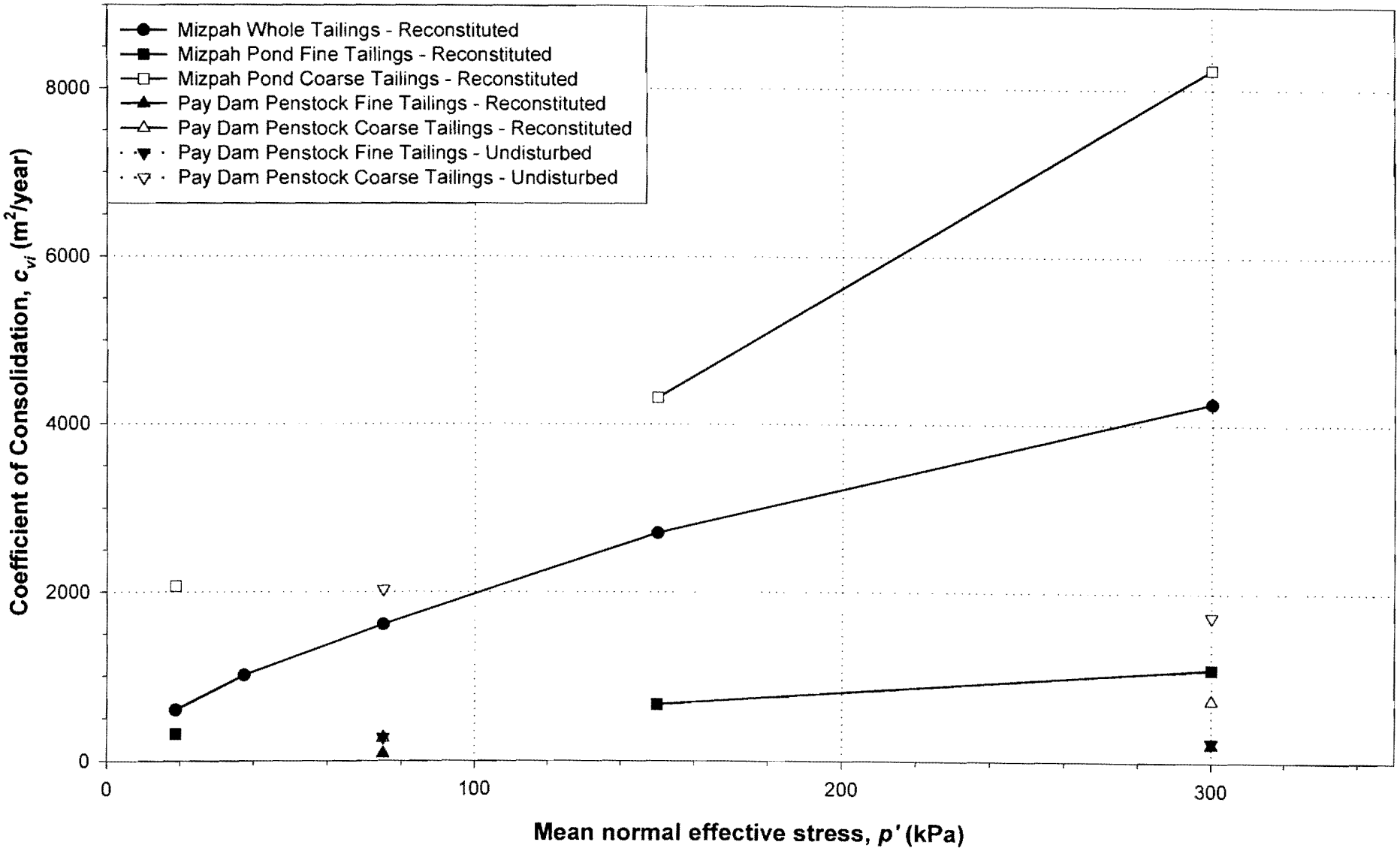

Figure 4-16: Gold Tailings: Coefficient of Consolidation data.

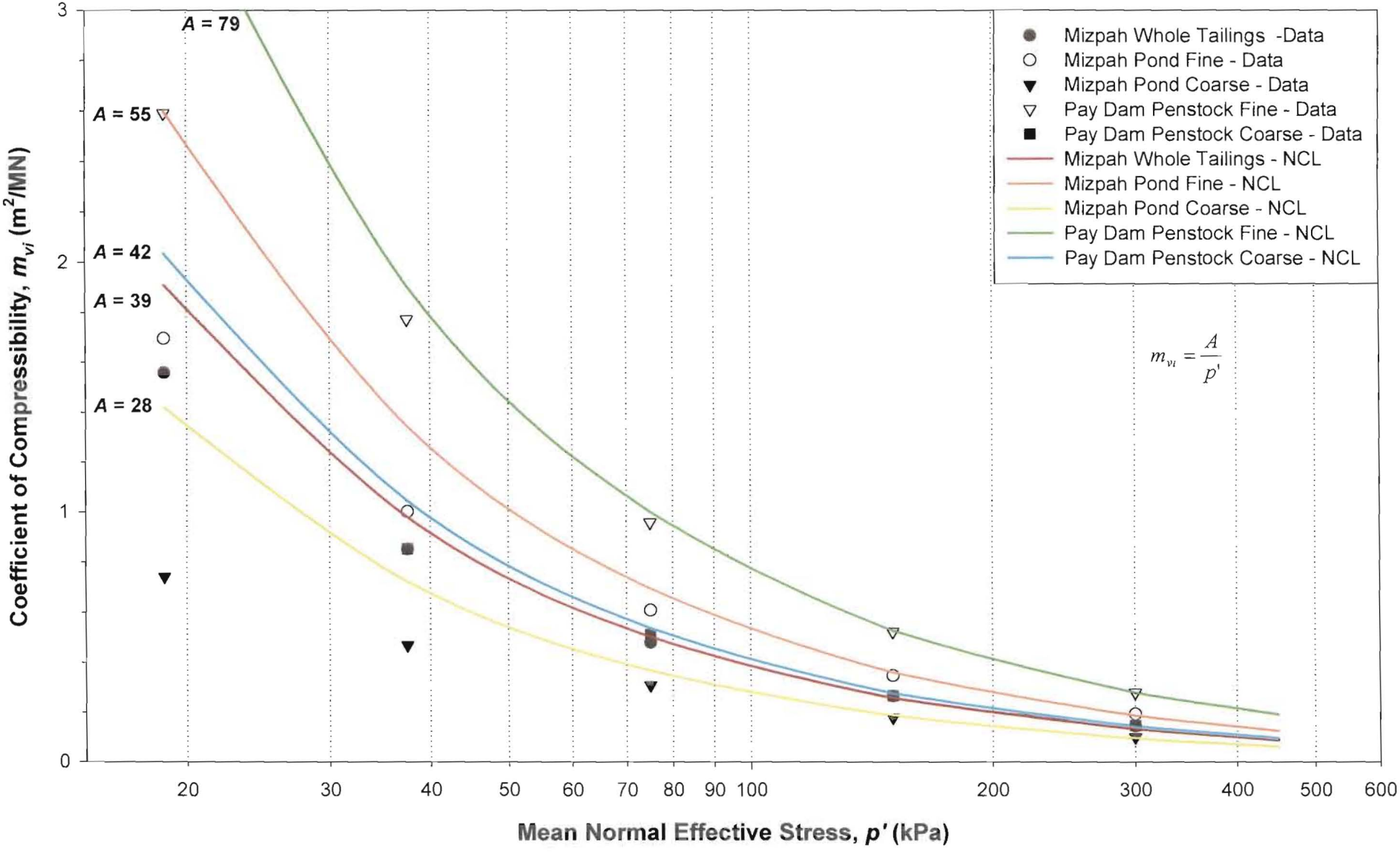

Figure 4-17: Coefficient of Compressibility as a function of the isotropic confinement pressure.

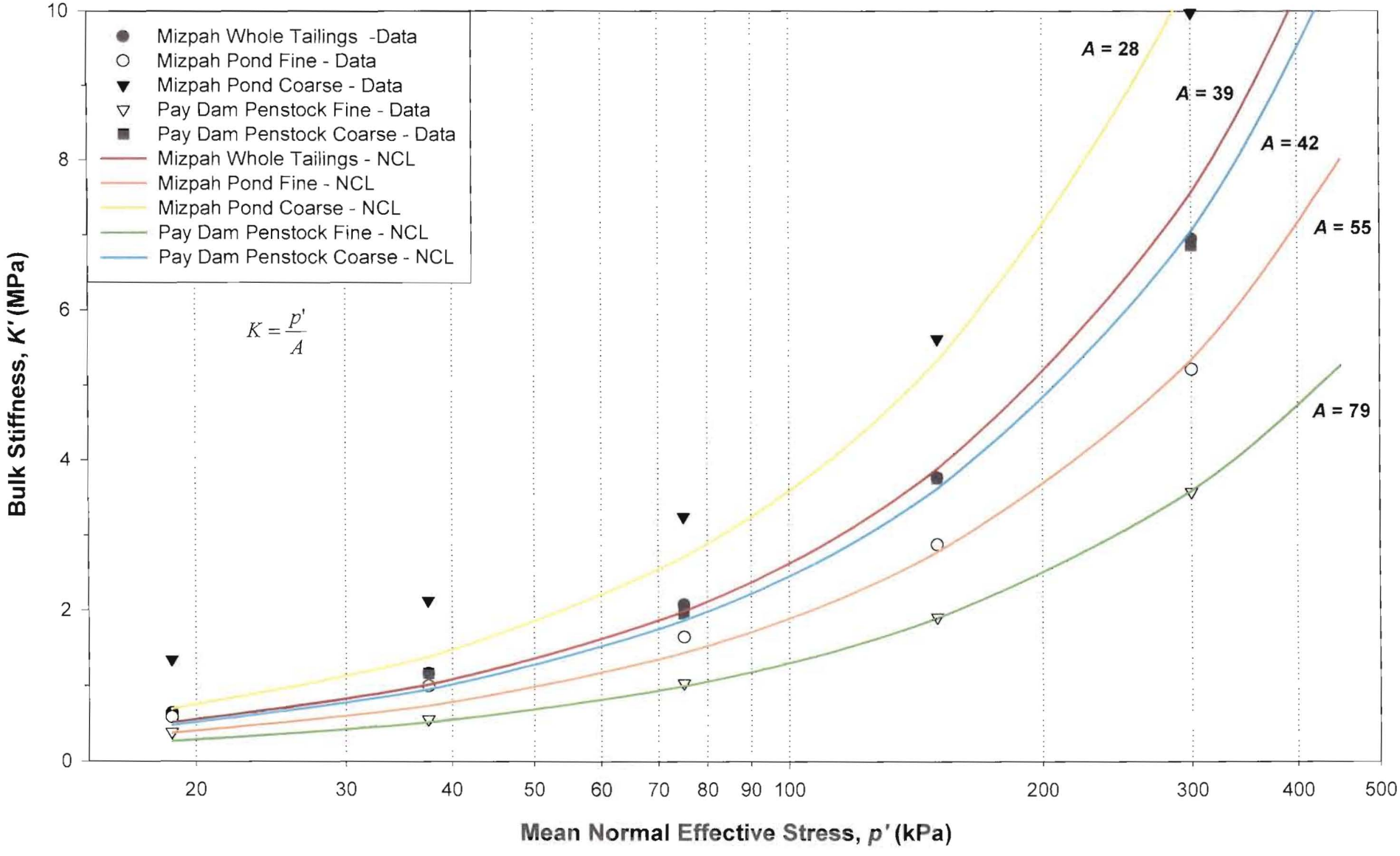

Figure 4-18: Bulk Stiffness as a function of the isotropic confinement pressure.

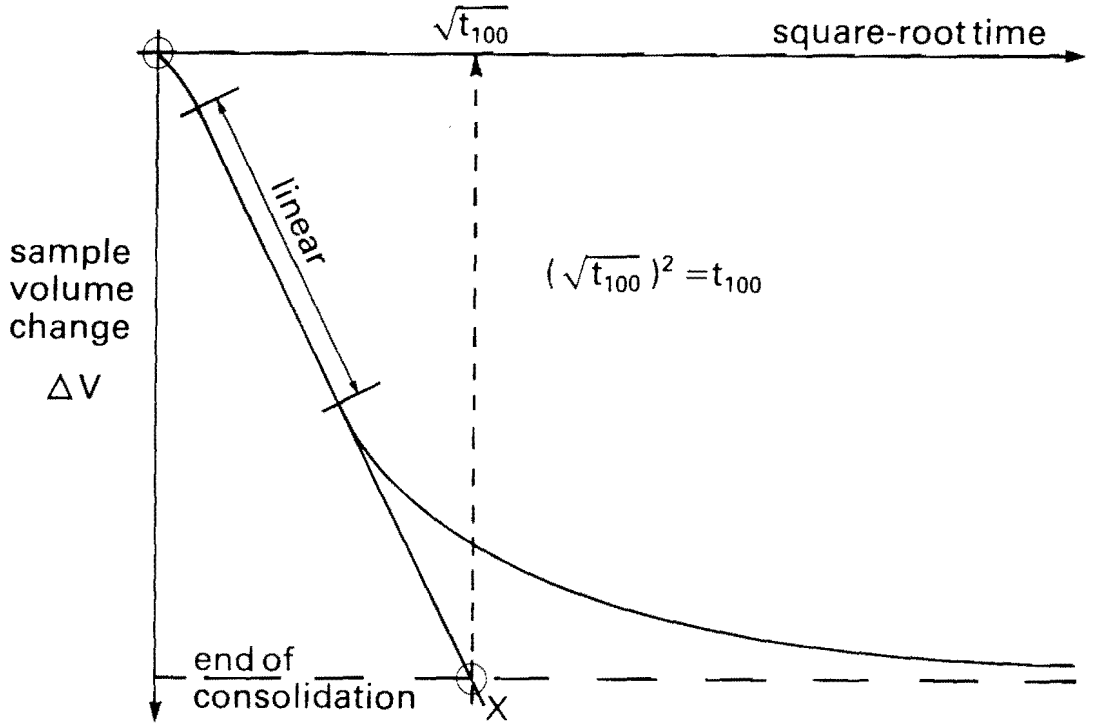

(a)

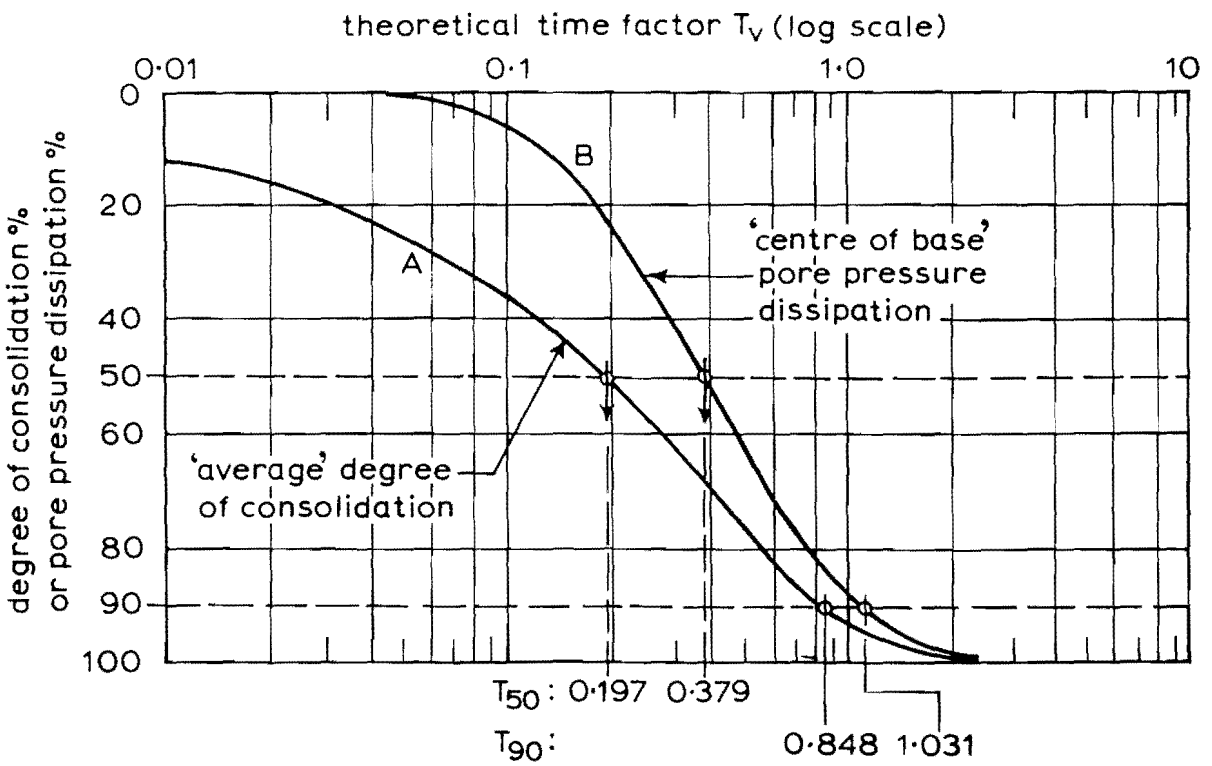

(b)

Figure 4-19: (a) Derivation of theoretical t_{100} from the volume change square root time consolidation curve for a triaxial specimen, (b) Theoretical relationships between time factor and degree of consolidation for vertical triaxial drainage for two methods of measurement.

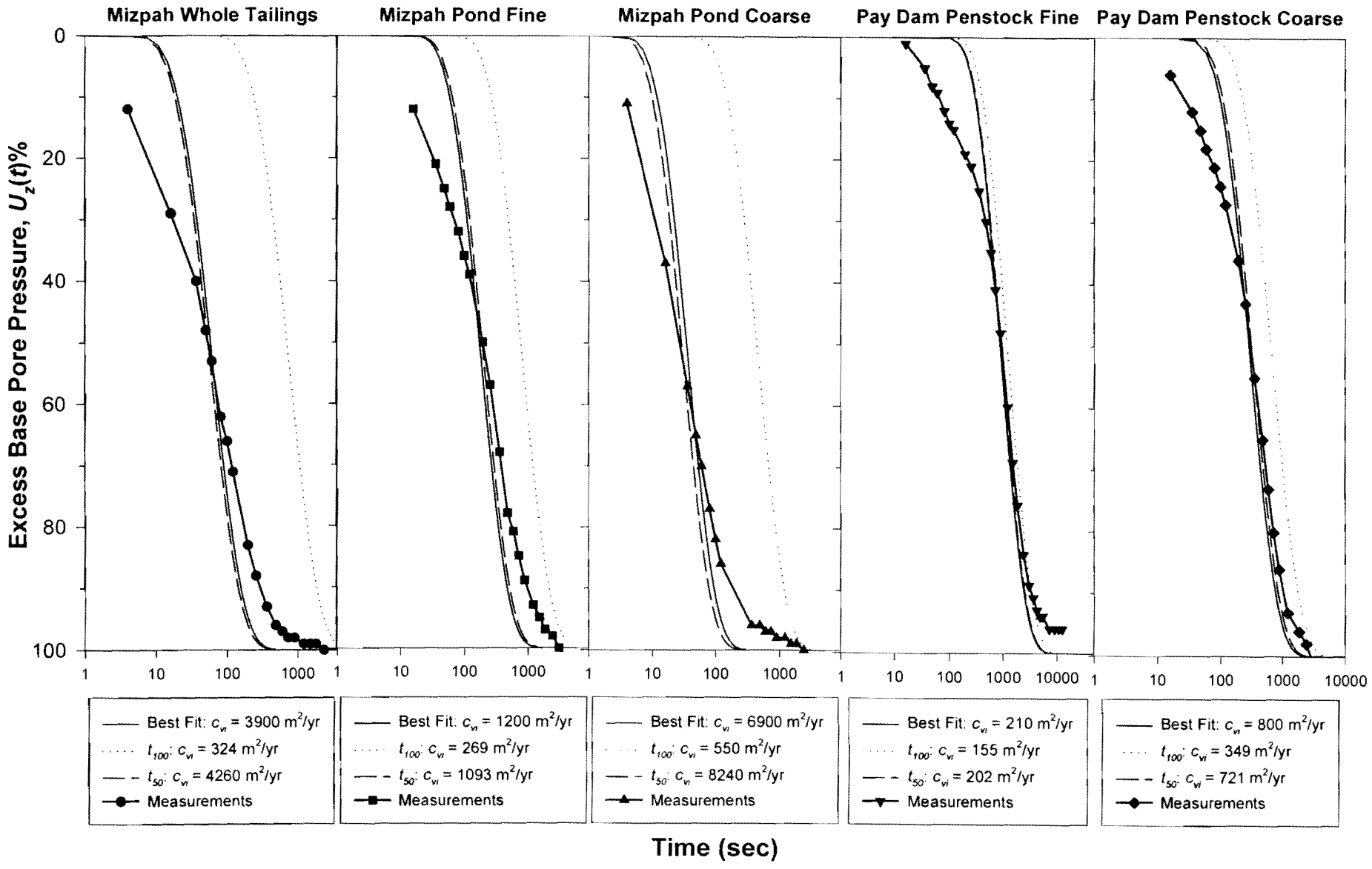

Figure 4-20: Pore pressure dissipation data compared with theoretical curves.

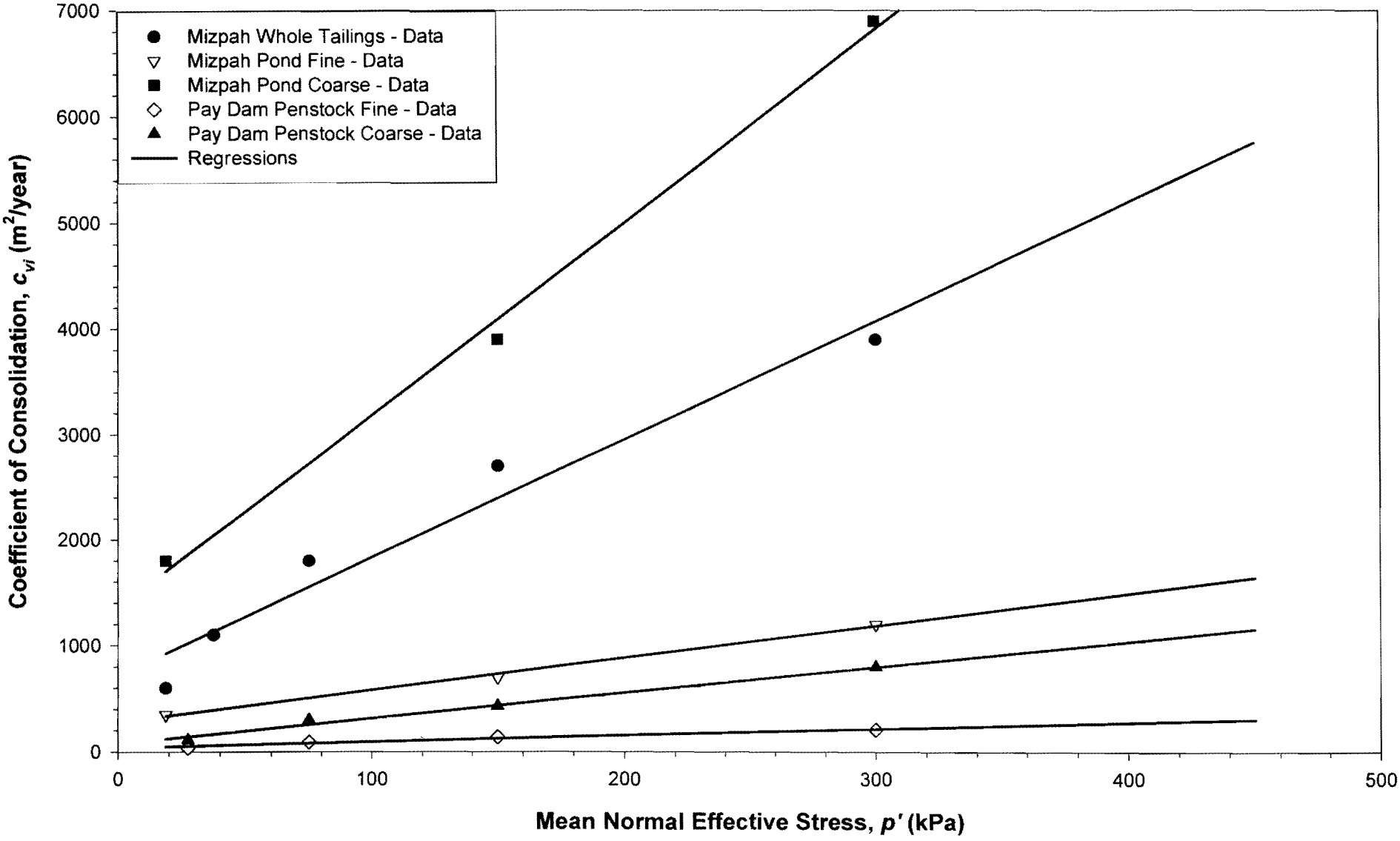

Figure 4-21: Coefficient of Consolidation as a function of the isotropic confinement pressure.

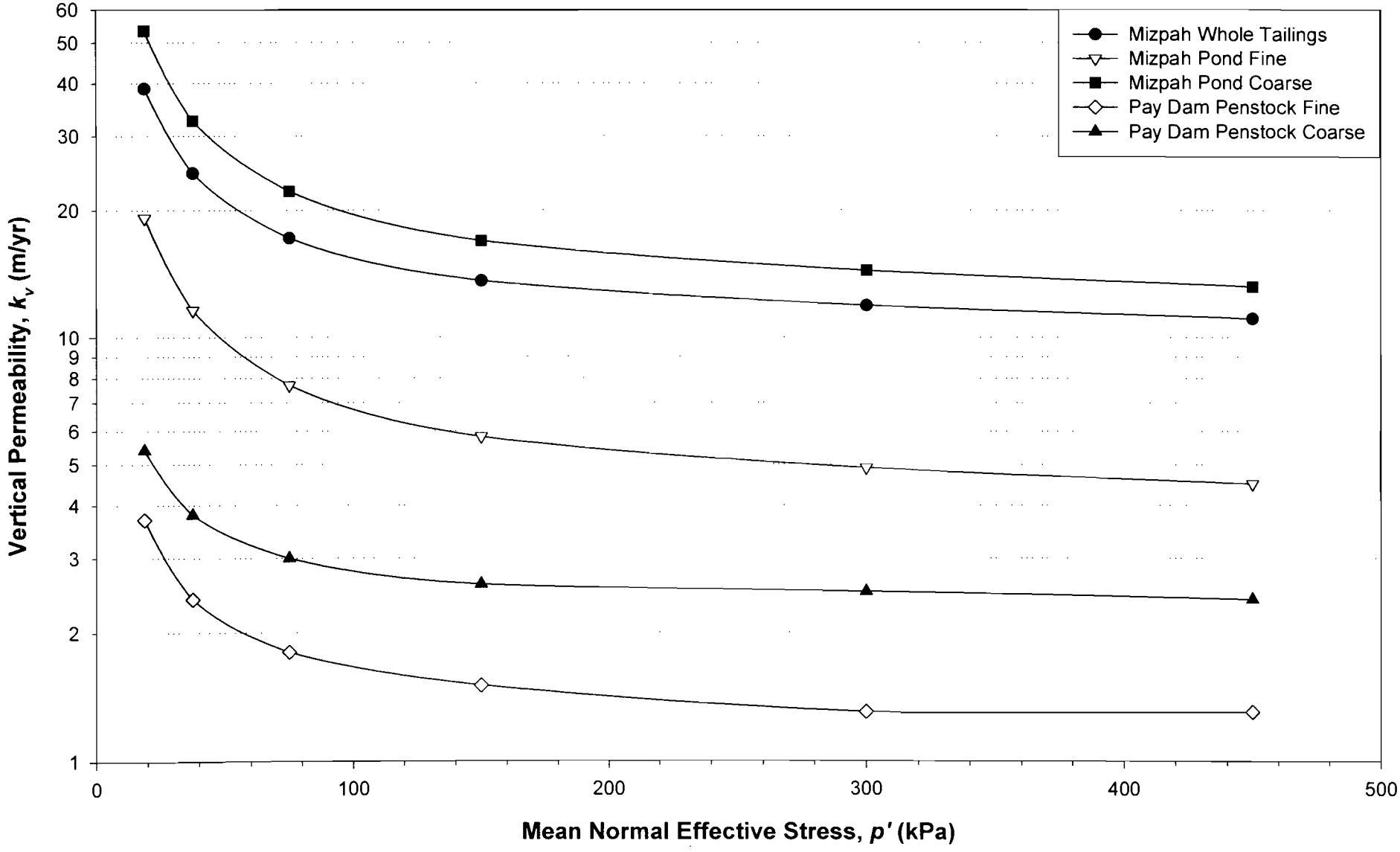

Figure 4-22: Vertical permeability as a function of the confinement pressure.

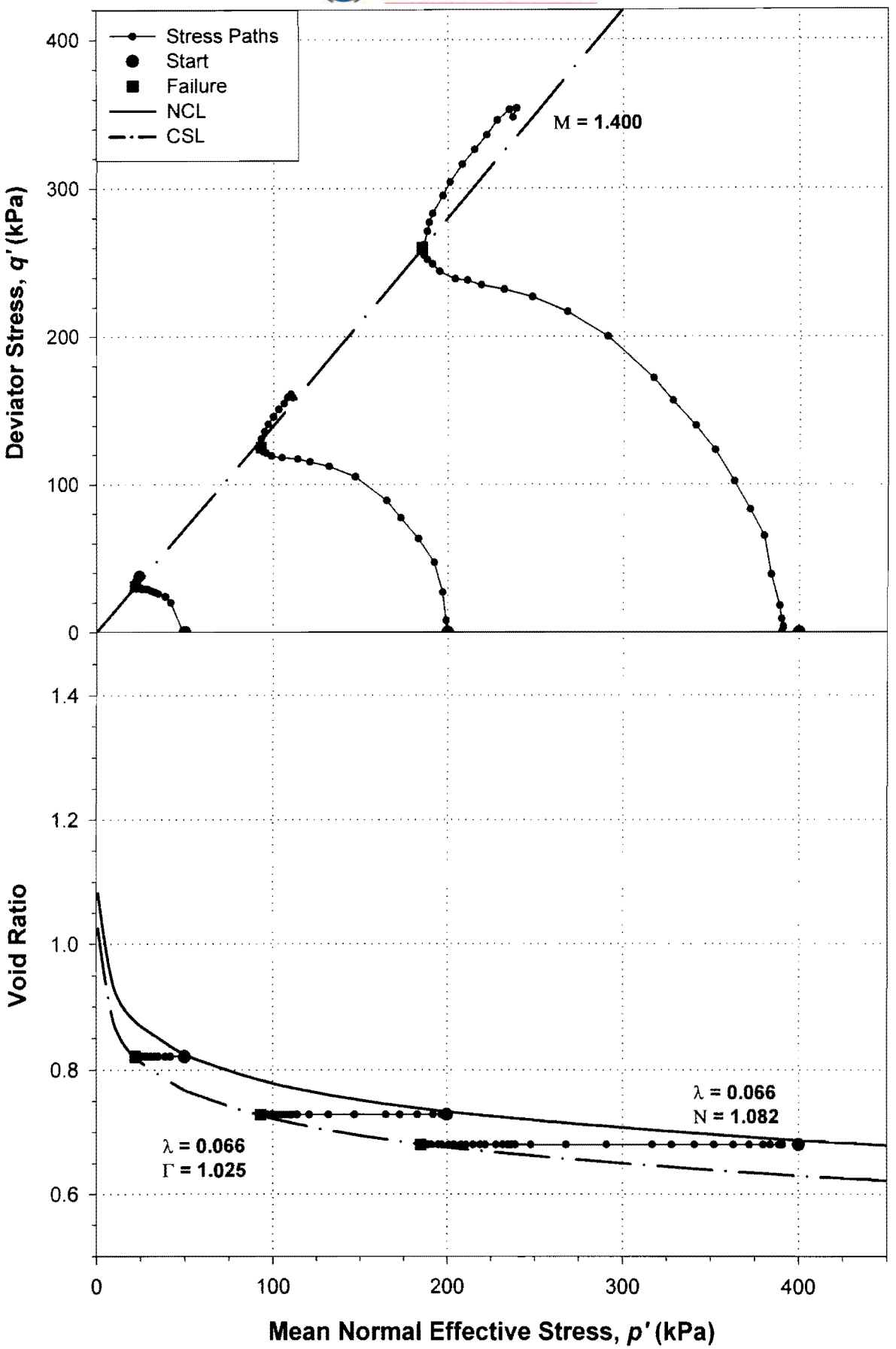

Figure 4-23: Critical state parameters for reconstituted Mizpah whole tailings.

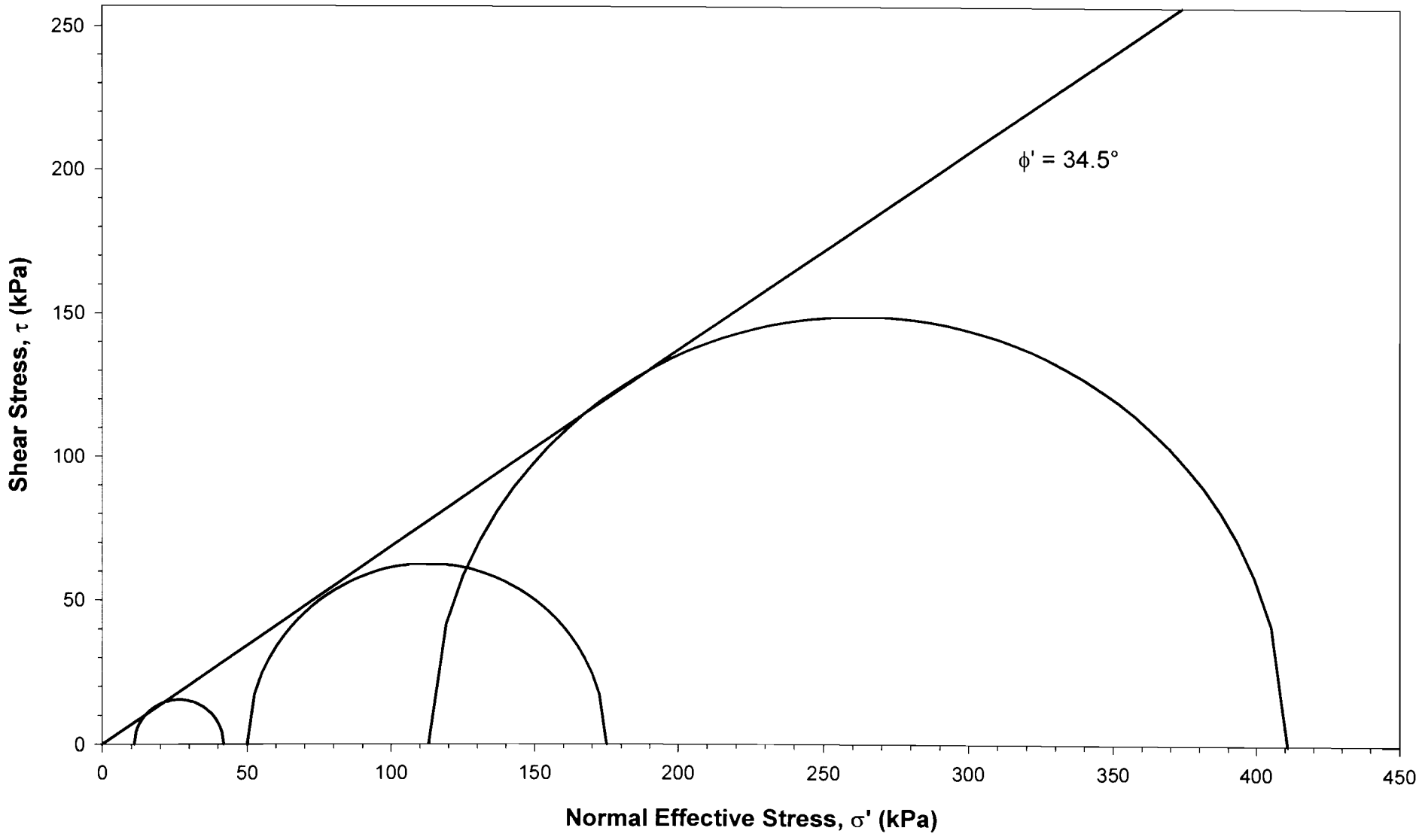

Figure 4-24: Mohr's Circles for reconstituted Mizpah whole tailings.

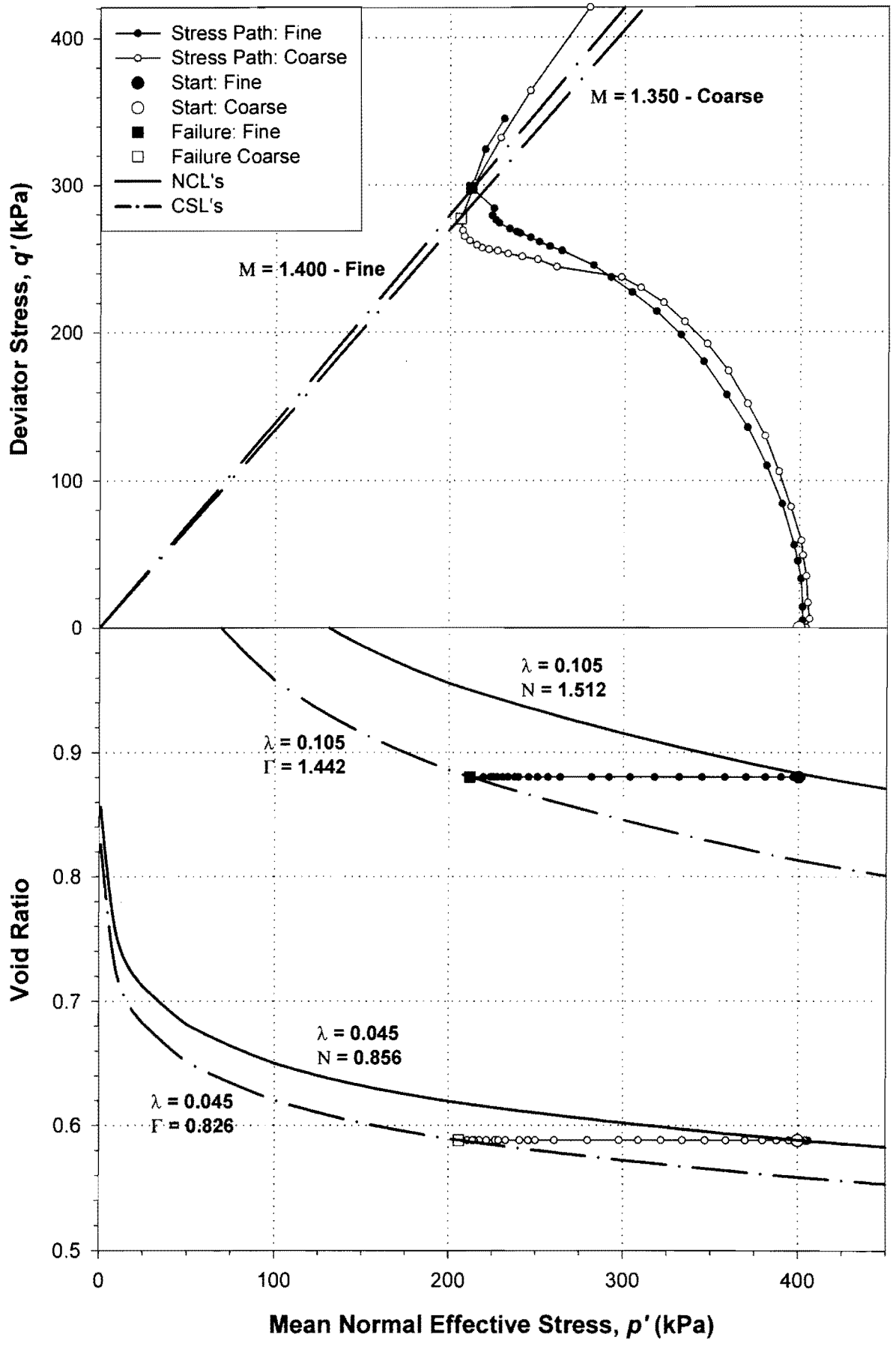

Figure 4-25: Critical state parameters for reconstituted Mizpah pond tailings.

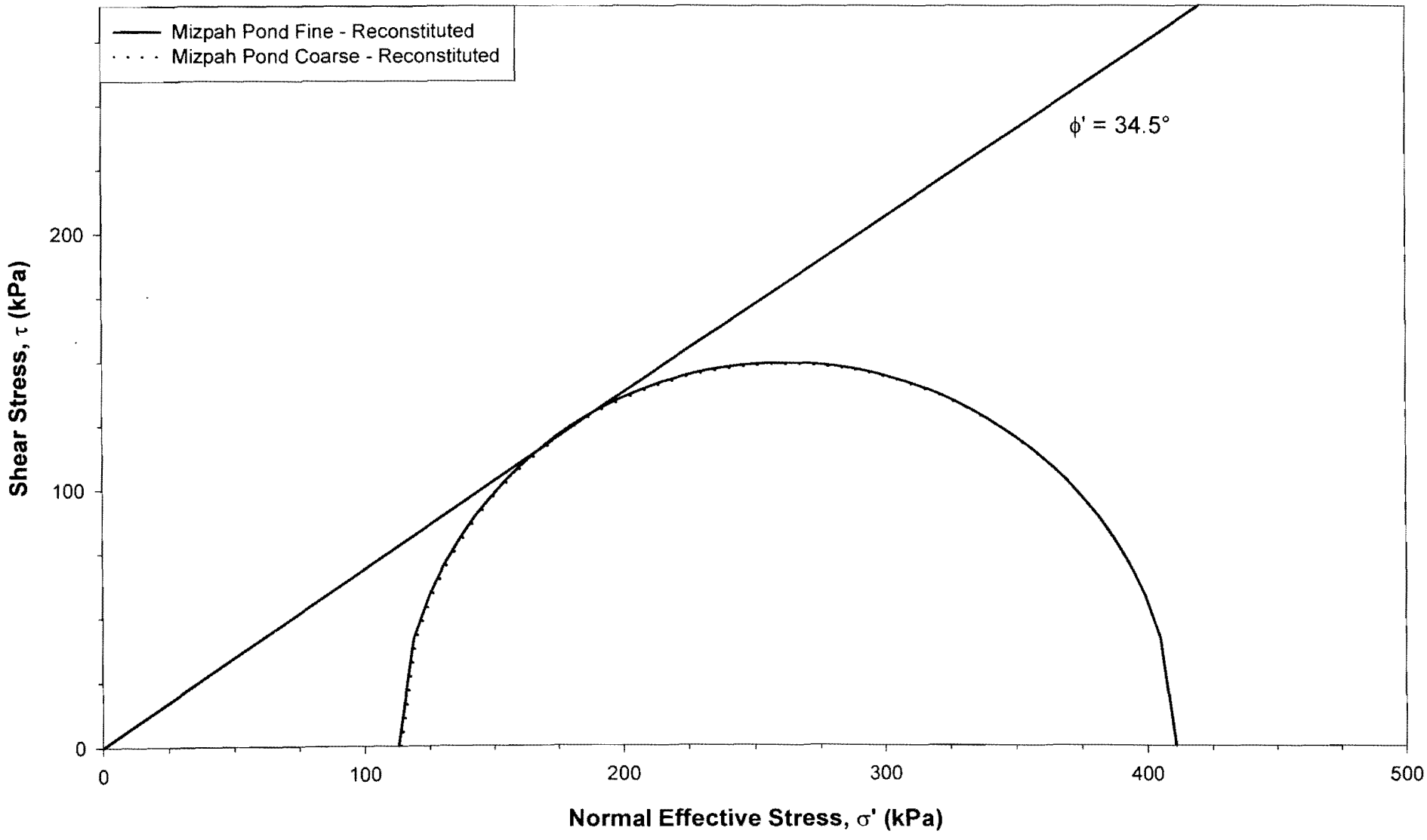

Figure 4-26: Mohr's Circles for reconstituted Mizpah pond tailings.

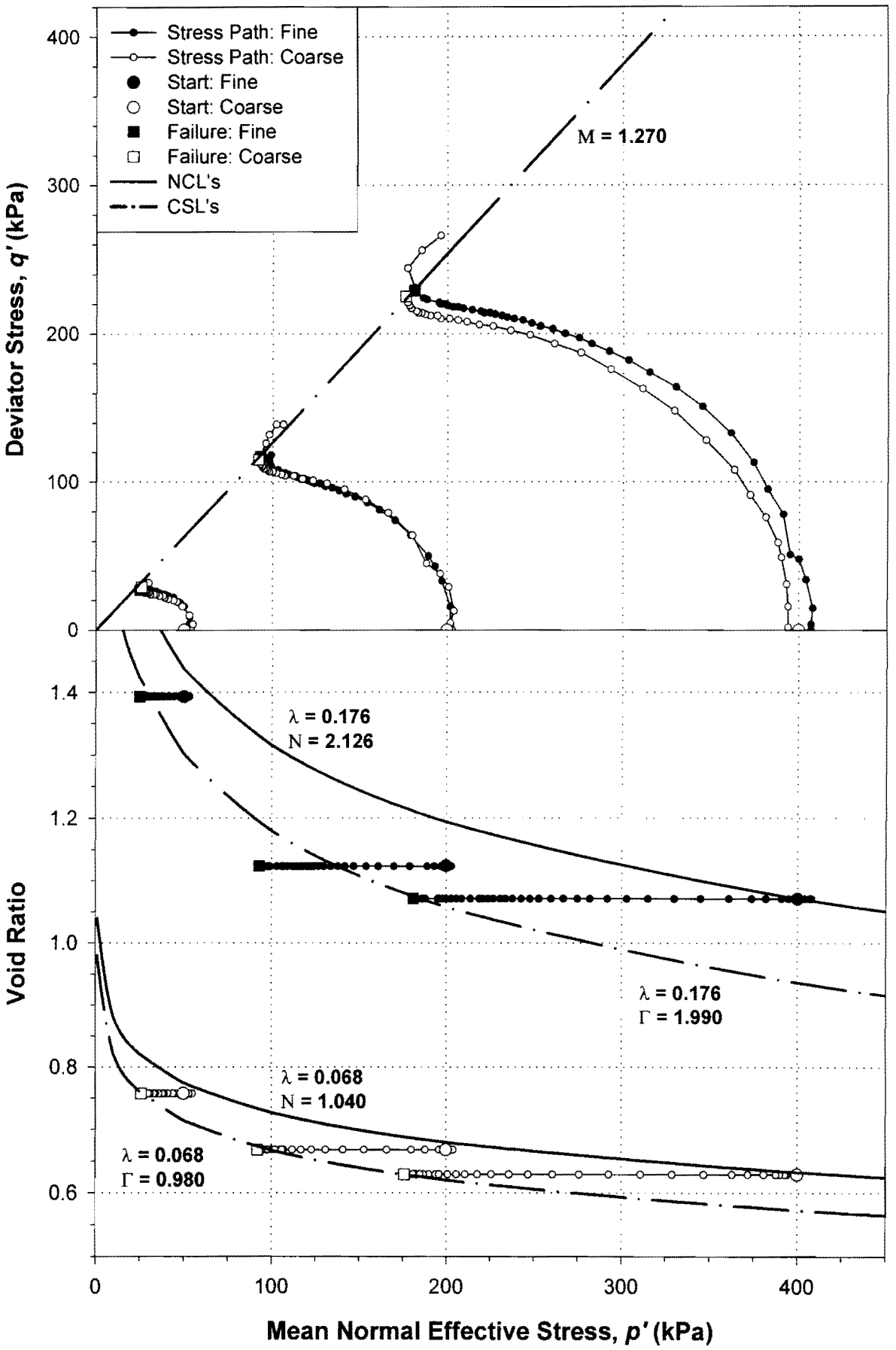

Figure 4-27: Critical state parameters for reconstituted Pay Dam penstock tailings.

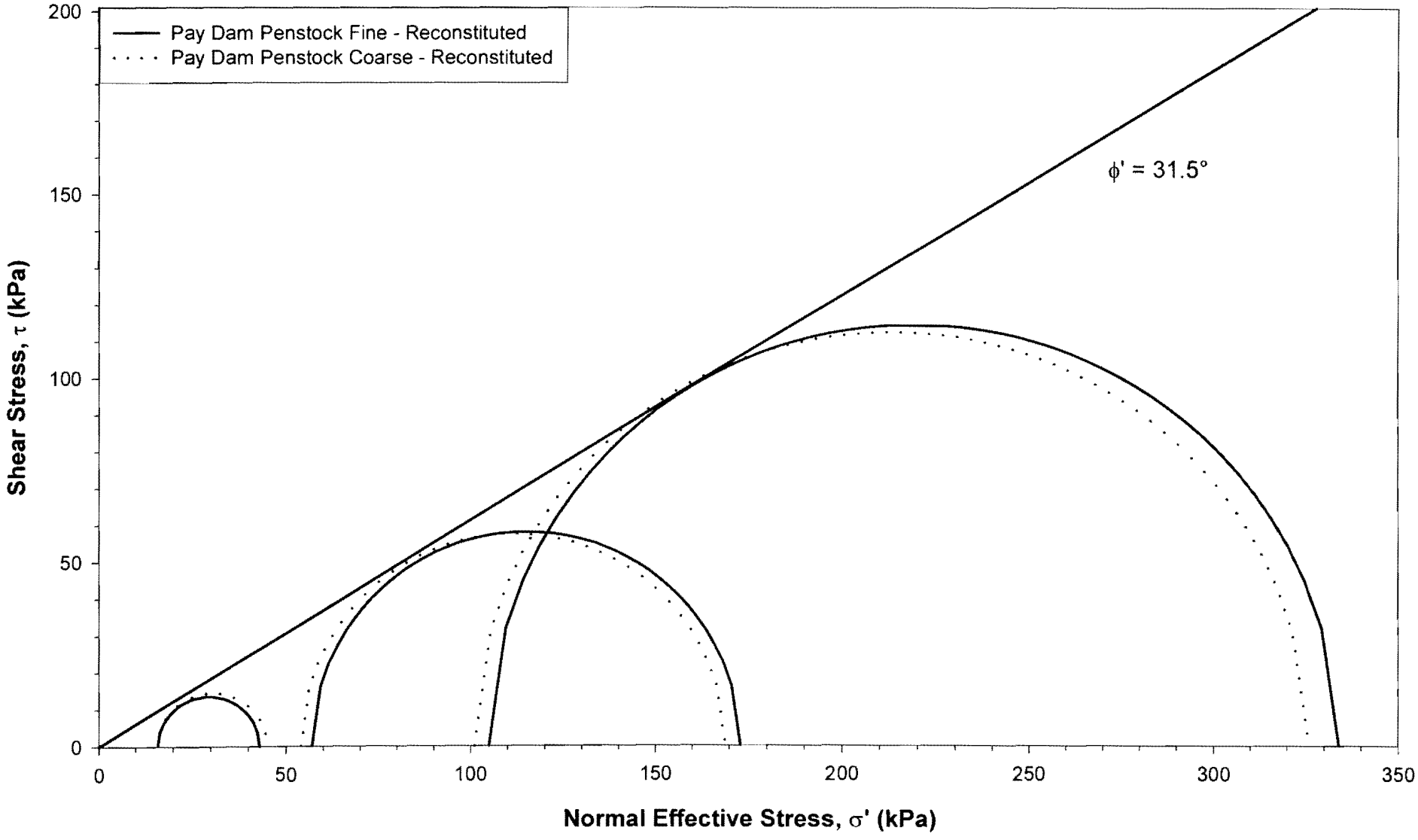

Figure 4-28: Mohr's Circles for reconstituted Pay Dam penstock tailings.

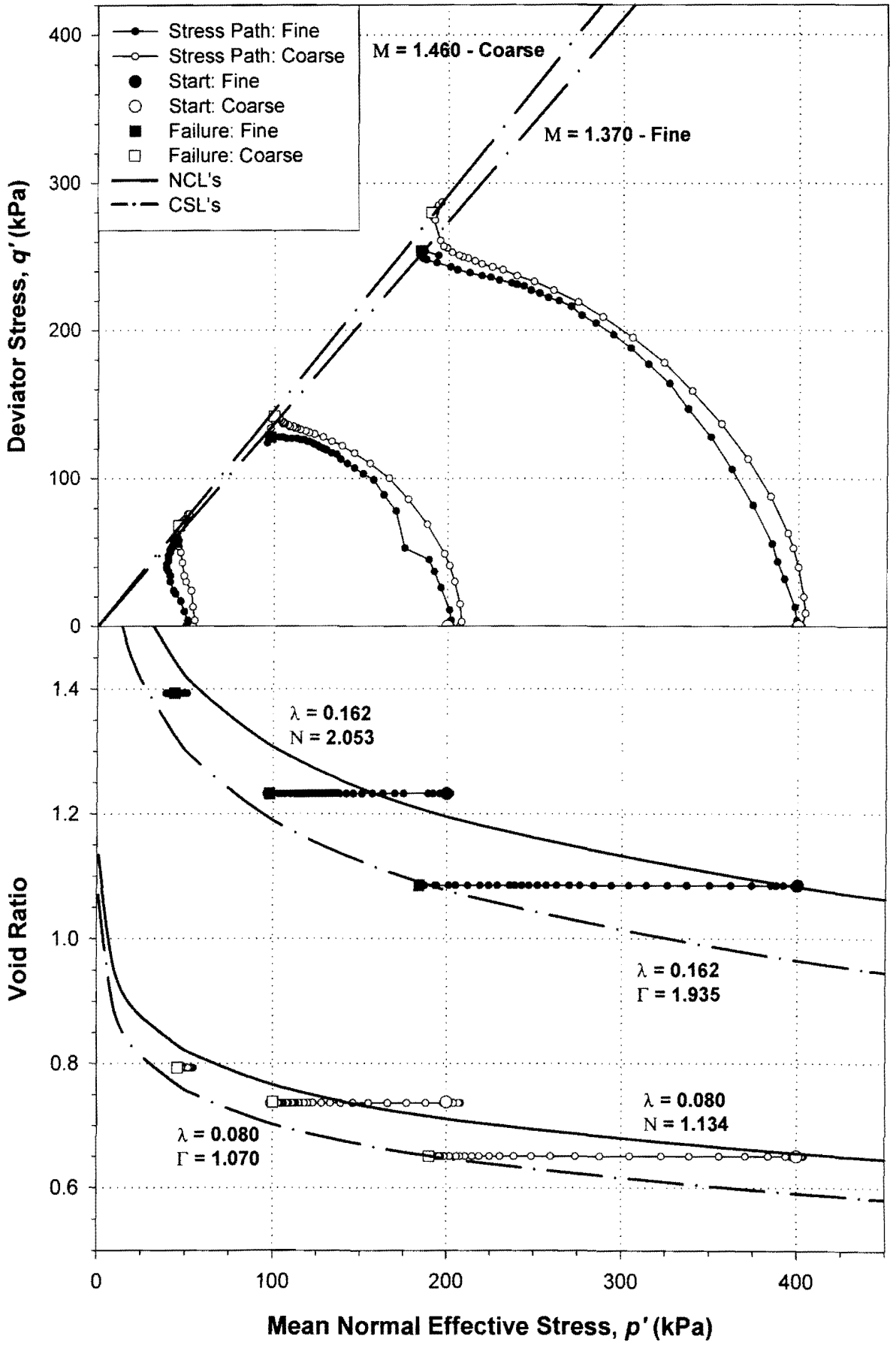

Figure 4-29: Critical state parameters for undisturbed Pay Dam penstock tailings.

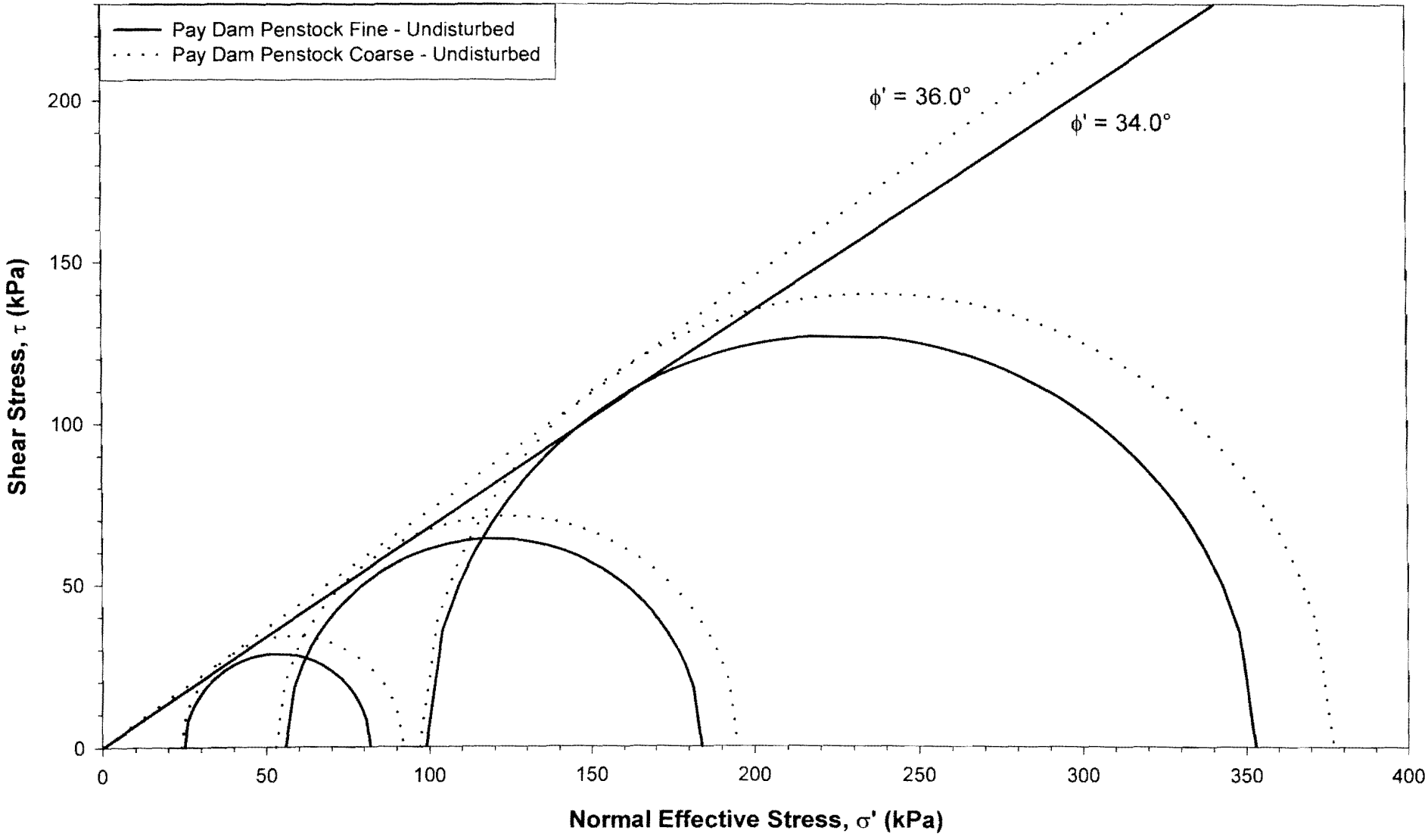

Figure 4-30: Mohr's Circles for undisturbed Pay Dam penstock tailings.

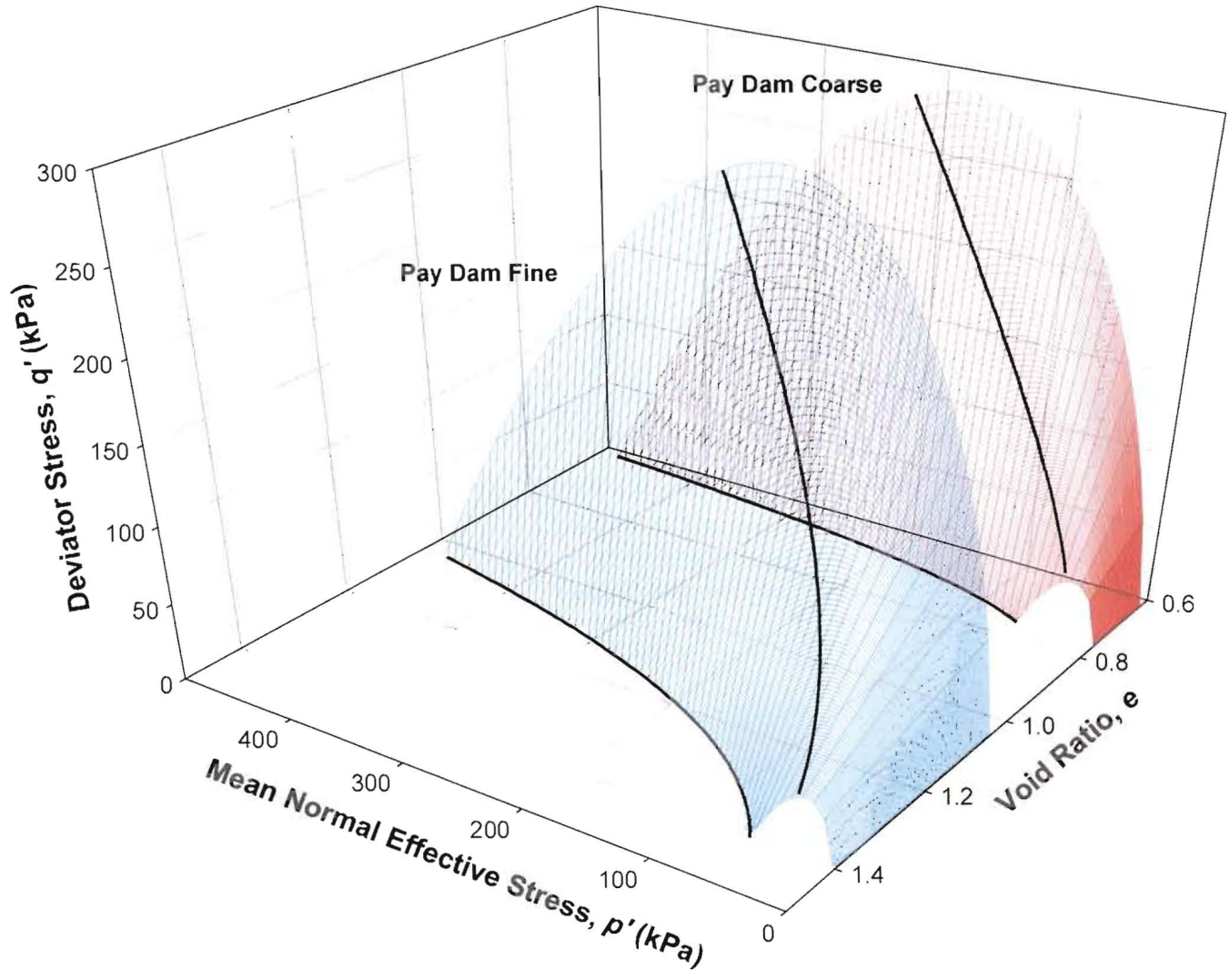

Figure 4-31: Isometric view of the Cam-Clay state boundary surfaces for Pay Dam penstock tailings.

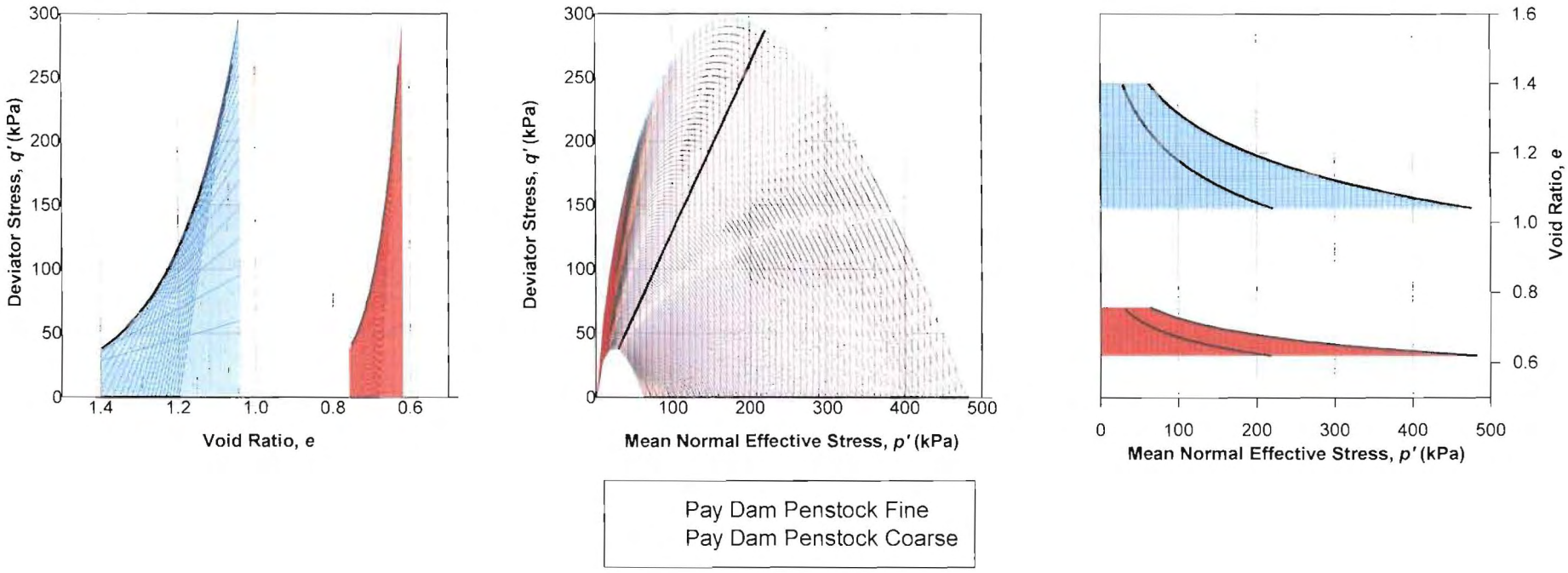

Figure 4-32: Two dimensional projections of the Pay Dam Cam-Clay state boundary surfaces.

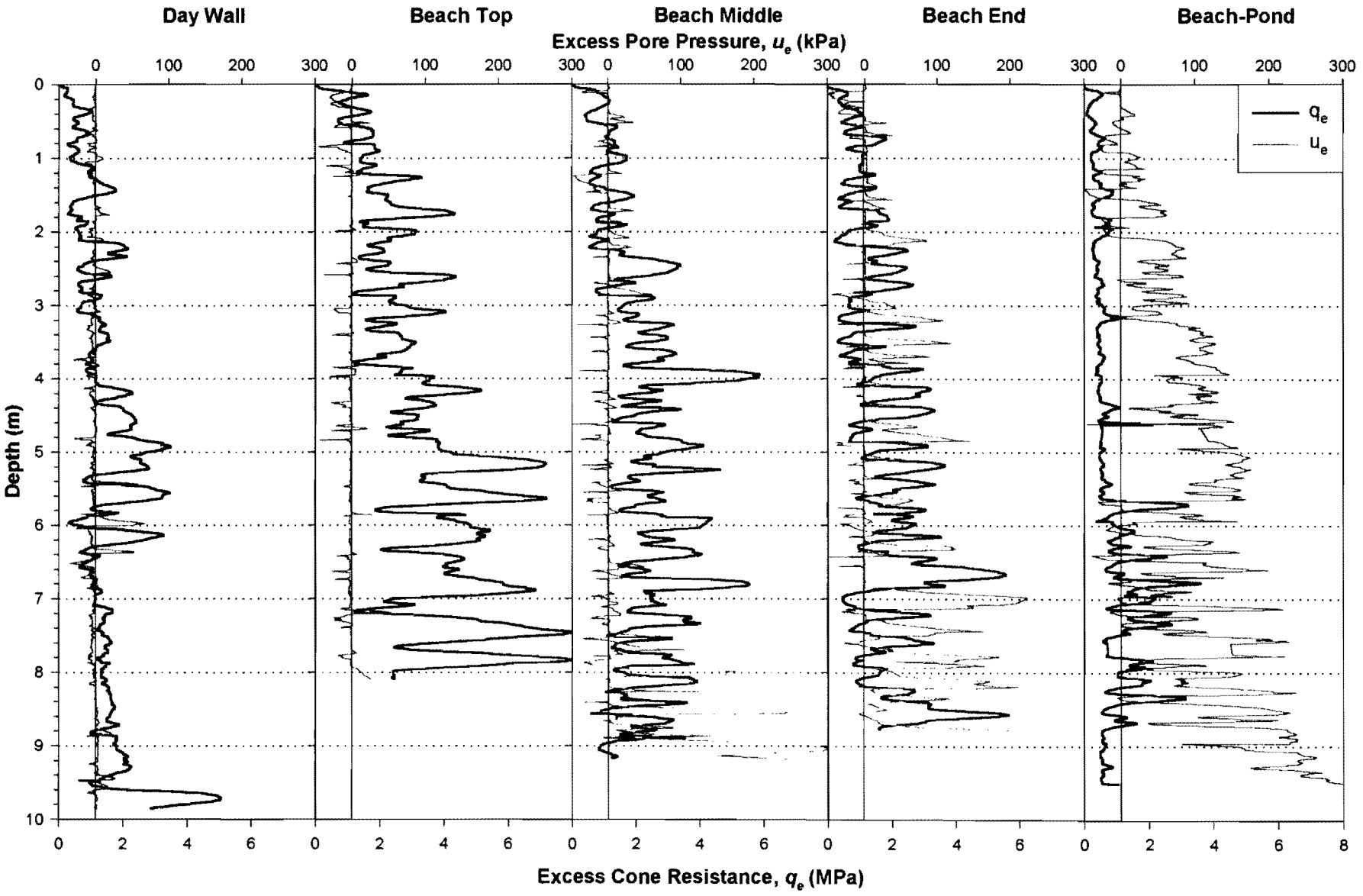

Figure 4-33: Piezocone probe results for a cross section of the Mizpah tailings dam.

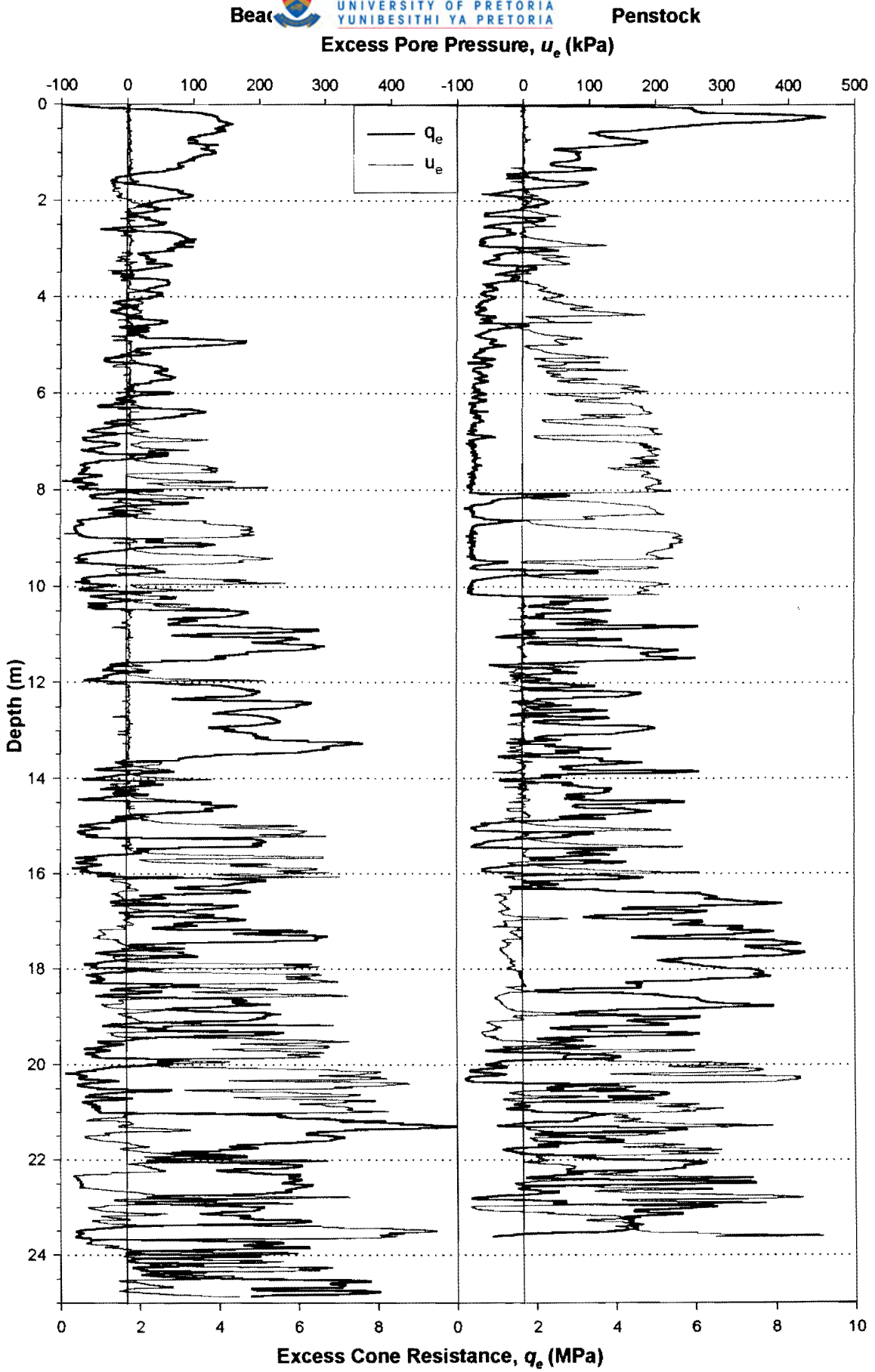

Figure 4-34: Piezocone probe results on Pay Dam for the Beach and Penstock locations.

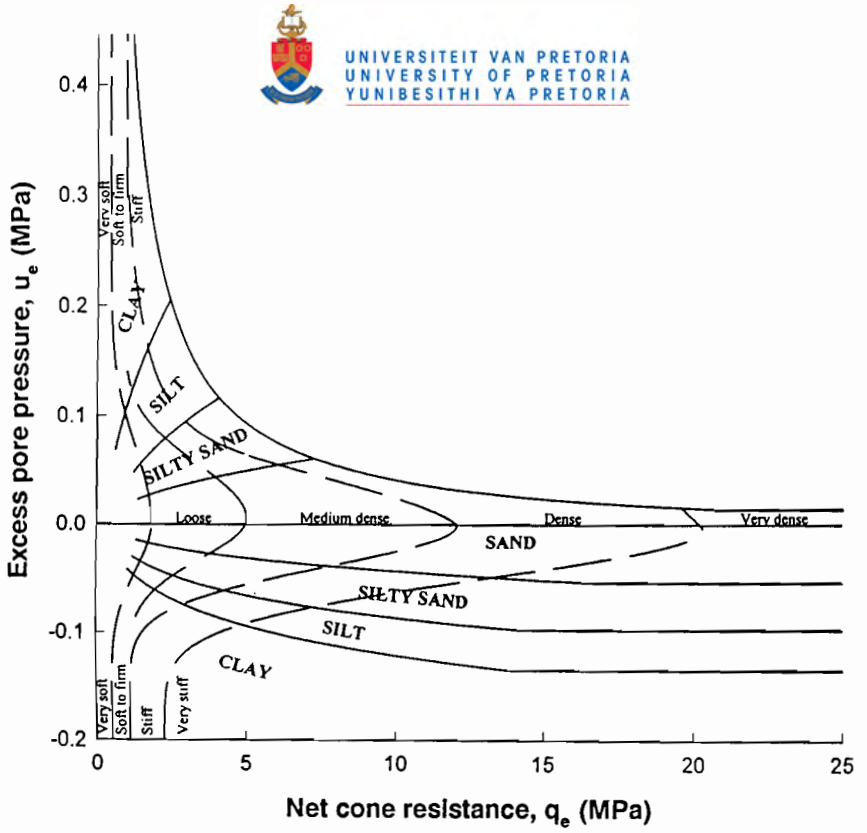

(a)

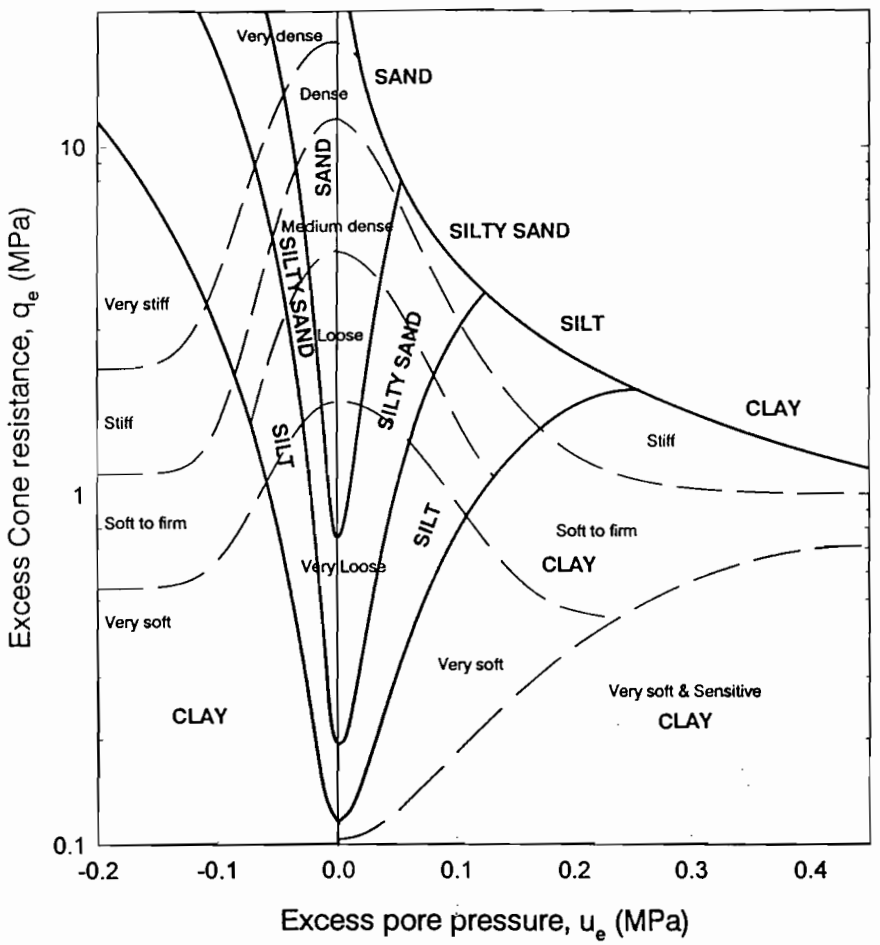

(b)

Figure 4-35: (a) The Jones and Rust (1982) soils identification chart for use with the piezocone, (b) as modified by the author.

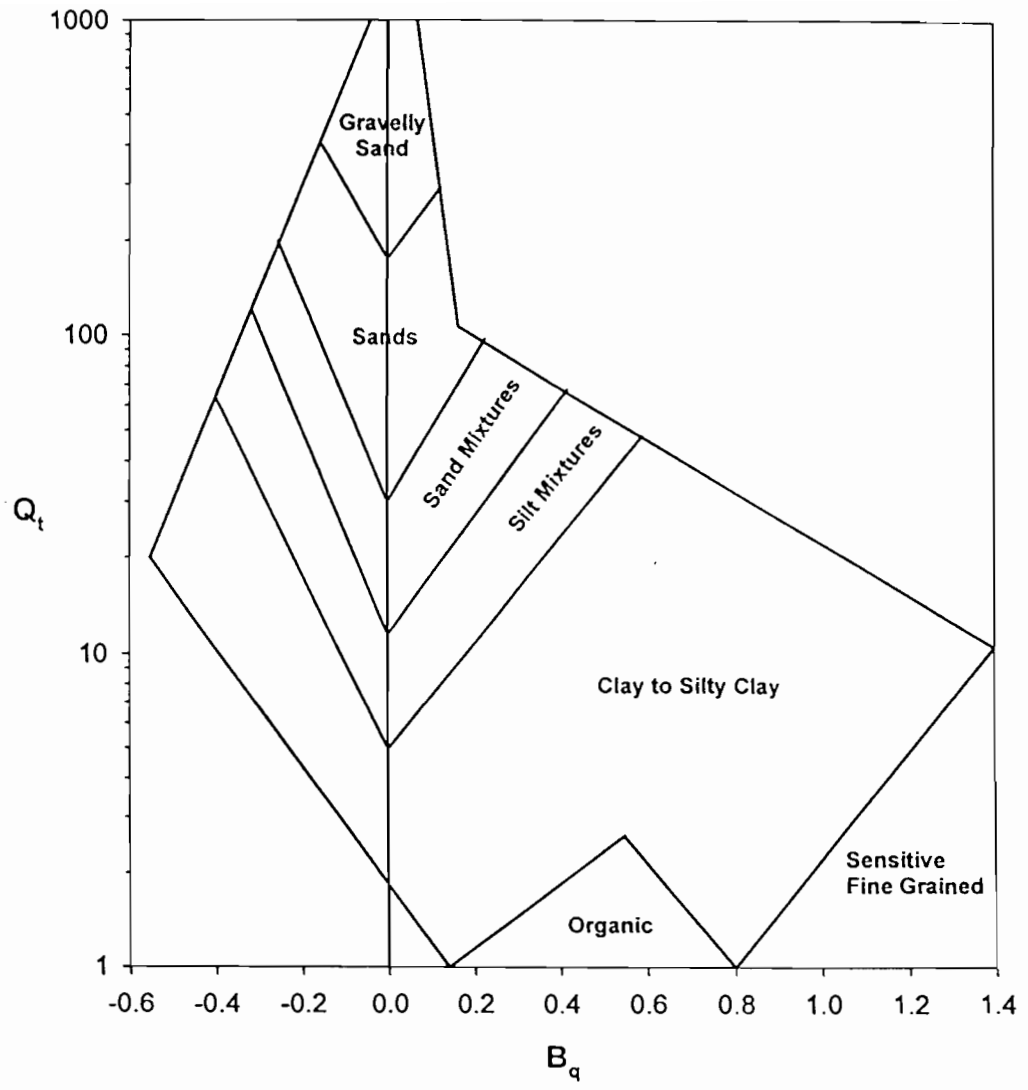

Figure 4-36: The Robertson and Campanella soils identification charts for use with the piezocone (Robertson, 1990).

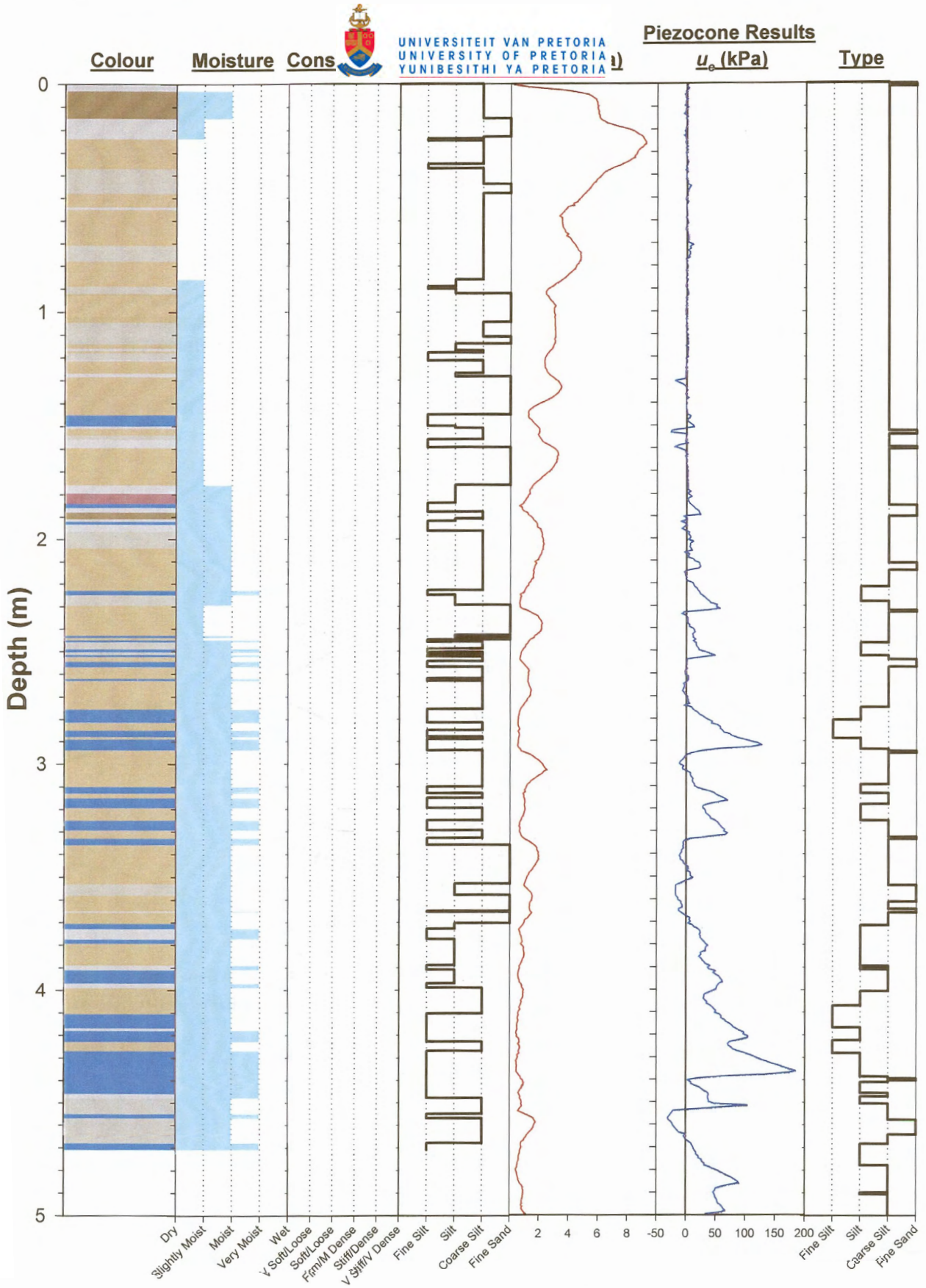

Figure 4-37: Piezocone penetration data compared with the in-situ profile for Pay Dam Penstock.

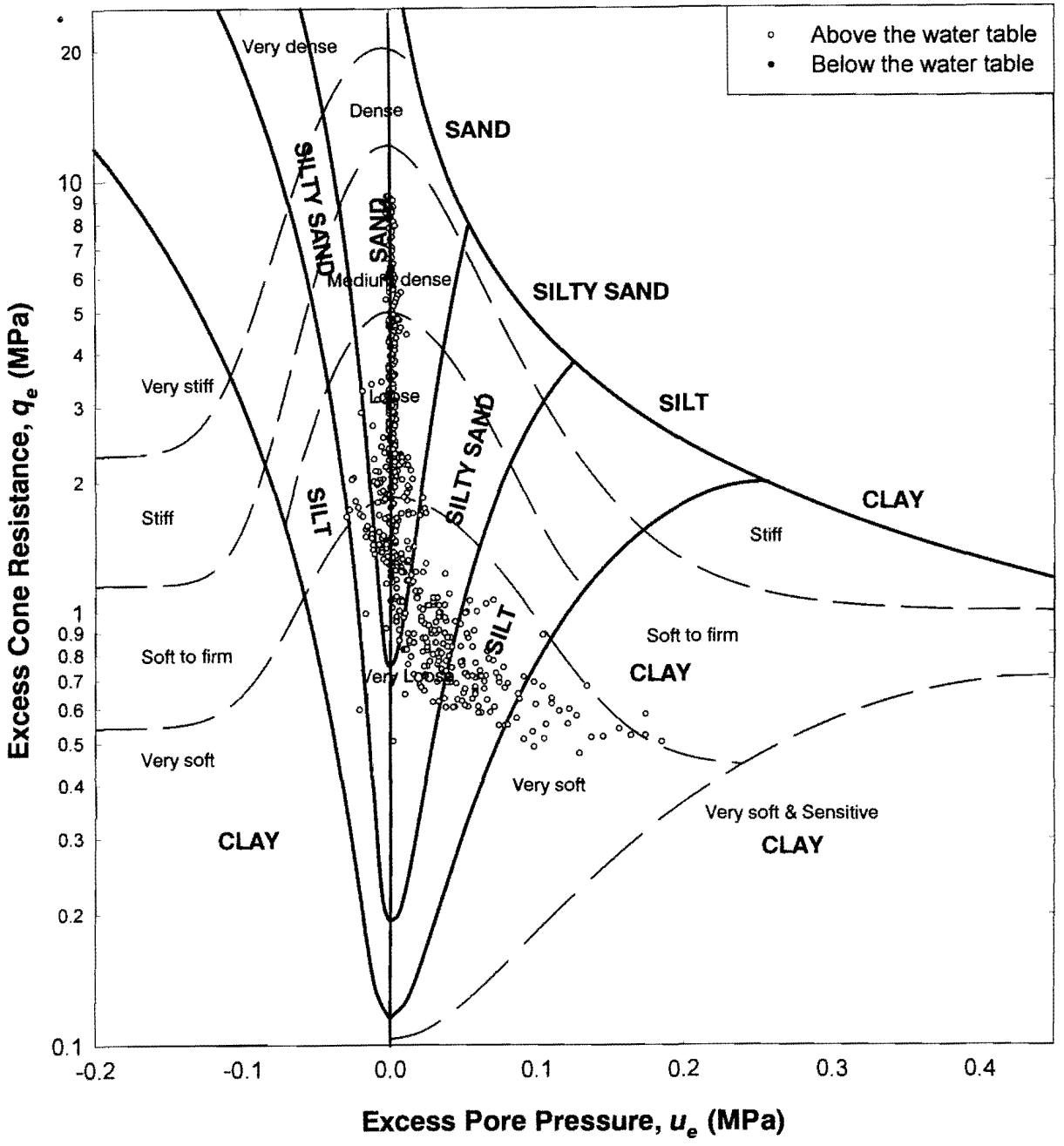

Figure 4-38: Penetration data for Pay Dam Penstock represented on the soils identification chart.

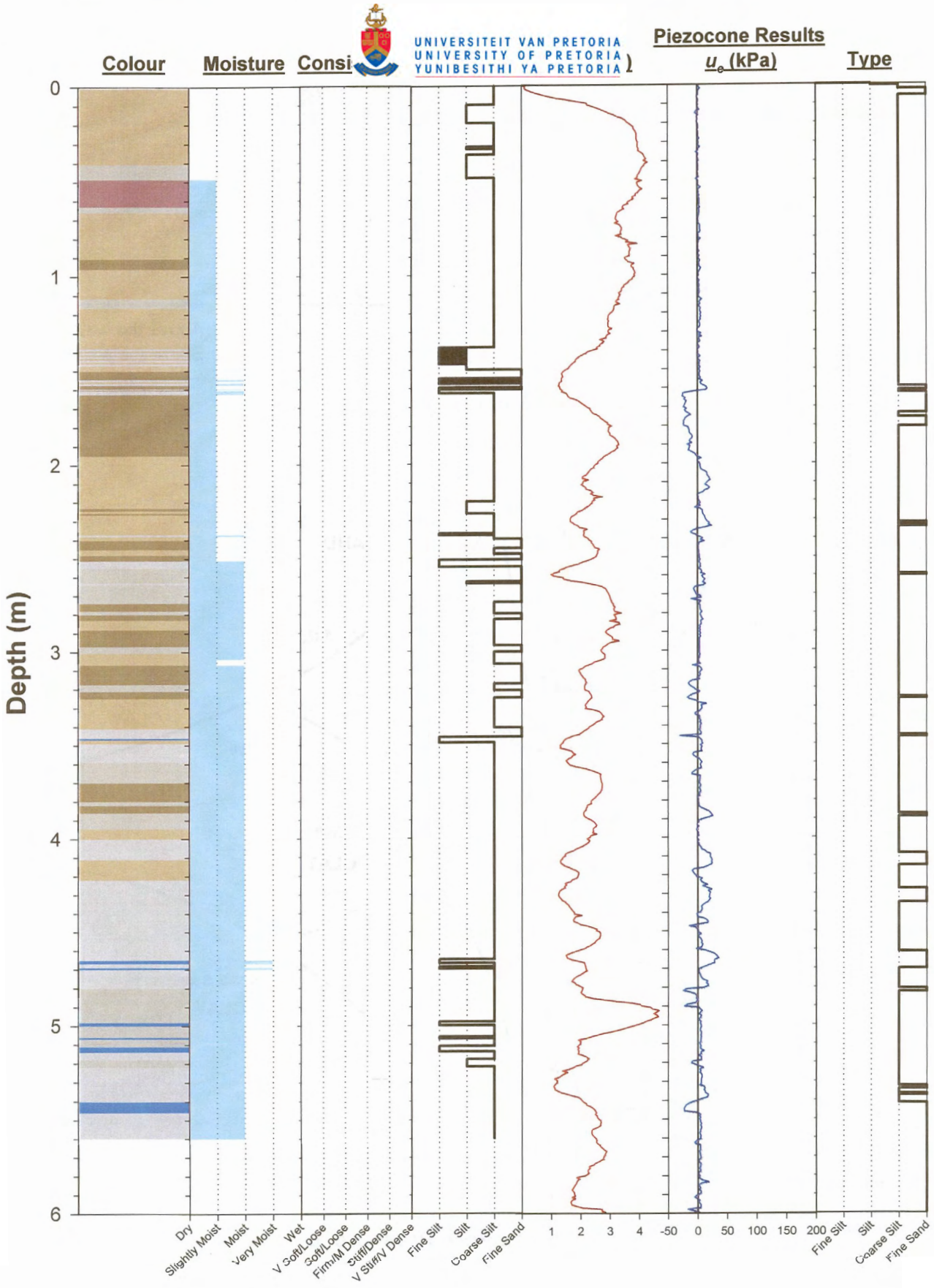

Figure 4-39: Piezocone penetration data compared with the in-situ profile for Pay Dam Beach.

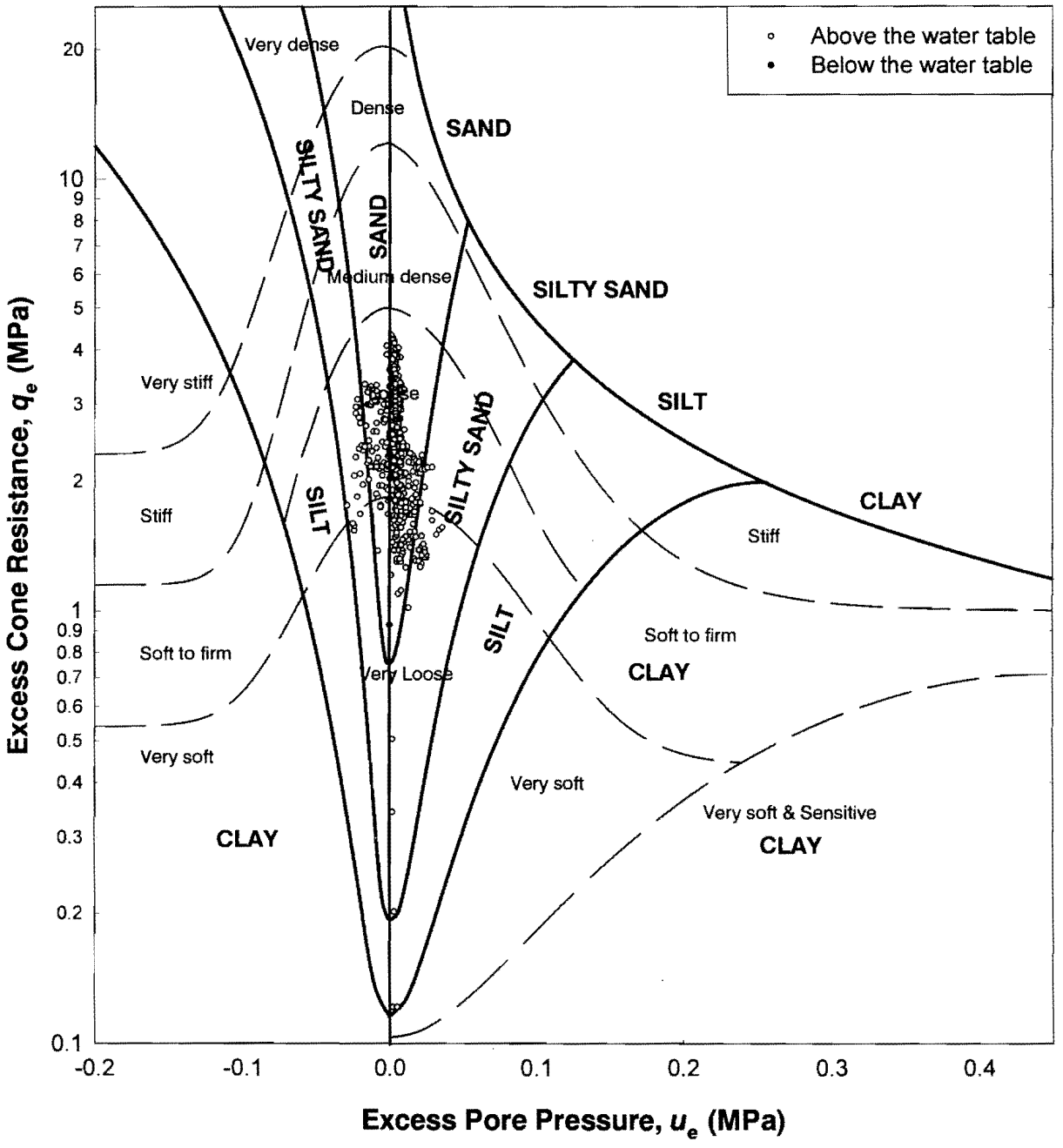

Figure 4-40: Penetration data for Pay Dam Beach represented on the soils identification chart.

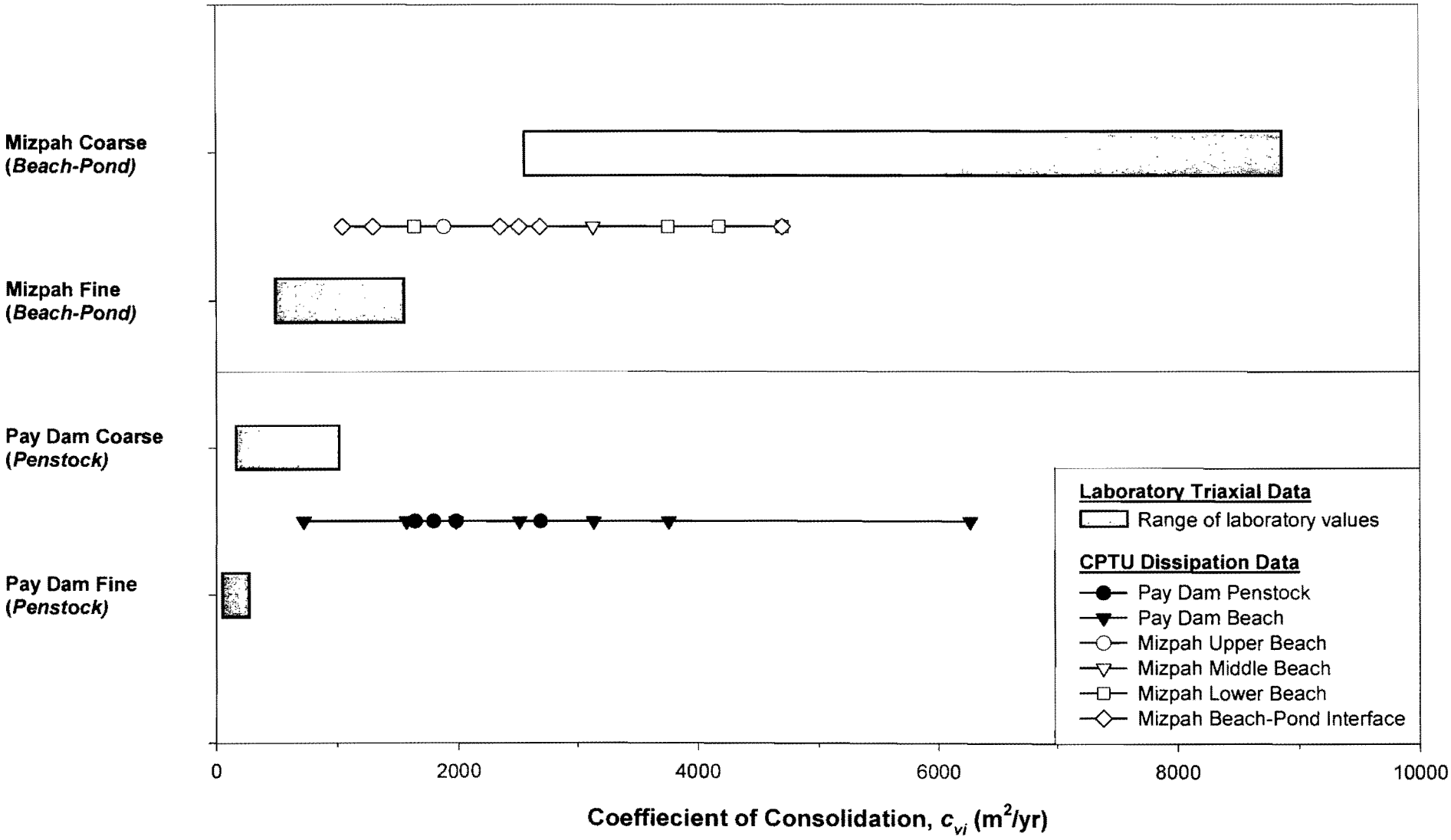

Figure 4-41: Estimates of the coefficient of consolidation based on Piezocone dissipation tests in Mizpah and Pay Dam.

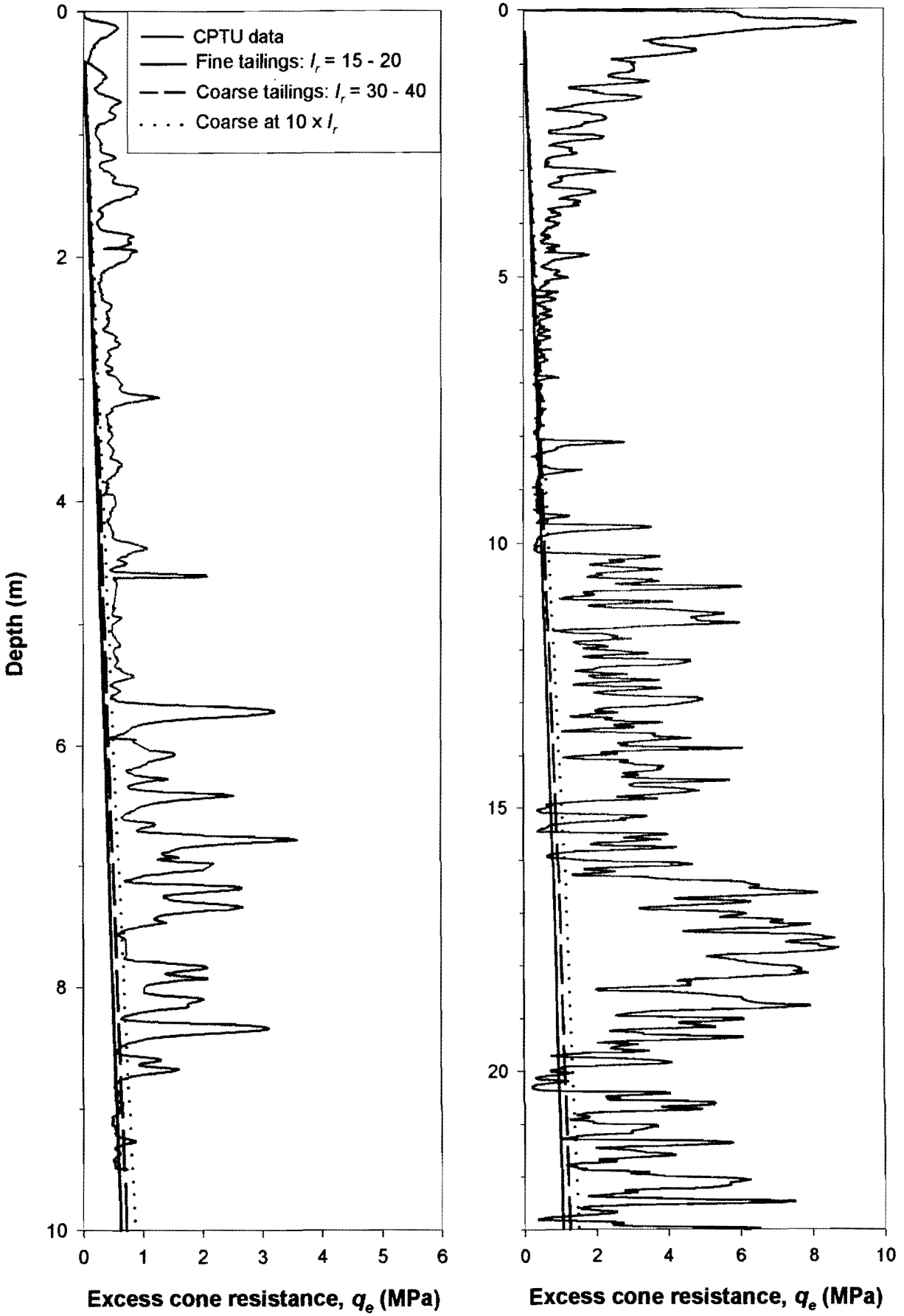

Figure 4-42: Use of cavity expansion theory to model cone penetration in saturated tailings.

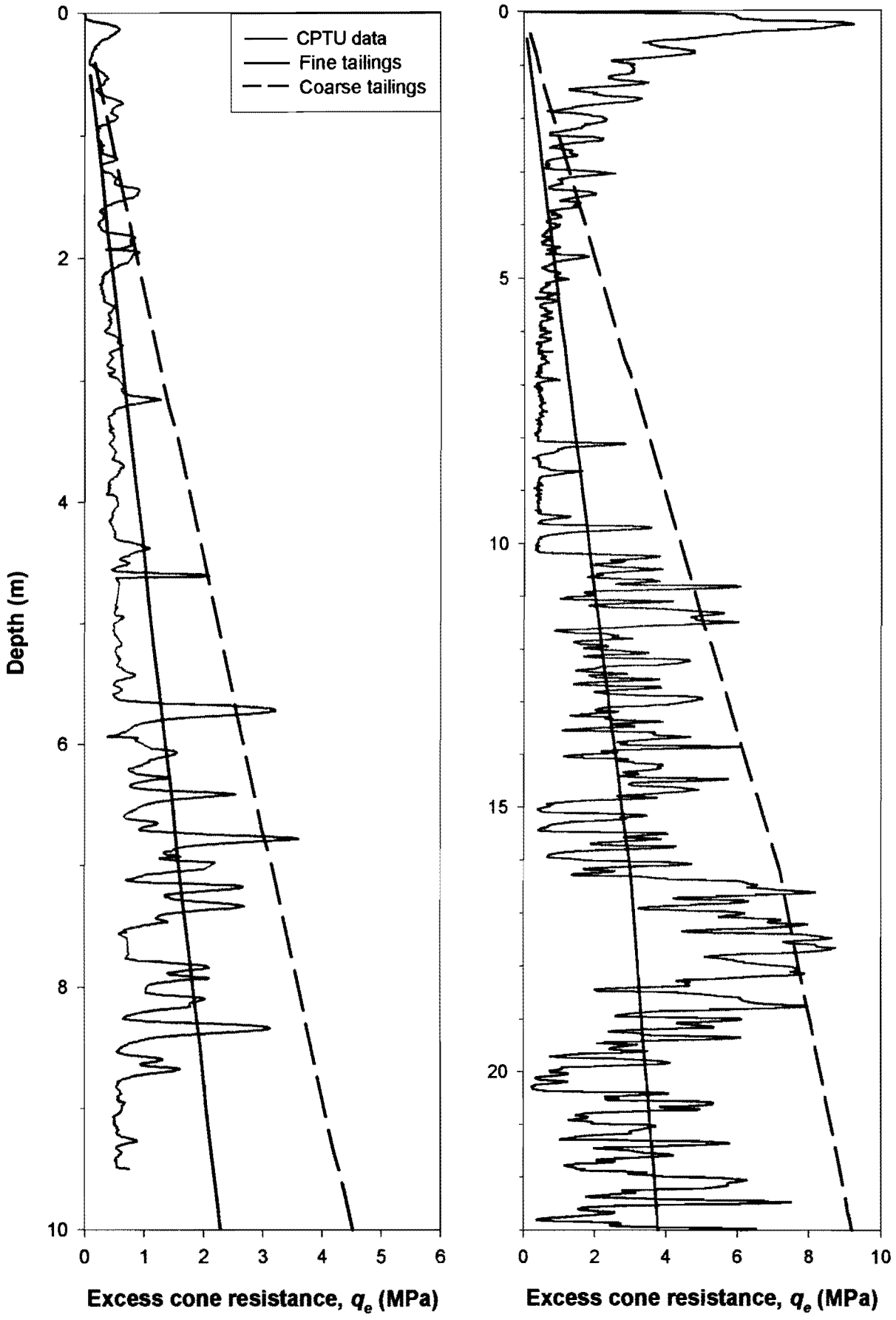

Figure 4-43: Use of the effective stress formulation proposed by Senneset et.al. (1982; 1988) to model the CPTU in tailings.

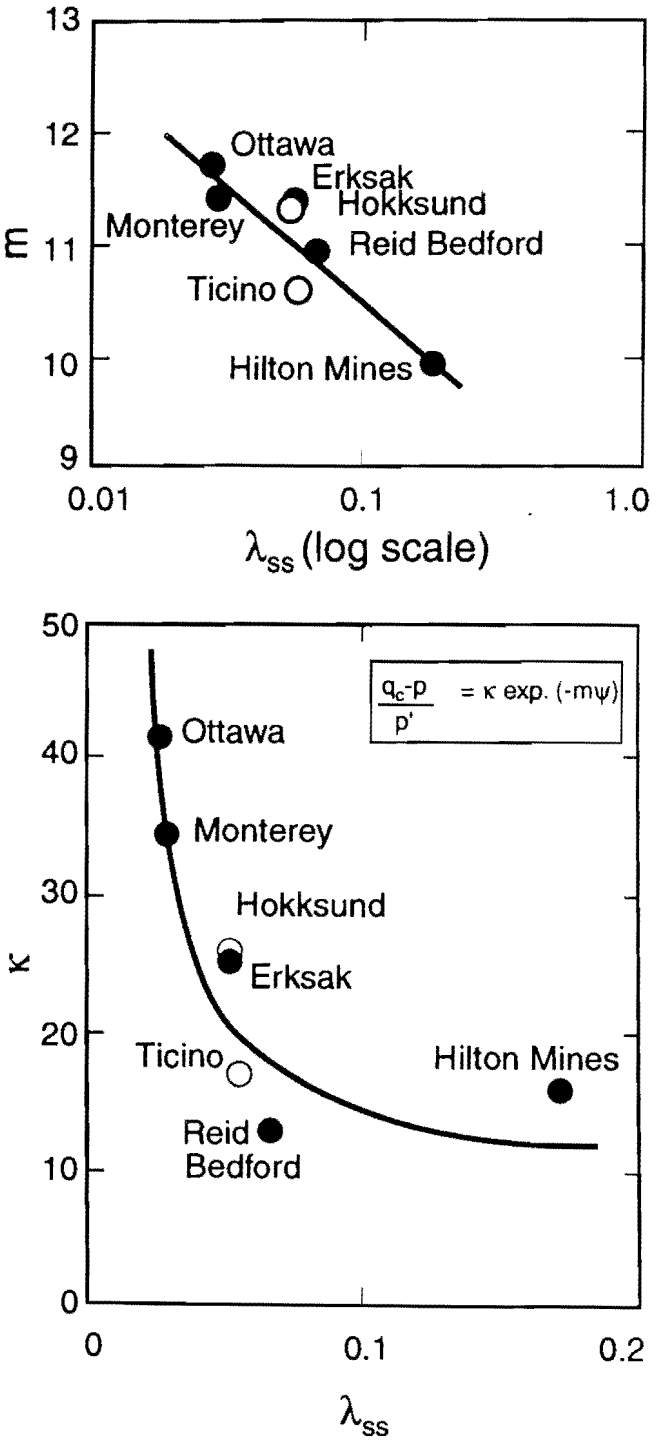

Figure 4-44: Normalised state parameters κ and *m* (Been et.al., 1986).

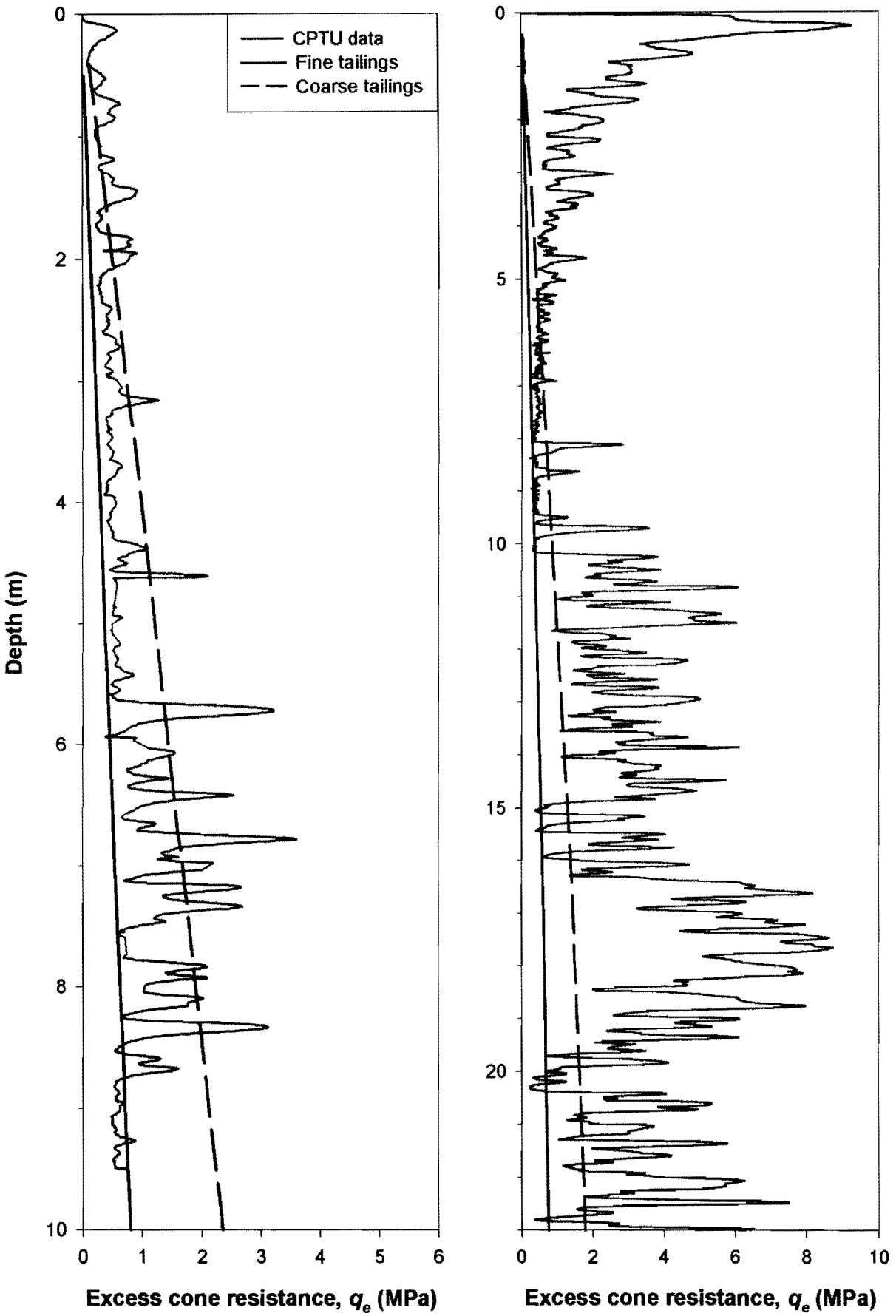

Figure 4-45: Use of the state parameter approach proposed by Been et.al. (1985) to model the CPTU in tailings.

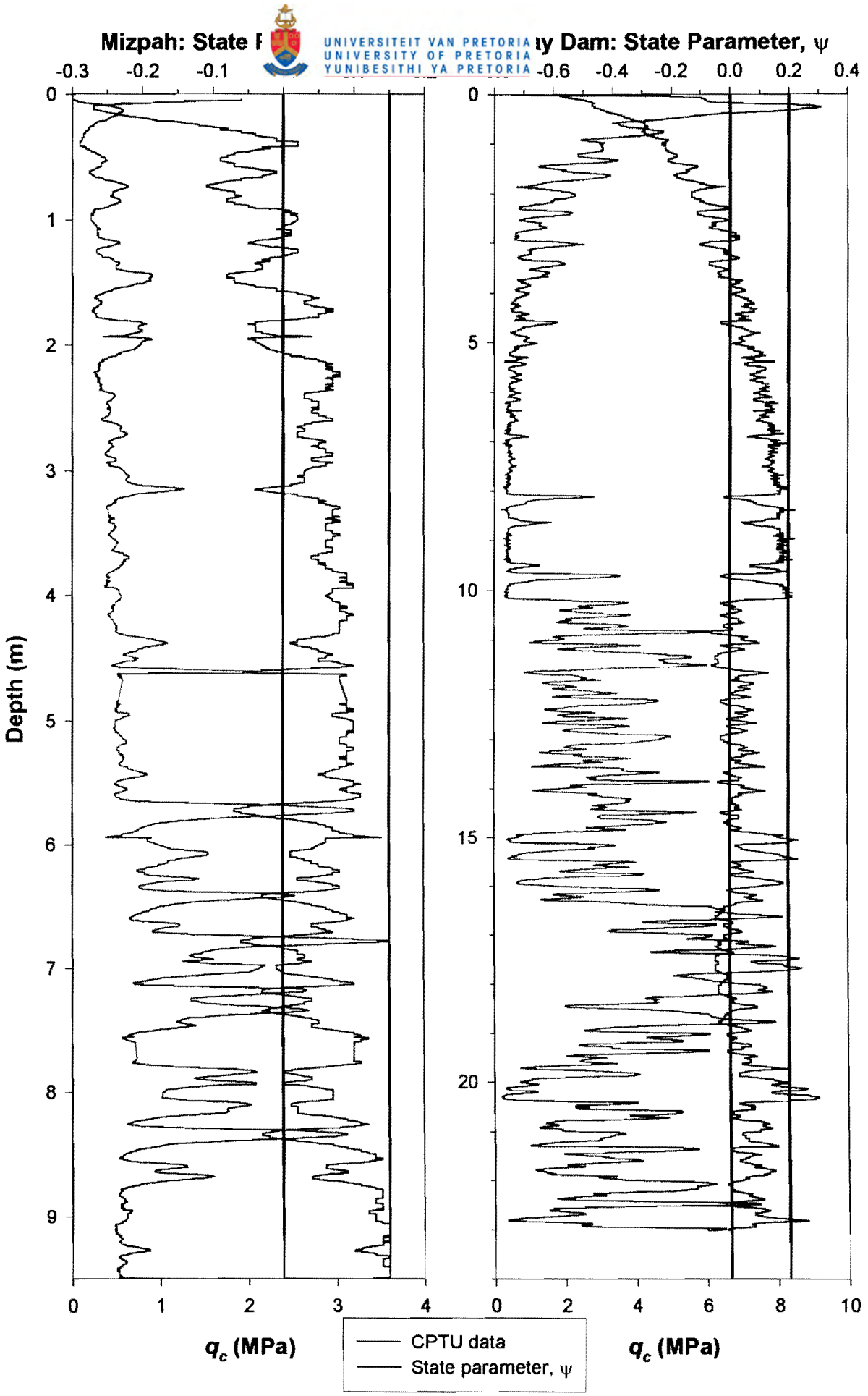

Figure 4-46: State parameter values from field penetration data.

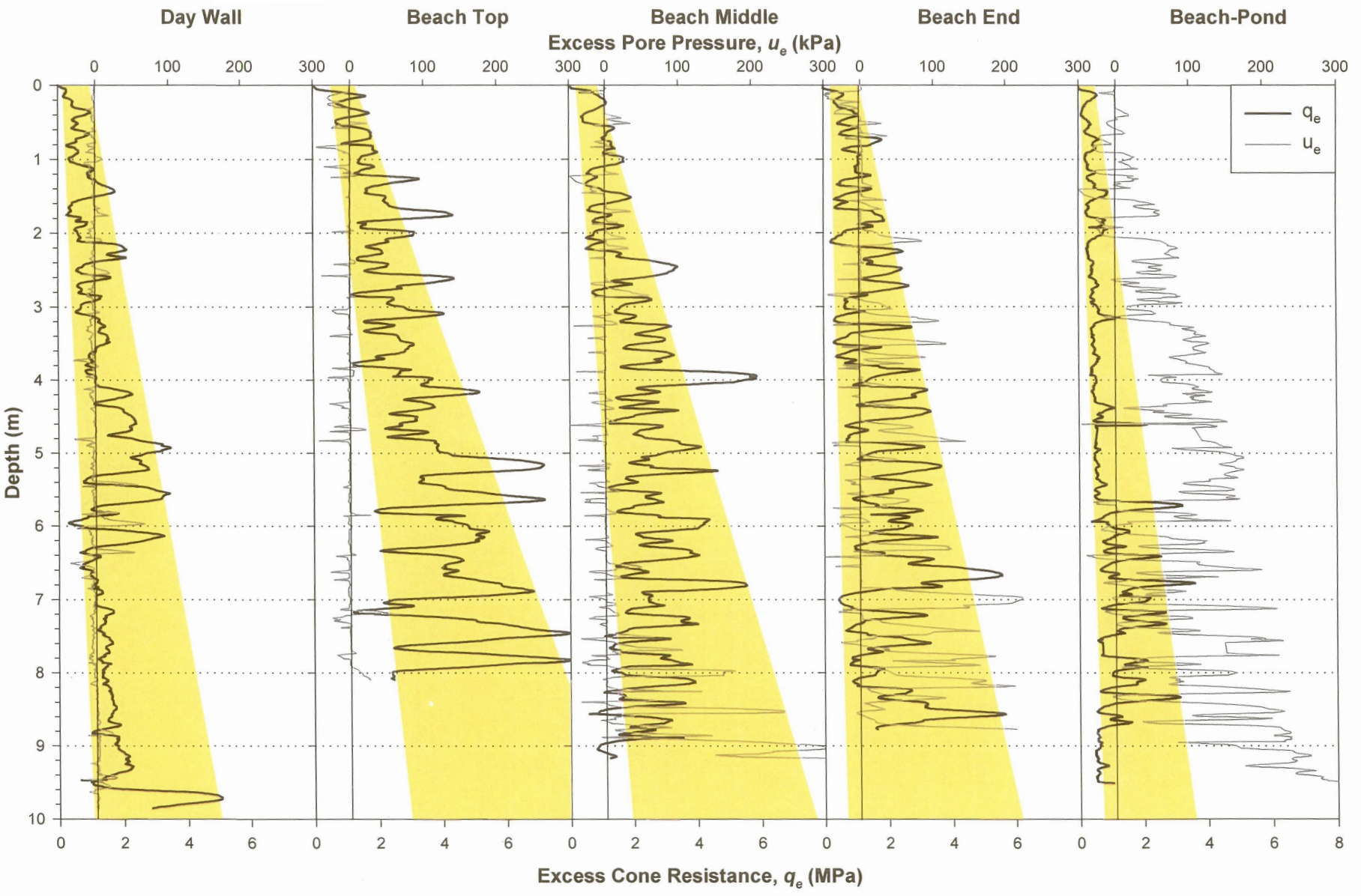

Figure 4-47: CPTU cross section of Mizpah highlighting the lower and upper boundary cone resistance measurements.

CHAPTER 5

CONCLUSIONS

The consequences of a tailings dam failure are devastating and evidence of these abounds in the literature. Apart from the more than 1000 fatalities in the last century, countless millions of rand in property damage and production losses, not to mention devastation of the environment, have resulted from tailings incidents. South Africa, today, is even more at risk as financial pressures are mounting on mining operators as a result of lower gold prices and dwindling gold reserves. Another major concern is the development of settlements adjacent to, and in some cases even on tailings structures.

The safe design, construction, operation and reclamation of impoundment structures require an understanding of the nature and behaviour of tailings as a construction material. Of particular interest is the composition of this man-made material and the influence it has on the in-situ state of tailings. A research program was, therefore, initiated at the University of Pretoria to investigate the composition and state of South African gold tailings from the Witwatersrand gold reefs. Samples for this study were collected from the tailings delivery slurry and from the pond areas of two tailings impoundments at Vaal River Operations in the far West Rand. Piezocone soundings were also made through a cross section of one of the dams and at the sampling locations on both dams.

This chapter brings together the main conclusions of the study. The work has provided a better understanding of the condition and behaviour of gold tailings in a typical impoundment, viz.:

(a) The composition of the tailings delivery slurry as well as typical fine and coarse deposits in an impoundment.

(b) The normalised compression behaviour of tailings.

(c) Strength characteristics with reference to pre- and post failure stress paths in undrained loading.

(d) Interpretation of in-situ piezocone data in tailings.

5.1 TAILINGS DISPOSAL IN SOUTH AFRICA

5.1.1 Impoundment design, construction and operation

- Tailings dams are generally not designed with the same conservatism as conventional water-retention dams, for economical reasons.
- South African gold tailings impoundments are almost exclusively designed and operated as perimeter ring dikes with the tailings embankment raised, upstream, throughout the lifetime of the impoundment using the daywall-nightpan paddock system. Deposition is sub-aerial by open-ended pipe discharge, or in some cases by spigotting or cycloning. The daywall is raised to provide adequate freeboard, but also allowing maximum time, three weeks on average, for evaporation and desiccation to improve the mechanical properties, especially density, of the material. The rate-of-rise of the embankment commonly ranges between 1 and 3 m per year. Impoundment complexes can be operated as one or more isolated compartments, each with its own delivery and decant facilities. Decant systems are almost always of the penstock type with internal drainage structures absent in all but the most recent developments. In addition to internal and surface drainage measures, ground level catchment paddocks are provided around the perimeter of the dam to intercept contaminated runoff from the side slopes.
- When impoundments are raised by cyclone construction, the properties of the embankment building material can be optimised by controlling the cyclone underflow. This underflow should preferably contain only the coarse and bulky sand particles. Impoundments that are raised by open ended pipe discharge rely on particle sorting processes to grade the deposited material from coarse to fine, from the embankment to the decant penstock. However, with the paddock system of construction, significant amounts of fines are deposited in the daywall, especially at low points between discharge stations. This study has shown that a piezocone profile at the daywall compares better to a profile at the beach-pond interface than ones at the upper or middle beach areas of the dam. These impoundments, although more cost effective, rely heavily on the effects of desiccation to improve the stability of the embankment, as well as on proper phreatic surface control and continuous monitoring.
- Control of the phreatic surface from a design and operational point of view is the single most important factor in maintaining the stability and serviceability of a tailings impoundment. The controlled rate-of-rise and sequence of deposition should be tailored in relation to the post depositional properties of the tailings and any internal drainage structures to ensure both adequate storage capacity and a safe structure. The drainage properties of tailings are highly dependent on the in-situ composition and

state of the material. Entrapment of significant amounts of fines in the embankment wall will severely affect the drainage conditions in this critical area of an impoundment.

- The soil forming process on a tailings impoundment includes transportation of sediments, sedimentation, primary consolidation and, as shown in this study, significant secondary consolidation or creep. Depositional practices, variations in the mill product, and soil forming processes result in a highly layered profile with fine and coarse deposits alternating over small depths. Gold tailings do not segregate readily on deposition and heavy reliance is placed on desiccation to improve the properties of material deposited on or close to the perimeter embankment.
- On a typical gold tailings impoundment, raised by the daywall-nightpan paddock system, the composition of material at any location is highly dependent on the depositional sequence. As discharge stations are cycled around the perimeter of the dam, alternating layers of fine and coarse tailings are deposited at a specific location. For example, during this investigation it was found that layers of coarse tailings had been deposited within the decant pond. This happens when coarse particles are carried directly into the pond by concentrated flow. Scour channels of concentrated flow are common on the beaches of active impoundments. During the next cycle of deposition, when the concentrated flow channel is located somewhere else, a fine layer is deposited over the coarse layer, etc.

5.2 COMPOSITION OF GOLD TAILINGS

5.2.1 Delivery Slurry

- Gold tailings have been classified as a low to high plasticity, fine, hard and angular rock flour, slurried with process water in a flocculated slightly alkaline state together with soluble salts.
- Pulp densities normally range between 25 and 50% (dry density of 300 to 750 kg/m^3) when delivered to the impoundment site.
- The rheology of a gold tailings slurry lies somewhere between a Bingham plastic and a Newtonian fluid.

5.2.2 In-situ Composition

Electron microscope, energy dispersive x-ray spectrometry and powder x-ray diffraction technologies were fully exploited, together with standard soil mechanics laboratory tests, to determine the composition of the tailings.

- *Mineralogy:* It is common practice in South Africa to separate tailings particles into two classes, i.e. tailings sands (particles fractioned by sieve tests, > 63 μm), and tailings slimes (particles fractioned by sedimentation, < 63 μm). This study has shown that tailings consist almost exclusively of tectosilicates and sheet-like phyllosilicates, with quartz being by far the most abundant mineral. The coarser tailings sands are predominantly pure silica quartz, with up to 10% illite clay minerals. Tailings slimes on the other hand, although still dominated by quartz, contain significant amounts of phyllosilicates (20% muscovite, 15% illite and 20% pyrophyllite, kaolin and clinochlore) as well as traces of pyrite and other sulphides. Gold tailings, therefore, contain significant amounts of clay fines, and these can be expected to have a major effect on the mechanical behaviour of the material.
- *Specific gravity:* G_s normally ranges between 2.5 and 3.0 Mg/m^3. In this study the tailings had a specific gravity of 2.74 Mg/m^3, including the delivery slurry and all other samples collected, irrespective of sampling location. It is suggested that segregation processes on a gold tailings impoundment are driven by gravity rather than size. The sizing of the particles, according to density, is such that deposited layers are all at a constant specific gravity, irrespective of grade.
- *Grading:* Fully dispersed gradings were uniformly distributed in the fine sand and silt-size ranges with approximately 2% coarser than 200 μm, 10% finer than 2 μm and at least 50% slimes. Variations in the gradings between fine and coarse tailings were largely around the median particle size, D_{50}, which ranged between 6 and 60 μm. These gradings are representative of the near full range of published gradings from gold tailings literature. Non-dispersed the fines were flocculated and/or attached to the coarser sands so that no particles smaller than 10 μm could be detected in the hydrometer sedimentation test without adding a dispersant.
- *Particle shape:* The coarser tailings sands consisted of highly angular to sub-rounded bulky but flattened particles. The finer slimes consisted mostly of thin and plate-like particles characteristic of clay minerals, containing some bulky silt sized particles with properties similar to the sands. The general flattened shape of the particles caused sieve and hydrometer tests to consistently under-estimate the actual size distribution. Operators of cyclone systems will benefit greatly from a knowledge of the size split between predominantly coarse bulky grains and flaky fines in the delivery slurry, roughly 10 μm in this case.
- *Surface texture:* Surface textures ranged from completely smooth to rough on a micro-scale.
- *Chemical Interactions:* The principal chemical reaction that takes place in gold tailings is the oxidation of the sulphide minerals in the presence of oxygen and water or through anaerobic biological processes. Pyrite oxidation results in the formation of iron

oxides and sulphuric acid. Resulting changes in pH may trigger precipitation of bonding agents including silica, metal oxides and carbonates. However, no evidence of this could be identified. Other than that, the only other interaction of significance is crust formation on drying and evaporating surfaces. These crusts are superficial, however, and do not have an effect on the strength properties of the deposit, although they can reduce evaporation from exposed surfaces.

5.3 STATE OF GOLD TAILINGS

Having defined the fundamental characteristics of the gold tailings mix, it is possible to consider the in-situ state and mechanical behaviour of this material. A coarse deposited layer with more bulky and angular tailings sands, could behave like a clean, but fine sand. The finer layers consisting mainly of thin plate-like slimes, should behave more like a clay.

Sampling of tailings has always been a major problem due to the silty nature, low in-situ density and highly layered structure of tailings deposits. High quality undisturbed samples were recovered for this study either by cutting block samples, or by using a well-designed tube sampler. However, this was only possible provided direct access could be gained to the material. To prepare reconstituted laboratory samples, a method of settling high water content slurries proved to be effective in providing samples that are representative of the in-situ state.

The tailings considered in this study had an abundance of fines so that, irrespective of grade, the state and behaviour was controlled by the fines.

- *Stress and Stress History:* The stress regime in a tailings impoundment is largely the result of self-weight loading of the impounded martial. Under sub-aqueous deposition in the pond the stress history follows a normally one-dimensionally consolidated state with low effective stress levels as a result of the low densities. Under sub-aerial deposition on the daywall and beach areas, evaporation and desiccation can build in some overconsolidation with resulting increases in density and effective stress levels. However, desiccation suctions are short-lived due to re-wetting by precipitation and seepage from successive deposition cycles.
- *Density:* The in-situ dry density of coarse layers of tailings range typically between 1250 and 1650 kg/m^3 with an average of 1450 kg/m^3. In-situ density of the finer slimes is closer to 1000 kg/m^3. Thus, following similar soil forming histories, layers of fine tailings exist at density states of almost half those of coarse layers. These contrasting states are a function only of differences in composition resulting from slurry properties and soil forming conditions, which vary constantly at a specific location.

- *Compressibility:* Similar to density, compressibility of tailings is highly dependent on composition, especially on the relative percentages of bulky sands and flaky slimes. However, the virgin compression curves of both fine and coarse tailings could be normalised successfully using the void index. It is, therefore, possible to derive density profiles and bulk stiffness properties of a tailings sediment as a function of the confinement stress levels and some fundamental constant based on material composition only.

  For the range of stresses to be expected in an impoundment the density state and bulk stiffness of the material considered in this study could well be predicted using the normalised void index and correlations with the Atterberg limits as follows:

$$I_v = \frac{e - e_{100}}{e_{100} - e_{1000}} = 2 - \frac{\ln p'}{2.303} \qquad \text{Eq. 5-1}$$

$$e_{100} = 0.647\left(\frac{PI}{2.24}\right) \qquad \text{Eq. 5-2}$$

$$e_{1000} = 0.53\ln\left(\frac{LL}{10}\right) \qquad \text{Eq. 5-3}$$

  If the in-situ range and extent of the layering can be established, estimates of density and stiffness can be made based on parameters derived from simple laboratory tests on reconstituted samples of a similar composition. Information of this kind is extremely useful in estimating rate-of-rise, storage capacity and other operational parameters for a tailings impoundment.

- *Consolidation:* Consolidation characteristics are also significantly affected by composition, with tailings slimes reported to be 6 orders of magnitude slower to consolidate than tailings sands. The fast draining properties of tailings demand special care when performing permeability tests in the laboratory.

  Laboratory triaxial and in-situ piezocone consolidation data indicated that the shape of the tailings consolidation curve deviates significantly from that of the theoretical one-dimensional equation after Terzaghi-Rendulic. Acceptable estimates of the coefficient of consolidation can, however, be obtained by fitting the time for 50% consolidation, t_{50}, to the one-dimensional theoretical T_{50} for the appropriate boundary conditions.

  An important observation was the large percentage of creep or secondary consolidation that took place during consolidation stages. Creep is often ignored or assumed negligible in tailings literature.

- *Shear Strength:* The shear strength properties of the tailings were: zero effective cohesion, with an effective angle of internal friction of $\phi' \approx 34°$. It was found, as reported in tailings literature, that the strength properties are independent of composition. The internal friction angle can be assumed independent of grading, density, overconsolidation and effective stress level up to the onset of particle crushing.

Fine and coarse tailings, sampled from the same location, not only had the same strength properties, but also followed exactly the same undrained stress path up to the failure state. However, this can only be true provided that a specific relationship exists between the compositions of the different grades and their respective density states. Such states, representative of the in-situ condition, could be set-up repeatedly in the laboratory by settling remoulded high water content slurries. It is concluded that following similar sub-aqueous sedimentation-consolidation histories, tailings of different compositions (fine and coarse) will exist at varying density states, but so that their specific gravity and undrained shear strengths are the same. The validity of this hypothesis has not yet been confirmed on sub-aerial beaches and daywall areas, but the effects of desiccation only, should not alter the relative states between fine and coarse deposits. Particle sorting and horizontal rolling during sub-aerial deposition could, however, result in alternative structures compared with those following sub-aqueous deposition.

Further observations on the shear behaviour of the tailings suggested that material of the finest composition will reach a stable ultimate critical state, while material of a coarser composition is particularly prone to post failure phase transfer dilation and strain hardening. In addition, the coarser material with greater permeability may shear partially drained at the same strain rates that cause the finer material to behave fully undrained. The drained shear strength should be significantly higher than the equivalent undrained strength at the same initial density.

When analysing the stability of a tailings embankment, the composition and state of the material should be considered. Layers of fine tailings are likely to be saturated and if sheared undrained should be assigned the undrained critical state shear strength. On the other hand layers of coarse tailings, even if saturated, are likely to shear partially to fully drained, with an increased effective shear strength. Nevertheless, if the coarser material is sheared undrained, it will generate additional strength, over and above the critical state strength, as a result of post failure stress dilatency. This assumes a normally consolidated initial state. If the material has been subjected to desiccation, the effects of overconsolidation on the stress paths should be considered.

- *Structure:* Phyllosilicate-minerals with their large surface areas in tailings slimes are subject to and may be dominated by surface forces compared with the body force of gravity. Low surface area bulky tailings sands, on the other hand, are primarily subject to gravity forces. Based upon the evidence on electron micrographs and triaxial test data on undisturbed samples, the structure of pond-area tailings is determined by the randomly orientated and flocculated slime flakes rather than the coarser bulky sands. This is in agreement with the constant and independent shear strength properties of all samples studied.

Natural fine silts have a tendency to form open meta-stable packing arrangements following sub-aqueous sedimentation. No such open structures could be identified in either the fine or coarse tailings, which rather behaved like loose but stable particle arrangements that strain hardened to failure. Collapsible structure has only been evident in laboratory specimens artificially prepared by wet-tamping techniques, as reported in the literature.

The possibility of inter-particle bonding as a result of precipitating agents is dependent on pH fluctuations, following the oxidation of sulphide minerals in tailings. Oxidation, in the absence of anaerobic oxidising bacteria, can only take place to a limited depth on exposed surfaces, such as daywall and beach surfaces. Structural bonding could not be detected in any of the undisturbed samples considered in this study.

5.4 USE OF THE PIEZOCONE IN TAILINGS

The piezocone today is one of the most popular instruments used to probe and characterise tailings impoundments. Difficulties with sampling virtually eliminate the feasibility of controlled laboratory tests on undisturbed samples. Of all other in-situ devices, the piezocone is the one device which provides a continuous record of sub-surface conditions with depth at reasonable cost.

- *Stratigraphy:* The piezocone has been used by many engineers worldwide to successfully delineate the sub-surface stratigraphy of tailings impoundments. The small, localised nature and quick response-time of the pore pressure sensor, makes it ideal for locating layer interfaces in the highly layered tailings profile.

  A modified version of the Jones and Rust identification chart was used in this study to classify the tailings profile, which compared well to an exposed profile next to the CPTU sounding. Some aspects that need consideration in the classification process are:

  - The classification chart must comply with the location of the filter element on the piezocone probe.
  - Most classification systems were designed for saturated conditions.
  - Due to the small depth of individual layers the measured values of the pore pressure and especially cone resistance may not be fully developed.
- *Seepage Regime:* The piezocone is considered by many as the most reliable tool to determine the in-situ seepage regime in a tailings dam. It gives excellent data on the location of the phreatic surface and distribution of ambient pore pressures. In addition, it can be used to estimate the in-situ anisotropy in permeability. However, calculation of the coefficient of consolidation from pore pressure dissipation data is only practical in

the finest layers, as dissipation in the coarser layers is almost instantaneous. The highly layered nature of the tailings profile, often with alternating fine and coarse layers over small depths, makes interpretation of the drainage boundary conditions around the cone extremely difficult.

Due to the difference in the shape between theoretical one-dimensional consolidation curves and piezocone consolidation curves, it is recommended that the coefficient of consolidation be calculated using the time for 50% dissipation or t_{50} rather than t_{90}.

- *Strength and Stiffness:* Confidence in the strength and stiffness interpretation of cone penetration data in tailings has been lacking in the past. Reasons for this include a need to understand the drainage conditions around the advancing cone and the large imposed strain field. With a better understanding of the composition and state of tailings, it is now possible to at least justify the typical upper and lower bound cone measurements in tailings. Upper and lower bound penetration resistances are not the result of large differences in strength and stiffness, as was initially thought. These result rather from differences in drainage conditions and post failure stress-dilatency between layers of different composition.

  The following conclusions were drawn from the combined results of theoretical cavity expansion, effective stress and state parameter interpretations:

  - Usually for gold tailings, the friction angle of layers of different composition remains constant. However, this fact should be verified by consolidated undrained triaxial tests on reconstituted laboratory samples.
  - Unless it can be proved otherwise, cohesion should be taken as zero. Although desiccation suctions will induce some apparent cohesion on the daywall and upper beaches, these are soon relieved on re-wetting.
  - Coarse and fine layers of tailings vary significantly in density and stiffness, but the absolute values are so low in tailings (I_r typically being 15 to 40) that it hardly affects penetration resistances.
  - Cone resistance profiles typically follow lower and upper bound trends in tailings. For strength and stiffness interpretation, the lower bound measurements should be considered. The cavity expansion and state parameter approaches are both adequate in this regard. The upper bound measurements result from a number of factors including partial drainage and post failure stress-dilatency in the coarser layers. An effective stress approach should provide a reasonable upper bound estimate.

Considering the above, a much more rational approach to the interpretation of in-situ strength properties, based on piezocone data, has been made possible. The lower trend of penetration resistances can be used to calculate the effective strength properties of the tailings, fine and coarse, using either the cavity expansion or state parameter approaches.

The upper trend of resistances serves as an indication of the effects of post failure dilation and partial drainage in the coarser layers.

REFERENCES

Abadjiev, C.B. (1976), Seepage through mill tailings dams, *Proceedings, 12th International Congress on Large Dams*, Mexico, Vol. 1, No. R42, 381-393.

Abadjiev, C.B. (1985), Estimation of the physical characteristics of deposited tailings in the tailings dam of non-ferrous metallurgy, *Proceedings, 11th International Conference on Soil Mechanics and Foundation Engineering, San Francisco, Vol. 3, 1231-1234.*

Abadjiev, C.B. (1988), Estimation of the physical characteristics of deposited tailings in the tailings dam of non-ferrous metallurgy, *Proceedings, 11th International Conference on Soil Mechanics and Foundation Engineering*, San Francisco, Vol. 3, 1231-1234.

Abadjiev, C.B. (1997), A practical method for estimating the grading of hydraulically deposited tailings across the beach, *Proceedings, 2nd International Conference on Mining and Industrial Waste Management*, Johannesburg.

Airey, D.W., and Wood, D.M. (1987), An evaluation of direct simple shear test on clay, *Géotechnique*, Vol. 37, No. 1, 25-35.

Alarcon-Guzman, A., Leonards, G.A., and Charmeau, J.L. (1988).Undrained monotonic and cyclic strength of sands, *ASCE Journal of Geotechnical Engineering*, Vol. 114, No. 10, 1089-1109.

Al-Hussaini, M.M., Goodings, D.J., Schofield, A.N., and Townsend, F.C. (1981), Centrifuge modelling of coal waste embankments, *ASCE, Journal of the Geotechnical Engineering Division*, 481-499.

Atkinson, J.H. and Bransby, P.L. (1978), *The mechanics of soils. An introduction to critical state soil mechanics*, Maidenhead: McGraw-Hill.

Aubertin, M., Bussiere, B., and Chapuis, R.P. (1996), Hydraulic conductivity of homogenised tailings from hard rock mines, *Canadian Geotechnical Journal*, Vol. 33, No. 3, 470-482.

Aubertin, M., Ricard, J-F, and Chapuis, R.P. (1998), A predictive model for the water retention curve: Application to tailings from hard-rock mines, *Canadian Geotechnical Journal*, Vol. 35, No. 1, 55-69.

Baldi, G., Bellotti, R., Ghionna, V., and Jamiolkowski, M. (1982), Design parameters for sands from CPT, *Proceedings, 2nd European Symposium on Penetration Testing, ESOPT II*, Amsterdam, Vol. 2, 425-432.

Baldi, G., Hight, D. W., and Thomas, G. E. (1988), A re-evaluation of conventional triaxial test methods, *Symposium on Advanced Triaxial Testing of Soil and Rock, ASTM STP 977*, Philadelphia, 219-263.

Baligh, M.M. (1975), *Theory of Deep Site Static Cone Penetration Resistance*, Publication No. R75-56, Department of Civil Engineering, MIT.

Baligh, M.M. (1985), Strain Path Method, *ASCE Journal of the Geotechnical Engineering Division*, Vol. 111, No. 9, 1108-1136.

Barrett, A.J. (1987), Seepage analysis in tailings impoundments using a finite element model: Two case histories, P*roceedings, International Conference on Mining and Industrial Waste Management, SAICE*, Johannesburg, 205-210.

Bartlett, C.L., and Van Zyl, D. (1984), Utilising numerical analysis of unsaturated seepage to design tailings management strategy, *Proceedings, 6th Annual Symposium on management of Uranium Tailings, Low-level Waste, and Hazardous Waste*, Fort Collins, Colorado, 627-638.

Bates, R.C., and Wayment, W.R. (1967), Laboratory study of factors influencing water flow in mine backfill, *U.S. Bureau of Mines, Report RI 7034*.

Been, K. (1980), *Stress Strain Behaviour of a Cohesive Soil Deposited Under Water*, PhD thesis, University of Oxford, UK.

Been, K., and Sills, G.C. (1981), Self-weight consolidation of soft soils: an experimental and theoretical study, *Géotechnique*, Vol. 31, No. 4, 519-535.

Been, K., and Jefferies, M.G. (1985), A state parameter for sands, *Géotechnique*, **35**(2), 99-112.

Been, K., Crooks, J.H.A., Becker, D.E., and Jefferies, M.G. (1986), The cone penetration test in sands: Part I, state parameter interpretation, *Géotechnique*, **36**(2), 239-249.

Been, K., Conlin, B.H., Crooks, J.H.A., Fitzpatrick, S.W., Jefferies, M.G., Rogers, B.T., and Shinde, S. (1987), Discussion: Back analyses of the Nerlerk berm liquefaction slides, *Canadian Geotechnical Journal*, Vol. 24, No. 1, 170-179.

Been, K., Crooks, J.H.A., Conlin, B.H., and Horsfield, D. (1988), Liquefaction of hydraulically placed sand fills, *Hydraulic Fill Structures, ASCE Geotechnical Special Publication No. 21*, 573-590.

Berti, G., Villa, F., Dovera, D., Genevois, R., and Brauns, J. (1988), Disaster of Stava, Northern Italy, *Hydraulic Fill Structures, ASCE Geotechnical Special Publication No. 21*, 492-510.

Bentel, G.M. (1981), Some aspects of the behaviour of hydraulic deposited tailings, *Research Project: University of the Witwatersrand*.

Bica, A.V.D., and Clayton, C.R.I. (1998), Experimental study of the behaviour of embedded lengths of cantilever walls, *Géotechnique*, Vol. 48No. 6 731-745.

Biot, M.A. (1941), General theory of three dimensional consolidation, *Journal of Applied Physics*, **12**, 155-164.

Bishop, A.W. (1973), The stability of tips and spoil heaps, *Quarterly Journal of Engineering Geology*, Vol. 6, 335-376.

Bishop, A.W., and Henkel, D.J. (1962), *The measurement of soil properties in the triaxial test*, London: Edward Arnold Publishers Ltd.

Bishop, A.W., Hutchinson, J.N., Penman A.D.M., and Evans, H.E. (1969), Geotechnical investigations into the causes and circumstances of the disaster of 21st October 1966, *A selection of technical report submitted to the Aberfan Tribunal*, Welsh Office, London: H.M.S.O.

Bjerrum, L., and Landva, A. (1966), Direct simple shear tests on Norwegian quick clay, *Géotechnique*, Vol. 16, No. 1, 1-20.

Blackshaw, J. (1951), Mill tailings disposal at Hollinger, *Bulletin, Canadian Institute of Mining and Metallurgy*, June.

Blight, G.E. (1969), Shear stability of dumps and dams of gold mining waste. *Transactions, South African Institution of Civil Engineers*, Vol. 11, No. 3, 49-54.

Blight, G.E. (1970), In-situ strength of rolled and hydraulic fill, *ASCE, Journal of the Soil Mechanics and Foundations Division*, Vol. 96, No. SM3, 881-889.

Blight, G.E. (1980), Properties of pumped tailings fill, *Journal of the South African Institute of Mining and Metallurgy*, Vol. 79, No. 15, 446-453.

Blight, G.E. (1981), Assessment for environmentally acceptable disposal of mine wastes, *The Civil Engineer in South Africa*, Vol. 23, No. 10, 480-499.

Blight, G.E. (1987), Erosion of the slopes of gold tailings dams, *Proceedings of a Speciality Conference on Geotechnical Practice for Waste Disposal '87, ASCE Geotechnical Special Publication no. 13*, 294-305.

Blight, G.E. (1988), Some less familiar aspects of hydraulic fill structures, *Hydraulic Fill Structures, ASCE Geotechnical Special Publication No. 21*, 1000-1027.

Blight, G.E. (1989), Erosion losses from the surfaces of gold-tailings dams, *Journal of the South African Institute of Mining and Metallurgy*, Vol. 89, No. 1, 23-29.

Blight, G.E. (1994), Master profile for hydraulic fill tailings beaches, *Proceedings of the Institution of Civil Engineers: Geotechnical Engineering*, **107**(1), 27-40.

Blight, G.E. (1997), Destructive mudflows as a consequence of tailings dyke failures, *Proceedings of the Institution of Civil Engineers: Geotechnical Engineering*, Vol. 125, 9-18.

Blight, G.E., and Steffen, K.H. (1979), Geotechnics of gold mining waste disposal, *Current Geotechnical Practice in Mine Waste Disposal*, ASCE, New York, 1-53.

Blight, G.E., and Bentel, G.M. (1983), The Behaviour of mine tailings during hydraulic deposition, *Journal of the South African Institute of Mining and Metallurgy*, 73-86.

Blight, G.E., Vorster, K., and Thomson, R.R. (1985), Profiles of hydraulic-fill tailings beaches, and seepage through hydraulically sorted tailings, *Journal of the South African Institute of Mining and Metallurgy*, Vol. 85, No.5, 157-161.

Brawner, C. (1979), Design, construction and repair of tailings dams for metal mine waste disposal, *ASCE, Current Geotechnical Practice in Mine Waste Disposal*.

Brawner, C.O., and Campbell, D.B. (1972), The tailing structure and its characteristics: A soils engineer's viewpoint, in G.O. Argall and C.L. Aplin (eds.) *Tailing Disposal Today, Proceedings of the First International Tailing Symposium*, Tuscon: Arizona, 59-101.

Brooks, R.H., and Corey, A.T. (1966), Properties of porous media affecting fluid flow, *ASCE, Journal of the Irrigation and Drainage Division*, Vol. 92, No. IR2, 61-89.

BS 1377-2:1990, *Methods of test for soils for civil engineering purposes. Classification tests*, British Standards Institution, London.

BS 1377-3:1990, *Methods of test for soils for civil engineering purposes. Chemical and electro-chemical tests*, British Standards Institution, London.

BS 1377-4:1990, *Methods of test for soils for civil engineering purposes. Compaction related tests*, British Standards Institution, London.

BS 1377-5:1990, *Methods of test for soils for civil engineering purposes. Compressibility, permeability and durability tests*, British Standards Institution, London.

BS 1377-6:1990, *Methods of test for soils for civil engineering purposes. Consolidation and permeability tests in hydraulic cells and with pore pressure measurement*, British Standards Institution, London.

BS 1377-8:1990, *Methods of test for soils for civil engineering purposes. Shear strength tests (effective stress)*, British Standards Institution, London.

BS 1377-9:1990, *Methods of test for soils for civil engineering purposes. In-situ tests*, British Standards Institution, London.

Bugno, W.T., and McNeilan, T.W. (1984), Cone penetration test results in offshore California silts, *Symposium on Strength Testing of Marine Sediments; Laboratory and In-situ Measurements, ASTM STP 883*, 55-71.

Burland, J.B. (1990), Rankine Lecture: On the compressibility and shear strength of clays, *Géotechnique*, Vol. 40, No. 3, 329-378.

Caldwell, J.A., and Stevenson, C. (1984) Geotechnical evaluations for tailings impoundments, in Boyce, J.R., Mackechnie, W.R., and Schwartz, K. (eds.) (1984), *Soil Mechanics and Foundation Engineering*, Vol. 1, 433-442.

Caldwell, J.A., Ferguson, K., Schiffman, R.L., and Van Zyl, D. (1984), Application of finite strain consolidation theory for engineering design and environmental planning of mine tailings impoundments, in R.W. Yong, and F.C. Townsend (eds.), *Sedimentation / Consolidation Models - Predictions and Validation, ASCE*, 581-606.

Caldwell, J.A., and Robertson, A. (1986), Geotechnical stability considerations in the design and reclamation of tailings impoundments, *Proceedings of the International Symposium on Geotechnical Stability in Surface Mining*, Calgary: Alberta, 255-258.

Campanella, R.G., Robertson, P.K., and Gillespie, D. (1983), Cone penetration testing in deltaic soils, *Canadian Geotechnical Journal*, Vol. 20, 23-35.

Campanella, R.G., Gillespie, D., Klohn, E.J., and Robertson, P.K. (1984), Piezometer friction cone investigation at a tailings dam, *Canadian Geotechnical Journal*, Vol. 21, No. 3, 551-562.

Carrier, W.D., Bromwell, L.G., and Somogyi, F. (1983), Design capacity of slurried mineral waste ponds, *ASCE, Journal of the Geotechnical Engineering Division*, Vol. 109, No. 5, 699-716.

Casagrande, A. (1965), Role of 'calculated risk' in earthwork foundation engineering: Terzaghi Lecture, *ASCE, Journal of the Soil Mechanics and Foundation Engineering Division*, Vol. 91, No. SM4, 1-40.

Casagrande, L., and McIver, B.N. (1970), Design and construction of tailings dams, *Proceedings, 1st International Conference on Stability in Open Pit Mining*, Vancouver, 181-203.

Castro, G. (1969), *Liquefaction of Sands*, PhD thesis, Harvard University, Cambridge, Massachusetts, USA.

Castro, G., and Christian, J.T. (1976), Shear strength of soils and cyclic loading, *ASCE, Journal of the Geotechnical Engineering Division*, Vol. 102, No. GT9, 887-894.

Castro, G., and Poulos, S.J. (1977), Factors affecting liquefaction and cyclic mobility, *ASCE, Journal of Geotechnical Engineering*, Vol. 103, No. GT6, 501-516.

Chamber of Mines of South Africa (1983), *Handbook of guidelines for Environmental Protection*, Vol. 1/1979, Revised 1983, "The design, operation and closure of metalliferous and coal residue deposits".

Chandler, R.J., and Tosatti, G. (1995), The Stava Tailings Dam failure, Italy, *Proceedings, Institution of Civil Engineers: Geotechnical Engineering*, **113**(2), 67-79.

Chapuis, R.P., and Montour, I. (1992), Évaluation de l'équation de Kozeny-Carman pour prédire la conductivité hydraulique (Evaluation of the Kozeny-Carman equation for predicting hydraulic conductivity), *Proceedings, 45th Canadian Geotechnical Conference, Toronto*, 78.1-78.10.

Chen, H.W., and Van Zyl, D.J.A. (1988), Shear strength and volume-change behaviour of copper tailings under saturated conditions, *Hydraulic Fill Structures, ASCE Geotechnical Special Publication No. 21*, 430-451.

Chen, P.K., Keshian, B., and Guros, F.B. (1988), Settlement of uranium mill tailings , *Hydraulic Fill Structures, ASCE Geotechnical Special Publication No. 21*, 310-329.

Clark, M., Weitz, T., Banning, W., Turk, D., and Patterson, J. (1989), Montana Tunnels - start-up efficiencies improved, expansion considered, *Mining Engineering*, February.

Clayton, C.R.I., Matthews, M.C., and Simons, N.E. (1995), *Site Investigation, Second Edition*, Blackwell Science.

Consoli, N.C. (1997), Comparison of the measured and predicted performance of tailings sedimentation, *Proceedings of the Institution of Civil Engineers: Geotechnical Engineering*, Vol. 125, No. 3, 179-187.

Consoli, N.C., and Sills, G.C. (2000), Soil formation from tailings: Comparison of predictions and field measurements, *Géotechnique*, Vol. 50, No. 1, 25-33.

Collins, I.E. (1954), Some foundation experiences in the Durban area, *Transactions, South African Institution of Civil Engineers*, Vol. 4, 219.

Cowey, A. (1994), *Mining and Metallurgy in South Africa - a pictorial history*, MINTEK, 17-36.

Dobry, R., and Alvarez, L. (1967), Seismic failures of Chilean tailings dams, *ASCE, Journal of the Soil Mechanics and Foundations Division*, Vol. 93, No. SM6, 237-260.

Donaldson, G. (1965), The effects of capillary action on the consolidation and shear strength of silt in a hydraulic fill dam, *Proceedings, 6th International Conference on Soil Mechanics and Foundation Engineering*, Montreal, 454-463.

Donaldson, G., Adamson, R., and Clausen, H. (1976), Slimes dams for gold mine tailings and other residues in South Africa, *Proceedings, 12th International Congress on Large Dams*, Vol. 1, ICOLD.

Dunbar, S., Garga, V., and Nguyen, T.S. (1991), Modelling the liquefaction potential of uranium tailings, *Proceedings of the 44th Canadian Geotechnical Conference*, Calgary Alberta, Vol. 1, 13/1-13/9.

East, D.R., and Ulrich, B.F. (1989), The electric piezocone for profiling of mine tailings deposits, in R.J. Watters (ed.), *Proceedings, 25th Symposium on Engineering Geology and Geotechnical Engineering*, Reno, 35-38.

East, D.R., Ransone, J.W., and Cincilla, W.A. (1988), Testing of the Homestake mine tailings deposit, *Proceedings, 2nd International Conference on Case Histories in Geotechnical Engineering*, 495-502.

East, D.R., Cincilla, W.A., Hughes, J.M.O., and Benoit, J. (1988a), The use of the electric piezocone for mine tailings deposits *Proceedings, 1st International Symposium on Penetration Testing, ISOPT-1*, Orlando, Vol. 2, 745-750.

Emerson, W.W., and Self, P.G. (1994), Neutralised tailings and sulphates: Evaluating bulk properties, *Géotechnique*, Vol. 44, No. 3, 495-501.

Emerson, W.W., Peter, P., McClure, S., and Weissmann, D. (1994), Neutralised tailings and sulphates: Settlement, drying and consolidation, *Géotechnique*, Vol. 44, No. 3, 503-512.

Fahey, M., and Fujiyasu, Y. (1994), The influence of evaporation on the consolidation behaviour of gold tailings, *Proceedings, 1st International Conference on Environmental Geotechnics*, Canada, 481-486.

Fan, X., and Masliyah, J. (1990), Laboratory investigation of beach profiles in tailings disposal, *Journal of Hydraulic Engineering*, Vol. 116, No. 11, 1357-1373.

Fell, R. (1988), Mine tailings, dispersants and flocculants, *Hydraulic Fill Structures, ASCE Geotechnical Special Publication No. 21*, 711-729.

Finn, W. (1982), Fundamental aspects of response of tailings dams to earthquakes, *Dynamic Stability of Tailings Dams, ASCE*, 46-72.

Finn, W., and Byrne, P. (1976), Liquefaction potential of mine tailings dams, *12th International Congress on Large Dams*, Mexico, 153-177.

Finn, W., Lee, K., Maartman, V., and Lo, R. (1978), Cyclic pore pressure under anisotropic conditions, *ASCE, Proceedings, Conference on Earthquake Engineering and Soil Dynamics*, Vol. 1, 457-470.

Follin, S.E., Chedsey, G.L., and Robertson, A.M.G. (1984), Unconventional uses of geotechnical tools for impoundment seepage investigations, *Proceedings, 6th Symposium on Uranium Mill Tailings Management*, Fort Collins: Colorado, 615-625.

Fourie, A. (1988), Beaching and permeability properties of tailings, *Hydraulic Fill Structures, ASCE Geotechnical Special Publication No. 21*, 142-154.

Fox, P.J., and Baxter, C.D.P. (1997), Consolidation properties of soil slurries from hydraulic consolidation test, *Journal of Geotechnical and Geo-environmental Engineering*, Vol. 123, No. 8, 770-776.

Fuller, W.B., and Thompson, S.E. (1907), The laws of proportioning concrete, *Transactions of the American Society of Civil Engineers*, Vol. 59.

Garga, V.K., and McKay, L.D. (1984), Cyclic triaxial strength of mine tailings, *ASCE, Journal of Geotechnical Engineering*, Vol. 110, No. 8, 1091-1105.

Gibson, R.E., and Lumb, P. (1953), Numerical solutions of some problems in the consolidation of clay, , *Proceedings, Institution of Civil Engineers: Geotechnical Engineering*, Vol. 2, No. 1, 182-198.

Gibson, R.E., England, L., and Hussey, M.J. (1967), The theory of one-dimensional consolidation of saturated clays, I: Finite non-linear consolidation of thin homogeneous layers, *Géotechnique*, Vol. 17, No. 3, 261-273.

Gibson, R.E., Schiffman, R.L., and Cargill, K.W. (1981), The theory of one-dimensional consolidation of saturated clays, II: Finite non-linear consolidation of thick homogeneous layers, *Canadian Geotechnical Journal*, Vol. 18, No. 2, 280-293.

Gilchrist, J.D. (1989), *Extraction Metallurgy, 3rd Edition*, Pergamon Press, 341-342.

Gowan, M.J., and Williamson, J.R.G. (1987), A review of tailings deposition techniques in South Africa and appropriate selection of application, *Proceedings, International Conference on Mining and Industrial Waste Management, SAICE*, Johannesburg, 81-87.

Guerra, F. (1972), Characteristics of tailings from a soils engineer's viewpoint, in G.O. Argall and C.L. Aplin (eds.) *Tailing Disposal Today, Proceedings of the First International Tailing Symposium*, Tuscon: Arizona, 102-137.

Hamel, J.V., and Gunderson, J.W. (1973), Shear strength of Homestake slimes tailings, *ASCE Journal of the Soil Mechanics and Foundation Engineering Division*, Vol. 99, SM5, 427-431.

Han, G., and Wang, D. (1996), Numerical modelling of Anhui debris flow, *ASCE, Journal of the Hydraulic Engineering Division*, **122**(5), 262-265.

Harper, T.G., McLeod, H.N., and Davies, M.P. (1992), Seismic assessment of tailings dams, *Civil Engineering (New York)*, Vol. 62, No. 12, 64-66.

Harr, M.E. (1977), *Mechanics of Particulate Media - A Probabilistic Approach*, McGraw-Hill, 543pp.

Hazen, A. (1892), Physical properties of sands and gravels with reference to their use in filtration, *Report, Massachusetts State Board of Health*.

Head, K.H. (1984), *Manual of soil laboratory testing, Volume 1*: Soil classification and compaction tests, London: Pentech Press Limited.

Head, K.H. (1984), *Manual of soil laboratory testing, Volume 2*: Permeability, shear strength and compressibility tests, London: Pentech Press Limited.

Head, K.H. (1984), *Manual of soil laboratory testing, Volume 3*: Effective stress tests, London: Pentech Press Limited.

Highter, W.H., and Tobin, R.F. (1980), Flow slides and the undrained brittleness index of some mine tailings, *Engineering Geology*, Vol. 16, No. 1-2, 71-82.

Highter, W.H., and Vallee, R.P. (1980), The liquefaction of different mine tailings under stress controlled loading, *Engineering Geology*, Vol. 16, No. 1-2, 147-150.

Hoare, B., and Hill, H.M. (1970), The hydraulic construction of mine tailings dams, *Canadian Mining Journal*, Vol. 91, No. 6, 51-58.

Hungr, O. (1995), A model for the run-out analysis of rapid flow slides, debris flows, and avalanches, *Canadian Geotechnical Journal*, Vol. 32, No. 4, 610-623.

Hutchinson, I., Ash, W., and Fisher, J. (1985), Cyanide control options - lessons from case histories, *Proceedings, Conference on Cyanide and the Environment*, Vol. 1.

Imai, G. (1980), Settling behaviour of clay suspensions, *Soils and Foundations*, Vol. 20, No. 2, 61-77.

Imai, G. (1981), Experimental studies on sedimentation mechanisms and sediment formation of clay materials, *Soils and Foundations*, Vol. 21, No. 1, 7-20.

Ishihara, K. (1993), 33rd Rankine Lecture: Liquefaction and flow failure during earthquakes, *Géotechnique*, Vol. 43, No. 3, 349-416.

Ishihara, K., Tatsuoka, F., and Yasuda, S. (1975), Undrained deformation and liquefaction of sand under cyclic stresses, *Soil and Foundations*, Vol. 15, No. 1, 29-44.

Ishihara, K, Yasuda, S., and Yoshida, Y. (1990), Liquefaction-induced flow failure of embankments and residual strength of silty sands, *Soils and Foundations*, Vol. 30, No. 3, 69-80.

ISSMFE (1989), International reference test procedure for cone penetration test (CPT), *Report of the ISSMFE Technical Committee on Penetration Testing of Soils - TC 16*, Swedish Geotechnical Institute, Linköping, No. 7, 6-16.

Jaky, J. (1944), The coefficient of earth pressure at rest, *Journal of the Society of Hungarian Architects and Engineers*, Vol. 7, 355-358.

Jefferies, M.G. (1993) Nor-Sand: a simple critical state model for sand, *Géotechnique*, **43**(1), 91-103.

Jennings, J.E. (1979), The failure of a slimes dam at Bafokeng: Mechanisms of failure and associated design considerations, *The Civil Engineer in South Africa*, Vol. 21, No. 6, 135-145.

Jennings, J.E., Brink, A.B.A., and Williams, A.A.B. (1973), Revised guide to soil profiling for civil engineering purposes in Southern Africa, *Transactions, South African Institution of Civil Engineers*, Vol. 15, 3-12.

Jerabek, F., and Hartman, H. (1965), Investigations of segregation and compressibility in discharged fill slurry, *Transactions of the Society of Mining Engineers*, March, 18-24.

Jeyapalan, J.K., Duncan, J.M., and Seed, H.B. (1982), Investigation of flow failures of tailings dams, *ASCE, Journal of the Geotechnical Engineering Division*, Vol. 109, GT2, 172-189.

Jeyapalan, J.K., Duncan, J.M., and Seed, H.B. (1982a), Analysis of flow failures of mine tailings dams, *ASCE, Journal of the Geotechnical Engineering Division*, Vol. 109, GT2, 150-171.

Jones, G.A., and Rust, E. (1982), Piezometer penetration testing, *Proceedings, 2nd European Symposium on Penetration Testing*, Amsterdam, 607-613.

Jones, G.A., and Rust, E. (1983), Piezometer probe (CUPT) for subsoil identification, *Proceedings, International Symposium on In-situ Testing*, Paris, Vol. 2, 303-308.

Jones, G.A., Van Zyl, D.J., and Rust, E. (1981), Mine tailings characterisation by piezometer cone, in G.M. Norris, and R.D. Holtz (eds.), *Proceedings, Cone Penetration Testing and Experience*, Session sponsored by ASCE, 303-324.

Kealy, C.D., and Busch, R. (1969), *Determining Seepage Characteristics of Mill Tailings Dams by the Finite Element Method*, US Department, Interior, Bureau of Mines, Report of Investigations 7477.

Kealy, C.D., and Busch, R. (1971), Determining seepage Characteristics of mill-tailings dams by the finite element method, *U.S. Bureau of Mines, RI 7477.*

Kealy, C.D., and Busch, R. (1979), Evaluation of mine tailings disposal, *Current Geotechnical Practice in Mine Waste Disposal, ASCE*, New York, 181-201.

Keshian, B., Rager, R.E. (1988), Geotechnical properties of hydraulically placed uranium mill tailings, *Hydraulic Fill Structures, ASCE Geotechnical Special Publication No. 21*, 227-254.

Kleinmann, R., Crerar, D., and Pacelli, R. (1981), Bio-geochemistry of acid mine drainage and a method to control acid formation, *Mining Engineering*, March, 300-305.

Klohn, E.J. (1980), The development of current tailings dam design and construction methods, *Proceedings, Symposium on Design and Construction of Tailings Dams*, Colorado, A1-A51.

Klohn, E.J. (1984), The Brenda Mines' cycloned-sand tailings dam, *ASCE, Conference on Case Histories in Geotechnical Engineering*, St Louis, 953-977.

Klohn, E.J., and Maartman, C.H. (1973), Construction of sound tailings dams by cycloning and spigotting, in Aplin, C.L., and Argall, G.O. (eds.) (1972), *Tailings Disposal Today: Proceedings of the 1st International Tailing Symposium, Tuscon: Arizona.*, 232-267.

Klohn, E., Maartman, C., Lo, C., and Finn, W. (1978), Simplified seismic analysis for tailings dams, *ASCE, Proceedings, Conference on Earthquake Engineering and Soil Dynamics*, Vol. 1, 540-556.

Konrad, J.-M. (1997), In situ sand state from CPT: evaluation of a unified approach at two CANLEX sites, *Canadian Geotechnical Journal*, Vol. 34, 120-130.

Kotzias, P.C., Stamatopoulos, A.C., and Karas, B. (1984), Stability of an erratic tailings deposit, *ASCE, Conference on Case Histories in Geotechnical Engineering*, St Louis, 755-758.

Kozeny, J. (1931), Grundwasserbewegung bei freim spiegel, fluss und kanalversickering, *Wasserkraft und Wasserwirtschaft*, No. 3.

Kramer, S.L., and Seed, H.B. (1988), Initiation of soil liquefaction under static loading conditions, *ASCE, Journal of Geotechnical Engineering*, Vol. 114, 412-430.

Kuerbis, R., Negussey, D., and Vaid, Y.P. (1988), Effect of gradation and fines content on the undrained response of sand, *Hydraulic Fill Structures, ASCE Geotechnical Special Publication No. 21*, 330-345.

Kynch, G.J. (1952), A theory of sedimentation, *Transactions of the Faraday Society*, Vol. 48, 166-176.

Ladanyi, B. (1967), Deep punching of sensitive clays, *Proceedings, 3rd Pan American Conference on Soil Mechanics and Foundation Engineering*, Caracas, Vol. 1, 533-546.

Ladd, C.C. (1991), Stability evaluation during staged construction, *Journal of Geotechnical Engineering*, Vol. 117, No. 4, 540-615.

Lambe, T.W., and Whitman, R.V. (1969), *Soil Mechanics.*, John Wiley & Sons, Inc.

Lappin, A.E. (1997), *Tailings Characterisation and Settlement Prediction*, MSc Thesis, University of Surrey.

Larson, N.B., and Mitchell, B. (1986), Cone penetrometer use on uranium mill tailings, *ASCE, Conference on the Use of In-situ Tests in Geotechnical Engineering, In-Situ '86*, Geotechnical Special Publication No.6, 700-713.

Lo, R.C., Klohn, E.J., and Finn, W.D.L. (1988), Stability of hydraulic sand-fill tailings dams, *Hydraulic Fill Structures, ASCE Geotechnical Special Publication No. 21*, 549-572.

Lucia, P.C., Duncan, J.M., and Seed, H.B. (1981), Summary of research on case histories of flow failures of mine tailings impoundments, *Mine Waste Disposal Technology, US Bureau of Mines Information Circular*, IC8857/1981, 46-53.

Lunne, T., Robertson, P.K., and Powell, J.J.M. (1997), *Cone Penetration Testing in Geotechnical Practice*, Blackie Academic and Professional.

Mabes, D., Hardcastle, J., and Williams, R. (1977), Physical properties of Pb-Zn mine-process wastes, *Proceedings, ASCE, Conference on Geotechnical Practice for Disposal of Solid Waste Materials*, 103-117.

Massarsch, K.R. (1979), Lateral earth pressure in normally consolidated clay, *Proceedings, 7th European Conference on Soil Mechanics and Foundation Engineering*, Brighton, Vol. 2, 245-250.

Matyas, E.L., Reades, D.W., and Welch, D.E. (1984), Geotechnical parameters and behaviour of uranium tailings, *Canadian Geotechnical Journal*, Vol. 21, No. 3, 489-504.

McPhail, G.I. (1995), *Prediction of the Beaching Characteristics of Hydraulically Placed Tailings*, PhD thesis, University of the Witwatersrand (WITS), South Africa.

McPhail, G.I., and Blight, G.E. (1997), Entropy, stream power and the prediction of tailings beach profiles, *Proceedings, 2nd International Conference on Mining and Industrial Waste Management*, Johannesburg.

McPhail, G.I., and Wagner, J.C. (1989), Disposal of residues, Chapter 11, in G.G. Stanley (ed.), The *Extractive Metallurgy of Gold in South Africa*, The Chamber of Mines of South Africa, Volume 2, 655-707.

McPhee, J. (1971), *Encounters with the Archdruid*, Farrar, Straus and Giroux, New York.

McRoberts, E.C., and Nixon, J.F. (1976), A theory of soil sedimentation, *Canadian Geotechnical Journal*, Vol. 13, 294-310.

McWilliams, P.C. (1983), Field determinations of a probabilistic density functions for slope stability analysis of tailings embankments, *Report of Investigations - United States, Bureau of Mines 8941*.

Melent'ev, V.A., Kolpashnikov, N.P., and Volmin, B.A. (1973), Hydraulic Fill Structures, *Energy*, Moscow, English Translation, D. van Zyl (ed.) (1973), 240pp.

Meyerhof, G.G. (1951), The ultimate bearing capacity of foundations, *Géotechnique*, Vol. 2, No. 4, 301-302.

Mittal, H.K. (1974), *Design and Performance of Tailings Dams*, PhD thesis, University of Alberta, Edmonton, Canada.

Mittal, H.K., and Morgenstern, N.R. (1975), Parameters for the design of Tailings dams, *Canadian Geotechnical Journal*, Vol. 12, 235-261.

Mittal, H.K., and Morgenstern, N.R. (1976), Seepage control in tailings dams, *Canadian Geotechnical Journal*, Vol. 13, 277-293.

Mittal, H.K., and Morgenstern, N.R. (1977), Design and performance of tailings dams, *Proceedings, Conference on Geotechnical Practice for Disposal of Solid Waste Materials, ASCE Speciality Conference of the Geotechnical Engineering Division*, 475-492.

Mlynarek, Z, Tschuschke, W., Sulikowska, I., and Werno, M. (1991), Predicting the strength parameters of post-flotation sediments using the CPT method, in Sorum (ed.), *Field Measurements in Geotechnics*, Vol. 2, 737-744.

Mlynarek, Z, Tschuschke, W., and Lunne, T. (1994), Technique for examining parameters of post-flotation sediments accumulated in the pond, *Proceedings, 3rd International Conference on Construction on Polluted and Marginal Land*, 17-23.

Mlynarek, Z, Tschuschke, W., and Lunne, T. (1995), Use of CPT in mine tailings, *Proceedings, International Symposium on Cone Penetration Testing, CPT'95*, Linköping, Vol. 3, 211-226.

Morris, P.H. (1993), Two-dimensional model for sub-aerial deposition of mine tailings slurry, *Transactions of the Institution of Mining & Metallurgy*, **102**, A181-A187.

Muir-Wood, D. (1990), *Soil behaviour and critical state soil mechanics*, New York: Cambridge University Press.

Nelson-Skornyakov, F.B. (1949), Seepage in homogeneous media, *Gosudarctvennoe Izd, Sovetskaya Nauka*, Moscow.

Nelson, J.D., Shepherd, T.A., and Charlie, W.A. (1977), Parameters affecting stability of tailings dams, *Proceedings, Conference on Geotechnical Practice for Disposal of Solid Waste Materials*, ASCE Speciality Conference of the Geotechnical Engineering Division, 444-460.

Okusa, S., and Anma, S. (1980), Slope failures and tailings dam damage in the 1978 Izu-Ohshima-Kinkai earthquake, *Engineering Geology*, Vol. 16, No. 3-4, 195-224.

Okusa, S., Anma, S., and Maikuma, H. (1980), Liquefaction of mine tailings in the 1978 Izu-Oshima-Kinkai earthquake, central Japan, *Proceedings, 4th Symposium on Uranium Mill Tailings Management*.

Olsen, H.W. (1966), Darcy's law in saturated kaolinite, *Water Resources Research*, Vol. 2, No. 6, 287-296.

Palmer, B., and Krizek, R.J. (1987), Thickened slurry disposal method for process tailings, *Proceedings of a Speciality Conference on Geotechnical Practice for Waste Disposal '87*, *ASCE Geotechnical Special Publication no. 13*, 728-743.

Pane, V. (1985), *Sedimentation and Consolidation of Clays*, PhD thesis, University of Colorado, USA.

Papageorgiou, G., Fourie, A.B., and Blight, G.E. (1997), Flow failures and static liquefaction of tailings dams, *Proceedings, 2nd International Conference on Mining and Industrial Waste Management*, Johannesburg.

Papageorgiou, G.P., Fourie, A.B., and Blight, G.E. (1999), Static liquefaction of Merriespruit gold tailings, *Proceedings, 12th Regional Conference for Africa on Soil Mechanics and Geotechnical Engineering*, Durban, South Africa, 61-72.

Parez, L., Bachelier, M., and Sechet, B. (1976), Pression interstitielle developpee au foncage des penetrometers (Pore pressure generation during cone penetration), *Proceedings, 6th European Regional Conference of the European Society of Soil Mechanics and Foundation Engineering*, Vol. 1.2, 533-538.

Patchet, S. (1977), Fill support systems for deep-level gold mines, *Journal of the South African Institute of Mining and Metallurgy*, Sept., 34-46.

Patton, F. (1952), Back-filling at Noranda, *Canadian Mining and Metallurgy Bulletin*, Vol. 45, 191-197.

Peck, R.B. (1969), Advantages and limitations of the observational method in applied soil mechanics, *Géotechnique*, Vol. 19, No 2., 171-187.

Penman, A.D.M. (1994), Tailings dams, some aspects of their design and construction, in K.R. Saxena (ed.), *Geotechnical Engineering: Emerging Trends in Design and Practice*, 247-277.

Pettibone, H., and Kealy, D. (1971), Engineering properties of mine tailings, *ASCE, Journal of the Soil Mechanics and Foundations Division*, Vol. 97, No. SM9, 1207-1225.

Phillips, R., and Byrne, P.M. (1995), Modelling flow slides caused by static loading, *Transportation Research Record*, **1504**, 12-21.

Plewes, H.D., McRoberts, E.C., and Chan, W.K. (1988), Downhole nuclear density logging in sand tailings, *Hydraulic Fill Structures, ASCE Geotechnical Special Publication No. 21*, 290-309.

Poorooshasb, H.B. (1989), Description of flow of sand using state parameters, *Journal of Computers and Geotechnics*, Vol. 8, 195-218.

Poulos, S.J. (1988), Strength for static and dynamic stability analysis, *Hydraulic Fill Structures, ASCE Geotechnical Special Publication No. 21*, 430-451.

Poulos, S.J., Robinsky, E.I, and Keller, T.O. (1985), Liquefaction resistance of thickened tailings, *Journal of Geotechnical Engineering*, Vol. 112, No. 12, 1300-1394.

Randolph, M.F., and Wroth, C.P. (1979), An analytical solution for the consolidation around a driven pile, *Proceedings, International Journal for Numerical and Analytical Methods in Geomechanics*, Vol. 3, No. 3, 217-229.

Ripley, E.A., Redmann, R.E., and Maxwell, J. (1982), Environmental impact of mining in Canada, *The National Impact of Mining Series*, Center for Resource Studies, Kingston, Ontario.

Ritcey, G.M. (1989), *Tailings Management, Problems and solutions in the mining industry*, Elsevier, Excerpts.

Rendulic, L. (1936), Prenziffer und Porenwasserdruck in Tonen, *Der Bauingenieur*, Vol. 17, No. 51/53, 559-564.

Robertson, P.K. (1990), Soil classification using the cone penetration test, *Canadian Geotechnical Journal*, Vol. 28 176-178.

Robertson, P.K., and Campanella, R.G. (1983), Interpretation of cone penetration tests, Part I Sand and Part II: Clay, *Canadian Geotechnical Journal*, Vol. 20, 718-745.

Robertson, P.K., and Hughes, J.M.O. (1986), Determination of the properties of sand from self-boring pressuremeter tests, *ASTM, Proceedings, 2nd International Symposium on the Pressuremeter and its Marine Applications, STP 950.*

Robinsky, E.I. (1975), Thickened discharge - A new approach to tailings disposal, *Bulletin: The Canadian Institute of Mining and Metallurgy*, December, 47-59.

Robinsky, E.I. (1978), Tailing disposal by the thickened discharge method for improved economy and environmental control, *Proceedings, 2nd International Conference on Tailings Disposal*, Denver, 75-92.

Roe, C.H., and Zahl, E.G. (1986), Experiments using low viscosity resins for in-situ sampling of sand and tailing and sample analysis by image processing, *Proceedings of the International Symposium on Geotechnical Stability in Surface Mining*, Calgary: Alberta, 277-282.

Roscoe, K.H. (1970), 10th Rankine Lecture: The influence of strains in soil mechanics, *Géotechnique*, Vol. 20, No. 2, 129-170.

Roscoe, K.H., and Burland, J.B. (1968), On the generalised stress-strain behaviour of 'wet' clay, in J. Heyman and F.A. Leckie (eds.), *Engineering plasticity*, Cambridge: Cambridge University Press, 535-609.

Roth, W.F. (1991), *A Systems Approach to Quality Improvement*, Stevens, London.

Rowe, P.W. (1959), Measurement of the coefficient of consolidation of lacustrine clay, *Géotechnique*, Vol. 9, No. 3, 107.

Ruhmer, W.T. (1974), Slimes-dam construction in the gold mines of the Anglo-American group, *Journal of the South African Institute of Mining and Metallurgy*, Vol. 74, No. 7, 273-284.

Rust, E. (1996), *Interpretation of Incomplete Piezocone Dissipation Tests*, PhD thesis, University of Surrey, UK.

Rust, E., Van Zyl, D.J.A., and Follin, S. (1984), Interpretation of piezometer cone testing of tailings, *Proceedings, 6th Symposium on Uranium Mill Tailings Management*, Fort Worth.

Rust, E., Van der Berg, J.P., and Jacobsz, S.W. (1995) Seepage analysis from piezocone dissipation tests, *Proceedings, International Symposium on Cone Penetration Testing*, Swedish Geotechnical Institute, Linköping, Sweden, Vol. 2, No. 2.26, 289-294.

Sandven, R., Senneset, K., and Janbu, N. (1988), Interpretation of piezocone tests in cohesive soils, *Proceedings, 1st International Symposium on Penetration Testing, ISOPT-1*, Orlando, Vol. 2, 939-953.

Sasitharan, S., Robertson, P.K., Sego, D.C., and Morgenstern, N.R. (1993), Collapse behaviour of sand, *Canadian Geotechnical Journal*, Vol. 30, 569-577.

Schiffman, R.L., Pane, V., and Gibson, R.E. (1984), The theory of one-dimensional consolidation of saturated clays: An overview of non-linear finite strain sedimentation and consolidation, in R.N. Yong & F.C. Townsend (eds.), *ASCE, Proceedings, Symposium on Sedimentation and Consolidation Models*, Montreal, 1-29.

Schiffman, R.L., Pane, V., and Sunara, V. (1986), Sedimentation and consolidation, in B.M. Moudgil, and P. Somasumdaran (eds.), *AICE, Conference on Flocculation, Sedimentation and Consolidation*, Cloister Sea Island, 57-124.

Schiffman, R.L., Vick, S.G., and Gibson, R.E. (1988), Behaviour and properties of hydraulic fills, *Hydraulic Fill Structures, ASCE Geotechnical Special Publication No. 21*, 166-202.

Schmertmann, J.H. (1978), Guidelines for cone penetration tests, *United States Department of Transport, Report FHWA TS-78-209*, 145pp.

Schofield, A.N., and Wroth, C.P. (1968), *Critical state soil mechanics*, London: McGraw-Hill.

Scott, M.D., Lo, R.C., Klohn, E.J., Liam Finn, W.D., and Yogendrakumar, M. (1989), Non-linear dynamic analysis of L-L tailings dam, *Proceedings of the 12th International Conference on Soil Mechanics and Foundation Engineering*, Rio de Janeiro: Brazil, Vol. 3, 1911-1914.

Senneset, K., and Janbu, N. (1985), Shear strength parameters obtained from static cone penetration tests, *Strength Testing of Marine Sediments: Laboratory and In-situ Measurements, ASTM Special Technical Publication STP 883*, 41-54.

Senneset, K., Janbu, N., and Svanø, G. (1982), Strength and deformation parameters from cone penetration tests, Proceedings, *2nd European Symposium on Penetration Testing*, Amsterdam, Vol. 2, 863-870.

Senneset, K., Sandven, R., Lunne, T., By, T., and Amundsen, T. (1988), Piezocone tests in silty soils, , *Proceedings, 1st International Symposium on Penetration Testing, ISOPT-1*, Orlando, Vol. 2, 955-966.

Senneset, K., Sandven, R., and Janbu, N. (1989), The evaluation of soil parameters from piezocone tests, *Transportation Research Record, No. 1235*, 24-37.

Seed, H.B., and De Alba, P. (1986), Use of SPT and CPT tests for evaluating the liquefaction potential of sands, *ASCE, Use of In-situ Tests in Geotechnical Engineering, Geotechnical Special Publication No.6*, Blacksburg, 281-302.

Senevirante, N.H., Fahey, M., Newson, T.A., and Fujiyasu, Y. (1996), Numerical modelling of consolidation and evaporation of slurried mine tailings, *International Journal for Numerical and Analytical Methods in Geomechanics*, Vol. 20, No. 9, 647-671.

Shakesby, R.A., and Whitlow, J.R. (1991), Failure of a mine waste dump in Zimbabwe: Causes and Consequences, *Environmental Geology and Water Sciences*, Vol. 18, No. 2, 143-153.

Sherard, J.L., Dunnigan, L.P., Talbot, J.R. (1984), Basic properties of sand and gravel filters, *ASCE, Journal of Geotechnical Engineering*, Vol. 110, No. 6, 684-700.

Sherard, J.L., Dunnigan, L.P., Talbot, J.R. (1984a), Filters for silts and clays, *ASCE, Journal of Geotechnical Engineering*, Vol. 110, No. 6, 700-718.

Shields, D. (1974), Innovations in tailings disposal, *Proceedings, 1st Symposium on Mine and Preparation Plant Refuse Disposal*, 86-90.

Sills, G.C. (1975), Some conditions under which Biot's equations of consolidation reduce to Terzaghi's equation, *Géotechnique*, Vol. 25, No. 1, 129-132.

Sills, G.C., Hoare, D.L., and Baker, N. (1986), An experimental assessment of the restricted flow consolidation test, in R.N. Yong, and F.C. Townsend (eds.), *ASTM, Consolidation of soils: Testing and Evaluation - STP 892*, 7-70.

Singh, S., and Chew, R.Y. (1988), Dynamic strain in silt and effect on ground motions, *Proceedings of the Speciality Conference on Earthquake Engineering and Soil Dynamics II - Recent Advances in Ground-Motion Evaluation*, Park City: Utah, 321-330.

Siriwardane, H.J., and Ho, S.Z. (1985), Plastic deformation and hardening behaviour of a mine tailings material, *Proceedings of the 5th International Conference on Numerical Methods in Geomechanics*, Nagoya: Japan, Vol. 1, 539-546.

Skempton, A.W. (1944), Notes on the compressibility of clays, *Quarterly Journal of the Geological Society*, Vol. 100, 119-135.

Skempton, A.W. (1954), The pore pressure coefficients A and B, *Géotechnique*, **4**(4), 143-147.

Sladen, J.A., D'Hollander, R.D., and Krahn, J. (1985), The liquefaction of sands, a collapse surface approach, *Canadian Geotechnical Journal*, Vol. 22, 564-578.

Smith, E.S. (1972), Tailings disposal - Failures and lessons, in Aplin, C.L., and Argall, G.O. (eds.) (1972), *Tailings Disposal Today: Proceedings of the 1st International Tailing Symposium, Tuscon: Arizona.*, 356-376.

Smith, G.M., Abt, S.R., and Nelson, J.D. (1986), Profile prediction of hydraulically deposited tailings, *Transactions of the American Institute of Mining, Metallurgy, and Petroleum Engineers*, Vol. 280, Pt. A, 2024-2027.

Smith, M.E., Bentel, D.L., and Robertze, J.B. (1987), Management guidelines for the construction of gold tailings dams, *Proceedings, International Conference on Mining and Industrial Waste Management, SAICE*, Johannesburg, 31-38.

Soderberg, R., and Busch, R. (1977), Design guide for metal and non-metal tailings disposal, *U.S. Bureau of Mines, IC8755*.

Sowers, G.F. (1979), *Introductory Soil Mechanics and Foundations: Geotechnical Engineering*, Fourth Edition, Macmillan Publishing Co.

Stanley, G.G. (ed.) (1987), *The Extractive Metallurgy of Gold in South Africa*, The S.A. Institute of Mining and Metallurgy Monograph Series M7, The Chamber of Mines of South Africa, Volume 1 & 2.

Stokes, Sir George G. (1891), *Mathematical and Physical Paper III*, Cambridge University Press.

Stone, K.J.L., Randolph, M.F., Toh, S., and Sales, A.A. (1994), Evaluation of consolidation behaviour of mine tailings, *Journal of Geotechnical Engineering*, **120**(3), 473-490.

Sugawara, N., and Chikaraishi, M. (1982), On estimation of ϕ' for normally consolidated mine tailings by using the pore pressure cone penetrometer, *Proceedings, 2nd European Symposium on Penetration Testing*, Amsterdam, Vol. 2, 883-888.

Sully, J.P. (1985), Geotechnical aspects of remedial design for a gold tailings dam, *International Journal for Numerical and Analytical Methods in Geomechanics*, Vol. 9, No. 6, 589-598.

Suthaker, N.N., and Scott, J.D. (1996), Measurement of hydraulic conductivity in oil sand tailings slurries, *Canadian Geotechnical Journal*, Vol. 33, No. 4, 642-653.

Suthaker, N.N., and Scott, J.D. (1997), Thixotropic strength measurement of oil sand fine tailings, *Canadian Geotechnical Journal*, Vol. 34, No. 6, 974-984.

Sutherland, H.J., and Rechard, R.P. (1984), Centrifuge simulations of stable tailings dam, *ASCE, Journal of Geotechnical Engineering*, Vol. 110, No. 3, 390-402.

Swarbrick, G.E. (1992), *Transient Unsaturated Consolidation in Desiccating Mine Tailings*, PhD thesis, University of New South Whales, Australia.

Swarbrick, G.E. (1993), An approximate method for the design of tailings dams using sub-aerial deposition, in R. Fell et. al. (eds.), *Geotechnical management of waste and contamination*, 463-471.

Swarbrick, G.E. (1994), The use of small scale experiments to predict desiccation of tailings, *Proceedings, 1st International Congress on Environmental Geomechanics*, Edmonton Alberta, 563-568.

Swarbrick, G., and Fell, R. (1990), Prediction of desiccation rates of mine tailings, *Proceedings, 3rd International Symposium on the Reclamation Treatment and Utilisation of Coal Mining Wastes*, Glasgow.

Swarbrick, G.E., and Fell, R. (1991), Prediction of the improvement of tailings properties by desiccation, *Proceedings, 9th Pan American Conference on Soil Mechanics and Foundation Engineering*, 995-1008.

Swarbrick, G.E., and Fell, R. (1992), Modelling desiccation behaviour of mine tailings, *Journal of Geotechnical Engineering*, Vol. 118, No. 4, 540-557.

Taylor, D.W. (1948), *Fundamentals of Soil Mechanics*, Wiley, New York.

Teh, C.I. (1987), *An Analytical Study of the Cone Penetration Test*, D.Phil. thesis, Oxford, UK.

Terzaghi, K. (1923), Die berechnung der durchlassigkeitsziffer des tones aus dem verlauf der hidrodynamischen spannungserscheinungen, *Akademie Wissenchaften Wien*, No. 132, 125-138.

Terzaghi, K. (1941), Undisturbed clay samples and undisturbed clays, *Journal of the Boston Society of Civil Engineers*, Vol. 28, No. 3, 45-65.

Terzaghi, K. (1943), *Theoretical Soil Mechanics*, John Wiley and Sons, New York.

Thomas, E. (1971), Cemented fill practice and research at Mount Isa, *Proceedings, Australian Institute of Mining and Metallurgy*, No. 240, 33-51.

Tjelta, T.I., Tiegges, A.W.W., Smits, F.P., Geise, J.M., and Lunne, T.A. (1987), In-situ measurements by nuclear backscatter for an offshore soil investigation, *Norwegian Geotechnical Institute, Publication No. 169*, Oslo.

TMH1 (1986), *Standard Methods of Testing Road Construction Materials - Technical Methods for Highways TMH1*, National Institute for Transport and Road Research of the Council for Scientific and Industrial Research (CSIR), Second edition.

Torstensson, B.A. (1975), Pore pressure sounding instrument, *Proceedings, ASCE Speciality Conference on In-situ Measurement of Soil Properties*, Raleigh, Vol. 2, 48-54.

Toorman, E.A. (1996), Sedimentation and self-weight consolidation: general unifying theory, *Géotechnique*, Vol. 46, No. 1, 103-113.

Troncoso, J.H. (1986), Critical state of tailing silty sands for earthquake loading, *Soil Dynamics and Earthquake Engineering*, Vol. 5, No. 4, 248-252.

Troncoso, J.H., (1988), Evaluation of seismic behaviour of hydraulic fill structures, *Hydraulic Fill Structures, ASCE Geotechnical Special Publication No. 21*, 475-491.

Truscott, S.J. (1923), *A Text-Book of Ore Dressing*, Macmillan and Co.

Tschuschke, W., Mlynarek, Z, and Massolt, P. (1992), The use of the CPT test for density determination of an embankment constructed from post-flotation sediments, *Proceedings, 2nd International Conference on Construction on Polluted and Marginal Land*, 169-175.

Tschuschke, W., Mlynarek, Z, and Werno, M. (1993), Assessment of subsoil variability with the cone penetration test, *Proceedings, Conference on Probabilistic Methods in Geotechnical Engineering, Canberra*, 215-220.

Tschuschke, W., Mlynarek, Z, and Graf, R. (1994), Geotechnical parameters of post-flotation sediments with CPTU, *Special Conference Agricultural University Poznan*, 101-117.

Tschuschke, W., Mlynarek, Z., and Lunne, T. (1995), Application of cone penetration test for evaluation of geotechnical parameters of post-flotation sediments, *Proceedings, International Symposium on Cone Penetration Testing, CPT'95*, Linkoping, Vol. 2, 329-336.

Ulrich, B.F., and Valera, J.E. (1995), Experiences using CPT data for assessing liquefaction potential of mine tailings, *Proceedings, International Symposium on Cone Penetration Testing, CPT'95*, Linköping, Vol. 2, 601-606.

USCOLD (1994), *Tailings Dam Incidents*, United States Committee on Large Dams, Denver Colorado.

Vaid, Y.P. (1994), Liquefaction of silty soils, *Ground Failures under Seismic Conditions, ASCE, Geotechnical Special Publication No. 44*.

Vaid, Y.P., and Chern, J.C. (1983), Mechanism of deformation during undrained loading of saturated sands, *Soil Dynamics and Earthquake Engineering*, Vol. 2, No. 3, 171-177.

Van der Berg, J.P. (1995), *Monitoring of the Phreatic Surface in a Tailings Dam and Subsequent Stability Implications*, MSc Dissertation, University of Pretoria.

Van der Berg, J.P., Jacobz, S.W., and Steenkamp, J.M. (1998), Obtaining material properties for slope stability analysis of gold tailings dams in South Africa, *Proceedings, 1st international Conference on Site Characterisation - ISC'98*, Atlanta, Vol. 2, 1189-1194.

Van Genuchten, M.Th. (1980), A close-form equation for predicting the hydraulic conductivity of unsaturated soils, *Journal of the Soil Science Society of America*, Vol. 44, 892-898.

Van Zyl, D. (1987), Seepage and drainage analysis of tailings impoundments - Is it really that simple?, *Proceedings, International Conference on Mining and Industrial Waste Management, SAICE*, Johannesburg, 211-222.

Van Zyl, D. (1993), Mine waste disposal, in D.E. Daniel (ed.), *Geotechnical Practice for waste disposal*, Chapman Hall, 269-286.

Van Zyl, D.J.A., and Harr, M.E. (1977), Modelling of seepage through mine tailings dams, *Proceedings, Conference on Geotechnical Practice for Disposal of Solid Waste Materials*, ASCE Speciality Conference of the Geotechnical Engineering Division, 727-743.

Vermeulen, N.J. (2000), Gold tailings under the electron microscope, *Proceedings, SAICE Young Geotechnical Engineers Conference*, Stellenbosch.

Vesic, A.S. (1975), *Principles of Pile Foundation Design*, Soil Mechanics Series No. 38, Duke University, Durham.

Vesic, A.S., and Clough, G.W. (1968), Behaviour of granular materials under high stresses, *Proceedings of the ASCE, Journal of the Soil Mechanics and Foundations Division*, **94**(SM3), 661-688.

Vick, S.G. (1983), *Planning, design and analysis of tailings dams*, New York: Wiley.

Vick, S.G. (1996), Tailings dam failure at Omai in Guyana, *Mining Engineering*, Vol. 48, No. 11, 34-37.

Vick, S.G., Wilmot, C.I., and Atkinson, G.M. (1985), Risk analysis for seismic design of tailings dams, *ASCE Journal of Geotechnical Engineering*, Vol. 111, No. 7, 916-933.

Vidic, S.D., Beckwith, G.H., and Mayne, P.W. (1995), Profiling mine tailings with CPT, *Proceedings, International Symposium on Cone Penetration Testing, CPT'95*, Linköping, Vol. 2, 607-612.

Volpe, R.L. (1979), Physical and engineering properties of copper tailings, *ASCE, Current Geotechnical Practice in Mine Waste Disposal*, 242-260.

Wagener, F. (1997), The Merriespruit slimes dam failure: Overview and lessons learnt, *South African Institute of Civil Engineering Journal*, Vol. 39, No. 3, 11-15.

Wagener, F., and Wates, J.A. (1982), Geotechnical investigation and design of tailings dams on dolomite, *Transactions, 14th International Congress on Large Dams*, Rio de Janeiro, Vol. 2, 719-736.

Wagener, F, and Jacobsz, S.W. (1999), Penstock failures on gold tailings dams in South Africa, *Proceedings, 12th Regional Conference for Africa on Soil Mechanics and Geotechnical Engineering*, Durban, South Africa, 95-100.

Wagener, F, Van der Berg, J.P., and Jacobsz, S.W. (1997), Monitoring of the seepage regime in tailings dams in practice, *Proceedings, 2nd International Conference on Mining and Industrial Waste Management*, Johannesburg.

Wagener, F, Craig, H.J., Blight, G.E., McPhail, G., Williams, A.A.B., and Strydom, J.H. (1997a), The Merriespruit Tailings Dam Failure – A review, *Proceedings, 2nd International Conference on Mining and Industrial Waste Management*, Johannesburg.

Wagener, F., Craig, H.J., Blight, G., McPhail, G., Williams, A.A.B., and Strydom, J.H. (1998), *The Merriespruit tailings dam failure - A review, Proceedings, 5th International Conference on Tailings and Mine Waste, Fort Collins*, 925-952.

Wahler, W.A. and Associates (1973), Analysis of coal refuse dam failure, Middle Fork Buffalo Creek, Saunders, West Virginia, *U.S. Bureau of Mines, OFR10(1)-7*.

Watermeyer, P., and Williamson, R. (1979), Ergo tailings dam - Cyclone separation applied to a fine grind product, *Proceedings, 2nd International Tailings Symposium*, San Francisco, 369-396.

Wates, J.A. (1983), Tailings disposal, the real cost of excess water in residues, *Journal of the South African Institute of Mining and Metallurgy*, Vol. 25, 257-262.

Wates, J.A. (1991), Design and construction of tailings dams - Some design considerations, *SAICE Geotechnical Division Evening Lecture.*

Wates, J.A., Stevenson, C., and Purchase, A.R. (1987), The effect of relative densities on beaching angles and segregation on gold and uranium tailings dams, *Proceedings, International Conference on Mining and Industrial Waste Management, SAICE*, Johannesburg, 89-94.

Wates, J.A., Strayton, G., and de Swardt, G. (1999), Long-term integrity of residue deposits, *Proceedings, 12th Regional Conference for Africa on Soil Mechanics and Geotechnical Engineering*, Durban, South Africa, 101-108.

White, H. (1917), Discussion: The construction and maintenance of slimes dams, *Journal of the Chemical Metallurgical And Mining Society Of South Africa*, Vol. 17, No. 12.

Wills, B.A. (1992), *Mineral Processing Technology*, Fifth Edition, Pergamon Press.

WISE Uranium Project (1998), Safety of tailings dams,
http://antenna.nl/~wise/uranium/mdas.html

Yoshimi, Y., and Goto, S. (1996), Liquefaction resistance of silty sand based on in-situ frozen samples, *Géotechnique*, Vol. 46, No. 1, 153-156.